TUMOR MICROENVIRONMENT SIGNALING NETWORKS IN PATHOPHYSIOLOGY AND THERAPEUTICS

EDITED BY: Francesca Pirini, Paola Parrella and Daniele Vergara
PUBLISHED IN: Frontiers in Cell and Developmental Biology and
Frontiers in Oncology

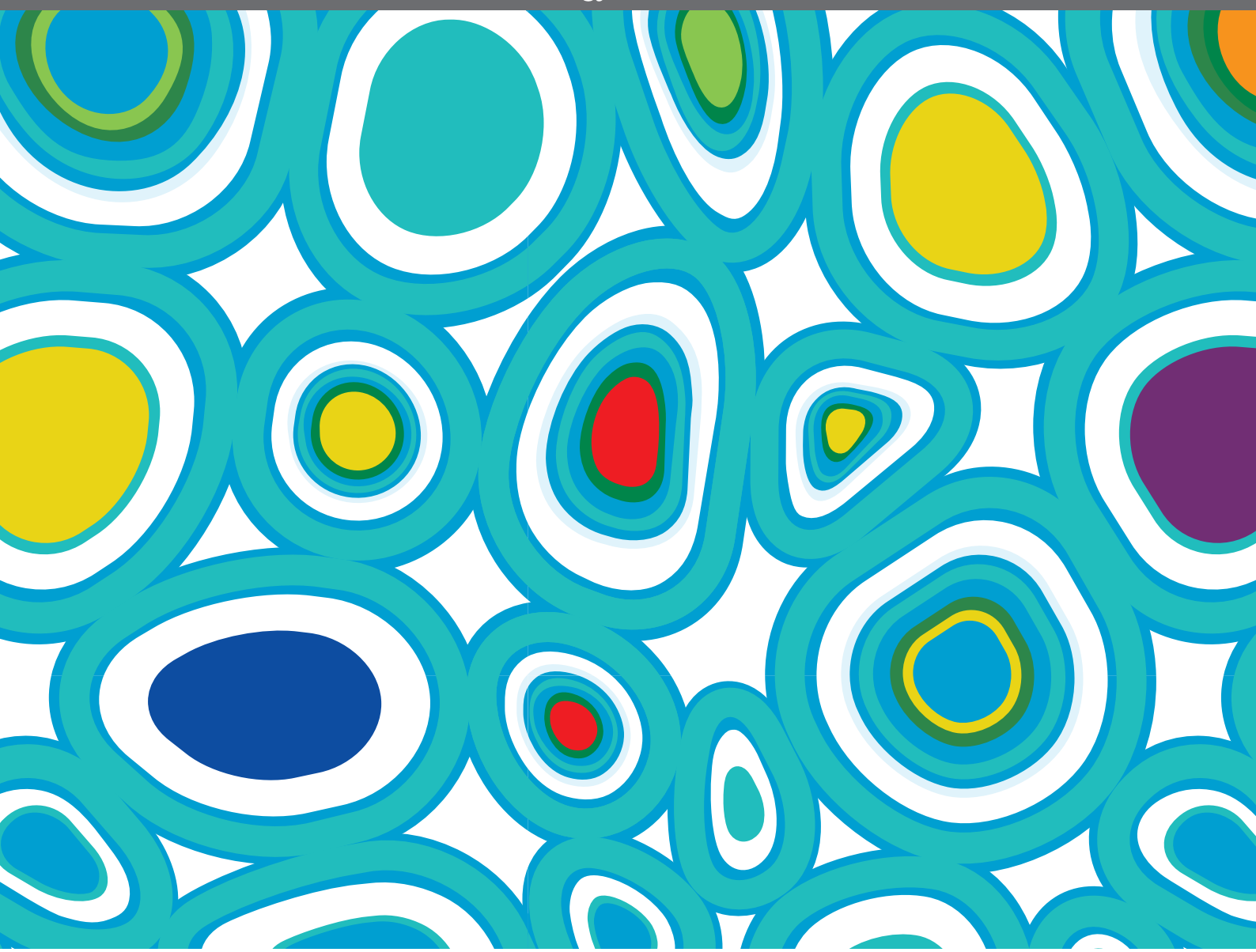

frontiers Research Topics

ISSN 1664-8714
ISBN 978-2-83250-287-7
DOI 10.3389/978-2-83250-287-7

About Frontiers

Frontiers is more than just an open-access publisher of scholarly articles: it is a pioneering approach to the world of academia, radically improving the way scholarly research is managed. The grand vision of Frontiers is a world where all people have an equal opportunity to seek, share and generate knowledge. Frontiers provides immediate and permanent online open access to all its publications, but this alone is not enough to realize our grand goals.

Frontiers Journal Series

The Frontiers Journal Series is a multi-tier and interdisciplinary set of open-access, online journals, promising a paradigm shift from the current review, selection and dissemination processes in academic publishing. All Frontiers journals are driven by researchers for researchers; therefore, they constitute a service to the scholarly community. At the same time, the Frontiers Journal Series operates on a revolutionary invention, the tiered publishing system, initially addressing specific communities of scholars, and gradually climbing up to broader public understanding, thus serving the interests of the lay society, too.

Dedication to Quality

Each Frontiers article is a landmark of the highest quality, thanks to genuinely collaborative interactions between authors and review editors, who include some of the world's best academicians. Research must be certified by peers before entering a stream of knowledge that may eventually reach the public - and shape society; therefore, Frontiers only applies the most rigorous and unbiased reviews.
Frontiers revolutionizes research publishing by freely delivering the most outstanding research, evaluated with no bias from both the academic and social point of view. By applying the most advanced information technologies, Frontiers is catapulting scholarly publishing into a new generation.

What are Frontiers Research Topics?

Frontiers Research Topics are very popular trademarks of the Frontiers Journals Series: they are collections of at least ten articles, all centered on a particular subject. With their unique mix of varied contributions from Original Research to Review Articles, Frontiers Research Topics unify the most influential researchers, the latest key findings and historical advances in a hot research area! Find out more on how to host your own Frontiers Research Topic or contribute to one as an author by contacting the Frontiers Editorial Office: frontiersin.org/about/contact

TUMOR MICROENVIRONMENT SIGNALING NETWORKS IN PATHOPHYSIOLOGY AND THERAPEUTICS

Topic Editors:
Francesca Pirini, Scientific Institute of Romagna for the Study and Treatment of Tumors (IRCCS), Italy
Paola Parrella, Home for Relief of Suffering (IRCCS), Italy
Daniele Vergara, University of Salento, Italy

Citation: Pirini, F., Parrella, P., Vergara, D., eds. (2022). Tumor Microenvironment Signaling Networks in Pathophysiology and Therapeutics. Lausanne: Frontiers Media SA. doi: 10.3389/978-2-83250-287-7

Table of Contents

frontiers | Frontiers in Oncology

TYPE Editorial
PUBLISHED 08 September 2022
DOI 10.3389/fonc.2022.1009187

OPEN ACCESS

EDITED AND REVIEWED BY
Tao Liu,
University of New South Wales,
Australia

*CORRESPONDENCE
Daniele Vergara
daniele.vergara@unisalento.it

SPECIALTY SECTION
This article was submitted to Molecular and Cellular Oncology, a section of the journal Frontiers in Oncology

RECEIVED 01 August 2022
ACCEPTED 04 August 2022
PUBLISHED 08 September 2022

CITATION
Pirini F, Vergara D and Parrella P (2022) Editorial: Tumor microenvironment signaling networks in pathophysiology and therapeutics. *Front. Oncol.* 12:1009187. doi: 10.3389/fonc.2022.1009187

Editorial: Tumor microenvironment signaling networks in pathophysiology and therapeutics

Francesca Pirini[1], Daniele Vergara[2*] and Paola Parrella[3]

[1]Biosciences Laboratory, IRCCS Istituto Romagnolo per lo Studio dei Tumori (IRST) "Dino Amadori", Meldola, Italy, [2]Department of Biological and Environmental Sciences and Technologies, University of Salento (DiSTeBA), Lecce, Italy, [3]Laboratory of Oncology, IRCCS 'Casa Sollievo della Sofferenza', San Giovanni Rotondo, Italy

Editorial on the Research Topic
Tumor microenvironment signaling networks in pathophysiology and therapeutics

The tumor microenvironment (TME) describes a variety of resident and infiltrating host non-cancerous cells including stromal cells, fibroblasts, endothelial cells, innate and adaptive immune cells, vessels, nerves and microbiota. The interplay of these different populations is the goal of numerous researches as it plays a fundamental role in tumor pathophysiology and response to treatments. Inside the tumor mass, the communication between cancer cells and the microenvironment is influenced by an intricate network modulated in time and space *via* metabolites, hormones, proteins and other molecules that influence crucial cellular processes including cell proliferation, apoptosis, cellular metabolism, genetic instability, angiogenesis, and metastasis promotion. Therefore, understanding the role of TME components and their integration adds important elements to the development and improvement of therapies. This Research Topic presents a collection of review and research articles that shed light on the molecular pathways and cellular processes involved in TME-cancer crosstalk at the signaling level, and how they influence cancer progression and response to treatments.

Ten papers of this collection focus specifically on the role of specific TME cell types in the regulation of cancer promotion and progression. As described, a range of well-orchestrated signaling mechanisms is required to coordinate their activities. In this scenario, the application of innovative techniques and increased computational power brings to a fine classification of the TME components.

Wei et al. investigated the intercellular interactions triggered by a hypoxic TME, identifying the cell population that plays a key prognostic role and the specific ligand – receptor pairs involved in tumorigenesis regulation. The authors performed a comprehensive analysis of single cell transcriptomic data collected on pan-cancer TME blueprint of six cancer types. They identified a specific subtype of macrophages characterized by the presence of secreted phosphoprotein 1 (SPP1) receptor (SPP1+ TAMs) and co-expression of MMP9. The SPP1+ TAMs are also strongly associated with hypoxia, and SPP1 expression is upregulated under this condition. Because of the

expression of MM9, they are associated with epithelial mesenchymal transition (EMT), with glycolysis and with worse outcomes. This study lays the foundations for a greater knowledge of the interactions between the components of TME and suggests possible new markers useful for improving patient stratification and the development of therapies.

Zhang Z. et al. reviewed the functional role of pancreatic stellate cells (PSC) in the progression of pancreatic cancer. PCS are stromal cells exclusively of the pancreas which function is to store vitamin A, lipid droplets and express protein markers such as synemin and desmin (1). PCSs are usually in a quiescent state but can be activated and recruited by pancreatic tumor cells. Recently, two subtypes of PCS have been identified, the myofibroblastic and inflammatory PCS subtypes, that are functionally complementary and cooperate to a favorable microenvironment for cancer survival.

Another TME component that has sparked attention for its role in supporting the proliferation of prostate cancer cells are osteoblasts. Ribelli et al. contributed to elucidate the signaling network that determines the interaction between castration resistant prostate cancer (CRPC) and osteoblast using *in vitro* co-colture models. This team reported a significant reduction of the expression of androgen receptor (AR) mRNA, protein and function after culturing C4-2B cell line with osteoblast-conditioned media (OCM), but an increase in proliferation. Among the soluble factors found in the OCM with a potential role in the reduction of AR, they found the matrix metalloproteinase-1 (MMP-1) protein. These results suggest that MMP-1 reduces AR expression and enhances proliferation binding PAR-1, a G protein-coupled receptor (GPCR). Thus, MMP-1/PAR-1 could be one of the potential pathways able to promote AR-independent CRPC proliferation.

It is now evident a direct role of nerves in the regulation of tumorigenesis. In fact, recent studies have demonstrated that nerves support tumor progression and dissemination, and that a specialized niche might be established between cancer cells and nerves. Specific signaling molecules including neurotrophins, neurotransmitters, adhesion molecules, matrix metalloproteinase and other mediators are highly enriched in this niche, suggesting that neoplastic invasion of nerves might be a key hallmark of cancer. Even if the perineural invasion (PNI) does not appear to be a common feature of colorectal cancer (CRC), PNI-positive CRC patients show a more than 20% decrease in overall and disease-free survival. As suggested by Zhang L. et al. nerves may stimulate tumor growth by releasing neurotransmitters and activating multiple downstream pathways leading to a higher risk of lymph node metastasis. An important mechanism of communication involved in both tumor promotion and tumor suppression, is the erythropoietin-producing hepatocellular carcinoma (Eph) receptor B2 (EphB2) pathway. EphB2 is a transmembrane receptor expressed in tumor cells and endothelial cells that binds transmembrane-ephrin ligands therefore them activation requires cell-cell contact, leading to a bidirectional intracellular signaling that activates various molecules, such as MAP kinases, Src family kinases, GTPases, PI3K and phosphatases. EphB2 can generate bidirectional signals and is aberrantly expressed in many cancer types. In tumors where EphB2 is overexpressed it acts as tumor promoter (hepatocarcinoma, breast cancer, glioma and malignant mesothelioma) while in colorectal cancer and bladder cancer is low expressed indicating a tumor suppression role. Recently, its expression has been detected also in immunocytes and monocytes reporting a role in immunity. Liu et al. summarized the role of EphB2 in cancer and the potential use as biomarker for cancer diagnosis, prognosis and treatment.

In addition to these different cellular types, other factors can impact on TME. For instance, chronic stress but also more physical and mechanical characteristics can activate signaling pathways that stimulate tumor initiation and progression. In particular, two articles deal with these topics. Sheth and Esfandiari discusses the fact that cancer is characterized by a bioelectric dysregulation which can be explained by the change in electrical state of the membrane potential and in an altered extracellular vesicles production which in turn can alter the tissue organization. Membrane potential is a property belonging to all cells and an integral contributor of the microenvironment that guides cellular behavior (2) spatially and temporally. The role of bioelectric dysregulation in cell signaling and its influence in EV production needs to be studied in depth for a more complete view of the mechanisms that regulate tumor initiation and metastasis and because it is manipulable thanks to the application of new technologies, as explained by the authors.

Some organs are subjected to continuous movements. The cells of the lungs and in particular lung cancer associated fibroblasts (CAFs) are constantly subjected to stretching and retraction because of the movements associated with breathing and this mechanical load plays a role in tumorigenesis. (3, 4). It is not to be forgotten that cells respond also to mechanical signals *via* mechanoreceptors that often encounter the ECM where the signals are converted in physiological responses. These signals affect cell proliferation, differentiation, and migration (5). Mechanical stimulation can regulate fibroblasts and the ECM components within the tumor microenvironment and studies suggest that CAFs play a crucial role in tumor progression. This topic has been reviewed by Gong et al. that provided an overview of factors involved in cell mechanics with a role in tumorigenesis.

Chronic stress occurs frequently in cancer patients during cancer diagnosis and treatment (6) and extensive studies determined the influence of these factors in altering TME. As reviewed by Tian et al., chronic stress leads to a constant release of stress hormones due to a constant activation of hypothalamic-pituitary adrenal (HPA) axis and the sympathetic nervous system (SNS). In detail, the TME of patients with chronic stress is characterized by changes in the number and types of immune cells, such as an increase of macrophages and NK. Chronic stress also affects the type and quantity of cytokines, angiogenesis, enhanced epithelial mesenchymal transition (EMT), and damaged ECM.

The review by Tian et al. also summarizes the mechanisms that lead to TME changes, under chronic stress. Mechanistically, androgen receptor (AR) and glucocorticoid signalling can modulate TME stress in distinct ways, for instance by inducing hypoxia (7). These findings suggest that the integration of cancer therapies with α-blockers, β-blockers, antidepressants, and interventions, like meditation and mindfulness, may be introduced in treatment plans to improve response to therapies.

A precise TME characterization also allows the identification of personalized strategies to improve cancer prognosis. Authophagy is an important doble player in tumorigenesis, acting in a positive and negative way, and is also associated with immunity. Zhang M.Y. et al. through an analysis of the gene expression profile and clinical information of 594 lung samples (LUAD), establish a risk model based on 10 autophagy related genes (ARGs) to predict the prognosis of LUAD. They also used five pooled ARG expression signatures as independent prognostic factors.

In recent years, the introduction of immune checkpoint inhibitors (ICIs) have revolutionized the treatment of solid tumors. However not all patients benefit from the treatment, and secondary resistance is widely reported. It is well known that *in vitro*, the immune system can recognize tumor antigens and kill tumor cells, but the recognition of the tumor antigen alone is not sufficient for the host to eliminate an established tumor *in vivo*. Indeed, the TME usually prevents effective lymphocyte priming, and tumor infiltration, and suppresses effector cells, which leads to a failure of the host to control tumor growth. The predominance of specific cell phenotypes in the TME may exert pro- or anti-tumoral and their modulation can affect the responses to treatments, making them more or less effective. In this collection, Russo and Nastasi reported the latest knowledge about the role of tumour-associated macrophages and neutrophils, their interactions with tumor cells, their role in response to current treatments and the development of therapeutic strategies.

The recognition of tumour cells by the immune system depends on a delicate balance between activating and inhibitory signals mediated by specific receptors. In particular the T cell immunoreceptor with immunoglobulin and ITIM domain (TIGIT) is an inhibitory receptor that regulates T cell-mediated tumor recognition and represents a putative target for checkpoint blockade immunotherapy. Annese et al. discuss the latest development on the role of TIGIT in cancer progression as possible therapeutic strategies to avoid tumor progression, drug resistance, and drug safety.

Three studies of the collection address the relationship among TME markers and response to immunotherapy in NSCLC. Wenhao Oyung by using bioinformatic and algorithms, established a risk model for overall survival based on hypoxia, immune, and EMT gene signatures. The model was established by using the TCGA-Lung Adenocarcinoma dataset (8) as training cohort and the Gene Expression Omnibus (GEO) database (GSE68465, GSE72094) (9) as validation cohorts. Overall survival differed significantly between the high-risk and low-risk groups with AUCs for predicting 1-, 3-, and 5-year survival of 0.763, 0.766, and 0.728 on the three datasets. In the TCGA dataset, the alterations in immune checkpoint genes, and the TME markers immunoscore and stromal score (10), were negatively correlated with the risk score indicating stronger tumor immune activity in low-risk patients than in high-risk patients. In addition, the risk score formula was associated with progression-free survival (PFS) in patients with NSCLC undergoing anti-PD-1/PD-L1 therapy (GSE135222 dataset) and was higher in patients with NSCLC who had experienced no benefit from nivolumab or pembrolizumab than in those who had experienced a benefit (GSE126044 dataset). Interestingly, the risk score was associated with worse immunotherapy response in patients with metastatic urothelial cancer (IMvigor210 dataset) (11, 12) resulting also in other tumour types.

Bravaccini et al. evaluated the expression of the immune checkpoint PD-L1 and the EMT marker vimentin expression in tumor cells, immune infiltrate and PD-L1 positive immune infiltrate through immunohistochemistry in tissue samples from resected non-metastatic NSCLC patients. A weak positive correlation was found between PD-L1 and vimentin expressions in tumor cells ($r=0.25$; $p< 0.001$) and a trend towards a shorter overall survival in patients with both PD-L1 and vimentin expression >1% (HR 1.36; 95% CI:0.96–1.93, p 0.087) suggesting that the interplay between PD-L1 and vimentin may affect the risk of tumour progression through the effect of EMT on immune evasion exerted through the regulation of PD-L1 expression (13) as a consequence of the action of TNF-α on NF-κB stimulation, which increases EMT induction by TGF-β1. NF-κB inhibition also blocks PD-L1 (13).

Although Immune checkpoint inhibitors (ICIs) have revolutionized the treatment of NSCLC, not all patients can benefit from the treatment, and secondary resistance to ICIs is widely reported. In addition to T lymphocytes, which are the major target for immunotherapies, a variety of other cells present in the tumor microenvironment (TME) act in a complex cross-talk between tumor, stromal, and immune cells. Gemelli et al. reviewed the potential role of Natural Killer (NK) cells as predictive biomarkers for immunotherapy response and putative targets to overcome resistance in NSCLC. In physiological conditions, NKs can coordinate the anticancer response together with T cells. However, cancer cells and TME act by modulating NK functions inducing the switch toward a pro-tumor phenotype influencing the treatment response and effectiveness of ICIs. Indeed a growing amount of evidence suggests that NKs can act as predictor as well as a prognostic factor but they may also represent a, may also be a promising therapeutic strategy (14, 15).

Patients affected by advanced gastric cancer show a very poor prognosis with a median survival of less than one year (16). The introduction of immunotherapy is able to improve the overall survival but not all patients show the same benefits (17). Thus, there is the need for novel and more effective biomarkers that could be used to predict progression and response to immunotherapy. In their study Liang et al. investigated the putative role of as biomarkers of chemokine related long non coding (lnc-RNA). By using TCGA expression analysis data, they constructed a risk model including 10 chemokine-related lncRNAs that were able to predict patient survival, immune cell infiltration and immunotherapy response.

In recent years post-transcriptional mRNA modifications have emerged as one of the main mechanisms of gene regulation in eukaryotes. In particular, the methylation of adenosine at messenger RNA to form m6A is the most frequent mRNA modification. Several recent studies suggest that m6A modification play an important role in the interplay between the immune system and cancer (18). Liao et al. screened 23 m6A regulatory factors in 369 colorectal cancers. The modification patterns of m6A were correlated with the characteristics of TME cell infiltration. They identified three different m6A modification patterns related to different and biological pathways and clinical outcome, that allowed the stratification of patients into high and low score groups.

In conclusion, all the collected articles provide a deeper insight into the role of TME components and the interplay between them in pathophysiology of cancer and response to treatment. Published contributions range from focus on specific TME cell types to comprehensive bioinformatic analysis of publicly online cancer-related databases, combined with experimental models in order to provide prognostic biomarkers and risk models based on TME characteristics which could improve the clinical decision making and personalized approaches. We hope that this Research Topic will contribute to increasing the comprehension of TME network thus facilitating the application of this knowledge in clinical settings.

Author contributions

All authors listed have made a substantial, direct, and intellectual contribution to the work and approved it for publication.

Conflict of interest

The authors declare that the research was conducted in the absence of any commercial or financial relationships that could be construed as a potential conflict of interest.

Publisher's note

References

1. Roife D, Sarcar B, Fleming JB. Stellate cells in the tumor microenvironment. *Adv Exp Med Biol* (2020) 1263:67–84. doi: 10.1007/978-3-030-44518-8_6

2. Silver BB, Nelson CM. The bioelectric code: Reprogramming cancer and aging from the interface of mechanical and chemical microenvironments. *Front Cell Dev Biol* (2018) 6:21. doi: 10.3389/fcell.2018.00021

3. Najrana T, Mahadeo A, Abu-Eid R, Kreienberg E, Schulte V, Uzun A, et al. Mechanical stretch regulates the expression of specific miRNA in extracellular vesicles released from lung epithelial cells. *J Cell Physiol* (2020) 235:8210–23. doi: 10.1002/jcp.29476

4. Roshanzadeh A, Nguyen TT, Nguyen KD, Kim D-S, Lee B-K, Lee D-W, et al. Mechanoadaptive organization of stress fiber subtypes in epithelial cells under cyclic stretches and stretch release. *Sci Rep* (2020) 10:18684. doi: 10.1038/s41598-020-75791-2

5. Jang I, Beningo KA. Integrins, CAFs and mechanical forces in the progression of cancer. *Cancers (Basel).* (2019) 11:1–7. doi: 10.3390/cancers11050721

6. Gil F, Costa G, Hilker I, Benito L. First anxiety, afterwards depression: Psychological distress in cancer patients at diagnosis and after medical treatment. *Stress Heal J Int Soc Investig Stress* (2012) 28:362–7. doi: 10.1002/smi.2445

7. Chiarugi P, Filippi L. β3-adrenoreceptor and tumor microenvironment: A new hub. *Oncoimmunology* (2015) 4:e1026532. doi: 10.1080/2162402X.2015.1026532

8. Schabath MB, Welsh EA, Fulp WJ, Chen L, Teer JK, Thompson ZJ, et al. Differential association of STK11 and TP53 with KRAS mutation-associated gene expression, proliferation and immune surveillance in lung adenocarcinoma. *Oncogene* (2016) 35:3209–16. doi: 10.1038/onc.2015.375

9. Zhang A, Yang J, Ma C, Li F, Luo H. Development and validation of a robust ferroptosis-related prognostic signature in lung adenocarcinoma. *Front Cell Dev Biol* (2021) 9:616271. doi: 10.3389/fcell.2021.616271

10. Yoshida C, Kadota K, Ikeda T, Ibuki E, Go T, Haba R, et al. Tumor-associated macrophage infiltration is associated with a higher rate of tumor spread through air spaces in resected lung adenocarcinomas. *Lung Cancer* (2021) 158:91–6. doi: 10.1016/j.lungcan.2021.06.009

11. Cho J-W, Hong MH, Ha S-J, Kim Y-J, Cho BC, Lee I, et al. Genome-wide identification of differentially methylated promoters and enhancers associated with response to anti-PD-1 therapy in non-small cell lung cancer. *Exp Mol Med* (2020) 52:1550–63. doi: 10.1038/s12276-020-00493-8

12. Yu Y, Lin D, Li A, Chen Y, Ou Q, Hu H, et al. Association of immune checkpoint inhibitor therapy with survival in patients with cancers with MUC16 variants. *JAMA Netw Open* (2020) 3:e205837. doi: 10.1001/jamanetworkopen.2020.5837

13. Asgarova A, Asgarov K, Godet Y, Peixoto P, Nadaradjane A, Boyer-Guittaut M, et al. PD-L1 expression is regulated by both DNA methylation and NF-kB during EMT signaling in non-small cell lung carcinoma. *Oncoimmunology* (2018) 7:e1423170. doi: 10.1080/2162402X.2017.1423170

14. Albini A, Noonan DM. Decidual-like NK cell polarization: From cancer killing to cancer nurturing. *Cancer Discovery* (2021) 11:28–33. doi: 10.1158/2159-8290.CD-20-0796

15. Daher M, Rezvani K. Outlook for new CAR-based therapies with a focus on CAR NK cells: What lies beyond CAR-engineered T cells in the race against

cancer. *Cancer Discovery* (2021) 11:45–58. doi: 10.1158/2159-8290.CD-20-0556

16. Smyth EC, Nilsson M, Grabsch HI, van Grieken NC, Lordick F. Gastric cancer. *Lancet (London England)* (2020) 396:635–48. doi: 10.1016/S0140-6736(20)31288-5

17. Herbst RS, Baas P, Kim D-W, Felip E, Pérez-Gracia JL, Han J-Y, et al. Pembrolizumab versus docetaxel for previously treated, PD-L1-positive, advanced non-small-cell lung cancer (KEYNOTE-010): A randomised controlled trial. *Lancet (London England)* (2016) 387:1540–50. doi: 10.1016/S0140-6736(15)01281-7

18. Fridman WH, Zitvogel L, Sautès-Fridman C, Kroemer G. The immune contexture in cancer prognosis and treatment. *Nat Rev Clin Oncol* (2017) 14:717–34. doi: 10.1038/nrclinonc.2017.101

frontiers in Cell and Developmental Biology

ORIGINAL RESEARCH
published: 05 October 2021
doi: 10.3389/fcell.2021.749210

Characterizing Intercellular Communication of Pan-Cancer Reveals SPP1+ Tumor-Associated Macrophage Expanded in Hypoxia and Promoting Cancer Malignancy Through Single-Cell RNA-Seq Data

Jinfen Wei[1†], Zixi Chen[1†], Meiling Hu[1], Ziqing He[1], Dawei Jiang[1], Jie Long[2] and Hongli Du[1]*

[1] School of Biology and Biological Engineering, South China University of Technology, Guangzhou, China, [2] Department of Thoracic Surgery, Guangdong Provincial People's Hospital, Guangdong Academy of Medical Sciences, Guangzhou, China

OPEN ACCESS

Edited by:
Daniele Vergara,
University of Salento, Italy

Reviewed by:
Sandhya Prabhakaran,
Moffitt Cancer Center, United States
Xiaoshu Zhu,
Yulin Normal University, China
Smrati Bhadauria,
Council of Scientific and Industrial Research (CSIR), India

***Correspondence:**
Hongli Du
hldu@scut.edu.cn

[†]These authors share first authorship

Specialty section:
This article was submitted to Molecular and Cellular Oncology, a section of the journal Frontiers in Cell and Developmental Biology

Received: 29 July 2021
Accepted: 09 September 2021
Published: 05 October 2021

Citation:
Wei J, Chen Z, Hu M, He Z, Jiang D, Long J and Du H (2021) Characterizing Intercellular Communication of Pan-Cancer Reveals SPP1+ Tumor-Associated Macrophage Expanded in Hypoxia and Promoting Cancer Malignancy Through Single-Cell RNA-Seq Data. Front. Cell Dev. Biol. 9:749210. doi: 10.3389/fcell.2021.749210

Hypoxia is a characteristic of tumor microenvironment (TME) and is a major contributor to tumor progression. Yet, subtype identification of tumor-associated non-malignant cells at single-cell resolution and how they influence cancer progression under hypoxia TME remain largely unexplored. Here, we used RNA-seq data of 424,194 single cells from 108 patients to identify the subtypes of cancer cells, stromal cells, and immune cells; to evaluate their hypoxia score; and also to uncover potential interaction signals between these cells *in vivo* across six cancer types. We identified SPP1+ tumor-associated macrophage (TAM) subpopulation potentially enhanced epithelial–mesenchymal transition (EMT) by interaction with cancer cells through paracrine pattern. We prioritized SPP1 as a TAM-secreted factor to act on cancer cells and found a significant enhanced migration phenotype and invasion ability in A549 lung cancer cells induced by recombinant protein SPP1. Besides, prognostic analysis indicated that a higher expression of *SPP1* was found to be related to worse clinical outcome in six cancer types. *SPP1* expression was higher in hypoxia-high macrophages based on single-cell data, which was further validated by an *in vitro* experiment that *SPP1* was upregulated in macrophages under hypoxia-cultured compared with normoxic conditions. Additionally, a differential analysis demonstrated that hypoxia potentially influences extracellular matrix remodeling, glycolysis, and interleukin-10 signal activation in various cancer types. Our work illuminates the clearer underlying mechanism in the intricate interaction between different cell subtypes within hypoxia TME and proposes the guidelines for the development of therapeutic targets specifically for patients with high proportion of SPP1+ TAMs in hypoxic lesions.

Keywords: tumor microenvironment, single-cell RNA sequencing, pan-cancer, SPP1+ tumor-associated macrophage, intercellular crosstalk network, hypoxia

INTRODUCTION

Tumor is a complex and heterogeneous ecosystem, composed of various cell types and its surrounding tumor microenvironment (TME). Hypoxia is one characteristic of TME, linked to metabolic reprogramming (Xiao et al., 2019) and increased genomic instability (Bhandari et al., 2019), and promotes cancer progression and drug resistance (Hompland et al., 2021). Experimental and clinical studies suggest that T cells, as well as cancer-associated fibroblasts (CAFs) and (TAMs), play significant roles in cancer development and progression under hypoxia TME. For instance, IL1β-IL1R signaling is involved in the stimulatory effects triggered by hypoxia in breast cancer cells, and CAFs promote cancer progression (Lappano et al., 2020). Galectin-3 expressed and secreted from TAMs induced by hypoxia promotes breast tumor growth (Wang et al., 2020). T cell exhaustion, as a common phenomenon in solid tumors, can be mediated by TME. As T cells infiltrated cholesterol-enriched tumor tissues, it would express high levels of immune checkpoints and become exhausted through increasing endoplasmic reticulum stress (Ma et al., 2019). Therefore, explaining the molecular crosstalk between various cells and changes of cellular compositions to environmental pressure is significant for understanding how cancer develops. However, the interaction between tumor cells and other cells has been obtained using cell culture models in most studies (Chen et al., 2019), which reveals the relationship to a certain extent. Tumor and other cells in cell culture settings are not enough to reflect the true conditions of cancer patients' lesions. Besides, the molecular interaction between tumors and hypoxia TME remains largely unknown.

Recent studies, including The Cancer Genome Atlas (TCGA) project, have achieved molecular subtyping based on various characteristics and identified immune infiltration by using deconvolution on tissue samples in many cancer types (Thorsson et al., 2019). Although these studies have revealed cell proportion in cancer, it remains unresolved how the cells may interact with others to influence cancer development at a very intuitive data level and cannot effectively dissect the heterogeneity of TME. In addition, the gene expression analysis based on bulk cell population averages may be incomplete to reveal the biological properties between cell types in responses to hypoxia stress. The recently developed single-cell transcriptomic technology has great advantages for distinguishing complex cellular compositions and unravelling cell states in tumor tissues (Xiao et al., 2019). Most single-cell studies have focused on distinguishing exhausted CD8+ T cells, TAMs, and CAFs subtypes and also studied the impact of tumor heterogeneity on the effect of drug treatment in a specific cancer type (Kieffer et al., 2020; Lee et al., 2020). However, the heterogeneity and similarity of molecular interaction between distinct cell subtypes across different cancer types and their functional consequences on cancer-promoting effect remain poorly characterized. Moreover, to our knowledge, the direct role of hypoxia on the biological characteristics of each cell subtype as well as on cellular interaction mode between them has not yet been addressed in pan-cancer.

Here, we use single-cell transcriptomic data covering six cancer types and perform a comprehensive analysis to identify the cell subtypes, evaluate their hypoxia score, and to deduce their possible interrelationships in the complex pan-cancer ecosystem landscape. We further identify specific ligand–receptor pairs involved in regulating tumorigenesis and identify specific macrophage subpopulations co-occurring in multiple cancers as key roles linking to poor prognosis and tumor malignancy. Our study illuminates the nature of interactions between cancer cells and the TME and proposes the guidelines for the development of novel therapeutic interventions by targeting hypoxia and cellular crosstalk triggered by hypoxia.

MATERIALS AND METHODS

Data Collection

The single-cell gene expression matrices in the present study were retrieved from the following database: pan-cancer TME blueprint[1] [including the data of breast cancer (BC), colorectal cancer (CRC), lung cancer (LC), and ovarian cancer (OV; Qian et al., 2020)]; Gene Expression Omnibus [accession numbers: GSE13246, GSE132257, GSE144735 (Lee et al., 2020), and GSE144240 (Ji et al., 2020), including the data of CRC and squamous skin cancer (SCC)]; and Genome Sequence Archive (project number: PRJCA001063) (Peng et al., 2019), including the data of pancreatic ductal cancer (PDAC). Level 3 RNA-seq data and clinical data were downloaded from The Cancer Genome Atlas (TCGA) database[2]. Moreover, the microarray sequencing data of macrophages in hypoxic culture was obtained in GEO database (accession number: GSE4630) (Boström et al., 2006).

Single-Cell RNA-Seq Data Processing

The raw gene expression matrices were processed using Seurat (v3.2.0) R toolkit. The following quality control steps were applied: (1) genes expressed by <50 cells were not considered and (2) cells that had either fewer than 800 (low-quality cells), over 6,000 expressed genes (possible doublets or multiplets), or over 10% of reads mapping to mitochondrial RNA were filtered out. The sample and remaining cell number in each cancer type is listed in **Supplementary Table 1**. We obtained the S and G2/M phase score of each cell using the CellCycleScoring function, then normalized the gene expression matrices and regressed out confounding factors such as cell cycle, mitochondrial gene percentage, and total UMI counts using the SCTransform wrapper in Seurat. We constructed principal components (PCs) using highly variable genes generated in the former steps, then selected the first 30 PCs for graph-based clustering with functions FindNeighbors and FindClusters in Seurat. To obtain major cell clusters, the resolution parameter of FindClusters function was set to a small value; to obtain subclusters, we extracted the data of major cell types and reperformed RunPCA, FindNeighbors, and FindClusters. The resolution for each cluster and subcluster analysis is presented in **Supplementary Table 2**. For visualization

[1]http://blueprint.lambrechtslab.org

[2]https://portal.gdc.cancer.gov/

of clustering analysis, we performed t-distributed stochastic neighbor embedding (t-SNE) using RunTSNE function in Seurat. As the CRC samples are from different platforms, to increase the accuracy of cell-type designation, we jointly applied a canonical correlation analysis (CCA) before cell-type identification.

We discriminated differentially expressed genes (DEGs) based on Wilcoxon rank-sum test and Model-based Analysis of Single-cell Transcriptomics (MAST) using the Seurat function FindAllMarkers; each cluster was compared to the union of the rest clusters. Genes with a P-value < 0.05 were considered as DEGs detected by both Wilcoxon and MAST methods.

Cell Type and Subtype Annotation

The clusters and subclusters were annotated based on the top-ranking DEGs among the canonical marker genes known from previous studies and literatures. To improve the accuracy of the annotation, we implemented reference-based cell type annotation with SingleR (v1.4.0) and celldex (v1.1.0) R package. Highly expressed markers in each cluster were identified for specific T/NK cells, fibroblasts, myeloid cells, mast cells, endothelial cells, B/plasma cells, and epithelial cells (**Supplementary Table 2**). To facilitate the identification of numerous cell types, each subcluster was labeled according to the sequence of cells in the cluster tag. Subclusters 0, 1, 2, 3, and 4 of stromal cells were labeled FS1, FS2, FS3, FS4, and FS5 in each cancer type. Subclusters 0, 1, 2, 3, and 4 of cancer cells were labeled CS1, CS2, CS3, CS4, and CS5 in each cancer type. Subclusters 0, 1, 2, 3, and 4 of macrophages/monocytes/dendritic cells were labeled M-S1/Mon-S1/DC-S1, M-S2/Mon-S2/DC-S2, M-S3/Mon-S3/DC-S3, M-S4/Mon-S4/DC-S4, and M-S5/Mon-S5/DC-S5 in each cancer type. Subclusters 0, 1, 2, 3, and 4 of CD8 T cells/CD4 T cells/natural killer cells were labeled CD8-S1/CD4-S1/NK-S1, CD8-S2/CD4-S2/NK-S2, CD8-S3/CD4-S3/NK-S3, CD8-S4/CD4-S4/NK-S4, and CD8-S5/CD4-S5/NK-S5 in each cancer type. Detailed information of cluster including subcluster annotation and cell type markers used in this pipeline are addressed in **Supplementary Table 2**. In some subclusters, we also found few cells expressing markers from other cell types, which we define as unknown clusters and were removed from further analysis.

Evaluation of Developmental Trajectory of Myeloid Cells

In order to reveal the cell state transitions, we constructed cell trajectory for monocytes and macrophages using Monocle (v2.18.0) R package (Trapnell et al., 2014). We first excluded dendritic cell clusters from myeloid cells, then substituted Monocle variable genes with the union of DEGs in each subcluster. Dimensional reduction and cell ordering were performed using reduceDimension and orderCells function. The myeloid cells' cell differentiation trajectory was deduced with the default parameters of Monocle after dimension reduction and cell ordering.

Definition of Gene Signature Scores Involved in Cell-Specific Function

To make a comparison with the transcriptional signatures of tumor cells, we used the hallmark gene sets from MsigDB[3] to define cell characteristics by calculating gene set variation analysis (GSVA) score (Hänzelmann et al., 2013). GSVA scores of gene signatures (CAF related, M1/M2 macrophages, pro-inflammatory, anti-inflammatory, etc.) were obtained from previous researches (Azizi et al., 2018; Chen and Song, 2019) to distinguish the features of each cluster in fibroblasts and myeloid cells, respectively. Hypoxia and glycolysis scores were also calculated by GSVA using gene signatures (Wei et al., 2020) across cells and samples in each cancer type. The cytotoxicity and exhaustion activity scores were defined as described in a previous study (Guo et al., 2018). All gene signatures are listed in **Supplementary Table 3**.

Gene Signatures of SPP1+ Tumor-Associated Macrophage Cluster

Specific gene signatures of SPP1+ TAM clusters were identified by performing a differential analysis (overlap of Wilcoxon rank-sum test and MAST) between myeloid cell clusters in CRC, LC, and SCC. Differentially expressed genes between clusters (one cluster vs. all other clusters) with an adjusted P-value < 0.05 were selected. We used the DEGs in SPP1+ cluster from CRC, LC, and SCC for detecting if these genes were expressed specifically in SPP1+ cluster, and we excluded the genes if it showed an expression level higher than 1 in more than 10% of tumor cells or fibroblasts in CRC, LC, or SCC, respectively. Then, the overlapped genes between three cancer types were defined as SPP1+ TAM signature (**Supplementary Table 3**). SPP1+ TAM signature score was calculated in bulk RNA-seq data as described above.

Cell–Cell Interaction Analysis

In order to reveal the molecular mechanism of crosstalk between cells in TME, CellPhoneDB (Efremova et al., 2020) (v2.1.4) was used to calculate ligand–receptor interaction scores in each cell subcluster. This method infers the potential interaction strength between two cell subclusters based on gene expression level and provides the significance through permutation test (1,000 times). To identify biologically relevant interactions, only receptors and ligands expressed in more than a 10% threshold of the cells in the specific cluster were considered for the analysis; log-normalized gene expression matrices were input to CellPhoneDB and ran with the statistical method. We prioritized interactions that were highly enriched between different cell types based on the number of significant pairs, then manually selected biologically relevant pairs by considering the P-value (P-value < 0.05) and mean expression of the average ligand and receptor level in the present clusters.

[3]http://www.gsea-msigdb.org/gsea/msigdb/

Survival Analysis

The samples were grouped into high and low groups according to the specific gene expression, signature score, or percentage of particular cell types by the median values. Macrophage fractions were estimated by CIBERSORT[4] with default parameters to eradicate the effects of different cell proportions.

For *SPP1* expression, we performed survival analysis using the top and bottom 50% expression as high and low groups. For *SPP1* expression and TAM proportion, the samples with top and bottom 50% *SPP1* expression and TAM proportion were defined as high and low groups, respectively. The R package "survival" was used to perform the overall survival analysis and produce Kaplan–Meier survival plots. HR and the 95% CI were generated using Cox proportional hazards models.

Cell Culture, RNA Isolation, and qPCR

The human A549 lung cancer cells were cultured in RPMI-1640 replenished with 10% fetal bovine serum (FBS). All cells were cultured at 37°C in a humidified 5% CO_2 incubator. The digested cells were counted and inoculated in six-well plates until cell attachment, and then, cells were cultured in a medium added with 100 ng/ml recombinant TNFSF12 (R&D Systems) or 200 ng/ml recombinant SPP1 (R&D Systems), respectively. After 48-h culture, the total RNA was isolated from cells using TRIzol reagent (Magen) according to the manufacturer's protocol. Reverse-transcribed complementary DNA was synthesized using the Evo-M-MLV RT Kit (AG11705, Accurate Biotechnology). qRT-PCR was performed using the Applied Biosystems QuantStudio 1 Real-Time PCR System (Thermo Fisher) and the PowerUp^{TM} SYBR Green Mix (Thermo Fisher). The fold-change in the expression of target genes was calculated by the $2^{-\Delta\Delta Ct}$ method. The primer sequence is listed in **Supplementary Table 4**.

Wound Healing Assay

We conducted a wound healing assay based on the description of a previous research (Grada et al., 2017). The dissociated cells by trypsin were counted (8×10^5) and inoculated in six-well plates. The cells were cultured until a 90–100% fused cell monolayer formed after 24 h. We then scratched the cells in the fused monolayer with a pipette tip causing an experimental injury and created a linear thin scratch "wound." Subsequently, cells were cultured in FBS-free medium treated with 100 ng/ml recombinant TNFSF12 (R&D Systems) or 200 ng/ml recombinant SPP1 (R&D Systems), respectively. The wound healing was observed, and images were photographed in 8–15 fields of view that were randomly selected under the MF53-N inverted microscope (MSHOT) in 24 and 48 h. We did three biological repeat experiments. Finally, images of healing were measured and analyzed using ImageJ software (National Institutes of Health).

Cell Invasion Assay

Matrigel (BD) was diluted by FBS-free 1640 medium and coated on Transwell membrane filter inserts (Corning) to enable analysis of cell invasion. The dissociated cells by trypsin cells were washed by PBS for three times and resuspended by FBS-free 1640 medium. A 200-μl cell suspension with 1×10^5 cells treated with 100 ng/ml recombinant TNFSF12 or 200 ng/ml recombinant SPP1 was inoculated in the upper chamber, respectively, and 700 μl 1640 medium with 10% FBS was added to the lower chamber and cultured at 37°C in a 5% CO_2 environment. After 24 h, the upper chamber was washed with PBS, and cells were fixed with methanol for 30 min then dyed with 5% crystal violet for 30 min. The images were photographed in five fields of view that were randomly selected under the MF53-N inverted microscope (MSHOT). We did three biological repeat experiments. Finally, images of invasive cells were measured and analyzed using ImageJ software (National Institutes of Health).

Cell Viability Assays

Logarithmically growing cells were plated into a 96-well plate at a density of 1×10^3 cells/well and 100 ng/ml recombinant TNFSF12 (R&D Systems) or 200 ng/ml recombinant SPP1 (R&D Systems) was added after 12 h and then incubated for 0, 24, 48, 72, 96, and 120 h. Recombinant protein was added to cultured media once, and the media were not changed for 24, 48, 72, 96, and 120 h. Before proliferation ability was detected, 10 μl of Cell Counting Kit-8 (CCK8) solution (GlpBio) was added to the cultures. After incubation for 1 h in a humidified incubator containing 5% CO_2 at 37°C, absorbance was detected at 450 nm.

Hypoxia Treatment of THP-1-Derived Macrophages

Human monocyte cell THP-1 were cultured in RPMI-1640 replenished with 10% FBS, and 100 U/ml penicillin and 100 mg/ml streptomycin were added. All cells were cultured at 37°C in a humidified 5% CO_2 incubator. For cell differentiation, THP-1 monocytes were seeded at 8×10^5 cells/well in six-well plates and directly differentiated into macrophages by 24-h incubation with 100 ng/ml phorbol 12-myristate 13-acetate (PMA, Sigma), followed by a 24-h rest period in complete RPMI-1640 medium without PMA. At the end of 48 h, THP-1 macrophages were used as M0 macrophages. The total RNA was immediately isolated from cells using TRIzol reagent (Magen) according to the manufacturer's protocol.

THP-1-derived M0 macrophages were cultured in a six-well plate and incubated at 37°C under normoxia (21% O_2 and 5% CO_2) or hypoxia (1% O_2, 5% CO_2, and balanced N_2) in a hypoxic environment chamber (Maworde), respectively, for 24 h. The total RNA was immediately isolated from cells using TRIzol reagent (Magen) according to the manufacturer's protocol.

Statistical Analysis

All statistical analyses and graphical representation of data were performed in the R environment (version 4.0.3) or using GraphPad Prism software (version 7.0). The correlation analysis including gene expression, gene signature score, and cell proportion between the two groups used in this study was based on Spearman correlation. For the cell subtype abundance correlation matrix, we defined the number ratio of cell subtype

[4]https://cibersort.stanford.edu

to the belonging major cell type as the relative abundance of each cell subtype, then computed the Spearman correlation coefficient between the relative abundance of each cell subtype in six cancer types.

For the difference analysis between groups, we used Wilcoxon rank-sum test throughout the analysis on single-cell and bulk RNA-seq data. For the differential gene analysis between hypoxia-high and -low groups in TCGA, we used edgeR (Robinson et al., 2010) to get DEGs and used Metascape (Zhou et al., 2019) for gene enrichment analysis. For the cell experiment, the unpaired two-tailed *t*-test was used to compare the difference between experimental groups and control groups.

RESULTS

Global Cellular Landscape of Six Cancer Types Revealed by scRNA-Seq Analysis

After strict quality control (QC) and filtration, we collected 25,318, 15,347, 6,019, 14,991, and 21,447 single cells originating from normal tissues; 57,486, 32,509, 17,732, 40,940, and 25,772 tumor-derived cells in CRC, LC, OV, PDAC, and SCC, respectively; and 24,160 tumor-derived cells in BC. We divided all cells for each cancer type into 6–10 major clusters and identified epithelial cells, stromal cells (fibroblasts, pericytes, and endothelial cells), and immune cells (T/NK cells, B/plasma cells, myeloid, and mast cells) as the major cell types (**Figure 1**). We observed that the cell proportion of each cell type was different among cancer types. T/NK cells were only 4% in SCC, 7% in PDAC, and 10% in OV, while they were 32% in CRC, 42% in LC, and 45% in BC (**Supplementary Figure 1A** and **Supplementary Table 1**). Besides, the proportion of cells in each patient also varied, indicating intertumoral heterogeneity (**Supplementary Figure 1B**).

Hypoxia Score of Cell Subtypes in Stromal Cells, Myeloid Cells, and T Cells

In order to evaluate the hypoxia level of these major cell types in the TME, we performed a subcluster analysis on cells from cancer tissues and calculated hypoxia score in each subtype across cancer types. Subclustering of stromal cells mainly revealed three broad classes: pericytes, myofibroblasts, and fibroblasts (**Supplementary Figure 2A**). As there were few fibroblasts (710 cells) in SCC, we failed to subcluster stromal cells in this cancer, and the remaining studies of stromal cells focused on the other five cancer types. We named fibroblast clusters in order in the form of labels (e.g., FS1 and FS2 are clusters 0 and 1, respectively). According to the markers from previous studies (Costa et al., 2018; Kieffer et al., 2020) and significant up-regulated genes in each cluster, we then termed fibroblasts into collagen-related CAFs, chemokine-related CAFs, and interleukin (IL) signal-related CAFs in specific cancer types. IL signal-related CAFs [FS5 (cluster 4) in BC] up-expressed inflammatory signatures such as interferon response and inflammatory response in BC (**Figure 2A**). Collagen-related CAFs [FS1 (cluster 0) in six cancer types] exhibited the highest extracellular matrix (ECM) remodeling score (**Supplementary Figure 2B**). However, there was no consistent trend among CAFs in hypoxia scores across cancer types.

Myeloid cells were investigated in two aspects, including identification of subtypes and evaluation inflammatory features. Using conventional marker genes, we identified dendritic cells, monocytes, and macrophages and found the common subsets across all cancer types (**Supplementary Figure 2C**). We distinguished the pro-inflammatory and anti-inflammatory monocyte/macrophages according to the markers/gene sets referenced in previous studies (Azizi et al., 2018; **Figure 2B** and **Supplementary Figure 3A**). However, some specific TAMs had a mixed phenotype, expressing both pro-inflammatory and anti-inflammatory signatures as well as M1 and M2 gene signatures (**Figure 2B** and **Supplementary Figures 2C**, **3A**), consistent with previous studies (Lee et al., 2020). The noteworthy phenomenon was that *SPP1* was expressed higher in one subtype, such as M-S1 (cluster 0) in BC; M-S3 (cluster 2) in CRC; M-S1 (cluster 0) and M-S2 (cluster 1) in LC; M-S1 (cluster 0) and M-S5 (cluster 4) in OV; M-S2 (cluster 1) in PDAC; and M-S3 (cluster 2) in SCC, which were universal across six cancer types (**Figure 2B** and **Supplementary Table 2**). We named these subtypes as SPP1+ TAMs and found matrix metallopeptidase 9 (*MMP9*), associated with ECM remodeling, was also highly expressed in SPP1+ TAMs (**Figure 2B**). It was worth noting that the hypoxia score was higher in SPP1+ TAMs compared with other subtypes (**Figure 2B**). Given the above characteristics of SPP1+ TAMs, they might play a central role in tumor progress under the influence of hypoxia TME.

As TAMs can be either tissue-resident or monocyte-derived (Yona et al., 2013), a cell trajectory analysis was employed to explore the lineage trajectories of the macrophage and monocyte populations (**Figure 2C** and **Supplementary Figure 3B**). The Monocle trajectory analysis suggested that some TAM clusters could be monocyte derived, such as M-S1 and M-S2 derived from Mon-S4 in BC and M-S1, M-S3, and M-S4 derived from Mon-S7 in SCC, while others appeared to be tissue-resident macrophages in origin, such as M-S1 in CRC (**Figure 2C**). Taken together, our findings illustrate that TAMs may undergo different transcriptional reprogramming like the pro- and anti-inflammatory differentiation axis and also suggest a more complex phenotype of TAMs in the TME across different cancer types.

Subclustering of T/NK cells led to the identification of CD4+ T cells, CD8+ T cells, and NK cells (**Supplementary Figure 3C**). We intended to identify the exhaustion status of CD8+ T cells from the gene expression of key inhibitory receptors (*PDCD1*, *TIGIT*, *HAVCR2*, *LAG3*, and *CTLA4*) (**Supplementary Figure 3C**). However, cells expressing exhaustion genes also highly express cytotoxicity markers (*GZMB* and *IFNG*) in CD8+ T cells, which further confirmed that one specific subcluster highly exhibited both cytotoxicity score and exhaustion score (**Supplementary Figure 3D**). As shown in **Supplementary Figure 3D**, CD8-S3 (cluster 4) in CRC expressed both higher cytotoxicity and exhaustion scores compared with other clusters. This observation appeared to an activation-dependent exhaustion expression program similar to the previous scRNA-seq study

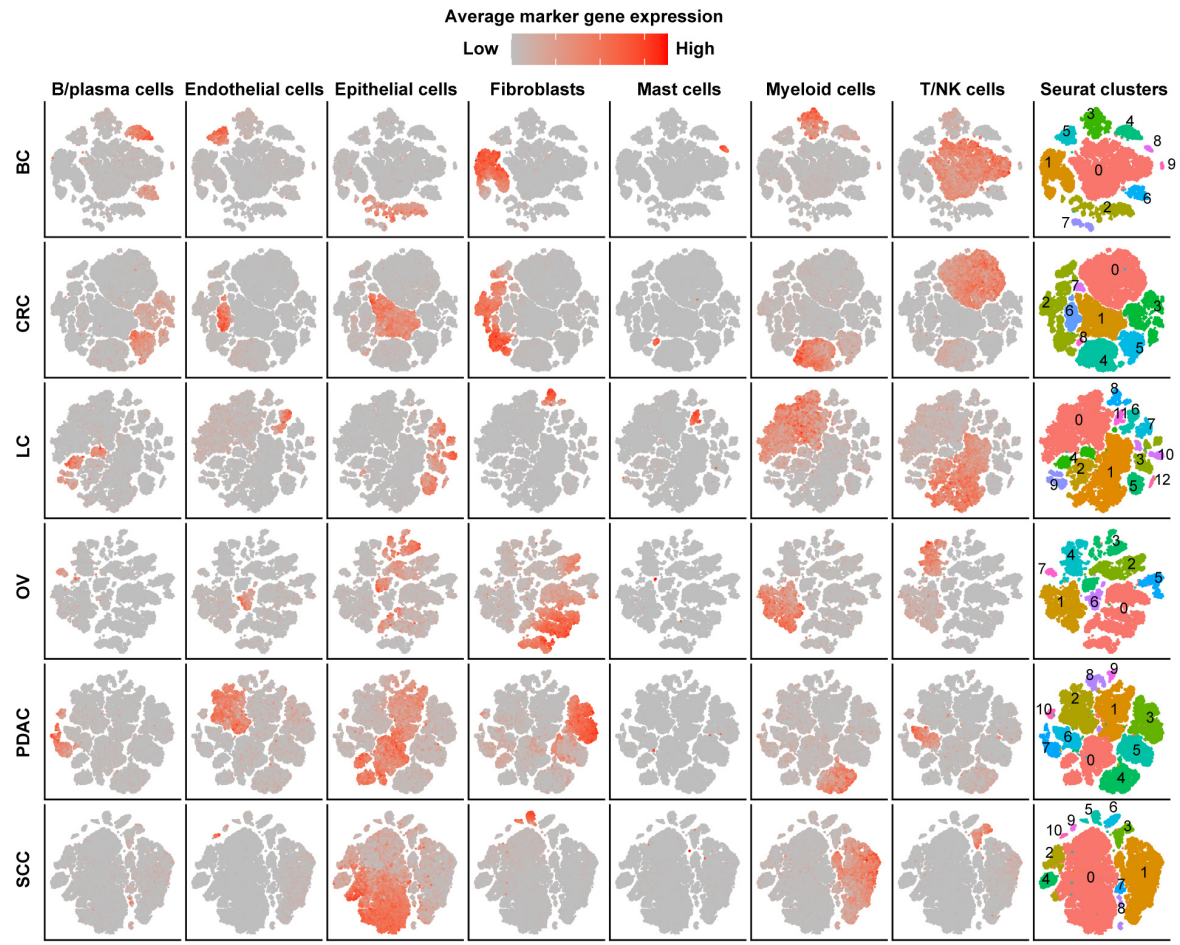

FIGURE 1 | Cell-type identification in pan-cancer. t-SNE map of single cells from cancer tissues to visualize cell-type clusters based on the expression of known marker genes [T/NK cells (*CD2*, *CD3D*, *CD3E*, *CD3G*, *FGFBP2*, *XCL1*, *FCGR3A*, *KLRD1*, and *KLRF1*), fibroblasts (*FAP*, *PDPN*, *COL1A2*, *DCN*, *COL3A1*, *COL6A1*, and *LUM*), myeloid cells (*CD14*, *CD16*, and *CD68*), mast cells (*CMA1*, *MS4A2*, *TPSAB1*, *TPSB2*, and *CPA3*), endothelial cells (*PECAM1*, *VWF*, *ENG*, *PLVAP*, and *SELE*), B/plasma cells (*SLAMF7*, *CD79A*, *BLNK*, *FCRL5*, and *CD79A*), and epithelial cells (*EPCAM*, *KRT19*, *KRT7*, *KRT18*, *KRT1*, *DMKN*, and *KRT6C*)].

(Guo et al., 2018). Unexpectedly, the exhausted CD4+ T cells [CD4-S5 (cluster 4) in BC; CD4-S9 (cluster 8) in CRC; CD4-S6 (cluster 5) in LC; CD4-S4 (cluster 3) in PDAC; and CD4-S4 (cluster 3) in SCC] were distinguished across five cancer types. As a previous study (Scharping et al., 2021) showed that T cell exhaustion was driven under hypoxic environment, it was suggested that there may be an association between hypoxia and exhaustion. We then preformed a correlation analysis and found that hypoxia score was highly correlated with exhaustion score but not cytotoxicity score in T cells across six cancer types (**Figure 2D**).

Transcriptional Heterogeneity of Malignant Cells and the Association With Hypoxia

We obtained the malignant epithelial cell subclusters and DEGs of each subcluster. We next explored how expression states varied among different cancer cells within the same cancer type, and the GSVA reflecting the activity of cancer-related hallmark pathways was applied. GSVA distribution of some subclusters revealed a significant enrichment of genes related to epithelial–mesenchymal transition (EMT) and angiogenesis, while some subclusters were highly enriched in cell cycle-related hallmarks: E2F/MYC targets and G2M checkpoint, indicating intratumoral heterogeneity (**Figure 3**). Notably, it was observed that subclusters with high hypoxia was the same as the subclusters with EMT program.

Crosstalk Between Stromal and Myeloid Cells and Cancer Cells

To decipher the molecular associations underlying cell–cell interactions, we constructed a cellular communication network between different cell subtypes using potential ligand–receptor (L–R) pair interactions (**Supplementary Figure 4A** and **Supplementary Table 5**). Importantly, the numbers of interaction between cancer cells and myeloid cells were predicted to be the most universal within the cellular network across six cancer types (**Supplementary Figure 4A**). Besides, we

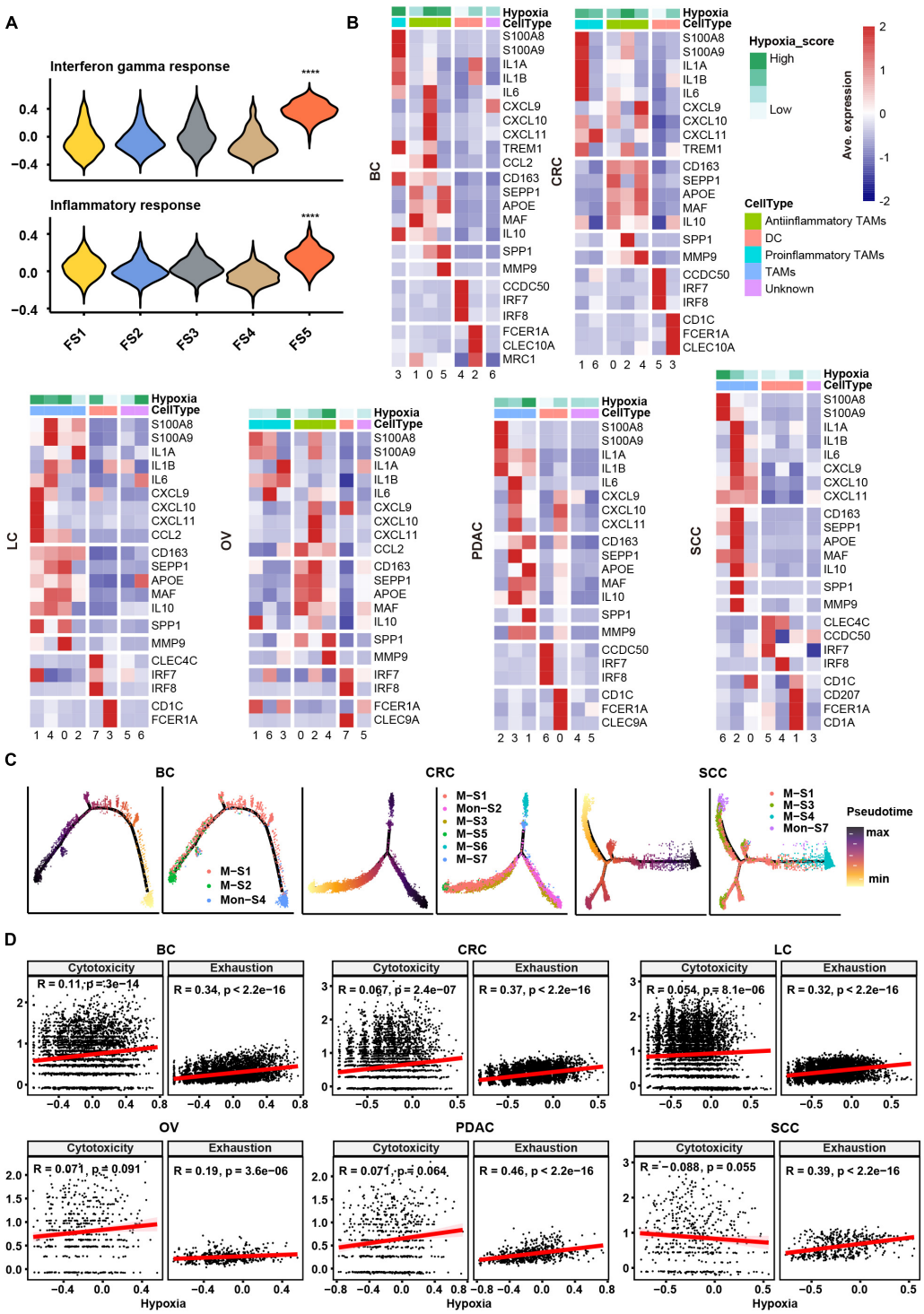

FIGURE 2 | Subtype classification and characteristics of non-malignant cells across cancer types. **(A)** Hallmark gene set scores for interferon gamma response (top) and inflammatory response (bottom), computed for all fibroblast clusters in BC. FS1, FS2, FS3, FS4, and FS5 are subclusters 0, 1, 2, 3, and 4 in stromal cells, see *Materials and Methods* and **Supplementary Figure 2A**. $^{****}p \leq 0.0001$, two-sided Wilcoxon rank sum test. **(B)** Heatmap of Z-score-normalized $\log_2$ (count+ 1) expression of canonical marker genes for myeloid cells. The color of the square on the top map indicates the average hypoxia score for each myeloid cell cluster (low to high, light green to green). **(C)** The branched trajectory of myeloid cell state transition in cancer (BC), colorectal cancer (CRC), and squamous skin cancer (SCC) inferred by Monocle 2. Each dot corresponds to one single cell, colored according to its cluster label. Subclusters 0, 1, 2, 3, and 4 of macrophages/monocytes were labeled M-S1/Mon-S1, M-S2/Mon-S2, M-S3/Mon-S3, M-S4/Mon-S4, and M-S5/Mon-S5 in each cancer type, see *Materials and Methods*. **(D)** Correlation scatter plot between gene set variation analysis (GSVA) scores of hypoxia, cytotoxicity, or exhaustion.

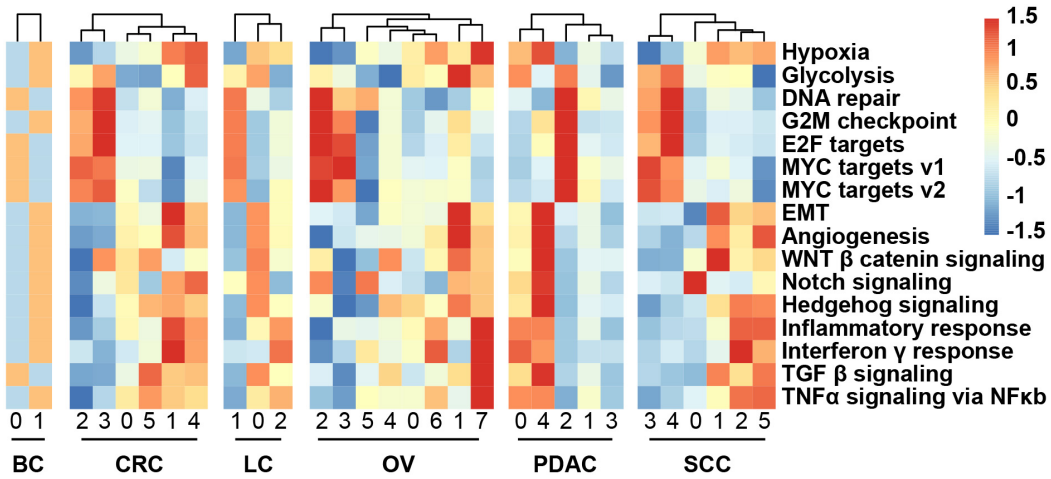

FIGURE 3 | Heatmap showing different hallmark gene sets enriched in the cancer cell subclusters by GSVA, colored by *Z*-score-transformed mean GSVA scores.

next analyzed whether there was any correlation between the respective proportions between these subclusters across patients and found some co-occurring cell subclusters (**Supplementary Figure 4B** and **Supplementary Table 6**), such as proportions between some fibroblast and cancer cell subclusters that were correlated in BC and OV.

Given that crosstalk between cancer cells and myeloid cells as well as stromal cells was predicted to be universal, we focused an analysis on interactions between these cell types and interrogated how they influenced each other in a particular way to promote cancer progression (**Figure 4A** and **Supplementary Figure 5**). In BC and OV, the stromal cells were the widespread cell types interacting with cancer cells (**Figure 4A** and **Supplementary Figure 5**). Insulin-like growth factor 1 (*IGF1*) may be secreted by stromal cells to regulate cancer cell growth through binding their receptors on the cancer cell. Insulin-like growth factor 1 receptor (*IGF1R*) gene expressed by cancer cells was highly associated with estrogen response signatures in BC, which may demonstrate that the binding effect of IGF1 on IGF1R as well as activating estrogen signaling enhanced cancer growth (**Figure 4B**). Protein tyrosine phosphatase receptor type S (*PTPRS*) was highly expressed in OV cancer cells and correlated with MYC/E2F targets, indicating that pleiotrophin (*PTN*) was secreted by fibroblasts binding to its receptor to promote the cancer cell growth (**Figure 4B**). Correspondingly, the expression of *IGF1R* and *PTPRS* was positively correlated with estrogen response-related gene *ESR1* and MYC target gene *SLC2A1* in BC and OV, respectively, (**Figure 4B**). Furthermore, the proportion of cancer cell subcluster [CS1 (cluster 0)] and stroma cell subcluster (FS3 and FS4) also displayed positive correlations in BC (**Figure 4C**). These results showed that fibroblasts potentially promoted tumor cell proliferation by expressing and secreting different growth factors.

Obviously, some L–R pairs between myeloid cell and cancer cell interaction were universal. For example, *TNFSF12-TNFRSF12A* and *SPP1-CD44* were shown in LC, CRC, and SCC (**Figure 4A** and **Supplementary Figure 5**), indicating that myeloid cells might express and secrete TNFSF12 and SPP1, signaling to their receptors TNFRSF12A and CD44 on cancer cells, respectively. Conversely, we also predicted the interaction between ligand on cancer cells and receptor on myeloid cells. The result showed TAMs would receive activated signals from cancer cells through *GAS6-AXL*, *RPS19-C5AR1*, *FAM3C-LAMP1*, *CD47-SIRPA*, and *VEGFA-NRP1/NRP2* L–R pairs in TME (**Supplementary Table 5**). Besides, these receptors of TAMs were correlated with M2 macrophage polarization (**Figure 4D**), suggesting cancer cells could possibly serve as the potential source of the ligand for activation of M2-like TAMs in TME. It is worth noting that hypoxia score also had a positive correlation with M2 macrophage polarization, which could speculate that hypoxia is a potential factor affecting cell communication (**Figure 4D**). Overall, these results indicated that tumor cells and macrophages formed a positive feedback interaction *via* ligand–receptor signaling in the TME.

Tumor-Associated Macrophages Potentially Promote Epithelial–Mesenchymal Transition of Cancer Cells

In order to study the specific effect of macrophages on tumor cells through the common L–R pairs (*TNFSF12–TNFRSF12A* and *SPP1–CD44*), we further calculated the correlation between the *TNFRSF12A* or *CD44* expression and hallmark signature scores in cancer cells. The results revealed that angiogenesis, glycolysis, and EMT were the biological process most correlated with *CD44* expression, while the TNFα signaling *via* NFκB, angiogenesis, IL6_JAK_STAT3 pathway, and EMT were correlated with *TNFRSF12A* in cancer cells across CRC, LC, and SCC (**Figure 5A** and **Supplementary Table 7**). As *SPP1* was mainly expressed in macrophage (**Supplementary Figure 6A**), we further detected that the relative abundances of SPP1+ TAMs [M-S2 (cluster 1) in LC and M-S3 (cluster 2) in CRC] and cancer cell subclusters with high EMT [CS1 (cluster 0) in LC and CS2 (cluster 1) in CRC] were

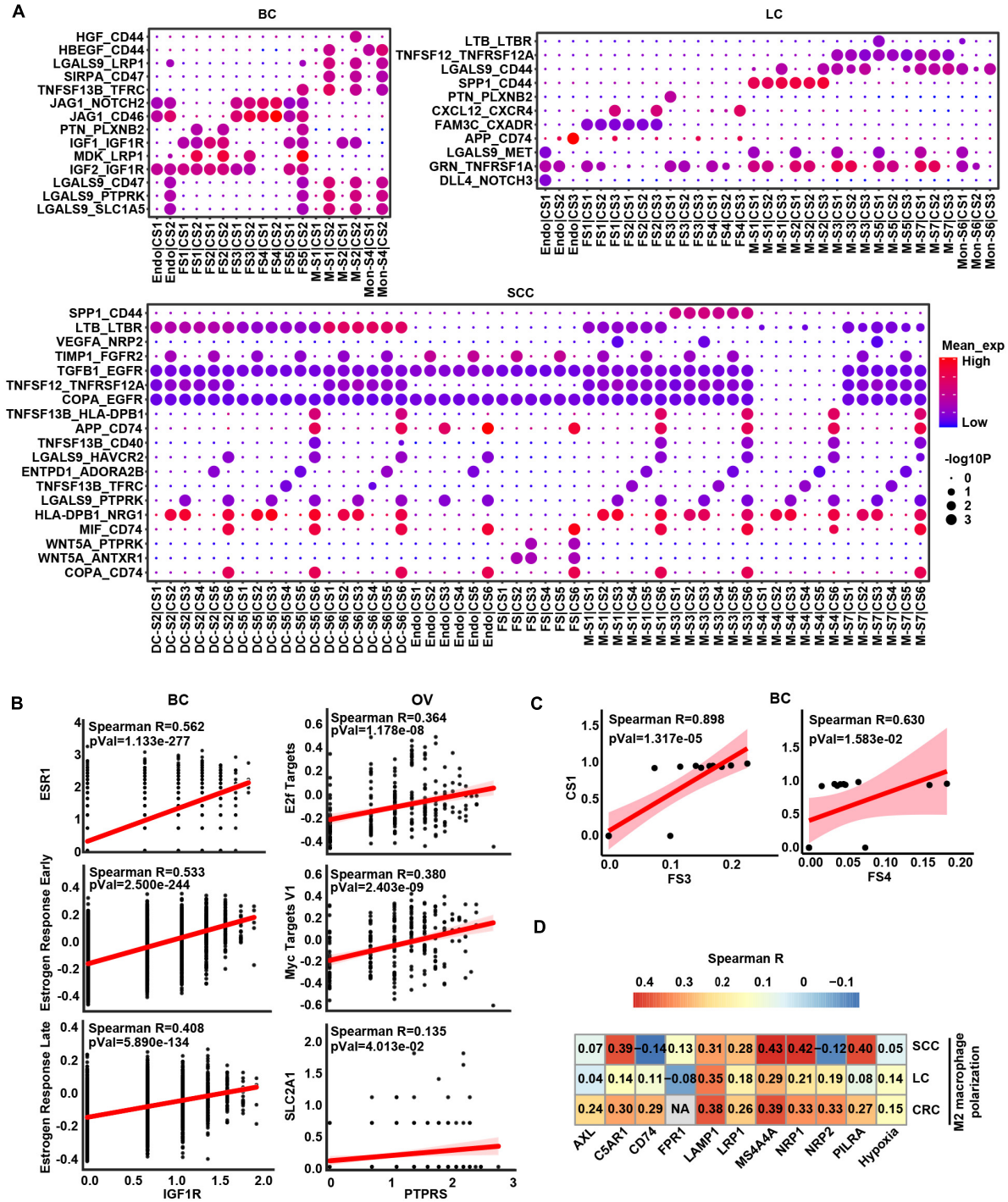

FIGURE 4 | The intercellular interactions between non-malignant cells and cancer cells. **(A)** Significant ligand–receptor genes accounting for specific intercellular interactions in BC, LC, and SCC. *P*-values are indicated by circle size. The means of the average expression level of interacting molecule (ligand or receptor genes) 1 in cluster 1 and interacting molecule 2 in cluster 2 are indicated by color. Subclusters 0, 1, 2, 3, and 4 of stroma cells were labeled FS1, FS2, FS3, FS4, and FS5 in each cancer type. Subclusters 0, 1, 2, 3, and 4 of cancer cells were labeled CS1, CS2, CS3, CS4, and CS5 in each cancer type. Subclusters 0, 1, 2, 3, and 4 of macrophages/monocytes/dendritic cells were labeled M-S1/Mon-S1/DC-S1, M-S2/Mon-S2/DC-S2, M-S3/Mon-S3/DC-S3, M-S4/Mon-S4/DC-S4, and M-S5/Mon-S5/DC-S5 in each cancer type. Endo is endothelial cells. **(B)** Correlation scatter plot between main receptors expressed on cancer cells and specific pathways as well as genes in BC and OV. **(C)** Correlation between proportional changes in specific stromal cell cluster and cancer cell cluster in BC. **(D)** Heatmap depicts the correlations between M2 macrophage polarization and hypoxia as well as main receptors expressed on macrophage.

correlated together in LC and CRC, which further strengthens the function of SPP1+ TAMs in promoting EMT (**Supplementary Table 2** and **Figure 5B**).

To evaluate the functional significance of the above key L–R interactions in lung cancer, A549 lung cancer cells were exposed to human recombinant protein SPP1 or TNFSF12 for 24 and 48 h, respectively. Compared with the control, cells exposed to recombinant protein TNFSF12 exhibited significantly enhanced migration and invasion ability but a slightly reduced proliferation of lung cancer cells (**Figures 5C–E** and **Supplementary Figures 6B–D**). In line with the phenotypic changes, TNFSF12 treatment led to a decreased expression of the epithelial marker E-cadherin (*CDH1*) (**Figure 5E**). It is known that VEGF is an NFκB-inducible protein and is one of the most potent angiogenic factors crucial for tumor metastasis (Leung et al., 1989), and qRT-PCR analysis showed that *VEGFA* expression was remarkably upregulated in lung cancer cells with recombinant protein TNFSF12 treatment at 48 h (**Figure 5E**). However, *TNFRSF12A* expression was reduced after TNFSF12 treatment, which needs a further extensive study to investigate its molecular mechanism. We observed an enhancement of cell migration and invasive behavior in lung cancer cells induced after SPP1 treatment (**Figures 5C,D** and **Supplementary Figures 6B,C**). By performing qRT-PCR, we observed that cancer cells exposed to SPP1 exhibited a significantly increased gene expression in EMT-related molecule *CD44* and glycolytic genes including *SLC2A1* and *ENO2* at 48 h (**Figure 5F**).

To further verify our single-cell analysis and *in vitro* experiment results, we then extended our analysis to TCGA LUAD database and found that *TNFSF12* expression was positively correlated with EMT score, but negatively correlated with proliferation score (**Supplementary Figure 6E**). There was a strong correlation between *SPP1* expression and glycolysis, EMT score, and related genes (**Supplementary Figure 6E**), which further reinforced that SPP1+ TAM-derived SPP1 might participate in facilitating glycolysis and EMT in lung cancer cells. Taken together, our results of the paracrine interactions analysis and *in vitro* experiment highlight the cancer-promoting role of SPP1 and TNFSF12 signaling.

SPP1 Is Upregulated in Hypoxia Tumor Microenvironment and Associated With Poor Prognosis

As SPP1+ TAMs were revealed to harbor higher hypoxia score (**Figure 2B**) and co-occur with EMT cancer cells (**Figure 5B**), we focused on exploring the functions of SPP1 and SPP1+ TAMs. *SPP1* was upregulated in macrophage derived from tumor samples compared with that from normal tissues (**Figure 6A**); we reasoned that *SPP1* was a specific TME-induced expression program in TAMs. These findings were further confirmed by TCGA cancer samples, which showed that compared with adjacent normal tissues, a much higher expression of *SPP1* in tumor tissues was observed in corresponding cancer types (**Supplementary Figure 7A**). Meanwhile, PDAC and LC were found to harbor a higher proportion (>50%) of SPP1+ TAMs (**Supplementary Figure 7B**). Using clinical data collected from the TCGA project, we confirmed that patients with a higher level of *SPP1* gene expression showed worse prognosis in six cancer types, including lung cancer studied in this study (**Figure 6B**), and a higher proportion of SPP1+ TAMs was also associated with a worse clinical outcome (**Supplementary Figure 7C**), suggesting the clinical impact of *SPP1* and SPP1+ TAMs in cancer.

As showed above, *SPP1* and *MMP9* were co-expressed in SPP1+ TAMs (**Figure 2B**); we reasoned that SPP1+ TAMs might participate in ECM remodeling. Using the ECM remodeling signatures, we assessed the functional phenotypes of each macrophage subtypes across different cancer types. As expected, the SPP1+ TAMs showed preferential ECM remodeling (**Supplementary Figure 7D**), while other TAMs exhibited lower performance. Due to the role of ECM remodeling in cancer glycolysis, angiogenesis, and metastasis, we investigated the association between SPP1+ TAM signature, SPP1 expression with glycolysis, and EMT program, respectively, and found that there was a positive correlation between them in multiple cancer types (**Figure 6C**). These results may underscore the potential cancer-promoting role of SPP1+ TAMs in complex TME.

As showed in **Figure 6D** and **Supplementary Figure 7E**, *SPP1* expression was higher in hypoxia-high macrophages, and the hypoxia score was higher in SPP1+ TAMs. Consistent with the results in single-cell data, the expression of *SPP1* was higher in hypoxia-high samples than that in low ones (**Supplementary Figure 8**). To further verify whether *SPP1* expression is directly regulated by hypoxic stress, we performed cell culture experiment and confirmed that *SPP1* expression was significantly upregulated in THP-1-derived macrophages exposed to hypoxic (1% O_2) than to normoxic (21% O_2) conditions for 24 h (**Supplementary Figures 7F,G** and **Figure 6E**). We observed a higher *SPP1* expression in human mononuclear cell-derived macrophages exposed to hypoxic (1% O_2) than to normoxic conditions for 24 h, which was further confirmed by an independent GEO dataset (Boström et al., 2006; **Figure 6F**). Thus, we reasoned that *SPP1* was upregulated, and SPP1+ TAMs were expanded in hypoxia TME, interacting with cancer cells to promote malignant biological characteristics and thus bring poor survival of patients.

Hypoxia Potentially Affecting the Biological Characteristics and Functions of Different Tumor-Infiltrating Cell Types

To discover the hypoxia effect on gene expression spectrum in different cell types, we compared the gene expression of the hypoxia-high and hypoxia-low cells by DEG analysis (1.5-fold difference, adj. $p < 0.05$) coupled with Reactome term enrichment analysis (adj. $p < 0.01$) of DEGs across T cells, fibroblasts, myeloid cells, and cancer cells. As the DEGs were fewer in T cells and fibroblasts, and we mainly focused on myeloid and cancer cells (**Supplementary Table 8**). Among the DEGs in myeloid cells, *SPP1* and *TIMP1* were the most significantly upregulated genes in hypoxia-high cells across cancers (**Supplementary Figure 9A**). As shown in **Figure 7A**, signaling by interleukins including IL4, IL13, and IL10 signals were enriched in hypoxia-high myeloid cells, indicating that immunosuppressive cytokines were activated in hypoxia TME.

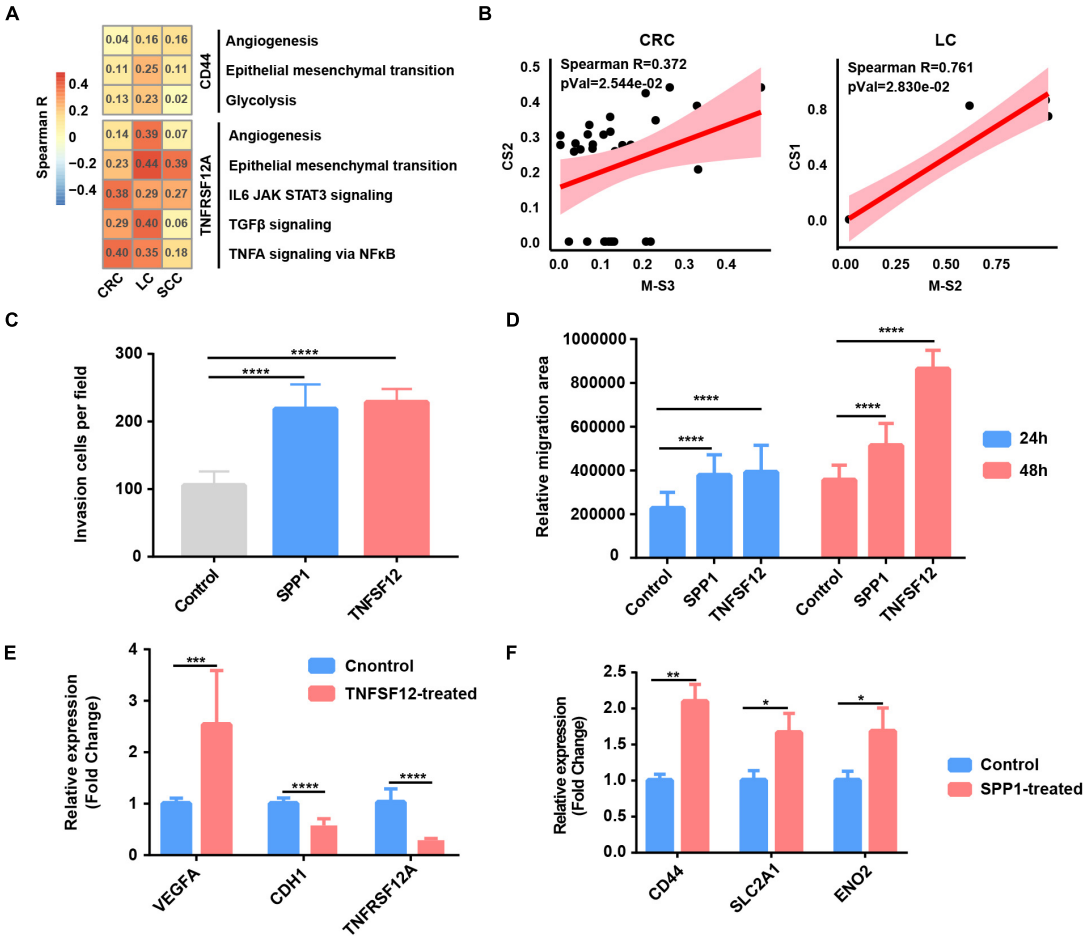

FIGURE 5 | Tumor-associated macrophages (TAMs) promote glycolysis, invasion, and migration phenotype of cancer cells. **(A)** Heatmap depicts the correlation between *CD44* or *TNFRSF12A* expression and hallmark signatures scores in cancer cells. **(B)** The correlation between proportional changes in SPP1+ TAM cluster (M-S3 and M-S2 in CRC and LC, respectively) and epithelial–mesenchymal transition (EMT)-related cancer cells (CS2 and CS1 in CRC and LC, respectively). **(C)** Box plot shows relative invasion cells per field of A549 cells treated by recombinant protein SPP1 and TNFSF12 for 24 and 48 h. $^{****}p \leq 0.0001$, two-sided unpaired *t*-test. **(D)** Box plot shows relative migration area of A549 cells treated by recombinant protein SPP1 and TNFSF12 for 24 and 48 h. $^{****}p \leq 0.0001$, two-sided unpaired *t*-test. **(E)** Relative mRNA expression of specific genes (*VEGFA*, *CDH1*, and *TNFRSF12A*) in A549 lung cancer cells exposed to TNFSF12 for 48 h. $^{**}p \leq 0.01$, two-sided unpaired *t*-test. **(F)** Relative mRNA expression of specific genes (*CD44*, *SLC2A1*, and *ENO2*) in A549 lung cancer cells exposed to SPP1 for 48 h. $^{*}p \leq 0.05$; $^{**}p \leq 0.01$, two-sided unpaired *t*-test.

Besides, degradation of ECM and glycolysis were active in hypoxia-high myeloid cells across six cancer types. However, except glycolysis, the enriched pathways in hypoxia-high cancer cells varied among cancer types, suggesting a tissue-specific response to hypoxia (**Supplementary Figure 9B**). Moreover, we included 25 TCGA cancer types and performed DEG analysis. From the DEGs, there were 489 genes upregulated in hypoxia-high tumors versus low tumors in more than 13 cancer types (**Supplementary Table 7**). We found that IL signaling and ECM degradation, as well as glycolysis, were significantly enriched in hypoxia-high tumors (**Figure 7B**). Biological processes of matrix proteoglycan, like collagen formation, collagen degradation, and integrin cell surface interactions, were also identified in TCGA cancers. Moreover, we found that the DEGs, upregulated in hypoxia myeloid cells across six cancer types, interacted with each other frequently in protein–protein interaction networks (**Figure 7C**). Taken together, these results suggest that cross-talk among these molecules up-expressing under hypoxia TME, may play critical roles in the development and progression of different cancer types.

In addition, we returned the key hypoxia-related molecular characteristics of above results back to individual samples to further inspect their relationship and distribution and found that most of the characteristics in the individual were consistent with the overall distribution across six cancer types (**Figure 7D**). For example, the extensive association between hypoxia and glycolysis in different types of cells was observed at the individual level. *SPP1* expression in myeloid cells along with EMT and glycolysis program in cancer cells was higher in hypoxia-high samples. Thus, this analysis provides a theoretical basis

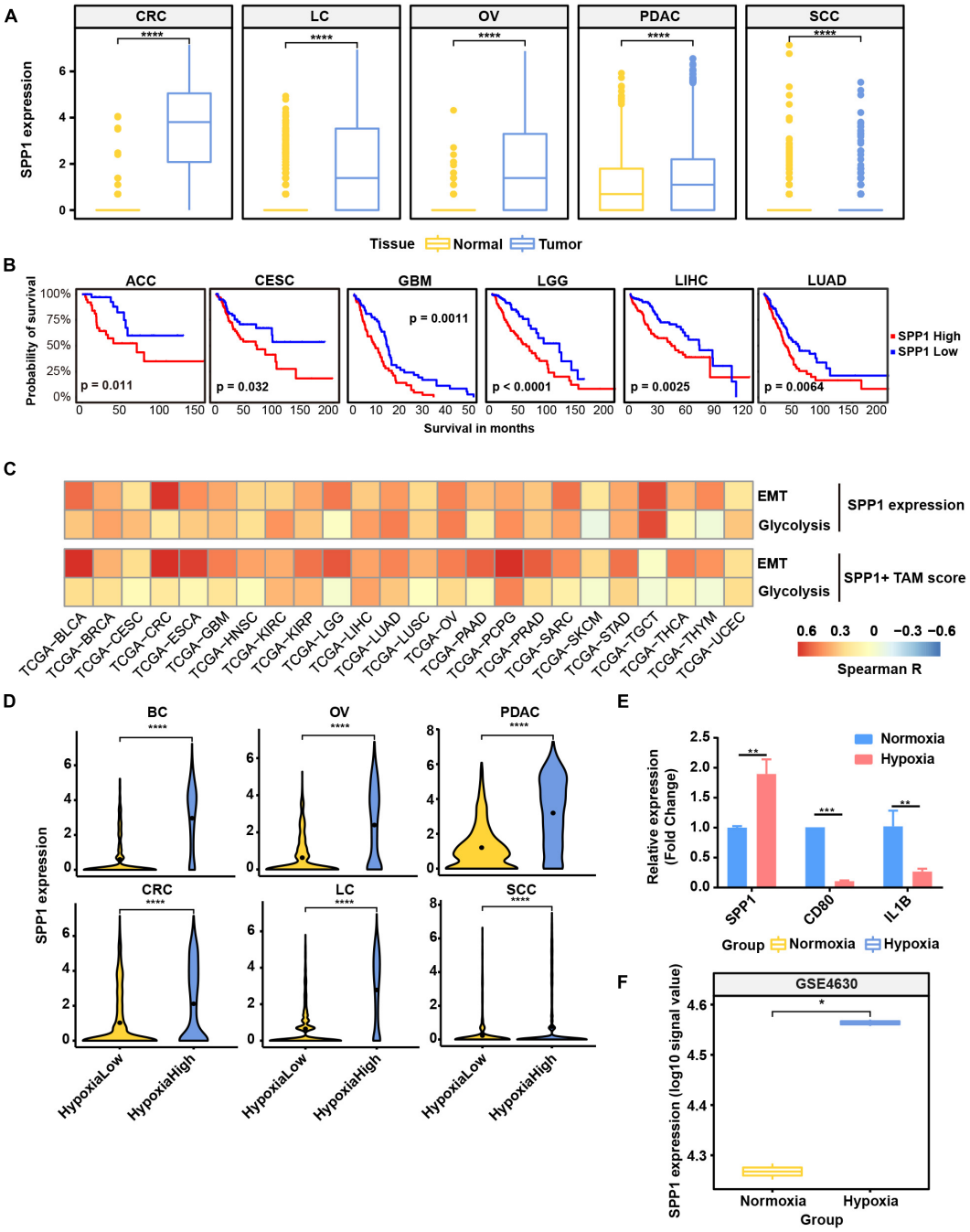

FIGURE 6 | *SPP1* is related to poor prognosis and upregulated in hypoxia tumor microenvironment (TME) to promote malignant phenotype of cancer. **(A)** The expression of *SPP1* in macrophage from tumor and normal samples. $^{****}p \leq 0.0001$, two-sided Wilcoxon rank sum test. **(B)** The Kaplan–Meier overall survival curves of The Cancer Genome Atlas (TCGA) patients grouped by gene expression of *SPP1*. **(C)** The correlation between *SPP1* expression and SPP1+ TAM signature score with glycolysis score and EMT score in TCGA cancer samples. **(D)** Violin plot shows the *SPP1* expression in hypoxia-high and -low macrophages in six cancer types. **(E)** Relative mRNA expression of *SPP1* and M1 marker genes in THP-1-derived macrophage exposed to hypoxia (1% O_2) for 24 h. **(F)** The expression of *SPP1* in macrophage exposed to hypoxia and normoxia from GSE4630 data.

for studying the intratumoral heterogeneity and intertumoral consistency within multiple cell types and also provides the clinical guidance value to single patients. In general, the above results show that hypoxia is disclosed to be the major factor to influence the intercellular crosstalk and shows different contributions to each cell types, participating in SPP1+ TAM expansion, ECM remodeling, and interleukin-10 signal activation to accelerate cancer EMT, glycolysis, and angiogenesis.

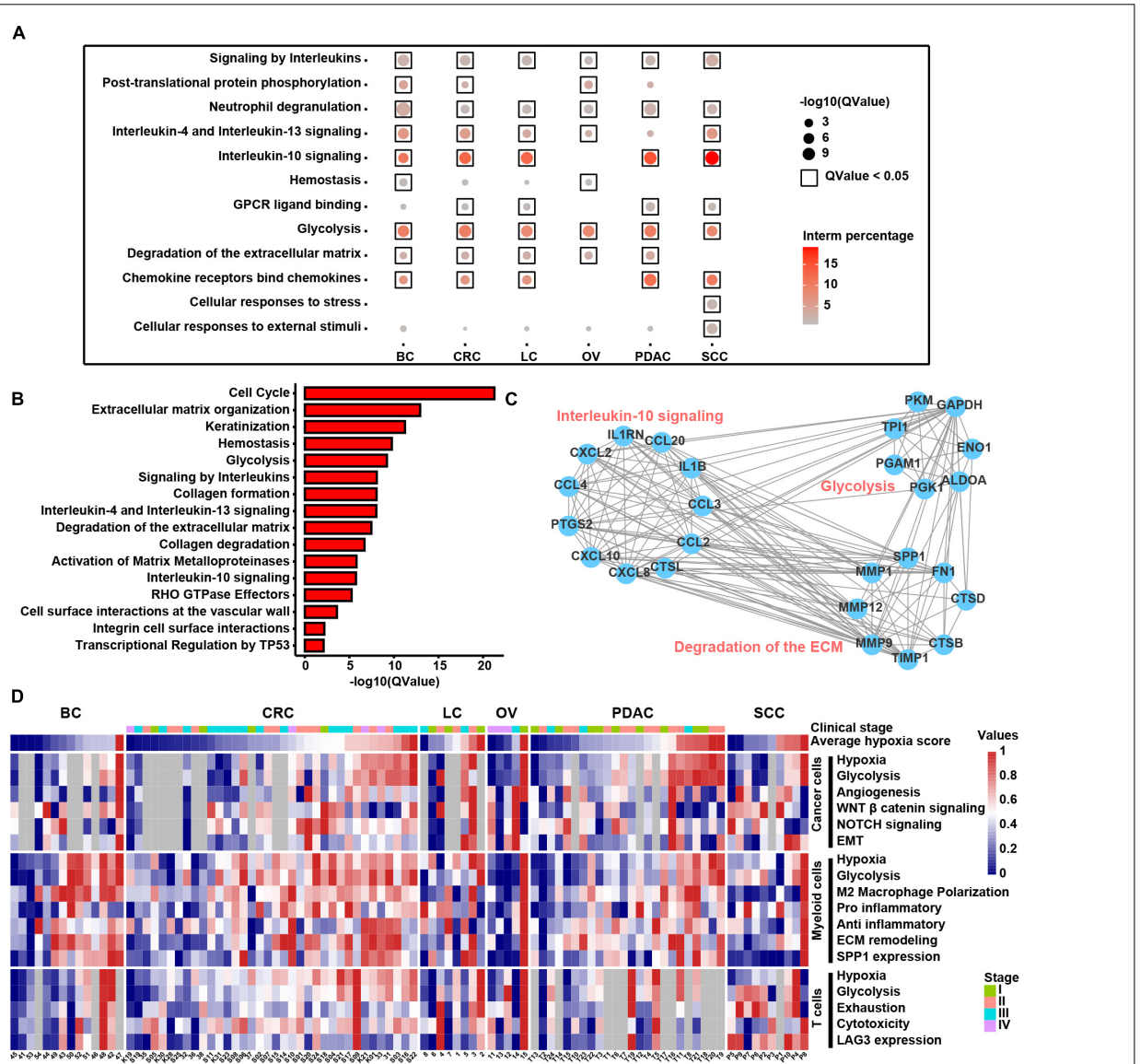

FIGURE 7 | Molecular characteristics of different cell types across samples under the hypoxia TME. **(A)** Enriched Reactome gene sets of upregulated genes in hypoxia-high myeloid cells across six cancer types. **(B)** Enriched Reactome gene sets of upregulated genes in hypoxia-high samples at least in 13 TCGA cancer types. **(C)** The protein–protein interactions among differentially expressed genes (DEGs) upregulated in hypoxia-high myeloid cells. **(D)** Clustered heatmap of 18 features across pan-cancer samples. Samples are arranged from low hypoxia score to high hypoxia score with the color blue to red, respectively. For tumors, the stage is indicated by color. Gray rectangles highlight that there were less than 50 cells in this sample. The values were normalized from 0 to 1 by Minmax.

DISCUSSION

In the present study, we identified multiple subclusters among different cell types that shape the heterogeneous TME and share consistency across different cancer types. We illustrated the cellular communication landscape between malignant and non-malignant cells and highlighted the reciprocal relationship between them. We distinguished that SPP1+ TAMs, expanded under hypoxia TME, might promote the EMT and glycolysis program of cancer cells and might be related to worse survival in multiple cancer types. This study depicts the comprehensive cellular interaction map of BC, CRC, OV, LC, PDAC, and SCC and provides a framework for future discoveries of molecular and cellular therapeutic targets to block the interactions between cancer cells and TME to inhibit cancer development more thoroughly and effectively.

Sufficient cells in this study enable us to distinguish different macrophage clusters and highlight the SPP1+ TAM subtype, which is activated under the hypoxia TME, and higher *SPP1* expression was linked to poor prognosis in multiple types. Studies have previously shown that stromal SPP1 promotes cancer cell survival and enhances invasion behavior in glioma (Lu et al., 2012), prostate cancer (Pang et al., 2019), and melanoma (Kale et al., 2015), suggesting a direct effect of SPP1 on tumor cells.

Besides, a recent study based on single-cell analysis showed that SPP1+ TAMs were associated with tumor angiogenesis in various cancer types (Cheng et al., 2021). Our current study shows that EMT is the biological process in cancer cells most associated with SPP1+ TAMs as revealed by single-cell analysis, and the potential effect of SPP1+ TAMs on cancer cells is further confirmed by TCGA bulk data. The results indicate that SPP1+ TAMs may interact with cancer cells in a paracrine pattern through expressing and secreting SPP1 then binding to cell-surface receptor CD44, consistent with a previous work, showing that CD44 is the receptor of SPP1 to regulate cancer metastasis (Wai and Kuo, 2004). One study indicates that SPP1 activates JNK signaling through a CD44v6-dependent pathway to promote clonogenicity of colorectal cancer cells, and the CD44v6 antibody is able to potently block the activation of JNK induced by SPP1 (Rao et al., 2013). Besides, another study on human optic nerve head astrocytes shows that a CD44-blocking antibody led to a significant increase of metabolic activity caused by SPP1 signaling (Neumann et al., 2014). Our results, combined with previous studies, suggest that the SPP1–CD44 interaction is important for cancer progression. Thus, the identification of SPP1 as an abundant TAM-secreted factor in cancer, coupled with the pro-tumor impact of SPP1, suggests that inhibiting SPP1 at transcriptional or protein level, blocking the interaction between SPP1+ TAMs and cancer cells through targeting SPP1 and CD44, may be an effective clinical strategy for tumor growth and metastasis inhibition. For example, small interfering RNA against SPP1 by intratumoral injection significantly suppressed breast tumor growth and angiogenesis in a mouse model (Cho et al., 2015). Blocking antibodies to SPP1 and its specific receptors CD44 showed an inhibitory role in cancer cell migration. Researchers showed that the blocking antibody targeting CD44 on stromal cells reduced the SPP1-induced breast cancer metastasis (Mi et al., 2011). SPP1-R3 aptamer was used to inactivate SPP1 and disturb surface binding of SPP1 to its cell surface CD44 receptor and mediators of ECM degradation, MMP-2, in human breast cancer cells (Mi et al., 2009). However, although there are a considerable number of therapeutic approaches by targeting SPP1 based on preclinical studies, only a few number of findings translate into clinical practice, and SPP1 inhibitors or combination drug therapy should still be further investigated from bench to clinic (Wei et al., 2017). Thus, future research is needed to elucidate the roles of SPP1 and explore the underlying molecular mechanism of SPP1 in cancer progression.

As hypoxia is one of the key environmental stresses in tumor tissues, resulting in aggressive cancer phenotypes (Haider et al., 2016), we go a step further by analyzing the association between hypoxia and cell characteristics. Although the association between hypoxia and TAMs has been studied by various researches (Henze and Mazzone, 2016), to our knowledge, this is the first study to discover a strong association between *SPP1* expression as well as SPP1+ TAM abundance and hypoxia. In exploring the link between SPP1 and hypoxia, we observed that *SPP1* gene expression was higher in hypoxia samples both in single-cell and tissue samples (**Figure 6D**; **Supplementary Figure 8**). *SPP1* expression is also upregulated under hypoxia conditions in cell culture system (**Figures 6E,F**), which indicated that *SPP1* expression was directly regulated by hypoxia. Disordered glycolysis, as an oncogenic event, is also higher in hypoxia cancer cells, which is consistent with the findings of a single-cell research where glycolysis and hypoxia signature were highly correlated in melanoma and HNSCC cancer cells (Xiao et al., 2019). Conceivably, the cancer EMT and glycolysis program promoted by SPP1+ TAMs may also be accelerated by hypoxia TME, as there is a strong correlation between the abundance of SPP1+ TAMs and EMT, glycolysis, and hypoxia. As reported by a previous work (Colegio et al., 2014) that M2 macrophage polarization is associated with the hypoxia TME and thus promotes tumor growth, we further uncover the specific molecules involved in these processes, including NRP1/NRP2 and LAMP1 expressed on TAMs. Moreover, hypoxia, in the current study, is disclosed to be a factor to influence the intercellular crosstalk, metabolic reprogramming, tumor heterogeneity, SPP1+ TAM expansion, and T cell exhaustion, thus promoting cancer development.

CONCLUSION

In summary, our work identifies the significant cell subpopulations and the interactions between them, which may provide a theoretical framework for understanding that tumor heterogeneity and diversity are driven not only by genetic and epigenetic factors but also by a combination of factors, including TME stress and other cell types surrounding tumors. The intercellular interactions suggest a tight molecular relationship between different cell types that may determine the progression and the prognosis in cancer and also encourage the development of therapeutic agents blocking interaction signals between SPP1+ TAMs and cancer cells or targeting SPP1+ TAMs in cancer patients. Although the putative interaction analysis and correlation analysis between ligand and receptor cannot define the accurate causality, this indicates a potential role for cell-to-cell interactions *in vivo*.

DATA AVAILABILITY STATEMENT

The original contributions presented in the study are included in the article/**Supplementary Material**, further inquiries can be directed to the corresponding author/s.

AUTHOR CONTRIBUTIONS

JW, ZC, and HD conceptualized the study and involved in writing—review and editing. ZC, JW, and MH were involved in the methodology. ZC, ZH, and DJ provided the software. MH, JW, and JL performed the experiment validation. ZC and JW conducted the formal analysis and performed the investigation. ZC curated the data. JW and ZC were involved in writing—original

draft preparation. HD was the project administrator and acquired funding. All authors contributed to the article and approved the submitted version.

FUNDING

This research was funded by the National Key R&D Program of China (2018YFC0910201), the Key R&D Program of Guangdong Province (2019B020226001), and the Science and the Technology Planning Project of Guangzhou (201704020176).

SUPPLEMENTARY MATERIAL

The Supplementary Material for this article can be found online at: https://www.frontiersin.org/articles/10.3389/fcell.2021.749210/full#supplementary-material

REFERENCES

Azizi, E., Carr, A. J., Plitas, G., Cornish, A. E., Konopacki, C., Prabhakaran, S., et al. (2018). Single-cell map of diverse immune phenotypes in the breast tumor microenvironment. *Cell* 174, 1293–1308.e36. doi: 10.1016/J.Cell.2018.05.060

Bhandari, V., Hoey, C., Liu, L. Y., Lalonde, E., Ray, J., Livingstone, J., et al. (2019). Molecular landmarks of tumor hypoxia across cancer types. *Nat. Genet.* 51, 308–318. doi: 10.1038/S41588-018-0318-2

Boström, P., Magnusson, B., Svensson, P. A., Wiklund, O., Borén, J., Carlsson, L. M., et al. (2006). Hypoxia converts human macrophages into triglyceride-loaded foam cells. *Arterioscler. Thromb. Vasc. Biol.* 26, 1871–1876. doi: 10.1161/01.Atv.0000229665.78997.0b

Chen, P., Zhao, D., Li, J., Liang, X., Li, J., Chang, A., et al. (2019). Symbiotic macrophage-glioma cell interactions reveal synthetic lethality in pten-null glioma. *Cancer Cell* 35, 868–884.e6. doi: 10.1016/J.Ccell.2019.05.003

Chen, X., and Song, E. (2019). Turning foes to friends: targeting cancer-associated fibroblasts. *Nat. Rev. Drug Discov.* 18, 99–115. doi: 10.1038/S41573-018-0004-1

Cheng, S., Li, Z., Gao, R., Xing, B., Gao, Y., Yang, Y., et al. (2021). A pan-cancer single-cell transcriptional atlas of tumor infiltrating myeloid cells. *Cell* 184, 792–809.e23. doi: 10.1016/J.Cell.2021.01.010

Cho, W. Y., Hong, S. H., Singh, B., Islam, M. A., Lee, S., Lee, A. Y., et al. (2015). Suppression of tumor growth in lung cancer xenograft model mice by poly(Sorbitol-Co-Pei)-mediated delivery of osteopontin sirna. *Eur. J. Pharm. Biopharm.* 94, 450–462. doi: 10.1016/J.Ejpb.2015.06.017

Colegio, O. R., Chu, N. Q., Szabo, A. L., Chu, T., Rhebergen, A. M., Jairam, V., et al. (2014). Functional polarization of tumour-associated macrophages by tumour-derived lactic acid. *Nature* 513, 559–563. doi: 10.1038/Nature13490

Costa, A., Kieffer, Y., Scholer-Dahirel, A., Pelon, F., Bourachot, B., Cardon, M., et al. (2018). Fibroblast heterogeneity and immunosuppressive environment in human breast cancer. *Cancer Cell* 33, 463–479.e10. doi: 10.1016/J.Ccell.2018.01.011

Efremova, M., Vento-Tormo, M., Teichmann, S. A., and Vento-Tormo, R. (2020). Cellphonedb: inferring cell-cell communication from combined expression of multi-subunit ligand-receptor complexes. *Nat. Protoc.* 15, 1484–1506. doi: 10.1038/S41596-020-0292-X

Grada, A., Otero-Vinas, M., Prieto-Castrillo, F., Obagi, Z., and Falanga, V. (2017). Research techniques made simple: analysis of collective cell migration using the wound healing assay. *J. Invest. Dermatol.* 137, e11–e16. doi: 10.1016/J.Jid.2016.11.020

Guo, X., Zhang, Y., Zheng, L., Zheng, C., Song, J., Zhang, Q., et al. (2018). Global characterization of T cells in non-small-cell lung cancer by single-cell sequencing. *Nat. Med.* 24, 978–985. doi: 10.1038/S41591-018-0045-3

Haider, S., Mcintyre, A., Van Stiphout, R. G., Winchester, L. M., Wigfield, S., Harris, A. L., et al. (2016). Genomic alterations underlie a pan-cancer metabolic shift associated with tumour hypoxia. *Genome Biol.* 17:140. doi: 10.1186/S13059-016-0999-8

Hänzelmann, S., Castelo, R., and Guinney, J. (2013). Gsva: gene set variation analysis for microarray and RNA-Seq data. *BMC Bioinformatics* 14:7. doi: 10.1186/1471-2105-14-7

Henze, A. T., and Mazzone, M. (2016). The impact of hypoxia on tumor-associated macrophages. *J. Clin. Invest.* 126, 3672–3679. doi: 10.1172/Jci84427

Hompland, T., Fjeldbo, C. S., and Lyng, H. (2021). Tumor hypoxia as a barrier in cancer therapy: why levels matter. *Cancers (Basel)* 13:499. doi: 10.3390/Cancers13030499

Ji, A. L., Rubin, A. J., Thrane, K., Jiang, S., Reynolds, D. L., Meyers, R. M., et al. (2020). Multimodal analysis of composition and spatial architecture in human squamous cell carcinoma. *Cell* 182, 1661–1662. doi: 10.1016/J.Cell.2020.08.043

Kale, S., Raja, R., Thorat, D., Soundararajan, G., Patil, T. V., and Kundu, G. C. (2015). Osteopontin signaling upregulates cyclooxygenase-2 expression in tumor-associated macrophages leading to enhanced angiogenesis and melanoma growth via A9β1 integrin. *Oncogene* 34, 5408–5410. doi: 10.1038/Onc.2015.315

Kieffer, Y., Hocine, H. R., Gentric, G., Pelon, F., Bernard, C., Bourachot, B., et al. (2020). Single-cell analysis reveals fibroblast clusters linked to immunotherapy resistance in cancer. *Cancer Discov.* 10, 1330–1351. doi: 10.1158/2159-8290.Cd-19-1384

Lappano, R., Talia, M., Cirillo, F., Rigiracciolo, D. C., Scordamaglia, D., Guzzi, R., et al. (2020). The Il1β-Il1r signaling is involved in the stimulatory effects triggered by hypoxia in breast cancer cells and Cancer-Associated Fibroblasts (Cafs). *J. Exp. Clin. Cancer Res.* 39:153. doi: 10.1186/S13046-020-01667-Y

Lee, H. O., Hong, Y., Etlioglu, H. E., Cho, Y. B., Pomella, V., Van Den Bosch, B., et al. (2020). Lineage-dependent gene expression programs influence the immune landscape of colorectal cancer. *Nat. Genet.* 52, 594–603. doi: 10.1038/S41588-020-0636-Z

Leung, D. W., Cachianes, G., Kuang, W. J., Goeddel, D. V., and Ferrara, N. (1989). Vascular endothelial growth factor is a secreted angiogenic mitogen. *Science* 246, 1306–1309. doi: 10.1126/Science.2479986

Lu, D. Y., Yeh, W. L., Huang, S. M., Tang, C. H., Lin, H. Y., and Chou, S. J. (2012). Osteopontin increases heme oxygenase-1 expression and subsequently induces cell migration and invasion in glioma cells. *Neuro. Oncol.* 14, 1367–1378. doi: 10.1093/Neuonc/Nos262

Ma, X., Bi, E., Lu, Y., Su, P., Huang, C., Liu, L., et al. (2019). Cholesterol induces Cd8+ T cell exhaustion in the tumor microenvironment. *Cell Metab.* 30, 143–156.e5. doi: 10.1016/J.Cmet.2019.04.002

Mi, Z., Bhattacharya, S. D., Kim, V. M., Guo, H., Talbot, L. J., and Kuo, P. C. (2011). Osteopontin promotes CCL5-mesenchymal stromal cell-mediated breast cancer metastasis. *Carcinogenesis* 32, 477–487. doi: 10.1093/Carcin/Bgr009

Mi, Z., Guo, H., Russell, M. B., Liu, Y., Sullenger, B. A., and Kuo, P. C. (2009). RNA aptamer blockade of osteopontin inhibits growth and metastasis of MDA-MB231 breast cancer cells. *Mol. Ther.* 17, 153–161. doi: 10.1038/Mt.2008.235

Neumann, C., Garreis, F., Paulsen, F., Hammer, C. M., Birke, M. T., and Scholz, M. (2014). Osteopontin is induced by TGF-B2 and regulates metabolic cell activity in cultured human optic nerve head astrocytes. *PLoS One* 9:e92762. doi: 10.1371/Journal.Pone.0092762

Pang, X., Xie, R., Zhang, Z., Liu, Q., Wu, S., and Cui, Y. (2019). Identification Of SPP1 as an extracellular matrix signature for metastatic castration-resistant prostate cancer. *Front. Oncol.* 9:924. doi: 10.3389/Fonc.2019.00924

Peng, J., Sun, B. F., Chen, C. Y., Zhou, J. Y., Chen, Y. S., Chen, H., et al. (2019). Single-cell RNA-Seq highlights intra-tumoral heterogeneity and malignant progression in pancreatic ductal adenocarcinoma. *Cell Res.* 29, 725–738. doi: 10.1038/S41422-019-0195-Y

Qian, J., Olbrecht, S., Boeckx, B., Vos, H., Laoui, D., Etlioglu, E., et al. (2020). A pan-cancer blueprint of the heterogeneous tumor microenvironment revealed by single-cell profiling. *Cell Res.* 30, 745–762. doi: 10.1038/S41422-020-0355-0

Rao, G., Wang, H., Li, B., Huang, L., Xue, D., Wang, X., et al. (2013). Reciprocal interactions between tumor-associated macrophages and CD44-positive cancer cells via osteopontin/CD44 promote tumorigenicity in colorectal cancer. *Clin. Cancer Res.* 19, 785–797. doi: 10.1158/1078-0432.Ccr-12-2788

Robinson, M. D., Mccarthy, D. J., and Smyth, G. K. (2010). Edger: a bioconductor package for differential expression analysis of digital gene expression data. *Bioinformatics* 26, 139–140. doi: 10.1093/Bioinformatics/Btp616

Scharping, N. E., Rivadeneira, D. B., Menk, A. V., Vignali, P., Ford, B. R., Rittenhouse, N. L., et al. (2021). Mitochondrial stress induced by continuous stimulation under hypoxia rapidly drives T cell exhaustion. *Nat. Immunol.* 22, 205–215. doi: 10.1038/S41590-020-00834-9

Thorsson, V., Gibbs, D. L., Brown, S. D., Wolf, D., Bortone, D. S., Ou Yang, T. H., et al. (2019). The immune landscape of cancer. *Immunity* 51, 411–412. doi: 10.1016/J.Immuni.2019.08.004

Trapnell, C., Cacchiarelli, D., Grimsby, J., Pokharel, P., Li, S., Morse, M., et al. (2014). The dynamics and regulators of cell fate decisions are revealed by pseudotemporal ordering of single cells. *Nat. Biotechnol.* 32, 381–386. doi: 10.1038/Nbt.2859

Wai, P. Y., and Kuo, P. C. (2004). The role of osteopontin in tumor metastasis. *J. Surg. Res.* 121, 228–241. doi: 10.1016/J.Jss.2004.03.028

Wang, L., Li, Y. S., Yu, L. G., Zhang, X. K., Zhao, L., Gong, F. L., et al. (2020). Galectin-3 expression and secretion by tumor-associated macrophages in hypoxia promotes breast cancer progression. *Biochem. Pharmacol.* 178:114113. doi: 10.1016/J.Bcp.2020.114113

Wei, J., Huang, K., Chen, Z., Hu, M., Bai, Y., Lin, S., et al. (2020). Characterization of glycolysis-associated molecules in the tumor microenvironment revealed by pan-cancer tissues and lung cancer single cell data. *Cancers (Basel)* 12:1788. doi: 10.3390/Cancers12071788

Wei, R., Wong, J., and Kwok, H. F. (2017). Osteopontin – a promising biomarker for cancer therapy. *J. Cancer* 8, 2173–2183. doi: 10.7150/Jca.20480

Xiao, Z., Dai, Z., and Locasale, J. W. (2019). Metabolic landscape of the tumor microenvironment at single cell resolution. *Nat. Commun.* 10:3763. doi: 10.1038/S41467-019-11738-0

Yona, S., Kim, K. W., Wolf, Y., Mildner, A., Varol, D., Breker, M., et al. (2013). Fate mapping reveals origins and dynamics of monocytes and tissue macrophages under homeostasis. *Immunity* 38, 79–91. doi: 10.1016/J.Immuni.2012.12.001

Zhou, Y., Zhou, B., Pache, L., Chang, M., Khodabakhshi, A. H., Tanaseichuk, O., et al. (2019). Metascape provides a biologist-oriented resource for the analysis of systems-level datasets. *Nat. Commun.* 10:1523. doi: 10.1038/S41467-019-09234-6

Conflict of Interest: The authors declare that the research was conducted in the absence of any commercial or financial relationships that could be construed as a potential conflict of interest.

Publisher's Note: All claims expressed in this article are solely those of the authors and do not necessarily represent those of their affiliated organizations, or those of the publisher, the editors and the reviewers. Any product that may be evaluated in this article, or claim that may be made by its manufacturer, is not guaranteed or endorsed by the publisher.

frontiers in Cell and Developmental Biology

ORIGINAL RESEARCH
published: 18 November 2021
doi: 10.3389/fcell.2021.756911

Identification of a Five Autophagy Subtype-Related Gene Expression Pattern for Improving the Prognosis of Lung Adenocarcinoma

Meng-Yu Zhang[1†], Chen Huo[1†], Jian-Yu Liu[1], Zhuang-E. Shi[1], Wen-Di Zhang[1], Jia-Jia Qu[1], Yue-Liang Yue[1] and Yi-Qing Qu[2]*

[1]Department of Pulmonary and Critical Care Medicine, Qilu Hospital, Cheeloo College of Medicine, Shandong University; Shandong Key Laboratory of Infectious Respiratory Diseases, Jinan, China, [2]Department of Pulmonary and Critical Care Medicine, Qilu Hospital of Shandong University; Shandong Key Laboratory of Infectious Respiratory Diseases, Jinan, China

OPEN ACCESS

Edited by:
Daniele Vergara,
University of Salento, Italy

Reviewed by:
Anjing Chen,
Shandong University, China
Yaiza Potes,
University of Oviedo, Spain
Qing Chun Zhao,
Shenyang Pharmaceutical University, China

***Correspondence:**
Yi-Qing Qu
quyiqing@sdu.edu.cn

[†]These authors have contributed equally to this work

Specialty section:
This article was submitted to Molecular and Cellular Oncology, a section of the journal Frontiers in Cell and Developmental Biology

Received: 11 August 2021
Accepted: 27 October 2021
Published: 18 November 2021

Citation:
Zhang M-Y, Huo C, Liu J-Y, Shi Z-E, Zhang W-D, Qu J-J, Yue Y-L and Qu Y-Q (2021) Identification of a Five Autophagy Subtype-Related Gene Expression Pattern for Improving the Prognosis of Lung Adenocarcinoma. Front. Cell Dev. Biol. 9:756911. doi: 10.3389/fcell.2021.756911

Background: Autophagy plays an important role in lung adenocarcinoma (LUAD). In this study, we aimed to explore the autophagy-related gene (ARG) expression pattern and to identify promising autophagy-related biomarkers to improve the prognosis of LUAD.

Methods: The gene expression profiles and clinical information of LUAD patients were downloaded from the Cancer Genome Atlas (TCGA), and validation cohort information was extracted from the Gene Expression Omnibus database. The Human Autophagy Database (HADb) was used to extract ARGs. Gene expression data were analyzed using the limma package and visualized using the ggplot2 package as well as the pheatmap package in R software. Functional enrichment analysis was also performed for the differentially expressed ARGs (DEARGs). Then, consensus clustering revealed autophagy-related tumor subtypes, and differentially expressed genes (DEGs) were screened according to the subtypes. Next, the univariate Cox and multivariate Cox regression analyses were used to identify independent prognostic ARGs. After overlapping DEGs and the independent prognostic ARGs, the predictive risk model was established and validated. Correlation analyses between ARGs and clinicopathological variables were also explored. Finally, the TIMER and TISIDB databases were used to further explore the correlation analysis between immune cell infiltration levels and the risk score as well as clinicopathological variables in the predictive risk model.

Results: A total of 222 genes from the HADb were identified as ARGs, and 28 of the 222 genes were pooled as DEARGs. The most significant GO term was autophagy (p = 3.05E-07), and KEGG analysis results indicated that 28 DEARGs were significantly enriched in the ErbB signaling pathway ($p < 0.001$). Then, consensus clustering analysis divided the LUAD

Abbreviations: ARGs, autophagy-related genes; DEARGs, differentially expressed autophagy-related genes; GEPIA, Gene Expression Profiling Interactive Analysis; GO, Gene ontology; HADb, Human Autophagy Database; HRs, hazard ratios; KEGG, Kyoto Encyclopedia of Genes and Genomes; LUAD, lung adenocarcinoma; LUSC, lung squamous cell carcinoma; OS, overall survival; ROC, Receiver Operating Characteristic; SCNA, somatic copy number variation; TCGA, the Cancer Genome Atlas; TILs, tumor infiltrating lymphocytes.

into two clusters, and a total of 168 DEGs were identified according to cluster subtypes. Then univariate and multivariate Cox regression analyses were used to identify 12 genes that could serve as independent prognostic indicators. After overlapping 168 DEGs and 12 genes, 10 genes (ATG4A, BAK1, CAPNS1, CCR2, CTSD, EIF2AK3, ITGB1, MBTPS2, SPHK1, ST13) were selected for the further exploration of the prognostic pattern. Survival analysis results indicated that this risk model identified the prognosis (p = 4.379E-10). Combined with the correlation analysis results between ARGs and clinicopathological variables, five ARGs were screened as prognostic genes. Among them, SPHK1 expression levels were positively correlated with $CD4^+$ T cells and dendritic cell infiltration levels.

Conclusions: In this study, we constructed a predictive risk model and identified a five autophagy subtype-related gene expression pattern to improve the prognosis of LUAD. Understanding the subtypes of LUAD is helpful to accurately characterize the LUAD and develop personalized treatment.

Keywords: lung adenocarcinoma, ARGS, risk model, SPHK1, immune cell infiltration

BACKGROUND

According to the most recent global cancer statistics in 2018, lung cancer is the most commonly diagnosed cancer, whose diagnosis rate has reached 11.6% (Bray et al., 2018). Lung cancer is also the leading cause of cancer death, accounting for 18.4% of all the cancer deaths (Bray et al., 2018). Lung adenocarcinoma (LUAD) is the most common subtype and accounts for more than 40% of lung cancers, and its clinical outcome still remains grim (Nakamura and Saji, 2014; Zappa Mousa, 2016). Although great advances in surgery, radiotherapy, and systemic treatment have significantly prolonged the clinical survival time of LUAD patients (Wright et al., 2006; Hirsch et al., 2017; Gettinger et al., 2018), 5-year survival rates still vary from 4% to 17% depending on the pathological TNM stage (Hirsch et al., 2017). Early detection, diagnosis, and intervention contribute to a better clinical outcome as well as the prognosis of LUAD patients, such as early diagnosis based on low-dose computed tomography, which could finally improve lung cancer mortality by nearly 20% (Aberle et al., 2011). Hence, it is essential to identify new biomarkers for early diagnosis and intervention and eventually improve the prognosis of LUAD.

Autophagy has been illustrated to be related to various cancers. Autophagy has been proven to have opposing and context-dependent roles during the process of tumorigenesis, and interventions to both stimulate and inhibit the many processes of autophagy have been proposed as a cancer therapy (Levy et al., 2017). It is clear that autophagy is a key biological process and that it is associated with tumorigenesis (Martinet et al., 2009; Dikic et al., 2010). In the very recent years, autophagy-related genes (ARGs) have been investigated in both inflammatory diseases (including pulmonary diseases) (Wang, 2015; Racanelli et al., 2018; Kim et al., 2019; Larabi et al., 2020) and various cancers (Wang et al., 2019a; Wan et al., 2019; Zhu et al., 2020a). For lung cancer, there are some newly released studies that have identified ARG prognostic signatures in LUAD and lung squamous cell carcinoma (LUSC) (Zhu et al., 2020b; Zhang et al., 2020).

Existing studies further elucidated the crucial roles of ARGs in the biological processes. ARG expression patterns not only participate in inflammasome formation but also could serve as prognostic biomarkers in cancer. Various ARGs are involved in the maintenance of intestinal homeostasis, such as ATG16L1, IRGM, LRRK2, ATG7, p62, optineurin, and TFEB (Kim et al., 2019). A six autophagy-related gene expression signature (including EIF4EBP1, TP63, BNIP3, ATIC, ERO1A, and FADD) showed better performance for predicting the survival of LUAD and LUSC patients than other clinicopathological variables (Zhu et al., 2020b). Another study constructed a risk model based on five autophagy-related gene expression levels, which could also predict the prognosis and serve as a prognostic biomarker in LUAD patients (Zhang et al., 2020). All of the above findings confirm the role of autophagy in lung cancer and indicate that ARGs could serve as prognostic biomarkers. Autophagy plays vital roles in the innate immune system and the acquired immune system, which could influence the levels of infiltrating immune cells. Take antigen presentation as an example, autophagy could not only disrupt the process but also promote the antigen presentation. One study found that NBR1 targets and degrades the MHC I, thus disrupting its antigen presentation ability to $CD8^+$ T cells, which in turn can be reversed by autophagy inhibitor, for NBR1 is an autophagy cargo receptor gene (Yamamoto et al., 2020). Another two studies suggested that the activation of autophagy promotes antigen presentation to CD8+T lymphocytes mediated by dendritic cells, which then stimulate cytotoxic responses (Li et al., 2012; Wang et al., 2019b). Besides, TIM-4 can bind to AMPK-a1, activate autophagy, and degrade TAA, thereby disrupting antigen presentation and leading to a decrease in $CD8^+$ T cells (Baghdadi et al., 2013). Furthermore, previous studies have illustrated that the prognostic value of tumor-infiltrating lymphocytes (TILs) significantly differs according to histological type and other factors in non-

small cell lung cancer (NSCLC) patients (Kinoshita et al., 2017). Combining the previous existing studies, we found that autophagy is closely related to TILs, so we supposed that TILs may be affected by autophagy, further influencing the prognosis of LUAD patients.

In the current study, we pooled an autophagy subtype-related gene expression pattern in The Cancer Genome Atlas (TCGA) database and validated it in the Gene Expression Omnibus (GEO) database. We identified two tumor subgroups using consensus clustering analysis based on 28 prognostic ARGs, in which we found that cluster 2 had poor prognostic value in LUAD compared to cluster 1. Then, we analyzed the differentially expressed genes (DEGs) of these two clusters and performed univariate and multivariate Cox regression analyses to obtain the prognostic ARGs and overlapped the DEGs and prognostic ARGs. Finally, 10 genes were selected, and a risk model was constructed based on the coefficient value of each independent risk gene to predict the prognosis of LUAD patients. Many previously published works have simply focused either on consensus clustering analysis or on risk models. Few studies have focused on both at the same time. Therefore, in the current study, we combined both of these methods to explore the prognosis of LUAD. Furthermore, unlike existing studies, we further validated their expression and prognostic value and finally explored their associations with TILs.

MATERIALS AND METHODS

Data Collection and Validation of Differentially Expressed ARGs in LUAD

The gene expression profiles and clinical information of LUAD patients were downloaded from the TCGA database (https://tcga-data.nci.nih.gov/tcga/). The Human Autophagy Database (HADb; http://www.autophagy.lu) was used to extract genes involved in autophagy. In detail, TCGA contains a total of 594 patients (including 59 adjacent normal lung tissues and 535 NSCLC tissues). Gene expression data from TCGA were analyzed by the limma package in R software. The independent cohort GSE72094 was downloaded from the GEO database (http://www.ncbi.nlm.nih.gov/geo/) for data validation. The dataset contains both expression levels of related genes and clinical information such as age, sex, survival status, and survival time. All the raw data including expression data and survival data from TCGA and GSE72094 are displayed in the Supplementary Information file. The significant cutoff value was $p < 0.05$ and absolute fold change >2. In addition, all expression levels of the ARGs were visualized as volcano plots using the ggplot2 package in R software. Furthermore, all DEARGs were displayed with heat maps using the pheatmap package in R software.

Validation of 28 Significant ARGs Using Quantitative Reverse Transcription-Polymerase Chain Reaction

Human LUAD cells (A549) and normal bronchial epithelial cells (16HBE) were purchased from Cell Bank, Institute of Life Sciences, Chinese Academy of Sciences Cell Bank (Shanghai, China) and confirmed by short tandem repeat (STR) profiling. Total RNA was extracted from 16HBE and A549 cells using TRIzol reagent (Invitrogen, Carlsbad, CA, USA). After the purity and concentration of the total RNA were determined, the total RNA was reverse transcribed into cDNA using the PrimeScript RT Reagent Kit (Accurate Biology). The qRT-PCR was performed using the SYBR Green Premix Ex Taq II (Accurate Biology). The PCR conditions were set as follows: 95°C for 30 s, followed by 40 cycles at 95°C for 5 s and 60°C for 30 s for each specific primer. Finally, the relative mRNA expression levels of 28 genes were calculated using the $2^{-\Delta\Delta CT}$ method. The primer sequences are listed in a **Supplementary Table S1**.

Functional Enrichment Analysis

Functional enrichment analysis includes Gene Ontology (GO) and Kyoto Encyclopedia of Genes and Genomes (KEGG) in this study. In brief, GO enrichment analyses predict the function of the target genes and KEGG is a widely used database for systematic signaling pathway analysis according to gene functions. In this study, the clusterProfiler package in R software was used to perform the functional enrichment analysis of DEARGs in LUAD, and GOplot package in R software was employed to visualize all of the enrichment analysis results. The identification criterion of significant GO terms and KEGG pathways was $p < 0.050$.

Establishment of the Risk Model Based on Prognostic ARGs in LUAD

Consensus clustering analysis of the DEARGs inferred the optimal number of clusters, the lowest proportion of ambiguous clustering, and the best cumulative distribution function (CDF) value by taking the k value of 2. Finally, two clusters were identified and DEGs were analyzed. The Cox regression analysis, also called the proportional hazards model, chooses survival outcomes and survival time as dependent variables. This model not only analyzes the impact of many factors on survival at the same time but also analyzes data with censored survival time and does not require estimation of the survival distribution type of the data. In our present study, univariate Cox proportional hazard regression analysis was used to identify ARGs associated with overall survival (OS), which were selected as prognostic biomarkers and used for further multivariate Cox regression analysis. According to the multivariate Cox regression analysis and overlapping with DEGs based on the two clusters, 10 independent prognostic ARGs were identified. At the same time, the regression coefficient and hazard ratios (HRs) were also calculated using multivariate Cox regression analysis, and the coefficient value and the gene expression levels were used to construct the risk model based on the risk score. Finally, the median risk score was the cutoff value, dividing all of the LUAD patients into low-risk and high-risk groups. According to our description above, we used both univariate and multivariate Cox regression analyses to further investigate whether these identified ARGs could serve as independent prognostic factors. In addition, we pooled all LUAD patients with complete clinical information and calculated all expression levels and risk scores of prognostic

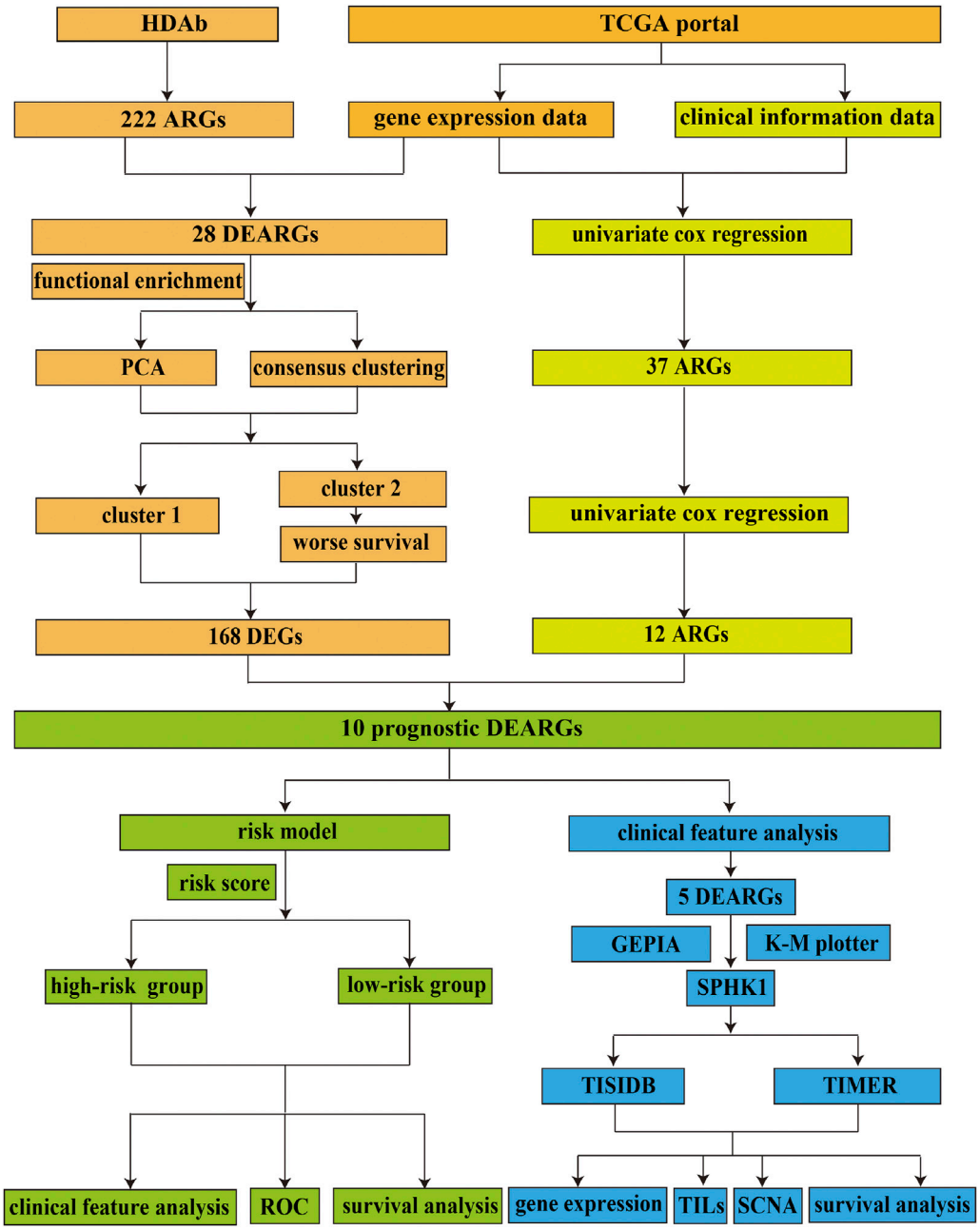

FIGURE 1 | Flowchart of the current study. HADb, Human Autophagy Database; TCGA, the Cancer Genome Atlas; ARGs, autophagy-related genes; DEARGs, differentially expressed autophagy-related genes; PCA, principal component analysis; DEGs, differentially expressed genes; ROC, receiver operating characteristic; GEPIA, Gene Expression Profiling Interactive Analysis; K-M plotter, Kaplan–Meier plotter; TILs, tumor-infiltrating lymphocytes; SCNA, somatic copy number variation.

ARGs to explore the value of the constructed risk model. Receiver operating characteristic (ROC) curve analysis was used to evaluate the predictive accuracy of our risk model.

Correlation Analysis Between ARGs and Clinicopathological Variables in LUAD

After screening ARGs and exploring their associations with OS, we moved our attention to the relationship between prognostic ARGs and clinicopathological variables. Therefore, in this study, correlation analysis was performed to further explore the correlation between prognostic ARGs and clinicopathological variables in LUAD, including age (≤65 years group and >65 years group), sex (female and male groups), stage (I&II and III&IV groups), pathological T stage (T1&T2 and T3&T4 groups), pathological N stage (N0 and N1–N3 groups), and pathological M stage (M0 and M1 groups).

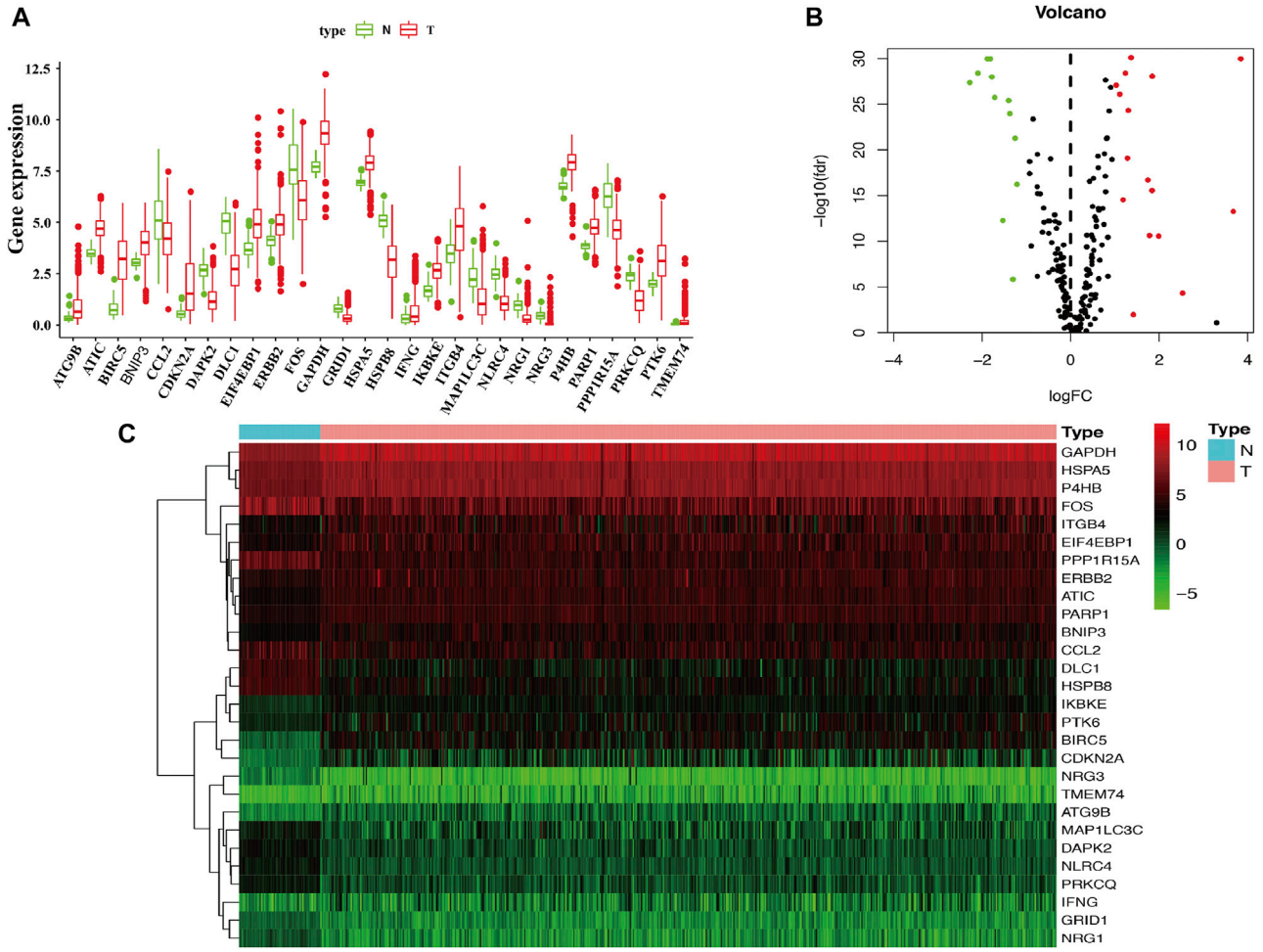

FIGURE 2 | Identification of differentially expressed ARGs in LUAD. **(A)** The boxplot of the differentially expressed ARGs. The red color indicates tumor tissues, and the green color indicated the non-tumor. **(B)** Volcano plot of the 222 ARGs analysis. There were 28 ARGs differentially expressed in LUAD, including 12 downregulated genes and 16 upregulated genes. X-axis: log 2-fold change; Y-axis: –log10 fdr for each probe. **(C)** Two-dimensional hierarchical clustering of the significant 28 differentially expressed ARGs in LUAD patients. LUAD, lung adenocarcinoma.

Validation of Prognostic ARGs in LUAD

Prognostic ARGs were validated using two public databases, Gene Expression Profiling Interactive Analysis (GEPIA) (http://gepia.cancer-pku.cn) and Kaplan–Meier Plotter (https://kmplot.com/analysis/). The GEPIA database contains information on a variety of cancers, including LUAD, and has expression data, survival data, and exact clinical stage data. The Kaplan–Meier plotter is a widely accepted and widely used online tool used to explore the survival rates of one and a list of genes as well as non-coding RNAs, including the survival time, survival status, clinical stages, and smoking histories. Therefore, in this study, these two databases were used to verify the prognostic value of the five well-explored prognostic ARGs.

Exploration of the Immune-Related Mechanism of Sphingosine Kinase 1

The immune-related mechanism of SPHK1 was explored using two databases, including TISIDB (http://cis.hku.hk/TISIDB/) and Tumor IMmune Estimation Resource (TIMER) (https://cistrome.shinyapps.io/timer/). In general, as the official website information, TISIDB is an integrated repository portal for tumor-immune system interactions. According to this database, we could explore the interaction between tumors and immunity because it is a powerful website containing a large amount of tumor immunity-related data. Meanwhile, TIMER is a comprehensive resource for systematic analysis of immune infiltrates across diverse cancer types, including LUAD. This database contains six kinds of immune cell infiltrates, including B cells, $CD4^+$ T cells, $CD8^+$ T cells, neutrophils, macrophages, and dendritic cells. All immune cell infiltrate levels were calculated using the TIMER algorithm. Finally, the resulting figures were dynamically displayed to conveniently assess the tumor immunological, clinical, and genomic features.

In our present study, we validated SPHK1 expression levels and its relationship with OS in both of these databases. Then,

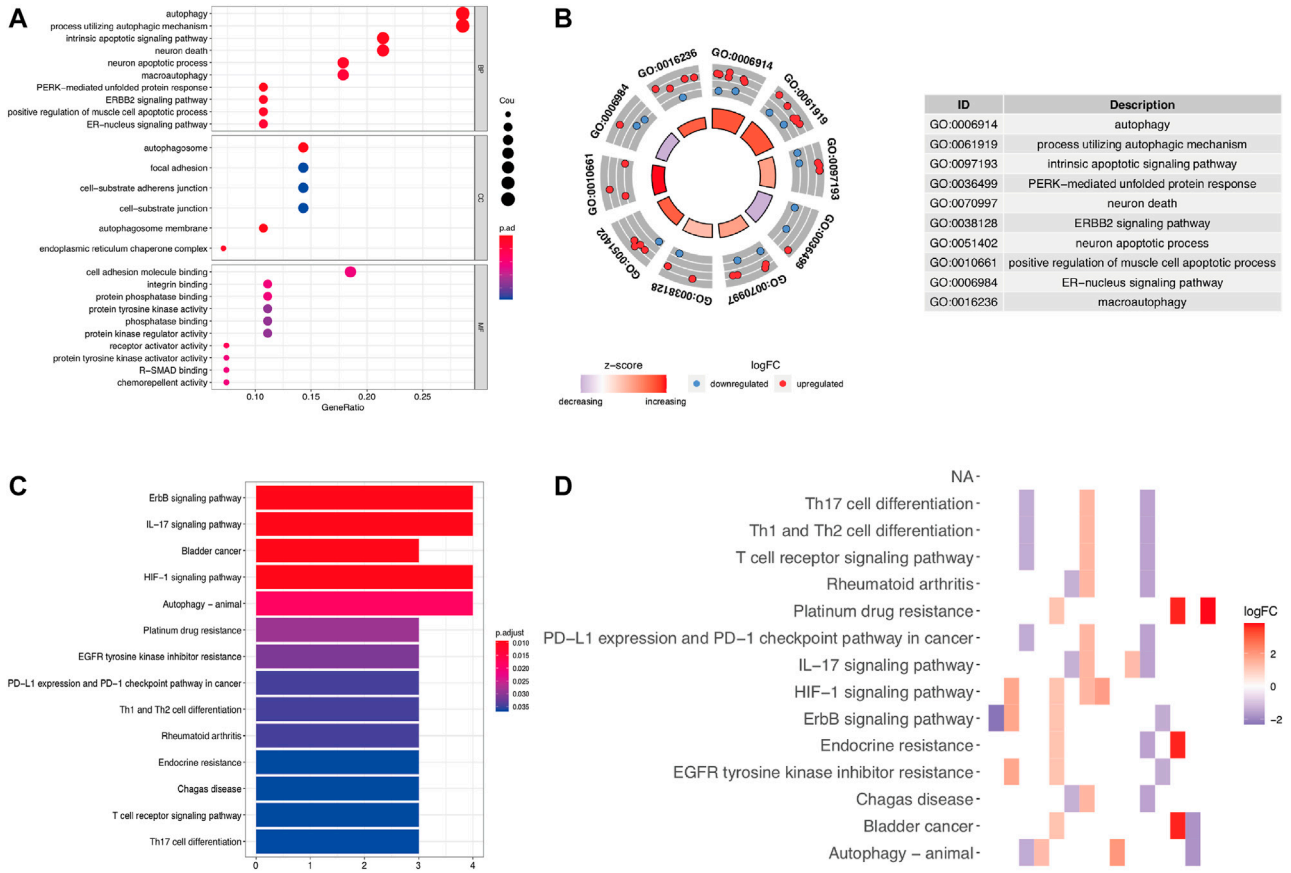

FIGURE 3 | Functional enrichment analysis of differentially expressed ARGs. **(A,B)** The bubble plot and circle plot of significant GO terms. **(C,D)** The bar plot and heat map of enriched KEGG pathways. GO, Gene Ontology; KEGG, Kyoto Encyclopedia of Genes and Genomes.

we further explored OS between low immune cell infiltration levels and high immune cell infiltration levels in TIMER. Next, correlation analysis between SPHK1 and immune cell infiltration levels was performed using both the TIMER and TISIDB databases. Furthermore, the correlation between somatic copy number variation (SCNA) levels of SPHK1 and immune cell infiltration levels was also determined. The purity-corrected partial Spearman method was used to analyze the data.

Statistical Analysis

Statistical analysis was performed using R software, and $p < 0.050$ was regarded as statistically significant. We divided patients into high-risk and low-risk groups of the 10 ARGs based on risk scores. Single comparisons of the expression rates between the two groups were performed using Student's t-test. The unpaired *t* test was used to assess expression levels of the ARGs between the high-expression and low-expression groups. Kaplan–Meier survival curves were generated for the TCGA cohort and GSE72094 and analyzed using the log-rank test. The correlation between gene expression levels and infiltrating immune cell levels was determined using the purity-corrected partial Spearman method.

RESULTS

Identification and Functional Enrichment Analysis of Differentially Expressed ARGs in Lung Adenocarcinoma From Cancer Genome Atlas Database

The flow diagram of this study is shown in **Figure 1**. In this study, gene expression profiles from TCGA database in LUAD were selected, and a total of 222 ARGs from HADb were identified (**Supplementary Table S1**). Genes with $p < 0.05$ and absolute fold change >2 were considered DEARGs. Finally, a total of 28 ARGs were pooled that were differentially expressed in LUAD, including 12 downregulated genes and 16 upregulated genes (**Figure 2**) (**Supplementary Table S1**).

To determine the biological functions of the 28 DEARGs, gene ontology and KEGG enrichment analyses were performed. The top five associated GO terms were autophagy (p = 3.05E-07), process utilizing autophagic mechanism (p = 3.05E-07), intrinsic apoptotic signaling pathway (p = 3.75E-06), neuron death (p = 9.09E-06), and neuron apoptotic process (p = 2.22E-05) according to both the functioned gene numbers and p-value (**Figures 3A,B**). Furthermore, all of these top five items were

TABLE 1 | Top 25 GO terms based on 28 differentially expressed autophagy-related genes.

Ontology	ID	Description	*p* value	Count
BP	GO:0006914	Autophagy	3.05E-07	8
BP	GO:0061919	Process utilizing autophagic mechanism	3.05E-07	8
BP	GO:0097193	Intrinsic apoptotic signaling pathway	3.75E-06	6
BP	GO:0036499	PERK-mediated unfolded protein response	4.06E-06	3
BP	GO:0070997	Neuron death	9.09E-06	6
BP	GO:0038128	ERBB2 signaling pathway	1.36E-05	3
BP	GO:0051402	Neuron apoptotic process	2.22E-05	5
BP	GO:0010661	Positive regulation of muscle cell apoptotic process	2.53E-05	3
BP	GO:0006984	ER-nucleus signaling pathway	4.52E-05	3
CC	GO:0005776	Autophagosome	7.39E-06	4
CC	GO:0000421	Autophagosome membrane	1.25E-05	3
CC	GO:0034663	Endoplasmic reticulum chaperone complex	0.000106742	2
CC	GO:0005925	Focal adhesion	0.002391067	4
CC	GO:0005924	Cell–substrate adherens junction	0.00245631	4
CC	GO:0030055	Cell–substrate junction	0.002545205	4
MF	GO:0030546	Receptor activator activity	0.000100852	2
MF	GO:0030296	Protein tyrosine kinase activator activity	0.000340315	2
MF	GO:0070412	R-SMAD binding	0.000560092	2
MF	GO:0050839	Cell adhesion molecule binding	0.000761564	5
MF	GO:0045499	Chemorepellent activity	0.000774116	2
MF	GO:0005178	Integrin binding	0.000919404	3
MF	GO:0019903	Protein phosphatase binding	0.001074992	3
MF	GO:0004713	Protein tyrosine kinase activity	0.002436602	3
MF	GO:0019902	Phosphatase binding	0.002475853	3
MF	GO:0019887	Protein kinase regulator activity	0.00255553	3

involved in biological processes, indicating that these 28 DEARGs participated in the biological processes of LUAD. In addition, the top 25 GO terms are shown in **Table 1**. Further KEGG analysis results indicated that the 28 ARGs were significantly enriched in the ErbB signaling pathway, IL-17 signaling pathway, and bladder cancer (all $p < 0.001$) (**Figure 3C**), and they were involved in a total of 14 KEGG pathways (**Figure 3D**). According to the results of functional enrichment of 28 DEARGs, we found that they were not only connected to autophagy but also involved in other biological processes. Therefore, in this study, we pooled the specific roles of ARGs in both autophagy and LUAD.

Identification of 2 Clusters Using Consensus Clustering and the Differentially Expressed Genes Shared Between These 2 Clusters in Lung Adenocarcinoma

Autophagy may exhibit different expression patterns among LUAD patients, potentially affecting the prognosis and gene expression signature. In this study, 28 DEARGs were used to identify autophagy subtypes associated with the overall survival of LUAD. Consensus clustering was used to explore the similarity of 28 DEARGs' expression patterns. By selecting a k value of 2, we obtained the optimal CDF value and classified the LUAD patients into two clusters (**Figures 4A,C**). Principal component analysis (PCA) results revealed two significantly different distribution patterns of LUAD patients. The samples of cluster 1 and cluster 2 were distributed on the left side and right sides, respectively (**Figure 4D**). Consensus clustering and principal component analysis suggested that autophagy may play a role in the occurrence and development of LUAD. In addition, to explore whether these two clusters of gene expression levels affect clinical outcomes, we constructed a prognostic classifier using Kaplan–Meier analysis. The results revealed that the prognosis of cluster 1 was better than that of cluster 2 ($p < 0.001$) (**Figure 4E**). Furthermore, since different clusters have shown variations in autophagy-related genes and patient prognosis, we explored the DEGs between cluster 1 and cluster 2. A total of 168 DEGs (76 upregulated genes in cluster 1 and 92 upregulated genes in cluster 2) were screened (**Supplementary Table S1**).

Establishment of the Risk Model Based on the Autophagy-Related Genes and Differentially Expressed Genes Between Cluster 1 and Cluster 2 to Improve the Prognostic Prediction of Lung Adenocarcinoma

To reveal the distinct expression signature of ARGs, we constructed a risk model to predict the prognosis of LUAD. First, univariate Cox regression analysis was used to identify the prognostic ARGs, and 37 ARGs were pooled as prognostic factors, among which 16 of 37 were identified as protective factors (HR < 1), while another 21 genes were identified as risk factors (HR > 1) (**Figure 5A**). Then, multivariate Cox regression analysis was conducted, and the results suggested that 12 genes (APOL1, ATG12, ATG4A, BAK1, CAPNS1, CCR2, CTSD, EIF2AK3, ITGB1, MBTPS2, SPHK1, ST13) represented independent prognostic indicators, which were selected for further exploration of the prognostic pattern (**Table 2**). Based on the previous important clustering, we overlapped the 12 independent prognostic indicators and 168

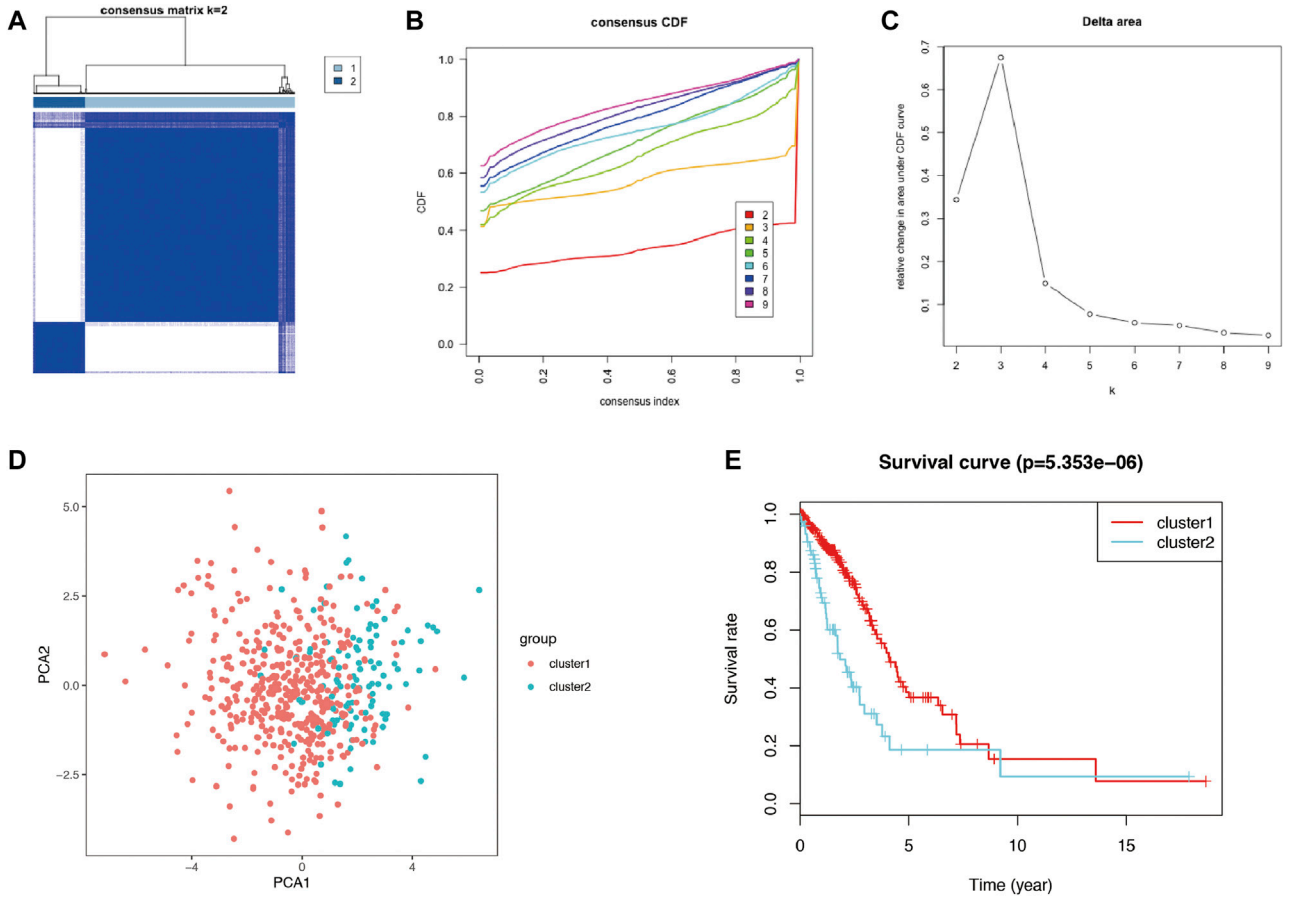

FIGURE 4 | The consensus clustering analysis and the principle components analysis. **(A–C)** The consensus clustering analysis of the 28-prognostic ARGs, inferring the optimal number of clusters, the lowest proportion of ambiguous clustering, and the best CDF value by taking the k value of 2. **(D)** The principle component analysis of the prognostic autophagy-related genes in LUAD patients. **(E)** Kaplan–Meier analysis between cluster 1 and cluster 2. ARGs, autophagy-related genes; CDF, cumulative distribution function; LUAD, lung adenocarcinoma.

DEGs between cluster 1 and cluster 2. Finally, 10 genes (ATG4A, BAK1, CAPNS1, CCR2, CTSD, EIF2AK3, ITGB1, MBTPS2, SPHK1, ST13) were selected for further analysis. Subsequently, the coefficient value of each independent risk gene was calculated, and our prognostic model based on the 10 genes was formed as follows: risk score = (−0.579 × ATG4A expression) + (0.224 × BAK1 expression) + (0.294 × CAPNS1 expression) + (−0.345 × CCR2 expression) + (−0.165 × CTSD expression) + (−0.561 × EIF2AK3 expression) + (0.230 × ITGB1 expression) + (0.479 × MBTPS2 expression) + (0.166 × SPHK1 expression) + (0.317 × ST13 expression). According to this formula, we calculated the risk score of each patient, and all of LUAD patients were divided into low-risk (n = 229) and high-risk groups (n = 229). Survival analysis results indicated that there was a difference between the high-risk and low-risk groups, and the low-risk group exhibited a significantly better prognosis than the high-risk group (p = 4.379E-10) (**Figure 5B**). The risk score plot, survival time, and status plot are shown in **Figures 5C,D**. In addition, these 10 independent risk genes are displayed in a heat map to show the different expression levels between the high-risk and low-risk groups (**Figure 5E**).

Validation of the 28 Differentially Expressed Autophagy-Related Genes Expression Pattern and Prognostic Value of the Risk Model Using Quantitative Reverse Transcription-Polymerase Chain Reaction and an Independent Cohort

To verify the risk model, the gene expression profile of GSE72094 was used for further analyses. The results showed that 28 DEARGs were pooled as differentially expressed in LUAD (**Figure 6**), in which the expression of 16 of 28 ARGs was significantly elevated and 12 genes were downregulated in LUAD tissues compared to adjacent normal lung tissues in GSE72094 (all $p < 0.050$), consistent with our previous results from TCGA database. For consensus clustering based on these 28 DEARGs, qRT-PCR was also performed. As we expected, the

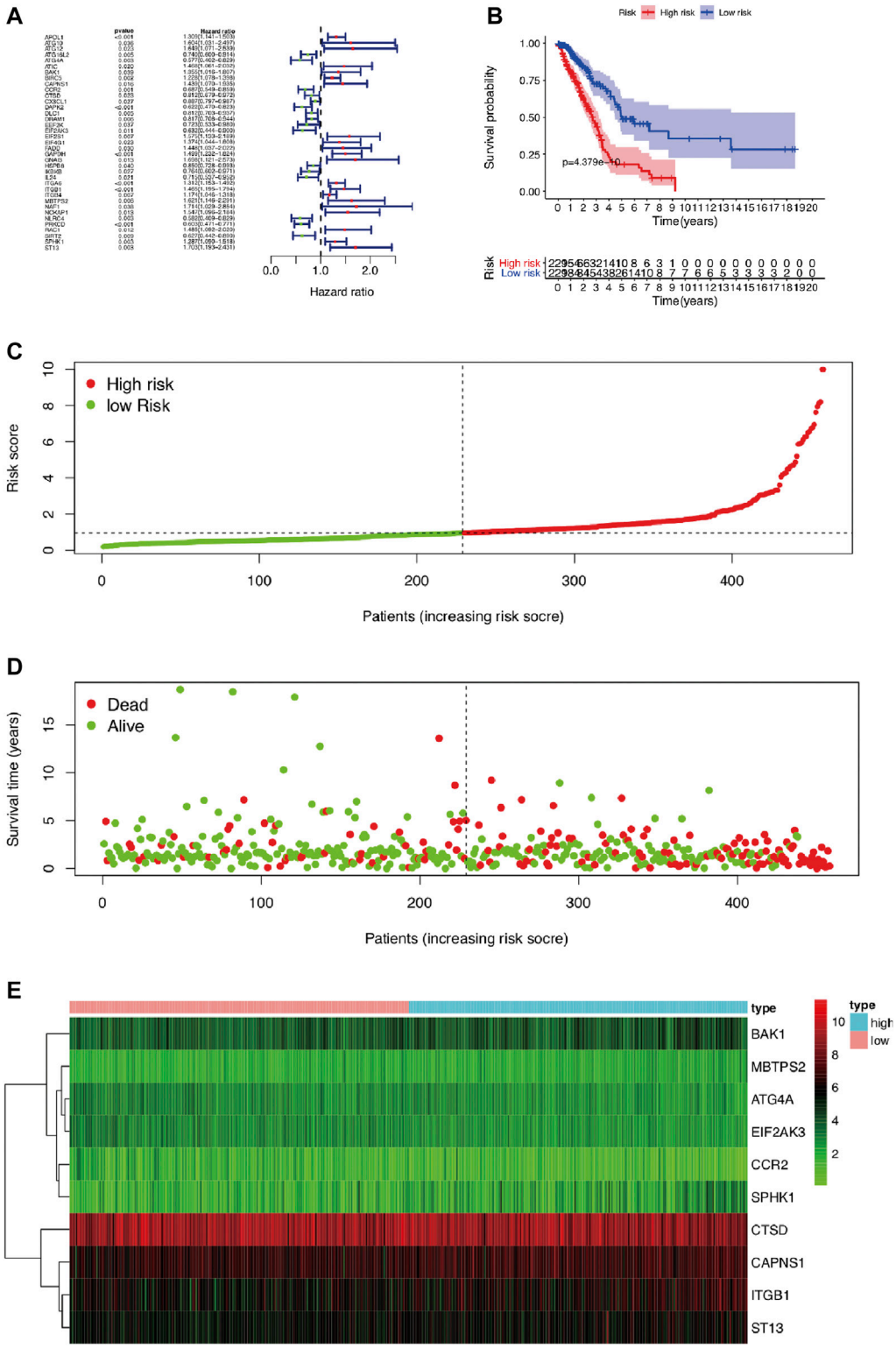

FIGURE 5 | The prognostic risk model based on ARGs in LUAD. **(A)** The univariate Cox regression analysis screened prognosis-related genes. **(B)** Kaplan–Meier analysis of OS between high-risk and low-risk groups in LUAD patients based on risk scores according to 12 autophagy-related gene signatures. **(C)** Visualization of the risk score plot of high-risk and low-risk groups in LUAD patients. **(D)** Survival status was displayed in red and green dots based on the risk model as the risk score increasing in LUAD patients. **(E)** Two-dimensional hierarchical clustering of the significant 10 differentially expressed prognostic ARGs in high-risk and low-risk LUAD patients. ARGs, autophagy-related genes; LUAD, lung adenocarcinoma; OS, overall survival.

TABLE 2 | Twelve autophagy-related genes are independent prognostic indicators using multivariate Cox regression analysis.

Gene	coef	HR	HR.95L	HR.95H	*p* value
APOL1	0.1239302	1.1319369	0.9835550	1.3027041	0.0838679
ATG12	0.7672543	2.1538443	1.3382951	3.4663844	0.0015767
ATG4A	−0.579587	0.5601290	0.3620170	0.8666568	0.0092520
BAK1	0.2235042	1.2504509	0.9328130	1.6762497	0.1349648
CAPNS1	0.2937850	1.3414955	0.9570607	1.8803512	0.0881531
CCR2	−0.344522	0.7085589	0.5469677	0.9178890	0.0090880
CTSD	−0.164576	0.8482525	0.6898705	1.0429961	0.1185853
EIF2AK3	−0.560724	0.5707951	0.3685623	0.8839945	0.0119893
ITGB1	0.2298494	1.2584104	0.9652966	1.6405287	0.0893375
MBTPS2	0.4789932	1.6144482	1.0610497	2.4564759	0.0253076
SPHK1	0.1659534	1.1805181	0.9692465	1.4378416	0.0990470
ST13	0.3170819	1.3731150	0.9276819	2.0324260	0.1130160

HR, hazard ratio.

results showed that 25 of the 28 genes were consistent with the above results. Three genes were not significantly different between the 16HBE and A549 cell lines (**Figure 7**), which could be caused by the differences between tissues and cell lines. Furthermore, univariate Cox regression analysis showed that 40 genes were pooled as prognostic factors (**Supplementary Table S1**), and multivariate Cox regression analysis results suggested that 17 genes represented independent prognostic indicators, including 10 genes (ATG4A, BAK1, CAPNS1, CCR2, CTSD, EIF2AK3, ITGB1, MBTPS2, SPHK1, ST13) mentioned above (**Supplementary Table S1**). Then, 393 LUAD patients in GSE72094 were divided into low-risk (n = 196) and high-risk groups (n = 197) according to the previous formula. Survival analysis results also validated that the low-risk group exhibited significantly better prognosis than the high-risk group (p < 0.001) (**Figure 8A**). The risk score plot, survival time, and status plot are also shown in **Figures 8B,C**. Finally, the heat map plot was visualized to further illustrate the distribution of 10 prognostic ARGs between the high-risk and low-risk groups (**Figure 8D**).

Survival Analysis of the Autophagy-Related Genes Expression Pattern and Clinicopathological Variables in Lung Adenocarcinoma

In this study, univariate and multivariate Cox regression analyses were performed to explore the prognostic value of autophagy-related gene expression patterns and clinicopathological variables. Univariate Cox regression analysis results indicated that stage, pathological T stage, pathological N stage, and risk score were correlated with OS (all p < 0.001) (**Figure 9A**). Multivariate Cox independent prognostic analysis results indicated that stage and risk score represented independent prognostic factors in LUAD (p = 0.006 and p < 0.001, respectively) (**Figure 9C**). In addition, given that the ARGs had different values in this model, ROC curves of OS were used to determine the predictive performance of the 10 ARG risk patterns (**Figure 9B**). The AUC value of the risk score (marks the 10 ARG risk pattern) for OS was 0.714, which was significantly higher than that of age (AUC = 0.513), sex (AUC = 0.581), pathological T stage (AUC = 0.673), pathological N stage (AUC = 0.505), and pathological M stage (AUC = 0.674). These results indicated that the risk score had a better ability to predict survival in LUAD patients than other clinical factors.

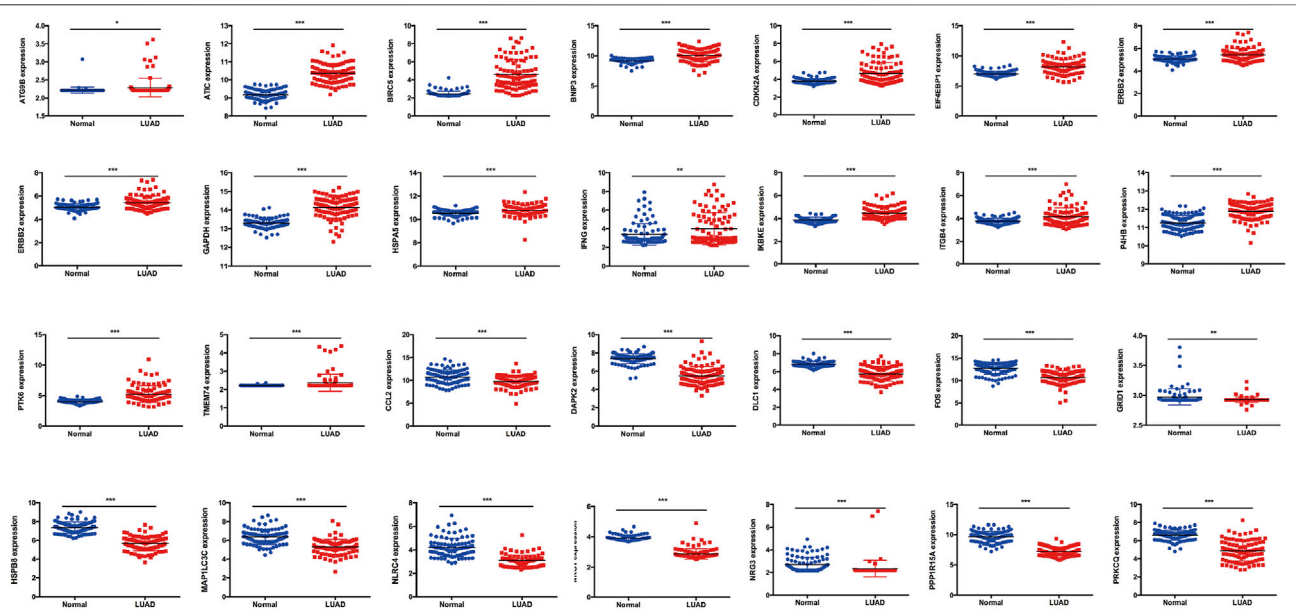

FIGURE 6 | The validation of 28 DEARGs in LUAD using an independent cohort GSE72094, in which expression of 16 of 28 ARGs was significantly elevated and 12 genes was downregulated in LUAD tissues compared with adjacent normal lung tissues in GSE72094 (all p < 0.050). DEARGs, differentially expressed autophagy-related genes; LUAD, lung adenocarcinoma.

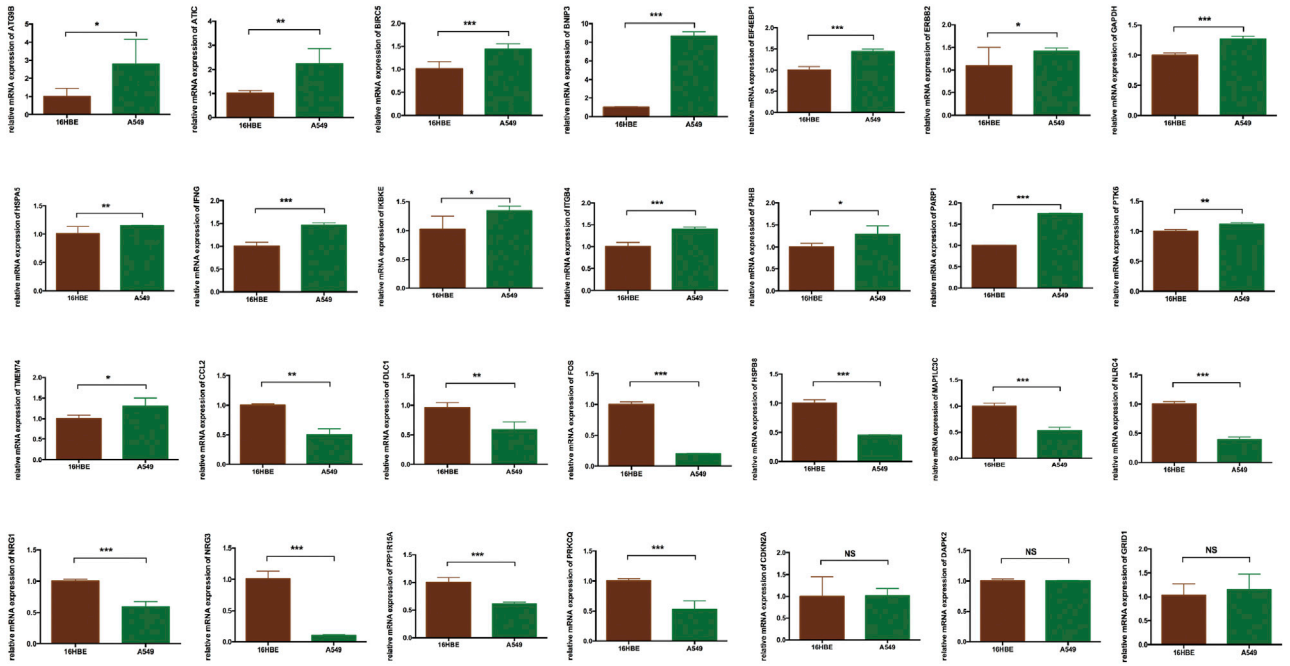

FIGURE 7 | The validation of 28 DEARGs in LUAD using qRT-PCR, in which 25 of the 28 genes showed the significance in 16HBE compared with A549 cell lines (all $p < 0.050$), while three genes showed that there is no significance between 16HBE and A549 cell lines (all $p > 0.050$). DEARGs, differentially expressed autophagy-related genes; LUAD, lung adenocarcinoma; qRT-PCR, quantitative reverse transcription–polymerase chain reaction.

Correlation Analysis Between Autophagy-Related Genes and Clinicopathological Variables in Lung Adenocarcinoma

After pooling 10 independent risk genes, we further performed correlation analysis between ARGs and clinicopathological variables, such as age, sex, stage, pathological T stage, pathological N stage, and pathological M stage. The risk score shows potential prognostic value because of its significant difference in LUAD patients with pathological N0 stage compared to pathological N1-N3 stages (p = 0.015) (**Figure 10A**), and expression levels of CAPNS1 (p = 0.017), CCR2 (p = 0.004), and SPHK1 (p = 0.016) showed the same results (**Figures 10B–D**). The risk score also exhibited potential prognostic value because of its significant difference in stage I and II LUAD patients compared to stage III and IV LUAD patients (p = 0.010) (**Figure 10E**), and the same results were observed in the expression levels of CAPNS1 (p = 0.042), CCR2 (p = 0.001), and CTSD (p = 0.004) (**Figures 10F–H**). In addition, the risk score and expression level of CCR2 were significantly different in LUAD patients between pathological T3–T4 stage and pathological T1–T2 stage (p = 0.049 and p = 0.009) (**Figures 10I,J**). For the pathological M stage, only CAPNS1 displayed a difference between M0 and M1 LUAD patients (p = 0.037) (**Figure 10K**). Expression levels of CCR2 were significantly different in LUAD patients aged ≤65 and >65 years (p = 0.003) (**Figure 10L**). Furthermore, sex was not a factor to be ignored and was associated with expression levels of BAK1 (p = 0.017) and CCR2 (p = 0.009) (**Figures 10M,N**). According to the results, five ARGs exhibited significant differences among clinicopathological variables.

Validation of Five Autophagy-Related Genes Expression Levels and Their Relationship With Overall Survival in Lung Adenocarcinoma

Five ARGs were screened as prognostic genes in TCGA database, and we validated their expression levels using the online GEPIA tool. The results showed that BAK1 and SPHK1 were highly expressed (**Supplementary Figures S1A,B**), while CAPNS1, CCR2, and CTSD were downregulated (**Supplementary Figures S1C–E**) in LUAD patients compared to controls. Unfortunately, these differences were not statistically significant. However, these five genes not only had prognostic value but also showed significant differences among clinicopathological variables according to our previous results, which attracted our attention. Furthermore, we performed Kaplan–Meier survival analysis using the Kaplan–Meier plotter online tool to validate the prognostic value of five ARGs, four of which, BAK1 (p = 2E-04), CAPNS1 ($p < 0.001$), CCR2 (p = 4.5E-12), and SPHK1 (p = 1.4E-06), exhibited prognostic value (**Supplementary Figures S1F–I**). However, in contrast to our previous findings, CTSD (also named CLN10) expression levels seemed to have no effect on OS in LUAD (p = 0.37) (**Supplementary Figure S1J**). SPHK1, as an

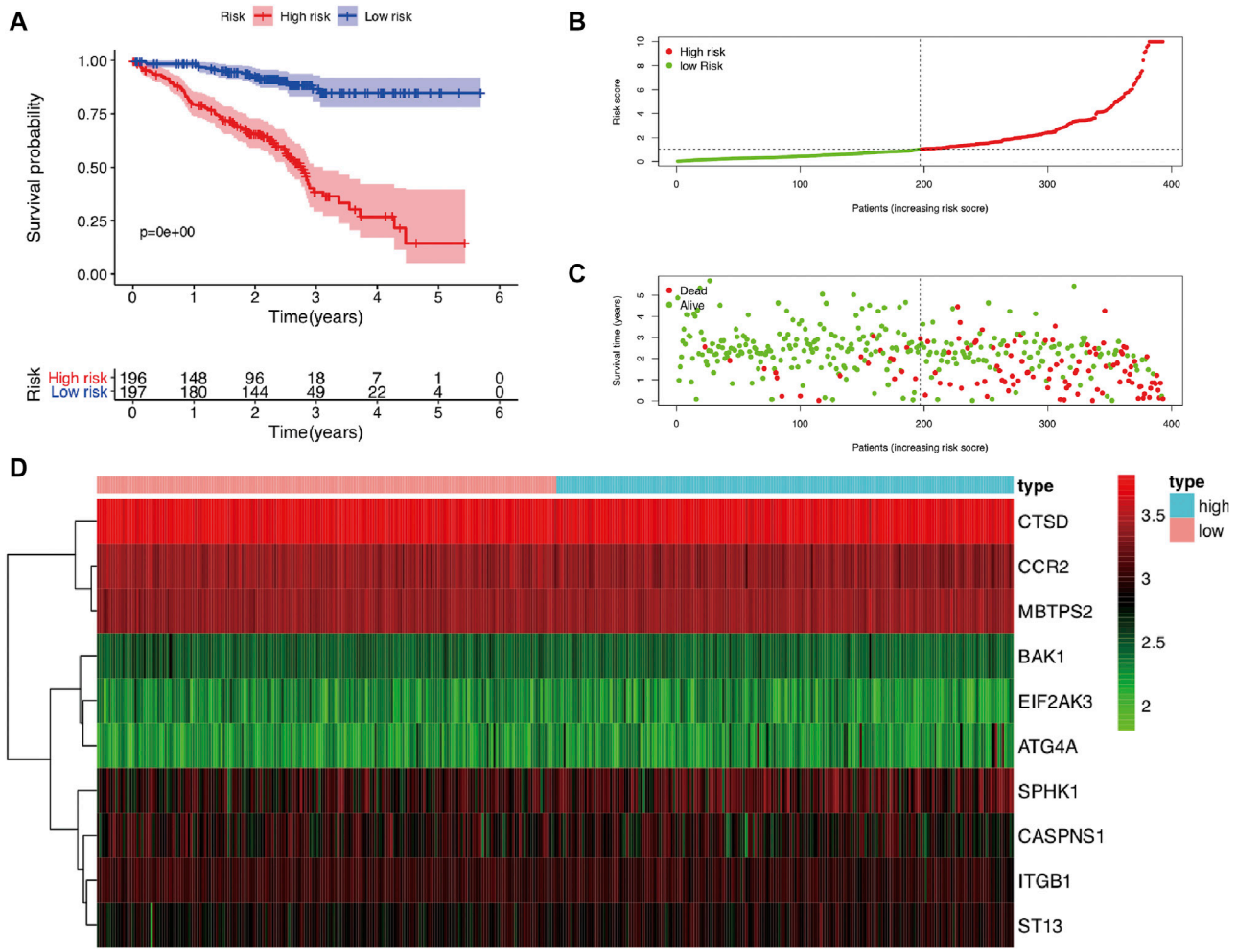

FIGURE 8 | The validation of the prognostic risk model based on ARGs in LUAD using an independent cohort GSE72094. **(A)** Kaplan–Meier analysis of OS between high-risk and low-risk groups in LUAD patients based on risk scores according to 10 ARGs signatures. **(B)** Visualization of the risk score plot of high-risk and low-risk groups in LUAD patients. **(C)** Survival status was displayed in red and green dots based on the risk model as the risk score increasing in LUAD patients. **(D)** Two-dimensional hierarchical clustering of the significant 10 differentially expressed prognostic ARGs in high-risk and low-risk LUAD patients. ARGs, autophagy-related genes; lung adenocarcinoma; OS, overall survival.

attractive gene, was selected for further specific study after considering its expression levels and prognostic value.

SPHK1 Expression Level and its Associations With Overall Survival and Tumor Infiltrating Lymphocytes

TIMER and TISIDB were used to explore the relationship between SPHK1 and TILs. First, we validated the high expression level of SPHK1 ($p < 0.010$) (**Figure 11A**) and its expression level in different stages ($p = 0.019$) (**Figure 11B**). In addition, we further explored the SPHK1 expression distribution across LUAD subtypes ($p = 4.73E-21$) (**Figure 11C**). Consequently, we performed a Kaplan–Meier analysis between high and low SPHK1 expression levels, and the results showed that low expression levels of SPHK1 were associated with a better prognosis ($p = 0.004$) (**Figure 11D**). After validating the expression level of SPHK1 and its prognostic value, we also examined whether this phenomenon was related to TILs.

For further exploration, we conducted an integrated analysis to predict the potential biological roles of SPHK1 in TILs of LUAD. The results indicated that as tumor purity increased, the SPHK1 expression levels were negatively correlated with B cells ($r = -0.144$, $p = 1.45E-03$) and positively correlated with $CD4^+$ T cell ($r = 0.132$, $p = 3.65E-03$), neutrophil ($r = 0.295$, $p = 3.89E-11$), and dendritic cell ($r = 0.186$, $p = 3.39E-05$) infiltration levels in the TIMER database (**Figure 12A**). Because data from one database seem to lack persuasiveness, we also validated the correlation between SPHK1 expression levels and immune cell infiltration using the TISIDB database. Consistent with our previous findings, except for the correlation between the SPHK1 expression level and B cell infiltration levels, SPHK1 expression levels were positively correlated with B cells ($r = 0.091$, $p = 0.039$; $r = 0.109$, $p = 0.013$; $r = 0.279$, $p = 1.27E-10$) (**Figures 12B–D**). The results

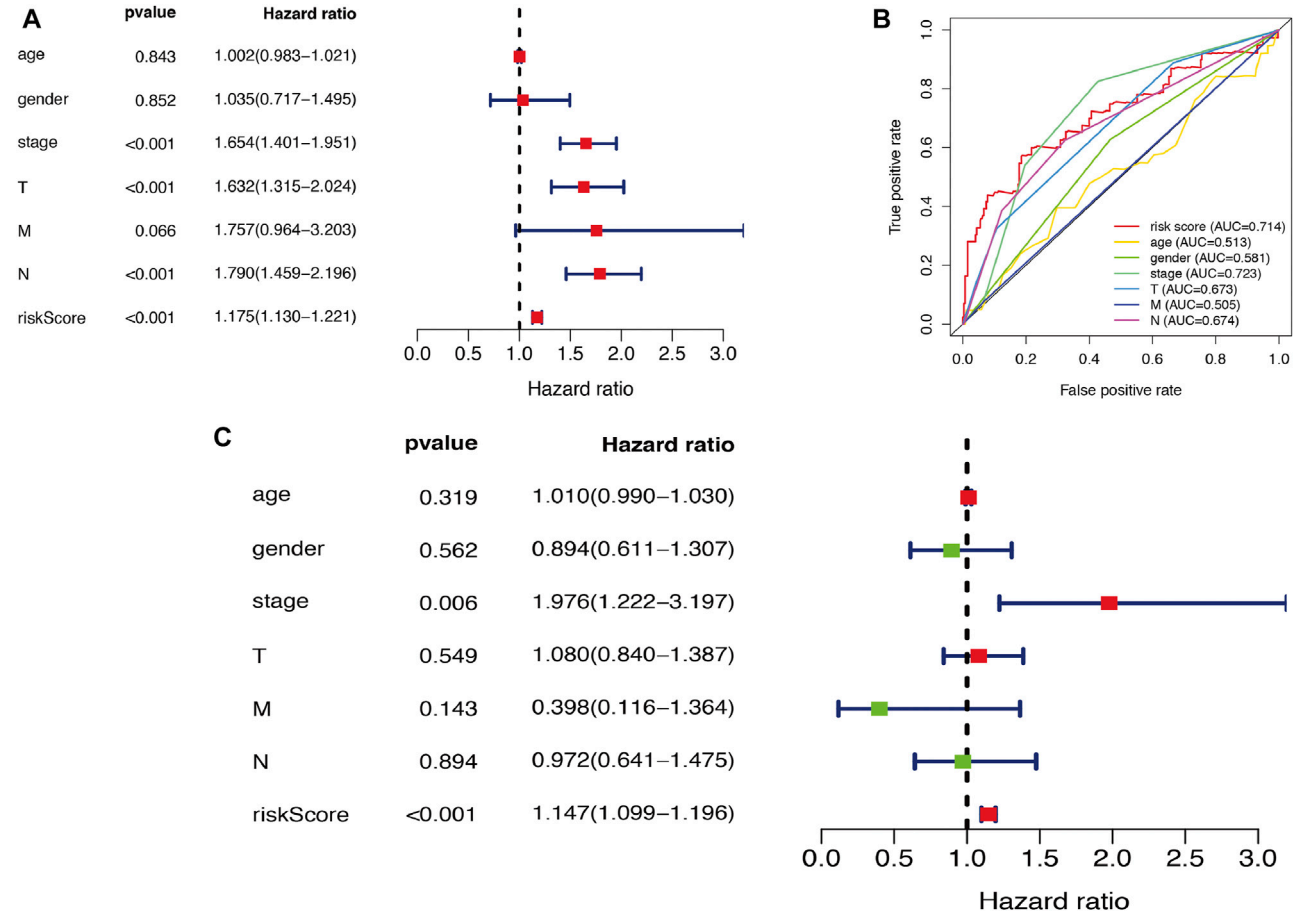

FIGURE 9 | Cox regression analysis of risk model and clinicopathological variables in LUAD. **(A)** Visualization of the forest map with single factor independent prognostic analysis. **(B)** The ROC analysis of OS for the risk model signature and the clinicopathologic variables. **(C)** Visualization of the forest map with multifactor independent prognostic analysis. LUAD, lung adenocarcinoma; ROC, receiver operating characteristic; OS, overall survival.

showed that SPHK1 was positively correlated with $CD4^+$ T cell ($r = 0.444$, $p < 2.2E\text{-}16$; $r = 0.349$, $p = 3.41E\text{-}16$; $r = 0.092$, $p = 0.037$) (**Figures 12E–G**), neutrophil ($r = 0.148$, $p < 0.001$) (**Figure 12H**), and dendritic cell ($r = 0.338$, $p = 3.33E\text{-}15$; $r = 0.152$, $p = 0.001$) infiltration levels, consistent with previous results.

Associations Among Overall Survival, Somatic Copy Number Variation of SPHK1 and Tumor Infiltrating Lymphocytes Levels

According to our previous results, we found that SPHK1 expression levels were correlated with B cell, $CD4^+$ T cell, neutrophil, and dendritic cell infiltration levels, which may be the reason that differentially expressed SPHK1 has a different prognosis. Therefore, we first investigated the prognosis between high and low TIL expression levels. Kaplan–Meier analysis results revealed that cumulative survival rates between low and high B cell ($p < 0.001$) and dendritic cell ($p = 0.048$) infiltration levels were significantly different, as were the different expression levels of SPHK1 ($p = 0.005$) (**Figure 13A**). The SCNA module provides a comparison of the abundance of TILs among tumors with different somatic copy number aberrations for SPHK1. Therefore, we first explored the association between the SCNA level of SPHK1 and immune cell infiltration. We found that the B cell infiltration level was associated with arm-level gain ($p < 0.050$), macrophage infiltration level was associated with arm-level deletion and high amplification (both $p < 0.010$), and $CD4^+$ T cell infiltration level was associated with arm-level gain ($p < 0.050$). For the dendritic cell infiltration level, there seemed to be no relationship with the SCNA level of SPHK1 (**Figure 13B**). Furthermore, TP53 mutation is one of the most common LUAD mutations and was correlated with $CD8^+$ T cell ($p < 0.010$), dendritic cell ($p < 0.050$), and neutrophil ($p < 0.010$) infiltration levels (**Figure 13C**). Heat map analysis between SPHK1 expression levels and tumor-infiltrating lymphocytes in the TISIDB database was also performed and is displayed in **Figure 13D**, which is consistent with our previous results using the TIMER database.

DISCUSSION

In our current study, the limma package in R software was first used to identify DEARGs, and then functional enrichment

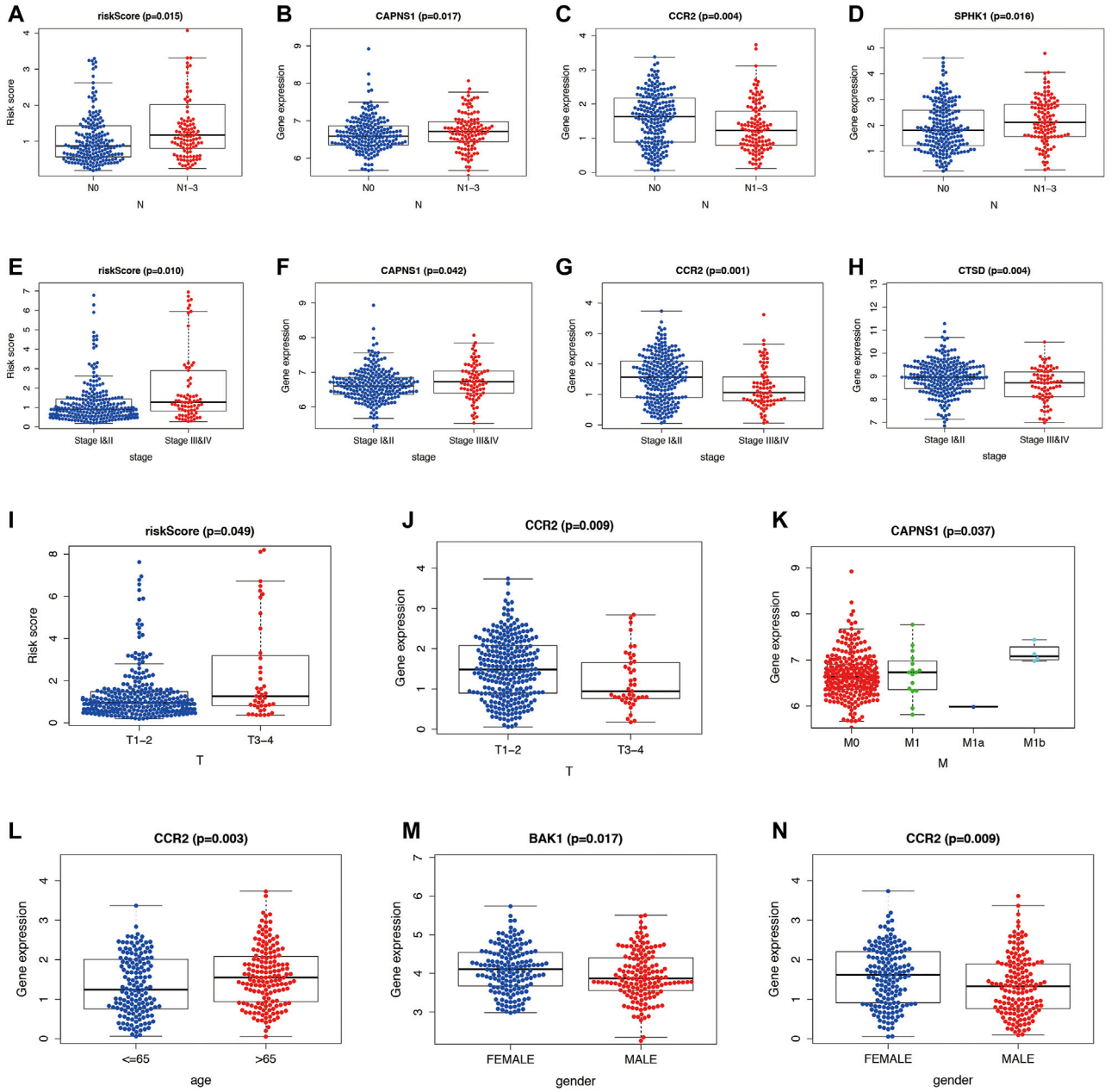

FIGURE 10 | Comparison of ARGs and clinicopathological variables in LUAD. **(A–D)** Difference in the risk score and expression levels of ARGs between pathological N0 stage and pathological N1–N3 stages. **(E–H)** Difference in the risk score and expression levels of ARGs in stage I and II and stage III and IV. **(I,J)** Difference in the risk score and expression levels of ARGs in pathological T3–T4 stage and pathological T1–T2 stage. **(K)** Difference in the expression levels of ARGs in pathological M0 and M1 stage. **(L)** Difference in the expression levels of ARGs in aged ≤65 and >65 years. **(M,N)** Difference in the expression levels of ARGs in gender (male and female). ARGs, autophagy-related genes; LUAD, lung adenocarcinoma.

analysis was performed to further refine the potential roles of DEARGs. Before performing Cox regression analysis, we classified LUAD cases into two subtypes according to consensus clustering based on the 28 prognostic ARGs. In addition, Kaplan–Meier analysis results showed differential prognoses between cluster 1 and cluster 2. Therefore, according to these two clusters, DEGs of each cluster were identified. Subsequently, univariate and multivariate Cox regression analyses were used to obtain the prognostic ARGs. After we overlapped the DEGs of clusters and the prognostic ARGs, 10 genes were selected for further study, and a risk model based on these genes was constructed to evaluate whether these genes could serve as independent prognostic factors for LUAD patients in TCGA database and performed subsequent validation using GSE72094. After we explored the associations between ARGs and clinicopathological variables, five ARGs were

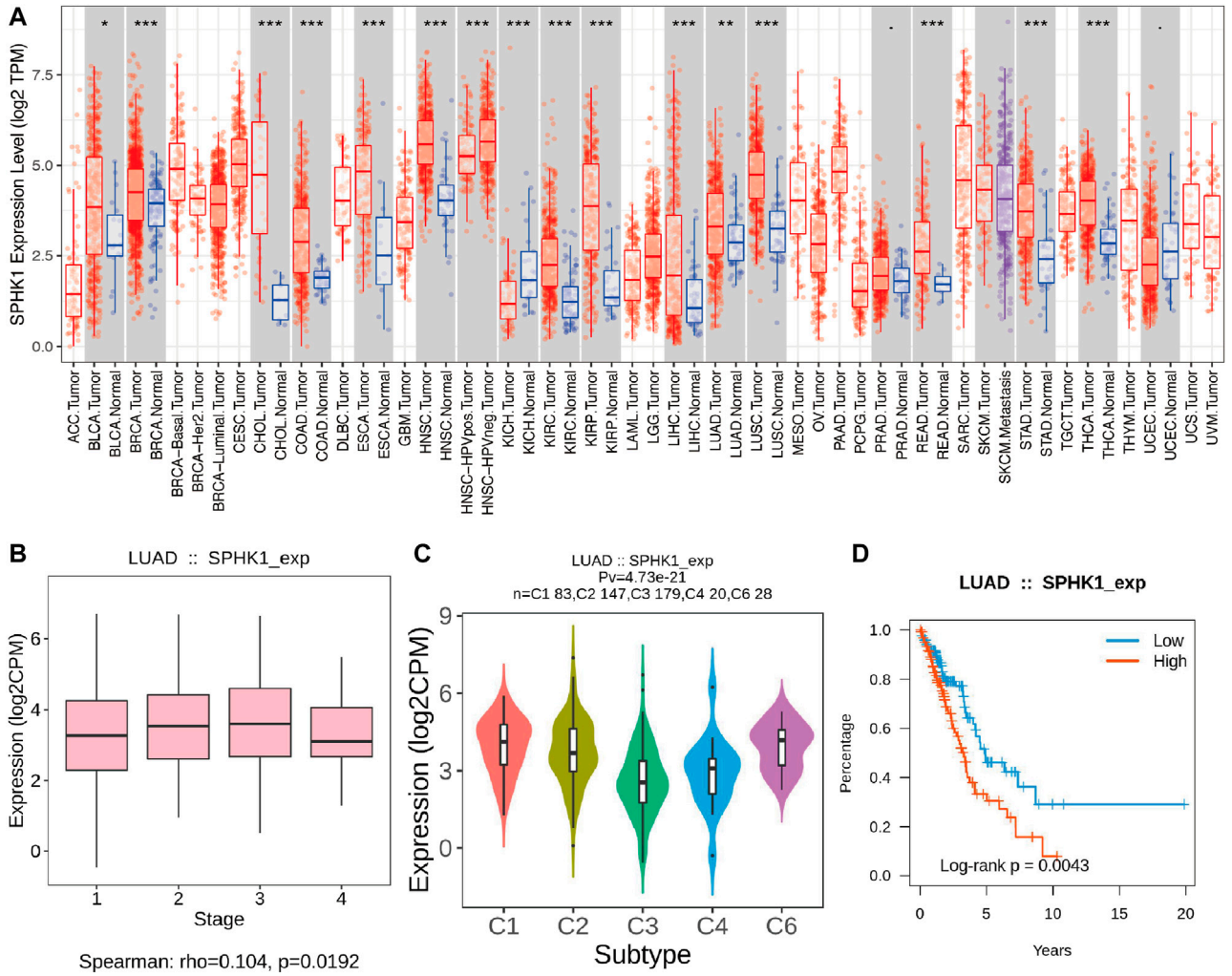

FIGURE 11 | Validation of SPHK1 expression level and its associations with OS. **(A)** SPHK1 expression level in various cancers compared with normal tissues. **(B)** SPHK1 expression level in different stages of LUAD. **(C)** SPHK1 expression distribution across LUAD subtype. **(D)** Kaplan–Meier survival analysis by different SPHK1 expression level of LUAD. OS, overall survival; LUAD, lung adenocarcinoma.

identified as prognostic genes. Then, we validated the expression levels of five ARGs and their relationships with OS in LUAD. SPHK1 was extracted for further study. In addition, the TIMER and TISIDB databases were used to further explore the correlation analysis between immune cell infiltration levels and the risk score as well as clinicopathological variables in the predictive risk model. In brief, a risk model associated with ARGs was constructed for monitoring immune cell infiltration levels and estimating the prognosis of LUAD.

Autophagy underlies the initiation, progression, and metastasis of various cancers, including LUAD, while aberrantly regulated autophagy affects the prognosis of LUAD, but the mechanisms are less well defined. Autophagy maintains cellular homeostasis by engulfing cytoplasmic proteins, complexes, or organelles within the autophagosome (Dikic et al., 2010; Macintosh and Ryan, 2013). Autophagosomes are cytoplasmic double-membraned vesicles that can be transported and fused with lysosomes to generate autolysosomes (Galluzzi et al., 2015). Autophagy has been reported to be associated with tumorigenesis (Martinet et al., 2009; Levy et al., 2017). Over the past few years, many studies have elucidated that autophagy participates in the development and progression of various diseases (Liu et al., 2017; Yao et al., 2018). In brief, autophagy exerts dual functions in tumorigenesis, including both positive and negative effects. Positive effects include autophagy clearing damaged proteins and organelles during the early stages of the tumor to inhibit tumor development (White et al., 2010). Negative effects are involved in the advanced stages of tumorigenesis, and autophagy promotes rapid growth of tumor cells by degrading and recycling damaged or aged organelle components (Janku et al., 2011). Furthermore, mechanisms related to autophagy have also been investigated in many studies (Chung et al., 2017; Bai et al., 2019; Chen et al., 2020; Liu et al., 2020; Peng et al., 2020). For example, PTBP1

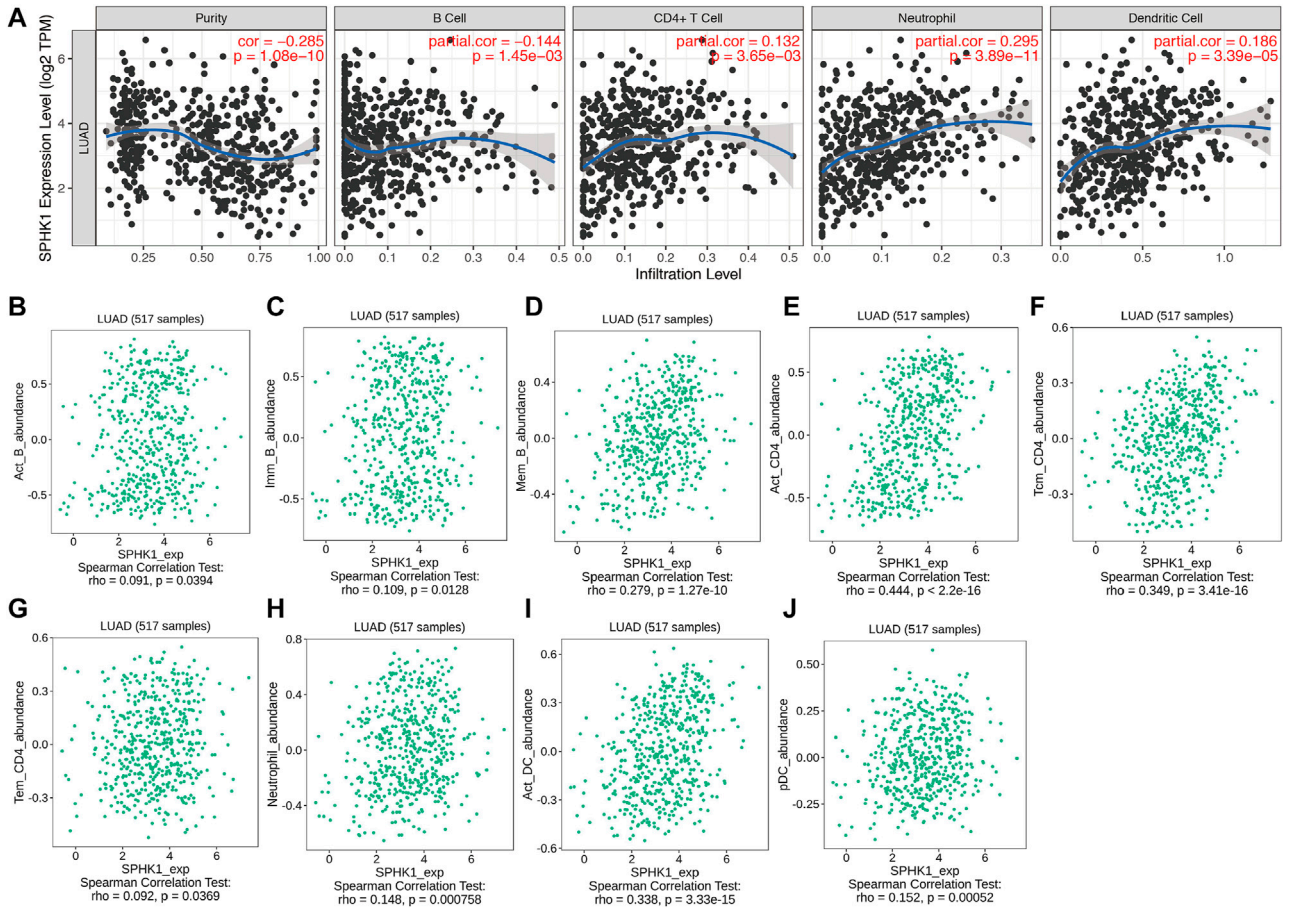

FIGURE 12 | SPHK1 expression level associated with immune cell infiltration levels. **(A)** Correlation between SPHK1 expression levels and immune cell infiltration levels. Correlation between SPHK1 expression level and B Cell infiltration levels **(B–D)**, $CD4^+$ T cells infiltration levels **(E–G)**, neutrophil cells infiltration levels **(H)**, dendritic cell infiltration levels **(I,J)**.

promotes the growth of cancer cells through the PTEN/Akt pathway and autophagy in breast cancer (Wang et al., 2018). In addition, ATG5 and ATG7 regulate autophagy, apoptosis, and the cell cycle through PERK signaling, which is a vital UPR branch pathway (Zheng et al., 2019a). ER stress and autophagy are reportedly involved in the apoptosis of lung cancer (Shi et al., 2016). Interestingly, both ER stress and PERK signaling could be connected to autophagy in the presence of ATG5 and ATG7, revealing that the interplay among these different mechanisms should also be evaluated in further studies. Naturally, ARGs have also attracted increasing attention for their significance to the development of various cancers (Gu et al., 2016; Lin et al., 2018; Jiang et al., 2019; Lin et al., 2020). However, next-generation sequencing associated with ARGs and the establishment of a predictive risk model has not been well elucidated thus far. In addition, owing to the worse prognosis of LUAD, it is vital to identify novel prognostic biomarkers based on different methods.

In recent years, the development of potential prognostic biomarkers associated with ARGs to reveal prognosis has rapidly emerged. One study proposed an ARG prognostic signature and divided all patients into high-risk and low-risk groups, and the author concluded that the autophagy-related gene prognostic signature was a promising independent biomarker for monitoring the outcomes of serous ovarian cancer (An et al., 2018). Another eight ARGs (BCL2, BIRC5, EIF4EBP1, ERO1L, FOS, GAPDH, ITPR1, and VEGFA) were explored, and the author found that these genes not only were significantly associated with overall survival but also could predict distant metastasis-free survival in breast cancer (Gu et al., 2016). In the present study, we also identified 10 ARGs using Cox regression analysis and consensus clustering, and the coefficient values and gene expression values were further used to explore the risk score of each gene. According to the median risk score, all LUAD patients were divided into high-risk and low-risk groups. Survival analysis suggested that the low-risk group exhibited a significantly better prognosis than the high-risk group. Therefore, these 10 genes could serve as independent prognostic indicators and were selected for further exploration of the prognostic pattern in LUAD.

To investigate these 10 genes, correlation analysis was performed, and we found that only five (BAK1, CAPNS1, CCR2, CTSD, and SPHK1) of 10 genes were correlated with

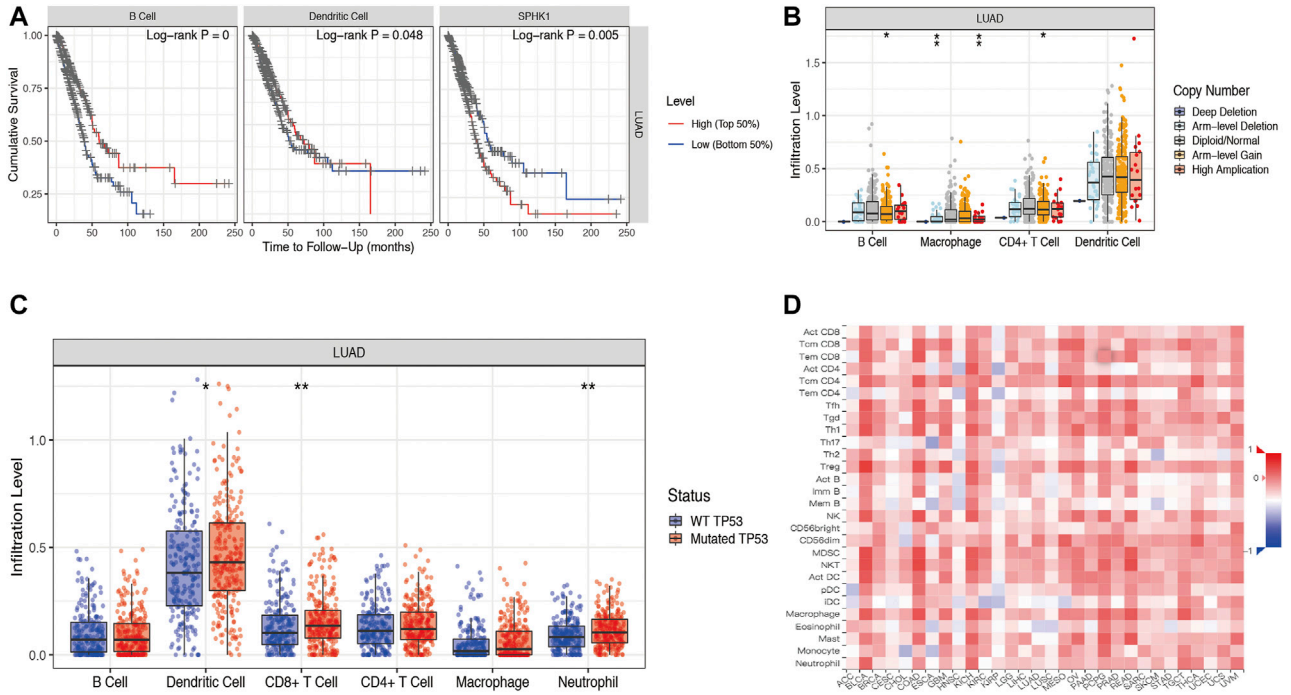

FIGURE 13 | Associations among OS, SCNA of SPHK1, and TIL levels. **(A)** Cumulative survival rates between low and high immune cell (B cell and dendritic cell) infiltration; Kaplan–Meier survival analysis by different SPHK1 expression levels of LUAD. **(B)** Correlation between SCNA level of SPHK1 and immune cell infiltration level. **(C)** TP53 mutation rates were associated with CD8$^+$ T cell, neutrophil, and dendritic cell infiltration levels. **(D)** Heat map analysis of SPHK1 expression level and tumor-infiltrating lymphocytes. OS, overall survival; SCNA, somatic copy number variation; TILs, tumor-infiltrating lymphocytes; LUAD, lung adenocarcinoma.

clinicopathological variables and prognosis in LUAD patients. BAK1 is associated with the development of oral squamous cell carcinoma and could serve as a prognostic biomarker in that malignancy (Baltaziak et al., 2004; Coutinho-Camillo et al., 2010). CAPNS1 has been explored as a crucial protein that could promote metastasis of hepatocellular carcinoma (Dai et al., 2014). Elevated expression levels of CCL2 were found to be correlated with tumor-associated macrophage accumulation, and both factors conveyed a poor prognosis in esophageal carcinogenesis (Yang et al., 2020). CTSD is one of the pivotal orchestrators in the occurrence and development of tumors, and its inhibition could increase autophagosome formation and decrease the formation of autolysosomes at the same time (Zheng et al., 2020). In this study, correlation analysis results suggested that these genes were correlated with age, sex, stage, pathological T stage, pathological N stage, or pathological M stage. Kaplan–Meier survival analysis suggested that CTSD (also called CLN10) expression levels seem to have no effects on OS in LUAD.

After screening the validated prognostic ARGs, SPHK1, as an attractive gene, was selected for further specific study after considering its expression level and prognostic value. Autophagy is involved in immune cell infiltration levels, and ARGs can affect immune responses. Autophagy is very important for the major functions of neutrophils, such as differentiation, phagocytosis, cytokine production, degranulation, and cell death (Germic et al., 2019). It has been demonstrated that enhanced autophagy or lysosome function in immune evasion could be achieved by selecting targets of MHC-I molecules for degradation, which could provide a therapeutic strategy against pancreatic ductal adenocarcinoma (Yamamoto et al., 2020). Various previous clinical studies have suggested that immune cell infiltration levels have a major impact on the clinical outcomes of several cancers (Bates et al., 2006; Galon et al., 2006; Johnson et al., 2000; Al-Shibli et al., 2008). SPHK1 is also known as SPHK. As characterized in a gene database (https://www.ncbi.nlm.nih.gov/gene/), this protein and its product S1P play a key role in immune processes. It has been observed that hypoxia-induced SPHK1 expression and its downstream S1P signaling promote ovarian cancer progression, and elevated expression levels of SPHK1 or S1P are sensitive to the cytotoxic effects of metformin (Hart et al., 2019). In addition, an increasing number of studies have shown the potential therapeutic value of SPHK1, which provides new strategies for cancer treatment to improve the prognosis of cancer patients (Plano et al., 2014; Wang et al., 2019c; Sukocheva et al., 2020). Another study suggested that enhanced SPHK activity promotes cell survival in Jurkat T cells in response to ceramide- or Fas-induced apoptosis (Zheng et al., 2019b). In this study, we found that SPHK1 expression is associated with the prognosis of LUAD. Furthermore, the SPHK1 expression levels were positively correlated with B cell, CD4$^+$ T cell, neutrophil, and dendritic cell infiltration

levels. In contrast, Kaplan–Meier analysis results showed that only B cell and dendritic cell infiltration levels were significantly correlated with prognosis.

In this study, gene expression profiles from TCGA database in LUAD were selected, and a risk model based on ARGs was established to predict the prognosis of LUAD. Subsequently, their prognostic value, association with clinicopathological variables, and the interesting association between SPHK1 and immune cell infiltration levels were validated. Compared to previous studies, the current study first constructed a risk model based on 10 ARGs, and we validated their prognostic value. Finally, five pooled ARG expression signatures were used as independent prognostic factors in patients with LUAD, which may provide new insight for monitoring and predicting the prognosis of LUAD patients.

DATA AVAILABILITY STATEMENT

The datasets presented in this study can be found in online repositories. The names of the repository/repositories and accession number(s) can be found in the article/**Supplementary Material**.

AUTHOR CONTRIBUTIONS

M-YZ developed the original idea, designed the research, performed the analysis and wrote the manuscript. CH helped to design the whole study. J-YL ran the most of data processing. Z-ES and W-DZ did data visualization. J-JQ and Y-LY helped to access the public data. M-YZ drafted the manuscript. Y-QQ revised the writings. All authors contributed to the article and approved the submitted version.

FUNDING

This work was supported by grants from the Major Scientific and Technological Innovation Project of Shandong Province (No. 2018CXGC1212), the CSCO-Qilu Cancer Research Fund (No. Y-Q201802-014), the Medical and Health Technology Innovation Plan of Jinan City (No. 201805002) and the Technology Development Project (6010120081).

ACKNOWLEDGMENTS

We are sincerely acknowledged the contributions from the TCGA project and the GEO project.

SUPPLEMENTARY MATERIAL

The Supplementary Material for this article can be found online at: https://www.frontiersin.org/articles/10.3389/fcell.2021.756911/full#supplementary-material

Supplementary Figure S1 | Expression levels of five prognostic ARGs and prognosis in LUAD patients according. **(A,B)** BAK1 and SPHK1 were highly expressed in LUAD compared with normal lung tissues. **(C–E)** CAPNS1, CCR2 and CTSD were down regulated in LUAD compared with normal lung tissues. **(F–I)** BAK1, CAPNS1, CCR2 and SPHK1 showed their prognostic value. **(J)** CTSD (also named CLN10) expression level seems have no relationship with OS in LUAD. LUAD, lung adenocarcinoma; OS, overall survival.

REFERENCES

Aberle, D. R., Adams, A. M., Berg, C. D., Black, W. C., Clapp, J. D., Fagerstrom, R. M., et al. (2011). Reduced Lung-Cancer Mortality With Low-Dose Computed Tomographic Screening. *N. Engl. J. Med.* 365, 395–409. doi:10.1056/NEJMoa1102873

Al-Shibli, K. I., Donnem, T., Al-Saad, S., Persson, M., Bremnes, R. M., and Busund, L.-T. (2008). Prognostic Effect of Epithelial and Stromal Lymphocyte Infiltration in Non-small Cell Lung Cancer. *Clin. Cancer Res.* 14, 5220–5227. doi:10.1158/1078-0432.CCR-08-0133

An, Y., Bi, F., You, Y., Liu, X., and Yang, Q. (2018). Development of a Novel Autophagy-Related Prognostic Signature for Serous Ovarian Cancer. *J. Cancer* 9, 4058–4071. doi:10.7150/jca.25587

Baghdadi, M., Yoneda, A., Yamashina, T., Nagao, H., Komohara, Y., Nagai, S., et al. (2013). TIM-4 Glycoprotein-Mediated Degradation of Dying Tumor Cells by Autophagy Leads to Reduced Antigen Presentation and Increased Immune Tolerance. *Immunity* 39, 1070–1081. doi:10.1016/j.immuni.2013.09.014

Bai, Y., Liu, X., Qi, X., Liu, X., Peng, F., Li, H., et al. (2019). PDIA6 Modulates Apoptosis and Autophagy of Non-Small Cell Lung Cancer Cells via the MAP4K1/JNK Signaling Pathway. *EBioMedicine* 42, 311–325. doi:10.1016/j.ebiom.2019.03.045

Baltaziak, M., Koda, M., Barwijuk-Machała, M., Musiatowicz, B., Duraj, E., Kańczuga-Koda, L., et al. (2004). The Role of Bak Expression in Apoptosis of the Oral Squamous Cell Carcinoma (OSCC) and Metastases to Lymph Nodes (LNMs). *Rocz Akad Med. Bialymst* 49 (Suppl. 1), 14–15.

Bates, G. J., Fox, S. B., Han, C., Leek, R. D., Garcia, J. F., Harris, A. L., et al. (2006). Quantification of Regulatory T Cells Enables the Identification of High-Risk Breast Cancer Patients and Those at Risk of Late Relapse. *J. Clin. Oncol.* 24, 5373–5380. doi:10.1200/JCO.2006.05.9584

Bray, F., Ferlay, J., Soerjomataram, I., Siegel, R. L., Torre, L. A., and Jemal, A. (2018). Global Cancer Statistics 2018: GLOBOCAN Estimates of Incidence and Mortality Worldwide for 36 Cancers in 185 Countries. *CA Cancer J. Clin.* 68, 394–424. doi:10.3322/caac.21492

Chen, X., Mao, R., Su, W., Yang, X., Geng, Q., Guo, C., et al. (2020). Circular RNA circHIPK3 Modulates Autophagy via MIR124-3p-STAT3-PRKAA/AMPKα Signaling in STK11 Mutant Lung Cancer. *Autophagy* 16, 659–671. doi:10.1080/15548627.2019.1634945

Chung, S. J., Nagaraju, G. P., Nagalingam, A., Muniraj, N., Kuppusamy, P., Walker, A., et al. (2017). ADIPOQ/Adiponectin Induces Cytotoxic Autophagy in Breast Cancer Cells Through STK11/LKB1-Mediated Activation of the AMPK-ULK1 Axis. *Autophagy* 13, 1386–1403. doi:10.1080/15548627.2017.1332565

Coutinho-Camillo, C. M., Lourenço, S. V., Nishimoto, I. N., Kowalski, L. P., and Soares, F. A. (2010). Expression of Bcl-2 Family Proteins and Association with Clinicopathological Characteristics of Oral Squamous Cell Carcinoma. *Histopathology* 57, 304–316. doi:10.1111/j.1365-2559.2010.03621.x

Dai, Z., Zhou, S.-L., Zhou, Z.-J., Bai, D.-S., Xu, X.-Y., Fu, X.-T., et al. (2014). Capn4 Contributes to Tumour Growth and Metastasis of Hepatocellular Carcinoma by Activation of the FAK-Src Signalling Pathways. *J. Pathol.* 234, 316–328. doi:10.1002/path.4395

Dikic, I., Johansen, T., and Kirkin, V. (2010). Selective Autophagy in Cancer Development and Therapy. *Cancer Res.* 70, 3431–3434. doi:10.1158/0008-5472.CAN-09-4027

Galluzzi, L., Pietrocola, F., Bravo-San Pedro, J. M., Amaravadi, R. K., Baehrecke, E. H., Cecconi, F., et al. (2015). Autophagy in Malignant Transformation and Cancer Progression. *EMBO J.* 34, 856–880. doi:10.15252/embj.201490784

Galon, J., Costes, A., Sanchez-Cabo, F., Kirilovsky, A., Mlecnik, B., Lagorce-Pagès, C., et al. (2006). Type, Density, and Location of Immune Cells within Human Colorectal Tumors Predict Clinical Outcome. *Science* 313, 1960–1964. doi:10.1126/science.1129139

Germic, N., Frangez, Z., Yousefi, S., and Simon, H.-U. (2019). Regulation of the Innate Immune System by Autophagy: Neutrophils, Eosinophils, Mast Cells, NK Cells. *Cell Death Differ* 26, 703–714. doi:10.1038/s41418-019-0295-8

Gettinger, S., Horn, L., Jackman, D., Spigel, D., Antonia, S., Hellmann, M., et al. (2018). Five-Year Follow-Up of Nivolumab in Previously Treated Advanced Non-Small-Cell Lung Cancer: Results From the CA209-003 Study. *J. Clin. Oncol.* 36, 1675–1684. doi:10.1200/JCO.2017.77.0412

Gu, Y., Li, P., Peng, F., Zhang, M., Zhang, Y., Liang, H., et al. (2016). Autophagy-Related Prognostic Signature for Breast Cancer. *Mol. Carcinog.* 55, 292–299. doi:10.1002/mc.22278

Hart, P. C., Chiyoda, T., Liu, X., Weigert, M., Curtis, M., Chiang, C.-Y., et al. (2019). SPHK1 is a Novel Target of Metformin in Ovarian Cancer. *Mol. Cancer Res.* 17, 870–881. doi:10.1158/1541-7786.MCR-18-0409

Hirsch, F. R., Scagliotti, G. V., Mulshine, J. L., Kwon, R., Curran, W. J., Jr., Wu, Y.-L., et al. (2017). Lung Cancer: Current Therapies and New Targeted Treatments. *The Lancet* 389, 299–311. doi:10.1016/S0140-6736(16)30958-8

Janku, F., McConkey, D. J., Hong, D. S., and Kurzrock, R. (2011). Autophagy as a Target for Anticancer Therapy. *Nat. Rev. Clin. Oncol.* 8, 528–539. doi:10.1038/nrclinonc.2011.71

Jiang, G.-M., Tan, Y., Wang, H., Peng, L., Chen, H.-T., Meng, X.-J., et al. (2019). The Relationship Between Autophagy and the Immune System and its Applications for Tumor Immunotherapy. *Mol. Cancer* 18, 17. doi:10.1186/s12943-019-0944-z

Johnson, S. K., Kerr, K. M., Chapman, A. D., Kennedy, M. M., King, G., Cockburn, J. S., et al. (2000). Immune Cell Infiltrates and Prognosis in Primary Carcinoma of the Lung. *Lung Cancer* 27, 27–35. doi:10.1016/s0169-5002(99)00095-1

Kim, S., Eun, H., and Jo, E.-K. (2019). Roles of Autophagy-Related Genes in the Pathogenesis of Inflammatory Bowel Disease. *Cells* 8, 77. doi:10.3390/cells8010077

Kinoshita, T., Kudo-Saito, C., Muramatsu, R., Fujita, T., Saito, M., Nagumo, H., et al. (2017). Determination of Poor Prognostic Immune Features of Tumour Microenvironment in Non-smoking Patients with Lung Adenocarcinoma. *Eur. J. Cancer* 86, 15–27. doi:10.1016/j.ejca.2017.08.026

Larabi, A., Barnich, N., and Nguyen, H. T. T. (2020). New Insights into the Interplay Between Autophagy, Gut Microbiota and Inflammatory Responses in IBD. *Autophagy* 16, 38–51. doi:10.1080/15548627.2019.1635384

Levy, J. M. M., Towers, C. G., and Thorburn, A. (2017). Targeting Autophagy in Cancer. *Nat. Rev. Cancer* 17, 528–542. doi:10.1038/nrc.2017.53

Li, Y., Hahn, T., Garrison, K., Cui, Z.-H., Thorburn, A., Thorburn, J., et al. (2012). The Vitamin E Analogue α-TEA Stimulates Tumor Autophagy and Enhances Antigen Cross-Presentation. *Cancer Res.* 72, 3535–3545. doi:10.1158/0008-5472.CAN-11-3103

Lin, P., He, Y., Wen, D.-Y., Li, X.-J., Zeng, J.-J., Mo, W.-J., et al. (2018). Comprehensive Analysis of the Clinical Significance and Prospective Molecular Mechanisms of Differentially Expressed Autophagy-Related Genes in Thyroid Cancer. *Int. J. Oncol.* 53, 603–619. doi:10.3892/ijo.2018.4404

Lin, Q.-G., Liu, W., Mo, Y.-z., Han, J., Guo, Z.-X., Zheng, W., et al. (2020). Development of Prognostic Index Based on Autophagy-Related Genes Analysis in Breast Cancer. *Aging* 12, 1366–1376. doi:10.18632/aging.102687

Liu, G., Pei, F., Yang, F., Li, L., Amin, A., Liu, S., et al. (2017). Role of Autophagy and Apoptosis in Non-Small-Cell Lung Cancer. *Ijms* 18, 367. doi:10.3390/ijms18020367

Liu, Z., Yang, L., Zhong, C., and Zhou, L. (2020). Retracted : EZH2 Regulates H2B Phosphorylation and Elevates colon Cancer Cell Autophagy. *J. Cell. Physiol.* 235, 1494–1503. doi:10.1002/jcp.29069

Macintosh, R. L., and Ryan, K. M. (2013). Autophagy in Tumour Cell Death. *Semin. Cancer Biol.* 23, 344–351. doi:10.1016/j.semcancer.2013.05.006

Martinet, W., Agostinis, P., Vanhoecke, B., Dewaele, M., and de Meyer, G. R. Y. (2009). Autophagy in Disease: A Double-Edged Sword With Therapeutic Potential. *Clin. Sci.* 116, 697–712. doi:10.1042/CS20080508

Nakamura, H., and Saji, H. (2014). A Worldwide Trend of Increasing Primary Adenocarcinoma of the Lung. *Surg. Today* 44, 1004–1012. doi:10.1007/s00595-013-0636-z

Peng, L., Sang, H., Wei, S., Li, Y., Jin, D., Zhu, X., et al. (2020). circCUL2 Regulates Gastric Cancer Malignant Transformation and Cisplatin Resistance by Modulating Autophagy Activation via miR-142-3p/ROCK2. *Mol. Cancer* 19, 156. doi:10.1186/s12943-020-01270-x

Plano, D., Amin, S., and Sharma, A. K. (2014). Importance of Sphingosine Kinase (SphK) as a Target in Developing Cancer Therapeutics and Recent Developments in the Synthesis of Novel SphK Inhibitors. *J. Med. Chem.* 57, 5509–5524. doi:10.1021/jm4011687

Racanelli, A. C., Kikkers, S. A., Choi, A. M. K., and Cloonan, S. M. (2018). Autophagy and Inflammation in Chronic Respiratory Disease. *Autophagy* 14, 221–232. doi:10.1080/15548627.2017.1389823

Shi, S., Tan, P., Yan, B., Gao, R., Zhao, J., Wang, J., et al. (2016). ER Stress and Autophagy are Involved in the Apoptosis Induced by Cisplatin in Human Lung Cancer Cells. *Oncol. Rep.* 35, 2606–2614. doi:10.3892/or.2016.4680

Sukocheva, O. A., Furuya, H., Ng, M. L., Friedemann, M., Menschikowski, M., Tarasov, V. V., et al. (2020). Sphingosine Kinase and Sphingosine-1-Phosphate Receptor Signaling Pathway in Inflammatory Gastrointestinal Disease and Cancers: A Novel Therapeutic Target. *Pharmacol. Ther.* 207, 107464. doi:10.1016/j.pharmthera.2019.107464

Wan, B., Liu, B., Yu, G., Huang, Y., and Lv, C. (2019). Differentially Expressed Autophagy-Related Genes are Potential Prognostic and Diagnostic Biomarkers in Clear-Cell Renal Cell Carcinoma. *Aging* 11, 9025–9042. doi:10.18632/aging.102368

Wang, K. (2015). Autophagy and Apoptosis in Liver Injury. *Cell Cycle* 14, 1631–1642. doi:10.1080/15384101.2015.1038685

Wang, P., Yuan, Y., Lin, W., Zhong, H., Xu, K., and Qi, X. (2019a). Roles of Sphingosine-1-Phosphate Signaling in Cancer. *Cancer Cell Int.* 19, 295. doi:10.1186/s12935-019-1014-8

Wang, X., Li, Y., Fan, Y., Yu, X., Mao, X., and Jin, F. (2018). PTBP1 Promotes the Growth of Breast Cancer Cells Through the PTEN/Akt Pathway and Autophagy. *J. Cell Physiol.* 233, 8930–8939. doi:10.1002/jcp.26823

Wang, Y., Lin, Y.-X., Wang, J., Qiao, S.-L., Liu, Y.-Y., Dong, W.-Q., et al. (2019b). *In Situ* Manipulation of Dendritic Cells by an Autophagy-Regulative Nanoactivator Enables Effective Cancer Immunotherapy. *ACS Nano* 13, 7568–7577. doi:10.1021/acsnano.9b00143

Wang, Z., Gao, L., Guo, X., Feng, C., Lian, W., Deng, K., et al. (2019c). Development and Validation of a Nomogram With an Autophagy-Related Gene Signature for Predicting Survival in Patients With Glioblastoma. *Aging* 11, 12246–12269. doi:10.18632/aging.102566

White, E., Karp, C., Strohecker, A. M., Guo, Y., and Mathew, R. (2010). Role of Autophagy in Suppression of Inflammation and Cancer. *Curr. Opin. Cell Biol.* 22, 212–217. doi:10.1016/j.ceb.2009.12.008

Wright, G., Manser, R. L., Byrnes, G., Hart, D., and Campbell, D. A. (2006). Surgery for Non-Small Cell Lung Cancer: Systematic Review and Meta-Analysis of Randomised Controlled Trials. *Thorax* 61, 597–603. doi:10.1136/thx.2005.051995

Yamamoto, K., Venida, A., Yano, J., Biancur, D. E., Kakiuchi, M., Gupta, S., et al. (2020). Autophagy Promotes Immune Evasion of Pancreatic Cancer by Degrading MHC-I. *Nature* 581, 100–105. doi:10.1038/s41586-020-2229-5

Yang, H., Zhang, Q., Xu, M., Wang, L., Chen, X., Feng, Y., et al. (2020). CCL2-CCR2 Axis Recruits Tumor Associated Macrophages to Induce Immune Evasion Through PD-1 Signaling in Esophageal Carcinogenesis. *Mol. Cancer* 19, 41. doi:10.1186/s12943-020-01165-x

Yao, C., Ni, Z., Gong, C., Zhu, X., Wang, L., Xu, Z., et al. (2018). Rocaglamide Enhances NK Cell-Mediated Killing of Non-Small Cell Lung Cancer Cells by Inhibiting Autophagy. *Autophagy* 14, 1831–1844. doi:10.1080/15548627.2018.1489946

Zappa, C., and Mousa, S. A. (2016). Non-Small Cell Lung Cancer: Current Treatment and Future Advances. *Transl. Lung Cancer Res.* 5, 288–300. doi:10.21037/tlcr.2016.06.07

Zhang, F., Xie, S., Zhang, Z., Zhao, H., Zhao, Z., Sun, H., et al. (2020). A Novel Risk Model Based on Autophagy Pathway Related Genes for Survival Prediction in Lung Adenocarcinoma. *Med. Sci. Monit.* 26, e924710. doi:10.12659/MSM.924710

Zheng, W., Chen, Q., Wang, C., Yao, D., Zhu, L., Pan, Y., et al. (2020). Inhibition of Cathepsin D (CTSD) Enhances Radiosensitivity of Glioblastoma Cells by Attenuating Autophagy. *Mol. Carcinog* 59, 651–660. doi:10.1002/mc.23194

Zheng, W., Xie, W., Yin, D., Luo, R., Liu, M., and Guo, F. (2019a). ATG5 and ATG7 Induced Autophagy Interplays with UPR via PERK Signaling. *Cell Commun. Signal* 17, 42. doi:10.1186/s12964-019-0353-3

Zheng, X., Li, W., Ren, L., Liu, J., Pang, X., Chen, X., et al. (2019b). The Sphingosine Kinase-1/sphingosine-1-Phosphate Axis in Cancer: Potential Target for Anticancer Therapy. *Pharmacol. Ther.* 195, 85–99. doi:10.1016/j.pharmthera.2018.10.011

Zhu, J., Wang, M., and Hu, D. (2020a). Development of an Autophagy-Related Gene Prognostic Signature in Lung Adenocarcinoma and Lung Squamous Cell Carcinoma. *PeerJ* 8, e8288. doi:10.7717/peerj.8288

Zhu, L., Yan, D., Chen, Y., Chen, S., Chen, N., and Han, J. (2020b). The Identification of Autophagy-Related Genes in the Prognosis of Oral Squamous Cell Carcinoma. *Oral Dis.* 26, 1659–1667. doi:10.1111/odi.13492

Conflict of Interest: The authors declare that the research was conducted in the absence of any commercial or financial relationships that could be construed as a potential conflict of interest.

The reviewer AC declared a shared affiliation with the authors to the handling editor at time of review.

Publisher's Note: All claims expressed in this article are solely those of the authors and do not necessarily represent those of their affiliated organizations, or those of the publisher, the editors, and the reviewers. Any product that may be evaluated in this article, or claim that may be made by its manufacturer, is not guaranteed or endorsed by the publisher.

frontiers in Cell and Developmental Biology

REVIEW
published: 19 November 2021
doi: 10.3389/fcell.2021.777018

Chronic Stress: Impacts on Tumor Microenvironment and Implications for Anti-Cancer Treatments

*Wentao Tian[1,2], Yi Liu[3], Chenghui Cao[1,2], Yue Zeng[1], Yue Pan[1], Xiaohan Liu[1], Yurong Peng[1] and Fang Wu[1,4,5,6]**

[1]Department of Oncology, The Second Xiangya Hospital, Central South University, Changsha, China, [2]Xiangya School of Medicine, Central South University, Changsha, China, [3]Xiangya School of Public Health, Central South University, Changsha, China, [4]Hunan Cancer Mega-Data Intelligent Application and Engineering Research Centre, Changsha, China, [5]Hunan Key Laboratory of Tumor Models and Individualized Medicine, The Second Xiangya Hospital, Central South University, Changsha, China, [6]Hunan Key Laboratory of Early Diagnosis and Precision Therapy in Lung Cancer, The Second Xiangya Hospital, Central South University, Changsha, China

Chronic stress is common among cancer patients due to the psychological, operative, or pharmaceutical stressors at the time of diagnosis or during the treatment of cancers. The continuous activations of the hypothalamic-pituitary-adrenal (HPA) axis and the sympathetic nervous system (SNS), as results of chronic stress, have been demonstrated to take part in several cancer-promoting processes, such as tumorigenesis, progression, metastasis, and multi-drug resistance, by altering the tumor microenvironment (TME). Stressed TME is generally characterized by the increased proportion of cancer-promoting cells and cytokines, the reduction and malfunction of immune-supportive cells and cytokines, augmented angiogenesis, enhanced epithelial-mesenchymal transition, and damaged extracellular matrix. For the negative effects that these alterations can cause in terms of the efficacies of anti-cancer treatments and prognosis of patients, supplementary pharmacological or psychotherapeutic strategies targeting HPA, SNS, or psychological stress may be effective in improving the prognosis of cancer patients. Here, we review the characteristics and mechanisms of TME alterations under chronic stress, their influences on anti-cancer therapies, and accessory interventions and therapies for stressed cancer patients.

Keywords: chronic stress, tumor microenvironment, glucocorticoid, catecholamine, anticancer treatment

OPEN ACCESS

Edited by:
Daniele Vergara, University of Salento, Italy

Reviewed by:
Marina Damato, University of Salento, Italy
Kristina Andrijauskaite, The University of Texas Health Science Center at San Antonio, United States

****Correspondence:***
Fang Wu
wufang4461@csu.edu.cn

Specialty section:
This article was submitted to Molecular and Cellular Oncology, a section of the journal Frontiers in Cell and Developmental Biology

Received: *14 September 2021*
Accepted: *02 November 2021*
Published: *19 November 2021*

Citation:
Tian W, Liu Y, Cao C, Zeng Y, Pan Y, Liu X, Peng Y and Wu F (2021) Chronic Stress: Impacts on Tumor Microenvironment and Implications for Anti-Cancer Treatments. Front. Cell Dev. Biol. 9:777018. doi: 10.3389/fcell.2021.777018

INTRODUCTION

Chronic stress, which is associated with the constant activation of the hypothalamic-pituitary-adrenal (HPA) axis and the sympathetic nervous system (SNS) and release of stress hormones including catecholamines and glucocorticoids, occurs frequently in cancer patients during cancer diagnosis and treatment (Gil et al., 2012). The catecholamines and glucocorticoids then activate the adrenergic receptors and glucocorticoid receptors, which belong to the G protein-coupled receptor (GPCR) family and nuclear receptor family respectively, to activate several signaling pathways or alter the transcriptions directly. Unlike the transient secretion of stress hormones in acute stress, lasting elevations of catecholamines and glucocorticoids not only cause mental diseases such as anxiety disorder and depression, but also takes part in the

tumorigenesis, progression, metastasis, and drug resistance of various cancers (Reiche et al., 2004). A meta-analysis suggested that stress-related psychosocial factors are associated with higher cancer incidence in initially healthy populations, poorer survival in patients with diagnosed cancer, and higher cancer-related mortality (Chida et al., 2008). Thus, chronic stress is a noteworthy issue in terms of anti-cancer treatments.

Tumor microenvironment (TME), consisting of tumor cells, tumor stromal cells, and non-cellular components, is largely involved in the formation, maintenance, and multidrug resistance (MDR) of cancers (Baghban et al., 2020). Initially, the pro-cancer effects of persistent activations of the HPA axis and SNS under chronic stress are thought to depend mostly on their regulations on systematic immune functions (Sloan et al., 2007; Silverman and Sternberg, 2012). Nowadays, extensive studies have revealed that chronic stress is also responsible for altering the TME, including the tumor cells, cancer stromal cells, and extracellular matrix (ECM), thus participants in cancer-promoting processes.

This review focuses on the consequences of chronic stress on TME and summarizes the characteristics and mechanisms of TME alterations under chronic stress, based on which we emphasize the negative effects of chronic stress on anti-tumor therapies and the implications for formulating well-rounded anti-cancer strategies.

FEATURES OF TME UNDER CHRONIC STRESS

The TME of patients with chronic stress is distinct from the TME of patients without it, manifested in the differences in the types, statuses, and quantities of immune cells, the class and amounts of cytokines, augmented angiogenesis, enhanced epithelial-mesenchymal transition (EMT), and damaged ECM.

Immune Cells

Generally, the effects of chronic stress on Immune cells in TME are embodied in decreased numbers or functions of immune-supportive cells and increased amounts of exhausted immune cells and immunosuppressive cells (**Figure 1**).

Dendritic cells (DCs) are essential in tumor antigen presentation and the initiation of cancer adaptive immunity (Gardner and Ruffell, 2016). Nonetheless, Chronic stress or exposure to glucocorticoids disabled immature DCs to undergo full maturation and prime Th1 cells and $CD8^+$ T cells efficiently in a rodent model with melanoma, yet the functions of mature DCs were unaffected (Matyszak et al., 2000; Sommershof et al., 2017).

T lymphocytes serve as the main force in cancer adaptive immunity, yet chronic stress leads to a reduction and dysfunction of immune-supportive T cells along with a raise of immunosuppressive T cells (Thommen and Schumacher, 2018). A reduction of cytotoxic T lymphocytes (CTLs) in TME occurred after impaired DC maturation in both healthy mice and the mice with melanoma (Bucsek et al., 2017; Sommershof et al., 2017). Endogenous glucocorticoids inhibited responses of DCs and T cells to type I interferons (IFNs) and IFN-γ, respectively, which compromised the differentiation or activations of these cells in the TME of mice (Yang et al., 2019). Endogenous glucocorticoid signaling led to dysfunctional CD8+ T cells characterized by increased expressions of PD-1, TIM-3, and Lag3 (Acharya et al., 2020). Stress-induced β-AR activation suppressed T-cell receptor (TCR) signaling in a rodent melanoma model and a rodent colon cancer model (Qiao et al., 2021). β2-AR activations in regulatory T (Treg) cells increased their immunosuppressive functions associated with decreased interleukin (IL-2) level and improved differentiation of CD4+ Foxp3- T cells into Foxp3+ Tregs in a rodent model (Guereschi et al., 2013). Stressed mice also had increased suppressive CD25+ cells in tumors of UV-induced squamous cell carcinoma (Saul et al., 2005).

Natural killer (NK) cells, acting through NK cell cytotoxicity (NKCC), represent pivotal cells in tumor innate immunity (DeNardo and Ruffell, 2019). Surgical stress reduced NKCC and NK cell expression of Fas ligand and CD11a in the blood of mice with melanoma or Lewis lung carcinoma (Glasner et al., 2010). Similar diminished NKCC was observed in blood samples from stressed rodent models with leukemia and breast cancer (Ben-Eliyahu et al., 1999). A study on 42 patients with epithelial ovarian cancer revealed that psychological distress was related to lower NK cytotoxicity in TIL (Lutgendorf et al., 2005). Another study revealed impaired NK cell lysis, associated with altered expression of killer immunoglobin-like receptors, in breast cancer patients with high levels of psychological stress (Varker et al., 2007).

Myeloid-derived suppressor cells (MDSCs), presenting in individuals with cancer or chronic stress, play a key role in immune suppression (Gabrilovich, 2017). The operative stress increased the number of immunosuppressive MDSCs in TME (Ma et al., 2019). Similarly, an increase of MDSCs and Treg cells was detected in another stressed male rodent model (Schmidt et al., 2016).

Macrophages are also important components of TME, with which tumors enhance cell proliferation, angiogenesis, and metastasis (DeNardo and Ruffell, 2019). Prostate cancer patients with a higher score of depression revealed higher $CD68^+$ tumor-associated macrophage (TAM) infiltration (Cheng et al., 2019), and daily restraint stress increased infiltration of CD68+ macrophages in rodent models of ovarian cancer as well (Colon-Echevarria et al., 2020). Moreover, β2-AR activation promoted macrophages to polarize to immunosuppressive M2 subtype in a rodent breast cancer model (Qin et al., 2015).

In addition, cancer-associated fibroblast (CAF) can regulate TME through cell-cell contact, releasing growth factors, and remodeling the extracellular matrix (Chen and Song, 2019). The activation of α2-ARs boosts the growth and proliferation of fibroblasts, increasing the concentration of growth factors in TME (Bruzzone et al., 2011; Shan et al., 2014).

Cytokines

Unsurprisingly, the cytokines originating from both tumor cells and stromal cells in stressed TME show cancer-

promoting properties (**Figure 1**). Glucocorticoids reduced the number of IFN-γ-producing cells and the amount of IFN-γ produced in TME of the rodent melanoma model (Matyszak et al., 2000; Sommershof et al., 2017). Increased MDSCs in TME up-regulated transforming growth factor-beta 1 (TGF-β1), vascular endothelial growth factor (VEGF), and Interleukin-10 (IL-10) in rodent breast cancer models (Ma et al., 2019). And glucocorticoid could upregulate the expression of TGF-β receptor type II on ovarian cancer cells and enhance their responsiveness to TGF-β1 (Chen et al., 2010). The activation of β-AR enhanced the secretion of neuropeptide Y (NPY) in a rodent prostate cancer model and subsequently promoted TAM trafficking (Cheng et al., 2019). The level of IL-6 was elevated in the TME of a prostate cancer model due to TAM activation and tumor cell secretion induced by β-AR signaling (Powell et al., 2013; Cheng et al., 2019). Elevations of matrix metalloproteinase (MMP)-9 in TAMs were detected in epithelial ovarian cancer tissue of patients with chronic stress (Lutgendorf et al., 2008). The expressions of VEGF, MMP-2, and MMP-9 were increased in a stressed rodent model of ovarian carcinoma and another stressed rodent model of lung carcinoma (Thaker et al., 2006; Wu et al., 2015), and the same upregulations were detected in nasopharyngeal carcinoma tumor cells treated with norepinephrine (Yang E. V. et al., 2006). Similar upregulations of VEGF and MMP-2 were observed in a rodent oral cancer model (Xie et al., 2015). The upregulated expression of VEGF, IL-8, and IL-6 was also observed in human melanoma tumor cell lines treated with norepinephrine (Yang et al., 2009). Elevated PGE2 secretion was detected in epinephrine-treated *ex vivo* human breast and colon cancer explant and mammary tumors of chronic stress-exposed mice due to activation (Muthuswamy et al., 2017). Additionally, the cytokine analyses in a stressed rodent ovarian cancer model revealed up-regulation of a large scale of cytokines, including platelet-derived growth factor AA (PDGF-AA), epithelial cell-derived neutrophil-activating peptide (ENA-78), angiogenin, VEGF, granulocyte-macrophage colony-stimulating factor (GM-CSF), IL-5, Lipocalin-2, macrophage migration inhibitory factor (MIF), and transferrin receptor (TfR) (Colon-Echevarria et al., 2020).

Angiogenesis

Overexpression of VEGF and other pro-angiogenic factors like IL-6, TGF-beta, and MMPs, as one of the critical features of stressed TME, leads to enhanced angiogenesis of solid tumors (Kerbel, 2008). This effect was observed in the stressed rodent models of ovarian cancer, oral cancer, and lung cancer, as mentioned above (Thaker et al., 2006; Wu et al., 2015; Xie et al., 2015). Additionally, the expression of VEGFR-2 on endothelial cells was upregulated in the stressed rodent lung cancer model, which also contributes to enhanced angiogenesis (Wu et al., 2015). Moreover, Chronic stress promoted VEGF/FGF2-mediated angiogenesis in a rodent model of breast cancer by down-regulating peroxisome proliferator-activated receptor γ (PPARγ) (Zhou et al., 2020). Enhanced angiogenesis induced by chronic stress and β-adrenergic signaling *via* histone deacetylase-2 (HDAC2)-mediated suppression of thrombospondin-1 was also observed in a stressed model of prostate cancer (Hulsurkar et al., 2017). What's worse, chaotic and unfunctional vessels induced by intense angiogenesis lead to other problems like acidosis and hypoxia in TME (Neri and Supuran, 2011; Rey et al., 2017).

Epithelial-Mesenchymal Transition

As TGF-β family signaling is crucial in EMT, chronic stress also promotes EMT because TGF-β1 is markedly upregulated in stressed TME (Lamouille et al., 2014). A high concentration of TGF-β1 induces EMT of tumor cells and promotes tumor metastasis in stressed rodent models with breast cancer (Ma et al., 2019). Norepinephrine induced EMT, reflected in E-cadherin downregulation and vimentin upregulation, *via* β-AR/TGF-β1/p-Smad3/Snail pathway or β-AR/TGF-β1/HIF-1α/Snail pathway in gastric, colonic, and pneumonic cancer cell lines *in vitro* (Shan et al., 2014; Zhang et al., 2016). In addition, Chronic stress downregulates E-cadherin expression and upregulates vimentin expression through the activation of miR-337-3p/STAT3 in a stressed rodent model with breast cancer (Du et al., 2020).

Moreover, given that the activation of ARs can induce the activations of protein kinase A (PKA) and protein kinase C (PKC) (Biazi et al., 2018; Durkee et al., 2019; Cole and Sood, 2012) (**Figure 2**), chronic stress can be associated with EMT *via* PKA and PKC signaling. It is well established that PKC promotes EMT by activating various downstream molecules. PKCα was regarded as a central signaling node for EMT in breast cancer (Tam et al., 2013). PKCθ was reported to induce EMT through TGF-βand NF-κB signaling (Zafar et al., 2014; Zafar et al., 2015), and PKCδ could induce EMT via phosphorylation of Bcl-2 associated athanogene 3 (BAG3) (Li et al., 2013). Moreover, a study showed that PKC-induced EMT was associated with a down-regulation of carbonic anhydrase 12 (CAXII) (Vergara et al., 2020). In contrast, the activation of PKA favored the epithelial type and contributed to the mesenchymal-epithelial transition (MET) of the tumor cells (Nadella et al., 2008; Pattabiraman et al., 2016). Yet, research showed that PKA promoted TGF-βinduced EMT (Yang Y. et al., 2006), and enhanced activity of PKA plays an important role in hypoxia-mediated EMT (Shaikh et al., 2012). However, research on PKA/PKC-induced EMT using stress or stress hormone-treated models is lacking, so the exact roles of PKA and PKC in chronic stress-induced EMT still need further investigations.

Additionally, it is notable that chronic stress is also associated with deteriorations of gut microbiota (Gao et al., 2018), which can facilitate EMT through microbiota-host interactions (Vergara et al., 2019).

Extracellular Matrix

Elevations of MMPs were present in TME of various cancers (Thaker et al., 2006; Lutgendorf et al., 2008; Wu et al., 2015; Xie et al., 2015), which are likely to cause damages to ECM and

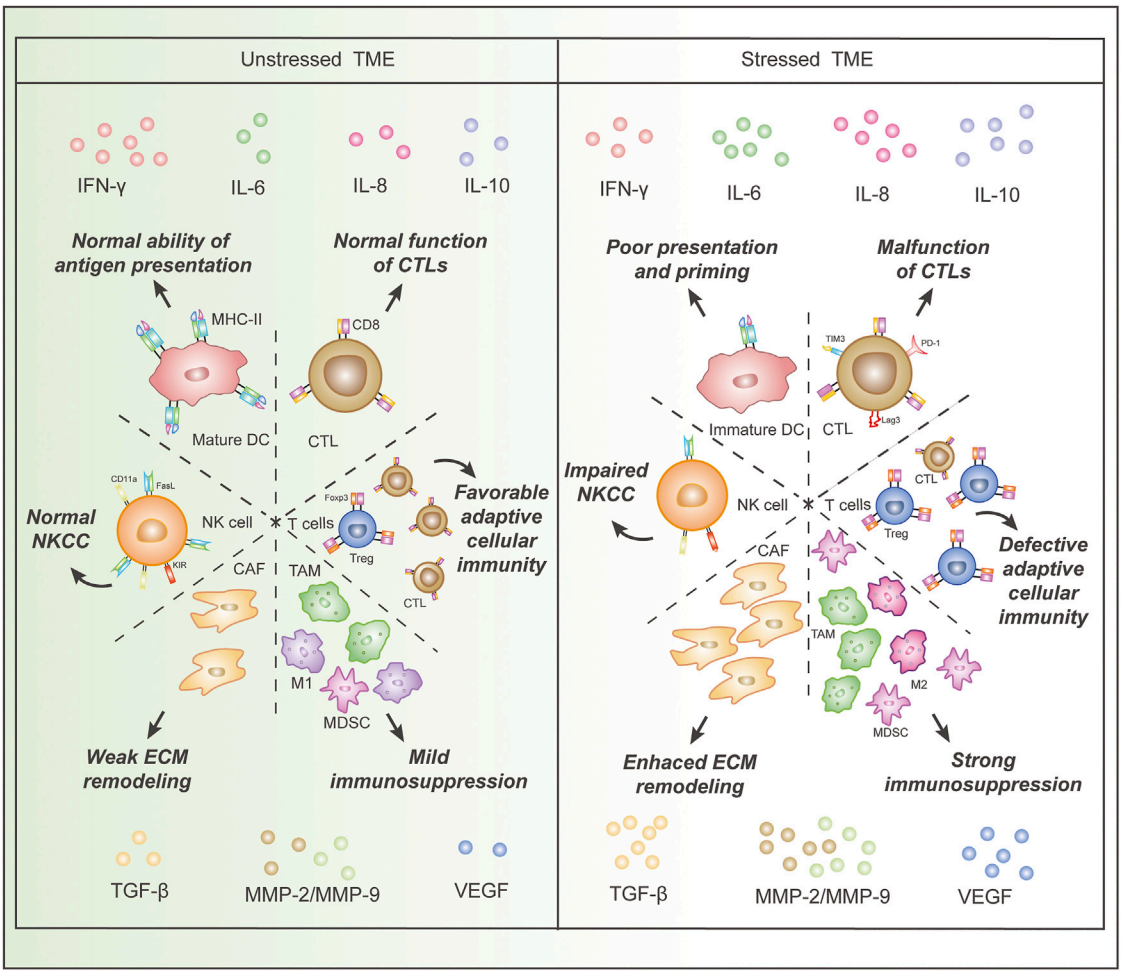

FIGURE 1 | Comparison of immune cells and cytokines in the stressed and unstressed tumor microenvironment (TME). Stressed TME is characterized by (I), decreased proportion and dysfunction of immune-supportive cells, including DCs and CTLs, as well as an increased proportion of cancer-promoting cells, such as MDSCs, Treg cells, CAFs, TAMs, and M2 macrophages; (II), increased concentrations of cytokines that impair anti-cancer immunity and induce angiogenesis, epithelial-mesenchymal transition, and extracellular matrix damage, as well as a decreased concentration of IFN-γ. Abbreviations: IFN, interferon; MMP, matrix metalloproteinase; IL, interleukin; TGF, transforming growth factor; VEGF, vascular endothelial growth factor; DC, dendritic cell; CTL, cytotoxic T lymphocyte, CAF, cancer-associated fibroblast; Treg, regulatory T cell; MDSC, myeloid-derived suppressor cell; TAM, tumor-associated macrophage;NK cell, natural killer cell; FasL, Fas ligand; NKCC, NK cell cytotoxicity; ECM, extracellular matrix.

promote cancer metastasis (Najafi et al., 2019). Additionally, glucocorticoids can downregulate the synthesis of tenascin-C, a vital protein in the extracellular matrix, in a rodent Wilms' tumor model, even though local stimulatory growth factors are present (Talts et al., 1995).

Metabolism

Chronic stress can cause molecular and functional recalibrations of mitochondria and metabolic disorders in immune cells (Picard and McEwen, 2018; Fan et al., 2019), which can alter the metabolic features in TME. Also, hostile TME with limited oxygen and nutrients can lead to metabolic reprogramming of local T cells and impair their functions (Pearce et al., 2013). Chronic stress-induced up-regulation of epinephrine could activate lactate dehydrogenase A (LDHA) to generate lactate and promote breast cancer stem-like properties in a rodent model (Cui et al., 2019). Besides, β-AR activation depressed endothelial oxidative phosphorylation and turned on the angiogenic switch for tumor progression in a rodent prostate cancer model (Zahalka et al., 2017). Additionally, the activations of PKC and PKA can lead to unfavorable metabolic alterations and fuel cancer progression (Aggarwal et al., 2019; Liu et al., 2019; Vergara et al., 2020).

MECHANISMS FOR TME ALTERATIONS UNDER CHRONIC STRESS

The TME alterations under chronic stress are mainly derived from activated AR signaling and glucocorticoid signaling. Under chronic stress, SNS is constantly activated, resulting in a high concentration of catecholamine in solid tumor tissues, which drives from both circulating blood and local sympathetic neurons

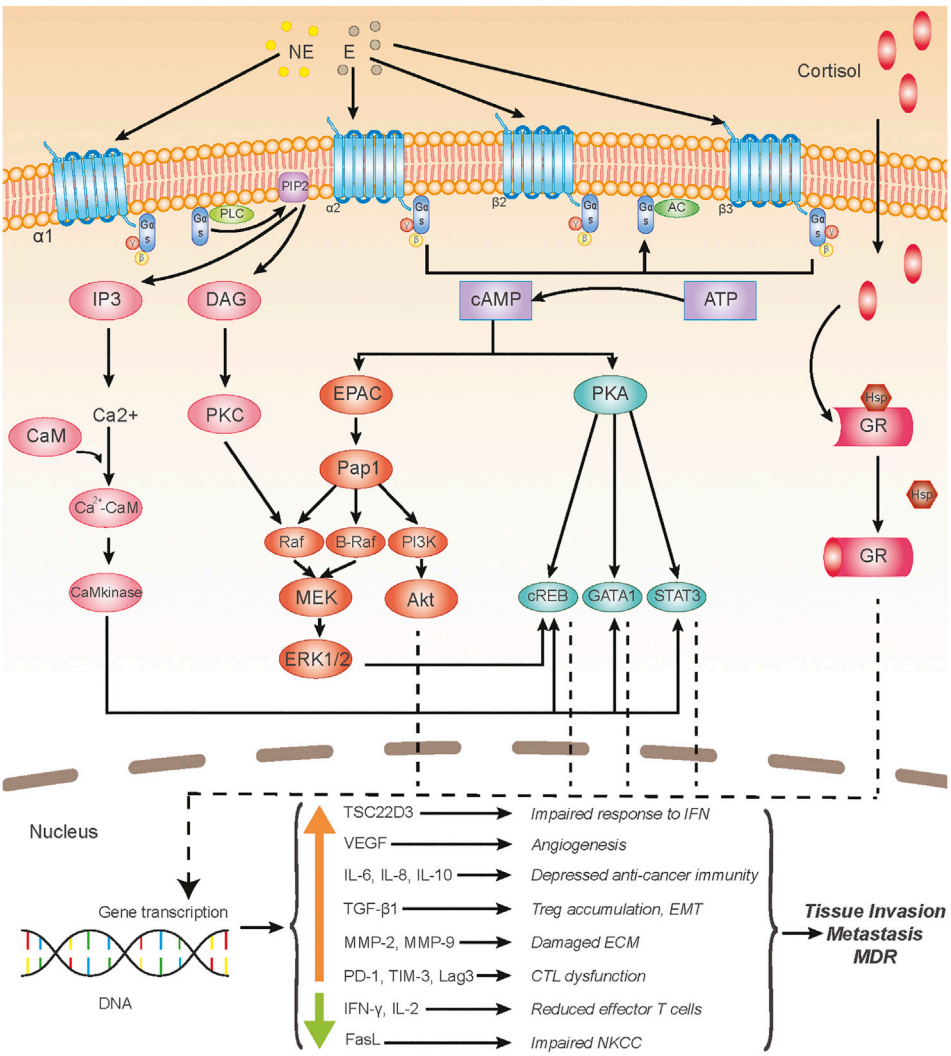

FIGURE 2 | Chronic stress-induced signaling pathways acting upon tumor microenvironment. Adrenergic receptors (ARs), including α-AR, β2-AR, and β3-AR get involved in chronic stress-induced tumor microenvironment (TME) alterations; ARs are G protein-coupled receptors (GPCRs), the binding of AR agonists, such as norepinephrine and epinephrine, to which activates intracellular Gαs protein. Activated Gαs either activates PLC (α1-AR) or AC (α1-AR, β2-AR, and β3-AR), which subsequently induces an intracellular increase of IP3 and DAG, or cAMP, respectively, and then the second messengers initiate activation of several signaling pathways, including the PKA, PKC, EPAC, and Ca^{2+}-CaM pathways. Glucocorticoid receptors (GRs), consisting of the glucocorticoid-binding subunit and Hsp 90 protein, belong to the nuclear receptor family and locate intracellularly; after glucocorticoids permeate through the cell membrane and bind to GRs, the Hsp protein depolymerizes from the polymeric substance and the main subunits of GRs translocate into the nucleus and initiate gene transcriptions. Transcriptions of various genes of cytokines or ligands are up-regulated or down-regulated, altogether causing the deterioration of the TME, which leads to a large scale of cancer-promoting effects. Abbreviation: NE, norepinephrine; E, epinephrine; PLC, phospholipase C; PIP2, phosphatidylinositol (4,5) bisphosphate; AC, adenylatecyclase; IP3, inositol triphosphate; DAG, diacylglycerol; CaM, calmodulin; PKC, protein kinase C; ATP, adenosine triphosphate; cAMP, cyclic adenosine monophosphate; PKA, protein kinase A; EPAC, exchange protein activated by adenylyl cyclase; Pap1, production of anthocyanin pigment 1; PI3K, phosphatidylinositol 3-kinase; MEK, mitogen-activated protein kinase kinase (MAPKK); ERK, extracellular regulated protein kinase; CREB, cAMP-responsive element-binding protein; GATA1, GATA Binding Protein 1; STAT3, signal transducer and activator of transcription 3; GR, glucocorticoid receptor; Hsp, heat shock protein; IFN, interferon; NKCC, NK cell cytotoxicity; ECM, extracellular matrix; CTL, cytotoxic T lymphocyte; EMT, epithelial-mesenchymal transition; MDR, multidrug resistance.

(Reiche et al., 2004). Additionally, endogenous glucocorticoids, deriving from the adrenal cortex, of which the concentration in the blood increases under chronic stress *via* the HPA axis, easily diffuse across the membrane of various cells in TME (Kadmiel and Cidlowski, 2013). One thing to point out here is that the enhanced β-adrenergic signaling and glucocorticoid signaling in TME can be induced by not only chronic stress, but also TME hypoxia (Chiarugi and Filippi, 2015).

α-AR signaling is partly responsible for TME alterations. There are two subtypes of α-ARs, including α1-AR and α2-AR, both of which belong to the GPCR family (Taylor and Cassagnol, 2021). The activation of α1-AR leads to the increase of intracellular calcium concentration *via* the PLC-IP3/DAG pathway, while the activation of α2-AR results in the inhibition of adenylyl cyclase, which decreases the concentration of cytoplasmic calcium and cAMP (Biazi et al., 2018; Durkee et al., 2019) (**Figure 2**).

β-ARs are expressed on the membranes of various tumor cells and tumor-related cells, such as immune cells, fibroblast, and epithelial cells, and epithelial cells, and two of the three subtypes of β-ARs, including β2-AR and β3-AR, take part in tumorous β-signaling (Daly and McGrath, 2011; Calvani et al., 2020). The binding of catecholamine, like epinephrine and norepinephrine, to β-ARs, contributes to the activation of guanylate cyclase, leading to transient cyclic adenosine monophosphate (cAMP) flux, which subsequently activates protein kinase A (PKA) and guanine nucleotide exchange protein activated by adenylyl cyclase (EPAC) (Cole and Sood, 2012). The two latter proteins activate a variety of intracellular pathways which switch on or off the transcriptions of genes, associating with inflammation, angiogenesis, tissue invasion, distant metastasis (Thaker et al., 2006; Cole and Sood, 2012; Duan et al., 2019) (**Figure 2**).

Glucocorticoids can be produced by the adrenal cortex and translocated to the tumor, or produced locally by TAMs (Acharya et al., 2020). Glucocorticoid receptors (GRs), located intracellularly, once activated by glucocorticoid, get involved in the formation of a complex and translocate to nuclei, which induce transcriptionally activation or suppression of gene expressions *via* direct interactions with DNA (Timmermans et al., 2019). For instance, TSC22D3 is upregulated in response to stress by glucocorticoid signaling, which blocks the response of DC to type I IFN and IFN-γ^+ T cell activation (Yang et al., 2019) (**Figure 2**).

CHRONIC STRESS INFLUENTS ANTI-CANCER THERAPY

It has been widely accepted that the TME profile plays a dominant role in determining the efficacies of anti-cancer therapies (Roma-Rodrigues et al., 2019). Not surprisingly, the TME alterations under chronic stress have negative impacts on the efficacies of cancer treatments, including chemotherapy, immunotherapy, and targeted therapy.

Chemotherapy

Chronic stress-induced endogenous glucocorticoids have unfavorable effects on the therapeutic response to chemotherapy. Dexamethasone increased the adhesion to ECM and the resistance to cisplatin and paclitaxel in two human ovarian cancer cells (Chen et al., 2010). The therapeutic of oxaliplatin (OXA)-based chemotherapy effect was largely compromised in social-defeat (SD)-conditioned mice (Yang et al., 2019). And a high expression of the glucocorticoid receptors (GR) was correlated with shorter metastasis-free survival in triple-negative breast cancer (TNBC) patients undergoing chemotherapy (Chen et al., 2015).

Endogenous catecholamines, such as norepinephrine and epinephrine, also interfere with chemotherapy. Catecholamines reduced p53 protein concentrations in cancer cells and increased the genetic instability of these cells, which significantly inhibited paclitaxel-induced and cisplatin-induced apoptosis in ovarian cancer cells (Hara et al., 2011; Kang et al., 2016). Yet, reduction of stress-related signaling potentiated the effect of chemotherapy in cancer patients has also been demonstrated (Mravec et al., 2020).

Immunotherapy

Chronic-stress induced reductions of CD8+ T cells and CTLs result in a cancer vaccine failure in a rodent melanoma model (Sommershof et al., 2017). Dysfunction of $CD8^+$ TILs induced by endogenous glucocorticoid signaling is associated with failure to respond to checkpoint blockade in both preclinical models and melanoma patients (Acharya et al., 2020). Increased infiltration of regulatory T-cells, decreased amount of CD8+ lymphocytes in tumor sites were observed in bladder-tumor-bearing mice treated with anti-PD-L1 under chronic stress. Therefore, chronic psychological stress could weaken the potency of anti-PD-L1 immunotherapy (Zhou et al., 2021).

A glucocorticoid-inducible molecule, TSC22D3 plays an important role in stress-induced immunosuppression as well as perturb responses to prophylactic tumor vaccination and PD-1-targeted immunotherapy (Yang et al., 2019). In addition, psychological stress down-regulated the expression of interleukin-2 (IL-2) receptor in peripheral blood leukocytes, affects the therapeutic efficacy of IL-2 immunotherapy in renal cell cancer patients (Zhang et al., 2020).

Molecule-Targeted Therapy

Since chronic stress increases VEGF secretion in TME, it can impair the efficacies of anti-angiogenic agents. By upregulating the VEGF expression *via* the β-AR-cAMP-PKA signaling pathway, chronic stress and exogenous norepinephrine markedly weakened the efficacy of sunitinib in rodent models of colorectal cancer and melanoma respectively (Deng et al., 2014; Liu et al., 2015).

Chronic stress-induced stress hormone norepinephrine (NE) promotes afatinib resistance by upregulating Cx32 expression which could decrease the degradation of EGFR-TKI resistance-associated proteins (MET, IGF-1R) and increase their transcription levels (Xie et al., 2019). β2-AR activation on non-small cell lung cancer (NSCLC) cell induces epidermal growth factor receptor (EGFR) tyrosine kinase inhibitor (TKI) resistance by inactivating liver kinase B1 (LKB1), elevating IL-6 expression, and MAPK pathway in a rodent model (Nilsson et al., 2017). Indeed, in treatment-naive patients with advanced lung adenocarcinoma receiving first-line EGFR-TKIs, prior b-blocker use was associated with a longer time-to-discontinuation (TTD) and overall survival (OS) (Chang et al., 2020).

ANTI-CANCER TREATMENTS AND INTERVENTIONS TARGETING CHRONIC STRESS

β-Blocker

β-blockers, such as propranolol and metoprolol, can block the interactions between catecholamine and β-AR, which inhibits the subsequent cancer-promoting effects induced by β-AR signaling as mentioned above (Fumagalli et al., 2020). Blocking β-AR interrupts the differentiation of exhausted T progenitors and

decreases the number of exhausted T cells in TME (Qiao et al., 2021). Propranolol reduced MDSC accumulation in the TME of thermal-stressed mice treatments and controlled tumor growth (MacDonald et al., 2021). Blocking β-AR also increases glycolysis and oxidative phosphorylation in tumor-infiltrating lymphocytes (TIL), which leads to increased CD28 expression and enhanced anti-tumor functions (Qiao et al., 2021). Propranolol can enhance the sensitivity of gastric cancer cells to radiation *in vitro* by inhibiting NF-κB-VEGF/EGFR/COX-2 pathway (Liao et al., 2010).

Combined administration of propranolol and etodolac, a cyclooxygenase-2 inhibitor, improved the survival rate of mice with melanoma or Lewis lung carcinoma (Glasner et al., 2010). A prospective pilot study showed that the combination of propranolol with chemotherapy improved the quality of life (QOL) of patients with epithelial ovarian cancer (Ramondetta et al., 2019).

The combination of propranolol with targeted therapy may improve the efficacy. An exploratory analysis of the LUX-Lung3 study revealed a significant PFS prolongation of NSCLC patients taking β-blockers with EGFR-TKI afatinib compared with those taking afatinib alone (median 11.1 vs. 6.9 months, $p = 0.0001$), indicating there is a synergic effect combining β-blockers with anti-EGFR therapy (Nilsson et al., 2017).

As the favorable efficacy of immunotherapy is based on the premise of an immune-supportive TME, β-blockers may be ideal companions for immunotherapy owing to their capacity of inhibiting β-AR-induced TME deterioration. The increased density of CTLs and decreased expression of PD-1 induced by propranolol enhanced the efficacy of anti-PD-1 agents in a rodent model. Propranolol strongly improved the efficacy of an anti-tumor STxBE7 vaccine by enhancing the frequency of CTLs in a rodent model (Daher et al., 2019). Propranolol increased the concentration of IL-12, IL-17, 1L-2, and IFN-γ in the breast tumor of mice and assisted with a tumor lysate vaccine (Ashrafi et al., 2017). A phase I study showed promising safety and activity of combining propranolol and pembrolizumab in the first-line treatment of metastatic melanoma (Gandhi et al., 2021). A meta-analysis revealed that β-blockers significantly improved DFS (HR 0.03, 95% CI 0.01–0.17) and OS (HR 0.04, 95% CI 0.00–0.38) in melanoma patients, but the beneficial effect is quite tumor-specific (Yap et al., 2018).

α-Blocker

α-blockers can also function as anti-cancer agents. Quinazoline α-1 blockers, such as prazosin, doxazosin, and terazosin, have shown promising anti-cancer effects in various types of cancer, and benefit chemotherapy, radiotherapy, and anti-EGFR therapy (Ashrafi et al., 2017). The VEGF-induced angiogenesis is inhibited by an α-blocker, doxazosin, in human umbilical vein endothelial cells (Keledjian et al., 2005). Another selective α1-blocker, naftopidil, presents with anti-proliferative and cytotoxic effects on prostate cancer as well as several other cancer types *in vitro*, *ex vivo*, and *in vivo* (Florent et al., 2020).

Stress-Reducing Interventions

Moreover, interventions targeting directly on physical or psychological stressors may ameliorate the TME and benefit anti-cancer treatments as well. The activation of the brain reward system decreased SNS activity and β-adrenergic signaling, which led to less immunosuppressive MDSCs in a murine model (Ben-Shaanan et al., 2018). Thermal treatments, including weekly whole-body hyperthermia and housing mice at their thermoneutral or sub-thermoneutral temperature, also decreased MDSC accumulation and tumor growth of mice (MacDonald et al., 2021). A similar enhancement of immune checkpoint inhibitor efficacy was observed in a rodent model with physiologically reduced stress (Bucsek et al., 2017). Mice housed in an enriched environment displayed enhanced NK-cell activity and increased infiltration of NK cells into TME (Song et al., 2017). Stress-reducing approaches, such as yoga, mindfulness, and cognitive behavioral therapy, have shown broad clinical benefits of increasing proportions of anti-tumor immune cells and cytokines in several studies, yet the results of these studies were limited with small sample sizes and short follow-ups (Antoni and Dhabhar, 2019).

Others

Additionally, a variety of other drugs may also reverse the unfavorable TME alterations in terms of chronic stress. Zoledronic acid, an anti-cancer adjuvant drug, is proficient in abrogating stress-induced macrophage infiltration, and PDGF-AA expression in a rodent ovarian cancer model (Colon-Echevarria et al., 2020). Antidepressants, such as fluoxetine and sertraline, can also alleviate chronic stress and have the potential in associating with cancer treatments, which still need further clinical confirmation (Di Rosso et al., 2018).

Some other strategies targeting chronic stress-inducible inflammatory signaling have shown promising efficacies in clinical practice. Bevacizumab, an anti-VEGF agent, is now applicable for a wide range of solid tumors and has shown favorable efficacies combined with chemotherapy, immune checkpoint inhibitors, anti-EGFR therapy, and PARP inhibitors (Garcia et al., 2020). Anti-IL-6 or Anti-IL-6 receptor agents, such as tocilizumab and siltuximab, have not shown satisfactory efficacies in cancers (Rossi et al., 2015), yet tocilizumab has been widely used to treat cytokine release syndrome induced by CAR T-cell toxicity (Brudno and Kochenderfer, 2019).

DISCUSSION

In summary, the TME under chronic stress is differentiated from others by increased numbers and enhanced functions of immunosuppressive cells, decreased amounts and impaired functions of immunosupportive cells, associated with corresponding changes in cytokines, which results in intense angiogenesis, boosted tumor cell proliferation and enhanced EMT inside of the TME. The over-secretion of glucocorticoid and catecholamines deriving from persistent activations of the

HPA axis and SNS mostly contribute to the TME alterations under chronic stress. These alterations can reduce the efficacies of anti-tumor therapies, like chemotherapy, immunotherapy, and targeted therapy. Drugs, such as α-blockers, β-blockers, antidepressants, and interventions, like meditation and mindfulness, may cut down the negative effects of chronic stress, which should draw the attention of clinical oncologists in adopting treatment plans for patients with chronic stress.

Still, recent studies for the interactions of chronic stress and TME have limitations, such as absences of evaluation of animal stress levels within the group and assessments for stress levels before investigations in animal models (Hylander et al., 2019). Therefore, researchers should value the importance of stress quantification in research, and approaches, such as detections of serum glucocorticoids and catecholamines before further procedures, should be taken to control potential bias.

AUTHOR CONTRIBUTIONS

WT searched for the literature and wrote the original draft; YL helped write a part of the manuscript; CC processed the images; YZ, YPA, XL, and YPE revised the whole manuscript; FW contributed to the conception of the review, and supervised the whole process of this work.

FUNDING

This work was supported by: 1) Natural Science Foundation of Hunan Province for Excellent Young Scholars (Grant No. 2021JJ20088); 2) Beijing Xisike Clinical Oncology Research Foundation (Grant No. Y-HS202102-0130); 3) Guangdong Association of Clinical Trials (GACT) /Chinese Thoracic Oncology Group (CTONG); 4) Guangdong Provincial Key Lab of Translational Medicine in Lung Cancer (Grant No. 2017B030314120); 5) Changsha Science and Technology Bureau (Grant No. kq1907077).

ACKNOWLEDGMENTS

The authors would like to thank the multi-disciplinary team (MDT) for thoracic tumors of the Second Xiangya Hospital of Central South University for the inspiration and guidance of this paper.

REFERENCES

Acharya, N., Madi, A., Zhang, H., Klapholz, M., Escobar, G., Dulberg, S., et al. (2020). Endogenous Glucocorticoid Signaling Regulates CD8+ T Cell Differentiation and Development of Dysfunction in the Tumor Microenvironment. *Immunity.* 53 (3), 658–671. e656. doi:10.1016/j.immuni.2020.08.005

Aggarwal, S., Gabrovsek, L., Langeberg, L. K., Golkowski, M., Ong, S.-E., Smith, F. D., et al. (2019). Depletion of dAKAP1-Protein Kinase A Signaling Islands From the Outer Mitochondrial Membrane Alters Breast Cancer Cell Metabolism and Motility. *J. Biol. Chem.* 294 (9), 3152–3168. doi:10.1074/jbc.RA118.006741

Antoni, M. H., and Dhabhar, F. S. (2019). The Impact of Psychosocial Stress and Stress Management on Immune Responses in Patients With Cancer. *Cancer.* 125 (9), 1417–1431. doi:10.1002/cncr.31943

Ashrafi, S., Shapouri, R., and Mahdavi, M. (2017). Immunological Consequences of Immunization With Tumor Lysate Vaccine and Propranolol as an Adjuvant: A Study on Cytokine Profiles in Breast Tumor Microenvironment. *Immunol. Lett.* 181, 63–70. doi:10.1016/j.imlet.2016.11.014

Baghban, R., Roshangar, L., Jahanban-Esfahlan, R., Seidi, K., Ebrahimi-Kalan, A., Jaymand, M., et al. (2020). Tumor Microenvironment Complexity and Therapeutic Implications at a Glance. *Cell Commun Signal.* 18 (1), 59. doi:10.1186/s12964-020-0530-4

Ben-Eliyahu, S., Page, G. G., Yirmiya, R., and Shakhar, G. (1999). Evidence that Stress and Surgical Interventions Promote Tumor Development by Suppressing Natural Killer Cell Activity. *Int. J. Cancer.* 80 (6), 880–888. doi:10.1002/(sici)1097-0215(19990315)80:6<880:aid-ijc14>3.0.co;2-y

Ben-Shaanan, T. L., Schiller, M., Azulay-Debby, H., Korin, B., Boshnak, N., Koren, T., et al. (2018). Modulation of Anti-Tumor Immunity by the Brain's Reward System. *Nat. Commun.* 9 (1), 2723. doi:10.1038/s41467-018-05283-5

Biazi, G. R., Frasson, I. G., Miksza, D. R., de Morais, H., de Fatima Silva, F., Bertolini, G. L., et al. (2018). Decreased Hepatic Response to Glucagon, Adrenergic Agonists, and CAMP in Glycogenolysis, Gluconeogenesis, and Glycolysis in Tumor-Bearing Rats. *J. Cell Biochem.* 119 (9), 7300–7309. doi:10.1002/jcb.27027

Brudno, J. N., and Kochenderfer, J. N. (2019). Recent Advances in CAR T-Cell Toxicity: Mechanisms, Manifestations and Management. *Blood Rev.* 34, 45–55. doi:10.1016/j.blre.2018.11.002

Bruzzone, A., Perez Pinero, C., Rojas, P., Romanato, M., Gass, H., Lanari, C., et al. (2011). α2-Adrenoceptors Enhance Cell Proliferation and Mammary Tumor Growth Acting Through Both the Stroma and the Tumor Cells. *Curr. Cancer Drug. Targets.* 11 (6), 763–774. doi:10.2174/156800911796191051

Bucsek, M. J., Qiao, G., MacDonald, C. R., Giridharan, T., Evans, L., Niedzwecki, B., et al. (2017). β-Adrenergic Signaling in Mice Housed at Standard Temperatures Suppresses an Effector Phenotype in CD8+ T Cells and Undermines Checkpoint Inhibitor Therapy. *Cancer Res.* 77 (20), 5639–5651. doi:10.1158/0008-5472.CAN-17-0546

Calvani, M., Dabraio, A., Subbiani, A., Buonvicino, D., De Gregorio, V., Ciullini Mannurita, S., et al. (2020). β3-Adrenoceptors as Putative Regulator of Immune Tolerance in Cancer and Pregnancy. *Front. Immunol.* 11, 2098. doi:10.3389/fimmu.2020.02098

Chang, C.-H., Lee, C.-H., Ko, J.-C., Chang, L.-Y., Lee, M.-C., Zhang, J.-F., et al. (2020). Effect of β-Blocker in Treatment-Naïve Patients With Advanced Lung Adenocarcinoma Receiving First-Generation EGFR-TKIs. *Front. Oncol.* 10, 583529. doi:10.3389/fonc.2020.583529

Chen, X., and Song, E. (2019). Turning Foes to Friends: Targeting Cancer-Associated Fibroblasts. *Nat. Rev. Drug Discov.* 18 (2), 99–115. doi:10.1038/s41573-018-0004-1

Chen, Y.-X., Wang, Y., Fu, C.-C., Diao, F., Song, L.-N., Li, Z.-B., et al. (2010). Dexamethasone Enhances Cell Resistance to Chemotherapy by Increasing Adhesion to Extracellular Matrix in Human Ovarian Cancer Cells. *Endocr. Relat. Cancer.* 17 (1), 39–50. doi:10.1677/ERC-08-0296

Chen, Z., Lan, X., Wu, D., Sunkel, B., Ye, Z., Huang, J., et al. (2015). Ligand-Dependent Genomic Function of Glucocorticoid Receptor in Triple-Negative Breast Cancer. *Nat. Commun.* 6, 8323. doi:10.1038/ncomms9323

Cheng, Y., Tang, X.-Y., Li, Y.-X., Zhao, D.-D., Cao, Q.-H., Wu, H.-X., et al. (2019). Depression-Induced Neuropeptide Y Secretion Promotes Prostate Cancer Growth by Recruiting Myeloid Cells. *Clin. Cancer Res.* 25 (8), 2621–2632. doi:10.1158/1078-0432.CCR-18-2912

Chiarugi, P., and Filippi, L. (2015). β3-Adrenoreceptor and Tumor Microenvironment: a New Hub. *Oncoimmunology.* 4 (11), e1026532. doi:10.1080/2162402X.2015.1026532

Chida, Y., Hamer, M., Wardle, J., and Steptoe, A. (2008). Do Stress-Related Psychosocial Factors Contribute to Cancer Incidence and Survival? *Nat. Rev. Clin. Oncol.* 5 (8), 466–475. doi:10.1038/ncponc1134

Cole, S. W., and Sood, A. K. (2012). Molecular Pathways: Beta-Adrenergic Signaling in Cancer: Figure 1. *Clin. Cancer Res.* 18 (5), 1201–1206. doi:10.1158/1078-0432.CCR-11-0641

Colon-Echevarria, C. B., Ortiz, T., Maldonado, L., Hidalgo-Vargas, M. J., Pérez-Morales, J., Aquino-Acevedo, A. N., et al. (2020). Zoledronic Acid Abrogates Restraint Stress-Induced Macrophage Infiltration, PDGF-AA Expression, and Ovarian Cancer Growth. *Cancers.* 12 (9), 2671. doi:10.3390/cancers12092671

Cui, B., Luo, Y., Tian, P., Peng, F., Lu, J., Yang, Y., et al. (2019). Stress-Induced Epinephrine Enhances Lactate Dehydrogenase A and Promotes Breast Cancer Stem-Like Cells. *J. Clin. Invest.* 129 (3), 1030–1046. doi:10.1172/JCI121685

Daher, C., Vimeux, L., Stoeva, R., Peranzoni, E., Bismuth, G., Wieduwild, E., et al. (2019). Blockade of β-Adrenergic Receptors Improves CD8+ T-Cell Priming and Cancer Vaccine Efficacy. *Cancer Immunol. Res.* 7 (11), 1849–1863. doi:10.1158/2326-6066.CIR-18-0833

Daly, C. J., and McGrath, J. C. (2011). Previously Unsuspected Widespread Cellular and Tissue Distribution of β-Adrenoceptors and its Relevance to Drug Action. *Trends Pharmacol. Sci.* 32 (4), 219–226. doi:10.1016/j.tips.2011.02.008

DeNardo, D. G., and Ruffell, B. (2019). Macrophages as Regulators of Tumour Immunity and Immunotherapy. *Nat. Rev. Immunol.* 19 (6), 369–382. doi:10.1038/s41577-019-0127-6

Deng, G.-H., Liu, J., Zhang, J., Wang, Y., Peng, X.-C., Wei, Y.-Q., et al. (2014). Exogenous Norepinephrine Attenuates the Efficacy of Sunitinib in a Mouse Cancer Model. *J. Exp. Clin. Cancer Res.* 33, 21. doi:10.1186/1756-9966-33-21

Di Rosso, M. E., Sterle, H. A., Cremaschi, G. A., and Genaro, A. M. (2018). Beneficial Effect of Fluoxetine and Sertraline on Chronic Stress-Induced Tumor Growth and Cell Dissemination in a Mouse Model of Lymphoma: Crucial Role of Antitumor Immunity. *Front. Immunol.* 9, 1341. doi:10.3389/fimmu.2018.01341

Du, P., Zeng, H., Xiao, Y., Zhao, Y., Zheng, B., Deng, Y., et al. (2020). Chronic Stress Promotes EMT-Mediated Metastasis Through Activation of STAT3 Signaling Pathway by miR-337-3p in Breast Cancer. *Cell Death Dis.* 11 (9), 761. doi:10.1038/s41419-020-02981-1

Duan, M., Goswami, S., Shi, J.-Y., Wu, L.-J., Wang, X.-Y., Ma, J.-Q., et al. (2019). Activated and Exhausted MAIT Cells Foster Disease Progression and Indicate Poor Outcome in Hepatocellular Carcinoma. *Clin. Cancer Res.* 25 (11), 3304–3316. doi:10.1158/1078-0432.ccr-18-3040

Durkee, C. A., Covelo, A., Lines, J., Kofuji, P., Aguilar, J., and Araque, A. (2019). G I/o Protein-Coupled Receptors Inhibit Neurons but Activate Astrocytes and Stimulate Gliotransmission. *Glia.* 67 (6), 1076–1093. doi:10.1002/glia.23589

Fan, K.-q., Li, Y.-y., Wang, H.-l., Mao, X.-t., Guo, J.-x., Wang, F., et al. (2019). Stress-Induced Metabolic Disorder in Peripheral CD4+ T Cells Leads to Anxiety-Like Behavior. *Cell.* 179 (4), 864–879. doi:10.1016/j.cell.2019.10.001

Florent, R., Poulain, L., and N'Diaye, M. (2020). Drug Repositioning of the α1-Adrenergic Receptor Antagonist Naftopidil: A Potential New Anti-Cancer Drug? *Int. J. Mol. Sci.* 21 (15), 5339. doi:10.3390/ijms21155339

Fumagalli, C., Maurizi, N., Marchionni, N., and Fornasari, D. (2020). β-Blockers: Their New Life From Hypertension to Cancer and Migraine. *Pharmacol. Res.* 151, 104587. doi:10.1016/j.phrs.2019.104587

Gabrilovich, D. I. (2017). Myeloid-Derived Suppressor Cells. *Cancer Immunol. Res.* 5 (1), 3–8. doi:10.1158/2326-6066.CIR-16-0297

Gandhi, S., Pandey, M. R., Attwood, K., Ji, W., Witkiewicz, A. K., Knudsen, E. S., et al. (2021). Phase I Clinical Trial of Combination Propranolol and Pembrolizumab in Locally Advanced and Metastatic Melanoma: Safety, Tolerability, and Preliminary Evidence of Antitumor Activity. *Clin. Cancer Res.* 27 (1), 87–95. doi:10.1158/1078-0432.CCR-20-2381

Gao, X., Cao, Q., Cheng, Y., Zhao, D., Wang, Z., Yang, H., et al. (2018). Chronic Stress Promotes Colitis by Disturbing the Gut Microbiota and Triggering Immune System Response. *Proc. Natl. Acad. Sci. USA.* 115 (13), E2960–E2969. doi:10.1073/pnas.1720696115

Garcia, J., Hurwitz, H. I., Sandler, A. B., Miles, D., Coleman, R. L., Deurloo, R., et al. (2020). Bevacizumab (Avastin) in Cancer Treatment: A Review of 15 Years of Clinical Experience and Future Outlook. *Cancer Treat. Rev.* 86, 102017. doi:10.1016/j.ctrv.2020.102017

Gardner, A., and Ruffell, B. (2016). Dendritic Cells and Cancer Immunity. *Trends Immunol.* 37 (12), 855–865. doi:10.1016/j.it.2016.09.006

Gil, F., Costa, G., Hilker, I., and Benito, L. (2012). First Anxiety, Afterwards Depression: Psychological Distress in Cancer Patients at Diagnosis and After Medical Treatment. *Stress and Health.* 28 (5), 362–367. doi:10.1002/smi.2445

Glasner, A., Avraham, R., Rosenne, E., Benish, M., Zmora, O., Shemer, S., et al. (2010). Improving Survival Rates in Two Models of Spontaneous Postoperative Metastasis in Mice by Combined Administration of a β-Adrenergic Antagonist and a Cyclooxygenase-2 Inhibitor. *J.I.* 184 (5), 2449–2457. doi:10.4049/jimmunol.0903301

Guereschi, M. G., Araujo, L. P., Maricato, J. T., Takenaka, M. C., Nascimento, V. M., Vivanco, B. C., et al. (2013). Beta2-Adrenergic Receptor Signaling in CD4+Foxp3+Regulatory T Cells Enhances Their Suppressive Function in a PKA-Dependent Manner. *Eur. J. Immunol.* 43 (4), 1001–1012. doi:10.1002/eji.201243005

Hara, M. R., Kovacs, J. J., Whalen, E. J., Rajagopal, S., Strachan, R. T., Grant, W., et al. (2011). A Stress Response Pathway Regulates DNA Damage through β2-Adrenoreceptors and β-Arrestin-1. *Nature.* 477 (7364), 349–353. doi:10.1038/nature10368

Hulsurkar, M., Li, Z., Zhang, Y., Li, X., Zheng, D., and Li, W. (2017). Beta-Adrenergic Signaling Promotes Tumor Angiogenesis and Prostate Cancer Progression through HDAC2-Mediated Suppression of Thrombospondin-1. *Oncogene.* 36 (11), 1525–1536. doi:10.1038/onc.2016.319

Hylander, B. L., Gordon, C. J., and Repasky, E. A. (2019). Manipulation of Ambient Housing Temperature To Study the Impact of Chronic Stress on Immunity and Cancer in Mice. *J.I.* 202 (3), 631–636. doi:10.4049/jimmunol.1800621

Kadmiel, M., and Cidlowski, J. A. (2013). Glucocorticoid Receptor Signaling in Health and Disease. *Trends Pharmacol. Sci.* 34 (9), 518–530. doi:10.1016/j.tips.2013.07.003

Kang, Y., Nagaraja, A. S., Armaiz-Pena, G. N., Dorniak, P. L., Hu, W., Rupaimoole, R., et al. (2016). Adrenergic Stimulation of DUSP1 Impairs Chemotherapy Response in Ovarian Cancer. *Clin. Cancer Res.* 22 (7), 1713–1724. doi:10.1158/1078-0432.Ccr-15-1275

Keledjian, K., Garrison, J. B., and Kyprianou, N. (2005). Doxazosin Inhibits Human Vascular Endothelial Cell Adhesion, Migration, and Invasion. *J. Cell. Biochem.* 94 (2), 374–388. doi:10.1002/jcb.20240

Kerbel, R. S. (2008). Tumor Angiogenesis. *N. Engl. J. Med.* 358 (19), 2039–2049. doi:10.1056/NEJMra0706596

Lamouille, S., Xu, J., and Derynck, R. (2014). Molecular Mechanisms of Epithelial-Mesenchymal Transition. *Nat. Rev. Mol. Cell Biol.* 15 (3), 178–196. doi:10.1038/nrm3758

Li, N., Du, Z.-X., Zong, Z.-H., Liu, B.-Q., Li, C., Zhang, Q., et al. (2013). Pkcδ-Mediated Phosphorylation of BAG3 at Ser187 Site Induces Epithelial–Mesenchymal Transition and Enhances Invasiveness in Thyroid Cancer FRO Cells. *Oncogene.* 32 (38), 4539–4548. doi:10.1038/onc.2012.466

Liao, X., Che, X., Zhao, W., Zhang, D., Long, H., Chaudhary, P., et al. (2010). Effects of Propranolol in Combination with Radiation on Apoptosis and Survival of Gastric Cancer Cells *In Vitro*. *Radiat. Oncol.* 5, 98. doi:10.1186/1748-717X-5-98

Liu, J., Deng, G.-H., Zhang, J., Wang, Y., Xia, X.-Y., Luo, X.-M., et al. (2015). The Effect of Chronic Stress on Anti-angiogenesis of Sunitinib in Colorectal Cancer Models. *Psychoneuroendocrinology.* 52, 130–142. doi:10.1016/j.psyneuen.2014.11.008

Liu, L., Lei, B., Wang, L., Chang, C., Yang, H., Liu, J., et al. (2019). Protein Kinase C-Iota-Mediated Glycolysis Promotes Non-Small-Cell Lung Cancer Progression. *Onco Targets Ther.* 12, 5835–5848. doi:10.2147/OTT.S207211

Lutgendorf, S. K., Lamkin, D. M., Jennings, N. B., Arevalo, J. M. G., Penedo, F., DeGeest, K., et al. (2008). Biobehavioral Influences on Matrix Metalloproteinase Expression in Ovarian Carcinoma. *Clin. Cancer Res.* 14 (21), 6839–6846. doi:10.1158/1078-0432.CCR-08-0230

Lutgendorf, S. K., Sood, A. K., Anderson, B., McGinn, S., Maiseri, H., Dao, M., et al. (2005). Social Support, Psychological Distress, and Natural Killer Cell Activity in Ovarian Cancer. *J. Clin. Oncol.* 23 (28), 7105–7113. doi:10.1200/JCO.2005.10.015

Ma, X., Wang, M., Yin, T., Zhao, Y., and Wei, X. (2019). Myeloid-Derived Suppressor Cells Promote Metastasis in Breast Cancer After the Stress of Operative Removal of the Primary Cancer. *Front. Oncol.* 9, 855. doi:10.3389/fonc.2019.00855

MacDonald, C., Ministero, S., Pandey, M., Robinson, D., Forti Hong, E., Hylander, B., et al. (2021). Comparing thermal Stress Reduction Strategies that Influence MDSC Accumulation in Tumor Bearing Mice. *Cell Immunol.* 361, 104285. doi:10.1016/j.cellimm.2021.104285

Matyszak, M. K., Citterio, S., Rescigno, M., and Ricciardi-Castagnoli, P. (2000). Differential Effects of Corticosteroids During Different Stages of Dendritic Cell

Maturation. *Eur. J. Immunol.* 30 (4), 1233–1242. doi:10.1002/(sici)1521-4141(200004)30:4<1233:aid-immu1233>3.0.co;2-f

Mravec, B., Tibensky, M., and Horvathova, L. (2020). Stress and Cancer. Part II: Therapeutic Implications for Oncology. *J. Neuroimmunology.* 346, 577312. doi:10.1016/j.jneuroim.2020.577312

Muthuswamy, R., Okada, N. J., Jenkins, F. J., McGuire, K., McAuliffe, P. F., Zeh, H. J., et al. (2017). Epinephrine Promotes COX-2-Dependent Immune Suppression in Myeloid Cells and Cancer Tissues. *Brain Behav. Immun.* 62, 78–86. doi:10.1016/j.bbi.2017.02.008

Nadella, K. S., Jones, G. N., Trimboli, A., Stratakis, C. A., Leone, G., and Kirschner, L. S. (2008). Targeted Deletion of Prkar1a Reveals a Role for Protein Kinase A in Mesenchymal-To-Epithelial Transition. *Cancer Res.* 68 (8), 2671–2677. doi:10.1158/0008-5472.CAN-07-6002

Najafi, M., Farhood, B., and Mortezaee, K. (2019). Extracellular Matrix (ECM) Stiffness and Degradation as Cancer Drivers. *J. Cell Biochem.* 120 (3), 2782–2790. doi:10.1002/jcb.27681

Neri, D., and Supuran, C. T. (2011). Interfering With pH Regulation in Tumours as a Therapeutic Strategy. *Nat. Rev. Drug Discov.* 10 (10), 767–777. doi:10.1038/nrd3554

Nilsson, M. B., Sun, H., Diao, L., Tong, P., Liu, D., Li, L., et al. (2017). Stress Hormones Promote EGFR Inhibitor Resistance in NSCLC: Implications for Combinations With β-blockers. *Sci. Transl. Med.* 9 (415), eaao4307. doi:10.1126/scitranslmed.aao4307

Pattabiraman, D. R., Bierie, B., Kober, K. I., Thiru, P., Krall, J. A., Zill, C., et al. (2016). Activation of PKA Leads to Mesenchymal-To-Epithelial Transition and Loss of Tumor-Initiating Ability. *Science.* 351 (6277), aad3680. doi:10.1126/science.aad3680

Pearce, E. L., Poffenberger, M. C., Chang, C.-H., and Jones, R. G. (2013). Fueling Immunity: Insights into Metabolism and Lymphocyte Function. *Science.* 342 (6155), 1242454. doi:10.1126/science.1242454

Picard, M., and McEwen, B. S. (2018). Psychological Stress and Mitochondria: A Systematic Review. *Psychosom Med.* 80 (2), 141–153. doi:10.1097/PSY.0000000000000545

Powell, N. D., Tarr, A. J., and Sheridan, J. F. (2013). Psychosocial Stress and Inflammation in Cancer. *Brain Behav. Immun.* 30 (Suppl. l), S41–S47. doi:10.1016/j.bbi.2012.06.015

Qiao, G., Chen, M., Mohammadpour, H., MacDonald, C. R., Bucsek, M. J., Hylander, B. L., et al. (2021). Chronic Adrenergic Stress Contributes to Metabolic Dysfunction and an Exhausted Phenotype in T Cells in the Tumor Microenvironment. *Cancer Immunol. Res.* 9, 651–664. doi:10.1158/2326-6066.CIR-20-0445

Qin, J.-f., Jin, F.-j., Li, N., Guan, H.-t., Lan, L., Ni, H., et al. (2015). Adrenergic Receptor β2 Activation by Stress Promotes Breast Cancer Progression Through Macrophages M2 Polarization in Tumor Microenvironment. *BMB Rep.* 48 (5), 295–300. doi:10.5483/bmbrep.2015.48.5.008

Ramondetta, L. M., Hu, W., Thaker, P. H., Urbauer, D. L., Chisholm, G. B., Westin, S. N., et al. (2019). Prospective Pilot Trial With Combination of Propranolol With Chemotherapy in Patients With Epithelial Ovarian Cancer and Evaluation on Circulating Immune Cell Gene Expression. *Gynecol. Oncol.* 154 (3), 524–530. doi:10.1016/j.ygyno.2019.07.004

Reiche, E. M. V., Nunes, S. O. V., and Morimoto, H. K. (2004). Stress, Depression, the Immune System, and Cancer. *Lancet Oncol.* 5 (10), 617–625. doi:10.1016/s1470-2045(04)01597-9

Rey, S., Schito, L., Wouters, B. G., Eliasof, S., and Kerbel, R. S. (2017). Targeting Hypoxia-Inducible Factors for Antiangiogenic Cancer Therapy. *Trends Cancer.* 3 (7), 529–541. doi:10.1016/j.trecan.2017.05.002

Roma-Rodrigues, C., Mendes, R., Baptista, P., and Fernandes, A. (2019). Targeting Tumor Microenvironment for Cancer Therapy. *Int. J. Mol Sci.* 20 (4), 840. doi:10.3390/ijms20040840

Rossi, J.-F., Lu, Z.-Y., Jourdan, M., and Klein, B. (2015). Interleukin-6 as a Therapeutic Target. *Clin. Cancer Res.* 21 (6), 1248–1257. doi:10.1158/1078-0432.CCR-14-2291

Saul, A. N., Oberyszyn, T. M., Daugherty, C., Kusewitt, D., Jones, S., Jewell, S., et al. (2005). Chronic Stress and Susceptibility to Skin Cancer. *J. Natl. Cancer Inst.* 97 (23), 1760–1767. doi:10.1093/jnci/dji401

Schmidt, D., Peterlik, D., Reber, S. O., Lechner, A., and Männel, D. N. (2016). Induction of Suppressor Cells and Increased Tumor Growth Following Chronic Psychosocial Stress in Male Mice. *PLoS One.* 11 (7), e0159059. doi:10.1371/journal.pone.0159059

Shaikh, D., Zhou, Q., Chen, T., Ibe, J. C. F., Raj, J. U., and Zhou, G. (2012). CAMP-Dependent Protein Kinase Is Essential for Hypoxia-Mediated Epithelial-Mesenchymal Transition, Migration, and Invasion in Lung Cancer Cells. *Cell Signal.* 24 (12), 2396–2406. doi:10.1016/j.cellsig.2012.08.007

Shan, T., Cui, X., Li, W., Lin, W., Li, Y., Chen, X., et al. (2014). Novel Regulatory Program for Norepinephrine-Induced Epithelial-Mesenchymal Transition in Gastric Adenocarcinoma Cell Lines. *Cancer Sci.* 105 (7), 847–856. doi:10.1111/cas.12438

Silverman, M. N., and Sternberg, E. M. (2012). Glucocorticoid Regulation of Inflammation and its Functional Correlates: from HPA axis to Glucocorticoid Receptor Dysfunction. *Ann. N. Y Acad. Sci.* 1261, 55–63. doi:10.1111/j.1749-6632.2012.06633.x

Sloan, E. K., Capitanio, J. P., Tarara, R. P., Mendoza, S. P., Mason, W. A., and Cole, S. W. (2007). Social Stress Enhances Sympathetic Innervation of Primate Lymph Nodes: Mechanisms and Implications for Viral Pathogenesis. *J. Neurosci.* 27 (33), 8857–8865. doi:10.1523/JNEUROSCI.1247-07.2007

Sommershof, A., Scheuermann, L., Koerner, J., and Groettrup, M. (2017). Chronic Stress Suppresses Anti-tumor TCD8+ Responses and Tumor Regression Following Cancer Immunotherapy in a Mouse Model of Melanoma. *Brain Behav. Immun.* 65, 140–149. doi:10.1016/j.bbi.2017.04.021

Song, Y., Gan, Y., Wang, Q., Meng, Z., Li, G., Shen, Y., et al. (2017). Enriching the Housing Environment for Mice Enhances Their NK Cell Antitumor Immunity via Sympathetic Nerve-Dependent Regulation of NKG2D and CCR5. *Cancer Res.* 77 (7), 1611–1622. doi:10.1158/0008-5472.CAN-16-2143

Talts, J. F., Weller, A., Timpl, R., Ekblom, M., and Ekblom, P. (1995). Regulation of Mesenchymal Extracellular Matrix Protein Synthesis by Transforming Growth Factor-Beta and Glucocorticoids in Tumor Stroma. *J. Cell Sci.* 108 (Pt 6) (Pt 6), 2153–2162. doi:10.1242/jcs.108.6.2153

Tam, W. L., Lu, H., Buikhuisen, J., Soh, B. S., Lim, E., Reinhardt, F., et al. (2013). Protein Kinase C α Is a Central Signaling Node and Therapeutic Target for Breast Cancer Stem Cells. *Cancer Cell.* 24 (3), 347–364. doi:10.1016/j.ccr.2013.08.005

Taylor, B. N., and Cassagnol, M. (2021). *"Alpha Adrenergic Receptors," in StatPearls.* (Treasure Island (FL): StatPearls Publishing Copyright © 2021, StatPearls Publishing LLC).

Thaker, P. H., Han, L. Y., Kamat, A. A., Arevalo, J. M., Takahashi, R., Lu, C., et al. (2006). Chronic Stress Promotes Tumor Growth and Angiogenesis in a Mouse Model of Ovarian Carcinoma. *Nat. Med.* 12 (8), 939–944. doi:10.1038/nm1447

Thommen, D. S., and Schumacher, T. N. (2018). T Cell Dysfunction in Cancer. *Cancer Cell.* 33 (4), 547–562. doi:10.1016/j.ccell.2018.03.012

Timmermans, S., Souffriau, J., and Libert, C. (2019). A General Introduction to Glucocorticoid Biology. *Front. Immunol.* 10, 1545. doi:10.3389/fimmu.2019.01545

Varker, K. A., Terrell, C. E., Welt, M., Suleiman, S., Thornton, L., Andersen, B. L., et al. (2007). Impaired Natural Killer Cell Lysis in Breast Cancer Patients With High Levels of Psychological Stress Is Associated with Altered Expression of Killer Immunoglobin-like Receptors. *J. Surg. Res.* 139 (1), 36–44. doi:10.1016/j.jss.2006.08.037

Vergara, D., Ravaioli, S., Fonzi, E., Adamo, L., Damato, M., Bravaccini, S., et al. (2020). Carbonic Anhydrase XII Expression Is Modulated During Epithelial Mesenchymal Transition and Regulated Through Protein Kinase C Signaling. *Int. J. Mol Sci.* 21 (3), 715. doi:10.3390/ijms21030715

Vergara, D., Simeone, P., Damato, M., Maffia, M., Lanuti, P., and Trerotola, M. (2019). The Cancer Microbiota: EMT and Inflammation as Shared Molecular Mechanisms Associated With Plasticity and Progression. *J. Oncol.* 2019, 1–16. doi:10.1155/2019/1253727

Wu, X., Liu, B.-J., Ji, S., Wu, J.-F., Xu, C.-Q., Du, Y.-J., et al. (2015). Social Defeat Stress Promotes Tumor Growth and Angiogenesis by Upregulating Vascular Endothelial Growth Factor/Extracellular Signal-Regulated Kinase/Matrix Metalloproteinase Signaling in a Mouse Model of Lung Carcinoma. *Mol. Med. Rep.* 12 (1), 1405–1412. doi:10.3892/mmr.2015.3559

Xie, H., Li, C., He, Y., Griffin, R., Ye, Q., and Li, L. (2015). Chronic Stress Promotes Oral Cancer Growth and Angiogenesis with Increased Circulating

Catecholamine and Glucocorticoid Levels in a Mouse Model. *Oral Oncol.* 51 (11), 991–997. doi:10.1016/j.oraloncology.2015.08.007

Xie, J., Wang, X., Ge, H., Peng, F., Zheng, N., Wang, Q., et al. (2019). Cx32 Mediates Norepinephrine-Promoted EGFR-TKI Resistance in a Gap Junction-Independent Manner in Non-Small-Cell Lung Cancer. *J. Cell Physiol.* 234 (12), 23146–23159. doi:10.1002/jcp.28881

Yang, E. V., Kim, S.-j., Donovan, E. L., Chen, M., Gross, A. C., Webster Marketon, J. I., et al. (2009). Norepinephrine Upregulates VEGF, IL-8, and IL-6 Expression in Human Melanoma Tumor Cell Lines: Implications for Stress-Related Enhancement of Tumor Progression. *Brain Behav. Immun.* 23 (2), 267–275. doi:10.1016/j.bbi.2008.10.005

Yang, E. V., Sood, A. K., Chen, M., Li, Y., Eubank, T. D., Marsh, C. B., et al. (2006a). Norepinephrine Up-Regulates the Expression of Vascular Endothelial Growth Factor, Matrix Metalloproteinase (MMP)-2, and MMP-9 in Nasopharyngeal Carcinoma Tumor Cells. *Cancer Res.* 66 (21), 10357–10364. doi:10.1158/0008-5472.CAN-06-2496

Yang, Y., Pan, X., Lei, W., Wang, J., Shi, J., Li, F., et al. (2006b). Regulation of Transforming Growth Factor-β1-Induced Apoptosis and Epithelial-To-Mesenchymal Transition by Protein Kinase A and Signal Transducers and Activators of Transcription 3. *Cancer Res.* 66 (17), 8617–8624. doi:10.1158/0008-5472.CAN-06-1308

Yang, H., Xia, L., Chen, J., Zhang, S., Martin, V., Li, Q., et al. (2019). Stress-Glucocorticoid-TSC22D3 Axis Compromises Therapy-Induced Antitumor Immunity. *Nat. Med.* 25 (9), 1428–1441. doi:10.1038/s41591-019-0566-4

Yap, A., Lopez-Olivo, M. A., Dubowitz, J., Pratt, G., Hiller, J., Gottumukkala, V., et al. (2018). Effect of Beta-Blockers on Cancer Recurrence and Survival: a Meta-Analysis of Epidemiological and Perioperative Studies. *Br. J. Anaesth.* 121 (1), 45–57. doi:10.1016/j.bja.2018.03.024

Zafar, A., Hardy, K., Wu, F., Li, J., and Rao, S. (2015). The Role of Protein Kinase-C Theta in Control of Epithelial to Mesenchymal Transition and Cancer Stem Cell Formation. *Genomics Data.* 3, 28–32. doi:10.1016/j.gdata.2014.11.002

Zafar, A., Wu, F., Hardy, K., Li, J., Tu, W. J., McCuaig, R., et al. (2014). Chromatinized Protein Kinase C-θ Directly Regulates Inducible Genes in Epithelial to Mesenchymal Transition and Breast Cancer Stem Cells. *Mol. Cell Biol.* 34 (16), 2961–2980. doi:10.1128/MCB.01693-13

Zahalka, A. H., Arnal-Estapé, A., Maryanovich, M., Nakahara, F., Cruz, C. D., Finley, L. W. S., et al. (2017). Adrenergic Nerves Activate an Angio-Metabolic Switch in Prostate Cancer. *Science.* 358 (6361), 321–326. doi:10.1126/science.aah5072

Zhang, J., Deng, Y.-t., Liu, J., Wang, Y.-q., Yi, T.-w., Huang, B.-y., et al. (2016). Norepinephrine Induced Epithelial-Mesenchymal Transition in HT-29 and A549 Cells *In Vitro*. *J. Cancer Res. Clin. Oncol.* 142 (2), 423–435. doi:10.1007/s00432-015-2044-9

Zhang, L., Pan, J., Chen, W., Jiang, J., and Huang, J. (2020). Chronic Stress-Induced Immune Dysregulation in Cancer: Implications for Initiation, Progression, Metastasis, and Treatment. *Am. J. Cancer Res.* 10 (5), 1294–1307.

Zhou, J., Liu, Z., Zhang, L., Hu, X., Wang, Z., Ni, H., et al. (2020). Activation of β2-Adrenergic Receptor Promotes Growth and Angiogenesis in Breast Cancer by Down-Regulating PPARγ. *Cancer Res. Treat.* 52 (3), 830–847. doi:10.4143/crt.2019.510

Zhou, Q., Qian, Z., Ding, W., Jiang, G., Sun, C., and Xu, K. (2021). Chronic Psychological Stress Attenuates the Efficacy of Anti-PD-L1 Immunotherapy for Bladder Cancer in Immunocompetent Mice. *Cancer Invest.* 39 (6-7), 571–581. doi:10.1080/07357907.2021.1943746

Conflict of Interest: The authors declare that the research was conducted in the absence of any commercial or financial relationships that could be construed as a potential conflict of interest.

Publisher's Note: All claims expressed in this article are solely those of the authors and do not necessarily represent those of their affiliated organizations, or those of the publisher, the editors and the reviewers. Any product that may be evaluated in this article, or claim that may be made by its manufacturer, is not guaranteed or endorsed by the publisher.

frontiers in Cell and Developmental Biology

ORIGINAL RESEARCH
published: 30 November 2021
doi: 10.3389/fcell.2021.772216

The Expression of Programmed Death Ligand 1 and Vimentin in Resected Non-Metastatic Non-Small-Cell Lung Cancer: Interplay and Prognostic Effects

Sara Bravaccini[1†], Giuseppe Bronte[2†], Elisabetta Petracci[3†], Maurizio Puccetti[4], Manolo D'Arcangelo[5], Sara Ravaioli[1], Maria Maddalena Tumedei[1], Roberta Maltoni[2], Angelo Delmonte[2], Federico Cappuzzo[6] and Lucio Crinò[2]*

[1]Biosciences Laboratory, IRCCS Istituto Romagnolo per lo Studio dei Tumori (IRST) "Dino Amadori", Meldola, Italy, [2]Department of Medical Oncology, IRCCS Istituto Romagnolo per lo Studio dei Tumori (IRST) "Dino Amadori", Meldola, Italy, [3]Unit of Biostatistics and Clinical Trials, IRCCS Istituto Romagnolo per lo Studio dei Tumori (IRST) "Dino Amadori", Meldola, Italy, [4]Azienda Unità Sanitaria Locale (AUSL) Imola, Imola, Italy, [5]AUSL Romagna, Ospedale Santa Maria delle Croci, Ravenna, Italy, [6]Istituto Nazionale Tumori "Regina Elena", Rome, Italy

Programmed death ligand 1 (PD-L1) is an immune checkpoint with a role in cancer-related immune evasion. It is a target for cancer immunotherapy and its expression is detected for the use of some immune checkpoint inhibitors in advanced non-small cell lung cancer patients (NSCLC). Vimentin is a key component of the epithelial-to-mesenchymal transition phenotype. Its expression has negative prognostic effects in NSCLC. In this study, we retrospectively evaluated PD-L1 and vimentin expression in tumor cells, immune infiltrate and PD-L1 positive immune infiltrate via immunohistochemistry in tissue samples from resected non-metastatic NSCLC patients. We explored the interplay between PD-L1 and vimentin expression through Spearman's correlation test. We performed univariate analysis through the Cox models for demographic and clinico-pathological variables, and also for dichotomized biomarkers, i.e., PD-L1 and vimentin in tumor cells, both with 1 and 50% cutoffs. We used Kaplan-Meier method to estimate the overall survival, comparing both vimentin and PD-L1 positive patients with all the others. We found a weak positive correlation between PD-L1 and vimentin expressions in tumor cells ($r = 0.25$; $p = 0.001$). We also observed a statistically not significant trend towards a shorter overall survival in patients with both PD-L1 and vimentin expression >1% (HR = 1.36; 95% CI: 0.96–1.93, $p = 0.087$). In conclusion, these findings suggest that interplay between PD-L1 and vimentin may exist in non-metastatic NSCLC patients and the positivity of both markers in tumor tissue is associated with a trend towards a worse prognosis.

Keywords: NSCLC, PD-L1, vimentin, immune infiltrate, non-metastatic (M0) patients

OPEN ACCESS

Edited by:
Paola Parrella, Casa Sollievo della Sofferenza (IRCCS), Italy

Reviewed by:
Jiaxi Yao, Fudan University, China
Giulia Mazzaschi, University Hospital of Parma, Italy
Izidor Kern, University Clinic of Pulmonary and Allergic Diseases Golnik, Slovenia

***Correspondence:**
Giuseppe Bronte
giuseppe.bronte@irst.emr.it

[†]These authors have contributed equally to this work

Specialty section:
This article was submitted to Molecular and Cellular Oncology, a section of the journal Frontiers in Cell and Developmental Biology

Received: *07 September 2021*
Accepted: *12 November 2021*
Published: *30 November 2021*

Citation:
Bravaccini S, Bronte G, Petracci E, Puccetti M, D'Arcangelo M, Ravaioli S, Tumedei MM, Maltoni R, Delmonte A, Cappuzzo F and Crinò L (2021) The Expression of Programmed Death Ligand 1 and Vimentin in Resected Non-Metastatic Non-Small-Cell Lung Cancer: Interplay and Prognostic Effects. Front. Cell Dev. Biol. 9:772216. doi: 10.3389/fcell.2021.772216

Abbreviations: NSCLC, non-small cell lung cancer; IASLC, International Association for the Study of Lung Cancer; OS, overall survival; ICI, immune checkpoint inhibitor; PD-1, programmed death 1; PD-L1, programmed death ligand 1; IHC, immunohistochemistry; EMT, epithelial-to-mesenchymal transition; HR, hazard ratio; CI, confidence interval; KRAS, Ki-ras2 Kirsten rat sarcoma viral oncogene homolog; EGFR, epidermal growth factor receptor; ALK, anaplastic lymphoma kinase; ROS1, c-ros oncogene 1.

INTRODUCTION

Lung cancer is still the leading cause of mortality by cancer, despite recent therapeutic advances. In non-small cell lung cancer (NSCLC) 5-year survival rates are limited to 60% in patients with stage II and 36% in those with stage IIIA according to the 8th edition staging by the International Association for the Study of Lung Cancer (IASLC) (Goldstraw et al., 2016). The surgery remains the gold standard treatment for patients in early stages (I-II); it can be considered in selected cases with stage IIIA disease. Post-surgical adjuvant platinum-based chemotherapy is used to achieve a modest improvement of around 5% in 5-year overall survival (OS) in patients who underwent complete resection for stage II and IIIA (Pignon et al., 2008). It can be considered in those patients who underwent resection for stage IB NSCLC if the primary tumor is greater than 4 cm. For unresectable stage IIIA or IIIB disease the treatment of choice is represented by concurrent chemoradiation therapy or, as an alternative, sequential chemotherapy followed by definitive radiotherapy (Postmus et al., 2017). In both cases, concurrent or sequential therapy, a consolidation with durvalumab, an immune checkpoint inhibitor (ICI), is approved according to the results of PACIFIC trial (Antonia et al., 2017). ICIs are currently being evaluated as neoadjuvant/adjuvant therapy in combination with standard treatments (Mielgo-Rubio et al., 2020).

The interaction between Programmed Death-1 (PD–1) and its ligand, Programmed Death–Ligand 1 (PD–L1), is an immune checkpoint with a relevant role in the regulation of anti-tumor immune response. These molecules are expressed in tumor-infiltrating immune cells and tumor cells, respectively. In some cases, the expression of PD-L1 evaluated through immunohistochemistry (IHC) helped to provide a predictive biomarker for ICI. Specifically, it allowed patients to be selected for upfront pembrolizumab, an anti-PD-1 ICI, among those with metastatic NSCLC which expressed PD-L1 > 50%, before the approval of chemoimmunotherapy as first-line treatment.

Epithelial–mesenchymal transition (EMT) may be associated with higher aggressiveness in NSCLC.

It is characterized by the reduction of epithelial features and an increase of mesenchymal ones. In this biological condition tumor cells are more invasive and maintain longer survival leading to higher numbers of circulating tumor cells and metastases (Francart et al., 2018). EMT characteristics include a higher expression of vimentin EMT-related transcription factors, and a remodeling of cell–cell contacts (Tsoukalas et al., 2017). The EMT phenotype was related to PD-L1 upregulation by the combined effect of TGF-β1 and TNF-α. This could be due to the action of TNF-α on NF-κB stimulation, which increases EMT induction by TGF-β1. NF-κB inhibition also blocks PD-L1 expression (Asgarova et al., 2018). These results are supported by the fact that TGF-β1 and TNF-α induce global DNA demethylation, including the demethylation of the PD-L1 promoter, which causes higher PD-L1 expression.

Moreover, vimentin has been described as a negative prognostic marker in various cancers (Dongre and Weinberg, 2019), and also in NSCLC, as extensively documented by numerous studies, then pooled in a meta-analysis (Ye et al., 2016).

In this paper we evaluated the interplay between PD-L1 and vimentin in a wide population of non-metastatic NSCLC patients. We also explored a potential role of immune infiltrate in tumor tissue and analyzed the prognostic impact of these combined markers.

TABLE 1 | Patients characteristics (n = 247).

	N	%
Gender		
female	51	20.65
male	196	79.35
missing	–	
Age at surgery, yrs		
mean ± sd	68.20 ± 7.85	
Median (min-max)	69 (36–87)	
missing	–	
Smoking status		
Non-smoker	6	15.38
Former smoker	20	51.28
Current smoker	13	33.33
missing	*208*	
Histology		
Non squamous	148	59.92
Squamous	94	38.06
Mixed	5	2.02
missing	–	
Grading		
G1	10	4.31
G2	87	37.50
G3	135	58.19
missing	15	
Disease stage (8th edition)		
IA	22	11.70
IB	45	23.94
IIA	20	10.64
IIB	50	26.60
IIIA	51	27.13
missing	59	
Type of surgery		
lobectomy	153	61.94
bilobectomy	10	4.05
pneumonectomy	38	15.38
Atypical resection	44	17.81
Other	2	0.81
missing	–	
Neoadjuvant Chemotherapy		
no	20	83.33
yes	4	16.67
missing	223	
Adjuvant Chemotherapy		
no	19	90.48
yes	2	9.52
missing	226	
Post-surgery Radiotherapy		
no	21	100.00
yes	–	0.00
missing	226	

sd: standard deviation; min: minimum; max: maximum.

MATERIALS AND METHODS

Study Design

To investigate the association between Vimentin and PD-L1 expression and immune infiltrate and their separate and combined effects in terms of OS, retrospectively retrieved data for patients consecutively treated at Area Vasta Romagna (AVR) since July, 1997, were used. Our hypothesis is that the increase of vimentin expression levels is associated with an increase of PD-L1 expression levels. We also hypothesized that the patients with both Vimentin and PD-L1 positive IHC expression had a worse prognosis in terms of OS. Second aim of the study was to explore the role of immune infiltrate in terms of quantity and percentage of PD-L1 positive immune cells on OS.

Patients

Eligibility criteria were ≥18 years old, histological diagnosis of non-metastatic NSCLC (Stage I-IIIA defined by using the latest version of staging system). At least one primary tumor specimen had to be available. From the clinical records we extracted information about histology, stage at diagnosis, date of diagnosis, type of radical surgery, adjuvant chemotherapy, adjuvant radiotherapy, date of death or date of last follow-up visit.

Given that the setting of patients analyzed is early stage NSCLC, the assessment of genetic testing was not required.

The Ethics Committee of AVR reviewed and approved the study protocol (NCT03078959). Patients provided written informed consent according to Italian privacy law and following the principles laid down in the Declaration of Helsinki.

Immunohistochemistry

NSCLC obtained during surgery was fixed in neutral buffered formalin and embedded in paraffin. Four-micron sections were mounted on positive-charged slides (Bio Optica, Milan, Italy). Biomarker evaluations were done according to European Quality Assurance guidelines. PD-L1 and Vimentin Immunostaining expression was performed using PD-L1 SP263 and Confirm anti-Vimentin V9 (Ventana Medical Systems) antibody clones by Ventana BenchmarkXT staining system (Ventana Medical Systems, Tucson, AZ, United States) with the Optiview DAB Detection Kit (Ventana Medical Systems).

For their detection, tissue sections were incubated for 16 min with prediluted antibodies by the supplier. Sections were incubated for 16 min and automatically counterstained with hematoxylin II (Ventana Medical Systems). Placenta was used as positive control for both the biomarkers. Membranous biomarker positivity was detected and semiquantitatively quantified as the percentage ratio between immunopositive tumor cells and the total number of tumor cells.

We defined immune infiltrate considering mainly the tumor infiltrating lymphocytes (TILs). PD-L1 positivity was detected both on tumor cells and on the immune infiltrate. We considered the amount (%) of the whole immune infiltrate on the total of the cells present in the sample. The PD-L1 positivity on immune infiltrate was evaluated in terms of percentage of PD-L1 positive immune cells on the total number of immune cells without subtyping the TILs identified by using only morphological criteria, due to the low number of sections available to perform further IHC detections.

Vimentin expression has been evaluated only on tumor cells given that its expression in the cells of interstitial area is known to be ubiquitous.

All samples were evaluated by 2 independent observers and any disagreement (>10% of positive cells for the different markers) was resolved by consensus after joint review using a multihead microscope.

Statistical Analysis

Data were summarized using mean ± standard deviation (sd), median and minimum and maximum values, for continuous variables. Categorical variables were reported as natural frequency and percentage. Correlation among variables was measured through the Spearman correlation coefficient.

Given the heavily asymmetric distribution of the considered biomarkers, characterized by a "spike at zero," the association between demographic and clinical covariates as well as with the OS was assessed using dichotomized variables on the 1% value. Patients with expression values lower than 1% were considered "negative" for the biomarkers whereas those with values equal or greater than 1%, were considered as "positive." Additional exploratory analyses considering a 50% cutoff ("negative" less than 50%, "positive" if equal or greater than 50%) as well as considering the biomarkers as continuous variables were also performed. These cutoffs were chosen because these are commonly used in clinical practice for PD-L1 characterization for the use of pembrolizumab in first- or second-line treatment for advanced NSCLC. The Chi-square test or the Fisher Exact test was used for the association between the biomarker as dichotomous variable and categorical covariates whereas the Wilcoxon-Mann-Whitney or the Kruskal Wallis test was used for the association between the biomarker as continuous variable and categorical covariates.

OS was defined as the time from surgery until death for any cause or last patient visit by April, 2016. The Kaplan-Meier method was used to estimate the OS function whereas the Log-rank test was used for survival curves comparison. Hazard ratios (HRs) and corresponsing 95% confidence intervals (CIs) were obtained applying the Cox proportional hazards model. To investigate the association between the biomarkers as continuous variables, the method proposed by Royston and Lorenz was also applied (Royston et al., 2010; Lorenz et al., 2017; Lorenz et al., 2019). The proportional hazards assumption was tested using Schoenfeld residuals. For all the analyses a two-sided p-value <0.05 was considered statistically significant. The analyses were carried with STATA 15.0 (College Station, Texas, United States).

RESULTS

In this retrospective study we included 247 patients who met the eligibility criteria. The majority of patients were male (79%), former or current smokers (85%), with a non-squamous histology (60%). The mean age at surgery was 68.20 ± 7.85 years. The stages were variably distributed: 36% stage I, 37% stage II, 27% stage IIIA. As

TABLE 2 | Descriptive statistics of IHC biomarkers.

	missing	Mean	sd	Median	min	Max	IQR
PD-L1+ tumor cells	–	20.76	33.24	0	0	100	30
Vim + tumor cells	–	10.96	23.19	0	0	100	5
Immune infiltrate	12	16.01	14.99	10	1	90	15
PD-L1+ immune infiltrate	12	5.53	9.36	2	0	80	10

IHC: immunohistochemistry; PD-L1: programmed death ligand 1; Vim: vimentin; sd: standard deviation; min: minimum; max: maximum; IQR: interquartile range.

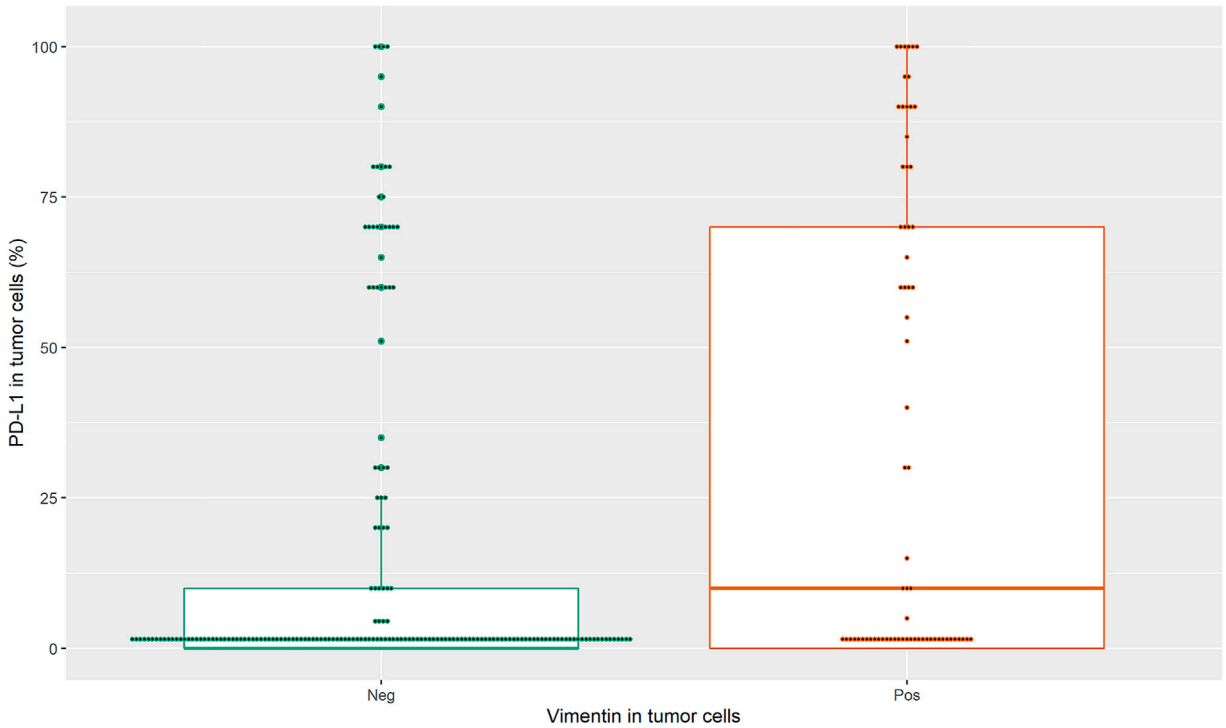

FIGURE 1 | Correlation between the IHC-defined biomarkers i.e. PD-L1 in tumor cells as continuous variable and vimentin in tumor cells as dichotomous variable.

regards surgery, the majority of patients (62%) underwent lobectomy. As regards cancer treatments, 17% received neoadjuvant chemotherapy, 10% received adjuvant chemotherapy and none of the patients was treated with post-surgical radiation therapy (**Table 1**). The mean values of PD-L1 expression in tumor cells, vimentin expression in tumor cells, immune infiltrate, and PD-L1-positive immune infiltrate with standard deviations are reported in **Table 2**, together with medians and minimum and maximum values. PD-L1 median percentage in tumor cells was equal to zero as well as the vimentin median percentage in tumor cells. The median values for the immune infiltrate and the PD-L1-positive immune infiltrate were equal to 10 and 2, respectively.

We measured the correlation between the IHC-defined biomarkers as continuous variables through the Spearman correlation coefficient. We found a weak positive correlation between PD-L1 and vimentin expressions in tumor cells (r = 0.25; p = 0.001). The comparison of PD-L1 expression in tumor cells between high and low vimentin expression (1% of cutoff value) by using Wilcoxon-Mann-Whitney resulted in a statistically significant difference (p-value<0.001), **Figure 1**.

A similar result was obtained using the 50% cutoff for vimentin expression (data not shown).

The tumor cells were negative for PD-L1 or vimentin with both the cutoff values in the majority of patients. Tumor cells were PD-L1-negative in 76% of cases with 50% cutoff and 57% with 1% cutoff. The same cells were vimentin-negative in 89% of cases with 50% cutoff and 72% with 1% cutoff. For the samples from 12 patients the information about immune infiltrate was missing. However, almost all cases (97%) were negative for immune infiltrate with 50% cutoff value, but all the samples had an immune infiltrate ≥1%. In 99% of cases the immune infiltrate had a PD-L1 expression <50%, but with 1% cutoff value PD-L1-positive immune infiltrate was present in the majority of patients (67%) (**Table 3**).

No significant associations were found between the biomarkers and demographic and clinico-pathological covariates (results not shown).

TABLE 3 | Distribution of biomarkers' values with different cutoffs.

	50% cutoff		1% cutoff	
	N	**%**	***n***	**%**
PD-L1 in tumor cells				
Negative	188	76.11	140	56.68
Positive	59	23.89	107	43.32
missing	–		–	
Vimentin in tumor cells				
Negative	220	89.07	207	71.63
Positive	27	10.93	82	28.37
missing	–		–	
Immune infiltrate				
Negative	227	96.60	0	0.00
Positive	8	3.40	235	100.00
missing	12		12	
PD-L1+ immune infiltrate				
Negative	233	99.15	78	33.19
Positive	2	0.85	157	66.81
missing	12		12	

TABLE 4 | Results from univariate Cox models for demographic and clinico-pathological variables.

	HR (95% CI)	P
Gender		
Female	1 (ref)	
Male	1.22 (0.88–1.70)	0.239
Age		
<70	1 (ref)	
≥70	1.40 (1.15–1.95)	**0.003**
Smoking status		
non smoker	1 (ref)	
ex smoker	0.64 (0.23–1.78)	0.399
Smoker	0.77 (0.26–2.26)	0.632
Histology		
non squamous	1 (ref)	
Squamous	1.03 (0.78–1.35)	0.848
Mixed	0.98 (0.36–2.65)	0.964
Grading		
G1	1 (ref)	
G2	1.71 (0.83–3.55)	0.148
G3	2.24 (1.09–4.59)	**0.027**
Disease stage		
I	1 (ref)	
II	1.40 (0.97–2.01)	0.072
III	2.15 (1.52–3.32)	**<0.001**

HR: hazard ratio; CI: confidence interval; P: p*-value; ref: reference.*
*The bold values refer to statistically significant values (*p *< 0.05).*

We also performed an univariate analysis for OS through the Cox models as regards the available demographic and clinico-pathological variables, including gender, age, smoking status, histology, grading and disease stage, and type of surgery. We found statistically significant differences for age (<70 vs. ≥ 70 years), grading (G1 vs. G3) and disease stage (I vs. III) (**Table 4**).

An univariate analysis for OS was also performed for the dichotomized biomarkers (**Table 5**). Note that for the immune infiltrate only eight patients had a value ≥ 50% whereas for the PD-L1+immune infiltrate only two patients presented with a value ≥50%. However, we did not find statistically significant

TABLE 5 | Results from univariate Cox models for dichotomized biomarkers.

	50% cutoff		1% cutoff	
	HR (95% CI)	**P**	**HR (95% CI)**	**P**
PD-L1 in tumor cells				
Negative	1 (ref)		1 (ref)	
Positive	0.95 (0.69–1.30)	0.732	1.01 (0.78–1.30)	0.961
Vimentin in tumor cells				
Negative	1 (ref)		1 (ref)	
Positive	1.14 (0.72–1.81)	0.565	1.19 (0.90–1.57)	0.219
Immune infiltrate				
Negative	1 (ref)		1 (ref)	
Positive	0.66 (0.29–1.48)	0.312	–[a]	
PD-L1+ immune infiltrate				
Negative	1 (ref)		1 (ref)	
Positive	1.33 (0.33–5.37)	0.687	1.19 (0.89–1.58)	0.243

HR: hazard ratio; CI: confidence interval; P: p*-value; ref: reference.*
[a]HRs, and 95% CIs, could not be estimated because no patients presented with a value < 1%.

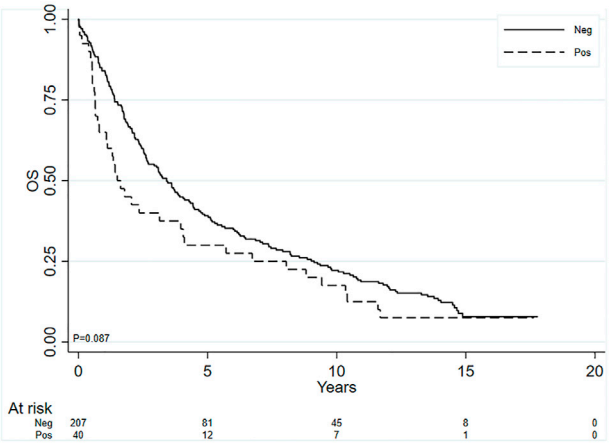

FIGURE 2 | Kaplan-Meier curves for OS, comparing the subgroup of patients with both PD-L1 and vimentin positive in tumor cells (cutoff value ≥ 1% for both the biomarkers) with all the others.

differences for the analyzed biomarkers (**Table 5**). No statistically significant associations for all four biomarkers were observed also when considered as continuous variables (results not shown).

Finally, given that we hypothesized that the patients with both Vimentin and PD-L1 positive (40 patients) could have a worse prognosis, we compared this subgroup of patients with all other patients (n = 207). We found a trend even if not statistically significant toward a worse survival in this double positive subgroup using 1% cutoff value for both the biomarkers (HR = 1.36; 95% CI: 0.96–1.93, p = 0.087). **Figure 2** shows the Kaplan-Meier curves for the two groups. Such a trend in significance disappeared when age and stage were also included in the Cox model. When considering the 50% cutoff no association was observed (HR = 1.03; 95% CI: 0.60–1.77, p = 0.912), **Figure 3**.

Figures 4, **5** show the expression of PD-L1 and vimentin in some tissue slides to highlight the differential expression of these biomarkers in tumor cells and infiltrate with immune cells.

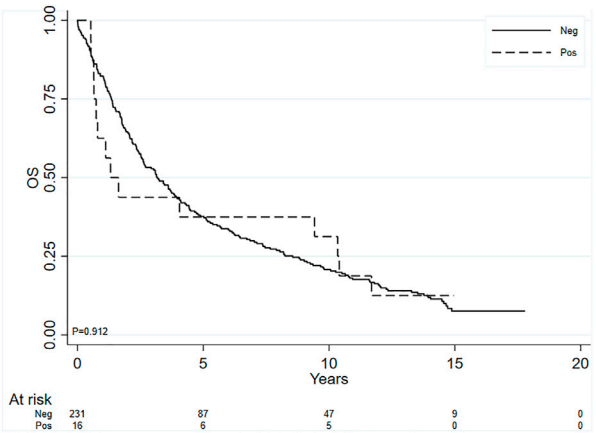

FIGURE 3 | Kaplan-Meier curves for OS, comparing the subgroup of patients with both PD-L1 and vimentin positive in tumor cells (cutoff value ≥ 50% for both the biomarkers) with all the others.

DISCUSSION

In the last few years PD-L1 expression in tumor tissue increased its importance because of the availability of ICIs which target the PD-1/PD-L1 pathway. However, these drugs have not yet reached a role in resected non-metastatic NSCLC. Vimentin expression is not directly involved in the treatment of this neoplasm, but it has a key role in the EMT process, which seems to be involved in resistance to various cancer treatments. Its prognostic role has been widely studied in NSCLC patients. Few studies explored its association with PD-L1 expression (Asgarova et al., 2018).

We previously retrospectively analyzed data on patients with advanced NSCLC consecutively enrolled in a clinical study in our center. PD-L1 and vimentin expression were detected by immunohistochemistry (Bronte et al., 2021). We used ≥1% and ≥50% as cutoff values to define PD-L1 positivity on immune cells because these cutoff values are the same used on tumor cells in the clinical practice to select patients for immunotherapy. A weak positive association between PD-L1 and vimentin in advanced NSCLC suggests a potential interplay between these biomarkers. Moreover, given our previous results (Bronte et al., 2021), the established prognostic value of these biomarkers in other subset of disease, we investigated their expression in an earlier disease setting, non-metastatic NSCLC patients. We also explored a potential role of immune infiltrate in tumor tissue and analyzed the prognostic impact of these combined markers.

We found a weak positive correlation between PD-L1 and vimentin expressions in tumor cells as well as a correlation between the quantity of immune cells and % of immune cells PD-L1 positive. In particular, we retrospectively analyzed Vimentin and PD-L1 expression in tumor cells and immune infiltrate to study their separate and combined effects in terms of OS.

In our study a positive association between the percentage of PD-L1 positive tumor cells and the percentage of vimentin in tumor cells was seen.

The interplay between EMT markers and immune checkpoint inhibitors (Chouaib et al., 2014; Chen et al., 2015; De Matteis et al., 2019) has been previously reported. The concurrent expression of PD-L1 and EMT phenotype was described both in tumor tissue and circulating tumor cells (Kim et al., 2016; Raimondi et al., 2017; Manjunath et al., 2019). The effect of EMT on immune evasion is exerted through the regulation of PD-L1 expression (Asgarova et al., 2018) as a consequence of a synergistic exposure to TGF-β1 and TNF-α. These factors determine global DNA demethylation, also in the promoter of

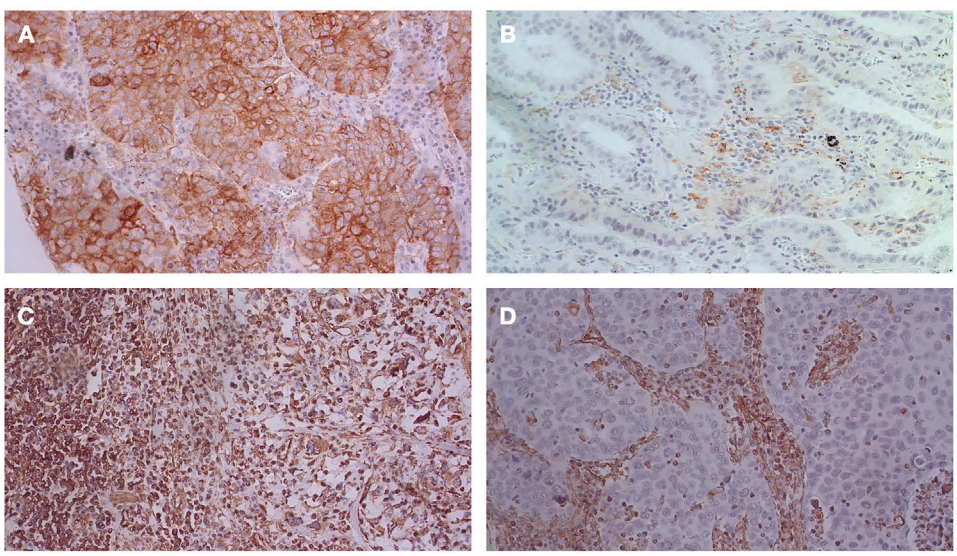

FIGURE 4 | IHC analysis for PD-L1 and vimentin: **(A)** PD-L1 positive in both tumor cells and infiltrate with immune cells (40X magnification); **(B)** PD-L1 positive in infiltrate with immune cells, but negative in tumor cells (40X magnification); **(C)** Vimentin expression observed both in tumor cells and immune cells (20X magnification); **(D)** Vimentin expression observed only in immune cells (20X magnification).

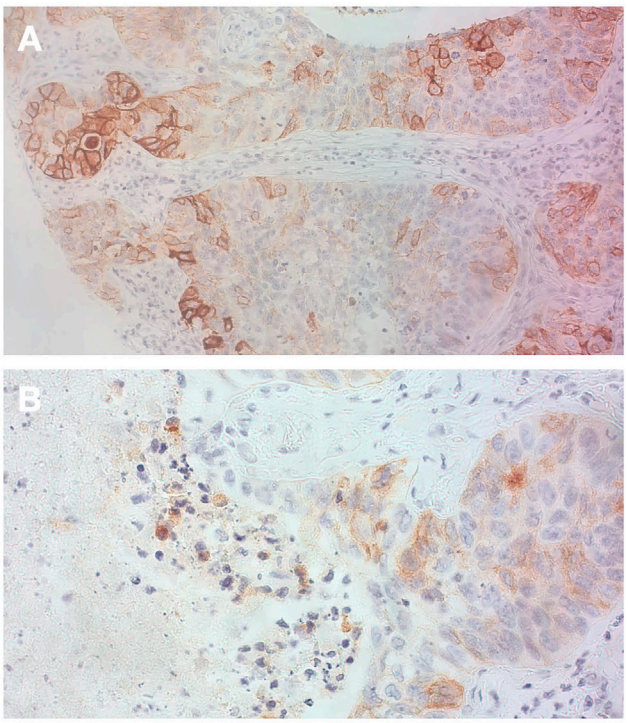

FIGURE 5 | IHC analysis for PD-L1 **(A)** This picture highlights heterogeneity in term of PD-L1 expression in tumor cells (20 X magnification); **(B)** Weak PD-L1 positivity mainly on tumor cells (also macrophages and very few stromal lymphocytes are positive) (40 X magnification).

the gene encoding for PD-L1, and consequently a higher PD-L1 expression is achieved.

Ancel and colleagues reported that a cut-off ≥ 25% vimentin-positive tumor cells was significantly associated with poor tumor differentiation even if it was not sufficient to predict a worse prognosis. However, these authors reported that concurrent high PD-L1 and vimentin expressions in early-stage NSCLC patients were more clearly associated with a shorter OS (Ancel et al., 2019). Such results are concordant with our finding of a trend even if it was not statistically significant of a worse survival in the patients harboring double positivity for PD-L1 and Vimentin using 1% cutoff value for both the biomarkers.

Our study has some limitations, because it is retrospective and this population of non-metastatic NSCLC patients is heterogeneous, mainly in terms of disease stage, type of surgery and subsequent treatments. Another strong limitation is the use of archival tissue for IHC analysis and the limited number of patients included in this study. A prospective study could allow the analysis in fresh tissue to evaluate more biomarkers associated with EMT and immune evasion. Moreover, proper cut-off values to define vimentin and PD-L1 positivity have to be established. Probably, we did not find any prognostic significance of immune infiltrate because the overall amount of lymphocytes is not sufficient to determine a prognostic effect, but perhaps the specific subsets of lymphocytes (e.g. $CD4^+$, $CD8^+$, etc.) could impact on prognosis, but we could not determine these subsets because of the few slides available. Anyway, our findings suggest that EMT markers and immune escape markers could be intended as components of the same process.

DATA AVAILABILITY STATEMENT

The raw data supporting the conclusion of this article will be made available by the authors, without undue reservation.

ETHICS STATEMENT

The studies involving human participants were reviewed and approved by the Ethics Committee of AVR. The patients/participants provided their written informed consent to participate in this study.

AUTHOR CONTRIBUTIONS

GB, FC, and LC conceived experiments; SB, RM, and EP conceived experiments and analysed data; SR, MMT, and MP carried out experiments; AD and MD'A collected data. All authors contributed to manuscript revision, read, and approved the submitted version.

ACKNOWLEDGMENTS

The authors thank Grainne Tierney and Cristiano Verna for editorial assistance.

REFERENCES

Ancel, J., Birembaut, P., Dewolf, M., Durlach, A., Nawrocki-Raby, B., Dalstein, V., et al. (2019). Programmed Death-Ligand 1 and Vimentin: A Tandem Marker as Prognostic Factor in NSCLC. *Cancers (Basel)* 11 (10). doi:10.3390/cancers11101411

Antonia, S. J., Villegas, A., Daniel, D., Vicente, D., Murakami, S., Hui, R., et al. (2017). Durvalumab after Chemoradiotherapy in Stage III Non-small-cell Lung Cancer. *N. Engl. J. Med.* 377 (20), 1919–1929. doi:10.1056/nejmoa1709937

Asgarova, A., Asgarov, K., Godet, Y., Peixoto, P., Nadaradjane, A., Boyer-Guittaut, M., et al. (2018). PD-L1 Expression Is Regulated by Both DNA Methylation and NF-kB during EMT Signaling in Non-small Cell Lung Carcinoma. *Oncoimmunology* 7 (5), e1423170. doi:10.1080/2162402x.2017.1423170

Bronte, G., Puccetti, M., Petracci, E., Landi, L., Cravero, P., Scodes, S., et al. (2021). The Interplay between Programmed Death Ligand 1 and Vimentin in Advanced Non-small-cell Lung Cancer. *Front. Oncol.* 11, 669839. doi:10.3389/fonc.2021.669839

Chen, L., Heymach, J. V., Qin, F. X.-F., and Gibbons, D. L. (2015). The Mutually Regulatory Loop of Epithelial-Mesenchymal Transition and Immunosuppression in Cancer Progression. *Oncoimmunology* 4 (5), e1002731. doi:10.1080/2162402x.2014.1002731

Chouaib, S., Janji, B., Tittarelli, A., Eggermont, A., and Thiery, J. P. (2014). Tumor Plasticity Interferes with Anti-tumor Immunity. *Crit. Rev. Immunol.* 34 (2), 91–102. doi:10.1615/critrevimmunol.2014010183

De Matteis, S., Canale, M., Verlicchi, A., Bronte, G., Delmonte, A., Crinò, L., et al. (2019). Advances in Molecular Mechanisms and Immunotherapy Involving the Immune Cell-Promoted Epithelial-To-Mesenchymal Transition in Lung Cancer. *J. Oncol.* 2019, 7475364. doi:10.1155/2019/7475364

Dongre, A., and Weinberg, R. A. (2019). New Insights into the Mechanisms of Epithelial-Mesenchymal Transition and Implications for Cancer. *Nat. Rev. Mol. Cel Biol.* 20 (2), 69–84. doi:10.1038/s41580-018-0080-4

Francart, M.-E., Lambert, J., Vanwynsberghe, A. M., Thompson, E. W., Bourcy, M., Polette, M., et al. (2018). Epithelial-mesenchymal Plasticity and Circulating Tumor Cells: Travel Companions to Metastases. *Dev. Dyn.* 247 (3), 432–450. doi:10.1002/dvdy.24506

Goldstraw, P., Chansky, K., Crowley, J., Rami-Porta, R., Asamura, H., Eberhardt, W. E., et al. (2016). The IASLC Lung Cancer Staging Project: Proposals for Revision of the TNM Stage Groupings in the Forthcoming (Eighth) Edition of the TNM Classification for Lung Cancer. *J. Thorac. Oncol.* 11 (1), 39–51. doi:10.1016/j.jtho.2015.09.009

Kim, S., Koh, J., Kim, M.-Y., Kwon, D., Go, H., Kim, Y. A., et al. (2016). PD-L1 Expression Is Associated with Epithelial-To-Mesenchymal Transition in Adenocarcinoma of the Lung. *Hum. Pathol.* 58, 7–14. doi:10.1016/j.humpath.2016.07.007

Lorenz, E., Jenkner, C., Sauerbrei, W., and Becher, H. (2019). Modeling Exposures with a Spike at Zero: Simulation Study and Practical Application to Survival Data. *Biostatistics Epidemiol.* 3 (1), 23–37. doi:10.1080/24709360.2019.1580463

Lorenz, E., Jenkner, C., Sauerbrei, W., and Becher, H. (2017). Modeling Variables with a Spike at Zero: Examples and Practical Recommendations. *Am. J. Epidemiol.* 185 (8), 650–660. doi:10.1093/aje/kww122

Manjunath, Y., Upparahalli, S. V., Avella, D. M., Deroche, C. B., Kimchi, E. T., Staveley-O'Carroll, K. F., et al. (2019). PD-L1 Expression with Epithelial Mesenchymal Transition of Circulating Tumor Cells Is Associated with Poor Survival in Curatively Resected Non-small Cell Lung Cancer. *Cancers* 11 (6), 806. doi:10.3390/cancers11060806

Mielgo-Rubio, X., Calvo, V., Luna, J., Remon, J., Martín, M., Berraondo, P., et al. (2020). Immunotherapy Moves to the Early-Stage Setting in Non-small Cell Lung Cancer: Emerging Evidence and the Role of Biomarkers. *Cancers* 12 (11), 3459. doi:10.3390/cancers12113459

Pignon, J.-P., Tribodet, H., Scagliotti, G. V., Douillard, J.-Y., Shepherd, F. A., Stephens, R. J., et al.LACE Collaborative Group (2008). Lung Adjuvant Cisplatin Evaluation: a Pooled Analysis by the LACE Collaborative Group. *Jco* 26 (21), 3552–3559. doi:10.1200/jco.2007.13.9030

Postmus, P. E., Kerr, K. M., Oudkerk, M., Senan, S., Waller, D. A., Vansteenkiste, J., et al.ESMO Guidelines Committee (2017). Early and Locally Advanced Non-small-cell Lung Cancer (NSCLC): ESMO Clinical Practice Guidelines for Diagnosis, Treatment and Follow-Up. *Ann. Oncol.* 28 (Suppl. l_4), iv1–iv21. doi:10.1093/annonc/mdx222

Raimondi, C., Carpino, G., Nicolazzo, C., Gradilone, A., Gianni, W., Gelibter, A., et al. (2017). PD-L1 and Epithelial-Mesenchymal Transition in Circulating Tumor Cells from Non-small Cell Lung Cancer Patients: A Molecular Shield to Evade Immune System?. *Oncoimmunology* 6 (12), e1315488. doi:10.1080/2162402x.2017.1315488

Royston, P., Sauerbrei, W., and Becher, H. (2010). Modelling Continuous Exposures with a 'spike' at Zero: a New Procedure Based on Fractional Polynomials. *Statist. Med.* 29 (11), 1219–1227. doi:10.1002/sim.3864

Tsoukalas, N., Aravantinou-Fatorou, E., Tolia, M., Giaginis, C., Galanopoulos, M., Kiakou, M., et al. (2017). Epithelial-Mesenchymal Transition in Non Small-Cell Lung Cancer. *Anticancer Res.* 37 (4), 1773–1778. doi:10.21873/anticanres.11510

Ye, Z., Zhang, X., Luo, Y., Li, S., Huang, L., Li, Z., et al. (2016). Prognostic Values of Vimentin Expression and its Clinicopathological Significance in Non-small Cell Lung Cancer: A Meta-Analysis of Observational Studies with 4118 Cases. *PLoS One* 11 (9), e0163162. doi:10.1371/journal.pone.0163162

Conflict of Interest: The authors declare that the research was conducted in the absence of any commercial or financial relationships that could be construed as a potential conflict of interest.

Publisher's Note: All claims expressed in this article are solely those of the authors and do not necessarily represent those of their affiliated organizations, or those of the publisher, the editors and the reviewers. Any product that may be evaluated in this article, or claim that may be made by its manufacturer, is not guaranteed or endorsed by the publisher.

frontiers in Oncology

ORIGINAL RESEARCH
published: 13 December 2021
doi: 10.3389/fonc.2021.789885

Osteoblasts Promote Prostate Cancer Cell Proliferation Through Androgen Receptor Independent Mechanisms

Giulia Ribelli[1†], Sonia Simonetti[1†], Michele Iuliani[1], Elisabetta Rossi[2,3], Bruno Vincenzi[1], Giuseppe Tonini[1], Francesco Pantano[1‡] and Daniele Santini[1‡]*

[1] Department of Medical Oncology, Campus Bio-Medico University of Rome, Rome, Italy, [2] Department of Immunology and Molecular Oncology, Istituto Oncologico Veneto (IOV) Istituto di Ricovero e Cura a Carattere Scientifico (IRCCS), Padua, Italy, [3] Department of Surgery, Oncology and Gastroenterology, University of Padua, Padua, Italy

OPEN ACCESS

Edited by:
Francesca Pirini, Istituto Scientifico Romagnolo per lo Studio e la Cura dei Tumori (IRCCS), Italy

Reviewed by:
Kenichi Takayama, Tokyo Metropolitan Institute of Gerontology, Japan
Swathi Ramakrishnan, University at Buffalo, United States

***Correspondence:**
Michele Iuliani
m.iuliani@unicampus.it

[†]These authors share first authorship

[‡]These authors share last authorship

Specialty section:
This article was submitted to Molecular and Cellular Oncology, a section of the journal Frontiers in Oncology

Received: *05 October 2021*
Accepted: *22 November 2021*
Published: *13 December 2021*

Citation:
Ribelli G, Simonetti S, Iuliani M, Rossi E, Vincenzi B, Tonini G, Pantano F and Santini D (2021) Osteoblasts Promote Prostate Cancer Cell Proliferation Through Androgen Receptor Independent Mechanisms. Front. Oncol. 11:789885. doi: 10.3389/fonc.2021.789885

Patients with metastatic prostate cancer frequently develop bone metastases that elicit significant skeletal morbidity and increased mortality. The high tropism of prostate cancer cells for bone and their tendency to induce the osteoblastic-like phenotype are a result of a complex interplay between tumor cells and osteoblasts. Although the role of osteoblasts in supporting prostate cancer cell proliferation has been reported by previous studies, their precise contribution in tumor growth remains to be fully elucidated. Here, we tried to dissect the molecular signaling underlining the interactions between castration-resistant prostate cancer (CRPC) cells and osteoblasts using *in vitro* co-culture models. Transcriptomic analysis showed that osteoblast-conditioned media (OCM) induced the overexpression of genes related to cell cycle in the CRPC cell line C4-2B but, surprisingly, reduced androgen receptor (AR) transcript levels. In-depth analysis of AR expression in C4-2B cells after OCM treatment showed an AR reduction at the mRNA ($p = 0.0047$), protein ($p = 0.0247$), and functional level ($p = 0.0029$) and, concomitantly, an increase of C4-2B cells in S-G2-M cell cycle phases ($p = 0.0185$). An extensive proteomic analysis revealed in OCM the presence of some molecules that reduced AR activation, and among these, Matrix metalloproteinase-1 (MMP-1) was the only one able to block AR function (0.1 ng/ml $p = 0.006$; 1 ng/ml $p = 0.002$; 10 ng/ml $p = 0.0001$) and, at the same time, enhance CRPC proliferation (1 ng/ml $p = 0.009$; 10 ng/ml $p = 0.033$). Although the increase of C4-2B cell growth induced by MMP-1 did not reach the proliferation levels observed after OCM treatment, the addition of Vorapaxar, an MMP-1 receptor inhibitor (Protease-activated receptor-1, PAR-1), significantly reduced C4-2B cell cycle (0.1 μM $p = 0.014$; 1 μM $p = 0.0087$). Overall, our results provide a novel AR-independent mechanism of CRPC proliferation and suggest that MMP-1/PAR-1 could be one of the potential pathways involved in this process.

Keywords: castration resistance prostate cancer, bone microenvironment, androgen receptor, osteoblasts, matrix metalloproteinase-1

INTRODUCTION

Androgen-deprivation therapy is the mainstay for advanced prostate cancer, but despite the initial success of these treatments, castration-resistant prostate cancer (CRPC) inevitably occurs within a few years (1). Multiple mechanisms of resistance contribute to the progression to castration-resistant disease and the androgen receptor (AR) remains the most important driver in this progression (2). At present, the approved chemotherapies for CRPC include systemic drugs (docetaxel and cabazitaxel) and agents that target androgen signaling such as enzalutamide, abiraterone, apalutamide, and daralutamide (3). Although these treatments confer a significant survival benefit, over time, the majority of patients inevitably develop resistance to treatment and their disease progresses. Several mechanisms have been attributed to these resistances including AR overexpression or mutations, the expression of constitutively active AR splice variants, the increase in intratumoral hormonal synthesis, and the activation of different growth factor pathways (4–7). At this stage, about 70% of patients develop bone metastases (8) usually associated with skeletal-related events (SREs) including pathological fractures, bone pain, and spinal cord compression that severely affect the patients' quality of life (9). As widely described in vicious cycle theory, bone microenvironment represents a fertile soil where the bi-directional interaction between bone and cancer cells promotes tumor growth and progression (10–14). Bone metastases from prostate cancer are predominantly characterized by an increased osteoblast (OB) activation that, in turn, influences prostate cancer proliferation. Despite increasing evidence supporting a key role of OBs within bone metastatic niche (15–17), their precise contribution in supporting tumor cell survival and proliferation is not completely elucidated. From these perspectives, our purpose was to better elucidate the biohumoral interactions between OBs and prostate cancer cells in the bone microenvironment.

MATERIALS AND METHODS

Prostate Cancer Cell Line

The C4-2B cell line was gently gifted by Thalman who isolated them in 1994 (18). C4-2B cells were grown in T-medium (80% Dulbecco's modified Eagle's medium, 20% F12K, 3 g/L $NaHCO_3$, 100 units/L Penicillin G, 100 µg/ml Streptomycin, 5 µg/ml insulin, 13.6 pg/ml triiodothyronine, 5 µg/ml apo-transferrin, 0.25 µg/ml biotin, and 25 µg/ml adenine) with 10% FBS. The cells were Mycoplasma free. Green Fluorescent Protein C4-2B (C4-2B GFP+) cells were obtained transfecting cells with MISSION® pLKO.1-puro-CMV Turbo GFP™ Positive Control Transduction Particles (multiplicity of infection: 0.5) (Sigma Aldrich). Transfected cells were isolated adding 2 µg/ml of Puromycin. C4-2B Firefly/Renilla (C4-2B FR) cells were generated transfecting C4-2B cells with androgen receptor (AR) two luciferase lentiviral particles using Cignal AR luciferase reporter assay (Qiagen). C4-2B FR were selected adding 100 µg/ml of Hygromycin and 2 µg/ml of Puromycin.

Primary Human Osteoblasts

Human primary OBs were obtained from bone marrow samples of healthy patients undergoing total hip replacement at Policlinico Universitario Campus Bio-Medico of Rome, Italy. The procedure was approved by the Ethical Committee of the Campus Bio-Medico University of Rome and informed consent from patients was collected in accordance with the Declaration of Helsinki principles (Prot 21/15 OSS). Bone marrow mesenchymal stem cells (BM-MSCs) were isolated and differentiated in OBs as previously described (19). At the end of the OB differentiation protocol, the positivity for alkaline phosphatase (ALP) and Alizarin red staining were tested as previously described (20).

OBs-C4-2B Cell Co-Cultures

For "indirect co-cultures", osteoblast-conditioned media (OCM) and C4-2B conditioned-media (C4-2B CM) were collected respectively from OBs and C4-2B cells after 48 h of androgen deprivation in T-medium supplemented with 10% of charcoal-stripped serum. OCM and C4-2B CM were added to C4-2B FR cells seeded at a confluency of 10^4 in 96-well plates for AR activity assay (see paragraph below) and 6×10^4 in 24-well plates for cell cycle analysis (see paragraph below). For "direct co-cultures", C4-2B FR cells were plated (10^4 in 96 well plates) on an OB layer for AR activity assay (see paragraph below) and GFP+ C4-2B cells were seeded (5×10^4 in 24-well plates) on an OB layer for proliferation analysis. To generate growth curves, GFP signal cells were measured at 24 h, 48 h, 96 h, and 120 h using Nikon NIS-Elements microscope imaging software. GFP-fluorescent signal at each time point was normalized to GFP-fluorescent signal at t0. As control, C4-2B FR cells were cultured on the C4-2B layer (for AR activity) and GFP+ C4-2B cells were cultured on the C4-2B layer (for proliferation analysis).

Real-Time PCR

Total RNA was extracted by Trizol reagent (Invitrogen) according to the manufacturer's instructions. cDNA was produced using the High-Capacity cDNA Reverse Transcription kit (Applied Biosystems) according to the manufacturer's instructions. mRNA levels were measured by quantitative real-time polymerase chain reaction (qRT-PCR) using TaqMan Gene Expression Assays in the 7900HT Real-Time PCR System (Applied Biosystems). AR (Hs00171172_m1), KLK3 (Hs02576345_m1), TMPRSS2 (Hs05024838_m1), and MMP-1 (Hs00899658_m1) expression levels were normalized to the endogenous housekeeping gene Glucuronidase Beta (GUSβ) (Hs99999908_m1).

Microarray

Gene expression profiling was performed using Clariom™ D Pico Assay, human (Affymetrix, USA) according to user guide. Quantile normalization and subsequent data processing were performed using Applied Biosystems™ Transcriptome Analysis Console (TAC) Software (Affymetrix, USA). A volcano plot representing differentially regulated genes was generated using R software (Vienna University of Economics and Business, Austria). According to the results of microarray, RNAs with

fold change > 1.5 were marked as significantly differentially expressed genes (21). Gene set enrichment analysis was performed using WEBGESTALT (22).

Western Blot

C4-2B FR cells were lysed in RIPA buffer (Sigma-Aldrich) with protease inhibitor cocktail (Sigma-Aldrich) and phosphatase inhibitor cocktail (Sigma-Aldrich). Protein concentration was measured using a DC protein assay (Bio-Rad) following the manufacturer's instruction. AR primary antibody (Rabbit mAb, Cell Signaling), β-actin primary antibody (Mouse mAb, Sigma), and secondary HRP-conjugated anti-Rabbit or anti-Mouse IgG Ab (Cell Signaling) were used. Immunoreactive bands were visualized by ChemiDoc MTP Imaging System (Bio-Rad) and their intensity was quantified using ImageJ software.

AR Luciferase Activity Assay

C4-2B FR cells were treated with OCM or C4-2B CM. After 24 h, AR activation was quantified using Dual-Luciferase Reporter Assay (Promega) following the manufacturer's instructions. Firefly and Renilla luciferase signals were measured sequentially by a spectrofluorometer (Tecan Infinite M200Pro). AR activity was determined normalizing firefly luciferase signal with Renilla luciferase signal (constitutively expressed signal). Specificity of the luciferase signal was checked treating C4-2B FR cells with AR agonist R1881 (1 nM) and AR-antagonist enzalutamide (35 μM) (**Supplementary Figure 1**).

Cell Cycle Analysis

Cell cycle analysis was performed on C4-2B FR cells treated with OCM or C4-2B CM for 96 h. Cell cycle was analyzed using the following gating strategy (**Figure 1**) (23). Briefly, cells were fixed and permeabilized with Foxp3/Transcription Factor Staining Buffer Set (Thermofisher eBioscience) for intracellular staining with anti-Ki67-APC antibody (clone 20Raj1 eBioscience) and a Propidium Iodide (PI) solution (50 μg/ml PI+ 40 ng/ml RNAseA+ 0.1% of Triton) (Sigma). Dead cell exclusion was performed with Fixable Viability Dye conjugated with eFluor780 fluorochrome (Affimetrix eBioscience). Samples were analyzed by CytoFlex instrument (Beckman Coulter) and using CytExpert Software, v.2.1. Raw data of cell cycle phases (percentage) are summarized in **Supplementary Figure 2**.

Proteomic Assay

Proteomic profile analysis was performed on OCM or C4-2B CM. A panel of 507 human target proteins was analyzed using the human antibody Array Membrane Kit (RayBiotech) according to the manufacturer's instructions. Band signal was detected by ChemiDoc MTP Imaging System (Bio-Rad), and their intensity was quantified using ImageLab Software (Bio-Rad).

Statistical Analysis

Data were analyzed using the Student's *t*-test and one-way ANOVA test followed by Tukey's multiple comparison tests. The graphics processing and statistical tests were performed using the program GraphPad Prism (San Diego, CA).

RESULTS

Osteoblasts Modulate CRPC Cell Gene Profile

To evaluate if OB-secreted factors influence gene expression profile of CRPC cells, transcriptomic analysis was performed on C4-2B cells treated with OCM and C4-2B CM (as control). Pathway enrichment analysis revealed a significant upregulation of cell cycle signaling pathways [false discovery rate (FDR) adjusted p-value ≤ 0.05] in C4-2B cells treated with OCM compared to control, suggesting that OCM could promote cancer proliferation. Surprisingly, AR, which represents the major driver in prostate cancer proliferation, resulted among the genes that were significantly downregulated (**Figure 2**).

Soluble Osteoblast Factors Inhibit AR and Promote CRPC Cell Proliferation

To dissect the effect of OB-secreted factors on AR signaling, we performed an "indirect" co-culture treating C4-2B FR cells with OCM or with C4-2B CM. Data confirmed that AR expression was downregulated in terms of mRNA (p = 0.0047), protein levels (p = 0.0247), and AR activity (p = 0.0029) when C4-2B FR cells grew in the presence of OCM compared to control (C4-2B CM) (**Figures 3A–C**). In addition, we found that OCM treatment significantly reduced mRNA levels of AR target genes such as Kallikrein Related Peptidase 3 (KLK3) (p = 0.02) and Transmembrane Serine Protease 2 (TMPRSS2) (p = 0.06) in C4-2B FR cells (**Figure 3D**). Next, we evaluated the effect of OCM on CRPC cell proliferation by flow cytometry. Data showed that OCM treatment increased the percentage of C4-2B in G1 (p = 0.0477) and S-G2-M (p = 0.0185) phases, but reduced the percentage of Ki-67-PI-resting cells in G0 phase (p = 0.0313) (**Figure 4**).

We obtained similar results co-culturing CRPC cells and OBs in cell–cell contact models. In particular, we set up a "direct" OBs/C4-2B FR co-culture seeding C4-2B FR cells on an OB monolayer or C4-2B FR cells on a C4-2B cell monolayer as control. Data confirmed a significant reduction of AR activity (p = 0.020) (**Figure 5A**) and a concomitant increase of C4-2B GFP+ cell proliferation when cancer cells grew in the presence of OBs. In particular, the presence of OBs augmented C4-2B GFP+ growth at 48 h (p = 0.006), 96 h (p = 0.006), and 120 h (p = 0.004) (**Figure 5B**).

Analysis of Osteoblast Secretome Identifies MMP-1 as a Key Mediator of CRPC Proliferation AR Independent

To identify potential OB soluble factors involved in AR reduction and/or CRPC proliferation, an extensive proteomic analysis was performed on OCM and C4-2B CM. Secretome analysis identified a subset of 154 molecules that were differentially expressed between OCM and C4-2B CM. After filtering analysis based on the factors overexpressed in OCM, with a fold change > 2, we identified 9 soluble molecules: TIMP metallopeptidase inhibitor 2 (TIMP-2), TIMP metallopeptidase inhibitor 1 (TIMP-1), Monocyte chemoattractant protein-1

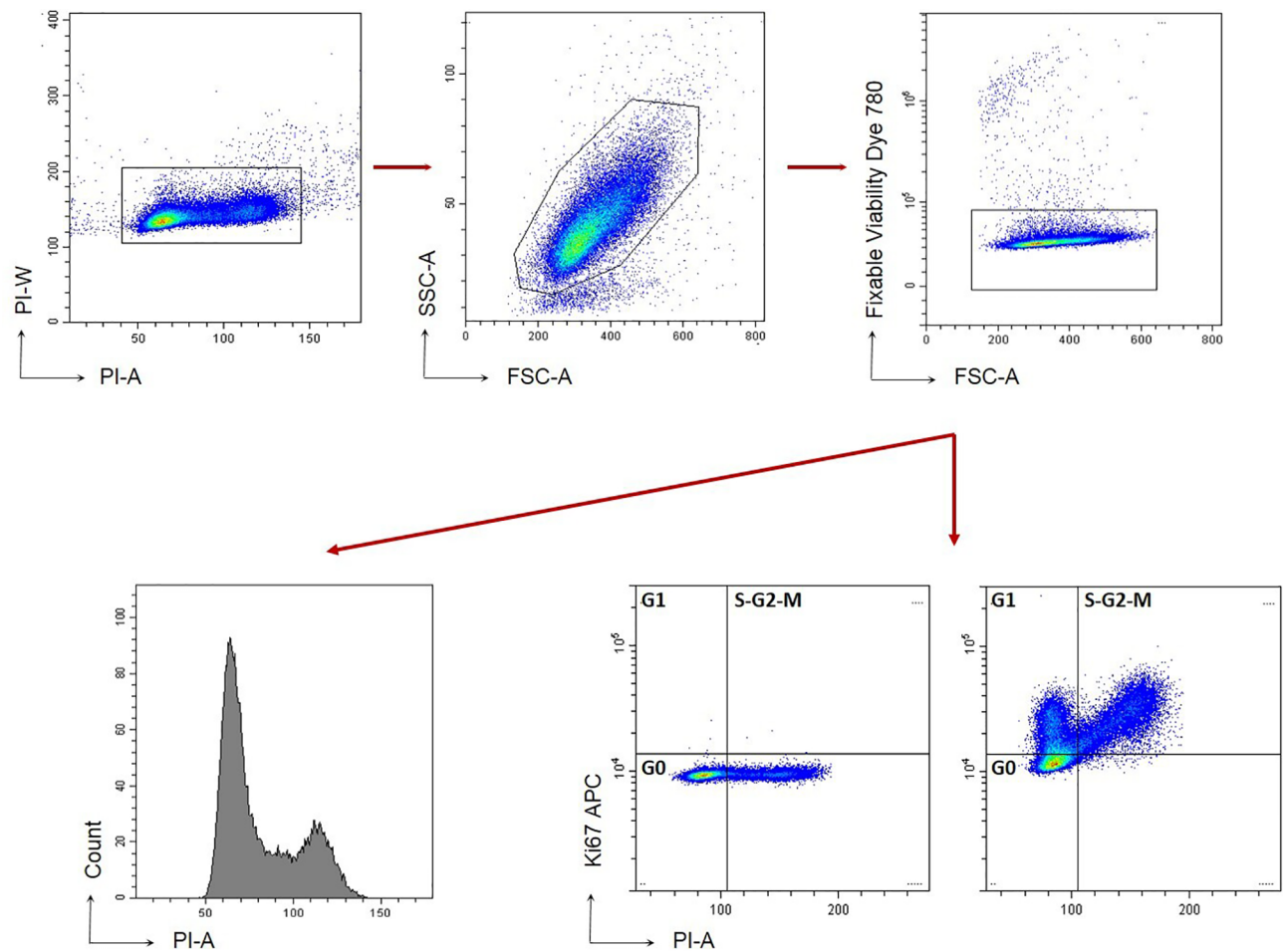

FIGURE 1 | Gating strategy for C4-2B cell cycle. Cells are stained with FVD to exclude death cells (FVD+). Gating strategy based on Forward and Side scatter is shown.

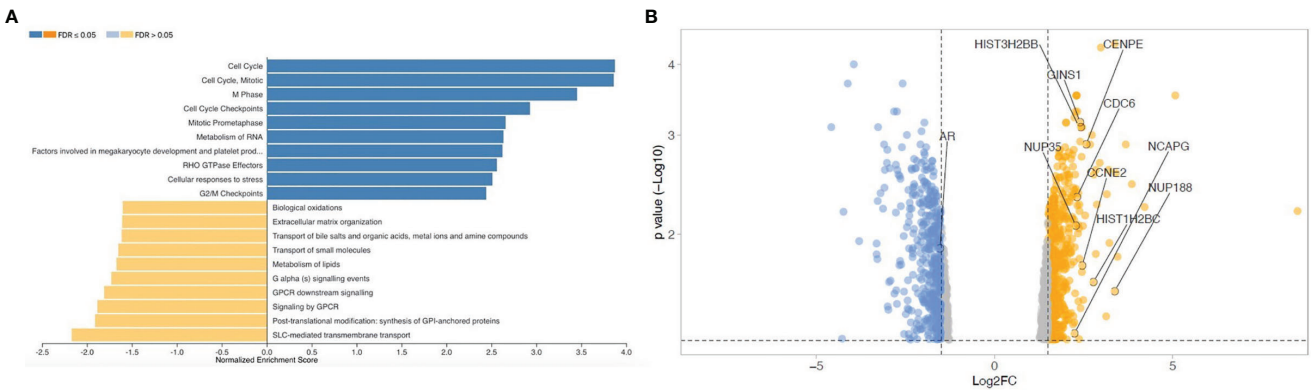

FIGURE 2 | Transcriptomic analysis on C4-2B FR treated with OCM and C4-2B CM. **(A)** Gene set enrichment analysis and **(B)** Volcano plot of down- (blue) and upregulated genes (red) in C4-2B FR treated with OCM (fold change ˃1.5). Top 10 genes ranked by enrichment score for gene set "cell cycle R-HAS-1640170 REACTOME" and androgen receptor (AR) are labeled.

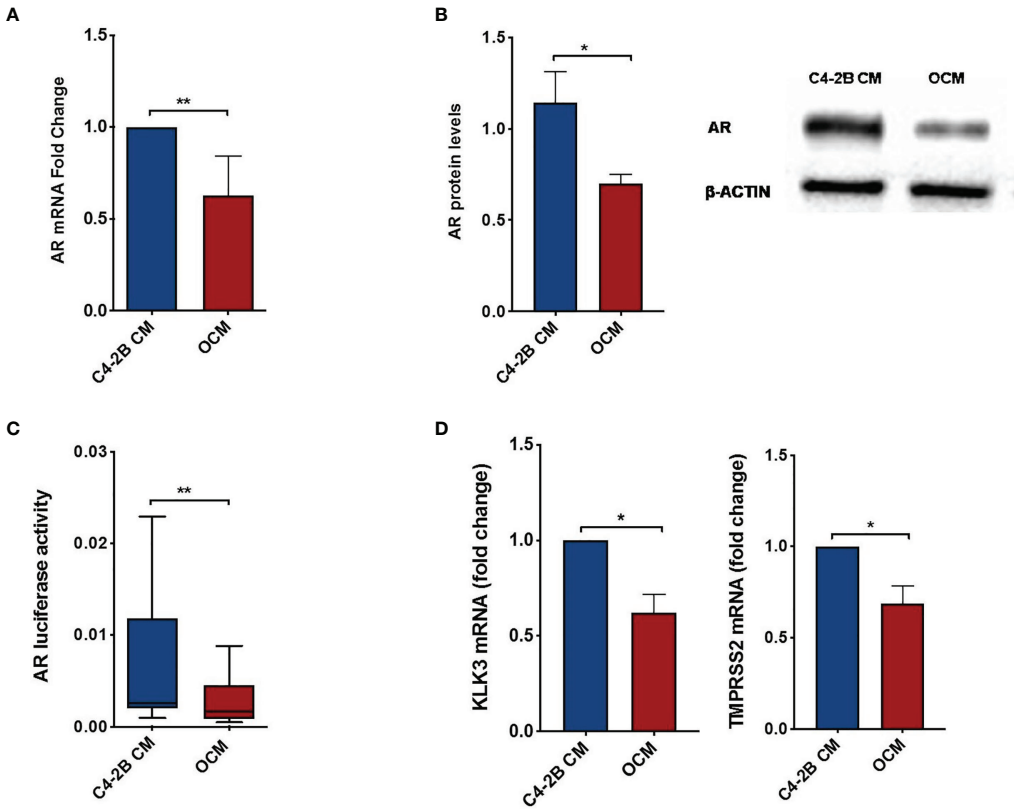

FIGURE 3 | AR and AR-target gene expression in C4-2B FR cells after OCM treatment. **(A)** AR mRNA levels normalized for the housekeeping β-glucoronidase (GUS-β). Values are expressed as fold change relative to the control. **(B)** Representative image and schematic representation of AR protein expression normalized for the housekeeping β-actin. **(C)** AR activity of C4-2B FR cells measured as firefly luciferase signal normalized with Renilla luciferase signal (housekeeping control). **(D)** KLK3 and TMPRSS2 mRNA levels were normalized for the housekeeping β-glucoronidase (GUS-β). Values are expressed as fold change relative to the control.*$p < 0.05$; **$p < 0.001$.

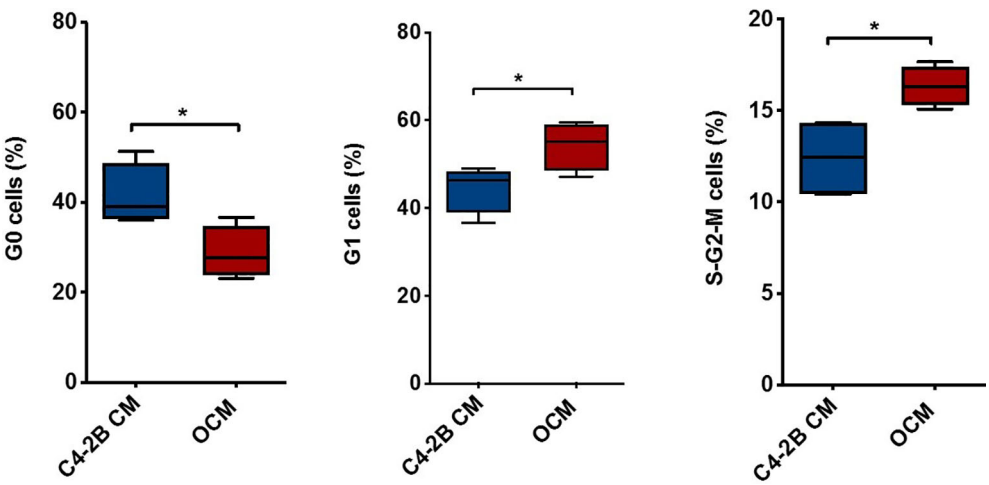

FIGURE 4 | Combination of PI and Ki-67 staining in C4-2B FR cells treated with OCM. Schematic representation of C4-2B cells percentage in G0, G1, and S-G2-M phases after OCM treatment with average value (bar). Cytometry profiles are representative of data from 4 different experiments. *$p < 0.05$.

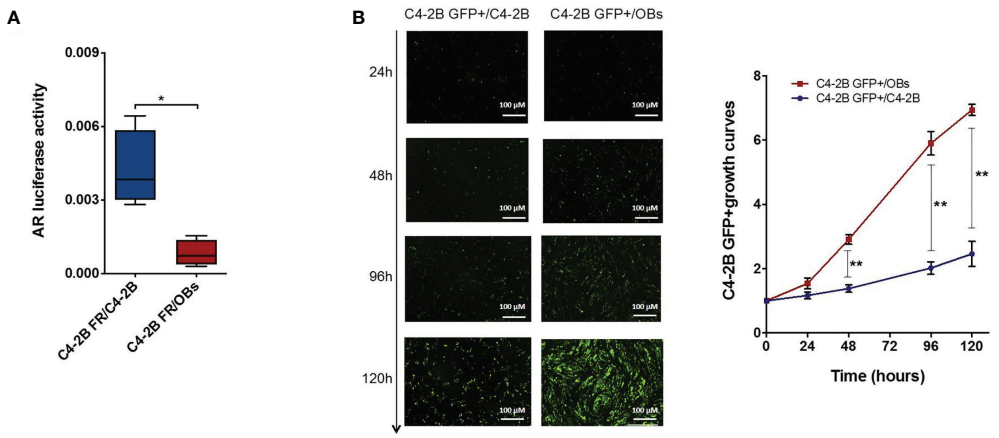

FIGURE 5 | AR activity C4-2B FR cells and proliferation analysis of C4-2B GFP+ cells in "direct" co-culture with OBs. **(A)** AR activity measured as firefly luciferase signal normalized with Renilla luciferase signal (housekeeping control). **(B)** Representative images of direct co-cultures captured at 24, 48, 96, and 120 h after C4-2B GFP+ cell (green) seeding; scale bar = 100 µm. Proliferation curves C4-2B GFP+ cells co-cultured with OBs (red) or C4-2B as control (blue). GFP+ signal at each time point was normalized with GFP signal at baseline *$p < 0.05$; **$p < 0.001$.

(MCP-1), C-X-C Motif Chemokine Ligand 2 (CXCL-2), C-X-C Motif Chemokine Ligand 1 (CXCL-1), Matrix metalloproteinase-1 (MMP-1), Dickkopf-1 (DKK-1), Ectodysplasin A2 (EDA-A2), and Insulin Like Growth Factor Binding Protein 7 (IGFBP-7) (**Figure 6**).

To investigate if one or some of these factors influenced AR activity, we treated C4-2B FR cells with C4-2B CM adding different dosages of each molecule (**Supplementary Figure 3A**). We found that DKK-1 (1 ng/ml $p = 0.03$; 10 ng/ml $p = 0.04$), EDA-A2 (1 ng/ml $p = 0.04$; 10 ng/ml $p = 0.03$), IGFBP-7 (50 ng/ml $p = 0.03$), and MMP-1 (0.1 ng/ml $p = 0.006$; 1 ng/ml $p = 0.002$; 10 ng/ml $p = 0.0001$) significantly reduced AR activity (**Figure 7**).

Then, we tested the effect of these factors on CRPC proliferation through flow cytometry. Data showed that only MMP-1 was able to increase S-G2-M phases (1 ng/ml $p = 0.009$; 10 ng/ml $p = 0.033$) (**Figure 8A** and **Supplementary Figure 3B**). Based on these results, we performed further analyses to confirm the direct involvement of MMP-1 in AR signal downregulation and CRPC proliferation. In particular, data showed that MMP-1 significantly reduced AR mRNA levels (0.1 ng/ml $p = 0.024$; 1 ng/ml $p < 0.001$; 10 ng/ml $p < 0.001$) (**Supplementary Figure 4**). Moreover, to confirm that MMP-1 is directly involved in CRPC proliferation through the activation of its receptor, Protease-activated receptor-1 (PAR-1), we treated C4-2B FR with OCM plus Vorapaxar (0.01 µM, 0.1 µM, and 1 µM), a specific PAR-1 inhibitor. As shown in **Figure 8B**, Vorapaxar significantly reduced S-G2-M cell cycle phases (0.1 µM $p = 0.014$; 1 µM $p = 0.0087$), confirming that MMP-1/PAR-1 could be one of the signaling pathways involved in AR-independent CRPC proliferation.

DISCUSSION

Our results provide a novel AR-independent mechanism of CRPC proliferation mediated by OBs. In the current study, we demonstrated that OB-secreted factors reduced AR activity, but, surprisingly, induced the growth of prostate cancer cells.

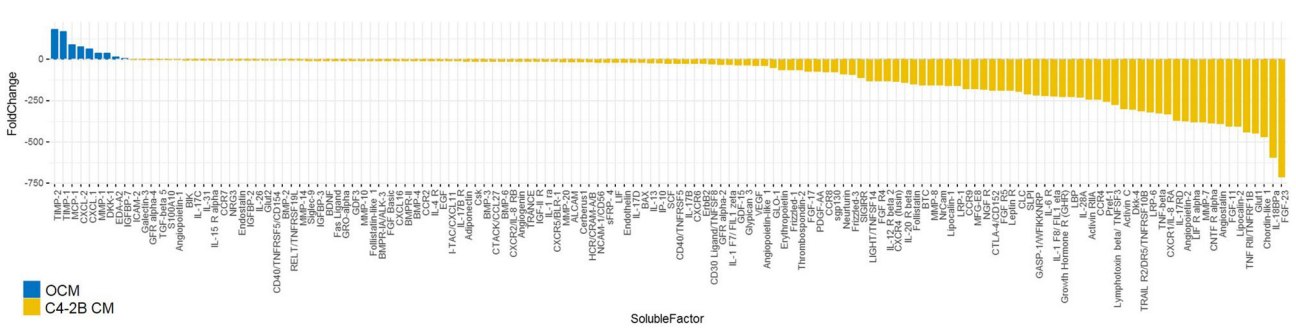

FIGURE 6 | Waterfall plot of soluble molecules differentially expressed in OCM compared to C4-2B CM (expressed as fold change). Proteomic analysis was performed on OCM pooled from three different donors and C4-2B CM from three different cell passages; molecules overexpressed in OCM with a fold change > 2 (blue) and downregulated fold change < 2 (yellow) are reported.

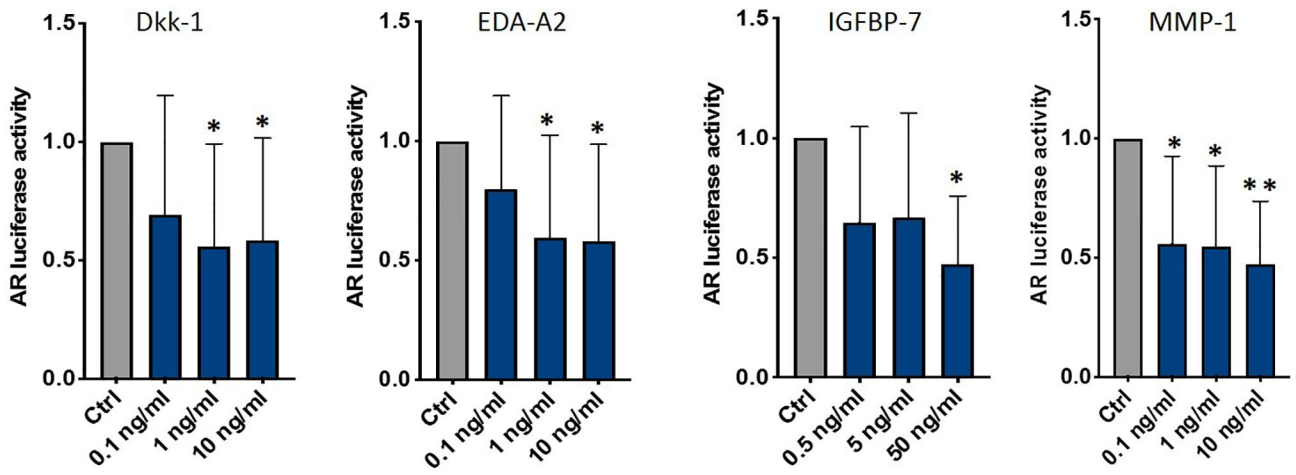

FIGURE 7 | AR activity of C4-2B FR cultured in C4-2B CM supplemented with DKK-1, EDA-A2, IGFBP-7, and MMP-1; *$p < 0.05$; **$p < 0.001$.

Proteomic analysis identified some soluble factors highly expressed in OCM compared to C4-2B CM, and, among these, four molecules were able to reduce AR activation, namely, DKK-1, MMP-1, EDA-A2, and IGFBP-7. Intriguingly, MMP-1 had the ability to decrease AR signal and, concomitantly, enhance prostate cancer cell proliferation. However, the increase in C4-2B cell growth induced by MMP-1 did not reach the proliferation levels observed after OCM treatment, suggesting that MMP-1 may not be the only factor responsible for AR-independent CRPC proliferation. MMP-1 is a potent agonist for PAR1, a G-protein-coupled receptor (GPCR) that plays critical roles in thrombosis, inflammation, and vascular biology (24). Moreover, several lines of evidence reported that PAR1 is also involved in the invasive and metastatic processes of various cancers (25–29). Thus, to evaluate if the MMP-1/PAR-1 axis was involved in OB-mediated CRPC proliferation, we treated C4-2B cells with Vorapaxar, a specific PAR-1 inhibitor. Intriguingly, C4-2B cell cycle was significantly reduced after treatment, confirming the potential role of MMP-1/PAR-1 pathway in tumor growth. Some studies reported that MMP-1 was mainly secreted by stromal cells, such as OBs and fibroblasts, in prostate and breast tumor microenvironment and promoted cancer cell migration and invasion through PAR-1 signaling (30, 31). In addition, cDNA microarray analysis revealed an increased

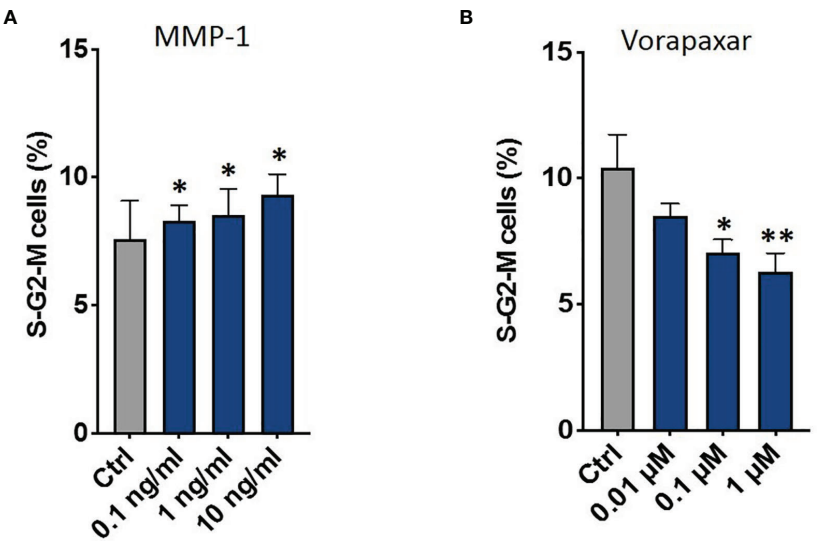

FIGURE 8 | Combination of PI and Ki-67 staining in C4-2B FR cells treated with OCM. Schematic representation of C4-2B cells percentage in S-G2-M phases treated with C4-2B CM supplemented with MMP-1 **(A)** and with OCM in the presence of different dosages of vorapaxar **(B)**. *p < 0.05; **p < 0.001.

expression of PAR1 on bone-derived prostate cancer cell lines (32), confirming the role of bone microenvironment in promoting MMP-1/PAR1 pathway activation.

Similar to the current study, previous papers reported that OBs contribute to prostate tumor proliferation in *in vitro* co-culture models of OBs and prostate cancer cell lines (33–36). In particular, Blaszczyket et al. demonstrated that interleukin-6 secreted by OBs stimulated the androgen-independent proliferation of prostate cancer cells by a mechanism that was partially AR dependent (33). However, data were obtained on LNCaP cells, a hormone-sensitive prostate cancer cell line that differs from C4-2B cells, which represent the best characterized castration-resistant bone metastatic model (37). In addition, Thulin and colleagues reported a key role of OBs as mediators of CRPC cell growth in bone through the stimulation of the intratumoral steroidogenesis. Differently from us, the authors used immortalized murine calvarial cell line MC3T3-E1 that did not completely resemble the physiological bone microenvironment (34). More recently, another study proposed an interesting *in vitro* 3D model to investigate the OBs/prostate cancer cell crosstalk. This more complex co-culture system highlighted the crucial involvement of OBs in prostate cancer progression (35). Moreover, preclinical studies showed that prostate cancer cells induced a strong osteogenic response (36) as well as the co-injection of bone stromal cells and human prostate cancer cells enhanced tumor formation in mice (17, 38). However, how osteoblasts supported tumor growth was not fully clarified. Sung et al. (17) identified extracellular matrix proteins versican and tenascin and chemokine ligands CXCL5 and CXCL16, released by stromal cells, as potential mediators of prostate cancer cell proliferation. Moreover, transcriptomic analysis of the stroma compartment of bones xenografted with human CRPC cells showed that some genes were upregulated in mouse stromal cells including PTN, EPHA3, and FSCN1 (39). These data suggest that a combination of stromal secreted factors, rather than one, could provide a support for prostate cancer cells. Taken together, these lines of evidence highlight the crucial role of bone microenvironment in supporting prostate cancer progression, but the identification of the cellular and molecular determinants remains an important unsolved question.

In this complex but fascinating scenario, our results reveal a novel potential mechanism of proliferation induced by OBs through an AR-independent mechanisms. Paradoxically, we found that AR signaling remained very low in bone microenvironment, and these findings have been confirmed at different levels, i.e., mRNA, protein, and functional activity. Although we consider this phenomenon real, we are not able to insert it in any biological frameworks given by previous literature data. Indeed, to our knowledge, no identified pathway can simultaneously inhibit AR and stimulate CRPC proliferation. Thus, MMP-1/PAR-1 could be one of the potential pathways able to promote AR-independent CRPC proliferation. However, further extensive investigations are warranted to completely elucidate the mechanisms that fully explain the data we observed. This represents the major limitation of the study.

To date, all mechanisms identified as responsible for CRPC progression or resistance to antiandrogens directly involved AR signaling. These include AR amplification and hypersensitivity (40), AR mutations (41), alterations in coactivators/corepressors (42), androgen-independent AR activation (43), intratumoral and alternative androgen production (44), and AR splice variants (45, 46). Here, we found that the AR axis could not be the only driver of disease progression, in bone metastatic niche, but it could be bypassed by alternative signaling pathways. Indeed, this inhibitory effect exerted by OB on AR activity could induce tumor cells to promote alternative molecular pathways of proliferation. Thus, bone microenvironment could provide novel potential mechanisms of resistance to second-generation AR inhibitors and, in particular, the MMP-1/PAR-1 axis could represent a new druggable pathway deserving of further studies.

DATA AVAILABILITY STATEMENT

The original contributions presented in the study are included in the article/**Supplementary Material**. Further inquiries can be directed to the corresponding author.

AUTHOR CONTRIBUTIONS

GR: Methodology and Data analysis. SS: Methodology and Data analysis. MI: Data analysis and Writing—Original draft preparation. ER: Methodology. BV: Data analysis. GT: Supervision and Reviewing. FP: Study design and Data interpretation. DS: Critical revision of the manuscript. All authors contributed to the article and approved the submitted version.

SUPPLEMENTARY MATERIAL

The Supplementary Material for this article can be found online at: https://www.frontiersin.org/articles/10.3389/fonc.2021.789885/full#supplementary-material

Supplementary Figure 1 | AR activity of C4-2B FR cells after treatment with R1881 (1nM) and enzalutamide (35μM) measured as firefly-luciferase signal normalized with renilla-luciferase signal. *p < 0.05.

Supplementary Figure 2 | Percentage of cell cycle phases (raw data).

Supplementary Figure 3 | (A) AR activity of C4-2B FR cultured in C4-2B CM supplemented with CXCL-1, CXCL-2, MCP-1, TIMP-1 and TIMP-2. **(B)** Schematic representation of C4-2B cells percentage in S-G2-M phases treated with C4-2B CM supplemented with DKK-1, IGFBP-7 and EDA-A2.

Supplementary Figure 4 | MMP-1 mRNA levels normalized for the housekeeping β-glucoronidase (GUS-β). Values are expressed as fold change relative to the control. *p < 0.05; **p < 0.001.

REFERENCES

1. Harris WP, Mostaghel EA, Nelson PS, Montgomery B. Androgen Deprivation Therapy: Progress in Understanding Mechanisms of Resistance and Optimizing Androgen Depletion. *Nat Clin Pract Urol* (2009) 6:76–85. doi: 10.1038/ncpuro1296
2. Chandrasekar T, Yang JC, Gao AC, Evans CP. Mechanisms of Resistance in Castration-Resistant Prostate Cancer (CRPC). *Trans Androl Urol* (2015) 4:365–80. doi: 10.3978/j.issn.2223-4683.2015.05.02
3. Rice MA, Malhotra SV, Stoyanova T. Second-Generation Antiandrogens: From Discovery to Standard of Care in Castration Resistant Prostate Cancer. *Front Oncol* (2019) 28:801. doi: 10.3389/fonc.2019.00801
4. Wadosky KM, Koochekpour S. Androgen Receptor Splice Variants and Prostate Cancer: From Bench to Bedside. *Oncotarget* (2017) 8:18550–76. doi: 10.18632/oncotarget.14537
5. Locke JA, Guns ES, Lubik AA, Adomat HH, Hendy SC, Wood CA, et al. Androgen Levels Increase by Intratumoral *De Novo* Steroidogenesis During Progression of Castration-Resistant Prostate Cancer. *Cancer Res* (2008) 68:6407–15. doi: 10.1158/0008-5472.CAN-07-5997
6. Takayama KI. Splicing Factors Have an Essential Role in Prostate Cancer Progression and Androgen Receptor Signaling. *Biomolecules* (2019) 9:131. doi: 10.3390/biom9040131
7. Kobayashi T, Inoue T, Kamba T, Ogawa O. Experimental Evidence of Persistent Androgen-Receptor-Dependency in Castration-Resistant Prostate Cancer. *Int J Mol Sci* (2013) 14:15615–35. doi: 10.3390/ijms140815615
8. Hensel J, Thalmann GN. Biology of Bone Metastases in Prostate Cancer. *Urology* (2016) 92:6–13. doi: 10.1016/j.urology.2015.12.039
9. Coleman RE. Clinical Features of Metastatic Bone Disease and Risk of Skeletal Morbidity. *Clin Cancer Res* (2006) 12:6243s–9s. doi: 10.1158/1078-0432.CCR-06-0931
10. Mundy GR. Metastasis to Bone: Causes, Consequences and Therapeutic Opportunities. *Nat Rev Cancer* (2002) 2:584–93. doi: 10.1038/nrc867
11. Logothetis CJ, Lin SH. Osteoblasts in Prostate Cancer Metastasis to Bone. *Nat Rev Cancer* (2005) 5:21–8. doi: 10.1038/nrc1528
12. Turner CJ, Edwards CM. The Role of the Microenvironment in Prostate Cancer-Associated Bone Disease. *Curr Osteoporos Rep* (2016) 14:170–7. doi: 10.1007/s11914-016-0323-2
13. Mundy GR. Malignancy and the Skeleton. *Horm Metab Res* (1997) 29:120–7. doi: 10.1055/s-2007-979004
14. Ottewell PD. The Role of Osteoblasts in Bone Metastasis. *J Bone Oncol* (2016) 5:124–7. doi: 10.1016/j.jbo.2016.03.007
15. Zhang S, Wang J, Bilen MA, Lin SH, Stupp SI, Satcher RL. Modulation of Prostate Cancer Cell Gene Expression by Cell-to-Cell Contact With Bone Marrow Stromal Cells or Osteoblasts. *Clin Exp Metastasis* (2009) 26:993–1004. doi: 10.1007/s10585-009-9289-0
16. Li Y, Sikes RA, Malaeb BS, Yeung F, Law A, Graham SE, et al. Osteoblasts can Stimulate Prostate Cancer Growth and Transcriptionally Down-Regulate PSA Expression in Cell Line Models. *Urol Oncol* (2011) 29:802–8. doi: 10.1016/j.urolonc.2009.09.016
17. Sung SY, Hsieh CL, Law A, Zhau HE, Pathak S, Multani AS, et al. Coevolution of Prostate Cancer and Bone Stroma in Three-Dimensional Coculture: Implications for Cancer Growth and Metastasis. *Cancer Res* (2008) 68:9996–10003. doi: 10.1158/0008-5472.CAN-08-2492
18. Thalmann N, Anezinis PE, Chang SM, Zhau HE, Kim EE, Hopwood VL, et al. Androgen-Independent Cancer Progression and Bone Metastasis in the LNCaP Model of Human Prostate Cancer. *Cancer Res* (1994) 54:2577–82.
19. Iuliani M, Simonetti S, Pantano F, Ribelli G, Di Martino A, Denaro V, et al. Antitumor Effect of Cabozantinib in Bone Metastatic Models of Renal Cell Carcinoma. *Biology (Basel)* (2021) 16:781. doi: 10.3390/biology10080781
20. Iuliani M, Pantano F, Buttigliero C, Fioramonti M, Bertaglia V, Vincenzi B, et al. Biological and Clinical Effects of Abiraterone on Anti-Resorptive and Anabolic Activity in Bone Microenvironment. *Oncotarget* (2015) 6:12520–8. doi: 10.18632/oncotarget.3724
21. Thomas JG, Olson JM, Tapscott SJ, Zhao LP. An Efficient and Robust Statistical Modeling Approach to Discover Differentially Expressed Genes Using Genomic Expression Profiles. *Genome Res* (2001) 11:1227–36. doi: 10.1101/gr.165101
22. Liao Y, Wang J, Jaehnig EJ, Shi Z, Zhang B. WebGestalt 2019: Gene Set Analysis Toolkit With Revamped UIs and APIs. *Nucleic Acids Res* (2019) 47: W199–205. doi: 10.1093/nar/gkz401
23. Simonetti S, Natalini A, Folgori A, Capone S, Nicosia A, Santoni A, et al. Antigen-Specific CD8 T Cells in Cell Cycle Circulate in the Blood After Vaccination. *Scand J Immunol* (2019) 89:e12735. doi: 10.1111/sji.12735
24. Gieseler F, Ungefroren H, Settmacher U, Hollenberg MD, Kaufmann R. Proteinase-Activated Receptors (PARs) - Focus on Receptor-Receptor-Interactions and Their Physiological and Pathophysiological Impact. *Cell Commun Signal* (2013) 11:86. doi: 10.1186/1478-811X-11-86
25. Even-Ram S, Uziely B, Cohen P, Grisaru-Granovsky S, Maoz M, Ginzburg Y, et al. Thrombin Receptor Overexpression in Malignant and Physiological Invasion Processes. *Nat Med* (1998) 4:909–14. doi: 10.1038/nm0898-909
26. Yang E, Cisowski J, Nguyen N, O'Callaghan K, Xu J, Agarwal A, et al. Dysregulated Protease Activated Receptor 1 (PAR1) Promotes Metastatic Phenotype in Breast Cancer Through HMGA2. *Oncogene* (2016) 35:1529–40. doi: 10.1038/onc.2015.217
27. Kancharla A, Maoz M, Jaber M, Agranovich D, Peretz T, Grisaru-Granovsky S, et al. PH Motifs in PAR1&2 Endow Breast Cancer Growth. *Nat Commun* (2015) 6:8853. doi: 10.1038/ncomms9853
28. Salah Z, Maoz M, Pokroy E, Lotem M, Bar-Shavit R, Uziely B. Protease-Activated Receptor-1 (Hpar1), A Survival Factor Eliciting Tumor Progression. *Mol Cancer Res* (2007) 5:229–40. doi: 10.1158/1541-7786.MCR-06-0261
29. Zhang Y, Zhan H, Xu W, Yuan Z, Lu P, Zhan L, et al. Upregulation of Matrix Metalloproteinase-1 and Proteinase-Activated Receptor-1 Promotes the Progression of Human Gliomas. *Pathol Res Pract* (2011) 207:24–9. doi: 10.1016/j.prp.2010.10.003
30. Boire A, Covic L, Agarwal A, Jacques S, Sherifi S, Kuliopulos A. PAR1 is a Matrix Metalloprotease-1 Receptor That Promotes Invasion and Tumorigenesis of Breast Cancer Cells. *Cell* (2005) 120:303–13. doi: 10.1016/j.cell.2004.12.018
31. Forbes K, Webb MA, Sehgal I. Growth Factor Regulation of Secreted Matrix Metalloproteinase and Plasminogen Activators in Prostate Cancer Cells, Normal Prostate Fibroblasts and Normal Osteoblasts. *Prostate Cancer Prostatic Dis* (2003) 6:148–53. doi: 10.1038/sj.pcan.4500640
32. Chay CH, Cooper CR, Gendernalik JD, Dhanasekaran SM, Chinnaiyan AM, Rubin MA, et al. A Functional Thrombin Receptor (PAR1) Is Expressed on Bone-Derived Prostate Cancer Cell Lines. *Urology* (2002) 60:760–5. doi: 10.1016/S0090-4295(02)01969-6
33. Blaszczyk N, Masri BA, Mawji NR, Ueda T, McAlinden G, Duncan CP, et al. Osteoblast-Derived Factors Induce Androgen-Independent Proliferation and Expression of Prostate-Specific Antigen in Human Prostate Cancer Cells. *Clin Cancer Res* (2004) 10:1860–9. doi: 10.1158/1078-0432.CCR-0974-3
34. Hagberg Thulin M, Nilsson ME, Thulin P, Céraline J, Ohlsson C, Damber JE, et al. Osteoblasts Promote Castration-Resistant Prostate Cancer by Altering Intratumoral Steroidogenesis. *Mol Cell Endocrinol* (2016) 422:182–91. doi: 10.1016/j.mce.2015.11.013
35. Bock N, Shokoohmand A, Kryza T, Röhl J, Meijer J, Tran PA, et al. Engineering Osteoblastic Metastases to Delineate the Adaptive Response of Androgen-Deprived Prostate Cancer in the Bone Metastatic Microenvironment. *Bone Res* (2019) 7:13. doi: 10.1038/s41413-019-0049-8
36. Li ZG, Mathew P, Yang J, Starbuck MW, Zurita AJ, Liu J, et al. Androgen Receptor-Negative Human Prostate Cancer Cells Induce Osteogenesis in Mice Through FGF9-Mediated Mechanisms. *J Clin Invest* (2008) 118:2697–710. doi: 10.1172/JCI33093
37. Pfitzenmaier J, Quinn JE, Odman AM, Zhang J, Keller ET, Vessella RL, et al. Characterization of C4-2 Prostate Cancer Bone Metastases and Their Response to Castration. *J Bone Miner Res* (2003) 18:1882–8. doi: 10.1359/jbmr.2003.18.10.1882
38. Gleave M, Hsieh JT, Gao CA, von Eschenbach AC, Chung LW. Acceleration of Human Prostate Cancer Growth *In Vivo* by Factors Produced by Prostate and Bone Fibroblasts. *Cancer Res* (1991) 51:3753–61.
39. Ozdemir BC, Hensel J, Secondini C, Wetterwald A, Schwaninger R, Fleischmann A, et al. The Molecular Signature of the Stroma Response in Prostate Cancer-Induced Osteoblastic Bone Metastasis Highlights Expansion of Hematopoietic and Prostate Epithelial Stem Cell Niches. *PloS One* (2014) 9: el 14530. doi: 10.1371/journal.pone.0114530
40. Gregory CW, Johnson RTJr, Mohler JL, French FS, Wilson EM. Androgen Receptor Stabilization in Recurrent Prostate Cancer Is Associated With Hypersensitivity to Low Androgen. *Cancer Res* (2001) 61:2892–8.

41. Taylor BS, Schultz N, Hieronymus H, Taylor BS, Schultz N, Hieronymus H, et al. Integrative Genomic Profiling of Human Prostate Cancer. *Cancer Cell* (2010) 18:11–22. doi: 10.1016/j.ccr.2010.05.026
42. Wolf IM, Heitzer MD, Grubisha M, DeFranco DB. Coactivators and Nuclear Receptor Transactivation. *J Cell Biochem* (2008) 104:1580–6. doi: 10.1002/jcb.21755
43. Wang Q, Li W, Zhang Y, Yuan X, Xu K, Yu J, et al. Androgen Receptor Regulates a Distinct Transcription Program in Androgen-Independent Prostate Cancer. *Cell* (2009) 138:245–56. doi: 10.1016/j.cell.2009.04.056
44. Montgomery RB, Mostaghel EA, Vessella R, Hess DL, Kalhorn TF, Higano CS, et al. Maintenance of Intratumoral Androgens in Metastatic Prostate Cancer: A Mechanism for Castration-Resistant Tumor Growth. *Cancer Res* (2008) 68:4447–54. doi: 10.1158/0008-5472.CAN-08-0249
45. Guo Z, Yang X, Sun F, Jiang R, Linn DE, Chen H, et al. A Novel Androgen Receptor Splice Variant Is Up-Regulated During Prostate Cancer Progression and Promotes Androgen Depletion-Resistant Growth. *Cancer Res* (2009) 69:2305–13. doi: 10.1158/0008-5472.CAN-08-3795
46. Obinata D, Lawrence MG, Takayama K, Choo N, Risbridger GP, Takahashi S, et al. Recent Discoveries in the Androgen Receptor Pathway in Castration-Resistant Prostate Cancer. *Front Oncol* (2020) 8:581515. doi: 10.3389/fonc.2020.581515

Conflict of Interest: The authors declare that the research was conducted in the absence of any commercial or financial relationships that could be construed as a potential conflict of interest.

Publisher's Note: All claims expressed in this article are solely those of the authors and do not necessarily represent those of their affiliated organizations, or those of the publisher, the editors and the reviewers. Any product that may be evaluated in this article, or claim that may be made by its manufacturer, is not guaranteed or endorsed by the publisher.

frontiers in Cell and Developmental Biology

REVIEW
published: 20 December 2021
doi: 10.3389/fcell.2021.783617

Heterogeneous Pancreatic Stellate Cells Are Powerful Contributors to the Malignant Progression of Pancreatic Cancer

Zhilin Zhang[1‡], Huan Zhang[1‡], Tian Liu[1], Tian Chen[1], Daorong Wang[2] and Dong Tang[2†]*

[1]Clinical Medical College, Yangzhou University, Yangzhou, China, [2]Department of General Surgery, Northern Jiangsu People's Hospital, Clinical Medical College, Institute of General Surgery, Yangzhou University, Yangzhou, China

Pancreatic cancer is associated with highly malignant tumors and poor prognosis due to strong therapeutic resistance. Accumulating evidence shows that activated pancreatic stellate cells (PSC) play an important role in the malignant progression of pancreatic cancer. In recent years, the rapid development of single-cell sequencing technology has facilitated the analysis of PSC population heterogeneity, allowing for the elucidation of the relationship between different subsets of cells with tumor development and therapeutic resistance. Researchers have identified two spatially separated, functionally complementary, and reversible subtypes, namely myofibroblastic and inflammatory PSC. Myofibroblastic PSC produce large amounts of pro-fibroproliferative collagen fibers, whereas inflammatory PSC express large amounts of inflammatory cytokines. These distinct cell subtypes cooperate to create a microenvironment suitable for cancer cell survival. Therefore, further understanding of the differentiation of PSC and their distinct functions will provide insight into more effective treatment options for pancreatic cancer patients.

Keywords: inflammation, fibrosis, pancreatic stellate cells, pancreatic neoplasms, antineoplastic protocols

OPEN ACCESS

Edited by:
Francesca Pirini,
Istituto Scientifico Romagnolo per lo Studio e la Cura dei Tumori (IRCCS), Italy

Reviewed by:
Yuan Seng Wu,
Sunway University, Malaysia
Shin Hamada,
Tohoku University, Japan
Richard T. Waldron,
Cedars Sinai Medical Center, United States

***Correspondence:**
Dong Tang
83392785@qq.com

***Present address:**
Dong Tang,
Department of General Surgery, Northern Jiangsu People's Hospital, Clinical Medical College, Institute of General Surgery, Yangzhou University, Yangzhou, China

These authors have contributed equally to this work

Specialty section:
This article was submitted to Molecular and Cellular Oncology, a section of the journal Frontiers in Cell and Developmental Biology

Received: *26 September 2021*
Accepted: *24 November 2021*
Published: *20 December 2021*

Citation:
Zhang Z, Zhang H, Liu T, Chen T, Wang D and Tang D (2021) Heterogeneous Pancreatic Stellate Cells Are Powerful Contributors to the Malignant Progression of Pancreatic Cancer. Front. Cell Dev. Biol. 9:783617. doi: 10.3389/fcell.2021.783617

1 INTRODUCTION

Pancreatic cancer is among the most deadly forms of cancer, with a mortality-to-incidence ratio of 0.82 in 2020 and a 5 year survival rate of about 9% (Mizrahi et al., 2020). Associated symptoms typically go undetected until the advanced stages of the disease, resulting in great difficulty in early diagnosis (Kamisawa et al., 2016). Although surgical resection remains the preferred treatment option for pancreatic cancer patients, it is not effective in cases involving distant metastases. Interstitial cells, especially pancreatic stellate cells (PSC), play an important role in the malignant progression and treatment resistance observed in pancreatic cancer patients. PSC promote the fibrosis and inflammatory response of the tumor microenvironment by producing a large number of collagen fibers, exosomes, and soluble factors, which provide the basis for the proliferation, migration, and immune escape of pancreatic cancer cells (Wang et al., 2020), (Wang et al., 2017). More importantly, PSC play an extremely critical role in promoting the epithelial-mesenchymal transition (EMT) of cancer cells and enhancing cancer cell stemness. PSC promote EMT in pancreatic cancer cells by secreting exosomal microRNA-21 (Ma et al., 2020). It was shown that PSC also induce cancer stem cell-like properties in cancer cells through the secretion of osteopontin (Cao et al., 2019). Moreover, PSC also promote EMT in cancer cells by

secreting hepatocyte growth factor (Xu et al., 2020), and the hepatocyte growth factor also promotes the expression of cancer stem cell pluripotency markers in cancer cells (Yan et al., 2018).

With the rapid development of single-cell sequencing technology, the heterogeneity of PSC populations has been recently investigated and attracted the attention of researchers, as this may provide a potential therapeutic route to targeting the tumor microenvironment (Pothula et al., 2020). Recently, researchers have identified two spatially separated, functionally complementary, and reversible subtypes of PSC in pancreatic cancer tissues, namely myofibroblastic and inflammatory PSC. Myofibroblastic PSC, characterized by elevated a-smooth muscle actin (α-SMA) expression, produce large amounts of pro-fibroproliferative collagen fibers, whereas inflammatory PSC express large amounts of inflammatory cytokines. Importantly, these two subtypes of PSC have been shown to operate synergistically to promote the progression of pancreatic cancer (Öhlund et al., 2017). Other PSC subtypes have also been identified. Cluster of differentiation (CD) 10-positive PSC assists in cancer cell invasion (Ikenaga et al., 2010). Bcl2-associated athanogene- or fibroblast activation protein (FAP)-positive PSC not only enhance cancer cell migration but also promote fibrosis (Yuan et al., 2019), (Feig et al., 2013). There are even examples of differentiation among tumor suppressor subtypes, such as subsets expressing CD271 or Meflin (Nielsen et al., 2018), (Mizutani et al., 2019). However, improving patient survival requires a more detailed understanding of the mechanisms underlying PSC differentiation and their role in tumor malignancy. In the present review, we discuss the differentiation mechanism and cancer-promoting functions of myofibroblastic and inflammatory PSC. Moreover, we propose a more effective approach to manage treatment resistance in pancreatic cancer, at the level of PSC heterogeneity.

ARTICLE CATEGORY: REVIEW

Differentiation Mechanism of Myofibroblastic and Inflammatory PSC

Cancer-associated fibroblasts (CAF) that are induced by cancer cells are mesenchymal-derived cells and play an active role in promoting pancreatic cancer progression. CAF in the pancreas are highly heterogeneous, and researchers have recently identified cancer-promoting inflammatory CAF and myofibroblastic CAF as well as cancer-suppressing CAF that exert antigen-presenting ability (Hosein et al., 2020). Different groups of CAF have very different functions, for example, inflammatory CAF mainly lead to the inflammatory response of cancer stroma, while myofibroblastic CAF mainly lead to stroma fibrosis. apCAF, which play an antigen-presenting role, can inhibit tumorigenesis (Sahai et al., 2020). In addition, the sources of CAF are again extensive. Currently, a prevailing view is that the main source of CAF is the quiescent PSC in the pancreas. However, it has also been shown that adipose-derived mesenchymal stem cells can differentiate into CAF *in vitro* and *in vivo* (Miyazaki et al., 2020), (Miyazaki et al., 2021). Moreover, bone marrow-derived macrophages also can differentiate into CAF (Iwamoto et al., 2021). Whereas the diverse source of CAF may lead to functional differences, it is necessary to study PSC as a well-defined concept.

How Do Cancer Cells Activate PSC?

PSC are stellate stromal cells unique to the pancreas and are usually located in a quiescent state on the outer side of the acinus (Pothula et al., 2016). In addition to storing vitamin A lipid droplets, quiescent PSC also express several protein markers such as synemin and desmin (Roife et al., 2020). Accumulating evidence shows that pancreatic cancer cells can recruit and activate PSC. The activity of PSC isolated from pancreatic cancer tissue is much higher than those associated with chronic pancreatitis (Lenggenhager et al., 2019). Pancreatic cancer cells secrete a large number of paracrine cytokines, as summarized in **Table 1**, such as transforming growth factor-beta (TGF-β), Sonic hedgehog (Shh), and Interleukin-1 (IL-1) alpha to activate PSC (Sherman, 2018), while direct contact between pancreatic cancer cells and PSC, stimulating the Notch signaling pathway in PSC, leads to the activation of PSC (Fujita et al., 2009). The Notch receptors Notch1 and Notch3 are known to be highly expressed in the pancreatic cancer stroma and are accompanied by a rise in delta-like ligands Dll1, Dll3, and Dll4. Binding of the receptor to the ligand leads to the entry of the intracellular portion of the receptor into the nucleus, which activates the CSL/RBPJ protein, to promote the transcription of collagen fibers (Song and Zhang, 2018), (Procopio et al., 2015). Studies suggest that Notch3 is involved in the activation of PSC (Procopio et al., 2015). Activated PSC proliferate and secrete a large number of growth factors, inflammatory mediators, and collagen fibers that reshape the tumor microenvironment.

Additionally, the rapid proliferation of cancer cells imposes significant pressure on the surroundings, including mechanical pressure which promotes the activation of PSC through a positive feedback loop (Sahai et al., 2020). G protein-coupled estrogen receptors, located within PSC membranes, sense interstitial mechanical signals and activate Ras homolog family member A (RhoA) (Cortes et al., 2019a). Both cell contraction and mechanosensation are dependent on RhoA activity, which regulates cell contractility and maintains the activated phenotype of PSC by regulating actomyosin (Cortes et al., 2019b), (Rodriguez-Hernandez et al., 2016). G protein-coupled estrogen receptor expression in the mesenchyme promotes stiffening and remodeling of the extracellular matrix (ECM), which also enhances the transmission of mechanical signals (Cortes et al., 2019c). PSC can maintain their activation state by autocrine TGF-β and other cytokines (Apte and Wilson, 2012). These cytokines effectively promote collagen synthesis and proliferation of PSC (Wu et al., 2020). Furthermore, pressure may be involved in the maintenance and enhancement of the activated state of PSC. Under conditions of high mechanical pressure, PSC will activate the injury-related stress response and synthesize a large number of reactive oxygen species (ROS) (Asaumi et al., 2007), which have been associated with the production of various cytokines and growth factors that

TABLE 1 | PSCs activating factor secreted by cancer cells.

Cytokines	Pathway	Main function
Transforming growth factor-α (Tahara et al., 2013)	Ras-ERK, PI3K/Akt	Induces MMP-1 expression
platelet derived growth factor (Apte et al., 1999)		Increase proliferation and collagen synthesis
Galectin-1 (Masamune et al., 2006)	ERK, JNK, Activator protein-1, and NF-kappaB	Induces chemokine production and proliferation
TNF-α (Mews et al., 2002)		Increases proliferation
Shh (Khan et al., 2020)	HH	Promotes fibrosis
Plasminogen activator inhibitor-1 (Wang et al., 2019)	PAI-1/LRP-1	Promotes fibrosis
Hepatoma-derived growth factor (Chen et al., 2019)		Promotes the antiapoptosis of PSCs
Chemokine (Roy et al., 2017)		Recruits PSCs
Fibrinogen (Masamune et al., 2009)	NF-kappaB, MAPK, and ERK	Induces cytokine and collagen production
IL1β (Das et al., 2020)		Promotes immunosuppression
IL-1α (Tjomsland et al., 2011)	JAK-STAT	Promotes the secretion of inflammatory factors
TGF-β1 (Qian et al., 2010)	Smads	Promotes fibrosis
Angiotensin II (Hama et al., 2006)	Protein kinase C pathway	Promotes the proliferation
Galectin-3 (Zhao et al., 2018)	Integrin subunit beta 1 (ITGB1)	Produces inflammatory cytokines

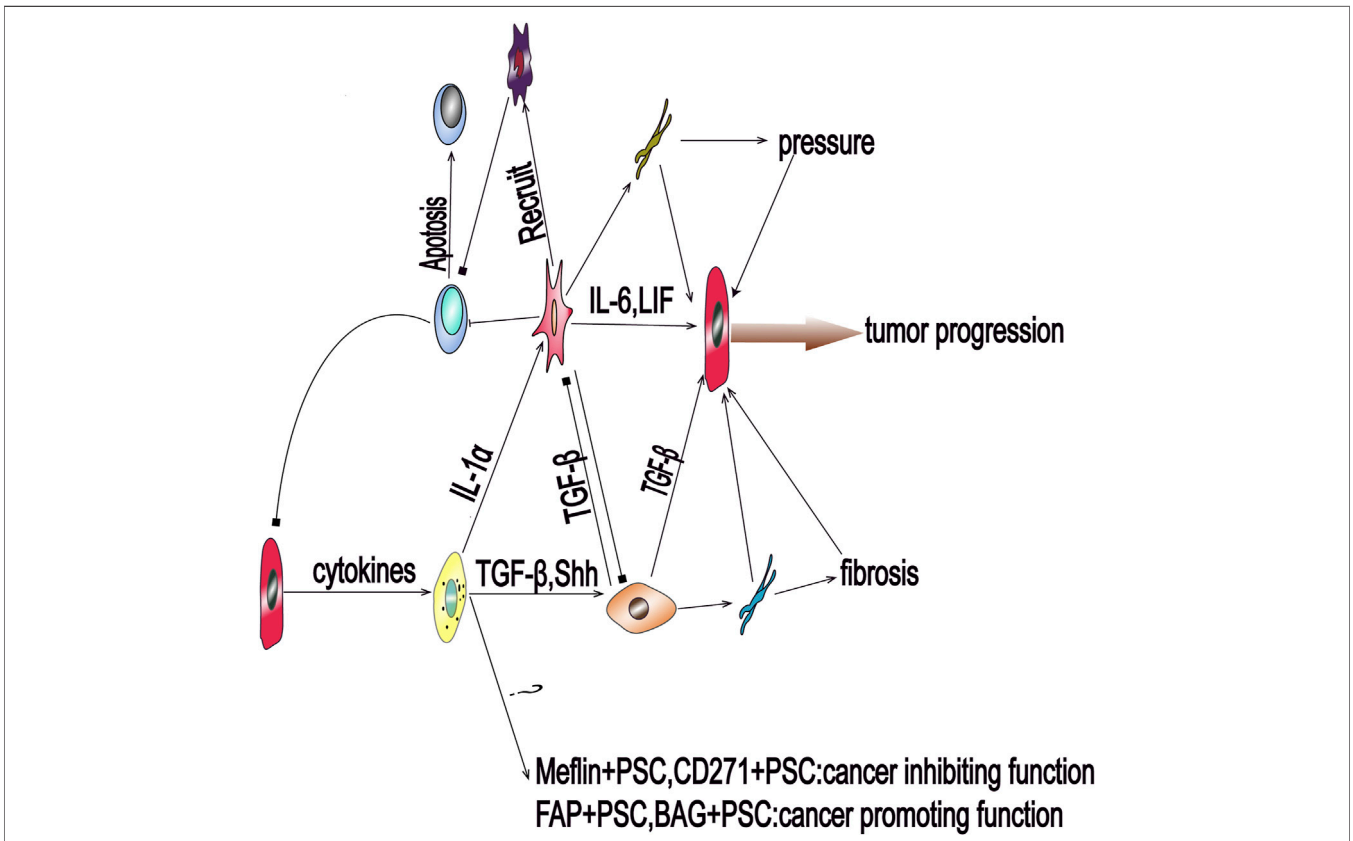

FIGURE 1 | Pancreatic cancer cells can send activation signals to quiescent pancreatic stellate cells (PSCs) via paracrine factors, resulting in the activation of PSCs and differentiation into multiple subsets that participate in the progression of pancreatic cancer. Transforming growth factor beta and Sonic hedgehog can promote the activation of PSCs to myofibroblastic PSCs. The cells of this subgroup mainly secrete collagen fibers and mediate environmental fibrosis and hypoxia. Interleukin-1 alpha can promote the differentiation of PSCs into inflammatory PSCs to induce the inflammatory response and interstitial hypertension. Inflammatory PSCs also induce immunosuppression by recruiting immunosuppressive cells; BAG: Bcl2-associated athanogene; FAP: fibroblast activation protein; IL-6: Interleukin-6; LIF: leukemia inhibitory factor; PSC: pancreatic stellate cell; Shh: Sonic hedgehog; TGF-β: transforming growth factor beta.

facilitate the continuous activation of PSC (Richter et al., 2015). Importantly, PSC can activate the ROS system under a diverse array of conditions, including inflammation, hypoxia, and a high glucose environment, which seem to be key mechanisms for the maintenance of PSC activity (Hu et al., 2007; Lei et al., 2014; Kim et al., 2016). Furthermore, the researchers identified a key role for

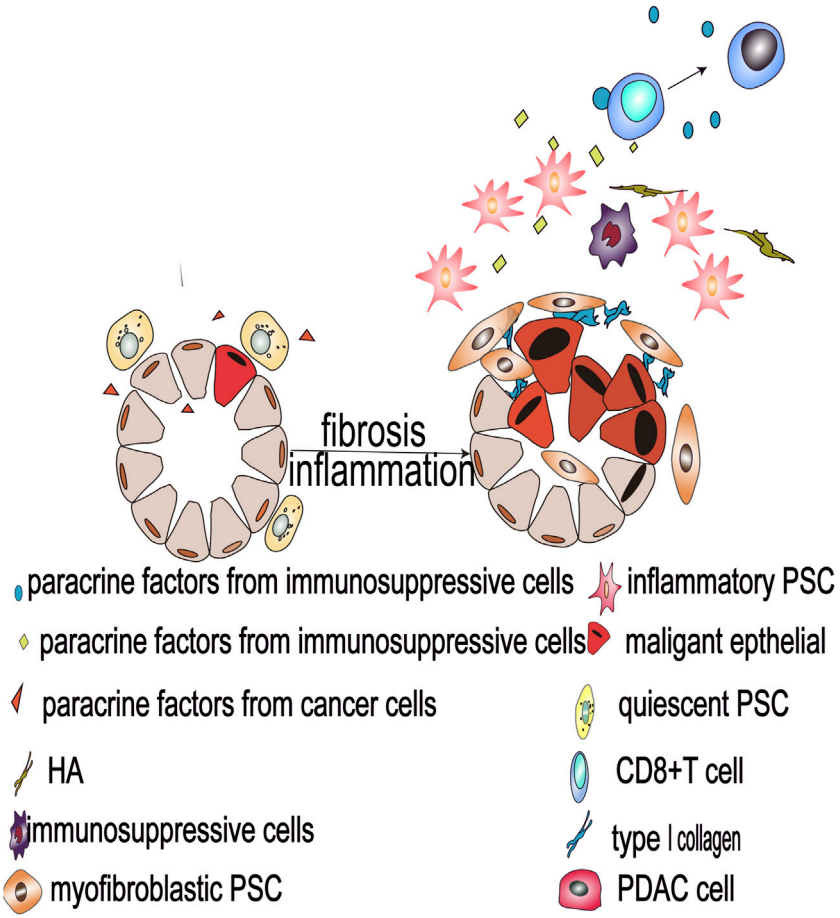

FIGURE 2 | Malignant pancreatic epithelial cells activate PSCs and secrete oncogenic factors that drive PSC differentiation into myofibroblastic and inflammatory PSC subtypes, and such heterogeneous PSCs reshape the tumor microenvironment and promote the development of pancreatic cancer.

the Keap1-Nrf2 signalling axis in influencing the functional status of PSC in pancreatic cancer through the regulation of ROS production (Shao et al., 2019).

The Driving Mechanism of PSC Differentiation Into Myofibroblastic and Inflammatory Subtypes

In mice and human pancreatic cancer tissues, researchers have identified two distinct subgroups of PSC. The first, myofibroblastic PSC, are associated with elevated *a*-SMA expression in immediately surrounding of cancer cells, and produce large amounts of pro-fibroproliferative collagen fibers, while the second type, inflammatory PSC, are not associated with elevated *a*-SMA expression, but are known to secrete large amounts of inflammatory cytokines further away from the cancer cells (Öhlund et al., 2017). Studies have shown that soluble cytokines secreted by cancer cells dominate this process and the differentiation of PSC into these two subtypes involves an antagonistic mechanism (**Figure 1** and **Figure 2**). Specifically, TGF-β activates Smads signaling to drive the expression of downstream target genes, including *a*-SMA and type 1 collagen (Col1), promoting the differentiation of myofibroblastic PSC. In contrast, IL-1α activates JAK-STAT signaling to mediate mass production of Interleukin-6 (IL-6) and leukemia inhibitory factor (LIF), promoting the differentiation of inflammatory PSC (Biffi et al., 2019). IL-1α-activated PSC can assist cancer cell migration, which is known to be inhibited by TGF-β *via* blocking IL-1α-mediated secretion of hepatocyte growth factor and reducing IL-1 receptor expression (Tjomsland et al., 2016a). These factors also act antagonistically in regulating the matrix metalloproteinase profile of PSC (Tjomsland et al., 2016b). Additionally, Shh protein shows a similar regulatory effect, as it promotes the differentiation of myofibroblastic PSC and inhibits the differentiation of inflammatory PSC in the tumor microenvironment (Steele et al., 2021). Furthermore, Shh activates Hedgehog signaling, in a dose-dependent manner, to enhance the proliferation of PSC and induce the expression of *a*-SMA (Bailey et al., 2008). Moreover, the differentiation of PSC is also regulated by mechanical signal transduction, and the mechanical pressure caused by glandular dilatation is known to induce the expression of *a*-SMA in surrounding stromal cells (Miyai et al., 2020).

Indeed, whereas Öhlund identified two typical PSC subgroups, myofibroblastic PSC and inflammatory PSC, other researchers revealed the mechanism of differentiation of the two subgroups (Pothula et al., 2020), (Biffi et al., 2019). But subgroups are not stable and can re-differentiate into other types under certain conditions, including the rapid re-differentiation of inflammatory PSC into myofibroblastic PSC, in the case of monolayer distribution (Öhlund et al., 2017). This work also implies that the differentiation of PSC is dominated by cancer cells and PSC present different phenotypes according to the spatial and biochemical ecological niches in the PDA microenvironment. For myofibroblastic PSC and inflammatory PSC, the essential difference is whether *a*-SMA is expressed at high levels or not. Whether this marking method is reasonable or not needs to be further examined. Additional markers are available to differentiate diverse subgroups of PSC, such as FAP, Platelet-derived growth factor receptors, and Vimentin (Nurmik et al., 2020). It was shown that the FAP-positive PSC may produce both ECM and inflammatory cytokines (Wen et al., 2019), and the ecological niche of FAP-positive PSC in the PDA microenvironment is located between myofibroblastic PSC and inflammatory PSC (Feig et al., 2013). Thus, FAP-positive PSC may be an intermediate state between the differentiation of myofibroblastic PSC and inflammatory PSC. We need more authoritative classification criteria for the study of subgroups of PSC, which is crucial for us to further investigate the functions of PSC. Different activators, markers, and ecological niche characteristics are key factors for further identification of PSC subgroups in the future. Based on existing studies, the following section will focus on the known features and functions of myofibroblastic PSC and inflammatory PSC to further explore the functions of PSC in pancreatic cancer.

THE FUNCTION OF MYOFIBROBLASTIC AND INFLAMMATORY PSC

Myofibroblastic PSC Mediate Characteristic Desmoplasia in Pancreatic Cancer

Pancreatic cancer has a high degree of desmoplasia, which is characterized by the differentiation of PSC into myofibroblastic PSC and overexpression of ECM proteins (Incio et al., 2016). Myofibroblastic PSC dominate the desmoplasia and form a physically protective barrier outside pancreatic cancer cells, protecting them from drug intervention and immune recognition, representing a significant impediment to the treatment of pancreatic cancer (Schnittert et al., 2019). This process is regulated by many myofibroblastic PSC differentiation drivers, such as TGF- β and Shh. Targeting TGF-β can improve patient prognosis, whereas targeting Shh has no observable effect (Melisi et al., 2019), (Kim et al., 2014). Alternatively, the depletion of the ECM, to dissolve the fibrous barrier, was conjectured, but its application to the treatment in pancreatic cancer has not been successful. Knockout *a*-SMA transgenic mice successfully deplete *a*-SMA positive PSC in the stroma, which was associated with earlier metastasis, a high inflammatory response, and immunosuppression of pancreatic cancer (Özdemir et al., 2014), while silencing Shh in mice leads to depletion of stromal a-SMA$^+$ cells, revealing a similar course of malignant progression (Rhim et al., 2014). Similarly, the depletion of Col1, which is the main component of the ECM, leads to immunosuppression and premature death in mice (Chen et al., 2021). Whether it is depletion of myofibroblast PSC or COL1, these are some drastic approaches. This does not directly confirm that they have a cancer-suppressive function. However, there are several possible reasons for immunosuppression and malignant progression: (Mizrahi et al., 2020): the self-protection mechanisms in pancreatic cancer cells were activated. (Kamisawa et al., 2016). the conditions created by inducing cell death in the cancer microenvironment may have primary responsibility for the adverse effects. This inspires us that targeting the mesenchymal component of pancreatic cancer requires more caution.

A novel treatment approach involves inducing PSC quiescence, which can not only effectively prevent the proliferation of connective tissue in pancreatic cancer, but also prevent the side effects caused by the depletion of the ECM. Calcipotriol, a ligand of the vitamin D receptor, is used to induce PSC quiescence and effectively reduce the degree of inflammation and fibrosis associated with pancreatic cancer in mice. The survival time of mice treated with calcipotriol chemotherapy increased by 57% (Sherman et al., 2014). All-trans retinoic acid (ATRA), an active metabolite of vitamin A, restores mechanical quiescence of PSC through a mechanism dependent on the contractile downregulation of actomyosin (Chronopoulos et al., 2016). ATRA also inhibits the ability of PSC to mechanically release active TGF-β, blocking the capacity of TGF-β to maintain the activity of PSC in an autocrine manner (Sarper et al., 2016). Recent studies have shown that ATRA-targeted stroma reduces pancreatic cancer aggressiveness (Froeling et al., 2011). A phase I clinical trial of ATRA-induced PSC quiescence demonstrates that patients tolerate ATRA well (Kocher et al., 2020); however, further clinical trials are required to verify the effectiveness of ATRA.

As the depletion of *a*-SMA positive stromal cells leads to the malignant progression of pancreatic cancer, an important question arises as to whether myofibroblastic PSC can inhibit tumor progression. This is likely not the case, and the expression of *a*-SMA in pancreatic cancer tissues is unstable and provides no predictive value in the prognosis of patients (Erkan et al., 2008; Moffitt et al., 2015; Haeberle et al., 2018). Studies have shown that the depletion of myofibroblastic PSC will lead to a substantial expansion of the number of inflammatory PSC, which then become the dominant subgroup in the tumor microenvironment, leading to the malignant progression of pancreatic cancer. This implies that an increase in the number of inflammatory PSC may be the main reason for the deterioration of a-SMA$^-$ mice (Steele et al., 2021). In addition, Col1 plays an important role in sending malignant signals to cancer cells (Grzesiak et al., 2007). Studies show that patients with low Col1 have a median survival time of 14.6 months, in comparison to 6.4 months for patients with high levels

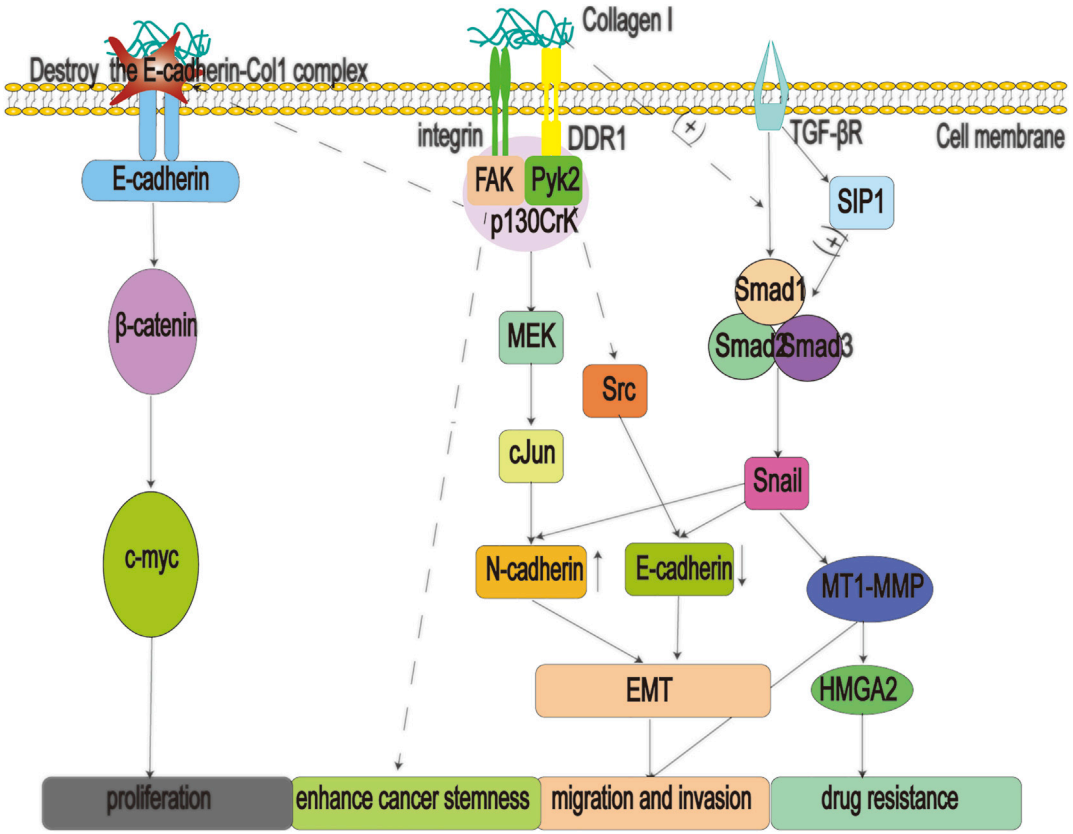

FIGURE 3 | Type 1 collagen (Col1) fibers are secreted by myofibroblastic pancreatic stellate cells (PSCs), which can promote multiple processes such as migration, proliferation, drug resistance, and stemness enhancement of pancreatic cancer cells, by binding to $\alpha 1\beta 2$ integrins and discoidin domain receptors 1 (DDR1). In addition, when the E-cadherin-Col1 complex is destroyed, it will lead to the accumulation of β-catenin in the nucleus, activate the oncogene c-myc, and eventually lead to the proliferation of pancreatic cancer cells; Col1: type 1 collagen; DDR1: Discoidin domain receptors one; EMT: epithelial mesenchymal transition; FAK: focal adhesion kinase; MET: metformin; HMGA2: high mobility group A2; MMPs: matrix metalloproteinases; MT1-MMP: membrane-type matrix metalloproteinase-1; SIP1: smad interacting protein one; TGF-βR: transforming growth factor beta receptor.

(Whatcott et al., 2015). $\alpha 1\beta 2$ integrin is an α/β heterodimer membrane protein and the main receptor mediating the adhesion of cancer cells to the surrounding Col1 (Naci et al., 2015). Once these two elements combine to form adhesion plaques on the cell surface, they provide an important medium for the ECM to transmit signals into the cell, activating downstream Src family kinases, focal adhesion kinase, and extracellular regulated kinase signaling pathways (Ivaska and Heino, 2011), (Cooper and Giancotti, 2019). Discoidin domain receptor 1 (DDR1) is a member of the receptor tyrosine kinase family and acts as an important receptor for Col1 (Baltes et al., 2020). DDR1 is widely expressed in epithelial cells, involved in the regulation of multiple signaling pathways, and is known to have a strong association with cancer progression (Henriet et al., 2018). Col1 can transmit a variety of carcinogenic signals to cells, through the two pathways described above, to promote the migration, proliferation, and drug resistance of pancreatic cancer.

Col1 makes an outstanding contribution in promoting the malignant procession of cancer (**Figure 3**). Col1 signals the p130Crk-associated substrate and activates the JNK signaling pathway to increase N-cadherin expression (Huang et al., 2016), (Shintani et al., 2006) DDR1 also activates downstream Src to decrease the expression of E-cadherin (Sun et al., 2008), (Chen et al., 2016). These factors reduce the adhesion of cancer cells to the adjacent extracellular matrix and help them to complete their EMT, greatly enhancing their ability to migrate. In addition, Col1 can engage in crosstalk with transforming growth factor-beta (TGF-β) signaling to promote EMT in cancer cells. Studies have shown that Col1 increases the expression of transcription factor Snail by interacting with TGF-β-Smads. Moreover, the up-regulation of Snail can not only promote the occurrence of EMT but also increase the expression of membrane-type matrix metalloproteinase-1, which further helps pancreatic cancer cells to dissolve collagen fibers and achieve metastasis (Shields et al., 2011). Furthermore, Col1 positively regulates the transcription of Snail via the Smad interacting protein 1, a positive regulator of Smads signal (Imamichi et al., 2007). Col1 also induces the proliferation of pancreatic cancer cells by disrupting the E-cadherin-Col1 complex, leading to the accumulation of β-catenin in the nucleus and activating the transcription of the oncogene c-Myc (Koenig et al., 2006; Katoh, 2018). Overexpression of

c-Myc promotes the immortalization of cancer cells (Dang, 2012) and alters the original signal transduction mode of cells, resulting in malignant cell proliferation, anti-apoptosis, and chromosome instability (Kolenda et al., 2020). Moreover, the $\alpha 1\beta 2$ integrin pathway can also assist cells to acquire a cancer stem cell phenotype (Begum et al., 2017). Finally, Col1 mediates drug resistance by activating MT1-MMP to increase the expression of high mobility group A2, a non-histone DNA-binding nuclear protein involved in chromatin remodeling and gene transcription (Dangi-Garimella et al., 2011).

Interstitial Hypertension Dominated by Inflammatory PSC Is a Natural Protective Barrier for Pancreatic Cancer

Hyaluronic acid (HA) is a linear glycosaminoglycan macromolecule composed of repeating units that are synthesized by hyaluronan synthase enzymes HAS1, HAS2, and HAS3, and is the main source of external pressure in the cancer stroma. HA can also specifically bind to the CD44 protein to affect the physiological activity of cancer cells (Sato et al., 2016; Caon et al., 2020). Studies have shown that the content of HA in pancreatic cancer is higher than in other cancer tissues, which leads to the characteristic interstitial hypertension observed in pancreatic cancer (Jacobetz et al., 2013). The content of HA in pancreatic cancer is 12 times higher than that in a healthy pancreas (Theocharis et al., 2000). Studies show that activated PSCs are the main source of HA (Junliang et al., 2019). Surprisingly, HA is not synthesized by myofibroblastic PSC, and their depletion does not affect the expression of HA in pancreatic cancer stroma (Özdemir et al., 2014). In contrast, inflammatory PSC express HAS1 and HAS2, suggesting that these cells represent the main source of HA (Elyada et al., 2019). Pancreatic cancer has extremely high external pressure in the interstitium, which contributes to difficulties associated with treatment (DuFort et al., 2016). HA-induced external pressure forms a physical barrier to help pancreatic cancer cells resist the effects of therapeutic intervention (Jacobetz et al., 2013). Studies have shown that low molecular weight HA enhances the migration of cancer cells (Junliang et al., 2019), whereas high molecular weight HA is the main cause of external pressure, leading to interstitial pressures of up to 100 mmHg, resulting in vascular collapse, impeding the delivery of nutrients, oxygen, and drugs, and reducing the infiltration of immune cells (Chauhan et al., 2014). A recent study shows a median survival time of 24.3 months for patients with low levels of HA, in comparison to 9.3 months for patients with high levels (Whatcott et al., 2015). The degradation of HA in pancreatic cancer tissue by administering halofuginone can significantly weaken the effect of the physical barrier, resulting in prolonged survival time in mice (Elahi-Gedwillo et al., 2019).

Dissolving HA with drugs represents a viable treatment option for pancreatic cancer patients (Sato et al., 2016). Compounds capable of dissolving HA in pancreatic tumor-bearing mice include 4-methylumbelliferone (Nagy et al., 2015), Minnelide (Banerjee et al., 2016), and PEGylated human recombinant hyaluronidase (PEGPH20) (Hingorani et al., 2016). PEGPH20 has been shown to significantly prolong disease-free survival of pancreatic cancer patients, especially in patients with high HA expression. Maximum survival was observed upon treatment with a combination therapy regimen including PEGPH20, albumin-bound paclitaxel, and gemcitabine (Hingorani et al., 2018; Ramanathan et al., 2019). Unfortunately, clinical trials of PEGPH20 were eventually discontinued due to pharmacological toxicity.

Several pancreatic cancer cell lines with HA receptor expression exhibit potential for hypo-differentiation and high migration (Abetamann et al., 1996; Sugahara et al., 2008). Research has shown that high levels of HA can lead to the malignant progression of pancreatic cancer. HA binding to the CD44 receptor mediates cancer cell EMT, drug resistance, and proliferation through both RAS/ERK and PI3K/AKT signaling pathway activation (Sato et al., 2016). Recently, researchers have developed a therapeutic approach involving a combination of HA and CD44 targeting. Specifically, the drug is modified by HA and targeted to CD44-positive tumor cells to improve the efficiency of drug utilization (Mattheolabakis et al., 2015). Many preclinical trials have revealed positive results using HA-modified drugs, as shown in **Table 2**.

Inflammatory PSC Lead to Malignant Inflammation of Pancreatic Cancer

Inflammation in the tumor microenvironment assists in the process of drug resistance, proliferation, metastasis, and immunosuppression in pancreatic cancer (Jarrin Jara et al., 2020). However, IL-6, secreted by inflammatory PSC, plays a significant role in mediating inflammation-related malignant progression of pancreatic cancer (**Figure 4**). Research has shown that IL-6 expression levels are significantly higher in patients with systemic metastases, and high levels of IL-6 reliably predict poor prognosis in patients treated with surgery (Palmquist et al., 2020). Additionally, high levels of IL-6 are often accompanied by large tumor size and distant metastases (Miura et al., 2015). IL-6 activates the JAK-STAT3 signaling pathway in cancer cells to exert its carcinogenic effect (Nagathihalli et al., 2016) and is regulated by both classical and trans-signaling pathways. In classical signaling, IL-6 can bind to the IL-6 receptor and induce a conformational change that triggers glycoprotein (gp) 130 dimerization. Subsequently, two IL-6-IL-R molecules bind to a gp130 dimer forming a 6-membered complex resulting in the activation of downstream JAK (Yu et al., 2014). In trans-signaling, the cleavage of IL-6R by specific enzymes, or alternative splicing of IL6R mRNA, produces soluble IL-6R (sIL-6R) (Johnson et al., 2018). IL-6R binds sIL-6R and forms an L-6-sIL-6R complex with the ability to induce gp130 dimerization to activate downstream JAK (104). Both types of regulation result in JAK activation and phosphorylation of the transcription factor STAT3, which regulates gene expression in cancer cells (van Duijneveldt et al., 19792020). Studies have shown that activating the JAK-STAT3 pathway enhances migration (Okitsu et al., 2010), drug resistance, proliferation (Zhang et al., 2017), and stemness (Alcalá et al., 2019) of pancreatic cancer cells. Inhibition of STAT3

TABLE 2 | Targeting CD44-positive pancreatic cancer cells with HA-modified drugs.

Drug	Auxiliary materials	Synthetic drug	Mechanism
3,4-difluorobenzylidene curcumin (CDF) (Kesharwani et al., 2015a)	Poly (amidoamine) (PAMAM)	HA-PAMAM-CDF	Inhibits NF-κB signaling and reduces CD44 expression
CDF (Kesharwani et al., 2015b)	styrene maleic acid (SMA)	HA-SMA-CDF	Inhibits NF-κB signaling and reduces CD44 expression
Gemcitabine and quercetin (Serri et al., 2019)	nanoparticles	Gemcitabine and quercetin encapsulated in HA modified nanoparticles	Anti-inflammatory effect and metabolic intervention of DNA
$Cu(DDC)_2$ (Marengo et al., 2019)	Liposome	Encapsulation of Cu (DDC) 2 complex in HA modified liposomes	ROS-mediated anticancer activity
Gemcitabine (Dalla Pozza et al., 2013)	Liposome	Gemcitabine complex encapsulated in HA modified liposomes	Interferes with DNA synthesis
Drugs (Wei et al., 2013)	nanogels	The drug encapsulated in HA modified nanogels	
5-FU (Nigam Joshi et al., 2017)	Ag-GQDs	5-FU encapsulated in HA modified Ag-GQDs	Anti-tumor proliferation
metformin (MET) (Farag et al., 2021)	Metformin-Phospholipid Sonocomplex (MPS)	HA-MPS-MET	Corrects microenvironment hypoxia

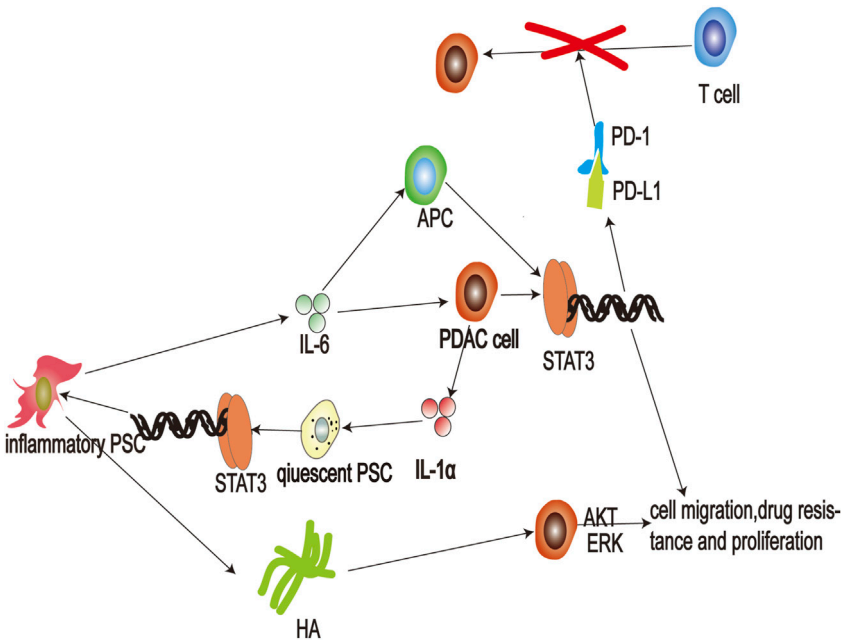

FIGURE 4 | Schematic representation of the interaction between pancreatic cancer cells and inflammatory pancreatic stellate cells (PSCs). Secretion of interleukin (IL)-1α by pancreatic cancer cells stimulates activation of JAK-STAT3 signaling in quiescent PSCs, and leads to differentiation of inflammatory PSCs. Thereafter, inflammatory PSCs produce hyaluronic acid that then binds to cluster of differentiation (CD) 44 to activate AKT and ERK signaling pathways and promote the malignant process of pancreatic cancer. Additionally, inflammatory PSCs can also secrete large amounts of the cytokine IL-6, which activates JAK-STAT3 signaling pathways in cancer cells, promoting their proliferation and invasion. In addition, IL-6 also promotes the transcription of PD-L1 in antigen-presenting cells and cancer cells, leading to suppression of T-cell immunity; APC: antigen-presenting cell; ERK: extracellular regulated kinase; HA: hyaluronic acid; HAS: hyaluronan synthase; IL-1: Interleukin-1 IL-6: Interleukin-6; PD-1: programmed cell death one; PD-L1: protein programmed cell death one ligand one; PSC: pancreatic stellate cell.

signaling leads to apoptosis of pancreatic cancer cells (Nagathihalli et al., 2015). IL-6-receptor blockers enhance chemotherapeutic efficacy in KPC (LSL-Kras G12D/+; LSL-Trp53 R172H/+; Pdx-1Cre) mice (Long et al., 2017).

Furthermore, inflammatory PSC also secrete IL-6 resulting in immunosuppression. PD-1 is one of the co-suppressor receptors of activated immune cells, and PD-L1 is mainly expressed in tumor cells and antigen-presenting cells (Ai et al., 2020). When PD-L1 binds to PD-1, this leads to suppression of activated immune cells and assists in the immune escape of tumor cells (Patel and Kurzrock, 2015). Anti-PD-1 targeted therapy has been successfully used in many cancers, but not in pancreatic cancer (Tsoukalas et al., 2019). This may be due to the persistent inflammatory response in pancreatic cancer (Antonangeli et al., 2020). Research has shown that transcription of PD-L1 is regulated by IL-6 in pancreatic cancer (Tsukamoto et al., 2018).

IL-6 accelerates bone marrow-derived myeloid-derived suppressor cell differentiation and leads to increased levels of PD-L1 expression on myeloid-derived suppressor cells (Marigo et al., 2010; Weber et al., 2021). IL-6 also induces apoptosis of conventional type 1 dendritic cells to prevent antigen presentation (Lin et al., 2020). Moreover, antibody blockade of IL-6 reduces the expression of PD-L1 in dendritic cells (Eriksson et al., 2019). JAK-STAT3 activation in pancreatic tumor-bearing mice inhibits the effect of anti-PD-1 treatment (Lu et al., 2017). Therefore, blocking IL-6 may represent an effective adjuvant method for anti-PD-1 therapy. The combination of anti-IL-6 and anti-PD-L1 therapy effectively increases the survival rates of pancreatic cancer mice (Mace et al., 2018).

Studies focused on blocking IL-6-mediated JAK-STAT3 signaling activation have been conducted in the following categories ((Kaur et al., 2020): (Mizrahi et al., 2020) IL-6 receptor antagonists: tocilizumab, sarilumab; (Kamisawa et al., 2016); IL-6 production inhibitors: olokizumab, sirukumab, siltuximab, clazakizumab, PF-423691; and (Wang et al., 2020) JAK1/2 and STAT3 inhibitors: ruxolitinib, momelotinib. Despite the success of blocking IL-6 in pancreatic cancer animal models, this approach was virtually ineffective in a clinical setting (Ng et al., 2019). Anti-IL-6 therapy as an adjuvant in combination with other targeted therapies may represent a novel area worthy of exploration in the treatment of pancreatic cancer.

Outlook: The diversity of PSC subsets represents an important factor in the therapeutic intervention of pancreatic cancer.

We have shown that different groups of PSC play different roles in the progression of pancreatic cancer. The discovery of PSC heterogeneity will provide the basis for the development of novel approaches for the treatment of pancreatic cancer. Finding therapeutic targets for the treatment of pancreatic cancer at the level of PSC heterogeneity represents an unexplored potential therapeutic strategy. Although most of our regimens targeting myofibroblastic PSC for pancreatic cancer (including depletion of *a*-SMA + PSC and blockade of Shh) have failed, we have still achieved some successes such as blocking TGF-β or inducing PSC quiescence. Simultaneous inhibition of inflammatory responses and fibroplasia caused by different PSC subgroups significantly prevented pancreatic cancer progression in mice with no side effects (Khan et al., 2020). These reveal that targeting PSC for pancreatic cancer is an extremely valuable idea, but it should be done rationally. Future research should focus on the following aspects: 1) Induction of PSC quiescence to effectively block the progression of pancreatic cancer, 2) Evaluation of how pancreatic cancer cells produce and regulate the production of PSC subsets, and how PSC tumor suppressor subsets, specifically CD271 + PSC (Nielsen et al., 2020) and Meflin + PSC (Mizutani et al., 2019), are formed, and 3) Simultaneous blockade of the oncogenic effects of different PSC subgroups to treat pancreatic cancer more effectively.

AUTHOR CONTRIBUTIONS

ZZ drafted the manuscript. HZ researched the literature and drafted figures. TL and TC counted and plotted the tables. DT and DW critically revised the article for important intellectual content. All authors read and approved the final manuscript.

FUNDING

This work was supported by grants from the Training Project of Key Talents of Youth Medicine in Jiangsu province, China (No. QNRC2016330), the Social Development-Health Care Project of Yangzhou, Jiangsu Province (No. YZ2018087), the Social Development-Health Care Project of Yangzhou, Jiangsu Province (No. YZ2021075), and High-level talent "six one projects" top talent scientific research project of Jiangsu Province (No. LGY2019034) the Graduate Research-Innovation Project in Jiangsu province (No. SJCX21_1644). The funding bodies had no role in the design of the study; in the collection, analysis, and interpretation of the data; and in writing the manuscript.

REFERENCES

Abetamann, V., Kern, H. F., and Elsässer, H. P. (1996). Differential Expression of the Hyaluronan Receptors CD44 and RHAMM in Human Pancreatic Cancer Cells. *Clin. Cancer Res.* 2 (9), 1607–1618. Epub 1996/09/01. PubMed PMID: 9816340.

Ai, L., Xu, A., and Xu, J. (2020). Roles of PD-1/pd-L1 Pathway: Signaling, Cancer, and beyond. *Adv. Exp. Med. Biol.* 1248, 33–59. Epub 2020/03/19PubMed PMID: 32185706. doi:10.1007/978-981-15-3266-5_3

Alcalá, S., Martinelli, P., Hermann, P. C., Heeschen, C., and Sainz, B., Jr (2019). The Anthrax Toxin Receptor 1 (ANTXR1) Is Enriched in Pancreatic Cancer Stem Cells Derived from Primary Tumor Cultures. *Stem Cell Int.* 2019, 1–13. Epub 2019/06/14PubMed PMID: 31191663; PubMed Central PMCID: PMCPMC6525821. doi:10.1155/2019/1378639

Antonangeli, F., Natalini, A., Garassino, M. C., Sica, A., Santoni, A., and Di Rosa, F. (2020). Regulation of PD-L1 Expression by NF-Kb in Cancer. *Front. Immunol.* 11, 584626, 2020 . Epub 2020/12/17PubMed PMID: 33324403; PubMed Central PMCID: PMCPMC7724774. doi:10.3389/fimmu.2020.584626

Apte, M. V., Haber, P. S., Darby, S. J., Rodgers, S. C., McCaughan, G. W., Korsten, M. A., et al. (1999). Pancreatic Stellate Cells Are Activated by Proinflammatory Cytokines: Implications for Pancreatic Fibrogenesis. *Gut* 44 (4), 534–541. Epub 1999/03/17PubMed PMID: 10075961; PubMed Central PMCID: PMCPMC1727467. doi:10.1136/gut.44.4.534

Apte, M. V., and Wilson, J. S. (2012). Dangerous Liaisons: Pancreatic Stellate Cells and Pancreatic Cancer Cells. *J. Gastroenterol. Hepatol.* 27 (Suppl. 2), 69–74. Epub 2012/02/15PubMed PMID: 22320920. doi:10.1111/j.1440-1746.2011.07000.x

Asaumi, H., Watanabe, S., Taguchi, M., Tashiro, M., and Otsuki, M. (2007). Externally Applied Pressure Activates Pancreatic Stellate Cells through the Generation of Intracellular Reactive Oxygen Species. *Am. J. Physiology-Gastrointestinal Liver Physiol.* 293 (5), G972–G978. Epub 2007/09/01PubMed PMID: 17761838. doi:10.1152/ajpgi.00018.2007

Bailey, J. M., Swanson, B. J., Hamada, T., Eggers, J. P., Singh, P. K., Caffery, T., et al. (2008). Sonic Hedgehog Promotes Desmoplasia in Pancreatic Cancer. *Clin. Cancer Res.* 14 (19), 5995–6004. Epub 2008/10/03PubMed PMID: 18829478; PubMed Central PMCID: PMCPMC2782957. doi:10.1158/1078-0432.ccr-08-0291

Baltes, F., Caspers, J., Henze, S., Schlesinger, M., and Bendas, G. (2020). Targeting Discoidin Domain Receptor 1 (DDR1) Signaling and its Crosstalk with β1-Integrin Emerges as a Key Factor for Breast Cancer Chemosensitization upon Collagen Type 1 Binding. *Ijms* 21 (14), 4956, 2020 . Epub 2020/07/17PubMed PMID: 32668815; PubMed Central PMCID: PMCPMC7404217. doi:10.3390/ijms21144956

Banerjee, S., Modi, S., McGinn, O., Zhao, X., Dudeja, V., Ramakrishnan, S., et al. (2016). Impaired Synthesis of Stromal Components in Response to Minnelide Improves Vascular Function, Drug Delivery, and Survival in Pancreatic Cancer. *Clin. Cancer Res.* 22 (2), 415–425. Epub 2015/09/26PubMed PMID: 26405195; PubMed Central PMCID: PMCPMC4716007. doi:10.1158/1078-0432.ccr-15-1155

Begum, A., Ewachiw, T., Jung, C., Huang, A., Norberg, K. J., Marchionni, L., et al. (2017). The Extracellular Matrix and Focal Adhesion Kinase Signaling Regulate Cancer Stem Cell Function in Pancreatic Ductal Adenocarcinoma. *PloS one* 12 (7), e0180181, 2017 . Epub 2017/07/12PubMed PMID: 28692661. doi:10.1371/journal.pone.0180181

Biffi, G., Oni, T. E., Spielman, B., Hao, Y., Elyada, E., Park, Y., et al. (2019). IL1-Induced JAK/STAT Signaling Is Antagonized by TGFβ to Shape CAF Heterogeneity in Pancreatic Ductal Adenocarcinoma. *Cancer Discov.* 9 (2), 282–301. Epub 2018/10/28PubMed PMID: 30366930; PubMed Central PMCID: PMCPMC6368881. doi:10.1158/2159-8290.cd-18-0710

Cao, J., Li, J., Sun, L., Qin, T., Xiao, Y., Chen, K., et al. (2019). Hypoxia-driven Paracrine Osteopontin/integrin αvβ3 Signaling Promotes Pancreatic Cancer Cell Epithelial-Mesenchymal Transition and Cancer Stem Cell-like Properties by Modulating Forkhead Box Protein M1. *Mol. Oncol.* 13 (2), 228–245. Epub 2018/10/28PubMed PMID: 30367545; PubMed Central PMCID: PMCPMC6360359. doi:10.1002/1878-0261.12399

Caon, I., Bartolini, B., Parnigoni, A., Caravà, E., Moretto, P., Viola, M., et al. (2020). Revisiting the Hallmarks of Cancer: The Role of Hyaluronan. *Semin. Cancer Biol.* 62, 9–19. Epub 2019/07/19PubMed PMID: 31319162. doi:10.1016/j.semcancer.2019.07.007

Chauhan, V. P., Boucher, Y., Ferrone, C. R., Roberge, S., Martin, J. D., Stylianopoulos, T., et al. (2014). Compression of Pancreatic Tumor Blood Vessels by Hyaluronan Is Caused by Solid Stress and Not Interstitial Fluid Pressure. *Cancer cell* 26 (1), 14–15. Epub 2014/07/16PubMed PMID: 25026209; PubMed Central PMCID: PMCPMC4381566. doi:10.1016/j.ccr.2014.06.003

Chen, H.-R., Yeh, Y.-C., Liu, C.-Y., Wu, Y.-T., Lo, F.-Y., Tang, M.-J., et al. (2016). DDR1 Promotes E-Cadherin Stability via Inhibition of Integrin-B1-Src Activation-Mediated E-Cadherin Endocytosis. *Sci. Rep.* 6, 36336, 2016 . Epub 2016/11/09PubMed PMID: 27824116; PubMed Central PMCID: PMCPMC5099905. doi:10.1038/srep36336

Chen, Y.-T., Chen, F.-W., Chang, T.-H., Wang, T.-W., Hsu, T.-P., Chi, J.-Y., et al. (2019). Hepatoma-derived Growth Factor Supports the Antiapoptosis and Profibrosis of Pancreatic Stellate Cells. *Cancer Lett.* 457, 180–190. Epub 2019/05/13PubMed PMID: 31078734. doi:10.1016/j.canlet.2019.05.001

Chen, Y., Kim, J., Yang, S., Wang, H., Wu, C.-J., Sugimoto, H., et al. (2021). Type I Collagen Deletion in αSMA+ Myofibroblasts Augments Immune Suppression and Accelerates Progression of Pancreatic Cancer. *Cancer cell* 39 (4), 548–565. e6. Epub 2021/03/06PubMed PMID: 33667385; PubMed Central PMCID: PMCPMC8423173. doi:10.1016/j.ccell.2021.02.007

Chronopoulos, A., Robinson, B., Sarper, M., Cortes, E., Auernheimer, V., Lachowski, D., et al. (2016). ATRA Mechanically Reprograms Pancreatic Stellate Cells to Suppress Matrix Remodelling and Inhibit Cancer Cell Invasion. *Nat. Commun.* 7, 12630, 2016 . Epub 2016/09/08PubMed PMID: 27600527; PubMed Central PMCID: PMCPMC5023948. doi:10.1038/ncomms12630

Cooper, J., and Giancotti, F. G. (2019). Integrin Signaling in Cancer: Mechanotransduction, Stemness, Epithelial Plasticity, and Therapeutic Resistance. *Cancer cell* 35 (3), 347–367. Epub 2019/03/20PubMed PMID: 30889378; PubMed Central PMCID: PMCPMC6684107. doi:10.1016/j.ccell.2019.01.007

Cortes, E., Lachowski, D., Rice, A., Thorpe, S. D., Robinson, B., Yeldag, G., et al. (2019). Tamoxifen Mechanically Deactivates Hepatic Stellate Cells via the G Protein-Coupled Estrogen Receptor. *Oncogene* 38 (16), 2910–2922. Epub 2018/12/24PubMed PMID: 30575816; PubMed Central PMCID: PMCPMC6755965. doi:10.1038/s41388-018-0631-3

Cortes, E., Lachowski, D., Robinson, B., Sarper, M., Teppo, J. S., Thorpe, S. D., et al. (2019). Tamoxifen Mechanically Reprograms the Tumor Microenvironment via HIF -1A and Reduces Cancer Cell Survival. *EMBO Rep.* 20 (1), e46557, 2019 . Epub 2018/12/13PubMed PMID: 30538116; PubMed Central PMCID: PMCPMC6322388. doi:10.15252/embr.201846557

Cortes, E., Sarper, M., Robinson, B., Lachowski, D., Chronopoulos, A., Thorpe, S. D., et al. (2019). GPER Is a Mechanoregulator of Pancreatic Stellate Cells and the Tumor Microenvironment. *EMBO Rep.* 20 (1), e46556, 2019 . Epub 2018/12/13PubMed PMID: 30538117; PubMed Central PMCID: PMCPMC6322386. doi:10.15252/embr.201846556

Dalla Pozza, E., Lerda, C., Costanzo, C., Donadelli, M., Dando, I., Zoratti, E., et al. (2013). Targeting Gemcitabine Containing Liposomes to CD44 Expressing Pancreatic Adenocarcinoma Cells Causes an Increase in the Antitumoral Activity. *Biochim. Biophys. Acta (Bba) - Biomembranes* 1828 (5), 1396–1404. Epub 2013/02/07PubMed PMID: 23384419. doi:10.1016/j.bbamem.2013.01.020

Dang, C. V. (2012). MYC on the Path to Cancer. *Cell* 149 (1), 22–35. Epub 2012/04/03PubMed PMID: 22464321; PubMed Central PMCID: PMCPMC3345192. doi:10.1016/j.cell.2012.03.003

Dangi-Garimella, S., Krantz, S. B., Barron, M. R., Shields, M. A., Heiferman, M. J., Grippo, P. J., et al. (2011). Three-dimensional Collagen I Promotes Gemcitabine Resistance in Pancreatic Cancer through MT1-MMP-mediated Expression of HMGA2. *Cancer Res.* 71 (3), 1019–1028. Epub 2010/12/15PubMed PMID: 21148071; PubMed Central PMCID: PMCPMC3076124. doi:10.1158/0008-5472.can-10-1855

Das, S., Shapiro, B., Vucic, E. A., Vogt, S., and Bar-Sagi, D. (2020). Tumor Cell-Derived IL1β Promotes Desmoplasia and Immune Suppression in Pancreatic Cancer. *Cancer Res.* 80 (5), 1088–1101. Epub 2020/01/10PubMed PMID: 31915130; PubMed Central PMCID: PMCPMC7302116. doi:10.1158/0008-5472.can-19-2080

DuFort, C. C., DelGiorno, K. E., Carlson, M. A., Osgood, R. J., Zhao, C., Huang, Z., et al. (2016). Interstitial Pressure in Pancreatic Ductal Adenocarcinoma Is Dominated by a Gel-Fluid Phase. *Biophysical J.* 110 (9), 2106–2119. Epub 2016/05/12PubMed PMID: 27166818; PubMed Central PMCID: PMCPMC4939548. doi:10.1016/j.bpj.2016.03.040

Elahi-Gedwillo, K. Y., Carlson, M., Zettervall, J., and Provenzano, P. P. (2019). Antifibrotic Therapy Disrupts Stromal Barriers and Modulates the Immune Landscape in Pancreatic Ductal Adenocarcinoma. *Cancer Res.* 79 (2), 372–386. Epub 2018/11/08PubMed PMID: 30401713; PubMed Central PMCID: PMCPMC6335156. doi:10.1158/0008-5472.can-18-1334

Elyada, E., Bolisetty, M., Laise, P., Flynn, W. F., Courtois, E. T., Burkhart, R. A., et al. (2019). Cross-Species Single-Cell Analysis of Pancreatic Ductal Adenocarcinoma Reveals Antigen-Presenting Cancer-Associated Fibroblasts. *Cancer Discov.* 9 (8), 1102–1123. Epub 2019/06/15PubMed PMID: 31197017; PubMed Central PMCID: PMCPMC6727976. doi:10.1158/2159-8290.cd-19-0094

Eriksson, E., Milenova, I., Wenthe, J., Moreno, R., Alemany, R., and Loskog, A. (2019). IL-6 Signaling Blockade during CD40-Mediated Immune Activation Favors Antitumor Factors by Reducing TGF-β, Collagen Type I, and PD-L1/pd-1. *J.I. Baltimore, Md*, 202(3), 787–798. Epub 2019/01/09PubMed PMID: 30617223. doi:10.4049/jimmunol.1800717

Erkan, M., Michalski, C. W., Rieder, S., Reiser–Erkan, C., Abiatari, I., Kolb, A., et al. (2008). The Activated Stroma index Is a Novel and Independent Prognostic Marker in Pancreatic Ductal Adenocarcinoma. *Clin. Gastroenterol. Hepatol.* 6 (10), 1155–1161. Epub 2008/07/22PubMed PMID: 18639493. doi:10.1016/j.cgh.2008.05.006

Farag, M. M., Abd El Malak, N. S., Yehia, S. A., and Ahmed, M. A. (2021). Hyaluronic Acid Conjugated Metformin-Phospholipid Sonocomplex: A Biphasic Complexation Approach to Correct Hypoxic Tumour Microenvironment. *Ijn* 16, 1005–1019. Epub 2021/02/20PubMed PMID: 33603365; PubMed Central PMCID: PMCPMC7885809. doi:10.2147/ijn.s297634

Feig, C., Jones, J. O., Kraman, M., Wells, R. J. B., Deonarine, A., Chan, D. S., et al. (2013). Targeting CXCL12 from FAP-Expressing Carcinoma-Associated Fibroblasts Synergizes with Anti-PD-L1 Immunotherapy in Pancreatic Cancer. *Proc. Natl. Acad. Sci.* 110 (50), 20212–20217. Epub 2013/11/28PubMed PMID: 24277834; PubMed Central PMCID: PMCPMC3864274. doi:10.1073/pnas.1320318110

Froeling, F. E. M., Feig, C., Chelala, C., Dobson, R., Mein, C. E., Tuveson, D. A., et al. (2011). Retinoic Acid-Induced Pancreatic Stellate Cell Quiescence Reduces Paracrine Wnt-β-Catenin Signaling to Slow Tumor Progression. *Gastroenterology* 141 (4), 1486–1497. Epub 2011/06/28PubMed PMID: 21704588. doi:10.1053/j.gastro.2011.06.047

Fujita, H., Ohuchida, K., Mizumoto, K., Egami, T., Miyoshi, K., Moriyama, T., et al. (2009). Tumor-stromal Interactions with Direct Cell Contacts Enhance Proliferation of Human Pancreatic Carcinoma Cells. *Cancer Sci.* 100 (12), 2309–2317. Epub 2009/09/09PubMed PMID: 19735487. doi:10.1111/j.1349-7006.2009.01317.x

Grzesiak, J. J., Ho, J. C., Moossa, A. R., and Bouvet, M. (2007). The Integrin-Extracellular Matrix axis in Pancreatic Cancer. *Pancreas* 35 (4), 293–301. Epub 2007/12/20PubMed PMID: 18090233. doi:10.1097/mpa.0b013e31811f4526

Haeberle, L., Steiger, K., Schlitter, A. M., Safi, S. A., Knoefel, W. T., Erkan, M., et al. (2018). Stromal Heterogeneity in Pancreatic Cancer and Chronic Pancreatitis. *Pancreatology* 18 (5), 536–549. Epub 2018/05/21PubMed PMID: 29778400. doi:10.1016/j.pan.2018.05.004

Hama, K., Ohnishi, H., Aoki, H., Kita, H., Yamamoto, H., Osawa, H., et al. (2006). Angiotensin II Promotes the Proliferation of Activated Pancreatic Stellate Cells by Smad7 Induction through a Protein Kinase C Pathway. *Biochem. biophysical Res. Commun.* 340 (3), 742–750. Epub 2005/12/29PubMed PMID: 16380081. doi:10.1016/j.bbrc.2005.12.069

Henriet, E., Sala, M., Abou Hammoud, A., Tuariihionoa, A., Di Martino, J., Ros, M., et al. (2018). Multitasking Discoidin Domain Receptors Are Involved in Several and Specific Hallmarks of Cancer. *Cell Adhes. Migration* 12 (4), 1–15. Epub 2018/04/28PubMed PMID: 29701112; PubMed Central PMCID: PMCPMC6411096. doi:10.1080/19336918.2018.1465156

Hingorani, S. R., Harris, W. P., Beck, J. T., Berdov, B. A., Wagner, S. A., Pshevlotsky, E. M., et al. (2016). Phase Ib Study of PEGylated Recombinant Human Hyaluronidase and Gemcitabine in Patients with Advanced Pancreatic Cancer. *Clin. Cancer Res.* 22 (12), 2848–2854. Epub 2016/01/28PubMed PMID: 26813359; PubMed Central PMCID: PMCPMC7787348. doi:10.1158/1078-0432.ccr-15-2010

Hingorani, S. R., Zheng, L., Bullock, A. J., Seery, T. E., Harris, W. P., Sigal, D. S., et al. (2018). HALO 202: Randomized Phase II Study of PEGPH20 Plus Nab-Paclitaxel/Gemcitabine versus Nab-Paclitaxel/Gemcitabine in Patients with Untreated, Metastatic Pancreatic Ductal Adenocarcinoma. *Jco* 36 (4), 359–366. Epub 2017/12/13PubMed PMID: 29232172. doi:10.1200/jco.2017.74.9564

Hosein, A. N., Brekken, R. A., and Maitra, A. (2020). Pancreatic Cancer Stroma: an Update on Therapeutic Targeting Strategies. *Nat. Rev. Gastroenterol. Hepatol.* 17 (8), 487–505. Epub 2020/05/13PubMed PMID: 32393771; PubMed Central PMCID: PMCPMC8284850. doi:10.1038/s41575-020-0300-1

Hu, R., Wang, Y.-L., Edderkaoui, M., Lugea, A., Apte, M. V., and Pandol, S. J. (2007). Ethanol Augments PDGF-Induced NADPH Oxidase Activity and Proliferation in Rat Pancreatic Stellate Cells. *Pancreatology* 7 (4), 332–340. Epub 2007/07/14PubMed PMID: 17627098; PubMed Central PMCID: PMCPMC2826430. doi:10.1159/000105499

Huang, H., Svoboda, R. A., Lazenby, A. J., Saowapa, J., Chaika, N., Ding, K., et al. (2016). Up-regulation of N-Cadherin by Collagen I-Activated Discoidin Domain Receptor 1 in Pancreatic Cancer Requires the Adaptor Molecule Shc1. *J. Biol. Chem.* 291 (44), 23208–23223. Epub 2016/10/30PubMed PMID: 27605668; PubMed Central PMCID: PMCPMC5087738. doi:10.1074/jbc.M116.740605

Ikenaga, N., Ohuchida, K., Mizumoto, K., Cui, L., Kayashima, T., Morimatsu, K., et al. (2010). CD10+ Pancreatic Stellate Cells Enhance the Progression of Pancreatic Cancer. *Gastroenterology* 139 (3), 1041–1051. PubMed PMID: 20685603. doi:10.1053/j.gastro.2010.05.084

Imamichi, Y., König, A., Gress, T., and Menke, A. (2007). Collagen Type I-Induced Smad-Interacting Protein 1 Expression Downregulates E-Cadherin in Pancreatic Cancer. *Oncogene* 26 (16), 2381–2385. Epub 2006/10/18PubMed PMID: 17043655. doi:10.1038/sj.onc.1210012

Incio, J., Liu, H., Suboj, P., Chin, S. M., Chen, I. X., Pinter, M., et al. (2016). Obesity-Induced Inflammation and Desmoplasia Promote Pancreatic Cancer Progression and Resistance to Chemotherapy. *Cancer Discov.* 6 (8), 852–869. Epub 2016/06/02PubMed PMID: 27246539; PubMed Central PMCID: PMCPMC4972679. doi:10.1158/2159-8290.cd-15-1177

Ivaska, J., and Heino, J. (2011). Cooperation between Integrins and Growth Factor Receptors in Signaling and Endocytosis. *Annu. Rev. Cel Dev. Biol.* 27, 291–320. Epub 2011/06/15PubMed PMID: 21663443. doi:10.1146/annurev-cellbio-092910-154017

Iwamoto, C., Ohuchida, K., Shinkawa, T., Okuda, S., Otsubo, Y., Okumura, T., et al. (2021). Bone Marrow-Derived Macrophages Converted into Cancer-Associated Fibroblast-like Cells Promote Pancreatic Cancer Progression. *Cancer Lett.* 512, 15–27. Epub 2021/05/08PubMed PMID: 33961925. doi:10.1016/j.canlet.2021.04.013

Jacobetz, M. A., Chan, D. S., Neesse, A., Bapiro, T. E., Cook, N., Frese, K. K., et al. (2013). Hyaluronan Impairs Vascular Function and Drug Delivery in a Mouse Model of Pancreatic Cancer. *Gut* 62 (1), 112–120. Epub 2012/04/03PubMed PMID: 22466618; PubMed Central PMCID: PMCPMC3551211. doi:10.1136/gutjnl-2012-302529

Jarrin Jara, M. D., Gautam, A. S., Peesapati, V. S. R., Sadik, M., and Khan, S. (2020). The Role of Interleukin-6 and Inflammatory Cytokines in Pancreatic Cancer-Associated Depression. *Cureus* 12 (8), e9969, 2020 . Epub 2020/08/28PubMed PMID: 32850269; PubMed Central PMCID: PMCPMC7444958. doi:10.7759/cureus.9969

Johnson, D. E., O'Keefe, R. A., and Grandis, J. R. (2018). Targeting the IL-6/JAK/STAT3 Signalling axis in Cancer. *Nat. Rev. Clin. Oncol.* 15 (4), 234–248. Epub 2018/02/07PubMed PMID: 29405201; PubMed Central PMCID: PMCPMC5858971. doi:10.1038/nrclinonc.2018.8

Junliang, L., Lili, W., Xiaolong, L., Xuguang, L., Huanwen, W., and Zhiyong, L. (2019). High-molecular-weight Hyaluronan Produced by Activated Pancreatic Stellate Cells Promotes Pancreatic Cancer Cell Migration via Paracrine Signaling. *Biochem. biophysical Res. Commun.* 515 (3), 493–498. Epub 2019/06/07PubMed PMID: 31171359. doi:10.1016/j.bbrc.2019.05.167

Kamisawa, T., Wood, L. D., Itoi, T., and Takaori, K. (2016). Pancreatic Cancer. *The Lancet* 388 (10039), 73–85. Epub 2016/02/03PubMed PMID: 26830752. doi:10.1016/s0140-6736(16)00141-0

Katoh, M. (2018). Multi-layered P-revention and T-reatment of C-hronic I-nflammation, O-rgan F-ibrosis and C-ancer A-ssociated with C-anonical WNT/β-catenin S-ignaling A-ctivation (Review). *Int. J. Mol. Med.* 42 (2), 713–725. Epub 2018/05/23PubMed PMID: 29786110; PubMed Central PMCID: PMCPMC6034925. doi:10.3892/ijmm.2018.3689

Kaur, S., Bansal, Y., Kumar, R., and Bansal, G. (2020). A Panoramic Review of IL-6: Structure, Pathophysiological Roles and Inhibitors. *Bioorg. Med. Chem.* 28 (5), 115327, 2020 . Epub 2020/01/30PubMed PMID: 31992476. doi:10.1016/j.bmc.2020.115327

Kesharwani, P., Banerjee, S., Padhye, S., Sarkar, F. H., and Iyer, A. K. (2015). Hyaluronic Acid Engineered Nanomicelles Loaded with 3,4-Difluorobenzylidene Curcumin for Targeted Killing of CD44+ Stem-like Pancreatic Cancer Cells. *Biomacromolecules* 16 (9), 3042–3053. Epub 2015/08/25PubMed PMID: 26302089. doi:10.1021/acs.biomac.5b00941

Kesharwani, P., Xie, L., Banerjee, S., Mao, G., Padhye, S., Sarkar, F. H., et al. (2015). Hyaluronic Acid-Conjugated Polyamidoamine Dendrimers for Targeted Delivery of 3,4-difluorobenzylidene Curcumin to CD44 Overexpressing Pancreatic Cancer Cells. *Colloids Surf. B: BiointerfacesBiointerfaces* 136, 413–423. Epub 2015/10/07PubMed PMID: 26440757. doi:10.1016/j.colsurfb.2015.09.043

Khan, M. A., Srivastava, S. K., Zubair, H., Patel, G. K., Arora, S., Khushman, M. d., et al. (2020). Co-targeting of CXCR4 and Hedgehog Pathways Disrupts Tumor-Stromal Crosstalk and Improves Chemotherapeutic Efficacy in Pancreatic Cancer. *J. Biol. Chem.* 295 (25), 8413–8424. Epub 2020/05/03PubMed PMID: 32358063; PubMed Central PMCID: PMCPMC7307206. doi:10.1074/jbc.RA119.011748

Kim, E. J., Sahai, V., Abel, E. V., Griffith, K. A., Greenson, J. K., Takebe, N., et al. (2014). Pilot Clinical Trial of Hedgehog Pathway Inhibitor GDC-0449 (Vismodegib) in Combination with Gemcitabine in Patients with Metastatic Pancreatic Adenocarcinoma. *Clin. Cancer Res.* 20 (23), 5937–5945. Epub 2014/10/04PubMed PMID: 25278454; PubMed Central PMCID: PMCPMC4254161. doi:10.1158/1078-0432.ccr-14-1269

Kim, J.-W., Park, S.-Y., You, Y.-H., Ham, D.-S., Lee, S.-H., Yang, H. K., et al. (2016). Suppression of ROS Production by Exendin-4 in PSC Attenuates the High Glucose-Induced Islet Fibrosis. *PloS one* 11 (12), e0163187, 2016 . Epub 2016/12/16PubMed PMID: 27977690; PubMed Central PMCID: PMCPMC5157943. doi:10.1371/journal.pone.0163187

Kocher, H. M., Basu, B., Froeling, F. E. M., Sarker, D., Slater, S., Carlin, D., et al. (2020). Phase I Clinical Trial Repurposing All-Trans Retinoic Acid as a Stromal Targeting Agent for Pancreatic Cancer. *Nat. Commun.* 11 (1), 4841, 2020 . Epub 2020/09/26PubMed PMID: 32973176. doi:10.1038/s41467-020-18636-w

Koenig, A., Mueller, C., Hasel, C., Adler, G., and Menke, A. (2006). Collagen Type I Induces Disruption of E-Cadherin-Mediated Cell-Cell Contacts and Promotes Proliferation of Pancreatic Carcinoma Cells. *Cancer Res.* 66 (9), 4662–4671. Epub 2006/05/03PubMed PMID: 16651417. doi:10.1158/0008-5472.can-05-2804

Kolenda, T., Guglas, K., Kopczyńska, M., Sobocińska, J., Teresiak, A., Bliźniak, R., et al. (2020). Good or Not Good: Role of miR-18a in Cancer Biology. *Rep. Pract. Oncol. Radiother.* 25 (5), 808–819. Epub 2020/09/05PubMed PMID: 32884453; PubMed Central PMCID: PMCPMC7451592. doi:10.1016/j.rpor.2020.07.006

Lei, J., Huo, X., Duan, W., Xu, Q., Li, R., Ma, J., et al. (2014). α-Mangostin Inhibits Hypoxia-Driven ROS-Induced PSC Activation and Pancreatic Cancer Cell Invasion. *Cancer Lett.* 347 (1), 129–138. Epub 2014/02/12PubMed PMID: 24513179; PubMed Central PMCID: PMCPMC4005872. doi:10.1016/j.canlet.2014.02.003

Lenggenhager, D., Amrutkar, M., Sántha, P., Aasrum, M., Löhr, J.-M., Gladhaug, I. P., et al. (2019). Commonly Used Pancreatic Stellate Cell Cultures Differ Phenotypically and in Their Interactions with Pancreatic Cancer Cells. *Cells* 8 (1), 23, 2019 . Epub 2019/01/10PubMed PMID: 30621293; PubMed Central PMCID: PMCPMC6356867. doi:10.3390/cells8010023

Lin, J. H., Huffman, A. P., Wattenberg, M. M., Walter, D. M., Carpenter, E. L., Feldser, D. M., et al. (2020). Type 1 Conventional Dendritic Cells Are Systemically Dysregulated Early in Pancreatic Carcinogenesis. *J. Exp. Med.* 217 (8). Epub 2020/05/27PubMed PMID: 32453421. doi:10.1084/jem.20190673

Long, K. B., Tooker, G., Tooker, E., Luque, S. L., Lee, J. W., Pan, X., et al. (2017). IL6 Receptor Blockade Enhances Chemotherapy Efficacy in Pancreatic Ductal Adenocarcinoma. *Mol. Cancer Ther.* 16 (9), 1898–1908. Epub 2017/06/15PubMed PMID: 28611107; PubMed Central PMCID: PMCPMC5587413. doi:10.1158/1535-7163.mct-16-0899

Lu, C., Talukder, A., Savage, N. M., Singh, N., and Liu, K. (2017). JAK-STAT-mediated Chronic Inflammation Impairs Cytotoxic T Lymphocyte Activation to Decrease Anti-PD-1 Immunotherapy Efficacy in Pancreatic Cancer. *Oncoimmunology* 6 (3), e1291106, 2017 . Epub 2017/04/14PubMed PMID: 28405527; PubMed Central PMCID: PMCPMC5384417. doi:10.1080/2162402x.2017.1291106

Ma, Q., Wu, H., Xiao, Y., Liang, Z., and Liu, T. (2020). Upregulation of Exosomal microRNA-21 in P-ancreatic S-tellate C-ells P-romotes P-ancreatic C-ancer C-ell M-igration and E-nhances Ras/ERK P-athway A-ctivity. *Int. J. Oncol.* 56 (4), 1025–1033. Epub 2020/04/23PubMed PMID: 32319558. doi:10.3892/ijo.2020.4986

Mace, T. A., Shakya, R., Pitarresi, J. R., Swanson, B., McQuinn, C. W., Loftus, S., et al. (2018). IL-6 and PD-L1 Antibody Blockade Combination Therapy Reduces Tumour Progression in Murine Models of Pancreatic Cancer. *Gut* 67 (2), 320–332. Epub 2016/11/01PubMed PMID: 27797936; PubMed Central PMCID: PMCPMC5406266. doi:10.1136/gutjnl-2016-311585

Marengo, A., Forciniti, S., Dando, I., Dalla Pozza, E., Stella, B., Tsapis, N., et al. (2019). Pancreatic Cancer Stem Cell Proliferation Is Strongly Inhibited by Diethyldithiocarbamate-Copper Complex Loaded into Hyaluronic Acid Decorated Liposomes. *Biochim. Biophys. Acta (Bba) - Gen. Subjects* 1863 (1), 61–72. Epub 2018/09/30PubMed PMID: 30267751. doi:10.1016/j.bbagen.2018.09.018

Marigo, I., Bosio, E., Solito, S., Mesa, C., Fernandez, A., Dolcetti, L., et al. (2010). Tumor-Induced Tolerance and Immune Suppression Depend on the C/EBPβ Transcription Factor. *Immunity* 32 (6), 790–802. Epub 2010/07/08PubMed PMID: 20605485. doi:10.1016/j.immuni.2010.05.010

Masamune, A., Kikuta, K., Watanabe, T., Satoh, K., Hirota, M., Hamada, S., et al. (2009). Fibrinogen Induces Cytokine and Collagen Production in Pancreatic Stellate Cells. *Gut* 58 (4), 550–559. Epub 2008/12/05PubMed PMID: 19052021. doi:10.1136/gut.2008.154401

Masamune, A., Satoh, M., Hirabayashi, J., Kasai, K., Satoh, K., and Shimosegawa, T. (2006). Galectin-1 Induces Chemokine Production and Proliferation in Pancreatic Stellate Cells. *Am. J. Physiology-Gastrointestinal Liver Physiol.* 290 (4), G729–G736. Epub 2005/12/24PubMed PMID: 16373424. doi:10.1152/ajpgi.00511.2005

Mattheolabakis, G., Milane, L., Singh, A., and Amiji, M. M. (2015). Hyaluronic Acid Targeting of CD44 for Cancer Therapy: from Receptor Biology to Nanomedicine. *J. Drug Target.* 23 (7-8), 605–618. Epub 2015/10/11PubMed PMID: 26453158. doi:10.3109/1061186x.2015.1052072

Melisi, D., Garcia-Carbonero, R., Macarulla, T., Pezet, D., Deplanque, G., Fuchs, M., et al. (2019). TGFβ Receptor Inhibitor Galunisertib Is Linked to Inflammation- and Remodeling-Related Proteins in Patients with Pancreatic Cancer. *Cancer Chemother. Pharmacol.* 83 (5), 975–991. Epub 2019/03/20PubMed PMID: 30887178. doi:10.1007/s00280-019-03807-4

Mews, P., Phillips, P., Fahmy, R., Korsten, M., Pirola, R., Wilson, J., et al. (2002). Pancreatic Stellate Cells Respond to Inflammatory Cytokines: Potential Role in Chronic Pancreatitis. *Gut* 50 (4), 535–541. Epub 2002/03/13PubMed PMID: 11889076; PubMed Central PMCID: PMCPMC1773172. doi:10.1136/gut.50.4.535

Miura, T., Mitsunaga, S., Ikeda, M., Shimizu, S., Ohno, I., Takahashi, H., et al. (2015). Characterization of Patients with Advanced Pancreatic Cancer and High Serum Interleukin-6 Levels. *Pancreas* 44 (5), 756–763. Epub 2015/05/02PubMed PMID: 25931255. doi:10.1097/mpa.0000000000000335

Miyai, Y., Esaki, N., Takahashi, M., and Enomoto, A. (2020). Cancer-associated Fibroblasts that Restrain Cancer Progression: Hypotheses and Perspectives. *Cancer Sci.* 111 (4), 1047–1057. Epub 2020/02/16PubMed PMID: 32060987; PubMed Central PMCID: PMCPMC7156845. doi:10.1111/cas.14346

Miyazaki, Y., Oda, T., Inagaki, Y., Kushige, H., Saito, Y., Mori, N., et al. (2021). Adipose-derived Mesenchymal Stem Cells Differentiate into Heterogeneous Cancer-Associated Fibroblasts in a Stroma-Rich Xenograft Model. *Sci. Rep.* 11 (1), 4690, 2021 . Epub 2021/02/27PubMed PMID: 33633222; PubMed Central PMCID: PMCPMC7907195. doi:10.1038/s41598-021-84058-3

Miyazaki, Y., Oda, T., Mori, N., and Kida, Y. S. (2020). Adipose-derived Mesenchymal Stem Cells Differentiate into Pancreatic Cancer-associated Fibroblasts *In Vitro*. *FEBS open bio* 10 (11), 2268–2281. Epub 2020/09/16PubMed PMID: 32931156; PubMed Central PMCID: PMCPMC7609785. doi:10.1002/2211-5463.12976

Mizrahi, J. D., Surana, R., Valle, J. W., and Shroff, R. T. (2020). Pancreatic Cancer. *Lancet Lond. Engl.* 395 (10242), 2008–2020. Epub 2020/07/01PubMed PMID: 32593337. doi:10.1016/s0140-6736(20)30974-0

Mizutani, Y., Kobayashi, H., Iida, T., Asai, N., Masamune, A., Hara, A., et al. (2019). Meflin-Positive Cancer-Associated Fibroblasts Inhibit Pancreatic Carcinogenesis. *Cancer Res.* 79 (20), 5367–5381. Epub 2019/08/24PubMed PMID: 31439548. doi:10.1158/0008-5472.can-19-0454

Moffitt, R. A., Marayati, R., Flate, E. L., Volmar, K. E., Loeza, S. G. H., Hoadley, K. A., et al. (2015). Virtual Microdissection Identifies Distinct Tumor- and Stroma-specific Subtypes of Pancreatic Ductal Adenocarcinoma. *Nat. Genet.* 47 (10), 1168–1178. Epub 2015/09/08PubMed PMID: 26343385; PubMed Central PMCID: PMCPMC4912058. doi:10.1038/ng.3398

Naci, D., Vuori, K., and Aoudjit, F. (2015). Alpha2beta1 Integrin in Cancer Development and Chemoresistance. *Semin. Cancer Biol.* 35, 145–153. Epub 2015/08/25PubMed PMID: 26297892. doi:10.1016/j.semcancer.2015.08.004

Nagathihalli, N. S., Castellanos, J. A., Shi, C., Beesetty, Y., Reyzer, M. L., Caprioli, R., et al. (2015). Signal Transducer and Activator of Transcription 3, Mediated Remodeling of the Tumor Microenvironment Results in Enhanced Tumor Drug Delivery in a Mouse Model of Pancreatic Cancer. *Gastroenterology* 149 (7), 1932–1943. e9. Epub 2015/08/11PubMed PMID: 26255562; PubMed Central PMCID: PMCPMC4863449. doi:10.1053/j.gastro.2015.07.058

Nagathihalli, N. S., Castellanos, J. A., VanSaun, M. N., Dai, X., Ambrose, M., Guo, Q., et al. (2016). Pancreatic Stellate Cell Secreted IL-6 Stimulates STAT3 Dependent Invasiveness of Pancreatic Intraepithelial Neoplasia and Cancer Cells. *Oncotarget* 7 (40), 65982–65992. Epub 2016/09/08PubMed PMID: 27602757; PubMed Central PMCID: PMCPMC5323208. doi:10.18632/oncotarget.11786

Nagy, N., Kuipers, H. F., Frymoyer, A. R., Ishak, H. D., Bollyky, J. B., Wight, T. N., et al. (2015). 4-methylumbelliferone Treatment and Hyaluronan

Inhibition as a Therapeutic Strategy in Inflammation, Autoimmunity, and Cancer. *Front. Immunol.* 6, 123, 2015 . Epub 2015/04/09PubMed PMID: 25852691; PubMed Central PMCID: PMCPMC4369655. doi:10.3389/fimmu.2015.00123

Ng, K., Hendifar, A., Starodub, A., Chaves, J., Yang, Y., Koh, B., et al. (2019). Phase 1 Dose-Escalation Study of Momelotinib, a Janus Kinase 1/2 Inhibitor, Combined with Gemcitabine and Nab-Paclitaxel in Patients with Previously Untreated Metastatic Pancreatic Ductal Adenocarcinoma. *Invest. New Drugs* 37 (1), 159–165. Epub 2018/08/15PubMed PMID: 30105668; PubMed Central PMCID: PMCPMC6510909. doi:10.1007/s10637-018-0650-5

Nielsen, M. F. B., Mortensen, M. B., Sørensen, M. D., Wirenfeldt, M., Kristensen, B. W., Schrøder, H. D., et al. (2020). Spatial and Phenotypic Characterization of Pancreatic Cancer-Associated Fibroblasts after Neoadjuvant Treatment. *Histol. Histopathol* 35 (8), 811–825. Epub 2020/01/22PubMed PMID: 31960942. doi:10.14670/hh-18-201

Nielsen, M. F. B., Mortensen, M. B., and Detlefsen, S. (2018). Typing of Pancreatic Cancer-Associated Fibroblasts Identifies Different Subpopulations. *Wjg* 24 (41), 4663–4678. Epub 2018/11/13PubMed PMID: 30416314; PubMed Central PMCID: PMCPMC6224473. doi:10.3748/wjg.v24.i41.4663

Nigam Joshi, P., Agawane, S., Athalye, M. C., Jadhav, V., Sarkar, D., and Prakash, R. (2017). Multifunctional Inulin Tethered Silver-Graphene Quantum Dots Nanotheranostic Module for Pancreatic Cancer Therapy. *Mater. Sci. Eng. C* 78, 1203–1211. Epub 2017/06/04PubMed PMID: 28575959. doi:10.1016/j.msec.2017.03.176

Nurmik, M., Ullmann, P., Rodriguez, F., Haan, S., and Letellier, E. (2020). In Search of Definitions: Cancer-associated Fibroblasts and Their Markers. *Int. J. Cancer* 146 (4), 895–905. Epub 2019/02/09PubMed PMID: 30734283; PubMed Central PMCID: PMCPMC6972582. doi:10.1002/ijc.32193

Öhlund, D., Handly-Santana, A., Biffi, G., Elyada, E., Almeida, A. S., Ponz-Sarvise, M., et al. (2017). Distinct Populations of Inflammatory Fibroblasts and Myofibroblasts in Pancreatic Cancer. *J. Exp. Med.* 214 (3), 579–596. Epub 2017/02/25PubMed PMID: 28232471; PubMed Central PMCID: PMCPMC5339682. doi:10.1084/jem.20162024

Okitsu, K., Kanda, T., Imazeki, F., Yonemitsu, Y., Ray, R. B., Chang, C., et al. (2010). Involvement of Interleukin-6 and Androgen Receptor Signaling in Pancreatic Cancer. *Genes & Cancer* 1 (8), 859–867. Epub 2011/07/23PubMed PMID: 21779469; PubMed Central PMCID: PMCPMC3092246. doi:10.1177/1947601910383417

Özdemir, B. C., Pentcheva-Hoang, T., Carstens, J. L., Zheng, X., Wu, C.-C., Simpson, T. R., et al. (2014). Depletion of Carcinoma-Associated Fibroblasts and Fibrosis Induces Immunosuppression and Accelerates Pancreas Cancer with Reduced Survival. *Cancer cell* 25 (6), 719–734. Epub 2014/05/27PubMed PMID: 24856586; PubMed Central PMCID: PMCPMC4180632. doi:10.1016/j.ccr.2014.04.005

Palmquist, C., Dehlendorff, C., Calatayud, D., Hansen, C. P., Hasselby, J. P., and Johansen, J. S. (2020). Prediction of Unresectability and Prognosis in Patients Undergoing Surgery on Suspicion of Pancreatic Cancer Using Carbohydrate Antigen 19-9, Interleukin 6, and YKL-40. *Pancreas* 49 (1), 53–61. Epub 2019/12/20PubMed PMID: 31856080. doi:10.1097/mpa.0000000000001466

Patel, S. P., and Kurzrock, R. (2015). PD-L1 Expression as a Predictive Biomarker in Cancer Immunotherapy. *Mol. Cancer Ther.* 14 (4), 847–856. Epub 2015/02/20PubMed PMID: 25695955. doi:10.1158/1535-7163.mct-14-0983

Pothula, S. P., Pirola, R. C., Wilson, J. S., and Apte, M. V. (2020). Pancreatic Stellate Cells: Aiding and Abetting Pancreatic Cancer Progression. *Pancreatology* 20 (3), 409–418. Epub 2020/01/14PubMed PMID: 31928917. doi:10.1016/j.pan.2020.01.003

Pothula, S. P., Xu, Z., Goldstein, D., Pirola, R. C., Wilson, J. S., and Apte, M. V. (2016). Key Role of Pancreatic Stellate Cells in Pancreatic Cancer. *Cancer Lett.* 381 (1), 194–200. Epub 2015/11/17PubMed PMID: 26571462. doi:10.1016/j.canlet.2015.10.035

Procopio, M.-G., Laszlo, C., Al Labban, D., Kim, D. E., Bordignon, P., Jo, S.-H., et al. (2015). Combined CSL and P53 Downregulation Promotes Cancer-Associated Fibroblast Activation. *Nat. Cel Biol* 17 (9), 1193–1204. Epub 2015/08/25PubMed PMID: 26302407; PubMed Central PMCID: PMCPMC4699446. doi:10.1038/ncb3228

Qian, Z. Y., Peng, Q., Zhang, Z. W., Zhou, L. A., and Miao, Y. (2010). Roles of Smad3 and Smad7 in Rat Pancreatic Stellate Cells Activated by Transforming Growth Factor-Beta 1. *Hepatobiliary Pancreat. Dis. Int.* 9 (5), 531–536. Epub 2010/10/15. PubMed PMID: 20943464.

Ramanathan, R. K., McDonough, S. L., Philip, P. A., Hingorani, S. R., Lacy, J., Kortmansky, J. S., et al. (2019). Phase IB/II Randomized Study of FOLFIRINOX Plus Pegylated Recombinant Human Hyaluronidase versus FOLFIRINOX Alone in Patients with Metastatic Pancreatic Adenocarcinoma: SWOG S1313. *Jco* 37 (13), 1062–1069. Epub 2019/03/01PubMed PMID: 30817250; PubMed Central PMCID: PMCPMC6494359. doi:10.1200/jco.18.01295

Rhim, A. D., Oberstein, P. E., Thomas, D. H., Mirek, E. T., Palermo, C. F., Sastra, S. A., et al. (2014). Stromal Elements Act to Restrain, rather Than Support, Pancreatic Ductal Adenocarcinoma. *Cancer cell* 25 (6), 735–747. Epub 2014/05/27PubMed PMID: 24856585; PubMed Central PMCID: PMCPMC4096698. doi:10.1016/j.ccr.2014.04.021

Richter, K., Konzack, A., Pihlajaniemi, T., Heljasvaara, R., and Kietzmann, T. (2015). Redox-fibrosis: Impact of TGFβ1 on ROS Generators, Mediators and Functional Consequences. *Redox Biol.* 6, 344–352. Epub 2015/09/04PubMed PMID: 26335400; PubMed Central PMCID: PMCPMC4565043. doi:10.1016/j.redox.2015.08.015

Rodriguez-Hernandez, I., Cantelli, G., Bruce, F., and Sanz-Moreno, V. (2016). Rho, ROCK and Actomyosin Contractility in Metastasis as Drug Targets. *F1000Res* 5, 783, 2016 . Epub 2016/05/10PubMed PMID: 27158478; PubMed Central PMCID: PMCPMC4856114. doi:10.12688/f1000research.7909.1

Roife, D., Sarcar, B., and Fleming, J. B. (2020). Stellate Cells in the Tumor Microenvironment. *Adv. Exp. Med. Biol.* 1263, 67–84. Epub 2020/06/27PubMed PMID: 32588324. doi:10.1007/978-3-030-44518-8_6

Roy, I., Boyle, K. A., Vonderhaar, E. P., Zimmerman, N. P., Gorse, E., Mackinnon, A. C., et al. (2017). Cancer Cell Chemokines Direct Chemotaxis of Activated Stellate Cells in Pancreatic Ductal Adenocarcinoma. *Lab. Invest.* 97 (3), 302–317. Epub 2017/01/17PubMed PMID: 28092365; PubMed Central PMCID: PMCPMC5334280. doi:10.1038/labinvest.2016.146

Sahai, E., Astsaturov, I., Cukierman, E., DeNardo, D. G., Egeblad, M., Evans, R. M., et al. (2020). A Framework for Advancing Our Understanding of Cancer-Associated Fibroblasts. *Nat. Rev. Cancer* 20 (3), 174–186. Epub 2020/01/26PubMed PMID: 31980749. doi:10.1038/s41568-019-0238-1

Sarper, M., Cortes, E., Lieberthal, T. J., and del Río Hernández, A. (2016). ATRA Modulates Mechanical Activation of TGF-β by Pancreatic Stellate Cells. *Sci. Rep.* 6, 27639, 2016 . Epub 2016/07/05PubMed PMID: 27375161; PubMed Central PMCID: PMCPMC4931506. doi:10.1038/srep27639

Sato, N., Kohi, S., Hirata, K., and Goggins, M. (2016). Role of Hyaluronan in Pancreatic Cancer Biology and Therapy: Once Again in the Spotlight. *Cancer Sci.* 107 (5), 569–575. Epub 2016/02/27PubMed PMID: 26918382; PubMed Central PMCID: PMCPMC4970823. doi:10.1111/cas.12913

Schnittert, J., Bansal, R., and Prakash, J. (2019). Targeting Pancreatic Stellate Cells in Cancer. *Trends Cancer* 5 (2), 128–142. Epub 2019/02/14PubMed PMID: 30755305. doi:10.1016/j.trecan.2019.01.001

Serri, C., Quagliariello, V., Iaffaioli, R. V., Fusco, S., Botti, G., Mayol, L., et al. (2019). Combination Therapy for the Treatment of Pancreatic Cancer through Hyaluronic Acid-decorated Nanoparticles Loaded with Quercetin and Gemcitabine: A Preliminary *In Vitro* Study. *J. Cel Physiol* 234 (4), 4959–4969. Epub 2018/10/20PubMed PMID: 30334571. doi:10.1002/jcp.27297

Shao, C., Tu, C., Cheng, X., Xu, Z., Wang, X., Shen, J., et al. (2019). Inflammatory and Senescent Phenotype of Pancreatic Stellate Cells Induced by Sqstm1 Downregulation Facilitates Pancreatic Cancer Progression. *Int. J. Biol. Sci.* 15 (5), 1020–1029. Epub 2019/06/12PubMed PMID: 31182922; PubMed Central PMCID: PMCPMC6535784. doi:10.7150/ijbs.27825

Sherman, M. H. (2018). Stellate Cells in Tissue Repair, Inflammation, and Cancer. *Annu. Rev. Cel Dev. Biol.* 34, 333–355. Epub 2018/07/22PubMed PMID: 30028641. doi:10.1146/annurev-cellbio-100617-062855

Sherman, M. H., Yu, R. T., Engle, D. D., Ding, N., Atkins, A. R., Tiriac, H., et al. (2014). Vitamin D Receptor-Mediated Stromal Reprogramming Suppresses Pancreatitis and Enhances Pancreatic Cancer Therapy. *Cell* 159 (1), 80–93.

Epub 2014/09/27PubMed PMID: 25259922; PubMed Central PMCID: PMCPMC4177038. doi:10.1016/j.cell.2014.08.007

Shields, M. A., Dangi-Garimella, S., Krantz, S. B., Bentrem, D. J., and Munshi, H. G. (2011). Pancreatic Cancer Cells Respond to Type I Collagen by Inducing Snail Expression to Promote Membrane Type 1 Matrix Metalloproteinase-dependent Collagen Invasion. *J. Biol. Chem.* 286 (12), 10495–10504. Epub 2011/02/04PubMed PMID: 21288898; PubMed Central PMCID: PMCPMC3060503. doi:10.1074/jbc.M110.195628

Shintani, Y., Hollingsworth, M. A., Wheelock, M. J., and Johnson, K. R. (2006). Collagen I Promotes Metastasis in Pancreatic Cancer by Activating C-Jun NH2-Terminal Kinase 1 and Up-Regulating N-Cadherin Expression. *Cancer Res.* 66 (24), 11745–11753. Epub 2006/12/21PubMed PMID: 17178870. doi:10.1158/0008-5472.can-06-2322

Song, H., and Zhang, Y. (2018). Regulation of Pancreatic Stellate Cell Activation by Notch3. *BMC cancer* 18 (1), 36, 2018 . Epub 2018/01/07PubMed PMID: 29304760; PubMed Central PMCID: PMCPMC5756326. doi:10.1186/s12885-017-3957-2

Steele, N. G., Biffi, G., Kemp, S. B., Zhang, Y., Drouillard, D., Syu, L., et al. (2021). Inhibition of Hedgehog Signaling Alters Fibroblast Composition in Pancreatic Cancer. *Clin. Cancer Res.* 27 (7), 2023–2037. Epub 2021/01/27PubMed PMID: 33495315; PubMed Central PMCID: PMCPMC8026631. doi:10.1158/1078-0432.ccr-20-3715

Sugahara, K. N., Hirata, T., Tanaka, T., Ogino, S., Takeda, M., Terasawa, H., et al. (2008). Chondroitin Sulfate E Fragments Enhance CD44 Cleavage and CD44-dependent Motility in Tumor Cells. *Cancer Res.* 68 (17), 7191–7199. Epub 2008/09/02PubMed PMID: 18757435. doi:10.1158/0008-5472.can-07-6198

Sun, C. K., Man, K., Ng, K. T., Ho, J. W., Lim, Z. X., Cheng, Q., et al. (2008). Proline-rich Tyrosine Kinase 2 (Pyk2) Promotes Proliferation and Invasiveness of Hepatocellular Carcinoma Cells through C-Src/ERK Activation. *Carcinogenesis* 29 (11), 2096–2105. Epub 2008/09/04PubMed PMID: 18765415. doi:10.1093/carcin/bgn203

Tahara, H., Sato, K., Yamazaki, Y., Ohyama, T., Horiguchi, N., Hashizume, H., et al. (2013). Transforming Growth Factor-α Activates Pancreatic Stellate Cells and May Be Involved in Matrix Metalloproteinase-1 Upregulation. *Lab. Invest.* 93 (6), 720–732. Epub 2013/04/24PubMed PMID: 23608755. doi:10.1038/labinvest.2013.59

Theocharis, A. D., Tsara, M. E., Papageorgacopoulou, N., Karavias, D. D., and Theocharis, D. A. (2000). Pancreatic Carcinoma Is Characterized by Elevated Content of Hyaluronan and Chondroitin Sulfate with Altered Disaccharide Composition. *Biochim. Biophys. Acta (Bba) - Mol. Basis Dis.* 1502 (2), 201–206. Epub 2000/10/21PubMed PMID: 11040445. doi:10.1016/s0925-4439(00)00051-x

Tjomsland, V., Pomianowska, E., Aasrum, M., Sandnes, D., Verbeke, C. S., and Gladhaug, I. P. (2016). Profile of MMP and TIMP Expression in Human Pancreatic Stellate Cells: Regulation by IL-1α and TGFβ and Implications for Migration of Pancreatic Cancer Cells. *Neoplasia New York, NY* 18 (7), 447–456. Epub 2016/07/21PubMed PMID: 27435927; PubMed Central PMCID: PMCPMC4954934. doi:10.1016/j.neo.2016.06.003

Tjomsland, V., Sandnes, D., Pomianowska, E., Cizmovic, S. T., Aasrum, M., Brusevold, I. J., et al. (2016). The TGFβ-SMAD3 Pathway Inhibits IL-1α Induced Interactions between Human Pancreatic Stellate Cells and Pancreatic Carcinoma Cells and Restricts Cancer Cell Migration. *J. Exp. Clin. Cancer Res.* 35 (1), 122, 2016 . Epub 2016/07/31PubMed PMID: 27473228; PubMed Central PMCID: PMCPMC4966589. doi:10.1186/s13046-016-0400-5

Tjomsland, V., Spångeus, A., Välilä, J., Sandström, P., Borch, K., Druid, H., et al. (2011). Interleukin 1α Sustains the Expression of Inflammatory Factors in Human Pancreatic Cancer Microenvironment by Targeting Cancer-Associated Fibroblasts. *Neoplasia New York, NY* 13 (8), 664–IN3. Epub 2011/08/19PubMed PMID: 21847358; PubMed Central PMCID: PMCPMC3156657. doi:10.1593/neo.11332

Tsoukalas, N., Kiakou, M., Tsapakidis, K., Tolia, M., Aravantinou-Fatorou, E., Baxevanos, P., et al. (2019). PD-1 and PD-L1 as Immunotherapy Targets and Biomarkers in Non-small Cell Lung Cancer. *J. BUON* 24 (3), 883–888. Epub 2019/08/20. PubMed PMID: 31424637.

Tsukamoto, H., Fujieda, K., Miyashita, A., Fukushima, S., Ikeda, T., Kubo, Y., et al. (2018). Combined Blockade of IL6 and PD-1/pd-L1 Signaling Abrogates Mutual Regulation of Their Immunosuppressive Effects in the Tumor Microenvironment. *Cancer Res.* 78 (17), 5011–5022. Epub 2018/07/04PubMed PMID: 29967259. doi:10.1158/0008-5472.can-18-0118

van Duijneveldt, G., Griffin, M. D. W., and Putoczki, T. L. (19792020). Emerging Roles for the IL-6 Family of Cytokines in Pancreatic Cancer. *Clin. Sci. Lond. Engl.* 134 (16), 2091–2115. Epub 2020/08/19PubMed PMID: 32808663; PubMed Central PMCID: PMCPMC7434989. doi:10.1042/cs20191211

Wang, H.-C., Lin, Y.-L., Hsu, C.-C., Chao, Y.-J., Hou, Y.-C., Chiu, T.-J., et al. (2019). Pancreatic Stellate Cells Activated by Mutant KRAS-Mediated PAI-1 Upregulation foster Pancreatic Cancer Progression via IL-8. *Theranostics* 9 (24), 7168–7183. Epub 2019/11/07PubMed PMID: 31695760; PubMed Central PMCID: PMCPMC6831292. doi:10.7150/thno.36830

Wang, L., Wu, H., Wang, L., Zhang, H., Lu, J., Liang, Z., et al. (2017). Asporin Promotes Pancreatic Cancer Cell Invasion and Migration by Regulating the Epithelial-To-Mesenchymal Transition (EMT) through Both Autocrine and Paracrine Mechanisms. *Cancer Lett.* 398, 24–36. Epub 2017/04/13PubMed PMID: 28400334. doi:10.1016/j.canlet.2017.04.001

Wang, S., Li, Y., Xing, C., Ding, C., Zhang, H., Chen, L., et al. (2020). Tumor Microenvironment in Chemoresistance, Metastasis and Immunotherapy of Pancreatic Cancer. *Am. J. Cancer Res.* 10 (7), 1937–1953. Epub 2020/08/11. PubMed PMID: 32774994; PubMed Central PMCID: PMCPMC7407356.

Weber, R., Groth, C., Lasser, S., Arkhypov, I., Petrova, V., Altevogt, P., et al. (2021). IL-6 as a Major Regulator of MDSC Activity and Possible Target for Cancer Immunotherapy. *Cell Immunol.* 359, 104254, 2021 . Epub 2020/12/10PubMed PMID: 33296753. doi:10.1016/j.cellimm.2020.104254

Wei, X., Senanayake, T. H., Warren, G., and Vinogradov, S. V. (2013). Hyaluronic Acid-Based Nanogel-Drug Conjugates with Enhanced Anticancer Activity Designed for the Targeting of CD44-Positive and Drug-Resistant Tumors. *Bioconjug. Chem.* 24 (4), 658–668. Epub 2013/04/04PubMed PMID: 23547842; PubMed Central PMCID: PMCPMC3677708. doi:10.1021/bc300632w

Wen, Z., Liu, Q., Wu, J., Xu, B., Wang, J., Liang, L., et al. (2019). Fibroblast Activation Protein α-positive Pancreatic Stellate Cells Promote the Migration and Invasion of Pancreatic Cancer by CXCL1-Mediated Akt Phosphorylation. *Ann. Transl. Med.* 7 (20), 532, 2019 . Epub 2019/12/07PubMed PMID: 31807514; PubMed Central PMCID: PMCPMC6861799. doi:10.21037/atm.2019.09.164

Whatcott, C. J., Diep, C. H., Jiang, P., Watanabe, A., LoBello, J., Sima, C., et al. (2015). Desmoplasia in Primary Tumors and Metastatic Lesions of Pancreatic Cancer. *Clin. Cancer Res.* 21 (15), 3561–3568. Epub 2015/02/20PubMed PMID: 25695692; PubMed Central PMCID: PMCPMC4526394. doi:10.1158/1078-0432.ccr-14-1051

Wu, Y., Zhang, C., Jiang, K., Werner, J., Bazhin, A. V., and D'Haese, J. G. (2020). The Role of Stellate Cells in Pancreatic Ductal Adenocarcinoma: Targeting Perspectives. *Front. Oncol.* 10, 621937, 2020 . Epub 2021/02/02PubMed PMID: 33520728; PubMed Central PMCID: PMCPMC7841014. doi:10.3389/fonc.2020.621937

Xu, J., Liu, S., Yang, X., Cao, S., and Zhou, Y. (2020). Paracrine HGF Promotes EMT and Mediates the Effects of PSC on Chemoresistance by Activating C-Met/PI3K/Akt Signaling in Pancreatic Cancer *In Vitro*. *Life Sci.* 263, 118523, 2020 . Epub 2020/10/12PubMed PMID: 33039386. doi:10.1016/j.lfs.2020.118523

Yan, B., Jiang, Z., Cheng, L., Chen, K., Zhou, C., Sun, L., et al. (2018). Paracrine HGF/c-MET Enhances the Stem Cell-like Potential and Glycolysis of Pancreatic Cancer Cells via Activation of YAP/HIF-1α. *Exp. Cel. Res.* 371 (1), 63–71. Epub 2018/07/30PubMed PMID: 30056064. doi:10.1016/j.yexcr.2018.07.041

Yu, H., Lee, H., Herrmann, A., Buettner, R., and Jove, R. (2014). Revisiting STAT3 Signalling in Cancer: New and Unexpected Biological Functions. *Nat. Rev.*

Cancer 14 (11), 736–746. Epub 2014/10/25PubMed PMID: 25342631. doi:10.1038/nrc3818

Yuan, Y., Jiang, J. Y., Wang, J. M., Sun, J., Li, C., Liu, B. Q., et al. (2019). BAG3-positive Pancreatic Stellate Cells Promote Migration and Invasion of Pancreatic Ductal Adenocarcinoma. *J. Cel Mol Med* 23 (8), 5006–5016. Epub 2019/05/24PubMed PMID: 31119886; PubMed Central PMCID: PMCPMC6653255. doi:10.1111/jcmm.14352

Zhang, Z., Wang, F., Du, C., Guo, H., Ma, L., Liu, X., et al. (2017). BRM/SMARCA2 Promotes the Proliferation and Chemoresistance of Pancreatic Cancer Cells by Targeting JAK2/STAT3 Signaling. *Cancer Lett.* 402, 213–224. Epub 2017/06/13PubMed PMID: 28602977. doi:10.1016/j.canlet.2017.05.006

Zhao, W., Ajani, J. A., Sushovan, G., Ochi, N., Hwang, R., Hafley, M., et al. (2018). Galectin-3 Mediates Tumor Cell-Stroma Interactions by Activating Pancreatic Stellate Cells to Produce Cytokines via Integrin Signaling. *Gastroenterology* 154 (5), 1524–1537. e6. Epub 2017/12/25PubMed PMID: 29274868. doi:10.1053/j.gastro.2017.12.014

Conflict of Interest: The authors declare that the research was conducted in the absence of any commercial or financial relationships that could be construed as a potential conflict of interest.

Publisher's Note: All claims expressed in this article are solely those of the authors and do not necessarily represent those of their affiliated organizations, or those of the publisher, the editors and the reviewers. Any product that may be evaluated in this article, or claim that may be made by its manufacturer, is not guaranteed or endorsed by the publisher.

GLOSSARY

ATRA: All-trans retinoic acid

CAF: Cancer-associated fibroblasts

Coll: type 1 collagen.

DDR1: Discoidin domain receptors one

ECM: extracellular matrix.

FAP: fibroblast activation protein

HA: hyaluronic acid.

HAS: hyaluronan synthase.

IL-1: Interleukin-1.

IL-6: Interleukin-6.

IL-6R: Interleukin-6 receptor.

LIF: leukemia inhibitory factor.

PD-1: programmed death-ligand 1.

PD-L1: protein programmed cell death one ligand 1.

PEGPH20: PEGylated human recombinant hyaluronidase.

PDGF: platelet derived growth factor.

PSC: pancreatic stellate cell.

a-SMA: a-smooth muscle actin.

RhoA: Ras homolog family member A

ROS: reactive oxygen species

Shh: Sonic hedgehog.

TGF-β: transforming growth factor beta

frontiers in Cell and Developmental Biology

REVIEW
published: 24 December 2021
doi: 10.3389/fcell.2021.781828

An Overview of the Role of Mechanical Stretching in the Progression of Lung Cancer

Fengying Gong[1], Yuchao Yang[2], Liangtao Wen[3], Congrong Wang[4], Jingjun Li[1] and Jingxing Dai[2]**

[1]Department of Traditional Chinese Medicine, Nanfang Hospital of Southern Medical University, Guangzhou, China, [2]Guangdong Provincial Key Laboratory of Medical Biomechanics and Guangdong Engineering Research Center for Translation of Medical 3D Printing Application and National Key Discipline of Human Anatomy, School of Basic Medical Sciences, Southern Medical University, Guangzhou, China, [3]Shiyue City Community Health Service Center, Shenzhen Integrated Traditional Chinese and Western Medicine Hospital, Shenzhen, China, [4]Department of Laboratory Medicine, Nanfang Hospital of Southern Medical University, Guangzhou, China*

Cells and tissues in the human body are subjected to mechanical forces of varying degrees, such as tension or pressure. During tumorigenesis, physical factors, especially mechanical factors, are involved in tumor development. As lung tissue is influenced by movements associated with breathing, it is constantly subjected to cyclical stretching and retraction; therefore, lung cancer cells and lung cancer-associated fibroblasts (CAFs) are constantly exposed to mechanical load. Thus, to better explore the mechanisms involved in lung cancer progression, it is necessary to consider factors involved in cell mechanics, which may provide a more comprehensive analysis of tumorigenesis. The purpose of this review is: 1) to provide an overview of the anatomy and tissue characteristics of the lung and the presence of mechanical stimulation; 2) to summarize the role of mechanical stretching in the progression of lung cancer; and 3) to describe the relationship between mechanical stretching and the lung cancer microenvironment, especially CAFs.

Keywords: mechanical stretching, mechanotransduction, lung cancer, cancer-associated fibroblasts (CAFs), cancer microenvironment

OPEN ACCESS

Edited by:
Daniele Vergara,
University of Salento, Italy

Reviewed by:
Andreas Stylianou,
European University Cyprus, Cyprus
Pranshu Sahgal,
Dana–Farber Cancer Institute, United States

****Correspondence:***
Jingjun Li
lijingjun@smu.edu.cn
Jingxing Dai
daijx@smu.edu.cn

Specialty section:
This article was submitted to Molecular and Cellular Oncology, a section of the journal Frontiers in Cell and Developmental Biology

Received: *23 September 2021*
Accepted: *09 December 2021*
Published: *24 December 2021*

Citation:
Gong F, Yang Y, Wen L, Wang C, Li J and Dai J (2021) An Overview of the Role of Mechanical Stretching in the Progression of Lung Cancer. Front. Cell Dev. Biol. 9:781828. doi: 10.3389/fcell.2021.781828

INTRODUCTION

The main function of the lungs is to exchange oxygen and carbon dioxide with the outside world. The lung and thorax are important organs in the human respiratory system (**Figure 1**) (Novak et al., 2021). The respiratory muscles contract rhythmically, causing the thoracic volume to change periodically and then causing changes in pulmonary pressure, driving oxygen and carbon dioxide in and out of the lung to achieve pulmonary ventilation (Hsia et al., 2016; Doryab et al., 2021; Novak et al., 2021). Therefore, mechanical transduction plays a crucial role in lung health and disease. There are many types of mesenchymal cells in lung tissues. The fibroblast is one of the most important mesenchymal cells to maintain the normal physiological function of the lung. The

Abbreviations: CAFs, Cancer-associated fibroblasts; ECM, extracellular matrix; FEV1/FVC, forced expiratory volume to full forced lung capacity in one second; TLC%, total lung capacity percentage; FEV1, forced expiratory volume in one second; PF, pulmonary fibrosis; α-SMA, osteopontin, alpha smooth muscle actin; TGF-β, transforming growth factor-β.

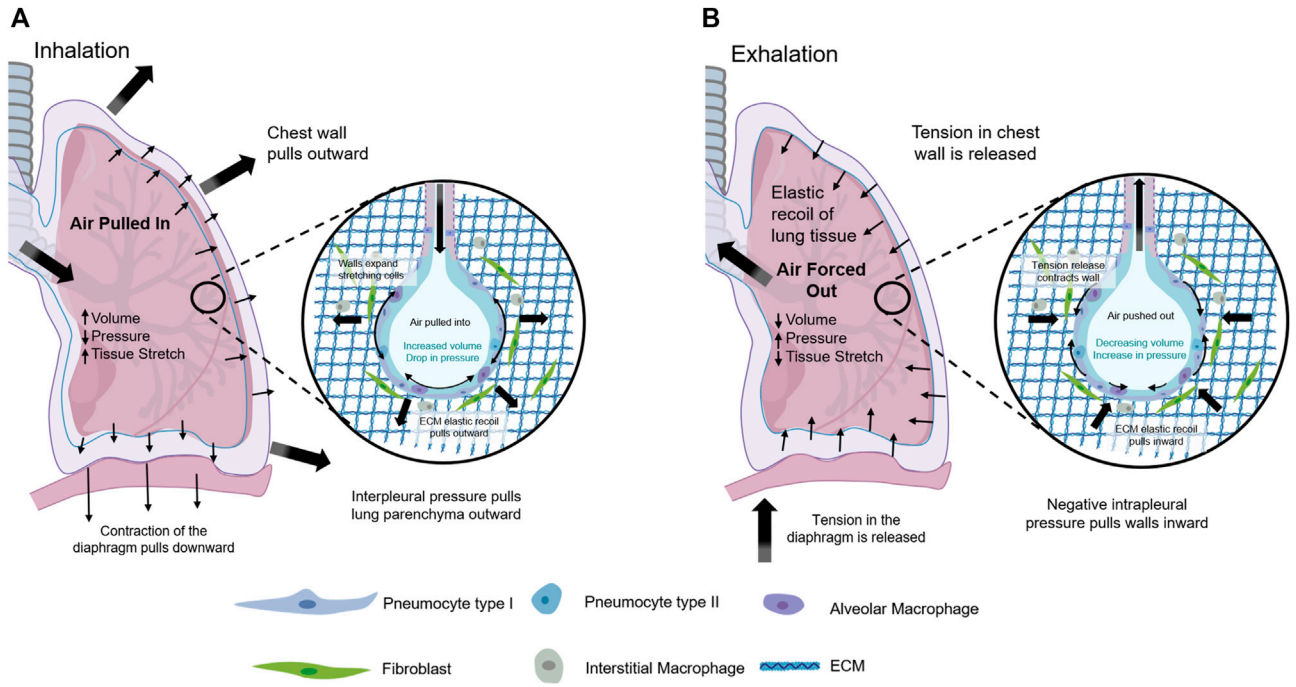

FIGURE 1 | Mechanical Forces within the lung. **(A)** Contraction of the diaphragm and muscles in chest wall during inhalation led to negative interpleural pressure that enlarged lung tissue, stretched the alveoli, and increased lung volume driving air pulled in. **(B)** Relaxation of the diaphragm and muscles in chest wall during expiration permitted for elastic retreat that decreased lung volume and air compression that drove air forced out.

heterogeneity of fibroblasts is responsible for their different phenotypes and activities (Kotaru et al., 2006).

Lung tissue is constantly influenced by breathing mechanics, and it is constantly exposed to a state of cyclical stretching and retraction. Therefore, lung cancer cells and lung cancer-associated fibroblasts (CAFs) are also influenced by mechanical load (Najrana et al., 2020; Roshanzadeh et al., 2020). Fibroblasts are the cells that make and sustain a structurally diverse array of ECM-rich connective tissues to support a wide-ranging of vital organ functions, like resistance to blunt and sharp damages in the skin or organ-wide stretching and flexible recoiling in the undamaged breathing lung. Three functions are generally assigned to fibroblasts: 1) secrete many of the same structural and signaling macromolecules that donate to the extracellular space; 2) adopt a transient and contractile myofibroblast phenotype in response to tissue injury; 3) play an important role in signaling extracellular cells for tissue-resident stem cells, or serve as mesenchymal stem cells, which can differentiate to specialized mesenchymal cells (Lemos and Duffield, 2018; Pittenger et al., 2019; Plikus et al., 2021). A main constituent of the tumor stroma is fibroblasts, and numerous studies have demonstrated a prominent functional role for these cells in cancer progression and metastasis (Kalluri and Zeisberg, 2006; Öhlund et al., 2014). Tumor related fibroblasts have been labeled CAFs, tumor associated fibroblasts, activated fibroblasts or activated myofibroblasts and could take in cancer-associated mesenchymal stem cells. To facilitate tissue repair, chemical and physical clues induce quiescent fibroblasts to myofibroblasts that secrete a lot of expressing contractile proteins in ECM such as α-SMA that coordinate biomechanical remodeling and contraction by traction (Plikus et al., 2017; Plikus et al., 2021).

Thus, to better explore the progression of lung cancer pathogenesis, it is necessary to combine cell mechanics factors to obtain a more comprehensive analysis. The purpose of this brief review is: 1) to provide an overview of the anatomy and tissue characteristics of the lung and the presence of mechanical stimulation; 2) to summarize the role of mechanical stretching in the progression of lung cancer; and 3) to describe the relationship between mechanical stretching and lung cancer microenvironment, especially CAFs.

PHYSIOLOGICAL AND BIOMECHANICAL CHARACTERISTICS OF THE LUNG

The lungs are in the chest cavity, on either side of the mediastinum, above the diaphragm. The lungs are composed of two functional areas: 1) the airways through which air enters and passes the pharynx, larynx, trachea, main bronchi, bronchioles, and terminal bronchioles; and 2) the respiratory zone (gas exchange zone), including the alveolar tubes, bronchioles, and alveolar sacs (Ahadian et al., 2018).

The main function of the lungs is to exchange gas with the outside world. Through the external respiration function of the lungs, oxygen (O_2) is continuously provided to the body and carbon dioxide (CO_2) is discharged to maintain the body's blood

and gas balance and internal environment in equilibrium. The alveoli, which provide a large surface area for gas exchange, are lined with a thin layer of epithelial cells that form a tight single membrane on the basement membrane (1.66 ± 0.128 μm) in normal lungs (Divertie et al., 1976) and are directly connected to the endothelial lining of the capillary network. The space between the epithelium and endothelial lining is called the lung interstitium and contains various cellular and extracellular matrix (ECM) components that provide structure and support for the lungs (Novak et al., 2021).

PATHOLOGICAL CHANGES OF LUNG

In general, lung diseases fall into two categories: 1) restrictive diseases, which include a reduction in the ability of the lungs to expand and 2) obstructive diseases, which cause increased airway resistance and restricted airflow. Restrictive or obstructive diseases a classified based on clinical measures, including the ratio of forced expiratory volume to full forced lung capacity in one second (FEV1/FVC) and total lung capacity percentage (TLC %) (Kouranos et al., 2020). The restrictive disease is characterized by a decrease in the TLC% with no change or increase in the FEV1/FVC ratio because either both indicators decrease simultaneously or forced expiratory volume in one second (FEV1) increases with decreased lung compliance. Restrictive diseases, such as pulmonary fibrosis, interstitial lung disease, and sarcoidosis, often result from the accumulation of components of the ECM and scar tissue around the alveoli that affects the stiffness of the lung parenchyma and limits the lung's ability to expand. Obstructive diseases, such as asthma, bronchopulmonary dysplasia, bronchiolitis obliteration, and chronic obstructive pulmonary disease, due to the degradation of lung connective tissue, lead to airway swelling, reduced matrix hardness and elasticity, and reduced lung retraction, and interfere with an individual's ability to exhale adequately (Novak et al., 2021).

Pulmonary fibrosis (PF) is a chronic, restrictive lung disease in which excessive collagen deposition results from the accumulation of scar tissue in the lung caused by lung injury, inflammation, and/or long-term exposure to toxins or particles. Idiopathic pulmonary fibrosis (IPF) is a chronic progressive pulmonary fibrosis disease with unknown reasons. In recent years, more and more studies have shown that IPF is closely related to the occurrence of lung cancer. Also, IPF diagnosis and treatment guidelines in 2011 clearly indicate that IPF is prone to lung cancer, pulmonary embolism, pulmonary hypertension, and other lung diseases (Raghu et al., 2011; Raghu et al., 2015). According to the latest research statistics, the incidence of lung cancer in IPF population is 2.7–48% (Ballester et al., 2019), which is significantly higher than that of the general population (2–6.4%) (Bouros et al., 2002). Undissolved scar tissue in the lungs hardens the lung parenchyma and limits lung dilation. Matrix over deposition occurs in the distal airway structure, where fibroblast lesions are composed of excess collagen, fibrin, and other ECM components that are insoluble and deteriorate over time (Burgess et al., 2016). Heterogeneous lung stiffness results in increased stress and strain, affecting cellular mechanical conduction and disease progression. Tsukui et al. (2013) constructed an *in vivo* model of bleomycin-induced pulmonary fibrosis to study the gene expression profile of fibroblast populations. They found that osteopontin is highly overexpressed in lung fibroblasts and can serve as a marker of CAFs activation. It has been reported that biomarkers commonly expressed by CAFs include α -smooth muscle actin (α-SMA), fibroblast specific protein-1 (FSP-1), fibroblast activating protein α (FAP-α), platelet-derived growth factor receptor -β (PDGFR-β), neural/glial antigen (NG2) (Kalluri, 2016; Nurmik et al., 2019), and Gamma-glutamyltransferase 5 (GGT5) (Wei et al., 2020). Su S et al. reported $CD10^{+}/GPR77^{+}$ CAFs promoted cancer development and chemoresistance by sustaining cancer stemness (Su et al., 2018). Interestingly, osteopontin expression is significantly increased in senescent fibroblasts and is a key mediator of senescent stroma promoting tumor progression (Pazolli et al., 2009).

ASSOCIATION BETWEEN MECHANICAL STRETCHING OF THE LUNG AND LUNG CANCER

Cells respond to both chemical and mechanical signals in their microenvironment. Various mechanical stimulus signals (e.g., basal rigidity, hydrostatic pressure, compression, tension, and shear stress) are detected and transmitted to cells *via* mechanoreceptors. These receptors often encounter the ECM, where external signals are converted into physiological responses that affect cell proliferation, differentiation, and migration (Jang and Beningo, 2019).

Studies on Cell Mechanics Involving Lung Tissue Cells

A major feature of the lung is its unique mechanical force. Each respiratory cycle imposes a periodic mechanical force, and this dynamic mechanical force exposes the lung to a challenging system of external reconstruction (Ahadian et al., 2018). The experiments by Tschumperlin and Margulies have shown that circulatory stretching stimulation of 5–12% is equivalent to 60–80% of the total lung volume and is associated with the physiological level of mechanical strain experienced by the alveolar epithelium and microvessels during low tidal volume mechanical ventilation, which is the protocol used in lung protection strategies (Tschumperlin and Margulies, 1998; Tschumperlin and Margulies, 1999). In contrast, circulatory stretching at 17–22% linear dilation is equivalent to 100% of total lung volume and is associated with pathophysiological conditions induced by mechanical ventilation of the organism volume and with inflammatory responses *in vivo* and with acute lung injury (Tschumperlin et al., 2000).

The lung is a dynamic organ with complex mechanical environment at microscale (Shikata et al., 2005). Thus, mechanotransduction plays a vital role in lung health and

TABLE 1 | Stimulation experiments of lung cancer cells by mechanical stretching.

Cell type	Mechanical stretching	Results	References
Lung epithelial cancer cells (A549) Fibroblast (IMR-90)	Short-term stretching (15, 30, and 60 min) and long-term stretching (24 h), 10% cell surface area, 1 Hz, incubated at 37°C	Cell rearrangement, cytoskeleton reorganization, and increased stretching time can prolong mitochondrial length	Wang et al. (2020)
AT II cell-like A549 serous glandular epithelial cell-like Calu-3 NCI-H322 NCI-H358 Lung epithelial cancer cells (BEAS-2B)	16% surface elongation, 12 min^{-1}	Several kinds of human lung epithelial cell lines can adapt to chronic cyclic strain	Wang et al. (2020)
Lung epithelial cancer cells (A549) NCI-H358	20% maximum strain and 15 cycles/minute	Decrease cell proliferation	Hendricks et al. (2012)

disease. The effects of mechanical force on proliferation, morphology, ECM composition, and alteration, gene regulation and the inflammatory response of lung cells and lung cancer cells have been recognized by most researchers (Novak et al., 2021). Nalayanda et al. (2009) observed that the growth rate of A549 cells decreased as the shear stress increased. However, Mahto et al. demonstrated that the effect of shear stress on alveolar cells was affected by cell species. The secretion of surface-active substances in human A549 cells showed no change below 8 dynes/cm^2, but was impaired when it was above 8 dynes/cm^2. The secretion of mouse MLE-12 cells increased with the growth of stimulation (Mahto et al., 2014). There are conflicting findings in the literature on the role of matrix rigidity on epithelial cell function. Eisenberg et al. (Jones, 2011) established that substrate rigidity affected cell morphology, microfilaments, and focal adhesion, but did not adjust the differentiation of EMT or cell types (from ATII into ATI) in mouse alveolar epithelial cells. In contrast, Marilyn M. Dysart et al. found that environmental particulate enhances stiffness induced alveolar epithelial cells mechanoactivation of TGF-β (Dysart et al., 2014). Markowski et al. (2012), reported that augmented matrix rigidity induced EMT, integrin binding, and TGF-β activation. The cell mechanics of lung cancer cells will discuss in the next section.

Many researchers have developed *in vitro* systems to detect the response of lung cells to mechanical forces. These models typically study how one type of mechanical force affects one cell type, and there is very little work combining multidimensional forces and multicellular models to accurately summarize the complex interactions that occur in the body. Typical devices *in vitro* mechanical stimulation involved: 1) cyclic uniaxial or biaxial, equi-biaxial strain for cell stretch stimulation (Felder et al., 2008; Rapalo et al., 2015) 2) static or cyclic pressure devices on cell stimulation (Huang et al., 2010); 3) microfluidic device for wall shear stress on cells (Mahto et al., 2014); 4) gradient stiffness hydrogel for cell culture (Liu et al., 2010); 5) cyclic strain device for capillary interface (Huh et al., 2010); 6) interstitial fluid flow custom device for cells seeded on the gel (Ng and Swartz, 2003). The effects of endothelial cells stimulated by shear stress have been widely studied. Shear stress is a known factor impacting endothelial cell morphology (Szulcek et al., 2016), cytoskeletal remodeling (Birukov et al., 2002), and Ca^{2+} levels in plasma (Yamamoto et al., 2018). Nitric oxide release is donated to maintain vasomotor action, anti-inflammatory mechanism, and cytoplasmic antioxidant ability (Tousoulis et al., 2012). Endothelial cells increased their ACE2 expression with pulsating shear stress stimulated, thereby enhancing the level of nitric oxide and decreasing proliferation and inflammation. ACE2 level was enlarged when endothelial cells were stimulated and stretched in the Flexcell device (Song et al., 2020).

Studies on Cell Mechanics on Lung Cancer Cells

Like normal cells, cancer cells recognize the mechanical changes provided by the tumor microenvironment and convert them into signaling pathways through mechanical transduction pathways (**Table 1**) (Sporn and Albini, 2007; Xu et al., 2017). Wang et al. (2020) found that after cyclic stretching of the A549 lung cancer and IMR-90 fibroblast cells, cells were rearranged, the cytoskeleton was restructured, and an increased stretching time could prolong mitochondrial length. Weber et al. (Wang et al., 2020) found that various human lung epithelial cell lines could adapt to chronic cyclic strain stimulation. Hendricks et al. (2012) studied the effects of the simulated force of near-normal respiration (20% maximum strain and 15 cycles/min) on proliferation and morphology of NCI-H358 and A549 cell lines. They showed that mechanical stimulation reduced cell proliferation. Shukla et al. (2016) demonstrated that higher substrate rigidity induced slower and directional migration of lung cancer cells by decreasing the phosphorylated focal adhesion kinase and paxillin, not the biomarkers of EMT. Furthermore, Barenholz Cohen et al. (2020) demonstrated that tumor-derived extracellular vesicles from breast carcinoma cells caused the lungs of cancer-free mice broadly variable, and being more elastic than viscous. Matrix rigidity encourages microtubules glutamylation by increasing glutamine metabolism and strengthening microtubules stabilization, thus stimulating the migration of cancer cells (Torrino et al., 2021).

CAFs and Studies on Cell Mechanics

Fibroblasts and Mechanical Stimulation

The lung is a complex organ, and types of mesenchymal cells are found in its tissues. Fibroblasts are one of the most important

TABLE 2 | Stimulation experiments of lung fibroblasts by mechanical stretching.

Cell type	Mechanical stretching	Results	References
Human embryonic lung fibroblast MRC-5	Flexcell FX-5000; mechanical tensile stimulation continuously for 48 h (0.1Hz; Sine waves, stretching amplitude of 5, 10, 15 and 20%)	Mechanical stimulation of 5% stretching increased cell proliferation. However, it had no significant effect on expression levels of TGF-β1 and collagen. Mechanical stimulation with 10% tensile force inhibited cell proliferation but increased expression levels of TGF-β1 and type I collagen. 15 and 20%, with significantly larger effects	Xie et al. (2020)
human lung fibroblasts	Strex ST-140; uniaxial tension (strain 10–30%); 30 cycle/min for 10 min	Mechanical stretching induces calcium influx and releases ATP independently of conventional stretch-sensitive ion channels, known as actin cytoskeleton	Murata et al. (2014)
human lung fibroblasts	Flexercell FX-4000; 0.2 HZ, maximum elongation 10%, 24 or 48 h of cyclic mechanical strain	The mRNA expressions of COL1A1, COL1A2, COL3A1, COL5A2 and Tenascin C were decreased. Cyclic mechanical loading on primary human lung fibroblasts for 48 h reduced the expression of fibrosis-related genes. Myofibroblast differentiation is reduced under these conditions. cyclic mechanical loading decreased the expression of endogenous TGF-β1	Blaauboer et al. (2011)
Mouse fetal lung fibroblasts: wild-type and EGFR knockout	Flexcell FX-4000; equibiaxial cyclic strain of 2.5% or 20% was applied at 40 cycles per min intervals for 48 h	Traumatic stretch (20% stretch) results in lactate dehydrogenase release at the same level in wild-type and knockout cells. EGFR does not alter the mechanical properties and damage resistance of fetal fibroblasts exposed to mechanical stretching	Giordani et al. (2013)
	A 2.5% stretching scheme was selected to simulate physiological stretching and 20% to simulate injury	20% stretching increased lysed caspase-3 and decreased proliferating nuclear antigen only in wild-type cells. 20% stretching increased macrophage inflammatory protein-2 and monocyte chemotactic protein-1 in wild-type cells. In knockout cells, miP-2 was reduced by 50% and McP-1 increased by only 60% compared to physiological stretching	
Mouse fetal lung fibroblasts	Flexcell FX-4000 Strain Unit; 20% cyclic stretch, 40 cycles/min for 48 h	After 24 h, LDH levels had increased by 50%. After 48 h mechanical stretching, fibroblast lysis increased	Hawwa et al. (2011a), Hawwa, et al. (2011b)

mesenchymal cells that contribute to maintaining the lung's normal physiological function. The heterogeneity of fibroblasts is the key reason for their different phenotypes and functions (Öhlund et al., 2014). Fibroblasts from different parts of the lung present significant differences and can be divided into different subgroups according to their heterogeneity (Chang et al., 2002; Kotaru et al., 2006). Kotaru et al. (2006) found that there are two kinds of fibroblasts at least: Airway fibroblasts (AFs) and distal lung fibroblasts (DLFs). AFs are larger, stellate-shaped with more cytoplasmic protrusions, and DLFs are spindle-shaped. AFs expressed more procollagen type I and eotaxin-1 than DLFs did at and after TGF-β treatment. In contrast, AFs had low proliferation rate than DLFs with serum treatment. Moreover, AFs expressed less α-SMA than DLFs in reference point. Pechkovsky et al. (2010) demonstrated results by comparing human proximal bronchi (B-FBR) and distal lung parenchyma (P-FBR). It indicated that P-FBR showed improved TGF-β/Smad signaling at the reference point, and the activated TGF-β significantly reduced basal a-SMA protein in P-FBR. Xie et al. (2018) segregated six subpopulations in adult pulmonary mesenchymal cells: myofibroblasts, Col13a1 matrix fibroblasts, Col14a1 matrix fibroblasts, lipofibroblasts, mesenchymal progenitors, and mesothelial cells.

Fibroblasts are cells that respond to mechanical stretching stimuli (**Table 2**). They maintain the structure and function of organ tissues by altering the expression of genes and proteins in their ECM in response to external physical (such as tensile force), chemical (such as chemical poisons), and biological (such as infectious toxins) factors (Amma et al., 2005; Sakamoto et al., 2010).

Pechkovsky et al. (2010) found that fibroblasts derived from the lung parenchyma cilia develop α-SMA, whose high expression characterizes a specific fibroblast phenotype. These cells are responsible for the composition of the ECM. Components, mainly cellular protein deposition, may be involved in the pathogenesis of idiopathic pulmonary fibrosis, and fiber proliferative disease and may play a key role in the occurrence and development of lung cancer. The cyclic load to which healthy lung cells are exposed during respiration prevents fibroblasts from differentiating into myofibroblasts (Blaauboer et al., 2011). suggesting that fibroblasts are static in their physiological state. Low levels of mechanical stretching may be important for interstitial remodeling during lung development. However, extensive stretching can damage the normal lung structure (Hawwa et al., 2011a; Sanchez-Esteban et al., 2002).

After the lung tissue is slightly injured, fibroblasts in the lung parenchyma differentiate into myofibroblasts (Tomasek et al., 2002) to promote wound healing. After tissue repair, apoptosis of myofibroblasts occurs once the remodeling balance of repaired tissue is restored. During fibrosis, however, myofibroblasts remain active after wound healing, producing an excess of strongly contracted ECM components. Xie et al. (2020) showed that (5–10%) mechanical stimulation could improve the proliferative activity of MRC-5 cells and may slightly

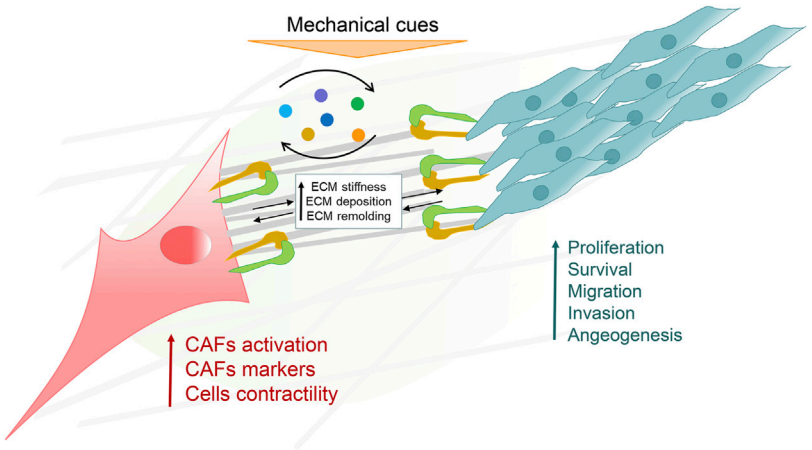

FIGURE 2 | The crosstalk of cancer associated fibroblasts (CAFs) and the cancer microenvironment (CME). CAFs and cancer cells are responsible for sensing and transducing various extracellular matrix (ECM) proteins and mechanical signals in the CME. CAFs and cancer cells also effect each other's physiological processes by releasing and receiving various factors in a paracrine manner.

stimulate the expression of transforming growth factor-β (TGF-β) 1 and type I collagen in human embryonic lung fibroblasts. Mechanical stimulation (15–20%) directly leads to cell damage, reduces cell proliferation activity, induces TGF-β1 expression, significantly increases collagen expression, and accelerates the process of pulmonary fibrosis.

After mechanical stimulation at different tensile ranges, the biomechanical properties of MRC-5 fibroblast cells decreased. And, the fibroblasts appeared to "soften", indicating that the degree of deformation of lung fibroblasts was lower than the linear stress-strain relationship. This feature is not a reflection of a specific molecular mechanism but indicates higher-level structural changes, which suggests that the cytoskeleton may have been damaged (Xie et al., 2020). Other *in vitro* studies have shown that mechanical stretching with higher strain ranges (20–30%) activates the Ca^{2+} influx pathway independently of the actin cytoskeleton and the conventional stretch sensitive ion channel (such as members of the transient receptor potential (TRP) family proteins, Piezo1, and Piezo2). Moreover, ATP is released in human lung fibroblasts after mechanical stretching (Murata et al., 2014). It is also suggested that Ca^{2+} is the second messenger that activates lung fibroblast functional activity (Hinz, 2012). However, an increase in the extracellular ATP concentration is considered a "danger signal" in the pathophysiology of pulmonary fibrosis (Riteau et al., 2010). Therefore, increased Ca^{2+} in lung fibroblasts responding to mechanical stress plays a role in the progression of pulmonary fibrosis.

Fibroblasts release more pro-inflammatory cytokines and chemokines after mechanical stretching, which actively participate in regulating the inflammatory response after mechanical injury (Hawwa et al., 2011a) and promote wound healing and tissue repair. Lung fibroblasts play a key role in pathophysiological events associated with pulmonary fibrosis (Barkauskas and Noble, 2014; Riteau et al., 2010; Yamauchi et al., 2020).

Cancer-Associated Fibroblasts Exposed to Stretching Stimulation

Cancer is known as "wounds that never heal", and fibroblasts activated in the tumor ECM can promote tumor inflammation and fibrosis (Kalluri, 2016); thus, they are also known as CAFs. Compared with resting fibroblasts, CAFs present a larger morphology, nuclear depression, and more branching cytoplasm (De Wever et al., 2008), and activated CAFs have stronger proliferation and migration ability (Chen and Song, 2019).

CAFs are cells with mechanical ability and are the most abundant stromal cell type in the tumor microenvironment (Bhowmick et al., 2004). They play a crucial role in cancer development and metastasis (Pereira et al., 2019). Once CAFs settle down in ECM of the tumor, they can benefit cancer cells in many aspects: 1) promote the growth and proliferation of tumor cells (Zhang et al., 2020); 2) assist in tumor-related angiogenesis (Fan et al., 2020; Lugano et al., 2020); 3) accelerate the invasion and metastasis of tumor cells (Birkbak and McGranahan, 2020); 4) cause drug resistance of some anti-tumor drugs (Wei et al., 2020). CAFs secrete soluble factors such as growth factors, cytokines, and ECM molecules during cancer progression to promote the self-differentiation of normal fibroblasts. TGF-β released by CAFs triggers the anisotropic matrix to stimulate myofibroblast differentiation of normal fibroblasts (Franco-Barraza et al., 2017). Meanwhile, excessive production of fibrillary ECM proteins and ECM remodeling by CAFs leads to cancer fibrosis, namely promoting connective tissue hyperplasia. As the stiffness of the ECM derived from CAFs increases, it usually leads to greater force (traction) exerted by cells on the matrix, as well as increased stress fibers and greater focal adhesion (Ladoux et al., 2016), thus promoting the differentiation of CAFs and supporting the progression of cancer.

There is an inverse relationship between traction stress and metastatic capacity of breast cancer cells, and the generation of force decreases with the increase of metastatic potential and capacity (Indra et al., 2011). Studies have shown that cell-

matrix adhesion dynamics and traction conversion regulate tumor cell migration (Fokkelman et al., 2016). Recent studies have shown that CAFs exert physical forces on cancer cells by stimulating phenotypically pro- or anti-tumorigenic interactions that allow them to invade en masse (Yamauchi et al., 2020).

Glentis et al. (2017) found that CAFs actively reshape the basement membrane by pulling, stretching, and softening it, leading to the formation of spaces where cancer cells can migrate. By applying contractile forces, CAFs alter the organizational and physical properties of the basement membrane, allowing cancer cells to invade. CAFs promote fracture of the bone matrix in a matrix metalloproteinase-independent manner. Therefore, it has been proposed that in addition to proteolysis, the mechanical forces exerted by CAFs represent another mechanism of basement membrane rupture.

In the tumor microenvironment, CAFs and cancer cells communicate through the ECM and other soluble factors to influence each other's cellular behavior (**Figure 2**). Numerous mechanical signals are detected and transmitted to cells by mechanoreceptors. These receptors often communicate with ECM, where external signals are converted into physiological replies. Integrin was a well-defined mechanoreceptor that directly connected the microfilaments to the ECM and conducted signals. The 18 α and 8 β subunits heterodimerize to produce more than 24 different receptors. These heterodimers are the link between cells and the tumor microenvironment. CAFs heterogeneity drives balancing processes in tumor growth and invasion (DiPersio and Van De Water, 2019; Jang and Beningo, 2019). Tumor growing accompanied with a heterogeneous population of CAFs. The subpopulations of CAFs can promote deposition and ECM remodeling, which interact directly with tumor cells in principal and subordinate structures to help tumor cell migration and invasion. Also, it provokes angiogenic factors by mediating new blood vessel growth and yield immune cell suppression *via* ECM modification and chemokine/cytokine secretion (Yamauchi et al., 2020). Although this communication is bi-directional, as shown in the figure, we mainly consider communication as unidirectional, from CAFs to cancer cells. Mechanical forces generated by ECM remodeling induced by CAFs contribute to the invasion efficiency of metastatic cells (Menon et al., 2011).

CONCLUDING REMARKS AND OUTSTANDING QUESTIONS

Mechanical stimulation is closely related to lung, lung cancer, and lung cancer-related fibroblasts. Mechanical strain is an important regulator of normal and abnormal lung growth and development. Mechanical forces are involved in biological processes ubiquitously (Kumar and Weaver, 2009), although the underlying mechanisms of cancer cell migration or metastasis are still not fully understood. Mechanical stimulation plays an important role in regulating fibroblasts and the ECM components within the tumor microenvironment. First, there is no literature available on the mechanisms induced in lung CAFs by mechanical stimulation. Secondly, a limited number of studies have described mechanisms induced by mechanical stimulation of other types of CAFs. However, these studies suggested that CAFs play a crucial role in tumor progression. Thirdly, the response of lung CAFs to mechanical stimulation may play a crucial role in the progression of lung cancer; thus, it will be of great clinical significance to study the response of lung CAFs to mechanical stimulation.

At present, lung biomechanics are mainly focused on mechanical ventilation, ventilation injury and fluid dynamics of vascular endothelial cells. There is a lack of research on mechanical factors affecting other lung cells (especially fibroblasts and immune cells) in normal respiration. There are few studies on the mechanism of lung tumors causing changes in lung physical properties and then affecting lung cells.

Due to the complexity of the lung cancer classification, there may be different types of lung CAFs, but once this role of mechanotransduction on lung cancer cells is recognized, this will be accompanied by further in-depth research. In the future, it will be extremely challenging and of practical significance to isolate different types of lung CAFs associated with different types of lung cancer, and elucidate the specific mechanisms involved in mechanical stimulation on tumor progression.

AUTHOR CONTRIBUTIONS

FG, JL, and JD organization of content and structure, writing and reviewing; YY preparation of figures, writing and reviewing; LW and CW writing and reviewing. All authors agree to be accountable for the content of the work.

FUNDING

This study was supported by Scientific research project of Traditional Chinese Medicine Bureau of Guangdong Province (20201232) and the President's Fund of Nanfang Hospital (2019C033).

REFERENCES

Ahadian, S., Civitarese, R., Bannerman, D., Mohammadi, M. H., Lu, R., Wang, E., et al. (2018). Organ-On-A-Chip Platforms: A Convergence of Advanced Materials, Cells, and Microscale Technologies. *Adv. Healthc. Mater.* 7 (2), 1700506. doi:10.1002/adhm.201700506

Albini, A., and Sporn, M. B. (2007). The Tumour Microenvironment as a Target for Chemoprevention. *Nat. Rev. Cancer* 7 (2), 139–147. doi:10.1038/nrc2067

Amma, H., Naruse, K., Ishiguro, N., and Sokabe, M. (2005). Involvement of Reactive Oxygen Species in Cyclic Stretch-Induced NF-Kb Activation in Human Fibroblast Cells. *Br. J. Pharmacol.* 145 (3), 364–373. doi:10.1038/sj.bjp.0706182

Ballester, B., Milara, J., and Cortijo, J. (2019). Idiopathic Pulmonary Fibrosis and Lung Cancer: Mechanisms and Molecular Targets. *Ijms* 20 (3), 593. doi:10.3390/ijms20030593

Barenholz-Cohen, T., Merkher, Y., Haj, J., Shechter, D., Kirchmeier, D., Shaked, Y., et al. (2020). Lung Mechanics Modifications Facilitating Metastasis Are

Mediated in Part by Breast Cancer-derived Extracellular Vesicles. *Int. J. Cancer* 147 (10), 2924–2933. doi:10.1002/ijc.33229

Barkauskas, C. E., and Noble, P. W. (2014). Cellular Mechanisms of Tissue Fibrosis. 7. New Insights into the Cellular Mechanisms of Pulmonary Fibrosis. *Am. J. Physiology-Cell Physiol.* 306 (11), C987–C996. doi:10.1152/ajpcell.00321.2013

Bhowmick, N. A., Neilson, E. G., and Moses, H. L. (2004). Stromal Fibroblasts in Cancer Initiation and Progression. *Nature* 432 (7015), 332–337. doi:10.1038/nature03096

Birkbak, N. J., and McGranahan, N. (2020). Cancer Genome Evolutionary Trajectories in Metastasis. *Cancer Cell* 37 (1), 8–19. doi:10.1016/j.ccell.2019.12.004

Birukov, K. G., Birukova, A. A., Dudek, S. M., Verin, A. D., Crow, M. T., Zhan, X., et al. (2002). Shear Stress-Mediated Cytoskeletal Remodeling and Cortactin Translocation in Pulmonary Endothelial Cells. *Am. J. Respir. Cel Mol Biol* 26 (4), 453–464. doi:10.1165/ajrcmb.26.4.4725

Blaauboer, M. E., Smit, T. H., Hanemaaijer, R., Stoop, R., and Everts, V. (2011). Cyclic Mechanical Stretch Reduces Myofibroblast Differentiation of Primary Lung Fibroblasts. *Biochem. Biophysical Res. Commun.* 404 (1), 23–27. doi:10.1016/j.bbrc.2010.11.033

Bouros, D., Hatzakis, K., Labrakis, H., and Zeibecoglou, K. (2002). Association of Malignancy with Diseases Causing Interstitial Pulmonary Changes. *Chest* 121 (4), 1278–1289. doi:10.1378/chest.121.4.1278

Burgess, J. K., Mauad, T., Tjin, G., Karlsson, J. C., and Westergren-Thorsson, G. (2016). The Extracellular Matrix - the Under-recognized Element in Lung Disease? *J. Pathol.* 240 (4), 397–409. doi:10.1002/path.4808

Chang, H. Y., Chi, J.-T., Dudoit, S., Bondre, C., van de Rijn, M., Botstein, D., et al. (2002). Diversity, Topographic Differentiation, and Positional Memory in Human Fibroblasts. *Proc. Natl. Acad. Sci.* 99 (20), 12877–12882. doi:10.1073/pnas.162488599

Chen, X., and Song, E. (2019). Turning Foes to Friends: Targeting Cancer-Associated Fibroblasts. *Nat. Rev. Drug Discov.* 18 (2), 99–115. doi:10.1038/s41573-018-0004-1

De Wever, O., Demetter, P., Mareel, M., and Bracke, M. (2008). Stromal Myofibroblasts Are Drivers of Invasive Cancer Growth. *Int. J. Cancer* 123 (10), 2229–2238. doi:10.1002/ijc.23925

DiPersio, C. M., and Van De Water, L. (2019). Integrin Regulation of CAF Differentiation and Function. *Cancers* 11 (5), 715. doi:10.3390/cancers11050715

Divertie, M. B., Cassan, S. M., and Brown, A. L. (1976). Ultrastructural Morphometry of the Blood-Air Barrier in Pulmonary Sarcoidosis. *Chest* 69 (2), 154–157. doi:10.1378/chest.69.2.154

Doryab, A., Taskin, M. B., Stahlhut, P., Schröppel, A., Orak, S., Voss, C., et al. (2021). A Bioinspired *In Vitro* Lung Model to Study Particokinetics of Nano-/Microparticles under Cyclic Stretch and Air-Liquid Interface Conditions. *Front. Bioeng. Biotechnol.* 9, 616830. doi:10.3389/fbioe.2021.616830

Dysart, M. M., Galvis, B. R., Russell, A. G., and Barker, T. H. (2014). Environmental Particulate (PM2.5) Augments Stiffness-Induced Alveolar Epithelial Cell Mechanoactivation of Transforming Growth Factor Beta. *PLoS One* 9 (9), e106821. doi:10.1371/journal.pone.0106821

Fan, J., Xu, G., Chang, Z., Zhu, L., and Yao, J. (2020). MiR-210 Transferred by Lung Cancer Cell-Derived Exosomes May Act as Proangiogenic Factor in Cancer-Associated Fibroblasts by Modulating JAK2/STAT3 Pathway. *Clin. Sci.* 134 (7), 807–825. doi:10.1042/CS20200039

Felder, E., Siebenbrunner, M., Busch, T., Fois, G., Miklavc, P., Walther, P., et al. (2008). Mechanical Strain of Alveolar Type II Cells in Culture: Changes in the Transcellular Cytokeratin Network and Adaptations. *Am. J. Physiology-Lung Cell Mol. Physiol.* 295 (5), L849–L857. doi:10.1152/ajplung.00503.2007

Fokkelman, M., Balcıoğlu, H. E., Klip, J. E., Yan, K., Verbeek, F. J., Danen, E. H. J., et al. (2016). Cellular Adhesome Screen Identifies Critical Modulators of Focal Adhesion Dynamics, Cellular Traction Forces and Cell Migration Behaviour. *Sci. Rep.* 6 (1), 31707. doi:10.1038/srep31707

Franco-Barraza, J., Francescone, R., Luong, T., Shah, N., Madhani, R., Cukierman, G., et al. (2017). Matrix-regulated Integrin αvβ5 Maintains α5β1-dependent Desmoplastic Traits Prognostic of Neoplastic Recurrence. *eLife* 6, e20600. doi:10.7554/eLife.20600

Giordani, V. M., DeBenedictus, C. M., Wang, Y., and Sanchez-Esteban, J. (2013). Epidermal Growth Factor Receptor (EGFR) Contributes to Fetal Lung Fibroblast Injury Induced by Mechanical Stretch. *J. Receptors Signal Transduction* 34 (1), 58–63. doi:10.3109/10799893.2013.862270

Glentis, A., Oertle, P., Mariani, P., Chikina, A., El Marjou, F., Attieh, Y., et al. (2017). Cancer-associated Fibroblasts Induce Metalloprotease-independent Cancer Cell Invasion of the Basement Membrane. *Nat. Commun.* 8 (1), 924. doi:10.1038/s41467-017-00985-8

Hawwa, R. L., Hokenson, M. A., Wang, Y., Huang, Z., Sharma, S., and Sanchez-Esteban, J. (2011b). Differential Expression of MMP-2 and -9 and Their Inhibitors in Fetal Lung Cells Exposed to Mechanical Stretch: Regulation by IL-10. *Lung* 189 (4), 341–349. doi:10.1007/s00408-011-9310-7

Hawwa, R. L., Hokenson, M. A., Wang, Y., Huang, Z., Sharma, S., and Sanchez-Esteban, J. (2011a). IL-10 Inhibits Inflammatory Cytokines Released by Fetal Mouse Lung Fibroblasts Exposed to Mechanical Stretch. *Pediatr. Pulmonol.* 46 (7), 640–649. doi:10.1002/ppul.21433

Hendricks, P., Diaz, F. J., Schmitt, S., Sitta Sittampalam, G., and Nirmalanandhan, V. S. (2012). Effects of Respiratory Mechanical Forces on the Pharmacological Response of Lung Cancer Cells to Chemotherapeutic Agents. *Fund. Clin. Pharmacol.* 26 (5), 632–643. doi:10.1111/j.1472-8206.2011.00964.x

Hinz, B. (2012). Mechanical Aspects of Lung Fibrosis. *Proc. Am. Thorac. Soc.* 9 (3), 137–147. doi:10.1513/pats.201202-017AW

Hsia, C. C. W., Hyde, D. M., and Weibel, E. R. (2016). Lung Structure and the Intrinsic Challenges of Gas Exchange. *Compr. Physiol.* 6 (2), 827–895. doi:10.1002/cphy.c150028

Huang, Y., Haas, C., and Ghadiali, S. N. (2010). Influence of Transmural Pressure and Cytoskeletal Structure on NF-Kb Activation in Respiratory Epithelial Cells. *Cel. Mol. Bioeng.* 3 (4), 415–427. doi:10.1007/s12195-010-0138-7

Huh, D., Matthews, B. D., Mammoto, A., Montoya-Zavala, M., Hsin, H. Y., and Ingber, D. E. (2010). Reconstituting Organ-Level Lung Functions on a Chip. *Science* 328 (5986), 1662–1668. doi:10.1126/science.1188302

Indra, I., Undyala, V., Kandow, C., Thirumurthi, U., Dembo, M., and Beningo, K. A. (2011). Anin Vitrocorrelation of Mechanical Forces and Metastatic Capacity. *Phys. Biol.* 8 (1), 015015. doi:10.1088/1478-3975/8/1/015015

Jang, I., and Beningo, K. (2019). Integrins, CAFs and Mechanical Forces in the Progression of Cancer. *Cancers* 11 (5), 721. doi:10.3390/cancers11050721

Jones, J. (2011). Substrate Stiffness Regulates Extracellular Matrix Deposition by Alveolar Epithelial Cells. *Rrb* 2, 1–12. doi:10.2147/RRB.S13178

Kalluri, R. (2016). The Biology and Function of Fibroblasts in Cancer. *Nat. Rev. Cancer* 16 (9), 582–598. doi:10.1038/nrc.2016.73

Kalluri, R., and Zeisberg, M. (2006). Fibroblasts in Cancer. *Nat. Rev. Cancer* 6 (5), 392–401. doi:10.1038/nrc1877

Kotaru, C., Schoonover, K. J., Trudeau, J. B., Huynh, M.-L., Zhou, X., Hu, H., et al. (2006). Regional Fibroblast Heterogeneity in the Lung. *Am. J. Respir. Crit. Care Med.* 173 (11), 1208–1215. doi:10.1164/rccm.200508-1218OC

Kouranos, V., Ward, S., Kokosi, M. A., Castillo, D., Chua, F., Judge, E. P., et al. (2020). Mixed Ventilatory Defects in Pulmonary Sarcoidosis. *Chest* 158 (5), 2007–2014. doi:10.1016/j.chest.2020.04.074

Kumar, S., and Weaver, V. M. (2009). Mechanics, Malignancy, and Metastasis: The Force Journey of a Tumor Cell. *Cancer Metastasis Rev.* 28 (1-2), 113–127. doi:10.1007/s10555-008-9173-4

Ladoux, B., Mège, R.-M., and Trepat, X. (2016). Front-Rear Polarization by Mechanical Cues: From Single Cells to Tissues. *Trends Cel Biol.* 26 (6), 420–433. doi:10.1016/j.tcb.2016.02.002

Lemos, D. R., and Duffield, J. S. (2018). Tissue-resident Mesenchymal Stromal Cells: Implications for Tissue-specific Antifibrotic Therapies. *Sci. Transl. Med.* 10 (426). doi:10.1126/scitranslmed.aan5174

Liu, F., Mih, J. D., Shea, B. S., Kho, A. T., Sharif, A. S., Tager, A. M., et al. (2010). Feedback Amplification of Fibrosis through Matrix Stiffening and COX-2 Suppression. *J. Cel Biol.* 190 (4), 693–706. doi:10.1083/jcb.201004082

Lugano, R., Ramachandran, M., and Dimberg, A. (2020). Tumor Angiogenesis: Causes, Consequences, Challenges and Opportunities. *Cell. Mol. Life Sci.* 77 (9), 1745–1770. doi:10.1007/s00018-019-03351-7

Mahto, S. K., Tenenbaum-Katan, J., Greenblum, A., Rothen-Rutishauser, B., and Sznitman, J. (2014). Microfluidic Shear Stress-Regulated Surfactant Secretion in Alveolar Epithelial Type II Cells *In Vitro*. *Am. J. Physiology-Lung Cell Mol. Physiol.* 306 (7), L672–L683. doi:10.1152/ajplung.00106.2013

Markowski, M. C., Brown, A. C., and Barker, T. H. (2012). Directing Epithelial to Mesenchymal Transition through Engineered Microenvironments Displaying

Orthogonal Adhesive and Mechanical Cues. *J. Biomed. Mater. Res.* 100A (8), 2119–2127. doi:10.1002/jbm.a.34068

Menon, S., Beningo, K. A., and Gullberg, D. (2011). Cancer Cell Invasion Is Enhanced by Applied Mechanical Stimulation. *PLoS One* 6 (2), e17277. doi:10.1371/journal.pone.0017277

Murata, N., Ito, S., Furuya, K., Takahara, N., Naruse, K., Aso, H., et al. (2014). Ca2+ Influx and ATP Release Mediated by Mechanical Stretch in Human Lung Fibroblasts. *Biochem. Biophysical Res. Commun.* 453 (1), 101–105. doi:10.1016/j.bbrc.2014.09.063

Najrana, T., Mahadeo, A., Abu-Eid, R., Kreienberg, E., Schulte, V., Uzun, A., et al. (2020). Mechanical Stretch Regulates the Expression of Specific miRNA in Extracellular Vesicles Released from Lung Epithelial Cells. *J. Cel. Physiol.* 235 (11), 8210–8223. doi:10.1002/jcp.29476

Nalayanda, D. D., Puleo, C. M., Fulton, W. B., Wang, T.-H., and Abdullah, F. (2009). Characterization of Pulmonary Cell Growth Parameters in a Continuous Perfusion Microfluidic Environment. *Exp. Lung Res.* 33 (6), 321–335. doi:10.1080/01902140701557754

Ng, C. P., and Swartz, M. A. (2003). Fibroblast Alignment under Interstitial Fluid Flow Using a Novel 3-D Tissue Culture Model. *Am. J. Physiology-Heart Circulatory Physiol.* 284 (5), H1771–H1777. doi:10.1152/ajpheart.01008.2002

Novak, C., Ballinger, M. N., and Ghadiali, S. (2021). Mechanobiology of Pulmonary Diseases: A Review of Engineering Tools to Understand Lung Mechanotransduction. *J. Biomechanical Eng.* 143 (11), 110801. doi:10.1115/1.4051118

Nurmik, M., Ullmann, P., Rodriguez, F., Haan, S., and Letellier, E. (2019). In Search of Definitions: Cancer-associated Fibroblasts and Their Markers. *Int. J. Cancer* 146 (4), 895–905. doi:10.1002/ijc.32193

Öhlund, D., Elyada, E., and Tuveson, D. (2014). Fibroblast Heterogeneity in the Cancer Wound. *J. Exp. Med.* 211 (8), 1503–1523. doi:10.1084/jem.20140692

Pazolli, E., Luo, X., Brehm, S., Carbery, K., Chung, J.-J., Prior, J. L., et al. (2009). Senescent Stromal-Derived Osteopontin Promotes Preneoplastic Cell Growth. *Cancer Res.* 69 (3), 1230–1239. doi:10.1158/0008-5472.CAN-08-2970

Pechkovsky, D. V., Hackett, T. L., An, S. S., Shaheen, F., Murray, L. A., and Knight, D. A. (2010). Human Lung Parenchyma but Not Proximal Bronchi Produces Fibroblasts with Enhanced TGF-β Signaling and α-SMA Expression. *Am. J. Respir. Cel Mol Biol* 43 (6), 641–651. doi:10.1165/rcmb.2009-0318OC

Pereira, B. A., Vennin, C., Papanicolaou, M., Chambers, C. R., Herrmann, D., Morton, J. P., et al. (2019). CAF Subpopulations: A New Reservoir of Stromal Targets in Pancreatic Cancer. *Trends Cancer* 5 (11), 724–741. doi:10.1016/j.trecan.2019.09.010

Pittenger, M. F., Discher, D. E., Péault, B. M., Phinney, D. G., Hare, J. M., and Caplan, A. I. (2019). Mesenchymal Stem Cell Perspective: Cell Biology to Clinical Progress. *NPJ Regen. Med.* 4, 22. doi:10.1038/s41536-019-0083-6

Plikus, M. V., Guerrero-Juarez, C. F., Ito, M., Li, Y. R., Dedhia, P. H., Zheng, Y., et al. (2017). Regeneration of Fat Cells from Myofibroblasts during Wound Healing. *Science* 355 (6326), 748–752. doi:10.1126/science.aai8792

Plikus, M. V., Wang, X., Sinha, S., Forte, E., Thompson, S. M., Herzog, E. L., et al. (2021). Fibroblasts: Origins, Definitions, and Functions in Health and Disease. *Cell* 184 (15), 3852–3872. doi:10.1016/j.cell.2021.06.024

Raghu, G., Collard, H. R., Egan, J. J., Martinez, F. J., Behr, J., Brown, K. K., et al. (2011). An Official ATS/ERS/JRS/ALAT Statement: Idiopathic Pulmonary Fibrosis: Evidence-Based Guidelines for Diagnosis and Management. *Am. J. Respir. Crit. Care Med.* 183 (6), 788–824. doi:10.1164/rccm.2009-040GL

Raghu, G., Rochwerg, B., Zhang, Y., Garcia, C. A. C., Azuma, A., Behr, J., et al. (2015). An Official ATS/ERS/JRS/ALAT Clinical Practice Guideline: Treatment of Idiopathic Pulmonary Fibrosis. An Update of the 2011 Clinical Practice Guideline. *Am. J. Respir. Crit. Care Med.* 192 (2), e3–e19. doi:10.1164/rccm.201506-1063ST

Rápalo, G., Herwig, J. D., Hewitt, R., Wilhelm, K. R., Waters, C. M., and Roan, E. (2015). Live Cell Imaging during Mechanical Stretch. *JoVE* 102, e52737. doi:10.3791/52737

Riteau, N., Gasse, P., Fauconnier, L., Gombault, A., Couegnat, M., Fick, L., et al. (2010). Extracellular ATP Is a Danger Signal Activating P2X7Receptor in Lung Inflammation and Fibrosis. *Am. J. Respir. Crit. Care Med.* 182 (6), 774–783. doi:10.1164/rccm.201003-0359OC

Roshanzadeh, A., Nguyen, T. T., Nguyen, K. D., Kim, D.-S., Lee, B.-K., Lee, D.-W., et al. (2020). Mechanoadaptive Organization of Stress Fiber Subtypes in Epithelial Cells under Cyclic Stretches and Stretch Release. *Sci. Rep.* 10 (1). doi:10.1038/s41598-020-75791-2

Sakamoto, Y., Ishijima, M., Kaneko, H., Kurebayashi, N., Ichikawa, N., Futami, I., et al. (2010). Distinct Mechanosensitive Ca2+influx Mechanisms in Human Primary Synovial Fibroblasts. *J. Orthop. Res.* 28 (7), a–n. doi:10.1002/jor.21080

Sanchez-Esteban, J., Wang, Y., Cicchiello, L. A., and Rubin, L. P. (2002). Cyclic Mechanical Stretch Inhibits Cell Proliferation and Induces Apoptosis in Fetal Rat Lung Fibroblasts. *Am. J. Physiology-Lung Cell Mol. Physiol.* 282 (3), L448–L456. doi:10.1152/ajplung.00399.2000

Shikata, Y., Rios, A., Kawkitinarong, K., Depaola, N., Garcia, J., and Birukov, K. (2005). Differential Effects of Shear Stress and Cyclic Stretch on Focal Adhesion Remodeling, Site-specific FAK Phosphorylation, and Small GTPases in Human Lung Endothelial Cells. *Exp. Cel Res.* 304 (1), 40–49. doi:10.1016/j.yexcr.2004.11.001

Shukla, V. C., Higuita-Castro, N., Nana-Sinkam, P., and Ghadiali, S. N. (2016). Substrate Stiffness Modulates Lung Cancer Cell Migration but Not Epithelial to Mesenchymal Transition. *J. Biomed. Mater. Res.* 104 (5), 1182–1193. doi:10.1002/jbm.a.35655

Song, J., Hu, B., Qu, H., Wang, L., Huang, X., Li, M., et al. (2020). Upregulation of Angiotensin Converting Enzyme 2 by Shear Stress Reduced Inflammation and Proliferation in Vascular Endothelial Cells. *Biochem. Biophysical Res. Commun.* 525 (3), 812–818. doi:10.1016/j.bbrc.2020.02.151

Su, S., Chen, J., Yao, H., Liu, J., Yu, S., Lao, L., et al. (2018). CD10+GPR77+ Cancer-Associated Fibroblasts Promote Cancer Formation and Chemoresistance by Sustaining Cancer Stemness. *Cell* 172 (4), 841–856. doi:10.1016/j.cell.2018.01.009

Szulcek, R., Happé, C. M., Rol, N., Fontijn, R. D., Dickhoff, C., Hartemink, K. J., et al. (2016). Delayed Microvascular Shear Adaptation in Pulmonary Arterial Hypertension. Role of Platelet Endothelial Cell Adhesion Molecule-1 Cleavage. *Am. J. Respir. Crit. Care Med.* 193 (12), 1410–1420. doi:10.1164/rccm.201506-1231OC

Tomasek, J. J., Gabbiani, G., Hinz, B., Chaponnier, C., and Brown, R. A. (2002). Myofibroblasts and Mechano-Regulation of Connective Tissue Remodelling. *Nat. Rev. Mol. Cel Biol* 3 (5), 349–363. doi:10.1038/nrm809

Torrino, S., Grasset, E. M., Audebert, S., Belhadj, I., Lacoux, C., Haynes, M., et al. (2021). Mechano-induced Cell Metabolism Promotes Microtubule Glutamylation to Force Metastasis. *Cel Metab.* 33 (7), 1342–1357. doi:10.1016/j.cmet.2021.05.009

Tousoulis, D., Kampoli, A.-M., Tentolouris Nikolaos Papageorgiou, C., and Stefanadis, C. (2012). The Role of Nitric Oxide on Endothelial Function. *Cvp* 10 (1), 4–18. doi:10.2174/157016112798829760

Tschumperlin, D. J., and Margulies, S. S. (1999). Alveolar Epithelial Surface Area-Volume Relationship in Isolated Rat Lungs. *J. Appl. Physiol.* 86 (6), 2026–2033. doi:10.1152/jappl.1999.86.6.2026

Tschumperlin, D. J., and Margulies, S. S. (1998). Equibiaxial Deformation-Induced Injury of Alveolar Epithelial Cells *In Vitro*. *Am. J. Physiology-Lung Cell Mol. Physiol.* 275 (6), L1173–L1183. doi:10.1152/ajplung.1998.275.6.L1173

Tschumperlin, D. J., Oswari, J., and Margulies, A. S. S. (2000). Deformation-Induced Injury of Alveolar Epithelial Cells. *Am. J. Respir. Crit. Care Med.* 162 (2), 357–362. doi:10.1164/ajrccm.162.2.9807003

Tsukui, T., Ueha, S., Abe, J., Hashimoto, S.-i., Shichino, S., Shimaoka, T., et al. (2013). Qualitative rather Than Quantitative Changes Are Hallmarks of Fibroblasts in Bleomycin-Induced Pulmonary Fibrosis. *Am. J. Pathol.* 183 (3), 758–773. doi:10.1016/j.ajpath.2013.06.005

Wang, W.-H., Hsu, C.-L., Huang, H.-C., and Juan, H.-F. (2020). Quantitative Phosphoproteomics Reveals Cell Alignment and Mitochondrial Length Change under Cyclic Stretching in Lung Cells. *Ijms* 21 (11), 4074. doi:10.3390/ijms21114074

Wei, J.-R., Dong, J., and Li, L. (2020). Cancer-associated Fibroblasts-Derived Gamma-Glutamyltransferase 5 Promotes Tumor Growth and Drug Resistance in Lung Adenocarcinoma. *Aging* 12 (13), 13220–13233. doi:10.18632/aging.103429

Xie, T., Wang, Y., Deng, N., Huang, G., Taghavifar, F., Geng, Y., et al. (2018). Single-Cell Deconvolution of Fibroblast Heterogeneity in Mouse Pulmonary Fibrosis. *Cel Rep.* 22 (13), 3625–3640. doi:10.1016/j.celrep.2018.03.010

Xie, Y., Qian, Y., Wang, Y., Liu, K., and Li, X. (2020). Mechanical Stretch and LPS Affect the Proliferation, Extracellular Matrix Remodeling and Viscoelasticity of Lung Fibroblasts. *Exp. Ther. Med.* 20 (5), 1. doi:10.3892/etm.2020.9133

Xu, F., Cui, W., Zhao, Z., Gong, W., Wei, Y., Liu, J., et al. (2017). Targeting Tumor Microenvironment: Effects of Chinese Herbal Formulae on Macrophage-Mediated Lung Cancer in Mice. *Evidence-Based Complement. Altern. Med.* 2017, 1–12. doi:10.1155/2017/7187168

Yamamoto, K., Imamura, H., and Ando, J. (2018). Shear Stress Augments Mitochondrial ATP Generation that Triggers ATP Release and Ca2+ Signaling in Vascular Endothelial Cells. *Am. J. Physiology-Heart Circulatory Physiol.* 315 (5), H1477–H1485. doi:10.1152/ajpheart.00204.2018

Yamauchi, M., Gibbons, D. L., Zong, C., Fradette, J. J., Bota-Rabassedas, N., and Kurie, J. M. (2020). Fibroblast Heterogeneity and its Impact on Extracellular Matrix and Immune Landscape Remodeling in Cancer. *Matrix Biol.* 91-92, 8–18. doi:10.1016/j.matbio.2020.05.001

Zhang, Y., Wang, S., Lai, Q., Fang, Y., Wu, C., Liu, Y., et al. (2020). Cancer-associated Fibroblasts-Derived Exosomal miR-17-5p Promotes Colorectal Cancer Aggressive Phenotype by Initiating a RUNX3/MYC/TGF-β1 Positive Feedback Loop. *Cancer Lett.* 491, 22–35. doi:10.1016/j.canlet.2020.07.023

Conflict of Interest: The authors declare that the research was conducted in the absence of any commercial or financial relationships that could be construed as a potential conflict of interest.

Publisher's Note: All claims expressed in this article are solely those of the authors and do not necessarily represent those of their affiliated organizations, or those of the publisher, the editors, and the reviewers. Any product that may be evaluated in this article, or claim that may be made by its manufacturer, is not guaranteed or endorsed by the publisher.

frontiers in Cell and Developmental Biology

ORIGINAL RESEARCH
published: 14 January 2022
doi: 10.3389/fcell.2021.797341

Identification and Comprehensive Prognostic Analysis of a Novel Chemokine-Related lncRNA Signature and Immune Landscape in Gastric Cancer

Xiaolong Liang[1†], Gangfeng Yu[2†], Lang Zha[1], Xiong Guo[1], Anqi Cheng[1], Chuan Qin[1,3], Han Zhang[3] and Ziwei Wang[1]*

[1]Department of Gastrointestinal Surgery, the First Affiliated Hospital of Chongqing Medical University, Chongqing, China, [2]Institute of Life Sciences, Chongqing Medical University, Chongqing, China, [3]Department of Digestive Oncology, Three Gorges Hospital, Chongqing University, Chongqing, China

OPEN ACCESS

Edited by:
Daniele Vergara,
University of Salento, Italy

Reviewed by:
Susana García-Silva,
Spanish National Cancer Research Center (CNIO), Spain
Xin Xie,
The First Affiliated Hospital of Xi'an Jiaotong University, China

***Correspondence:**
Ziwei Wang
wangziwei@hospital.cqmu.edu.cn

[†]These authors have contributed equally to this work

Specialty section:
This article was submitted to Molecular and Cellular Oncology, a section of the journal Frontiers in Cell and Developmental Biology

Received: 18 October 2021
Accepted: 28 December 2021
Published: 14 January 2022

Citation:
Liang X, Yu G, Zha L, Guo X, Cheng A, Qin C, Zhang H and Wang Z (2022) Identification and Comprehensive Prognostic Analysis of a Novel Chemokine-Related lncRNA Signature and Immune Landscape in Gastric Cancer. Front. Cell Dev. Biol. 9:797341. doi: 10.3389/fcell.2021.797341

Gastric cancer (GC) is a malignant tumor with poor survival outcomes. Immunotherapy can improve the prognosis of many cancers, including GC. However, in clinical practice, not all cancer patients are sensitive to immunotherapy. Therefore, it is essential to identify effective biomarkers for predicting the prognosis and immunotherapy sensitivity of GC. In recent years, chemokines have been widely reported to regulate the tumor microenvironment, especially the immune landscape. However, whether chemokine-related lncRNAs are associated with the prognosis and immune landscape of GC remains unclear. In this study, we first constructed a novel chemokine-related lncRNA risk model to predict the prognosis and immune landscape of GC patients. By using various algorithms, we identified 10 chemokine-related lncRNAs to construct the risk model. Then, we determined the prognostic efficiency and accuracy of the risk model. The effectiveness and accuracy of the risk model were further validated in the testing set and the entire set. In addition, our risk model exerted a crucial role in predicting the infiltration of immune cells, immune checkpoint genes expression, immunotherapy scores and tumor mutation burden of GC patients. In conclusion, our risk model has preferable prognostic performance and may provide crucial clues to formulate immunotherapy strategies for GC.

Keywords: chemokine, immune, prognosis, gastric cancer, tumor mutation burden

INTRODUCTION

Gastric cancer (GC) is one of the most common malignant tumors worldwide, and its morbidity and mortality rank fifth and fourth, respectively (Sung et al., 2021). Although progress has been made in the diagnosis and treatment of GC, the overall survival time of patients has not improved significantly especially for advanced gastric cancer (AGC). The effect of immune checkpoint inhibitors has been previously investigated in patients with AGC. First-line treatment of PD-1/PD-L1 inhibitors could prolong OS and PFS of GC patients with CPS>10 or MSI-H (Shitara et al., 2020; Janjigian et al., 2021; Moehler et al., 2021). Results from a randomized phase III KEYNOTE-062 study indicated that AGC patients with a combined positive score (CPS) more than 10 or greater could benefit from first-line pembrolizumab (Smyth and Moehler, 2020). Huang et al. reviewed the

efficacy and safety of third-line treatments for advanced gastric cancer (AGC). Among them, Nivolumab was one of the most effective third-line therapy drugs in prolonging overall survival (OS) of AGC especially for 1-year OS (Huang et al., 2021). These findings proved that PD-1/PD-L1 has an undeniable effect in patients with AGC. However, not all patients are sensitive to immunotherapy. Considering the poor outcome of GC and promising application use of immunotherapy, the identification of novel biomarkers for predicting prognosis and immune therapy response is helpful for disease stratification and developing GC treatment strategies.

Many biomarkers have been previously identified for predicting the prognosis of GC. Mismatch repair deficiency (MMRD) and microsatellite instability (MSI) were identified as positive prognostic biomarkers in GC patients treated with surgery alone and negative prognostic biomarkers in GC patients treated with chemotherapy (Smyth et al., 2017). Tumor mutation burden (TMB) was proved to be positively correlated with the disease-free survival (DFS) of microsatellite-stable (MSS) GC patients (Li et al., 2021). A combination of immune cell infiltration score and TMB score could be utilized to predict the survival of GC patients (Jiang et al., 2021a). Some noncoding RNAs such as circRNAs and lncRNAs could also act as diagnostic biomarkers or prognostic factors in GC (Yang et al., 2016; Shan et al., 2019). A recent study identified an immune-related signature composed of MAGED1, ACKR3, FZD2, and CTLA4 could be used to predict the prognosis of GC patients (Dai et al., 2021). These molecular analyses have increased our knowledge of GC biology and might provide new insights on GC therapy strategies.

Chemokines are a large class of cytokines with chemotactic activity. Chemokines were widely reported to regulate cancer progression and could be used as therapeutic targets (Mantovani et al., 2010). Dysregulation of chemokines and chemokine receptors were reported to be closely correlated with the progression of tumors including GC. For example, CC and CXC chemokines were reported to promote tumor angiogenesis, which is essential for tumor growth and metastasis (Santoni et al., 2014). CXCL5 chemokine could induce epithelial-mesenchymal transition (EMT) of GC cells thereby promoting GC metastasis (Mao et al., 2020). Another chemokine CXCL2 was reported to promote GC cell growth and peritoneal metastasis (Natsume et al., 2020). CXCL1 chemokine was reported to exert a tumor-promoting role through activating the VEGF pathway in GC (Wei et al., 2015). Chemokines and chemokine receptors also exert crucial roles in immunity and mainly affect the infiltration of various immune cells, thus affecting tumor progression. CCL2 chemokine and CCR2 chemokine receptor could regulate the infiltrating level of macrophages in hepatocellular carcinoma (Li et al., 2017). CCL2-CCR2 axis could affect the immune cell infiltration, which results in an induction of immune evasion in esophageal cancer (Yang et al., 2020). CCL28 chemokine could promote the infiltration of Treg cells, thereby promoting the progression of GC (Ji et al., 2020). CCL3 and CCL20 chemokines could recruit dendritic cell DCs, which could induce anti-tumor immunity of GC (He et al., 2010). In addition, some chemokines and chemokine receptors, such as CXCL8, CXCR4 and CXCL13, were proved to be promising prognostic biomarkers in GC (Jin K.et al., 2021; Pawluczuk et al., 2021; Xue et al., 2021). These findings indicated that chemokine-related genes exert crucial functions in tumors, especially in the tumor microenvironment.

LncRNAs are a subset of noncoding RNAs with a length of over 200 nucleotides that regulate the expression of many genes involved in cancer development (Chi et al., 2019; Fang et al., 2021; Yu et al., 2021). Apart from gene regulation, lncRNAs are also involved in regulating numerous biological processes involved in tumorigenesis (Bhan et al., 2017; Peng W.-X. et al., 2017; Fattahi et al., 2020). Mounting evidence indicated that lncRNAs have an undeniable prognosis prediction function in GC cancer. Prognostic signatures based on ferroptosis-related lncRNA, immune-related lncRNA and helicobacter pylori infection-related lncRNA were proved to have preferable prognosis prediction functions in GC (Ma et al., 2021; Pan J. et al., 2021; Wei et al., 2021; Xin et al., 2021). Apart from this, lncRNAs could be used for subtype identification and therapy response prediction of GC (Huang et al., 2021; Jiang et al., 2021b). LncRNAs have also been reported to modulate immunity (Yu et al., 2018). Various lncRNAs were identified as prognostic biomarkers and could be used to predict the immune landscape of multiple cancers (Hong et al., 2020; Shen et al., 2020; Xu et al., 2021).

At present, the role and type of immune landscape in the prognosis of gastric cancer remains largely unknown. Identification of infiltrating immune cells is associated with cancer prognosis and new immune therapeutic targets, which could provide meaningful clues for the future treatment of GC, especially for immunotherapy.

The correlation between chemokine-related lncRNAs and the immune landscape in GC has not been reported. In this study, we first constructed a multi-lncRNA risk model composed of 10 chemokine-related lncRNAs based on The Cancer Genome Atlas (TCGA) expression data. Then, we explored the prognostic efficiency and accuracy of the risk model. In addition, we explored the role of the risk model in predicting immune cell infiltration, immune checkpoint genes expression level and immunotherapy scores. Our results demonstrated that the lncRNA risk model shows preferable performance in predicting patient survival, immune cell infiltration and immunotherapy effectiveness.

RESULTS

Identification of Chemokine-Related lncRNAs

The workflow for this study was shown in **Figure 1**. First, we acquired the expression profiling data of 343 tumor samples and corresponding clinical information from The Cancer Genome Atlas (TCGA) database. We annotated the gene symbols to acquire the expression data of lncRNAs and mRNAs by using a human GTF file. Subsequently, we obtained 64 chemokine-related genes (**Supplementary Table S2**) (including chemokines and chemokine receptors) from four previous reviews concerned

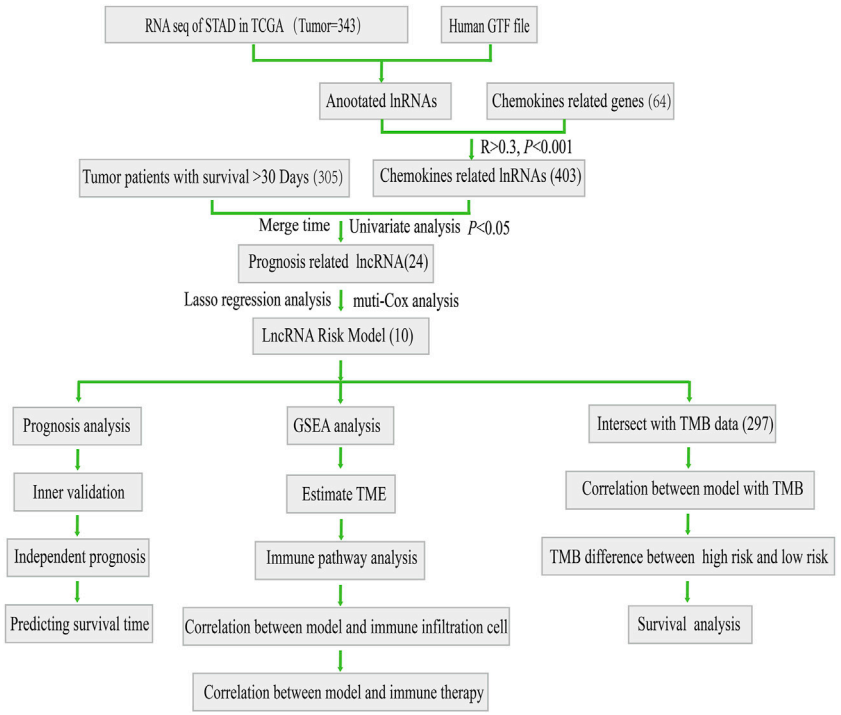

FIGURE 1 | Flow chart of this study.

with chemokines or chemokine recptors (Zlotnik and Yoshie, 2012; Griffith et al., 2014; Sokol and Luster, 2015; Tiberio et al., 2018). Pearson's correlation analysis (Pearson ratio > 0.3 and $p < 0.001$) was further conducted between these 64 chemokine-related genes and lncRNAs for screening chemokine-related lncRNAs. A total of 403 chemokine-related lncRNAs were identified and used for the subsequent analyses.

Construction and Validation of the Risk Model

After obtaining chemokine-related lncRNAs, we combined the survival status and survival time of gastric cancer (GC) patients with lncRNA expression data. We performed univariate analysis and obtained 24 prognostic chemokine-related lncRNAs. To further obtain the prognostic signature, we randomly divided 305 samples (the entire set) into two sets: training set (**Supplementary Table S7**) and testing set (**Supplementary Table S8**) at a ratio of 1:1. A total of 153 samples and 152 samples were enrolled in the training set and testing set, respectively. The training set was used for the establishment of the risk model. Then, lasso regression analysis was performed 1,000 times to recognize the potential survival-related combinations of the candidate chemokine-related lncRNAs in our study, which resulted in 17 optimal candidates (**Figures 2A,B**). To make our risk model more conducive to potential clinical application and cost-saving, we further conducted a multi-cox analysis on these 17 optimal candidates to reduce the number of lncRNAs in our model. Ten out of 17 lncRNAs were identified for the construction of the prognosis signature (**Figure 2C** and **Supplementary Table S6**). The coef value of each lncRNA was shown in **Supplementary Table S5**. The correlation between chemokines and 10 lncRNAs in the risk model was visualized by using a heatmap (**Figure 2D**). According to the median risk score, patients were divided into a high-risk group and a low-risk group. Principal component analysis (PCA) was used for dimensionality reduction of the entire genes, 403 chemokine-related genes and genes in the risk model according to the risk patterns of the risk model. Compared with the expression of all genes and 403 chemokine-related genes, only the risk model showed elevated efficiency in separating the high-risk and low-risk patients in all GC samples (**Supplementary Figures S1E–G**).

To further validate the efficiency of the risk model in predicting the survival of GC patients, we conducted survival analysis and found that low-risk group patients had a superior survival outcome than high-risk patients (**Figure 3A**). Next, we tested the accuracy of the risk model by using a time-dependent receiver operating characteristic (ROC) curve. The area under curve (AUC) value revealed that the risk model has enough efficiency in predicting the survival of GC patients (**Figure 3B**). In addition, we observed that there were more deaths in the high-risk group than in the low-risk group (**Figure 3C**). The expression of 10 lncRNAs in the risk model was visualized using a heatmap (**Figure 3D**).

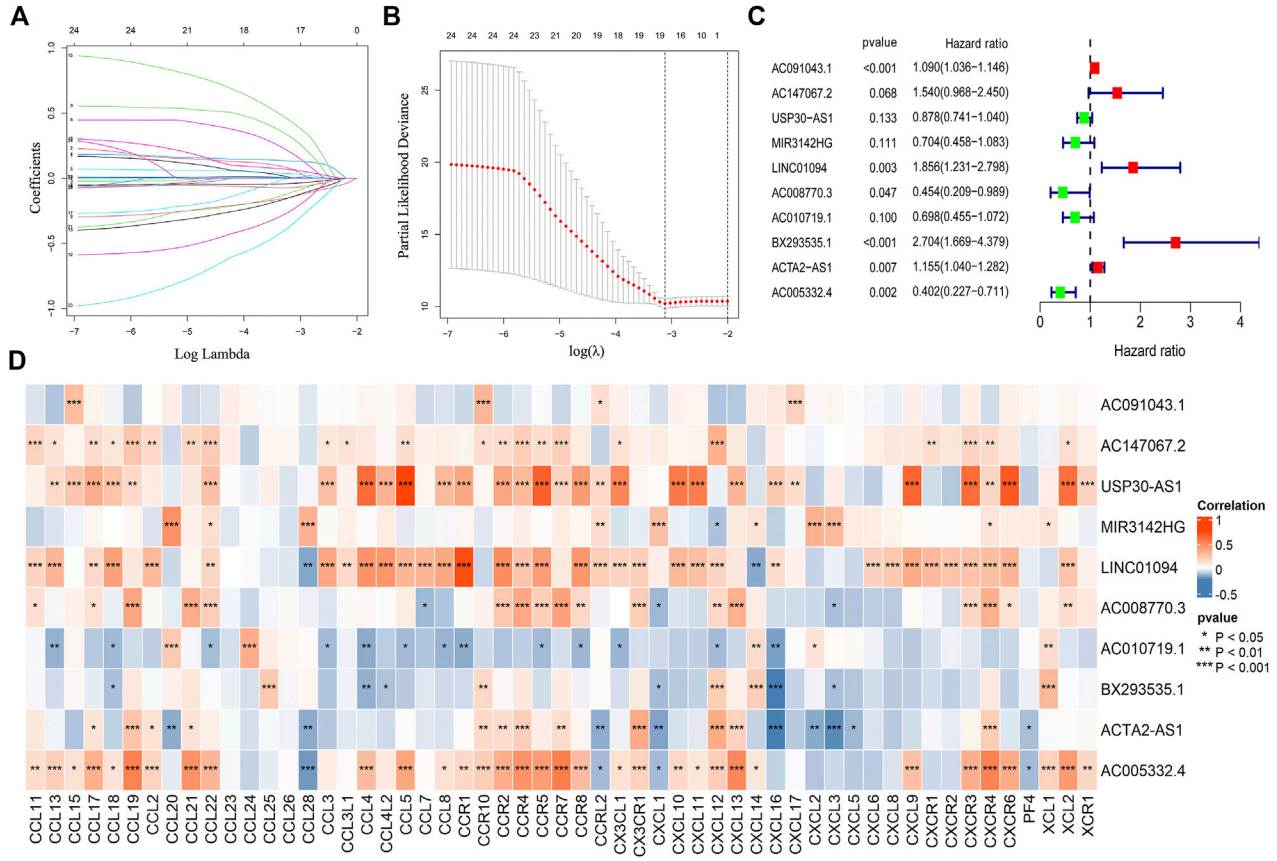

FIGURE 2 | Construction of the risk model. The lasso regression analysis (lasso) was conducted for the construction of the risk model **(A,B)**. A total of 10 chemokine-related lncRNA were identified in the risk model **(C)**. The correlation between chemokines and lncRNAs in the risk model (*$p < 0.05$, **$p < 0.01$, ***$p < 0.001$) **(D)**.

Inner Validation of Risk Model

To further validate the performance of the risk model, we conducted survival analysis in the testing set and the entire set. We observed that high-risk patients in the testing and entire set have poorer survival outcomes than low-risk patients (**Figure 3E** and **Supplementary Figure S1A**). Then, we tested the accuracy of the risk model in two sets by using a time-dependent ROC curve. As expected, we observed that our risk model has a preferable performance in both sets. The AUC values in the testing set and the entire set were 0.691 and 0.740 at one year (**Figure 3F** and **Supplementary Figure S1B**), respectively. After ranking the patients according to the median risk score, we found that the deaths incidence of low-risk patients in the training set and testing set were 11/77 (14.3%) and 28/85 (32.9%), respectively. However, the death rate of high-risk patients in the training set and testing set were 66/77 (85.7%) and 57/85 (67.1%), respectively (**Figure 3G** and **Supplementary Figure S1C**). We concluded that the high-risk group have more deaths than the low-risk group in both sets ($p = 0.006$). The expression of the 10 lncRNAs in two sets was shown in **Figure 3H** and **Supplementary Figure S1D**. These results indicated that our risk model has a good performance in predicting the survival outcome of GC patients.

Considering our risk model could not be validated in an external set, we obtained the expression data of colorectal cancer, the organ most closeted to stomach, (CRC) patients to validate the function of our risk model. We observed that our risk model has an undeniable value in predicting the survival time of CRC patients (**Supplementary Figures S1H, I**).

Independent Prognostic Value of the Risk Model

We also explored the correlation between the risk model and clinical characteristics of the GC patients. After excluding patients with unknown clinical features, no difference was observed in clinical characteristics between high-risk and low-risk patients (**Table 1**), which further validated the prognostic function of the risk model as not related to the clinical characteristics of the patients. To validate the independent prognostic value of the risk model, we conducted univariate analysis and multivariable analysis. We found that the risk score could be used as an independent prognostic index (**Figures 4A,B**). Then, we divided the patients into two groups according to different clinical characteristics and analyzed the survival outcome of the patients. Interestingly, we observed that

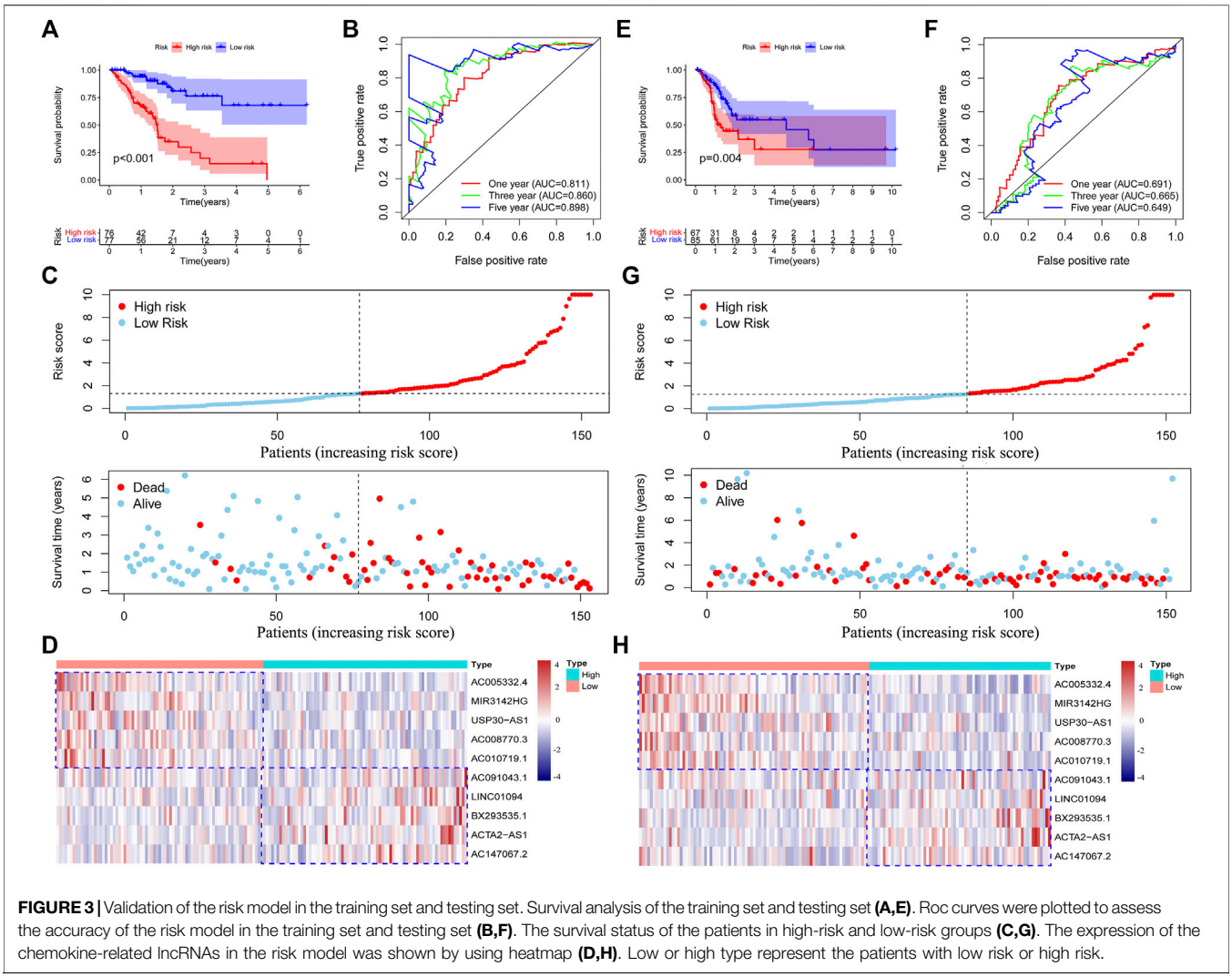

FIGURE 3 | Validation of the risk model in the training set and testing set. Survival analysis of the training set and testing set **(A,E)**. Roc curves were plotted to assess the accuracy of the risk model in the training set and testing set **(B,F)**. The survival status of the patients in high-risk and low-risk groups **(C,G)**. The expression of the chemokine-related lncRNAs in the risk model was shown by using heatmap **(D,H)**. Low or high type represent the patients with low risk or high risk.

low-risk group patients had better survival outcomes than high-risk group patients in all subgroups (**Supplementary Figures S2A–G**). In addition, we also divided 305 patients into a chemotherapy group (**Supplementary Table S13**) and a none-chemotherapy group (**Supplementary Table S14**). We tested the survival difference between low-risk and high-risk patients in two groups. Interestingly, we found that low-risk patients in the chemotherapy group have a better survival outcome than high-risk patients. However, there was no survival difference between low-risk and high-risk patients in the none-chemotherapy group (**Supplementary Figures S3A–C**). These findings indicated that the risk score could be used as an independent prognostic biomarker in all patients.

To further validate that the risk model is superior to other clinical characteristics in prognostic predicting function, we conducted ROC curve analysis and decision curve analysis (DCA) at 1, 3 and 5 years, respectively. The results demonstrated that the risk model has an elevated efficiency compared with other clinical characteristics (**Figures 4C,D** and **Supplementary Figures S3D–E**). In addition, nomogram and calibration curves were plotted to determine the accuracy in predicting patients' overall survival time (**Figures 4E,G**) and progression-free survival time (**Figures 4F,H**). The concordance index (C index) and ROC of the nomogram were also obtained to validate the accuracy of the nomogram. The value of C index is 0.739. As for the ROC of the OS nomogram, the AUC value of 1 year, 3 and 5 years were 0.753, 0.815 and 0.787, respectively (**Figure 4G**). We also observed that the predicted overall survival time and progression-free survival time were almost consistent with the actual survival time (**Figures 4G,H**), which further supports the risk model's accuracy.

Association Between the Risk Model and Immune-Related Pathways

To detect the difference in KEGG enrichment between the low-risk and high-risk patients, we performed gene set enrichment analyses (GSEAs) and identified 21 enrichment pathways in the low-risk patients. Among these pathways, 6 out of 21 were

TABLE 1 | Correlations between risk and clinicopathologic characteristics of GC patients.

Characteristic	Risk score			
	High (%) *n* = 127	Low (%) *n* = 145	χ2	*p*-value
Gender				
Male	75 (45.2)	91 (54.8)	0.39	$p = 0.532$
Female	52 (49.1)	54 (50.9)		
Age (Years)				
>65	63 (42.9)	84 (57.1)	1.889	$p = 0.169$
≤65	64 (51.2)	61 (48.8)		
Differentiation grade				
G1-G2	45 (45.0)	55 (55.0)	0.182	$p = 0.670$
G3	82 (47.7)	90 (52.3)		
Tumor size				
T1-T2	33 (45.8)	39 (54.2)	0.029	$p = 0.865$
T3-T4	94 (47.0)	106 (53.0)		
Metastasis				
M0	115 (45.1)	140 (54.9)	3.199	$p = 0.074$
M1	12 (70.5)	5 (29.5)		
Lymph node				
N0	37 (44.5)	46 (54.5)	0.214	$p = 0.643$
N1-N3	90 (50.3)	99 (49.7)		
Stages				
I-II	57 (44.9)	70 (54.1)	0.313	$p = 0.576$
III-IV	70 (48.3)	75 (51.7)		

immune-related pathways such as antigen processing and presentation, autoimmune thyroid disease, intestinal immune network, natural killer cell-mediated cytotoxicity, primary immunodeficiency and T cell receptor signaling pathway (**Figure 5A**). Subsequently, we determined the difference in 13 immune-related pathways between the high-risk group and low-risk group. Nine out of 13 pathways were identified to have a statistically significant difference between the two groups. Interestingly, among these nine immune-related pathways, eight pathways had a higher activity in the low-risk group, whereas one pathway showed a lower activity in the low-risk group (**Figure 5B**). This result was consistent with the enrichment of immune-related pathways in the low-risk group. These results indicated that the risk model is associated with the immune-related pathways in GC patients.

Correlation Between the Risk Model and Immune Infiltration Cells

Based on the above results, we speculated that the low-risk group and the high-risk group have different immune microenvironment statuses. To validate our hypothesis, the infiltration status was calculated by using the CIBERSORT analysis. The infiltration of 22 immune cells was visualized by using a bar plot graph (**Figure 6A**). We visualized the infiltration of 22 immune cells in groups according to the risk pattern. Results demonstrated that the infiltration pattern of 22 immune cells in low-risk group patients is obviously different from that in high-risk group (**Supplementary Figures S3F, G**). Then, we determined the correlation among 22 immune cells. The results demonstrated that most types of T cells have a negative correlation with macrophages, mast cells and dendritic cells (**Figure 6B**). In addition, we determined the difference in immune infiltration cells between the low-risk group and high-risk group. We observed that low-risk group patients had a higher infiltration of memory B cells, activated memory CD4 T cells, CD8 T cells and follicular helper T cells. However, a higher infiltration of naive B cells, M2 macrophages, resting mast cells, monocytes and resting memory T cells was detected in the high-risk group (**Figure 6C**). Furthermore, we detected the correlation between the infiltration of immune cells and the risk score. We observed that follicular helper T cells and memory B cells have a negative correlation with the risk score, which indicated that patients with lower risk scores have higher infiltration of these two immune cells (**Figure 6D**). In contrast, resting dendritic cells, M2 macrophages, resting mast cells and monocytes had a positive correlation with the risk score, which indicated that patients with higher risk score have more infiltration of these immune cells (**Figure 6D**). Our results suggested that the risk model could be used to predict the infiltration of immune cells.

Clinical Value of the Risk Model in Immunotherapy

The expression of immune checkpoint genes was reported to be associated with immunotherapy efficiency (Burugu et al., 2018). Patients with higher expression of PD-L1 have better immunotherapy outcomes in NSCLC (Sharma et al., 2021). In addition, we found that patients with PD-L1 combine positive score (CPS) > 10 could benefit more from PD-1 or PD-L1 immunotherapy (Shitara et al., 2020; Janjigian et al., 2021; Moehler et al., 2021). Elizabeth C et al. also analyzed the results of KEYNOTE-062 and found that AGC patients with PD-L1 combined positive score (CPS) more than 10 or greater could benefit more from pembrolizumab than patients with a

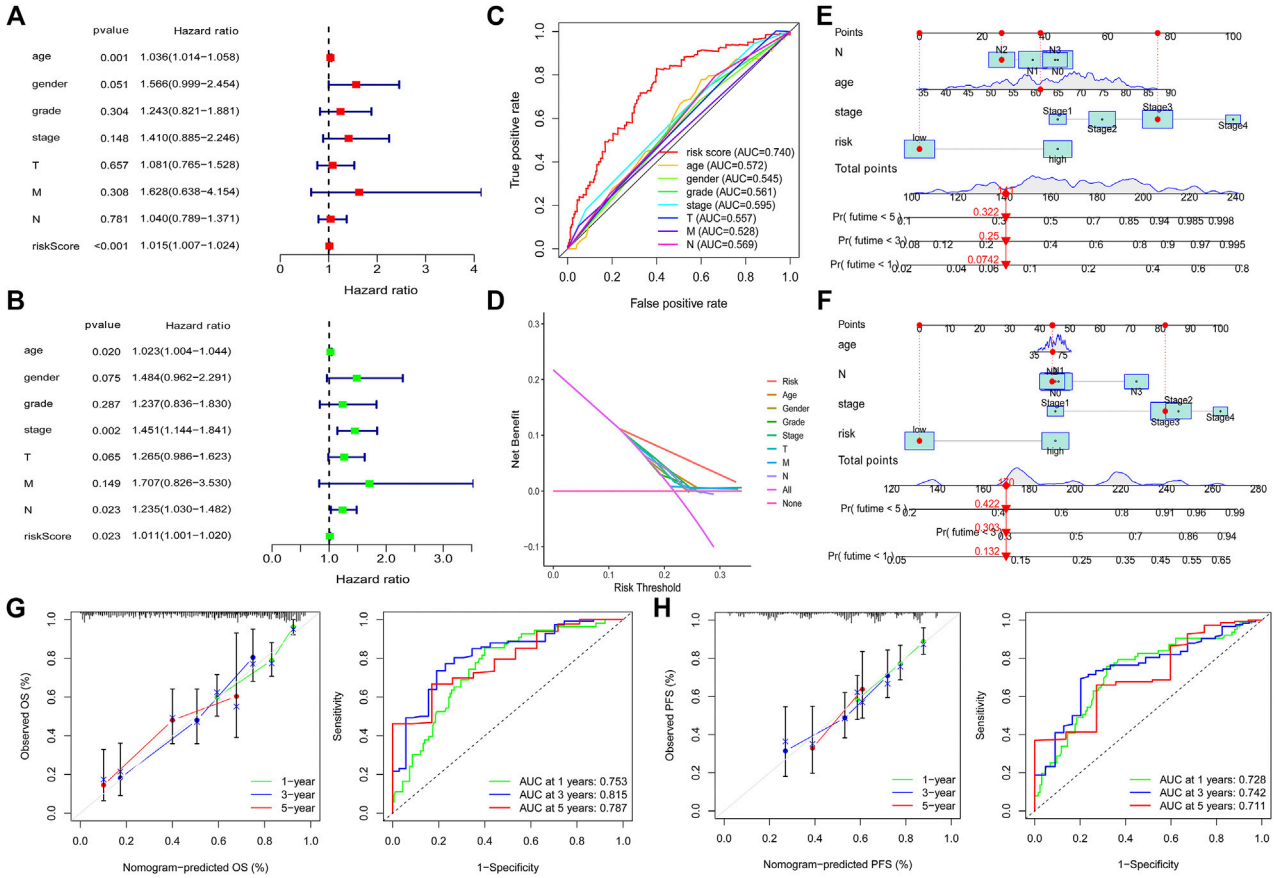

FIGURE 4 | Independent prognosis value of the risk model. Univariate analysis and multivariable analysis were conducted to validate the independent prognosis value of the model **(A,B)**. Roc curves were performed to validate the superiority of the risk score in predicting patient' survival **(C)**. Decision curve analysis (DCA) was conducted to confirm the superiority of the risk score in the clinical application **(D)**. Nomogram was plotted for the prediction of overall survival time **(E)** and progression-free survival time **(F)** in GC patients. The calibration curves and ROC curves were further plotted to determine the accuracy of the nomogram for OS and PFS at 1, 3 and 5 years, respectively **(G,H)**.

CPS of 1 or greater (Smyth and Moehler, 2020). To evaluate the expression difference of immune checkpoint genes, we compared the expression of immune checkpoint genes between the low-risk and high-risk patients. The results demonstrated that the low-risk patients showed elevated expression of most immune checkpoint genes (**Figure 7A**), which indicates that low-risk patients might be more sensitive to immunotherapy although clinical evidence should be required. To validate our results, we obtained the immunotherapy score data from TCIA (https://tcia.at/) and compared the difference in immunotherapy score between the two groups. Immunotherapy score was derived in an unbiased manner using machine learning by considering the four major categories of genes that determine immunogenicity (effector cells, immunosuppressive cells, MHC molecules, and immunomodulators) by the gene expression of the cell types these comprise (e.g., activated $CD4^+$ T cells, activated $CD8^+$ T cells). The immunotherapy score is positively correlated with immunogenicity. Results demonstrated that the low-risk group patients with single positivity for CTLA4 or PD-1 and double positivity for CTLA4 and PD-1 had higher immunotherapy scores (**Figures 7B–E**). We also utilized Tumor Immune Dysfunction and Exclusion (TIDE) score to prove immune response difference between the high-risk group and low-risk group. Result demonstrated that low-risk group has a relative lower TIDE prediction score, which indicated a potential better immune therapy response in low-risk group (**Supplementary Figure S3J**).

Correlation Between the Risk Model and Tumor Mutation Burden

By using "maftools" of R, we acquired the TMB data of GC. We compared the TMB difference between the low-risk group and high-risk group. We found that low-risk group patients had a higher TMB level (**Figure 8A**). The risk score is negatively correlated with TMB level (**Figure 8B**). We also analyzed the TMB status in the low-risk and high-risk groups. Except for the mutation of TP53, the mutation of other genes was higher in the low-risk group (**Figures 8C,D**). We grouped the patients according to the TMB level and analyzed the survival outcomes. We found that patients with higher TMB had better outcomes (**Figure 8E**). In addition, high TMB patients with lower

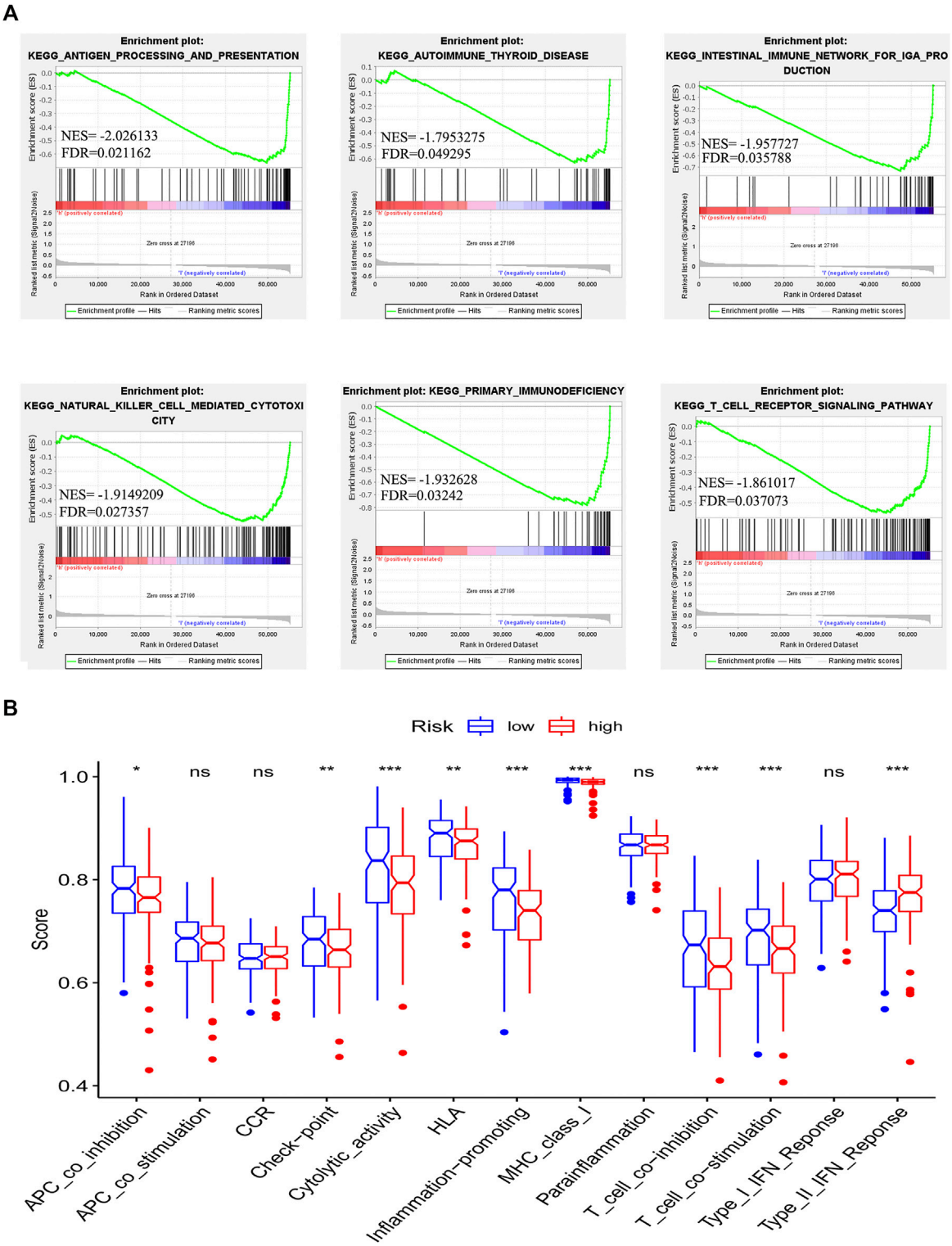

FIGURE 5 | Correlation between immune microenvironment and risk model. Gene set enrichment analysis based on the chemokine-related lncRNAs risk model **(A)**. The difference in the enrichment of thirteen immune-related pathways between the low-risk group and the high-risk group was assessed (*$p < 0.05$, **$p < 0.01$, ***$p < 0.001$) **(B)**.

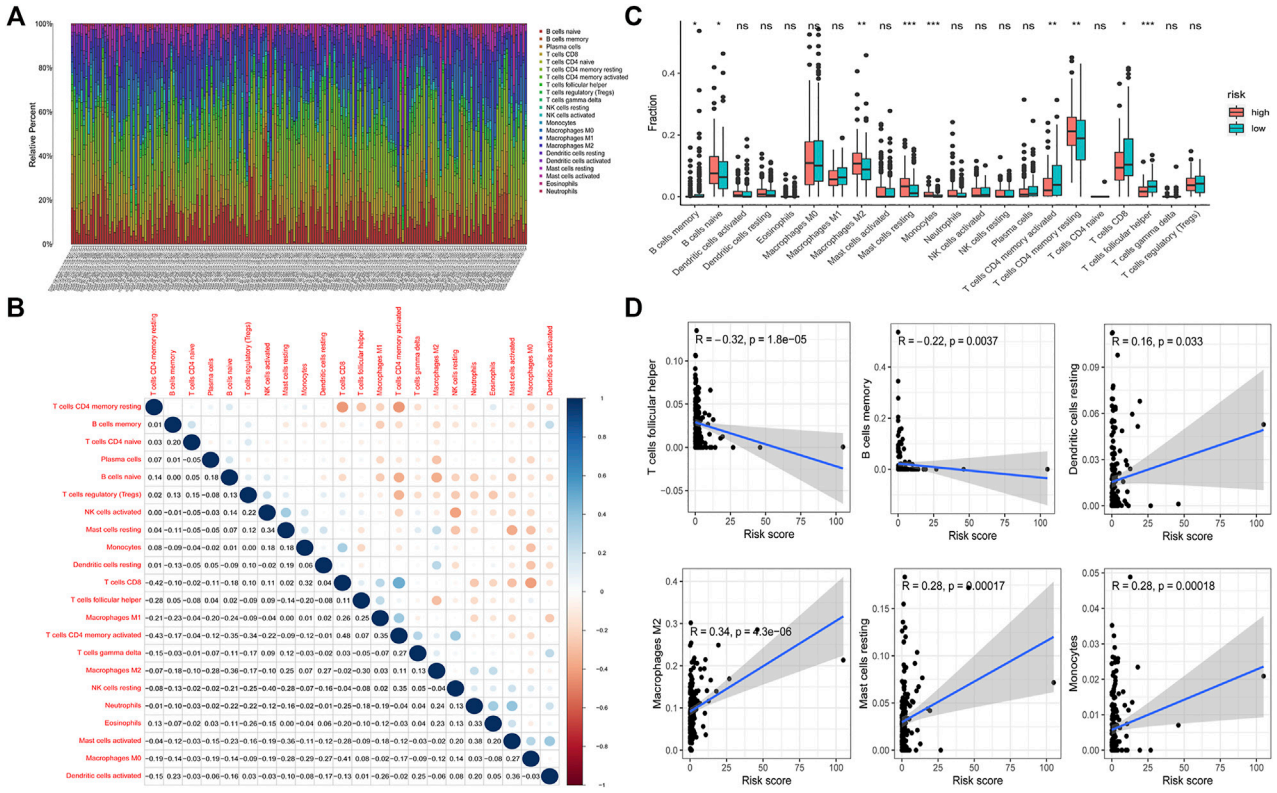

FIGURE 6 | Tumor infiltrating immune cells in GC. CIBERSORT calculation method was used to calculate the infiltrating level of 22 tumor immune cells in GC patients **(A)**. Correlation between 22 tumor infiltrating immune cells was visualized. The red plot represents the negative correlation between two immune cells, while the blue plot represents the positive correlation between two immune cells. The larger the shape of the point, the stronger the correlation **(B)**. The difference of the tumor infiltrating immune cells between the low-risk group and high-risk group (*$p < 0.05$, **$p < 0.01$, ***$p < 0.001$) **(C)**. Correlation between the risk score and infiltrating level of T cells follicular helper, B cells memory, dendritic cells resting, macrophages M2, mast cells resting and monocytes **(D)**.

risk scores had the best survival outcome. However, low TMB patients with higher risk scores have the worst survival outcome (**Figure 8F**).

Expression Validation of Ten lncRNAs in Our Risk Model

The above results indicated that ten chemokine-related lncRNAs of the risk model (AC010719.1, BX293535.1, LINC01094, AC008770.3, MIR3142HG, AC147067.2, AC005332.4, AC091043.1, ACTA2-AS1, USP30-AS1) were associated with patients' survival and immune landscape. To find the most valuable lncRNAs in our risk model, we determined the expression of each lncRNA in TCGA coherent. Six out of ten lncRNAs (AC010719.1, BX293535.1, LINC01094, AC008770.3, MIR3142HG and AC147067.2) were differentially expressed between tumor tissues and normal tissues (**Figures 9A–J**). Compared with normal tissues, only BX293535.1 exhibited a lower expression level in tumor tissues (**Figure 9B**). In addition, we collected 18 paired GC samples and performed qRT-PCR to validate the differences of these six lncRNAs in clinic samples. Interestingly, we observed that only LINC01094 and MIR3142HG were differentially expressed between tumor tissues and paired adjacent normal tissues (**Figure 9K–P**). These results indicated that LINC01094 and MIR3142HG might exert a more crucial function in GC development.

DISCUSSION

Traditionally, patients diagnosed with GC are treated with sequential chemotherapy such as the combination of platinum and fluoropyrimidine (Smyth et al., 2020). However, the overall survival of patients is still very low (Spolverato et al., 2014), especially the median survival time of advanced gastric cancer (AGC) is less than one year (Smyth et al., 2020). Immunotherapy can prolong the overall survival of many cancer patients (Herbst et al., 2016; McGranahan et al., 2016; Jin T. et al., 2021). However, immunotherapy is not effective for all patients. The effectiveness of immunotherapy is associated with many factors, such as the infiltration state of immune cells (Anfray et al., 2019; Zhang et al., 2019), the expression level of immune checkpoint genes (Burugu et al., 2018) and the state of somatic mutations (Allgäuer et al., 2018; Zhao et al., 2019). Therefore, it is very important to find effective biomarkers that could be used to predict patient prognosis and immunotherapy sensitivity.

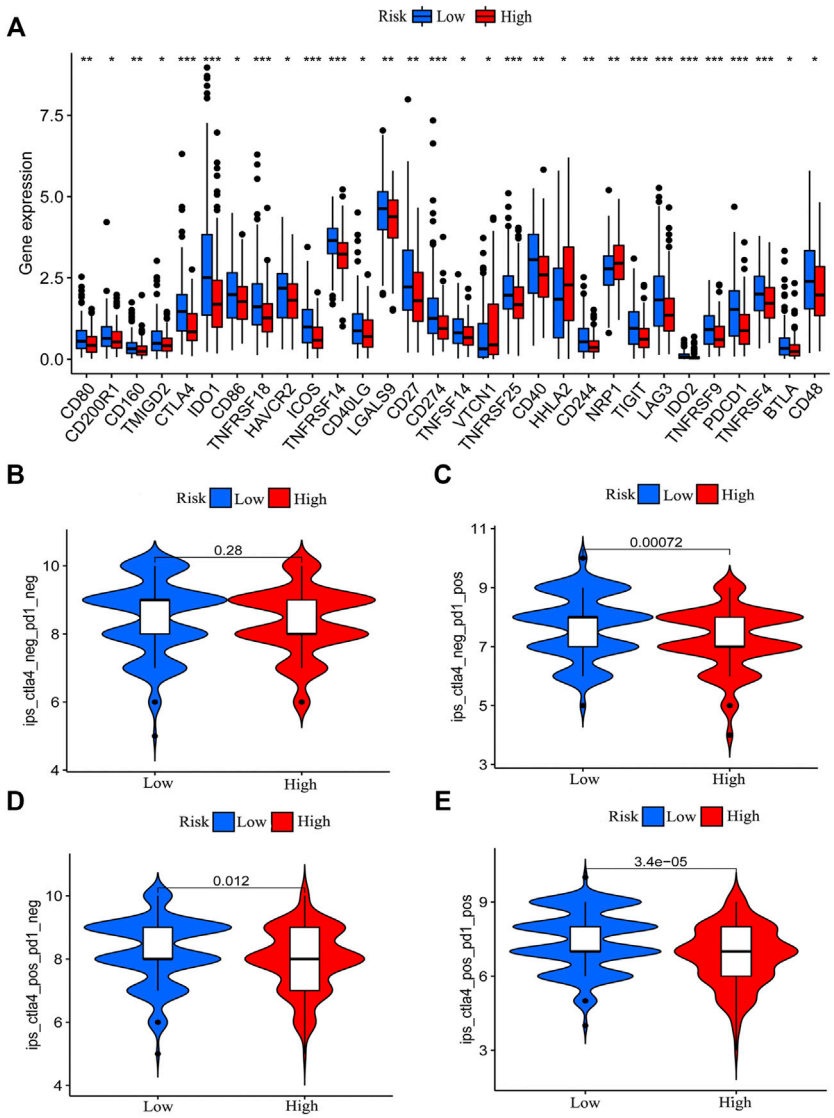

FIGURE 7 | Correlation between risk model and immune checkpoint genes and immunotherapy score. The difference in the expression of immune checkpoint genes between the low-risk group and the high-risk group was determined (*$p < 0.05$, **$p < 0.01$, ***$p < 0.001$) **(A)**. The immunotherapy scores of patients with positive status of CTLA4 or PD-1 in the low-risk group patients are higher than that of high-risk group patients **(B–E)**.

Chemokines are a large class of cytokines with chemotactic activity. It has been reported that chemokines exert crucial functions in the tumor microenvironment, especially in the immune microenvironment (Bian et al., 2019; Xun et al., 2020). Different types of immune cells could be recruited into the tumor microenvironment via interactions between chemokines and chemokine receptors (Nagarsheth et al., 2017). Altered expression levels of chemokines in malignant tumors are associated with angiogenesis, proliferation, metastasis and recruitment and activation of immune cells in multiple tumors (Strieter et al., 2005; Teicher and Fricker, 2010; Santoni et al., 2014; Li et al., 2017; Yang et al., 2017; Liang et al., 2018; Mo et al., 2020; Yang et al., 2020). Many anti-chemokine drugs have been used in combination with other antitumor drugs in cancer treatment (Feig et al., 2013; Salazar et al., 2018). Therefore, it is essential to explore the function of chemokines and their related genes.

In this study, we first identified a novel chemokine-related lncRNA prognostic signature based on the expression data of patients in the TCGA database. In brief, we acquired the RNA sequence profiles of 343 tumor samples from the TCGA database. By using the human GTF file, we annotated the mRNA and lncRNA from the RNA sequence results. To obtain chemokine-related lncRNAs, we conducted co-expression analysis between certified chemokine-related genes and lncRNAs (Zlotnik and Yoshie, 2012; Griffith et al., 2014; Sokol and Luster, 2015; Tiberio et al., 2018). A total of 403 chemokine-related lncRNAs were identified and used for univariate analysis to

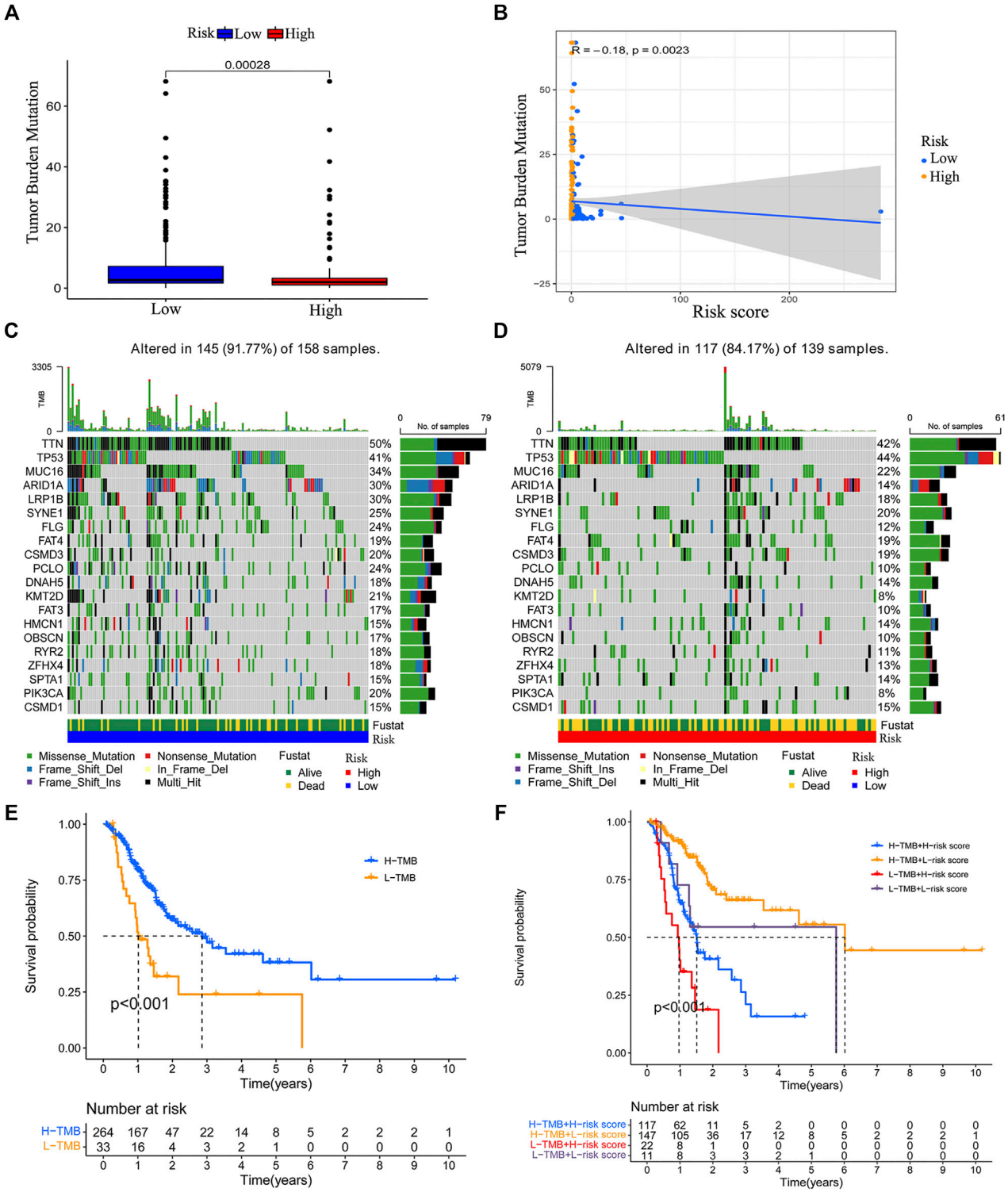

FIGURE 8 | Correlation between the risk model and tumor mutation burden (TMB). Boxplot was used to visualize the TMB level between the low-risk group and high-risk group **(A)**. The risk score is negatively correlated with the TMB level **(B)**. The top 20 genes' TMB in the low-risk group and high-risk group **(C–D)**. The survival difference between the high TMB group and low TMB group **(E)**. The survival status of patients with low or high risk-score in the high TMB group and low TMB group **(F)**.

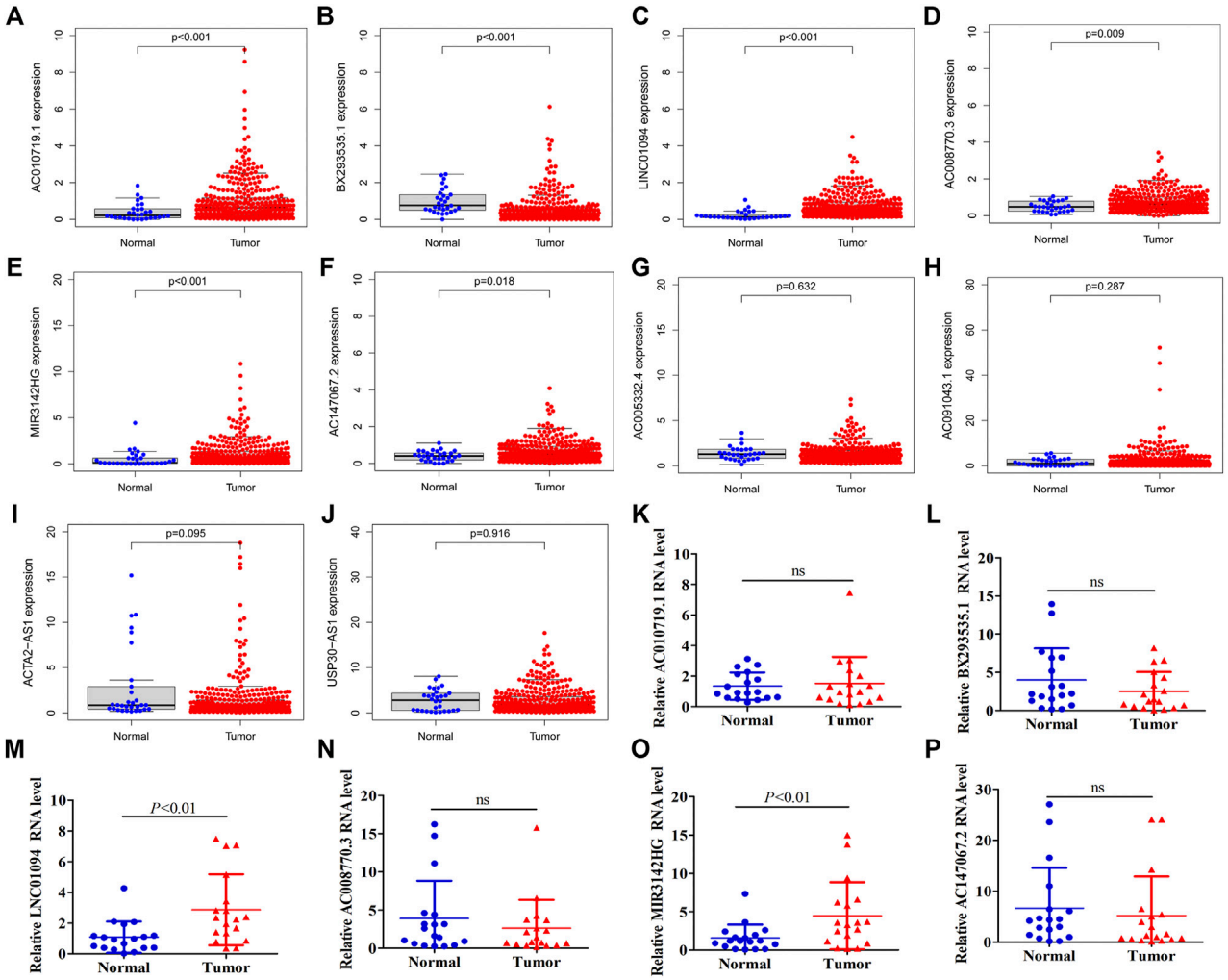

FIGURE 9 | Expression validation of ten lncRNAs in our risk model. A total of six lncRNAs were identified to be differentially expressed between normal tissues and tumor tissue of the TCGA dataset **(A–J)**. Expression of AC010719.1, BX293535.1, MIR3142HG, LINC01094, AC008770.3 and AC147067.2 between tumor tissues and adjacent normal tissues in 18 clinic samples **(K–P)**.

obtain prognostic chemokine-related lncRNAs. Then, lasso regression analysis (LASSO) and multi-cox analysis methods were performed to screen chemokine-related lncRNAs for the construction of the model. Ten chemokine-related lncRNAs (AC010719.1, BX293535.1, LINC01094, AC008770.3, MIR3142HG, AC147067.2, AC005332.4, AC091043.1, ACTA2-AS1, USP30-AS1) were identified in the risk model. Among these lncRNAs, AC091043.1, USP30-AS1, MIR3142HG, LINC01094 and ACTA2-AS1 were reported to regulate the progression of various tumors, while others were reported for the first time (Hadjicharalambous et al., 2018; Xu et al., 2020; Pan et al., 2021a; Wan et al., 2021). After obtaining the risk model, we divided patients into a high-risk group and a low-risk group according to the median risk score. Then, Principal component analysis (PCA) was performed for dimensionality reduction and model identification of the entire gene expression profile, 403 chemokine-related genes and a risk model (Li et al., 2020). As expected, we found that only the risk model showed elevated efficiency in separating the high-risk patients and low-risk patients, which further validates the efficiency of the risk model in separating high-risk patients and low-risk patients.

To explore the function of the risk model in predicting patients' survival outcomes. We performed survival analysis and found that low-risk group patients have better survival outcomes than high-risk group patients in the training set. The area under curve (AUC) values of the ROC curve at one, three and five years exceeded 0.8, which confirmed the accuracy of our risk model. The efficiency and accuracy of the risk model in the testing set and entire set were also determined. In addition, we explored the independent prognostic function of the risk model. The results demonstrated that the risk score could be used as an independent prognostic biomarker in GC. All patients with different clinical characteristics in the low-risk group had better survival outcomes. ROC curve and decision curve analysis (DCA) were conducted to validate the accuracy of the risk score in an independent prognostic function. In addition, the

predicted survival time from the nomogram was almost consistent with the actual survival time. These results indicated that our risk model has enough efficiency in predicting the prognosis of GC patients.

The immune system plays a crucial role in the development of cancer. Chemokines play crucial functions in the tumor microenvironment, especially in the immune microenvironment (Bian et al., 2019; Xun et al., 2020). To explore whether the chemokine-related lncRNA risk model also functions in the immune microenvironment, we performed gene set enrichment analyses (GSEA) and identified six immune-related pathways, antigen processing and presentation, autoimmune thyroid disease, intestinal immune network, natural killer cell-mediated cytotoxicity, primary immune deficiency and T cell receptor signaling pathway, that were enriched in the low-risk group (Tang et al., 2021). In addition, we observed that patients in the low-risk group showed an elevated score in immune-related pathways. Therefore, we speculated that the risk model may regulate immunotherapy by affecting the immune infiltration cells of GC. The status of immune infiltration cells was also reported to be associated with the response to immunotherapy (Anfray et al., 2019; Zhang et al., 2019). Then, we analyzed the proportion of infiltrating immune cells in GC tissue. We observed that the low-risk group had a higher infiltration of memory B cells, activated memory CD4 T cells, CD8 T cells and follicular helper T cells. However, the high-risk group had a higher infiltration of naive B cells, M2 macrophages, resting mast cells, monocytes and resting memory T cells. High infiltration of helper T cells, memory CD4 T cells and $CD8^+$ T cells is reported to be associated with better survival outcomes in patients with cancers (Melssen and SlingluffJr, 2017; Kim H. S. et al., 2021). Patients with more $CD4^+$ and $CD8^+$ T cell infiltration experienced a superior treatment response from immunotherapy than those with less infiltration (Zander et al., 2019; Niogret et al., 2021; Pan et al., 2021b). In contrast, M2 macrophages, resting mast cells and monocytes exert tumor-promoting functions. Monocytes can affect the tumor microenvironment through various mechanisms that induce angiogenesis, immune tolerance, and increased dissemination of tumor cells (Ugel et al., 2021). Infiltration of monocytes is associated with cancer progression, including GC (Peng L.-s. et al., 2017; Wang et al., 2017; Cavassani et al., 2018). Mast cells play a tumor-promoting role in gastric cancer by releasing angiogenic factors and lymphangiogenic factors (Sammarco et al., 2019). Macrophages in solid tumors are associated with poor prognosis and might enhance tumor progression and metastasis (Qian and Pollard, 2010; Cassetta and Pollard, 2018). M2 macrophages are related to the EMT and progression of GC (Guan et al., 2021). These results support the use of our risk model as a biomarker for predicting the GC immune landscape.

Immune checkpoint genes' expression level and tumor mutation burden (TMB) are effective indicators for immunotherapy. Patients with higher expression of immune checkpoint genes and higher somatic mutations might have better immunotherapy effectiveness (Allgäuer et al., 2018; Burugu et al., 2018; Zhao et al., 2019). To further understand the function of the risk model in the immune landscape, we analyzed the expression of immune factors and found that patients in the low-risk group had a relatively higher expression of various checkpoint genes. In addition, we compared the TMB status between the low-risk and high-risk patients. The risk score obtained from the risk model is negatively correlated with TMB. Patients with lower risk scores have a higher level of TMB. Thus, we speculated that low-risk patients might be more sensitive to immunotherapy. Based on this hypothesis, we downloaded the immunotherapy score data of GC and assessed the sensitivity of high-risk and low-risk group patients to immunotherapy. We found that low-risk patients with single positivity for CTLA4 or PD-1 and double positivity for CTLA4+PD-1 had higher immunotherapy scores. The survival analysis concerned with TMB revealed that high TMB patients with lower risk scores had the best survival outcome, and low TMB patients with higher risk scores had the worst survival outcome. According to the above results, we concluded that the chemokine-related lncRNA risk model could be used to predict the immunotherapy sensitivity of GC.

Recently, many studies constructed prognostic signatures in GC. All these studies aim to find a reliable signature for predicting prognosis, immune cells infiltration and immune response of GC. Dai identified that low-risk patients in their risk model have a higher tumor mutation burden (TMB) score and immunotherapy score than that in high-risk group (Dai et al., 2021), which is similar to our results. Ma established an immune-related lncRNA signature which has a preferable performance in prognosis and immune cell infiltration prediction. They observed that high-risk patients have a relatively higher infiltration of M2 macrophages and T cells regulatory (Ma et al., 2021). In our study, risk score was revealed to be positively correlated with the infiltration of M2 macrophages. Unexpectedly, there was no obvious difference in the infiltration of T cells regulatory between the two groups. Unlike other studies, Kim et al. constructed a novel tumor immune microenvironment (TIM) classification system. They found that TIM of GC could be influenced by frameshift mutations and tumor mutational burden (Kim H. et al., 2021). In our study, we only observed that risk score is closely correlated with immune cells infiltration and TMB. However, whether the infiltration of immune cells could be affected by TMB needs further research.

Despite our positive findings, we recognized that our study has some limitations. We obtained a risk model that could be used to predict patients' survival outcomes and immune landscape. We didn't perform independent validation of the risk model, which might lead to a risk of overfitting the model. In this regard, we performed 1,000 times lasso regression analysis. After obtaining the risk model from the training set, we validate the prognostic function of the model in the testing set and entire set. We also validated that our risk model has a good performance in predicting the survival time of CRC patients. These results indicated our model is reliable in predicting the prognosis of gastrointestinal cancer.

Additionally, these ten lncRNAs have not been previously reported to be associated with GC except LINC01094. LINC01094 was used for the construction of another

signature to predict the prognosis of GC patients (Zhang et al., 2021). To find the most valuable lncRNAs in our risk model, we determined the expression of ten lncRNAs in the TCGA dataset and 18 clinic samples. Two lncRNAs (LINC01094 and MIR3142HG) were identified to be differentially expressed between normal tissues and tumor tissues both in the TCGA dataset and 18 clinic samples. These results indicated that these two lncRNAs (LINC01094 and MIR3142HG) in the risk model might exert vital function in the prognosis and immune infiltration of GC patients. We will explore the association between these two lncRNAs and GC in further study.

In conclusion, we constructed a chemokine-related lncRNA risk model in GC. The risk model could be used to predict the prognosis of GC patients. The risk model also exerts a crucial function in predicting the immune landscape of GC patients. These results could provide insights for prognosis prediction of GC patients and might provide valuable clues for immunotherapy in GC.

MATERIALS AND METHODS

Data Acquisition and Processing

The RNA sequence data of gastric cancer (GC) and colorectal cancer (CRC) patients and their corresponding clinical information (**Supplementary Table S1**) were obtained from The Cancer Genome Atlas (TCGA) (https://tcga-data.nci.nih.gov/tcga/). Patients with survived time more than 30 days were enrolled. The human GTF file download from Ensembl (http://asia.ensembl.org) was used to acquire mRNA and lncRNA expression data from transcriptome data.

Acquiring of the Prognostic Chemokine-Related lncRNAs

According to four previous reviews concerned with chemokines or chemokine receptors (Zlotnik and Yoshie, 2012; Griffith et al., 2014; Sokol and Luster, 2015; Tiberio et al., 2018), we obtained 64 chemokine genes (**Supplementary Table S2**). Then, the expression of these 64 chemokine genes was extracted from the mRNA matrix of TCGA STAD by using the "limma" package of R software. Based on these 64 chemokines, we screened chemokine-related lncRNAs from lncRNA matrix by using Pearson's correlation analysis (Pearson ratio >0.3 and $p < 0.001$), and 403 chemokine-related lncRNAs were identified (**Supplementary Table S3**). Subsequently, univariate analysis was performed to determine prognosis-related lncRNAs. A total of 24 prognostic chemokine-related lncRNAs were identified (**Supplementary Table S4**).

Establishment of the Risk Model

The training set was used to construct the risk model, and the entire set (**Supplementary Table S6**) and testing set were used for the validation of the risk model. In brief, the lasso regression analysis and multi-cox analysis were utilized to construct the lncRNA risk model by using 24 prognostic chemokine-related lncRNAs. We identified 10 chemokine-related lncRNAs (**Supplementary Table S5**) to establish the risk model. The calculation formula of the risk score is as follows:

$$Risk\ score\,(patients) = \sum_{i=1}^{n} coef\,ficient\,(gene\,i) * expression\,(gene\,i)$$

In this formula, n, i, $coef\,ficient$, and $expression$ represent the number of selected lncRNA, lncRNA numbers, regression coefficient values and lncRNA expression value, respectively. Principal component analysis (PCA) was further used for dimensionality reduction, grouping visualization and model identification of the entire gene expression profiles, 403 chemokine-related genes and risk model according to the risk patterns of the risk model [25].

Validation of the Risk Model

According to the median risk score, all samples were divided into high-risk group and low-risk group. Kaplan-Meier survival analysis was used to determine the over survival (OS) difference between the two groups. A time-dependent receiver operating characteristic (ROC) curve was plotted to detect the accuracy of the risk model. The expression of the chemokine-related lncRNAs in the model was visualized by using a heatmap. All analyses were further performed in the entire set and testing set. R package of "survivalROC", "survival", "survminer" and "pheatmap" were used in the validation of the risk model.

Independent Prognostic Value of the Risk Model

The relationship between the risk model and clinicopathological characteristics was determined by using the chi-square test. Univariate analysis and multivariate analysis were used to detect the independent prognostic value of the risk model. Kaplan-Meier survival analysis was used to determine the over survival (OS) difference among patients with different clinical characteristics. The ROC curve and decision curve analysis (DCA) were performed to validate the clinical application value of the risk model. The "survival" and "regplot" R packages were utilized to construct a nomogram for the prediction of survival time in GC patients. The calibration curve was acquired to assess the accuracy of the nomogram by using "rms" package of R.

Correlation Between the Risk Model and Immune-Related Pathway

Gene set enrichment analyses (GSEA) were performed to define the lncRNAs signatures in the KEGG. Subsequently, we obtained and evaluated the difference in immune-related pathways between the high-risk group and low-risk group through the single-sample gene set enrichment analysis (ssGSEA). In ssGSEA analysis, the R packages of "limma", "GSVA", "GSEABase", "ggpubr", "reshape2" were used.

Evaluation of Immune Cell Infiltration

The CIBERSORT bioinformatic computational tool was used to predict the infiltration status of immune cells in tumors (**Supplementary Table S9**). The root mean squared error and *p*-value were counted for each sample file to improve the accuracy of the deconvolution algorithm. Only $p < 0.05$ was filtered and selected for further analysis, and the algorithm used a default signature matrix for 1000-loop computation. The "corrplot" package was used to visualize the correlation among 22 immune cells. The difference of immune infiltration cells between the high-risk and low-risk group was visualized by using R packages of "ggpubr", "ggplot2" and "data.table".

The Clinical Value of the Risk Model in Immunotherapy

The expression of immune checkpoint genes between the high-risk group and low-risk group patients was evaluated by using "limma", "reshape2", "ggplot2" and "ggpubr" package of R. In addition, the immunotherapy score data was obtained from TCIA (**Supplementary Table S10**). The sensitivity of high-risk and low-risk group patients to immunotherapy was calculated to further validate the prognostic function of our risk model. Tumor Immune Dysfunction and Exclusion (TIDE) score was acquired from http://tide.dfci.harvard.edu.

Correlation Between the Risk Model and Tumor Mutation Burden

Tumor mutation burden (TMB) data of GC was downloaded from the TCGA database (https://tcga-data.nci.nih.gov/tcga/). The correlation between the risk model and tumor mutation burden was acquired and visualized by using "ggpubr", "reshape2" and "ggplot2" packages of R software. The "maftools" package was utilized to obtain the TMB status in the high-risk group (**Supplementary Table S11**) and low-risk group patients (**Supplementary Table S12**). Kaplan-Meier analysis was performed to determine the survival difference among patients with different statuses of TMB and risk scores.

Human Tissue Samples Collection, RNA Isolation and Quantitative Real-Time PCR

A total of 18 pairs of GC tissues and adjacent normal tissues were collected from the First Affiliated Hospital of Chongqing Medical University (Chongqing, China). This study was approved by the Ethics Committee of the First Affiliated Hospital of Chongqing medical university. Total RNA of GC samples was isolated by using Trizol reagent according to the manufacturer's protocol (Takara, Japan). For the qRT-PCR assay, all primers were designed and synthesized by Sangon Biotech (Sangon Biotech, Wu Han, China). cDNA was synthesized by using PrimeScript RT Reagent Kit (#RR037A, Takara, Japan). qRT-PCR was performed by using TB Green Premix Ex Taq II (Takara, #RR820A). Results were normalized using GAPDH. The information of primers was exhibited in **Supplementary Table S15**.

Statistical Analysis

All data were acquired by using Perl (5.30.1) or R (version 4.1.0) software. Pearson correlation test was used for the correlation analysis. Survival analyses were performed using the Kaplan-Meier method with a log-rank test.

DATA AVAILABILITY STATEMENT

The original contributions presented in the study are included in the article/**Supplementary Material**, further inquiries can be directed to the corresponding authors.

ETHICS STATEMENT

The studies involving human participants were reviewed and approved by The Ethics Committee of the First Affiliated Hospital of Chongqing medical university. The patients/participants provided their written informed consent to participate in this study.

AUTHOR CONTRIBUTIONS

XL and XG designed the study. XL, GY, CQ, AC and HZ collected and analyzed data. XL, GY, XG, LZ and ZW wrote and revised the manuscript. ZW was responsible for supervising the study. All authors read and gave final approval of the manuscript.

FUNDING

This work was supported by the National Natural Science Foundation of China (81974385).

SUPPLEMENTARY MATERIAL

The Supplementary Material for this article can be found online at: https://www.frontiersin.org/articles/10.3389/fcell.2021.797341/full#supplementary-material

Supplementary Figure S1 | Validation of the risk model in the entire set. Prognosis of the risk model. Patients were ranked according to the risk score **(A)**. Survival analysis of the entire set **(A)**. Roc curves were plotted to assess the accuracy of the risk model in the entire set **(B)**. The survival status of the patients in the high-risk and low-risk group **(C)**. The expression of the chemokine-related lncRNA in the risk model was shown by using heatmap **(D)**. Principal component analysis (PCA) for the entire gene set **(E)**, chemokines **(F)** and lncRNAs in the risk model **(G)**. The green plots represent the patients with low risk, and the red plots represent the patients with high risk.

Supplementary Figure S2 | Survival analysis was conducted in high-risk and low-risk group patients with different ages **(A)**, genders **(B)**, grades **(C)**, stages **(D)**, T stages **(E)**, different N stages **(F)** and M stages **(G)**.

Supplementary Figure S3 | Survival analysis was conducted in patients without chemotherapy **(A)**. Survival analysis was conducted in patients receiving chemotherapy **(B)**. AUC value of the survival analysis in patients with chemotherapy **(C)**. 3 and 5 years DCA curves were plotted to validate the clinical application value of our risk model **(D and E)**. CIBERSORT was utilized

to visualize the infiltration of 22 immune cells in the high-risk group **(F)** and low-risk group **(G)**. Prognostic function of our risk model in colorectal cancer (CRC) patients **(H)**. AUC value of our risk model in predicting OS of CRC patients **(I)**. Tumor Immune Dysfunction and Exclusion (TIDE) score was obtained to prove the immune response difference between the high-risk group and low-risk group **(J)**.

Supplementary Table S1 | Clinical information of the GC patients

Supplementary Table S2 | Expression of 64 Chemokines related genes in 343 GC Samples

Supplementary Table S3 | Expression of 403 Chemokines related lncRNAs in 343 GC Samples

Supplementary Table S4 | Prognosis-related 24 lncRNAs

Supplementary Table S5 | Ten lncRNAs for the construction of the model

Supplementary Table S6 | Risk pattern of all GC patients

Supplementary Table S7 | Risk pattern of the training group

Supplementary Table S8 | Risk pattern of the testing group

Supplementary Table S9 | Immune cells infiltration status of GC patients

Supplementary Table S10 | Immune therapy sensitivity data

Supplementary Table S11 | Tumor mutation burden data of the high-risk group

Supplementary Table S12 | Tumor mutation burden data of the low-risk group

Supplementary Table S13 | The risk score of GC patients receiving chemotherapy

Supplementary Table S14 | The risk score of GC patients receiving no chemotherapy

Supplementary Table S15 | Quantitative real-time PCR primer sequences and R code used in our manuscript

REFERENCES

Allgäuer, M., Budczies, J., Christopoulos, P., Endris, V., Lier, A., Rempel, E., et al. (2018). Implementing Tumor Mutational burden (TMB) Analysis in Routine Diagnostics-A Primer for Molecular Pathologists and Clinicians. *Transl Lung Cancer Res.* 7, 703–715. doi:10.21037/tlcr.2018.08.14

Anfray, C., Ummarino, A., Andón, F. T., and Allavena, P. (2019). Current Strategies to Target Tumor-Associated-Macrophages to Improve Anti-tumor Immune Responses. *Cells* 9, 46. doi:10.3390/cells9010046

Bhan, A., Soleimani, M., and Mandal, S. S. (2017). Long Noncoding RNA and Cancer: A New Paradigm. *Cancer Res.* 77, 3965–3981. doi:10.1158/0008-5472.can-16-2634

Bian, X., Xiao, Y.-T., Wu, T., Yao, M., Du, L., Ren, S., et al. (2019). Microvesicles and Chemokines in Tumor Microenvironment: Mediators of Intercellular Communications in Tumor Progression. *Mol. Cancer* 18, 50. doi:10.1186/s12943-019-0973-7

Burugu, S., Dancsok, A. R., and Nielsen, T. O. (2018). Emerging Targets in Cancer Immunotherapy. *Semin. Cancer Biol.* 52, 39–52. doi:10.1016/j.semcancer.2017.10.001

Cassetta, L., and Pollard, J. W. (2018). Targeting Macrophages: Therapeutic Approaches in Cancer. *Nat. Rev. Drug Discov.* 17, 887–904. doi:10.1038/nrd.2018.169

Cavassani, K. A., Meza, R. J., Habiel, D. M., Chen, J. F., Montes, A., Tripathi, M., et al. (2018). Circulating Monocytes from Prostate Cancer Patients Promote Invasion and Motility of Epithelial Cells. *Cancer Med.* 7, 4639–4649. doi:10.1002/cam4.1695

Chi, Y., Wang, D., Wang, J., Yu, W., and Yang, J. (2019). Long Non-coding RNA in the Pathogenesis of Cancers. *Cells* 8, 1015. doi:10.3390/cells8091015

Dai, S., Liu, T., Liu, X.-Q., Li, X.-Y., Xu, K., Ren, T., et al. (2021). Identification of an Immune-Related Signature Predicting Survival Risk and Immune Microenvironment in Gastric Cancer. *Front. Cel Dev. Biol.* 9, 687473. doi:10.3389/fcell.2021.687473

Fang, P., Chen, H., Ma, Z., Han, C., Yin, W., Wang, S., et al. (2021). LncRNA LINC00525 Suppresses P21 Expression via mRNA Decay and Triplex-Mediated Changes in Chromatin Structure in Lung Adenocarcinoma. *Cancer Commun. (Lond)* 41 (7), 596–614.

Fattahi, S., Kosari-Monfared, M., Golpour, M., Emami, Z., Ghasemiyan, M., Nouri, M., et al. (2020). LncRNAs as Potential Diagnostic and Prognostic Biomarkers in Gastric Cancer: A Novel Approach to Personalized Medicine. *J. Cel Physiol* 235, 3189–3206. doi:10.1002/jcp.29260

Feig, C., Jones, J. O., Kraman, M., Wells, R. J. B., Deonarine, A., Chan, D. S., et al. (2013). Targeting CXCL12 from FAP-Expressing Carcinoma-Associated Fibroblasts Synergizes with Anti-PD-L1 Immunotherapy in Pancreatic Cancer. *Proc. Natl. Acad. Sci.* 110, 20212–20217. doi:10.1073/pnas.1320318110

Griffith, J. W., Sokol, C. L., and Luster, A. D. (2014). Chemokines and Chemokine Receptors: Positioning Cells for Host Defense and Immunity. *Annu. Rev. Immunol.* 32, 659–702. doi:10.1146/annurev-immunol-032713-120145

Guan, Y., Du, Y., Wang, G., Gou, H., Xue, Y., Xu, J., et al. (2021). Overexpression of PLXDC2 in Stromal Cell-Associated M2 Macrophages Is Related to EMT and the Progression of Gastric Cancer. *Front. Cel Dev. Biol.* 9, 673295. doi:10.3389/fcell.2021.673295

Hadjicharalambous, M. R., Roux, B. T., Feghali-Bostwick, C. A., Murray, L. A., Clarke, D. L., and Lindsay, M. A. (2018). Long Non-coding RNAs Are Central Regulators of the IL-1β-Induced Inflammatory Response in Normal and Idiopathic Pulmonary Lung Fibroblasts. *Front. Immunol.* 9, 2906. doi:10.3389/fimmu.2018.02906

He, S., Wang, L., Wu, Y., Li, D., and Zhang, Y. (2010). CCL3 and CCL20-Recruited Dendritic Cells Modified by Melanoma Antigen Gene-1 Induce Anti-tumor Immunity against Gastric Cancer *Ex Vivo* and *In Vivo*. *J. Exp. Clin. Cancer Res.* 29, 37. doi:10.1186/1756-9966-29-37

Herbst, R. S., Baas, P., Kim, D.-W., Felip, E., Pérez-Gracia, J. L., Han, J.-Y., et al. (2016). Pembrolizumab versus Docetaxel for Previously Treated, PD-L1-Positive, Advanced Non-small-cell Lung Cancer (KEYNOTE-010): A Randomised Controlled Trial. *The Lancet* 387, 1540–1550. doi:10.1016/s0140-6736(15)01281-7

Hong, W., Liang, L., Gu, Y., Qi, Z., Qiu, H., Yang, X., et al. (2020). Immune-Related lncRNA to Construct Novel Signature and Predict the Immune Landscape of Human Hepatocellular Carcinoma. *Mol. Ther. - Nucleic Acids* 22, 937–947. doi:10.1016/j.omtn.2020.10.002

Huang, M., Li, J., Yu, X., Xu, Q., Zhang, X., Dai, X., et al. (2021). Comparison of Efficacy and Safety of Third-Line Treatments for Advanced Gastric Cancer: A Systematic Review With Bayesian Network Meta-Analysis. *Front. Oncol.* 11, 734323. doi:10.3389/fonc.2021.734323

Huang, Y., Yang, Z., Huang, C., Jiang, X., Yan, Y., Zhuang, K., et al. (2021). Identification of N6-Methylandenosine-Related lncRNAs for Subtype Identification and Risk Stratification in Gastric Adenocarcinoma. *Front. Oncol.* 11, 725181. doi:10.3389/fonc.2021.725181

Janjigian, Y. Y., Shitara, K., Moehler, M., Garrido, M., Salman, P., Shen, L., et al. (2021). First-line Nivolumab Plus Chemotherapy versus Chemotherapy Alone for Advanced Gastric, Gastro-Oesophageal junction, and Oesophageal Adenocarcinoma (CheckMate 649): A Randomised, Open-Label, Phase 3 Trial. *Lancet* 398, 27–40. doi:10.1016/S0140-6736(21)00797-2

Ji, L., Qian, W., Gui, L., Ji, Z., Yin, P., Lin, G. N., et al. (2020). Blockade of β-Catenin-Induced CCL28 Suppresses Gastric Cancer Progression via Inhibition of Treg Cell Infiltration. *Cancer Res.* 80, 2004–2016. doi:10.1158/0008-5472.can-19-3074

Jiang, Q., Chen, H., Tang, Z., Sun, J., Ruan, Y., Liu, F., et al. (2021a). Stemness-related LncRNA Pair Signature for Predicting Therapy Response in Gastric Cancer. *BMC Cancer* 21, 1067. doi:10.1186/s12885-021-08798-1

Jiang, Q., Sun, J., Chen, H., Ding, C., Tang, Z., Ruan, Y., et al. (2021b). Establishment of an Immune Cell Infiltration Score to Help Predict the Prognosis and Chemotherapy Responsiveness of Gastric Cancer Patients. *Front. Oncol.* 11, 650673. doi:10.3389/fonc.2021.650673

Jin, K., Cao, Y., Gu, Y., Fang, H., Fei, Y., Wang, J., et al. (2021). Poor Clinical Outcomes and Immunoevasive Contexture in CXCL13+CD8+ T Cells Enriched Gastric Cancer Patients. *Oncoimmunology* 10, 1915560. doi:10.1080/2162402x.2021.1915560

Jin, T., Zhang, Q., Jin, Q.-F., Hua, Y.-H., and Chen, X.-Z. (2021). Anti-PD1 Checkpoint Inhibitor with or without Chemotherapy for Patients with

Recurrent and Metastatic Nasopharyngeal Carcinoma. *Translational Oncol.* 14, 100989. doi:10.1016/j.tranon.2020.100989

Kim, H., Heo, Y. J., Cho, Y. A., Kang, S. Y., Ahn, S., and Kim, K. (2021). Tumor Immune Microenvironment Is Influenced by Frameshift Mutations and Tumor Mutational burden in Gastric Cancer. *Clin. Transl Oncol* [Online ahead of print]. doi:10.1007/s12094-021-02714-6

Kim, H. S., Kim, M. G., Min, K.-W., Jung, U. S., and Kim, D.-H. (2021). High MMP-11 Expression Associated with Low CD8+ T Cells Decreases the Survival Rate in Patients with Breast Cancer. *PLoS One* 16, e0252052. doi:10.1371/journal.pone.0252052

Li, X., Li, Y., Yu, X., and Jin, F. (2020). Identification and Validation of Stemness-Related lncRNA Prognostic Signature for Breast Cancer. *J. Transl Med.* 18, 331. doi:10.1186/s12967-020-02497-4

Li, X., Yao, W., Yuan, Y., Chen, P., Li, B., Li, J., et al. (2017). Targeting of Tumour-Infiltrating Macrophages via CCL2/CCR2 Signalling as a Therapeutic Strategy against Hepatocellular Carcinoma. *Gut* 66, 157–167. doi:10.1136/gutjnl-2015-310514

Li, Z., Jia, Y., Zhu, H., Xing, X., Pang, F., Shan, F., et al. (2021). Tumor Mutation burden Is Correlated with Response and Prognosis in Microsatellite-Stable (MSS) Gastric Cancer Patients Undergoing Neoadjuvant Chemotherapy. *Gastric Cancer* 24, 1342–1354. doi:10.1007/s10120-021-01207-3

Liang, K., Liu, Y., Eer, D., Liu, J., Yang, F., and Hu, K. (2018). High CXC Chemokine Ligand 16 (CXCL16) Expression Promotes Proliferation and Metastasis of Lung Cancer via Regulating the NF-κB Pathway. *Med. Sci. Monit.* 24, 405–411. doi:10.12659/msm.906230

Ma, E., Hou, S., Wang, Y., Xu, X., Wang, Z., and Zhao, J. (2021). Identification and Validation of an Immune-Related lncRNA Signature to Facilitate Survival Prediction in Gastric Cancer. *Front. Oncol.* 11, 666064. doi:10.3389/fonc.2021.666064

Mantovani, A., Savino, B., Locati, M., Zammataro, L., Allavena, P., and Bonecchi, R. (2010). The Chemokine System in Cancer Biology and Therapy. *Cytokine Growth Factor. Rev.* 21, 27–39. doi:10.1016/j.cytogfr.2009.11.007

Mao, Z., Zhang, J., Shi, Y., Li, W., Shi, H., Ji, R., et al. (2020). CXCL5 Promotes Gastric Cancer Metastasis by Inducing Epithelial-Mesenchymal Transition and Activating Neutrophils. *Oncogenesis* 9, 63. doi:10.1038/s41389-020-00249-z

McGranahan, N., Furness, A. J. S., Rosenthal, R., Ramskov, S., Lyngaa, R., Saini, S. K., et al. (2016). Clonal Neoantigens Elicit T Cell Immunoreactivity and Sensitivity to Immune Checkpoint Blockade. *Science* 351, 1463–1469. doi:10.1126/science.aaf1490

Melssen, M., and Slingluff, C. L., Jr (2017). Vaccines Targeting Helper T Cells for Cancer Immunotherapy. *Curr. Opin. Immunol.* 47, 85–92. doi:10.1016/j.coi.2017.07.004

Mo, M., Tong, S., Li, T., Zu, X., and Hu, X. (2020). Serum CXCL13 Level Is Associated with Tumor Progression and Unfavorable Prognosis in Penile Cancer. *Ott* 13, 8757–8769. doi:10.2147/ott.s263980

Moehler, M., Dvorkin, M., Boku, N., Özgüroğlu, M., Ryu, M.-H., Muntean, A. S., et al. (2021). Phase III Trial of Avelumab Maintenance After First-Line Induction Chemotherapy Versus Continuation of Chemotherapy in Patients With Gastric Cancers: Results From JAVELIN Gastric 100. *Jco* 39, 966–977. doi:10.1200/jco.20.00892

Nagarsheth, N., Wicha, M. S., and Zou, W. (2017). Chemokines in the Cancer Microenvironment and Their Relevance in Cancer Immunotherapy. *Nat. Rev. Immunol.* 17, 559–572. doi:10.1038/nri.2017.49

Natsume, M., Shimura, T., Iwasaki, H., Okuda, Y., Hayashi, K., Takahashi, S., et al. (2020). Omental Adipocytes Promote Peritoneal Metastasis of Gastric Cancer through the CXCL2-VEGFA axis. *Br. J. Cancer* 123, 459–470. doi:10.1038/s41416-020-0898-3

Niogret, J., Berger, H., Rebe, C., Mary, R., Ballot, E., Truntzer, C., et al. (2021). Follicular Helper-T Cells Restore CD8+-dependent Antitumor Immunity and Anti-PD-L1/PD-1 Efficacy. *J. Immunother. Cancer* 9, e002157. doi:10.1136/jitc-2020-002157

Pan, J., Zhang, X., Fang, X., and Xin, Z. (2021). Construction on of a Ferroptosis-Related lncRNA-Based Model to Improve the Prognostic Evaluation of Gastric Cancer Patients Based on Bioinformatics. *Front. Genet.* 12, 739470. doi:10.3389/fgene.2021.739470

Pan, Q., Cheng, Y., and Cheng, D. (2021a). Identification of CD8+ T Cell-Related Genes: Correlations with Immune Phenotypes and Outcomes of Liver Cancer. *J. Immunol. Res.* 2021, 9960905. doi:10.1155/2021/9960905

Pan, Q., Huang, Y., Wang, Y., Li, D., and Lei, C. (2021b). LncRNA ACTA2-AS1 Suppress colon Adenocarcinoma Progression by Sponging miR-4428 Upregulation BCL2L11. *Cancer Cel Int* 21, 203. doi:10.1186/s12935-021-01769-3

Pawluczuk, E., Łukaszewicz-Zając, M., Gryko, M., Kulczyńska-Przybik, A., and Mroczko, B. (2021). Serum CXCL8 and Its Specific Receptor (CXCR2) in Gastric Cancer. *Cancers (Basel)* 13, 5186. doi:10.3390/cancers13205186

Peng, L.-s., Zhang, J.-y., Teng, Y.-s., Zhao, Y.-l., Wang, T.-t., Mao, F.-y., et al. (2017). Tumor-Associated Monocytes/Macrophages Impair NK-Cell Function via TGFβ1 in Human Gastric Cancer. *Cancer Immunol. Res.* 5, 248–256. doi:10.1158/2326-6066.cir-16-0152

Peng, W.-X., Koirala, P., and Mo, Y.-Y. (2017). LncRNA-mediated Regulation of Cell Signaling in Cancer. *Oncogene* 36, 5661–5667. doi:10.1038/onc.2017.184

Qian, B.-Z., and Pollard, J. W. (2010). Macrophage Diversity Enhances Tumor Progression and Metastasis. *Cell* 141, 39–51. doi:10.1016/j.cell.2010.03.014

Salazar, N., Carlson, J. C., Huang, K., Zheng, Y., Oderup, C., Gross, J., et al. (2018). A Chimeric Antibody against ACKR3/CXCR7 in Combination with TMZ Activates Immune Responses and Extends Survival in Mouse GBM Models. *Mol. Ther.* 26, 1354–1365. doi:10.1016/j.ymthe.2018.02.030

Sammarco, G., Varricchi, G., Ferraro, V., Ammendola, M., De Fazio, M., Altomare, D. F., et al. (2019). Mast Cells, Angiogenesis and Lymphangiogenesis in Human Gastric Cancer. *Int. J. Mol. Sci.* 20, 2106. doi:10.3390/ijms20092106

Santoni, M., Bracarda, S., Nabissi, M., Massari, F., Conti, A., Bria, E., et al. (2014). CXC and CC Chemokines as Angiogenic Modulators in Nonhaematological Tumors. *Biomed. Res. Int.* 2014, 768758. doi:10.1155/2014/768758

Shan, C., Zhang, Y., Hao, X., Gao, J., Chen, X., and Wang, K. (2019). Biogenesis, Functions and Clinical Significance of circRNAs in Gastric Cancer. *Mol. Cancer* 18, 136. doi:10.1186/s12943-019-1069-0

Sharma, P., Siddiqui, B. A., Anandhan, S., Yadav, S. S., Subudhi, S. K., Gao, J., et al. (2021). The Next Decade of Immune Checkpoint Therapy. *Cancer Discov.* 11, 838–857. doi:10.1158/2159-8290.cd-20-1680

Shen, Y., Peng, X., and Shen, C. (2020). Identification and Validation of Immune-Related lncRNA Prognostic Signature for Breast Cancer. *Genomics* 112, 2640–2646. doi:10.1016/j.ygeno.2020.02.015

Shitara, K., Van Cutsem, E., Bang, Y.-J., Fuchs, C., Wyrwicz, L., Lee, K.-W., et al. (2020). Efficacy and Safety of Pembrolizumab or Pembrolizumab Plus Chemotherapy vs Chemotherapy Alone for Patients With First-Line, Advanced Gastric Cancer. *JAMA Oncol.* 6, 1571–1580. doi:10.1001/jamaoncol.2020.3370

Smyth, E. C., and Moehler, M. (2020). Pembrolizumab in First-Line Gastric Cancer. *JAMA Oncol.* 6, 1539–1541. doi:10.1001/jamaoncol.2020.2436

Smyth, E. C., Nilsson, M., Grabsch, H. I., van Grieken, N. C., and Lordick, F. (2020). Gastric Cancer. *The Lancet* 396, 635–648. doi:10.1016/s0140-6736(20)31288-5

Smyth, E. C., Wotherspoon, A., Peckitt, C., Gonzalez, D., Hulkki-Wilson, S., Eltahir, Z., et al. (2017). Mismatch Repair Deficiency, Microsatellite Instability, and Survival. *JAMA Oncol.* 3, 1197–1203. doi:10.1001/jamaoncol.2016.6762

Sokol, C. L., and Luster, A. D. (2015). The Chemokine System in Innate Immunity. *Cold Spring Harb Perspect. Biol.* 7. doi:10.1101/cshperspect.a016303

Spolverato, G., Ejaz, A., Kim, Y., Squires, M. H., Poultsides, G. A., Fields, R. C., et al. (2014). Rates and Patterns of Recurrence after Curative Intent Resection for Gastric Cancer: A United States Multi-Institutional Analysis. *J. Am. Coll. Surgeons* 219, 664–675. doi:10.1016/j.jamcollsurg.2014.03.062

Strieter, R. M., Burdick, M. D., Gomperts, B. N., Belperio, J. A., and Keane, M. P. (2005). CXC Chemokines in Angiogenesis. *Cytokine Growth Factor. Rev.* 16, 593–609. doi:10.1016/j.cytogfr.2005.04.007

Sung, H., Ferlay, J., Siegel, R. L., Laversanne, M., Soerjomataram, I., Jemal, A., et al. (2021). Global Cancer Statistics 2020: GLOBOCAN Estimates of Incidence and Mortality Worldwide for 36 Cancers in 185 Countries. *CA A. Cancer J. Clin.* 71, 209–249. doi:10.3322/caac.21660

Tang, Y., Li, C., Zhang, Y.-J., and Wu, Z.-H. (2021). Ferroptosis-Related Long Non-coding RNA Signature Predicts the Prognosis of Head and Neck Squamous Cell Carcinoma. *Int. J. Biol. Sci.* 17, 702–711. doi:10.7150/ijbs.55552

Teicher, B. A., and Fricker, S. P. (2010). CXCL12 (SDF-1)/CXCR4 Pathway in Cancer: Fig. 1. *Clin. Cancer Res.* 16, 2927–2931. doi:10.1158/1078-0432.ccr-09-2329

Tiberio, L., Del Prete, A., Schioppa, T., Sozio, F., Bosisio, D., and Sozzani, S. (2018). Chemokine and Chemotactic Signals in Dendritic Cell Migration. *Cell Mol Immunol* 15, 346–352. doi:10.1038/s41423-018-0005-3

Ugel, S., Canè, S., De Sanctis, F., and Bronte, V. (2021). Monocytes in the Tumor Microenvironment. *Annu. Rev. Pathol. Mech. Dis.* 16, 93–122. doi:10.1146/annurev-pathmechdis-012418-013058

Wan, J., Guo, C., Fang, H., Xu, Z., Hu, Y., and Luo, Y. (2021). Autophagy-Related Long Non-coding RNA Is a Prognostic Indicator for Bladder Cancer. *Front. Oncol.* 11, 647236. doi:10.3389/fonc.2021.647236

Wang, Z., Yin, N., Zhang, Z., Zhang, Y., Zhang, G., and Chen, W. (2017). Upregulation of T-Cell Immunoglobulin and Mucin-Domain Containing-3 (Tim-3) in Monocytes/Macrophages Associates with Gastric Cancer Progression. *Immunological Invest.* 46, 134–148. doi:10.1080/08820139.2016.1229790

Wei, J., Zeng, Y., Gao, X., and Liu, T. (2021). A Novel Ferroptosis-Related lncRNA Signature for Prognosis Prediction in Gastric Cancer. *BMC Cancer* 21, 1221. doi:10.1186/s12885-021-08975-2

Wei, Z.-W., Xia, G.-K., Wu, Y., Chen, W., Xiang, Z., Schwarz, R. E., et al. (2015). CXCL1 Promotes Tumor Growth through VEGF Pathway Activation and Is Associated with Inferior Survival in Gastric Cancer. *Cancer Lett.* 359, 335–343. doi:10.1016/j.canlet.2015.01.033

Xin, Z., Zhang, L., Liu, M., Wang, Y., Zhang, Y., Zhao, W., et al. (2021). *Helicobacter pylori* Infection-Related Long Non-coding RNA Signatures Predict the Prognostic Status for Gastric Cancer Patients. *Front. Oncol.* 11, 709796. doi:10.3389/fonc.2021.709796

Xu, F., Huang, X., Li, Y., Chen, Y., and Lin, L. (2021). m6A-related lncRNAs Are Potential Biomarkers for Predicting Prognoses and Immune Responses in Patients with LUAD. *Mol. Ther. - Nucleic Acids* 24, 780–791. doi:10.1016/j.omtn.2021.04.003

Xu, H., Wang, X., Wu, J., Ji, H., Chen, Z., Guo, H., et al. (2020). Long Non-coding RNA LINC01094 Promotes the Development of Clear Cell Renal Cell Carcinoma by Upregulating SLC2A3 via MicroRNA-184. *Front. Genet.* 11, 562967. doi:10.3389/fgene.2020.562967

Xue, S., Ma, M., Bei, S., Li, F., Wu, C., Li, H., et al. (2021). Identification and Validation of the Immune Regulator CXCR4 as a Novel Promising Target for Gastric Cancer. *Front. Immunol.* 12, 702615. doi:10.3389/fimmu.2021.702615

Xun, Y., Yang, H., Li, J., Wu, F., and Liu, F. (2020). CXC Chemokine Receptors in the Tumor Microenvironment and an Update of Antagonist Development. *Rev. Physiol. Biochem. Pharmacol.* 178, 1–40. doi:10.1007/112_2020_35

Yang, H., Zhang, Q., Xu, M., Wang, L., Chen, X., Feng, Y., et al. (2020). CCL2-CCR2 axis Recruits Tumor Associated Macrophages to Induce Immune Evasion through PD-1 Signaling in Esophageal Carcinogenesis. *Mol. Cancer* 19, 41. doi:10.1186/s12943-020-01165-x

Yang, X. L., Liu, K. Y., Lin, F. J., Shi, H. M., and Ou, Z. L. (2017). CCL28 Promotes Breast Cancer Growth and Metastasis through MAPK-Mediated Cellular Anti-apoptosis and Pro-metastasis. *Oncol. Rep.* 38, 1393–1401. doi:10.3892/or.2017.5798

Yang, Z., Guo, X., Li, G., Shi, Y., and Li, L. (2016). Long Noncoding RNAs as Potential Biomarkers in Gastric Cancer: Opportunities and Challenges. *Cancer Lett.* 371, 62–70. doi:10.1016/j.canlet.2015.11.011

Yu, T., Li, G., Wang, C., Gong, G., Wang, L., Li, C., et al. (2021). MIR210HG Regulates Glycolysis, Cell Proliferation, and Metastasis of Pancreatic Cancer Cells through miR-125b-5p/HK2/PKM2 axis. *RNA Biol.* 18, 2513–2530. doi:10.1080/15476286.2021.1930755

Yu, W. D., Wang, H., He, Q. F., Xu, Y., and Wang, X. C. (2018). Long Noncoding RNAs in Cancer-immunity Cycle. *J. Cel Physiol* 233, 6518–6523. doi:10.1002/jcp.26568

Zander, R., Schauder, D., Xin, G., Nguyen, C., Wu, X., Zajac, A., et al. (2019). CD4+ T Cell Help Is Required for the Formation of a Cytolytic CD8+ T Cell Subset that Protects against Chronic Infection and Cancer. *Immunity* 51, 1028–1042. doi:10.1016/j.immuni.2019.10.009

Zhang, J., Endres, S., and Kobold, S. (2019). Enhancing Tumor T Cell Infiltration to Enable Cancer Immunotherapy. *Immunotherapy* 11, 201–213. doi:10.2217/imt-2018-0111

Zhang, S., Li, X., Tang, C., and Kuang, W. (2021). Inflammation-Related Long Non-coding RNA Signature Predicts the Prognosis of Gastric Carcinoma. *Front. Genet.* 12, 736766. doi:10.3389/fgene.2021.736766

Zhao, Q., Cao, L., Guan, L., Bie, L., Wang, S., Xie, B., et al. (2019). Immunotherapy for Gastric Cancer: Dilemmas and prospect. *Brief. Funct. Genomics* 18, 107–112. doi:10.1093/bfgp/ely019

Zlotnik, A., and Yoshie, O. (2012). The Chemokine Superfamily Revisited. *Immunity* 36, 705–716. doi:10.1016/j.immuni.2012.05.008

Conflict of Interest: The authors declare that the research was conducted in the absence of any commercial or financial relationships that could be construed as a potential conflict of interest.

Publisher's Note: All claims expressed in this article are solely those of the authors and do not necessarily represent those of their affiliated organizations, or those of the publisher, the editors, and the reviewers. Any product that may be evaluated in this article, or claim that may be made by its manufacturer, is not guaranteed or endorsed by the publisher.

frontiers in Cell and Developmental Biology

ORIGINAL RESEARCH
published: 24 January 2022
doi: 10.3389/fcell.2021.758777

A Prognostic Risk Score Based on Hypoxia-, Immunity-, and Epithelialto-Mesenchymal Transition-Related Genes for the Prognosis and Immunotherapy Response of Lung Adenocarcinoma

Wenhao Ouyang[1,2†], Yupeng Jiang[1†], Shiyi Bu[1,2], Tiantian Tang[1,2], Linjie Huang[1,2], Ming Chen[1,2], Yujie Tan[1], Qiyun Ou[1,3], Luhui Mao[1], Yingjie Mai[1], Herui Yao[1], Yunfang Yu[1,4]* and Xiaoling Lin[1,2]**

[1]Guangdong Provincial Key Laboratory of Malignant Tumor Epigenetics and Gene Regulation, Department of Medical Oncology, Breast Tumor Centre, Phase I Clinical Trial Centre, Sun Yat-Sen Memorial Hospital, Sun Yat-Sen University, Guangzhou, China, [2]Department of Pulmonary and Critical Care Medicine, Sun Yat-Sen Memorial Hospital, Sun Yat-Sen University, Guangzhou, China, [3]Department of Ultrasound in Medicine, Sun Yat-Sen Memorial Hospital, Sun Yat-Sen University, Guangzhou, China, [4]Artificial Intelligence and Digital Media Programme, Division of Science and Technology, Beijing Normal University-Hong Kong Baptist University United International College, Hong Kong Baptist University, Zhuhai, China

Background: Lung adenocarcinoma (LUAD), the most common subtype of non-small cell lung cancer (NSCLC), is associated with poor prognosis. However, current stage-based clinical methods are insufficient for survival prediction and decision-making. This study aimed to establish a novel model for evaluating the risk of LUAD based on hypoxia, immunity, and epithelial-mesenchymal transition (EMT) gene signatures.

Methods: In this study, we used data from TCGA-LUAD for the training cohort and GSE68465 and GSE72094 for the validation cohorts. Immunotherapy datasets GSE135222, GSE126044, and IMvigor210 were obtained from a previous study. Using bioinformatic and machine algorithms, we established a risk model based on hypoxia, immune, and EMT gene signatures, which was then used to divide patients into the high and low risk groups. We analyzed differences in enriched pathways between the two groups, following which we investigated whether the risk score was correlated with stemness scores, genes related to m^6A, m^5C, m^1A and m^7G modification, the immune microenvironment, immunotherapy response, and multiple anti-cancer drug sensitivity.

Results: Overall survival differed significantly between the high-risk and low-risk groups (HR = 4.26). The AUCs for predicting 1-, 3-, and 5-year survival were 0.763, 0.766, and 0.728, respectively. In the GSE68465 dataset, the HR was 2.03, while the AUCs for predicting 1-, 3-, and 5-year survival were 0.69, 0.651, and 0.618, respectively. The corresponding values in the GSE72094 dataset were an HR of 2.36 and AUCs of 0.653, 0.662, and 0.749, respectively. The risk score model could independently predict OS in patients with LUAD, and highly correlated with stemness scores and numerous m^6A, m^5C, m^1A and m^7G modification-related genes. Furthermore, the risk model was significantly

OPEN ACCESS

Edited by:
Daniele Vergara,
University of Salento, Italy

Reviewed by:
Jie Meng,
Central South University, China
Wangjun Liao,
Southern Medical University, China

***Correspondence:**
Herui Yao
yaoherui@mail.sysu.edu.cn
Yunfang Yu
yuyf9@mail.sysu.edu.cn
Xiaoling Lin
LinXL9@mail.sysu.edu.cn

†These authors have contributed equally to this work and share first authorship

Specialty section:
This article was submitted to Molecular and Cellular Oncology, a section of the journal Frontiers in Cell and Developmental Biology

Received: 15 August 2021
Accepted: 28 December 2021
Published: 24 January 2022

Citation:
Ouyang W, Jiang Y, Bu S, Tang T, Huang L, Chen M, Tan Y, Ou Q, Mao L, Mai Y, Yao H, Yu Y and Lin X (2022) A Prognostic Risk Score Based on Hypoxia-, Immunity-, and Epithelialto-Mesenchymal Transition-Related Genes for the Prognosis and Immunotherapy Response of Lung Adenocarcinoma. Front. Cell Dev. Biol. 9:758777. doi: 10.3389/fcell.2021.758777

correlated with multiple immune microenvironment characteristics. In the GSE135222 dataset, the HR was 4.26 and the AUC was 0.702. Evaluation of the GSE126044 and IMvigor210 cohorts indicated that PD-1/PD-LI inhibitor treatment may be indicated in patients with low risk scores, while anti-cancer therapy with various drugs may be indicated in patients with high risk scores.

Conclusion: Our novel risk model developed based on hypoxia, immune, and EMT gene signatures can aid in predicting clinical prognosis and guiding treatment in patients with LUAD.

Keywords: lung adenocarcinoma, hypoxia, immune, EMT, gene signature, immunotherapy response

1 INTRODUCTION

Lung adenocarcinoma (LUAD) is the most common subtype of non-small cell lung cancer (NSCLC) (Hyuna et al., 2021). Despite advances in standard treatment strategies based on clinical stage, the survival rate remains poor among patients with LUAD (Bi et al., 2020; Siegel et al., 2021), and the associated tumors are highly heterogeneous. Thus, developing a method for accurately stratifying risk and guiding treatment is essential.

Hypoxic conditions in the tumor microenvironment (TME) and immune microenvironment play a crucial role and are regarded as the major drivers of malignancy in LUAD. Further, both environments are strongly associated with malignant progression, therapeutic resistance, and poor prognosis (Wang D. D. et al., 2021; Wu et al., 2021; Zhang Y. et al., 2021). Several studies have recently shown that a hypoxic stimulus can alter the TME, decreasing the proportion of immune cells and increasing the expression of immunosuppressive cytokines (Zeng et al., 2021). Thus, hypoxia is considered the major immunosuppressive mechanism during cancer development (Labiano et al., 2015). Moreover, hypoxic stimulation can activate epithelial-mesenchymal transition (EMT), a key link in cancer progression (Jiang et al., 2011). Despite these findings, reliable prognostic signatures based on the fundamental combination of hypoxia, immunity, and EMT gene signatures have yet to be established.

Hence, to aid in improving clinical management strategies, the present study aimed to establish a novel model for evaluating LUAD risk based on genes related to hypoxia, immunity, and EMT.

2 MATERIALS AND METHODS

2.1 Data Acquisition

Gene expression data, clinical survival information, and gene mutation information for patients with LUAD were downloaded from The Cancer Genome Atlas (TCGA) database (TCGA-LUAD) (Schabath et al., 2016) and the Gene Expression Omnibus (GEO) database (GSE68465, GSE72094) (Zhang A. et al., 2021). The TCGA-LUAD data were used for the training cohort, while those for GSE68465 and GSE72094 were used for the validation cohorts. The TCGA-LUAD dataset was delivered via an Illumina HiSeq 2000 microarray, the GSE68465 dataset was delivered via the Affymetrix Human Genome U133A Array, and the GSE72094 dataset was delivered via the Rosetta/Merck Human RSTA Custom Affymetrix 2.0 microarray. The "sva" package of R software was used to correct the batch effect between different datasets using the "combat" algorithm.

Hypoxia- and EMT-related genes were extracted from the hallmark gene set in the Molecular Signatures Database v7.0(MSigDB, www.gsea-msigdb.org), which includes 200 hypoxia genes and 200 EMT-related genes; 2,498 immune-related genes were acquired in the ImmPort (http://www.immport.org/). This study was approved by the Ethics and Research Committees of Sun Yat-Sen Memorial Hospital and Sun Yat-Sen University.

2.2 Screening of Differentially Expressed Hypoxia-, Immunity-, and EMT-Related Genes

Information regarding the expression of 200 hypoxia-, 2,498 immune-, and 200 EMT-related genes was collected from the TCGA-LUAD database. Differentially expressed genes (DEGs) between LUAD and normal lung tissue were then identified using the Wilcoxon test according to $|\text{Log2FC}| > 1$ and $p < 0.05$ would considered as DEGs. $\text{Log2FC} > 1$ indicating upregulated genes and $\text{Log2FC} < -1$ indicating downregulated genes, respectively. Heat and volcano maps were then generated to show the expression of different genes.

2.3 Functional Exploration of DEGs

An R software package (clusterprofiler, version 3.12) was used to perform Gene Ontology (GO) and Kyoto Encyclopedia of Genes and Genomes (KEGG) pathway enrichment analysis. Using Fisher's exact test, those with false discovery rate (FDR)-corrected p values less than 0.05 were regarded as significant indicators.

2.4 Construction and Verification of the Risk Model

First, RNA expression in the TCGA-LUAD, GSE68465, and GSE72094 datasets was cross-checked to identify co-expressed and differentially expressed hypoxia-, immunity-, and EMT-related

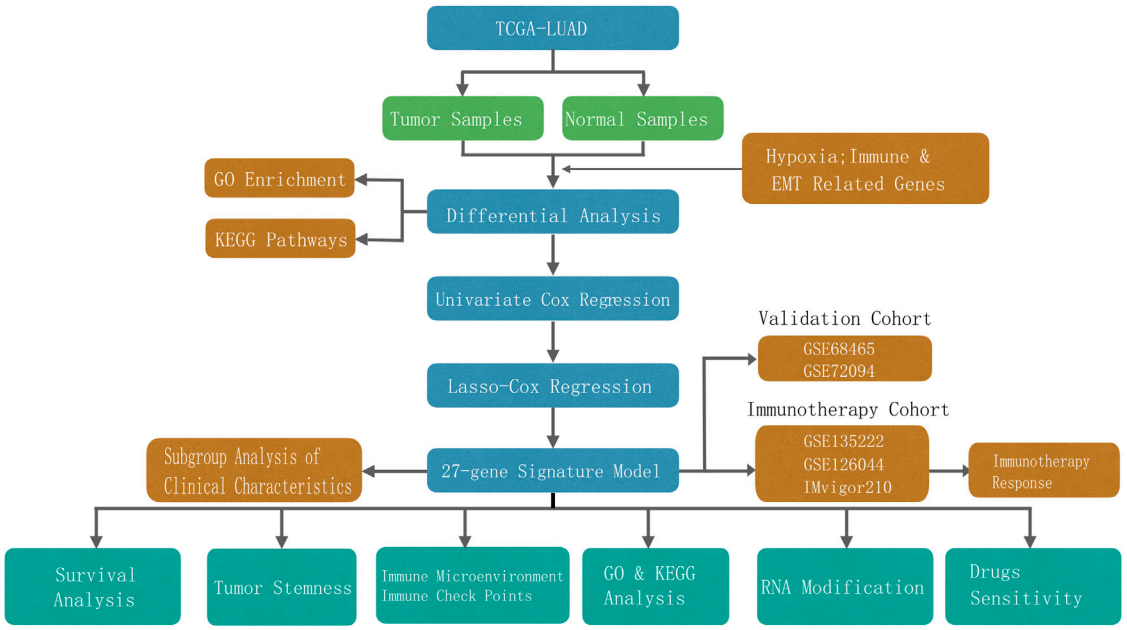

FIGURE 1 | Flow chart of this study.

genes. Consequently, univariate Cox analysis of overall survival (OS) was performed to screen for hypoxia-, immunity-, and EMT-related genes with prognostic values. Next, least absolute shrinkage and selection operator (LASSO) regression with 10-fold cross-validation was performed, and 1,000 cycles were run via the R software package "glmnet." For each cycle, 1,000 random simulations were performed. Based on the optimal lambda value, the best possible gene was selected to construct the model, and a risk formula was established.

The risk scores were calculated according to the expression of each gene and its corresponding regression coefficients using the following equation: risk score = ∑genes Cox coefficient × gene expression. The patients were then categorized into high-risk and low-risk groups based on the optimal cutoff value, which was computed using the "surv_cutpoint" function in the "survminer" R package. Receiver operating characteristic curves were drawn via the R Package "survivalROC" to estimate the predictive sensitivity of the formula. Model effectiveness was evaluated in the validation set using the same coefficients and cutoff values used in the training set. We then evaluated whether the risk score formula exhibited independent prognostic value when combined with clinical variables via multiple regression analysis.

2.5 Selection of m^6A, m^5C, m^1A and m^7G Genes

The expression matrices of m6A genes were including (METTL14, METTL3, RBM15, RBM15B, WTAP, CBLL1, ZC3H13, ALKBH5, FTO, YTHDC1, YTHDF1, YTHDC2, YTHDF2, IGF2BP1, YTHDF3, FMR1, HNRNPC, HNRNPA2B1, ELAVL1, and LRPPRC). The expression of m5C genes including (NSUN7, ALYREF, NSUN1, NSUN6, NSUN3, NSUN4, NSUN2 and NSUN5); The expression of m1A genes including (ALKBH3, ALKBH1 and YTHDF2); The expression of m7G genes including (METTL1, BUD23 and RNMT).

2.6 Differential Analysis of Immune Cell Infiltration, Immune Function, and Immune Checkpoint Function and the Validation of Immunotherapeutic Responses

Immune cell infiltration was identified using timer 2.0 (cistrome.shinyapps.io/timer/) *via* the Timer, QUANTISEQ, CIBERSORT, CIBERSORT-ABS, XCELL, MCPCOUNTER, and EPIC algorithms. The "gsva" R package was used to process the single-sample gene set of the enrichment analysis (ssGSEA) to calculate the activity status of 13 immune-related pathways. The selection of immune-checkpoint genes was based on the findings of a previous study (Isomura et al., 2021). The ESTIMATE algorithm was used to calculate the stromal score, immune score, and ESTIMATE score of TCGA-LUAD samples.

Given the lack of information on immune therapy in the TCGA-LUAD cohort, the predictive capability of the risk score formula was evaluated using the GSE135222 (NSCLC), GSE126044 (NSCLC), and IMvigor210 (metastatic urothelial cancer) cohorts (Charoentong et al., 2017; Mariathasan et al., 2018; Jung et al., 2019; Yu et al., 2019; Yu et al., 2020a; Cho et al., 2020).

2.7 Predicting Anti-Cancer Drug Response

To evaluate the ability of the risk score to predict the chemotherapeutic response, the half-maximal inhibitory

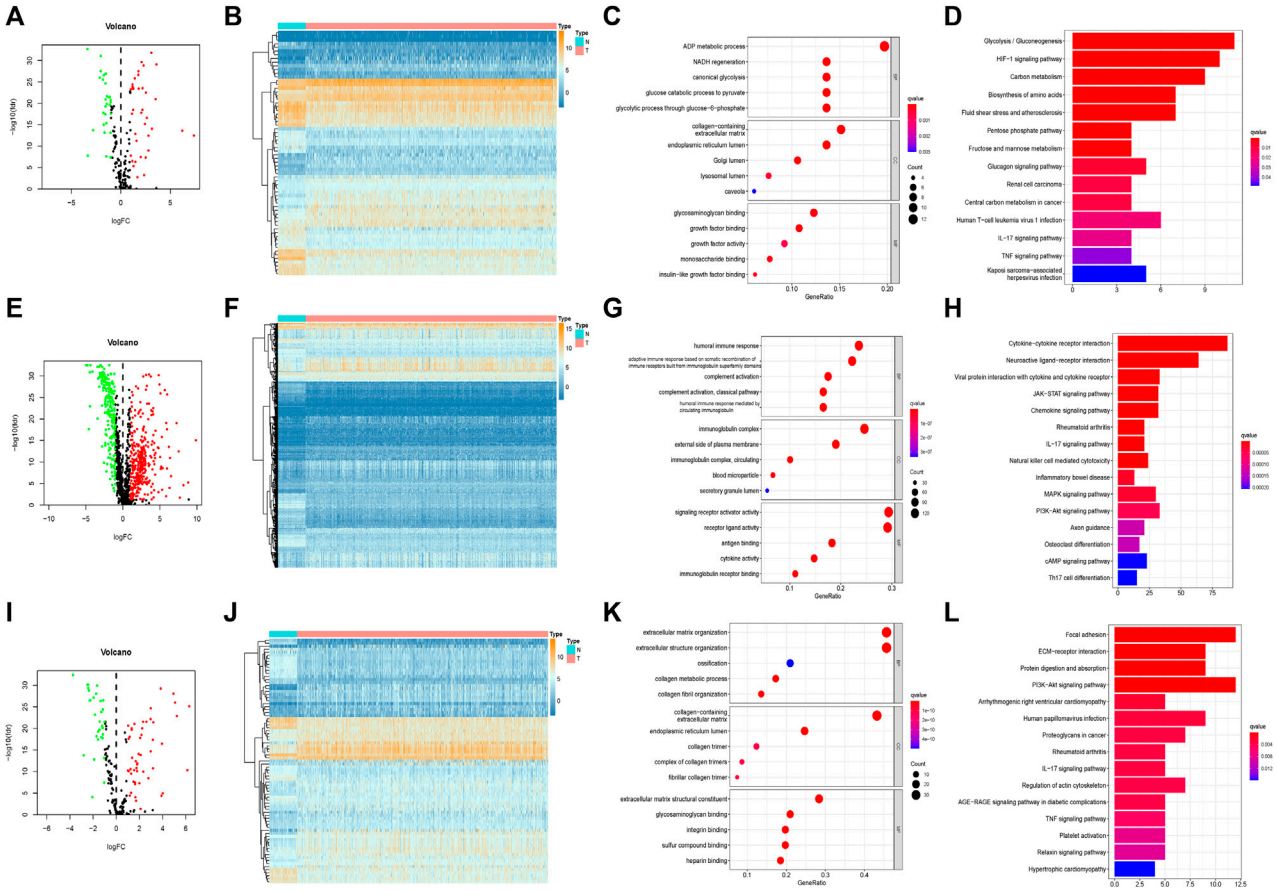

FIGURE 2 | Separatively screening of differentially expressed hypoxia, immunity and EMT related genes. **(A)** Volcano plots showing the hypoxia-related DEGs. **(B)** Heatmaps of differentially expressed hypoxia-related mRNAs. **(C)** GO enrichment of hypoxia-related DEGs. **(D)** KEGG pathways of hypoxia-related DEGs. **(E)** Volcano plots showing the immune-related DEGs. **(F)** Heatmaps of differentially expressed immune-related mRNAs. **(G)** GO enrichment of immune-related DEGs. **(H)** KEGG pathways of immune-related DEGs. **(I)** Volcano plots showing the EMT-related DEGs. **(J)** Heatmaps of differentially expressed EMT-related mRNAs. **(K)** GO enrichment of EMT-related DEGs. **(L)** KEGG pathways of EMT-related DEGs.

concentration (IC50) of common chemotherapeutic drugs was first calculated in the TCGA-LUAD training group, using the "pRRophetic" package in R software. The Wilcoxon rank test was then used to compare the difference in IC50 between the low- and high-risk groups. Finally, the R package "ggplot" was used to visualize the data.

2.8 Statistical Analysis

DEGs were screened using the Wilcoxon test. Univariate Cox analysis of overall survival (OS) was performed to screen relevant genes with prognostic values. Kaplan–Meier survival curves were generated and compared between the two groups using the log-rank test. The associations between the risk score determined using the prognostic model and the stromal score, stemness score, and immune score were assessed using Spearman correlation analysis. All statistical analyses were performed using R version 4.0.0 (R-project.org) and its adequate packages. Statistical significance was set at $p < 0.05$.

3 RESULTS

Totals of 500 and 840 patients with LUAD were selected from the training and validation sets, respectively. The detailed clinical features of these patients are summarized in **Supplementary Table S1**. The flowchart of the study is shown in **Figure 1**.

3.1 Differentially Expressed Hypoxia-, Immune-, and EMT-Related Genes

In the training set, 66 of 169 hypoxia-related genes, 556 of 1,214 immune-related genes, and 81 of 177 EMT-related genes were differentially expressed between LUAD and adjacent normal tissues. Of these, 37 hypoxia-related genes, 345 immune-related genes, and 50 EMT-related genes were upregulated, while 29 hypoxia-related genes, 211 immune-related genes, and 31 EMT-related genes were downregulated (**Figures 2A,B,E,F,I,J**). In total, there were 703 of 1,560 DEGS, 432 and

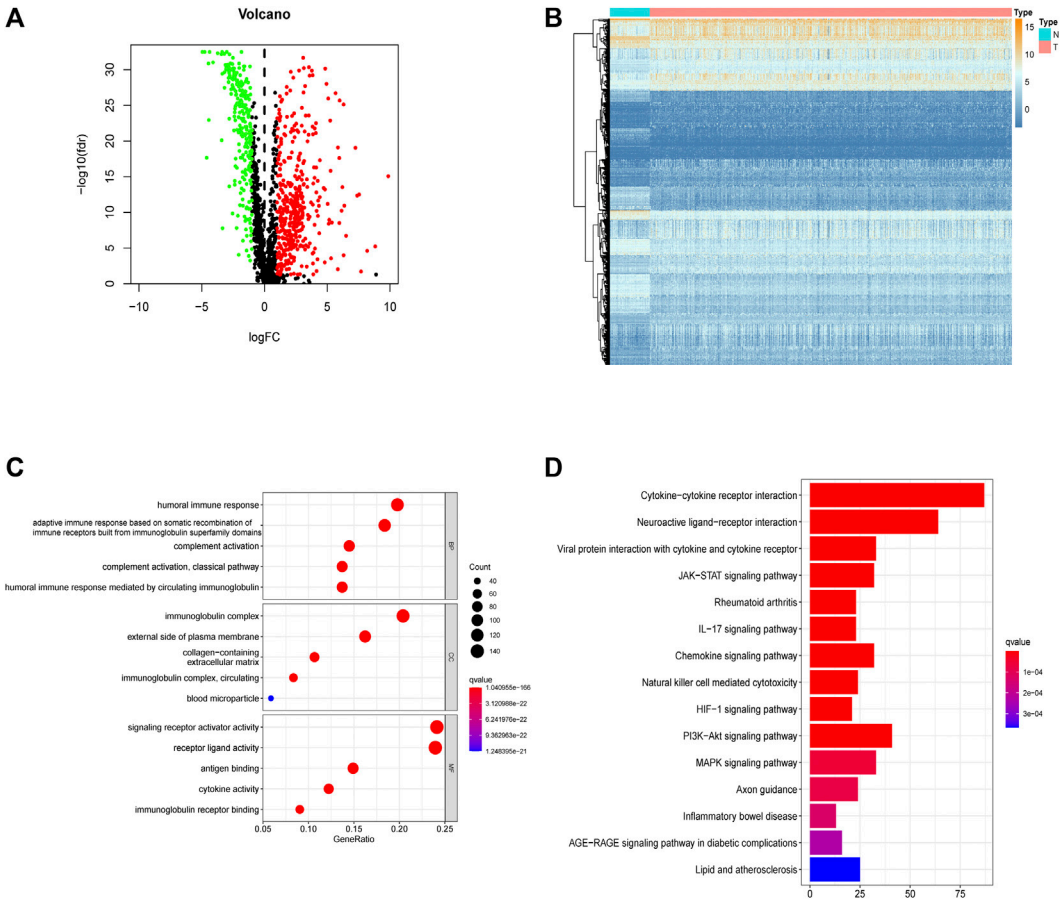

FIGURE 3 | Integrally screening of differentially expressed hypoxia, immunity and EMT related genes. **(A)** Volcano plots of the integrated DEGs. **(B)** Heatmaps of the integrated mRNAs. **(C)** GO enrichment based of integrated DEGs. **(D)** KEGG pathways of integrated DEGs.

271 of which were upregulated and downregulated, respectively (**Figures 3A,B**).

3.2 Functional Analysis of Hypoxia-, Immune-, and EMT-Related DEGs

In the GO enrichment analysis, we identified the top 5 GO categories with significant enrichment of genes related to hypoxia, immunity, or EMT. The most significantly altered hypoxia-, immune-, and EMT-related genes were involved in the metabolic processing of ADP, in signaling receptor activator activity, and in extracellular matrix organization, respectively (**Figures 2C,G,K**; **Supplementary Tables S2, S4, S6**). We then performed KEGG analysis and identified the top 15 KEGG categories with significant enrichment of hypoxia-, immune-, and EMT-related genes. The altered hypoxia-related genes were mostly associated with glycolysis, while the altered immune-related genes were mostly associated with cytokine–cytokine receptor reactions. The EMT-related genes exhibiting the most significant alterations were involved in focal adhesion (**Figures 2D,H,L**) (detailed in **Supplementary Tables S3, S5, S7**). Further, when these gene signatures were combined, the most correlated GO and KEGG categories were signaling receptor activator activity cytokine–cytokine receptor reactions, respectively (**Figures 3C,D**) (**Supplementary Tables S8, S9**).

3.3 Predictive Ability of the Risk Score

A total of 11,074 genes were co-expressed; among them, 430 of 668 hypoxia-, immune-, and EMT-related DEGs were selected (**Figures 4A,B**). Then, these 430 genes were used in the univariate Cox regression analysis. A total of 57 prognostic genes were identified (**Figure 5A**). To avoid overfitting the prognostic model, LASSO regression analysis was performed. Finally, 27 genes were selected and included in the risk score formula, as follows: Risk score = ADAM12 × 0.0537 + CCL20 × 0.1149 + LGR4 × 0.0481 − CTSG × 0.0435 + PDGFB × 0.2173 + INSL4×0.0526 + LIFR×0.0033 + LDHA × 0.1794 − FBP1 × 0.0417 − MAP3K8×0.3235 + SEMA3A × 0.0329 + MC1R × 0.1367 − CD79A × 0.1300 − WFDC2 × 0.0577 + PDYN × 0.2017 − GDF15 × 0.0710 + BCAN × 0.1043 + DDIT4 × 0.0715 − SPOCK1 ×

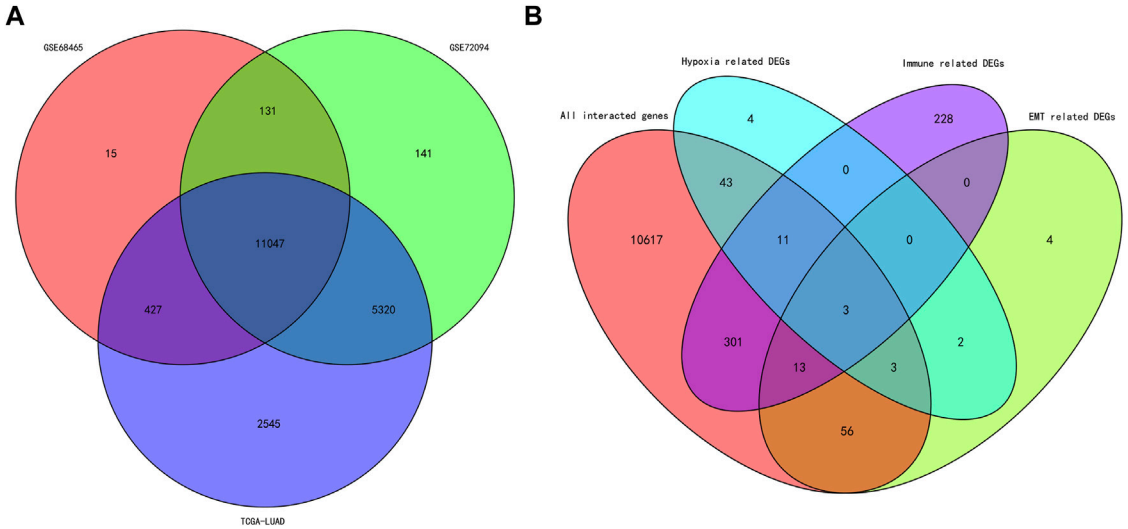

FIGURE 4 | Venn diagram of the intersected genes and DEGs. **(A)** Venn diagram of the intersected genes among the cohorts of TCGA, GSE68465 and GSE72094. **(B)** Venn diagram of the intersected hypoxia, immune and EMT related DEGs.

0.0148 + TNFRSF11A × 0.1982 − CX3CR1×0.1238 − AKAP12 × 0.0061 + ANGPTL4 × 0.0227 + GPI × 0.1924 − CAT × 0.0789 + FURIN × 0.0187 + F2RL1 × 0.1408 (**Figures 5B,C**). Based on am optimistic cut off, 144 and 356 patients were categorized into the high-risk and low-risk groups, respectively (**Figures 6A–C**). Kaplan–Meier survival analysis revealed that OS was lower in the high-risk group than in the low-risk group (**Figure 6E**). The area under the curve (AUC) values for predicting 1-, 3-, and 5-year OS were 0.763, 0.766, and 0.728, respectively (HR = 4.26; 95% CI 3.15–5.75; $p < 0.0001$; **Figure 6D**). These results show that the risk model based on the 27 genes listed above had high accuracy in predicting the OS of patients with LUAD. Besides, we also proved the novel risk score independently predict the OS of LUAD (**Supplementary Figure S1**).

3.4 Stability of the Risk Score Formula Constructed Using Hypoxia-Related Genes

To check the stability of the model developed from the training set, patients in the validation sets (GSE68465 and GSE72094) were also divided into a high-risk group and a low-risk group according to the same cut-off value and risk formula as those in TCGA cohort (**Figures 7A–C,F–H**). The results indicated that OS was markedly lower in the high-risk group than in the low-risk group (**Figures 7E,J**). In the GSE68465 set, the AUCs for predicting 1-, 3-, and 5-year OS were 0.69, 0.651, and 0.618, respectively (HR = 2.03; 95% CI = 1.55–2.65; $p < 0.0001$). In the GSE72094 cohort, the corresponding AUCs were 0.653, 0.662, and 0.749, respectively (HR = 2.36; 95% CI = 1.63–3.43; $p < 0.001$; **Figures 7D,I**).

3.5 Subgroup Analysis Using the Risk Score Formula

Next, we analyzed the association between clinical features (including stage, age, and sex) and the risk score in the TCGA-LUAD database. The risk score remained significantly effective across all subgroups based on tumor stage, sex, and age (**Figure 8**), supporting the reliability of the risk score formula. Moreover, in the univariate and multivariate Cox regression analysis, the risk score formula was identified as an independent prognostic indicator of poor outcomes in patients with LUAD (**Supplementary Figures S1A,B**).

3.6 Functional Analysis

Further analysis of the differences in enrichment pathways between the low-risk and high-risk groups showed that the most different pathways were related to the humoral immune response, collagen-containing extracellular matrix, and focal adhesion (**Figures 9A,B**; **Supplementary Tables S10, S11**). This may explain why OS was lower in the high-risk group than in the low-risk group.

3.7 Tumor Stemness Analysis and Gene Mutation Landscape

Growing evidence indicates that increased expression of stemness-related biomarkers in tumor cells is highly correlated with drug resistance, cancer recurrence, and tumor proliferation (Luo and Vögeli, 2020). Hence, we assessed the correlations of the DNA stemness score (DNAss) and RNA stemness score (RNAss) with the risk score. The results indicate that the risk score was

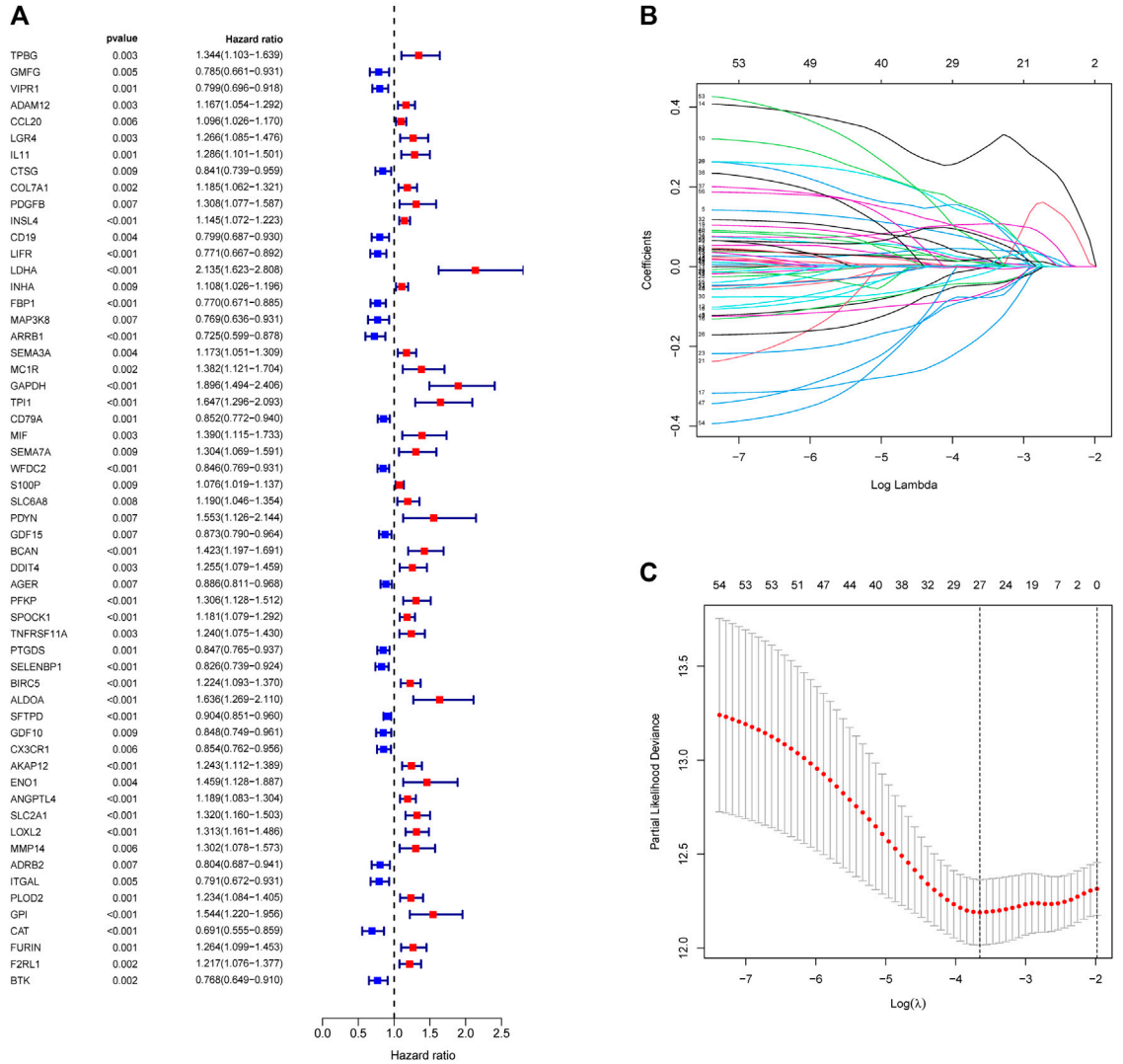

FIGURE 5 | Construction of risk score formula. **(A)** Forest plots showing the results of survival related gene via univariate Cox regression analysis between interacted genes and OS. **(B)** LASSO coefficient profile plots of the 57 prognostic related genes showing that the variations in the size of the coefficients of parameters shrink with an increasing value of the k penalty. **(C)** Penalty plot for the LASSO model for the 57 prognostic genes with error bars denoting the standard errors.

significantly positively correlated with the DNAss and RNAss (**Figures 10A,B**). Besides, this study also compared the gene mutation landscape between high and low risk score group. We found in high risk score group, the mutation frequency of TP53, TTN and KEAP were obviously higher than low risk score group (**Supplementary Figure S2**).

3.8 Expression of m^6A, m^5C, m^1A and m^7G Modification-Related Genes

Previous research has indicated that m^6A, m^5C, m^1A and m^7G modification, which were reversible epigenetic RNA process, significantly involved in the proliferation and migration of cancer cells (Dib et al., 2017; Barbieri and Kouzarides, 2020). In this study, the expression of m^6A modification genes WTAP, HNRNPA2B1, IGF2BP2, HNRNPC, CBLL1, ELAVL1, RBM15B, LRPPRC, and ELAVL1, the expression of m^5C modification gene ALYREF, NSUN1 and NSUN2 and the expression of m7G modification gene METTL1, BUD23 and RNMT were significantly higher in the high risk group, while the expression of m^6A modification gene METTL3, the expression of m^5C modification gene NSUN7 and NSUN6 were significantly higher in the low-risk group (**Figures 10C–F**).

3.9 Analysis of Immune Status

The relationship between the risk score and the immune status of the patients in the TCGA cohort is shown in **Figures 11A,B**. There were significant alterations in immune checkpoint genes. Thus, we further compared the expression of immune

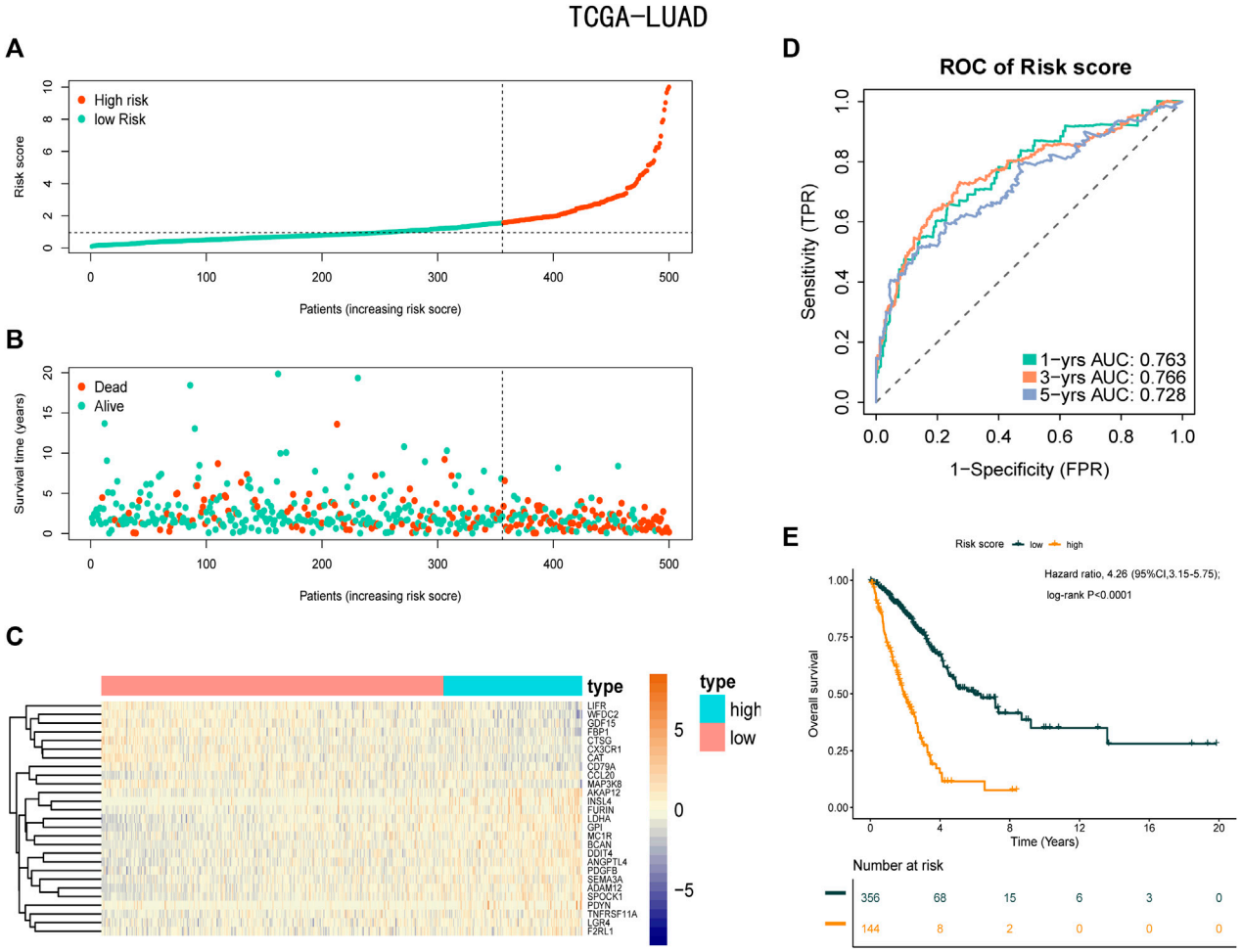

FIGURE 6 | Prognostic analysis of the risk score formula in the training set. **(A)** Distribution of risk score for the training set. **(B)** Patterns of the survival time and survival status between the high-risk and low-risk groups for training set. **(C)** Heatmaps of the 27 prognostic genes for each patient in training set. **(D)** Time-related ROC analysis proved the prognostic performance of the risk score in the training set. **(E)** Kaplan-Meier survival curve of the patients in the high-risk and low-risk groups for OS in the training set.

checkpoint-related genes between the high-risk group and the low-risk group. The tumor immune microenvironment was also assessed using the immune score, ESTIMATE score, and stromal score (Yoshida et al., 2021). All three scores were negatively correlated with the risk score (**Figures 11C–H**), indicating stronger tumor immune activity in low-risk patients than in high-risk patients.

3.10 Analysis of Anti-Cancer Treatment Sensitivity

To verify the prognostic value of the risk score formula for immunotherapy sensitivity, we selected three immunotherapy datasets from patients with NSCLC and metastatic urothelial cancer. The risk score formula was associated with progression-free survival (PFS) in patients with NSCLC undergoing anti-PD-1/PD-L1 therapy in the GSE135222 cohort (HR = 4.26; 95% CI = 3.15–5.75; p = 0.04) (**Figure 12A**), and the AUC value for predicting the 12-month PFS was 0.702 (**Figure 12B**). In the GSE126044 cohort, the risk score was higher in patients with NSCLC who had experienced no benefit (disease progression [PD]) from nivolumab or pembrolizumab than in those who had experienced a benefit (partial response [PR] + stable disease [SD]) (p = 0.017) (**Figure 12C**). Furthermore, the risk score was associated with worse immunotherapy response in patients with metastatic urothelial cancer (**Figures 12D,F**). The risk score was also significantly correlated with several immune checkpoint-related genes: *PD-1, CD8A, CTLA4, CXCL9, GZMA, HAVCR2, IDO1, PRF1, LAG3, IFNG, GZMB*, and *TBX2* (**Figure 13G**). Our analysis further revealed that a high risk score was associated with high sensitivity to common NCCN (National Comprehensive Cancer Network, https://www.nccn.org) recommended anti-

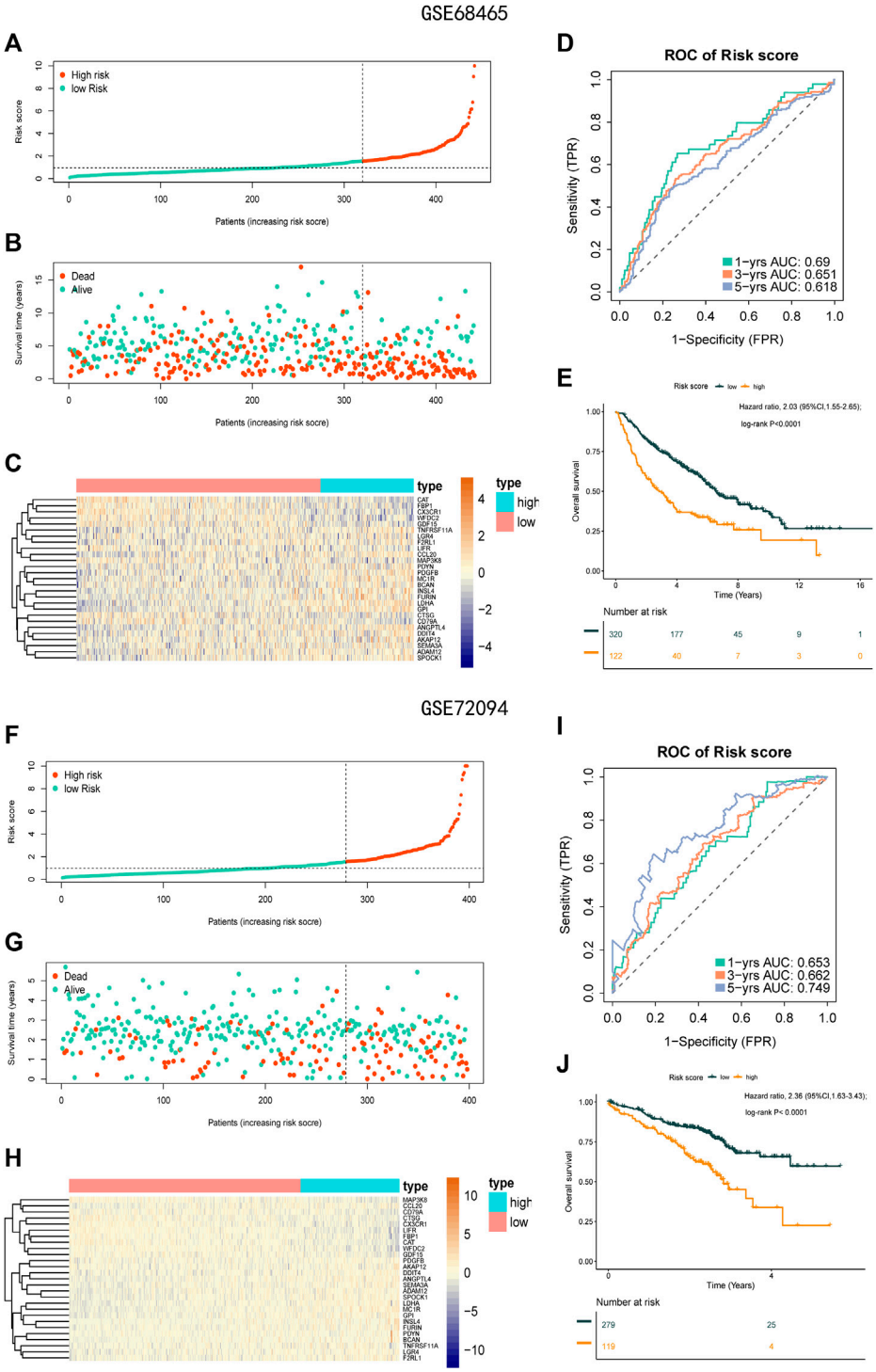

FIGURE 7 | Prognostic analysis of the 27-gene signature model in the validation sets GSE68465 and GSE72094. **(A)** Distribution of risk score for the GSE68465. **(B)** Patterns of the survival time and survival status between the high-risk and low-risk groups for GSE68465. **(C)** Heatmaps of the 27 prognostic genes for each patient in GSE68465. **(D)** Time-related ROC analysis proved the prognostic performance of the risk score in the GSE68465. **(E)** Kaplan-Meier survival curve of the patients in the high risk score and low risk score groups for OS in the GSE68465. **(F)** Distribution of risk score for the GSE72094. **(G)** Patterns of the survival time and survival status between the high-risk and low-risk groups for GSE72094. **(H)** Heatmaps of the 27 prognostic genes for each patient in GSE72094. **(I)** Time-related ROC analysis proved the prognostic performance of the risk score in the GSE72094. **(J)** Kaplan-Meier survival curve of the patients in the high-risk and low-risk groups for OS in the GSE72094.

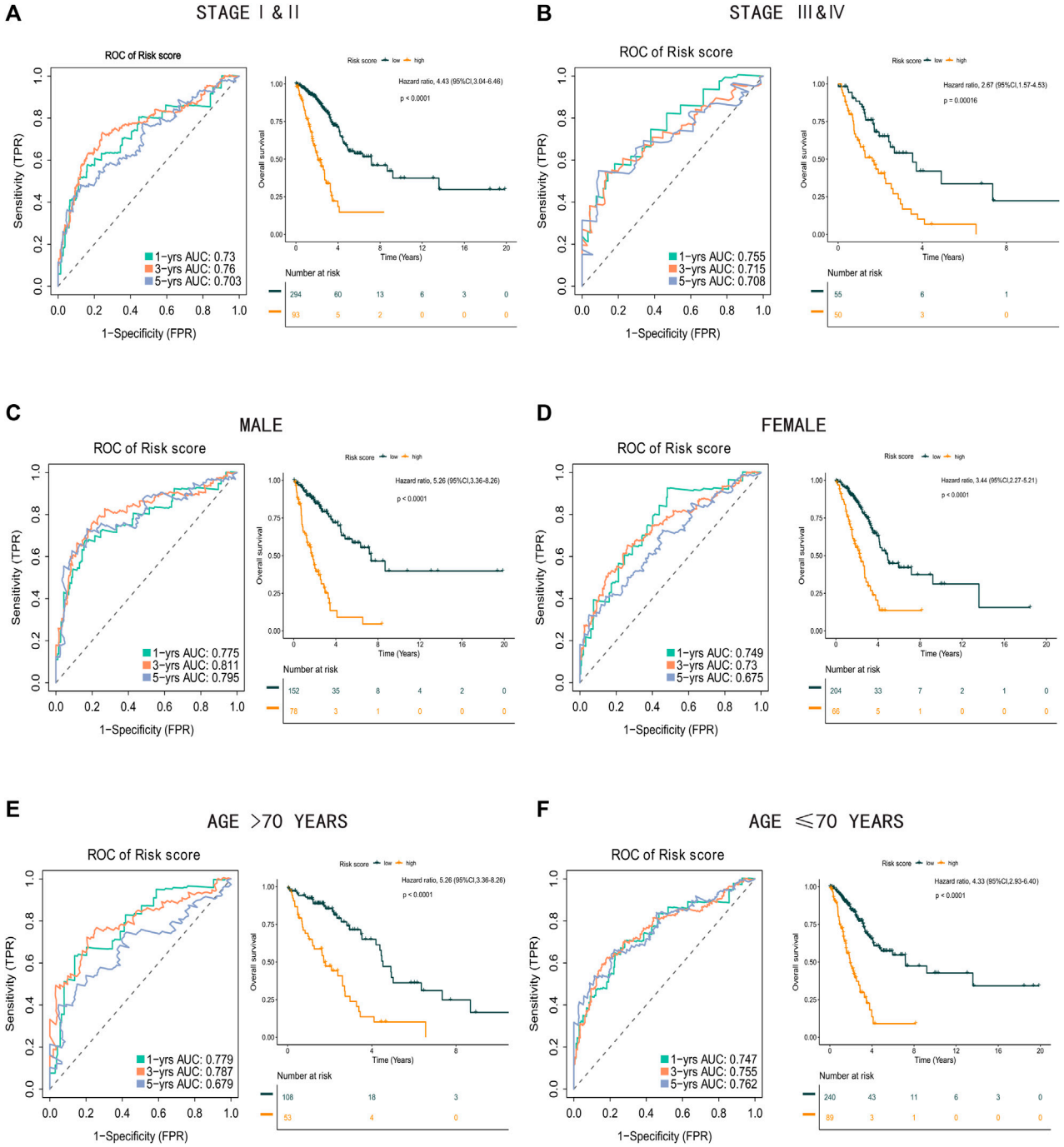

FIGURE 8 | Clinical subgroups analysis between high risk score group and low risk score group. **(A)** Time-related ROC analysis and Kaplan-Meier survival curve of the patients in stage I and stage II. **(B)** Time-related ROC analysis and Kaplan-Meier survival curve of the patients in stage III and stage IV. **(C)** Time-related ROC analysis and Kaplan-Meier survival curve of the male patients. **(D)** Time-related ROC analysis and Kaplan-Meier survival curve of the female patients. **(E)** Time-related ROC analysis and Kaplan-Meier survival curve of the patients more than 70 years old. **(F)** Time-related ROC analysis and Kaplan-Meier survival curve of the patients less than or equal to 70 years old.

LUAD drugs such as cisplatin, docetaxel, paclitaxel and gemcitabine (**Figure 13**). These results show that the risk score can be used as a potential predictor of chemosensitivity and that immunotherapy may be more appropriate for low-risk patients, while chemotherapy may be more appropriate for high-risk patients.

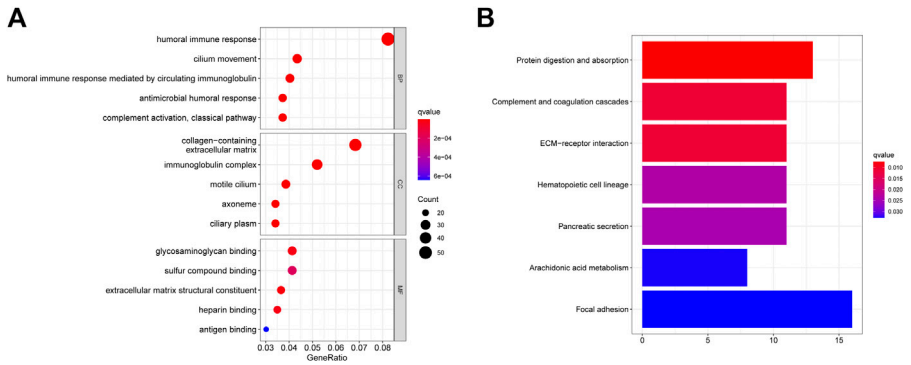

FIGURE 9 | GO and KEGG enrichment analysis between high risk score group and low risk score group. **(A)** GO enrichment between the high-risk patients and low-risk patients in TCGA cohort. **(B)** KEGG pathways between the high-risk patients and low-risk patients in TCGA cohort.

4 DISCUSSION

The current era of precision medicine highlights an urgent need to establish a more precise method for evaluating prognosis and guiding treatment in patients with LUAD. Hypoxia, the immune microenvironment, and EMT play crucial roles in tumorigenesis, progression, and drug resistance in LUAD (Isomura et al., 2021; Wu et al., 2021; Yoshida et al., 2021).

Numerous studies have identified the existence of a hypoxic area as one of the key characteristics of cancer growth (Shen et al., 2015). Indeed, hypoxia promotes cancer metastasis and reduces the survival rate in patients with cancer (Nobre et al., 2018), and the expression of hypoxia genes has been shown to increase metabolism in lung adenocarcinoma cells (Smolle et al., 2020). At the same time, the hypoxic microenvironment of the tumor suppresses the ability of immune cells to detect and kill tumor cells (Vito et al., 2020). Additional studies have reported that the hypoxic microenvironment influences the effect of tumor chemotherapy and immune checkpoint inhibitors, which explain the increasing mortality rate among patients with LUAD (Ando et al., 2019; Daniel et al., 2019; Gao et al., 2019). Hypoxia can also contribute to EMT in patients with LUAD (Ando et al., 2019). Moreover, the immune system plays a vital role in the development and progression of malignant tumors (Lin et al., 2021). Immunotherapy is a novel treatment for LUAD that has achieved multiple satisfactory results (Li et al., 2020). EMT has also been shown to play a critical role in tumor development from initiation to metastasis (Taki et al., 2021). After EMT, LUAD cells can produce more extracellular matrix, which can hasten tumor metastasis, aggravate immune evasion, and induce drug resistance (Pastushenko and Cédric, 2019; Cui et al., 2020; Taki et al., 2021). Based on these findings, the present study combined hypoxia-, immunity-, and EMT-related gene signatures to construct a prognostic model for LUAD risk. To our best knowledge, this is the first study to combine these gene signatures to predict prognosis in patients with LUAD.

Using the LASSO Cox algorithm, 200 hypoxia-related genes, 2,498 immune-related genes, and 200 EMT-related genes were used to identify the most robust biomarkers and establish a novel risk score. In total, 27 related genes were included in the risk formula for LUAD prognosis. Using this formula, we classified patients with LUAD into the high- and low-risk groups. The formula had AUCs of 0.763, 0.766, and 0.728 for predicting 1-, 3-, and 5-year OS, respectively, indicating that it has high accuracy and reliability. Further, OS was significantly lower in the high-risk group than in the low-risk group, and the risk score exhibited high predictive capability in the GSE68465 and GSE72094 validation sets.

Subsequent subgroup analysis by sex, age, and stage indicated that the formula exhibited good predictive capability across all categories. Prognosis was accurately predicted in male and female patients and in patients aged >70 years or <70 years. Importantly, patients in the high-risk group also had significantly lower OS than patients in the low-risk group, regardless of disease stage, indicating the need for a gene-based classification for clinical use. Functional analysis between each group revealed strong associations between a high risk score and genes related to the humoral immune response, collagen-containing extracellular matrix, and focal adhesion. All of these are highly correlated with the anti-tumor response, tumor metastasis, drug resistance, and tumor progression (Murphy et al., 2012; Lovitt et al., 2018; Kosibaty et al., 2021).

Stemness-related biomarkers in tumor cells are highly correlated with drug resistance, cancer recurrence, and tumor proliferation (Liu et al., 2021). In this study, stemness-related biomarkers were positively associated with the risk score, demonstrating the prognostic value of the formula. Modification of m^6A, m^5C, m^1A, and m^7G are the common type of modification in RNA and plays critical roles in cancer development (Teng et al., 2021; Xu F. et al., 2021; Xu R. et al., 2021). And RNA methylation highly interconnected with hypoxia, immune response and EMT(Lin et al., 2019; Chao et al., 2020; Wang E. et al., 2021). In previous study, researcher identified hypoxia can induced the sumolytion of m^6A enzyme(Hou et al., 2021), hypoxia-inducible factor-1 alpha (HIF-1α) can drive m^5C modification to promote tumorigenesis(Wang J. Z. et al., 2021), m^1A and m^6A modification can significantly affect the infiltration of immune

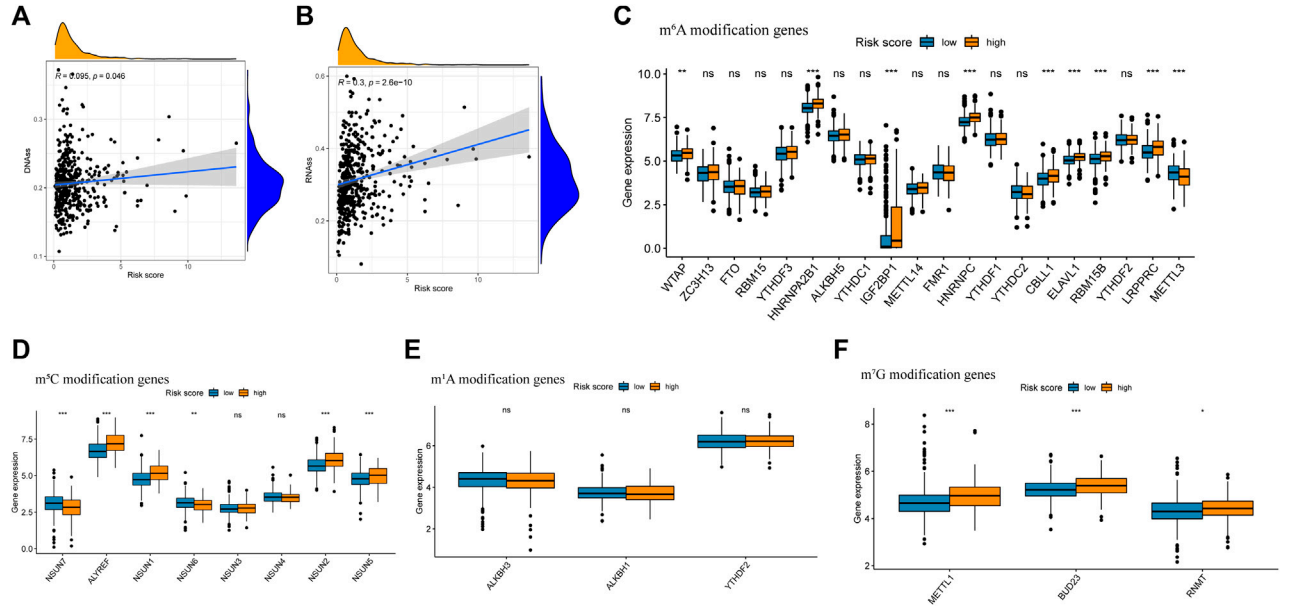

FIGURE 10 | Analysis of risk score with tumor stem cell score and Differential expression of m^{6}A related gene between high risk score group and low risk score group. **(A)** The relationship between risk score and RNAss. **(B)** The relationship between risk score and DNAss. **(C)** Differential expression analysis of m^{6}A related gene between high risk score group and low risk score group. **(D)** Differential expression analysis of m^{5}C related gene between high risk score group and low risk score group. **(E)** Differential expression analysis of m^{1}A related gene between high risk score group and low risk score group. **(F)** Differential expression analysis of m^{7}G related gene between high risk score group and low risk score group.

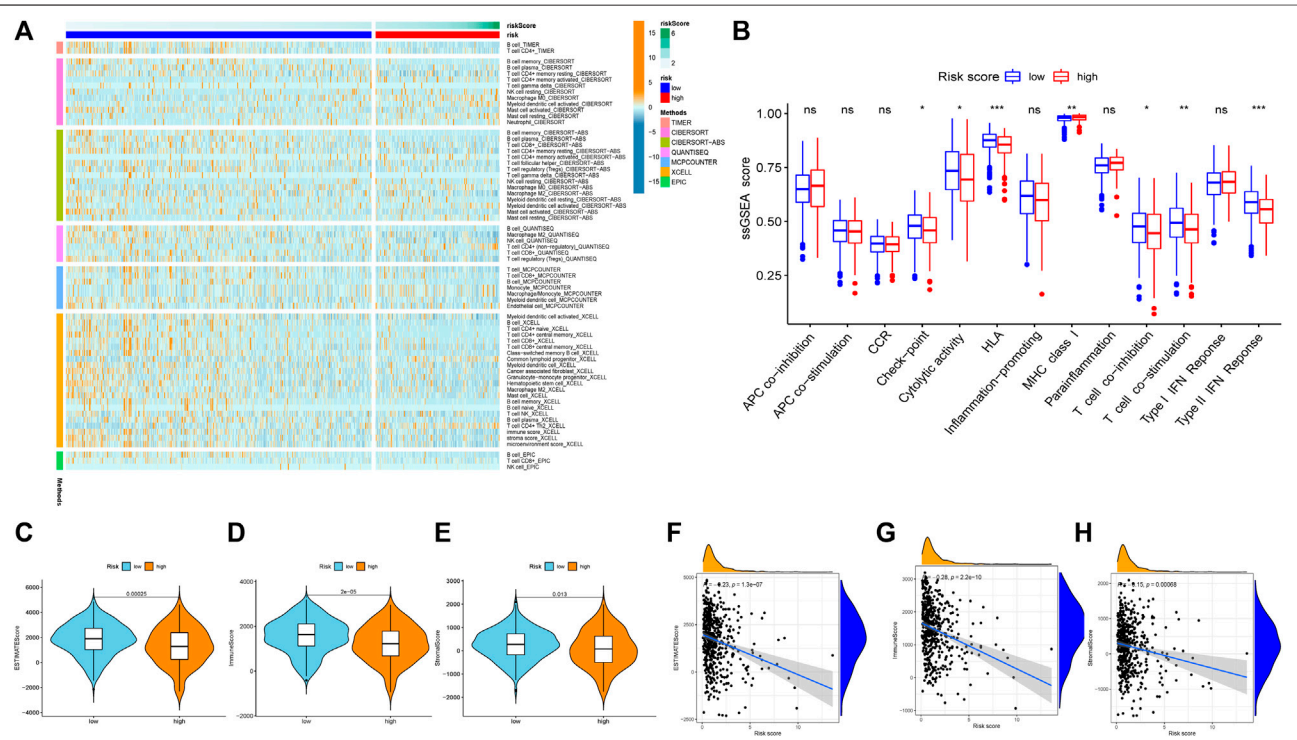

FIGURE 11 | Exploration of tumor immune microenvironment between high risk score group and low risk score group. **(A)** Heatmap for immune responses based on CIBERSORT, TIMER, CIBERSORT-ABS, QUANTISEQ, MCPCOUNTER, XCELL, EPIC algorithms among high risk score group and low risk score group. **(B)** ssGSEA for the association between immune cell subpopulations and related functions. **(C)** ESTIMATE score. **(D)** Immune score. **(E)** Stromal score. **(F)** The relationship between risk score and the ESTIMATE score. **(G)** The relationship between risk score and the Immune score. (H)The relationship between risk score and the Stromal score. *p < 0.05; **p < 0.01; ***p < 0.001, ns, not significant.

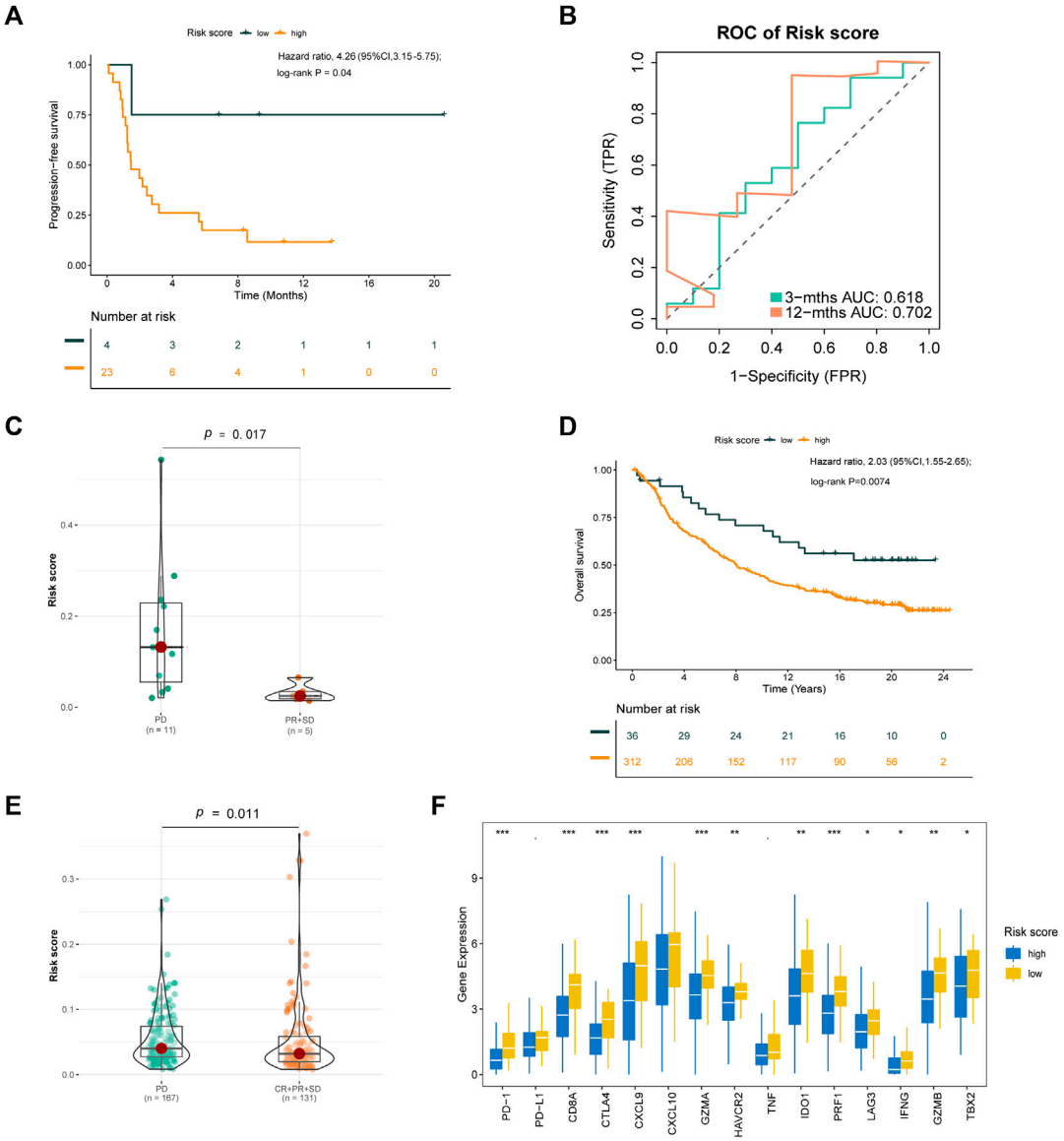

FIGURE 12 | Validation of the risk score formula for immunotherapy. **(A)** Kaplan-Meier survival curve of GSE135222 cohort for PFS. **(B)** Time-related ROC analysis proved the prognostic performance of the risk score in the GSE135222. **(C)** The difference of risk score in the subgroup of PD-1 treatment response in GSE126044. **(D)** Kaplan-Meier survival curve of IMvigor210 cohort for OS. **(E)** The difference of Risk score in the subgroup of PD-L1 treatment response. **(F)** The expression of immue-related checkpoints among high and low risk groups in IMvigor210 cohort. $^{*}p < 0.1$; $^{*}p < 0.05$; $^{**}p < 0.01$; $^{***}p < 0.001$.

cells(Cai et al., 2021; Gao et al., 2021), m^7G modification can drives immune evasion (Devarkar et al., 2016), and m^6A, m^7G modification can induce EMT in cancer development (Yu X. et al., 2020; Xia et al., 2021). Hence we investigate the correlation of RNA methylation with this risk score. In this study, the expression of WTAP, HNRNPA2B1, IGF2BP2, HNRNPC, CBLL1, ELAVL1, RBM15B, LRPPRC, ELAVL1, ALYREF, NSUN1, NSUN2, METTL1, BUD23, RNMT, METTL3, NSUN7 and NSUN6 differed significantly between the high-risk and low-risk groups. These results further support the value of our risk score formula.

Immune cells in the TME are associated with the development of cancer (Bruni et al., 2020). Our risk formula was highly correlated with markers of the immune microenvironment. Previous studies have reported that the characteristics of the immune microenvironment can predict sensitivity to immune checkpoint inhibitor treatment in patients with LUAD (Yu et al., 2020b; Park et al., 2020). In this study, patients in the low-risk group had higher immune activity. To validate the prognostic value of the risk score for immunotherapy sensitivity, we used two external datasets (GSE135222, GSE126044) containing information from patients with NSCLC treated with anti-PD-

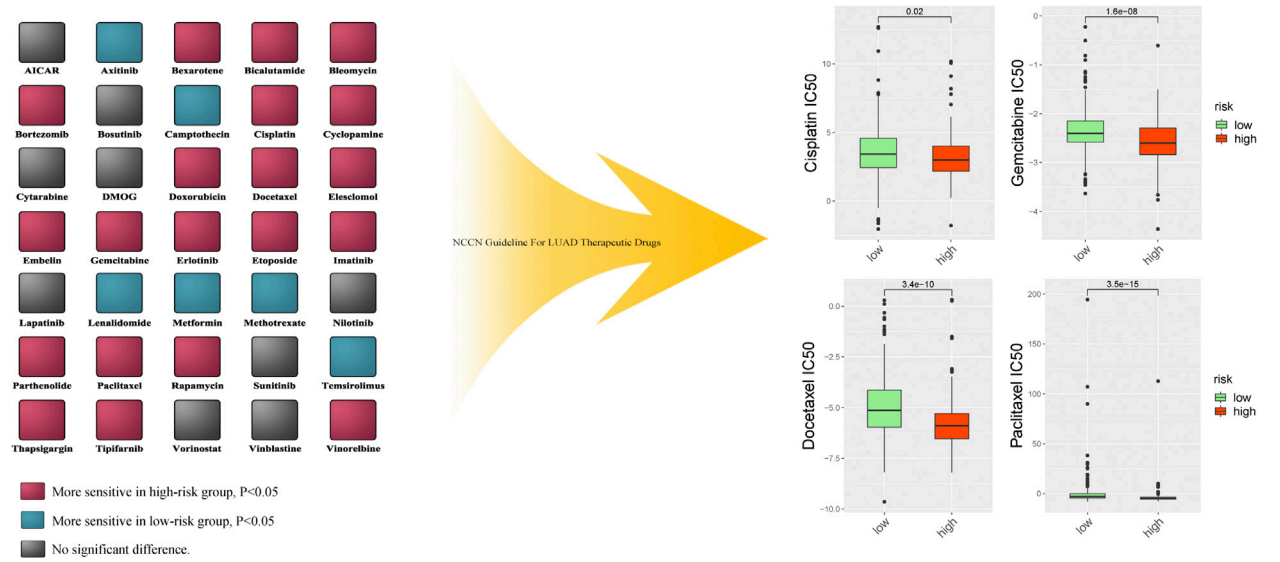

FIGURE 13 | The difference of multiple anti-cancer drugs sensitivity between high risk score group and low risk score group.

1/PD-L1 therapy. Our findings indicated that the risk score formula was associated with PFS and treatment responses in patients with NSCLC undergoing anti-PD-1/PD-L1 therapy. The IMvigor210 study examined the effect of PD-L1 inhibitor treatment in patients with metastatic urothelial cancer (Mariathasan et al., 2018; Wang S. et al., 2021). Because relatively few patients were enrolled in the GSE135222 and GSE126044 cohorts, we further evaluated the formula in the IMvigor210 cohort. Our results suggest that the risk score formula is not only suitable for predicting the effect of anti-PD-1/PD-L1 treatment in lung cancer, but that it may also be applicable in patients with other cancer types. Hence, a low-risk score may be an indicator for immunotherapy.

Previously, Sun et al. (2020) reported that the hypoxia-related signature could aid in predicting OS in patients with early-stage LUAD. However, whether hypoxia-related gene signatures can be used to develop a simple predictive formula for late-stage LUAD outcomes or immunotherapy sensitivity remains unknown. Other studies have also attempted to use immune- or EMT-related gene signatures to establish a prognostic model for LUAD (Tang et al., 2020; Wang et al., 2020). However, few of these studies used an authentic immune therapy cohort for validation. Given that multiple factors can have a substantial effect on the prognosis of LUAD and the intimate interconnections among hypoxia, immune responses, and EMT function, we aimed to establish a novel prognostic model based on the integration of multiple gene signatures. Our analysis indicated that the prognostic formula developed in this study exhibits precision for both early- and late-stage LUAD and is valid for predicting sensitivity to immunotherapy based on findings from a clinical cohort.

Currently, there are only a few methods for evaluating tumor sensitivity to chemotherapy (Rochigneux et al., 2020). In this study, the risk score was positively associated with drug sensitivity to cisplatin, docetaxel, paclitaxel and gemcitabine. This indicates that the risk score can be used to determine the appropriateness and benefit of chemotherapy in patients with LUAD, which may aid in the development of individualized treatment strategies.

This study also had some limitations. As the study was based on information within public databases, real-world prospective cohort studies are required to validate the risk score formula. The sequencing methods of the cohort included in this study were different, this may also affect the accuracy of this formula. Furthermore, most patients were Caucasian, highlighting the need to evaluate the predictive ability of the risk score in patients of other races.

5 CONCLUSION

In summary, this study established a novel 27-gene prognostic risk score for LUAD. The risk score was independently associated with OS in patients with LUAD and with functional analysis, tumor stemness, RNA methylation analysis, the immune microenvironment, and treatment response. Further, it accurately predicted prognosis in subgroups according to age, sex, and disease stage. These findings indicate that molecular risk stratification may be useful for predicting prognosis and guiding treatment in patients with LUAD.

DATA AVAILABILITY STATEMENT

The datasets presented in this study can be found in online repositories. The names of the repository/repositories and accession number(s) can be found in the article/ **Supplementary Material**.

ETHICS STATEMENT

The studies involving human participants were reviewed and approved the by Ethics and Research Committees of Sun Yat-Sen Memorial Hospital. Written informed consent for participation was not required for this study in accordance with the national legislation and the institutional requirements.

AUTHOR CONTRIBUTIONS

All authors contributed to study conception and design. WO, YJ, and YY analyzed and interpreted the data and performed the statistical analysis; WO, YJ, YY, and HY drafted and revised the manuscript. All authors provided administrative, technical, and material support. YY, HY, and XL supervised the study. All authors reviewed the manuscript and approved the final version of the manuscript.

FUNDING

This study was supported by grants 2017A030313822 and 2017A030313828 from the Natural Science Foundation of Guangdong Province, grant 2020ZX09201021 from the National Science and Technology Major Project, grant YXRGZN201902 from the Medical Artificial Intelligence Project of Sun Yat-Sen Memorial Hospital; Grant No. 2021M703771 from China Postdoctoral Science Foundation Funded Project; Grants 81572596, 81972471, and 82073408 from the National Natural Science Foundation of China, grant 201704020131 from the Guangzhou Science and Technology Major Program, grant 2017B030314026 from the Guangdong Science and Technology Department, grant 2018007 from the Sun Yat-Sen University Clinical Research 5010 Program, grant SYS-C-201801 from the Sun Yat-Sen Clinical Research Cultivating Program, grant A2020558 from the Guangdong Medical Science and Technology Program, grant SYSU-81000-20200311-0001 and SYSU-05160-20200506-0001 from Tencent Charity Foundation.

SUPPLEMENTARY MATERIAL

The Supplementary Material for this article can be found online at: https://www.frontiersin.org/articles/10.3389/fcell.2021.758777/full#supplementary-material

REFERENCES

Ando, A., Hashimoto, N., Sakamoto, K., Omote, N., Miyazaki, S., Nakahara, Y., et al. (2019). Repressive Role of Stabilized Hypoxia Inducible Factor 1α Expression on Transforming Growth Factor β-induced Extracellular Matrix Production in Lung Cancer Cells. *Cancer Sci.* 110 (6), 1959–1973. doi:10.1111/cas.14027

Barbieri, I., and Kouzarides, T. (2020). Role of RNA Modifications in Cancer. *Nat. Rev. Cancer* 20 (6), 303–322. doi:10.1038/s41568-020-0253-2

Bi, K.-W., Wei, X.-G., Qin, X.-X., and Li, B. (2020). BTK Has Potential to Be a Prognostic Factor for Lung Adenocarcinoma and an Indicator for Tumor Microenvironment Remodeling: A Study Based on TCGA Data Mining. *Front. Oncol.* 10, 424. doi:10.3389/fonc.2020.00424

Bruni, D., Angell, H. K., and Galon, J. (2020). The Immune Contexture and Immunoscore in Cancer Prognosis and Therapeutic Efficacy. *Nat. Rev. Cancer* 20 (11), 662–680. doi:10.1038/s41568-020-0285-7

Cai, C., Long, J., Huang, Q., Han, Y., Peng, Y., Guo, C., et al. (2021). M6A "Writer" Gene METTL14: A Favorable Prognostic Biomarker and Correlated with Immune Infiltrates in Rectal Cancer. *Front. Oncol.* 11, 615296. doi:10.3389/fonc.2021.615296

Chao, Y., Shang, J., and Ji, W. (2020). ALKBH5-m6A-FOXM1 Signaling axis Promotes Proliferation and Invasion of Lung Adenocarcinoma Cells under Intermittent Hypoxia. *Biochem. Biophysical Res. Commun.* 521 (2), 499–506. doi:10.1016/j.bbrc.2019.10.145

Charoentong, P., Finotello, F., Angelova, M., Mayer, C., Efremova, M., Rieder, D., et al. (2017). Pan-cancer Immunogenomic Analyses Reveal Genotype-Immunophenotype Relationships and Predictors of Response to Checkpoint Blockade. *Cell Rep* 18 (1), 248–262. doi:10.1016/j.celrep.2016.12.019

Cho, J.-W., Hong, M. H., Ha, S.-J., Kim, Y.-J., Cho, B. C., Lee, I., et al. (2020). Genome-wide Identification of Differentially Methylated Promoters and Enhancers Associated with Response to Anti-PD-1 Therapy in Non-small Cell Lung Cancer. *Exp. Mol. Med.* 52 (9), 1550–1563. doi:10.1038/s12276-020-00493-8

Cui, J., Song, Y., Han, X., Hu, J., Chen, Y., Chen, X., et al. (2020). Targeting 14-3-3ζ Overcomes Resistance to Epidermal Growth Factor Receptor-Tyrosine Kinase Inhibitors in Lung Adenocarcinoma via BMP2/Smad/ID1 Signaling. *Front. Oncol.* 10, 542007. doi:10.3389/fonc.2020.542007

Daniel, S. K., Sullivan, K. M., Labadie, K. P., and Pillarisetty, V. G. (2019). Hypoxia as a Barrier to Immunotherapy in Pancreatic Adenocarcinoma. *Clin. Transl Med.* 8 (1), 10. doi:10.1186/s40169-019-0226-9

Devarkar, S. C., Wang, C., Miller, M. T., Ramanathan, A., Jiang, F., Khan, A. G., et al. (2016). Structural Basis for m7G Recognition and 2′-O-Methyl Discrimination in Capped RNAs by the Innate Immune Receptor RIG-I. *Proc. Natl. Acad. Sci. USA* 113 (3), 596–601. doi:10.1073/pnas.1515152113

Dib, L., San-Jose, L., Ducrest, A.-L., Salamin, N., and Roulin, A. (2017). Selection on the Major Color Gene Melanocortin-1-Receptor Shaped the Evolution of the Melanocortin System Genes. *Ijms* 18, 2618. doi:10.3390/ijms18122618

Gao, X. Z., Wang, G. N., Zhao, W. G., Han, J., Diao, C. Y., Wang, X. H., et al. (2019). Blocking OLFM4/HIF-1α axis Alleviates Hypoxia-induced Invasion, Epithelial-Mesenchymal Transition, and Chemotherapy Resistance in Non-small-cell Lung Cancer. *J. Cel Physiol* 234, 15035–15043. doi:10.1002/jcp.28144

Gao, Y., Wang, H., Li, H., Ye, X., Xia, Y., Yuan, S., et al. (2021). Integrated Analyses of m1A Regulator-Mediated Modification Patterns in Tumor Microenvironment-Infiltrating Immune Cells in colon Cancer. *Oncoimmunology* 10 (1), 1936758. doi:10.1080/2162402x.2021.1936758

Hou, G., Zhao, X., Li, L., Yang, Q., Liu, X., Huang, C., et al. (2021). SUMOylation of YTHDF2 Promotes mRNA Degradation and Cancer Progression by Increasing its Binding Affinity with m6A-Modified mRNAs. *Nucleic Acids Res.* 49 (5), 2859–2877. doi:10.1093/nar/gkab065

Hyuna, S., Jacques., F., Siegel, R. L., Mathieu., L., Isabelle, S., Jemal, A., et al. (2021). Global Cancer Statistics 2020: GLOBOCAN Estimates of Incidence and Mortality Worldwide for 36 Cancers in 185 Countries. *CA Cancer J. Clin.* 71 (3), 209–249. doi:10.3322/caac.21660

Isomura, H., Taguchi, A., Kajino, T., Asai, N., Nakatochi, M., Kato, S., et al. (2021). Conditional Ror1 Knockout Reveals Crucial Involvement in Lung Adenocarcinoma Development and Identifies Novel HIF-1α Regulator. *Cancer Sci.* 112 (4), 1614–1623. doi:10.1111/cas.14825

Jiang, J., Tang, Y.-l., and Liang, X.-h. (2011). EMT: a New Vision of Hypoxia Promoting Cancer Progression. *Cancer Biol. Ther.* 11 (8), 714–723. doi:10.4161/cbt.11.8.15274

Jung, H., Kim, H. S., Kim, J. Y., Sun, J.-M., Ahn, J. S., Ahn, M.-J., et al. (2019). DNA Methylation Loss Promotes Immune Evasion of Tumours with High Mutation and Copy Number Load. *Nat. Commun.* 10 (1), 4278. doi:10.1038/s41467-019-12159-9

Kosibaty, Z., Murata, Y., Minami, Y., Noguchi, M., and Sakamoto, N. (2021). ECT2 Promotes Lung Adenocarcinoma Progression through Extracellular Matrix Dynamics and Focal Adhesion Signaling. *Cancer Sci.* 112 (2), 703–714. doi:10.1111/cas.14743

Labiano, S., Palazon, A., and Melero, I. (2015). Immune Response Regulation in the Tumor Microenvironment by Hypoxia. *Semin. Oncol.* 42 (3), 378–386. doi:10.1053/j.seminoncol.2015.02.009

Li, F., Huang, Q., Luster, T. A., Hu, H., Zhang, H., Ng, W.-L., et al. (2020). *In Vivo* Epigenetic CRISPR Screen Identifies Asf1a as an Immunotherapeutic Target in Kras-Mutant Lung Adenocarcinoma. *Cancer Discov.* 10 (2), 270–287. doi:10.1158/2159-8290.cd-19-0780

Lin, J., Wu, C., Ma, D., and Hu, Q. (2021). Identification of P2RY13 as an Immune-Related Prognostic Biomarker in Lung Adenocarcinoma: A Public Database-Based Retrospective Study. *PeerJ* 9, e11319. doi:10.7717/peerj.11319

Lin, X., Chai, G., Wu, Y., Li, J., Chen, F., Liu, J., et al. (2019). RNA m6A Methylation Regulates the Epithelial Mesenchymal Transition of Cancer Cells and Translation of Snail. *Nat. Commun.* 10 (1), 2065. doi:10.1038/s41467-019-09865-9

Liu, X., He, M., Li, L., Wang, X., Han, S., Zhao, J., et al. (2021). EMT and Cancer Cell Stemness Associated with Chemotherapeutic Resistance in Esophageal Cancer. *Front. Oncol.* 11, 672222. doi:10.3389/fonc.2021.672222

Lovitt, C. J., Shelper, T. B., and Avery, V. M. (2018). Doxorubicin Resistance in Breast Cancer Cells Is Mediated by Extracellular Matrix Proteins. *BMC Cancer* 18 (1), 41. doi:10.1186/s12885-017-3953-6

Luo, Q., and Vögeli, T.-A. (2020). A Methylation-Based Reclassification of Bladder Cancer Based on Immune Cell Genes. *Cancers* 12, 3054. doi:10.3390/cancers12103054

Mariathasan, S., Turley, S. J., Nickles, D., Castiglioni, A., Yuen, K., Wang, Y., et al. (2018). TGFβ Attenuates Tumour Response to PD-L1 Blockade by Contributing to Exclusion of T Cells. *Nature* 554 (7693), 544–548. doi:10.1038/nature25501

Murphy, M. A., O'Leary, J. J., and Cahill, D. J. (2012). Assessment of the Humoral Immune Response to Cancer. *J. Proteomics* 75 (15), 4573–4579. doi:10.1016/j.jprot.2012.01.021

Nobre, A. R., Entenberg, D., Wang, Y., Condeelis, J., and Aguirre-Ghiso, J. A. (2018). The Different Routes to Metastasis via Hypoxia-Regulated Programs. *Trends Cel Biol.* 28 (11), 941–956. doi:10.1016/j.tcb.2018.06.008

Park, C., Na, K. J., Choi, H., Ock, C.-Y., Ha, S., Kim, M., et al. (2020). Tumor Immune Profiles Noninvasively Estimated by FDG PET with Deep Learning Correlate with Immunotherapy Response in Lung Adenocarcinoma. *Theranostics* 10 (23), 10838–10848. doi:10.7150/thno.50283

Pastushenko, I., and Blanpain, C. (2019). EMT Transition States during Tumor Progression and Metastasis. *Trends Cel Biol.* 29 (3), 212–226. doi:10.1016/j.tcb.2018.12.001

Rochigneux, P., Garcia, A. J., Chanez, B., Madroszyk, A., Olive, D., and Garon, E. B. (2020). Medical Treatment of Lung Cancer: Can Immune Cells Predict the Response? A Systematic Review. *Front. Immunol.* 11, 1036. doi:10.3389/fimmu.2020.01036

Schabath, M. B., Welsh, E. A., Fulp, W. J., Chen, L., Teer, J. K., Thompson, Z. J., et al. (2016). Differential Association of STK11 and TP53 with KRAS Mutation-Associated Gene Expression, Proliferation and Immune Surveillance in Lung Adenocarcinoma. *Oncogene* 35 (24), 3209–3216. doi:10.1038/onc.2015.375

Shen, H., Feng, G., Cui, J., Du, Q., Qin, Y., Cai, J., et al. (2015). Clinical Implications of Serum Hypoxia Inducible Factor-1α and Vascular Endothelial Growth Factor in Lung Cancer. *Tumori* 101 (4), 404–411. doi:10.5301/tj.5000320

Siegel, R. L., Miller, K. D., Fuchs, H. E., and Jemal, A. (2021). Cancer Statistics, 2021. *CA A. Cancer J. Clin.* 71 (1), 7–33. doi:10.3322/caac.21654

Smolle, E., Leko, P., Stacher-Priehse, E., Brcic, L., El-Heliebi, A., Hofmann, L., et al. (2020). Distribution and Prognostic Significance of Gluconeogenesis and Glycolysis in Lung Cancer. *Mol. Oncol.* 14 (11), 2853–2867. doi:10.1002/1878-0261.12780

Sun, J., Zhao, T., Zhao, D., Qi, X., Bao, X., Shi, R., et al. (2020). Development and Validation of a Hypoxia-Related Gene Signature to Predict Overall Survival in Early-Stage Lung Adenocarcinoma Patients. *Ther. Adv. Med. Oncol.* 12, 1758835920937904. doi:10.1177/1758835920937904

Taki, M., Abiko, K., Ukita, M., Murakami, R., Yamanoi, K., Yamaguchi, K., et al. (2021). Tumor Immune Microenvironment during Epithelial-Mesenchymal Transition. *Clin. Cancer Res.* 27, 4669–4679. doi:10.1158/1078-0432.CCR-20-4459

Tang, Y., Jiang, Y., Qing, C., Wang, J., and Zeng, Z. (2020). Systematic Construction and Validation of an Epithelial-Mesenchymal Transition Risk Model to Predict Prognosis of Lung Adenocarcinoma. *Aging* 13 (1), 794–812. doi:10.18632/aging.202186

Teng, P. C., Liang, Y., Yarmishyn Aliaksandr, A., Hsiao, Y. J., Lin, T. Y., Lin, T. W., et al. (2021). RNA Modifications and Epigenetics in Modulation of Lung Cancer and Pulmonary Diseases. *Int. J. Mol. Sci.* 22, 10592. doi:10.3390/ijms221910592

Vito, A., El-Sayes, N., and Mossman, K. (2020). Hypoxia-Driven Immune Escape in the Tumor Microenvironment. *Cells* 9, 992. doi:10.3390/cells9040992

Wang, D. D., Shaver, L. G., Shi, F. Y., Wei, J. J., Qin, T. Z., Wang, S. Z., et al. (2021). Comparative Efficacy and Safety of PD-1/pd-L1 Immunotherapies for Non-small Cell Lung Cancer: a Network Meta-Analysis. *Eur. Rev. Med. Pharmacol. Sci.* 25 (7), 2866–2884. doi:10.26355/eurrev_202104_25541

Wang, E., Li, Y., Ming, R., Wei, J., Du, P., Zhou, P., et al. (2021). The Prognostic Value and Immune Landscapes of a m6A/m5C/m1A-Related LncRNAs Signature in Head and Neck Squamous Cell Carcinoma. *Front. Cel Dev. Biol.* 9, 718974. doi:10.3389/fcell.2021.718974

Wang, J. Z., Zhu, W., Han, J., Yang, X., Zhou, R., Lu, H. C., et al. (2021). The Role of the HIF-1α/ALYREF/PKM2 axis in Glycolysis and Tumorigenesis of Bladder Cancer. *Cancer Commun.* 41 (7), 560–575. doi:10.1002/cac2.12158

Wang, Q., Li, M., Yang, M., Yang, Y., Song, F., Zhang, W., et al. (2020). Analysis of Immune-Related Signatures of Lung Adenocarcinoma Identified Two Distinct Subtypes: Implications for Immune Checkpoint Blockade Therapy. *Aging* 12 (4), 3312–3339. doi:10.18632/aging.102814

Wang, S., Ma, H., Li, H., Liu, Q., Huang, S., Huang, L., et al. (2021). Alternatively Expressed Transcripts Analysis of Non-small Cell Lung Cancer Cells under Different Hypoxic Microenvironment. *J. Oncol.* 2021, 5558304. doi:10.1155/2021/5558304

Wu, J., Li, L., Zhang, H., Zhao, Y., Zhang, H., Wu, S., et al. (2021). A Risk Model Developed Based on Tumor Microenvironment Predicts Overall Survival and Associates with Tumor Immunity of Patients with Lung Adenocarcinoma. *Oncogene* 40, 4413–4424. doi:10.1038/s41388-021-01853-y

Xia, P., Zhang, H., Xu, K., Jiang, X., Gao, M., Wang, G., et al. (2021). MYC-targeted WDR4 Promotes Proliferation, Metastasis, and Sorafenib Resistance by Inducing CCNB1 Translation in Hepatocellular Carcinoma. *Cell Death Dis* 12 (7), 691. doi:10.1038/s41419-021-03973-5

Xu, F., Huang, X., Li, Y., Chen, Y., and Lin, L. (2021). m6A-related lncRNAs Are Potential Biomarkers for Predicting Prognoses and Immune Responses in Patients with LUAD. *Mol. Ther. - Nucleic Acids* 24, 780–791. doi:10.1016/j.omtn.2021.04.003

Xu, R., Pang, G., Zhao, Q., Yang, L., Chen, S., Jiang, L., et al. (2021). The Momentous Role of N6-methyladenosine in Lung Cancer. *J. Cel Physiol* 236 (5), 3244–3256. doi:10.1002/jcp.30136

Yoshida, C., Kadota, K., Ikeda, T., Ibuki, E., Go, T., Haba, R., et al. (2021). Tumor-associated Macrophage Infiltration Is Associated with a Higher Rate of Tumor Spread through Air Spaces in Resected Lung Adenocarcinomas. *Lung Cancer* 158, 91–96. doi:10.1016/j.lungcan.2021.06.009

Yu, X., Zhao, H., and Cao, Z. (2020). The m6A Methyltransferase METTL3 Aggravates the Progression of Nasopharyngeal Carcinoma through Inducing EMT by m6A-Modified Snail mRNA. *Minerva Med.* doi:10.23736/S0026-4806.20.06653-7

Yu, Y., Lin, D., Li, A., Chen, Y., Ou, Q., Hu, H., et al. (2020a). Association of Immune Checkpoint Inhibitor Therapy with Survival in Patients with Cancers with MUC16 Variants. *JAMA Netw. Open* 3 (6), e205837. doi:10.1001/jamanetworkopen.2020.5837

Yu, Y., Zeng, D., Ou, Q., Liu, S., Li, A., Chen, Y., et al. (2019). Association of Survival and Immune-Related Biomarkers with Immunotherapy in Patients with Non-small Cell Lung Cancer. *JAMA Netw. Open* 2 (7), e196879. doi:10.1001/jamanetworkopen.2019.6879

Yu, Y., Zhang, W., Li, A., Chen, Y., Ou, Q., He, Z., et al. (2020b). Association of Long Noncoding RNA Biomarkers with Clinical Immune Subtype and Prediction of Immunotherapy Response in Patients with Cancer. *JAMA Netw. Open* 3 (4), e202149. doi:10.1001/jamanetworkopen.2020.2149

Zeng, F., Zhang, Y., Han, X., Zeng, M., Gao, Y., and Weng, J. (2021). Employing Hypoxia Characterization to Predict Tumour Immune Microenvironment,

Treatment Sensitivity and Prognosis in Hepatocellular Carcinoma. *Comput. Struct. Biotechnol. J.* 19, 2775–2789. doi:10.1016/j.csbj.2021.03.033

Zhang, A., Yang, J., Ma, C., Li, F., and Luo, H. (2021). Development and Validation of a Robust Ferroptosis-Related Prognostic Signature in Lung Adenocarcinoma. *Front. Cel Dev. Biol.* 9, 616271. doi:10.3389/fcell.2021.616271

Zhang, Y., Bian, Y., Wang, Y., Wang, Y., Duan, X., Han, Y., et al. (2021). HIF-1α Is Necessary for Activation and Tumour-promotion Effect of Cancer-associated Fibroblasts in Lung Cancer. *J. Cel Mol Med* 25, 5457–5469. doi:10.1111/jcmm.16556

Conflict of Interest: The authors declare that the research was conducted in the absence of any commercial or financial relationships that could be construed as a potential conflict of interest.

Publisher's Note: All claims expressed in this article are solely those of the authors and do not necessarily represent those of their affiliated organizations, or those of the publisher, the editors and the reviewers. Any product that may be evaluated in this article, or claim that may be made by its manufacturer, is not guaranteed or endorsed by the publisher.

frontiers in Cell and Developmental Biology

REVIEW
published: 10 February 2022
doi: 10.3389/fcell.2022.788587

The Roles of EphB2 in Cancer

Wei Liu[1,2], *Chengpeng Yu*[3], *Jianfeng Li*[3] *and Jiwei Fang*[1]*

[1]Department of Geriatrics, The First Affiliated Hospital of Nanchang University, Nanchang, China, [2]Second Clinical Medical College, Nanchang University, Nanchang, China, [3]Department of General Surgery, The First Affiliated Hospital of Nanchang University, Nanchang, China

The erythropoietin-producing hepatocellular carcinoma (Eph) receptors and their Eph receptor-interacting (ephrin) ligands together constitute a vital cell communication system with diverse roles. Experimental evidence revealed Eph receptor bidirectional signaling with both tumor-promoting and tumor-suppressing activities in different cancer types and surrounding environment. Eph receptor B2 (EphB2), an important member of the Eph receptor family, has been proved to be aberrantly expressed in many cancer types, such as colorectal cancer, gastric cancer and hepatocellular carcinoma, resulting in tumor occurrence and progression. However, there are no reviews focusing on the dual roles of EphB2 in cancer. Thus, in this paper we systematically summarize and discuss the roles of EphB2 in cancer. Firstly, we review the main biological features and the related signaling regulatory mechanisms of EphB2, and then we summarize the roles of EphB2 in cancer through current studies. Finally, we put forward our viewpoint on the future prospects of cancer research focusing on EphB2, especially with regard to the effects of EphB2 on tumor immunity.

Keywords: receptor tyrosine kinase, EphB2 receptor, cancer, tumor progression, biomarker

OPEN ACCESS

Edited by:
Daniele Vergara,
University of Salento, Italy

Reviewed by:
Kayoko Hosaka,
Karolinska Institutet (KI), Sweden
Marina Damato,
University of Salento, Italy

***Correspondence:**
Jiwei Fang
fangjiwei1364@163.com

Specialty section:
This article was submitted to Molecular and Cellular Oncology, a section of the journal Frontiers in Cell and Developmental Biology

Received: *02 October 2021*
Accepted: *17 January 2022*
Published: *10 February 2022*

Citation:
Liu W, Yu C, Li J and Fang J (2022) The Roles of EphB2 in Cancer. Front. Cell Dev. Biol. 10:788587. doi: 10.3389/fcell.2022.788587

INTRODUCTION

The erythropoietin-producing hepatocellular carcinoma (Eph) receptors constitute the largest subfamily of receptor tyrosine kinases (RTKs) identified until now (Eph Nomenclature Committee, 1997). The Eph receptors have diverse activities, including effects on the actin cytoskeleton, cell attachment, cell shape, and cell mobility. Moreover, recent work has also found that these receptors also influence cell proliferation, survival, secretion, and differentiation. These activities depend on the interaction between the Eph receptors and the ephrins (Eph receptor interacting proteins) (Pasquale, 2005; Pasquale, 2008). Based on sequence identity, structure, and their binding affinity for ligands, the Eph receptors are grouped into two subclasses, EphA receptor (EphA1-10) and EphB receptor (EphB1–6). The ligands for Eph receptors, ephrins, are cell-surface bound proteins that are divided into two subclasses ephrin-A (ephrin-A1 to -A6) and ephrin-B (ephrin-B1 to -B3) according to how they bind to the plasma membrane (Pasquale, 2004; Pasquale, 2005). Ephrin-A ligands are glycosylphosphatidylinositol (GPI) anchored, and ephrin-A ligands can transmit signals despite the lack of a cytoplasmic domain. The reverse signaling mechanisms of ephrin-A ligands are considered to be related to ephrin-A clustering and recruitment of regulatory proteins (Davy et al., 1999). Ephrin-A ligands are anchored to the membrane via covalent linkage to GPI, and rely on transmembrane coreceptors to transmit signals intracellularly (Bonanomi et al., 2012). Ephrin-B ligands are similar to Eph receptors in that they contain a cytoplasmic region, a single transmembrane domain, and a PDZ-binding motif. Ephrin-B reverse signaling also involves the Src family kinases, which are responsible for ephrin-B phosphorylation after the binding of Eph receptor (Pasquale, 2005; Arvanitis and Davy, 2008). Phosphorylated ephrin-B can initiate reverse

signaling via SH2 or PDZ domain-containing proteins (Cowan and Henkemeyer, 2001; Lu et al., 2001). In general, EphA receptors are promiscuously activated by glycosylphosphatidylinositol (GPI)-linked ephrin-A ligands, and EphB receptors are promiscuously activated by transmembrane ephrin-B ligands. However, there are some exceptions, cross interactions have been observed between EphA4 and ephrin-B2/B3 as well as between EphB2 and ephrin-A5 (Himanen et al., 2004; Kania and Klein, 2016; Royet et al., 2017). Furthermore, the membrane attachment of both Eph receptors and ephrin ligands provides a mechanism whereby Eph-ephrin receptors signaling activation requires cell-cell contacts. Eph receptors interact with their membrane-bound ligands the ephrins and promote cell-cell contacts, leading to bidirectional intracellular signaling and downstream signaling cascades that induce autophosphorylation of tyrosine residues in the juxtamembrane region and kinase domain, which further drive the recruitment of downstream signaling molecules (Kullander and Klein, 2002). These include Src family kinases, mitogen-activated protein (MAP) kinases, Src homology 2 and 3 adapter proteins, guanine nucleotide exchange factors, phosphatidylinositol 3-kinase (PI3K), small GTPases, and phosphatases. They are all involved in complex cell-cell repulsion and adhesion pathways, which modulate cell morphology, motility and attachment (Pasquale, 2005).

It is widely known that Eph receptors have essential roles in embryonic development, and in the past decade their critical roles in the occurrence and progression of human disease, especially in tumorigenesis, have become more and more clear (Pasquale, 2008; Xi et al., 2012; Husa et al., 2016). Undoubtedly, enriching our understanding of the roles Eph receptors play in the potential biomarkers, stemness, and drug resistance of cancer will provide new opportunities for tumor therapy (Pasquale, 2010; Leung et al., 2021). Eph receptor B2 (EphB2) has been demonstrated to play a crucial modulatory role in tumor progression (Guo et al., 2006; Lam et al., 2014; Buckens et al., 2020; Morales et al., 2021). Perplexingly, EphB2 can function as both tumor promoters and suppressors in different cellular contexts. In many different human tumors, such as breast cancer, cervical cancer, and medulloblastoma (Wu et al., 2004; Sikkema et al., 2012; Duan et al., 2018), EphB2 acts as a tumor promoter that promotes migration and invasion of tumor cells, and its expression is upregulated. On the contrary, in colorectal cancer and bladder cancer (Xi et al., 2012; Lee et al., 2021), EphB2 functions as a tumor suppressor and its expression level is reduced. However, there are no reviews focusing on the dual roles of EphB2 in cancer. Hence, in the subsequent chapters we first review the main biological features and the related signaling regulatory mechanisms of EphB2, and then we summarize the roles of EphB2 in cancer through current studies, in order to provide some fundamental knowledge for following studies. Finally, we provide our viewpoint on the future prospects of cancer research focusing on EphB2, especially with regard to the effects of EphB2 on tumoral immunity.

THE BIOLOGICAL FEATURES OF EPHB2

The EphB2 receptor is a 117-kDa transmembrane protein consisting of 1,055 amino acids, which is encoded on chromosome 1p36.12 in humans. It was cloned from chicken cDNA in 1991 (Pasquale, 1991). EphB2 has a prototypical RTK topology including an N-terminal multidomain extracellular region, a membrane spanning region, and an intracellular region (**Figure 1**) (Beckmann et al., 1994; Lisabeth et al., 2013). The extracellular region includes two fibronectin type-III repeats, a cysteine-rich domain (containing an epidermal growth factor (EGF)-like motif), and an ephrin-binding region (Himanen et al., 2001; Pasquale, 2005). The ephrin-binding region of EphB2 is a spherical ligand-binding region containing a cavity that accommodates a hydrophobic loop protruding from the ephrin (Himanen et al., 2001).

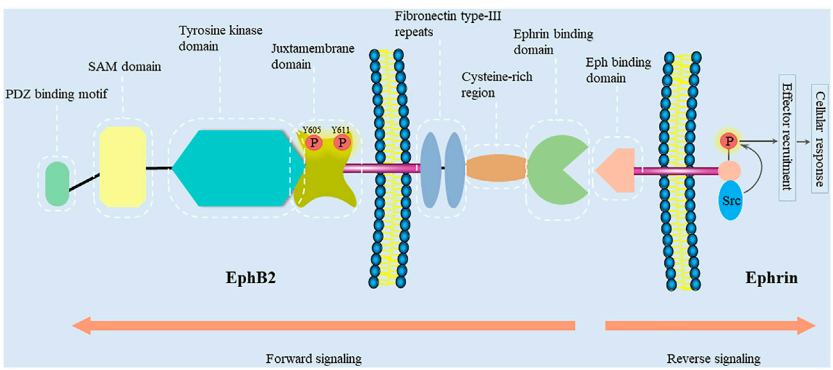

FIGURE 1 | EphB2 and ephrin domain structure and their interacting proteins. Eph receptors contain an N-terminal multidomain extracellular region, a membrane spanning region, and an intracellular region. The intracellular region encompasses a juxtamembrane region, a tyrosine kinase domain, a sterile-α-motif (SAM) domain, and a PDZ-binding motif. The extracellular region includes two fibronectin type-III repeats, a cysteine-rich domain (containing an epidermal growth factor (EGF)-like motif), and an ephrin-binding region. Bidirectional signaling causes forward signaling via Eph receptors and reverse signaling via ephrin ligands. The cellular response caused by Eph/ephrin reverse signaling depends on the intracellular environment. In general, ephrin-B binding of EphB receptors results in the recruitment of Src family kinase and the phosphorylation of the intracellular region of ephrin-B (Kania and Klein, 2016).

Interestingly, so as to accommodate to ephrin-A5 or ephrin-B2, different conformational changes occur in the ligand-binding cavity of EphB2 (Toth et al., 2001; Himanen et al., 2004). Moreover, EphB2 can also bind ephrin-B1 and ephrin-B3 (Tanaka et al., 2007; McClelland et al., 2010).

The intracellular region encompasses a juxtamembrane region, a tyrosine kinase domain, a sterile-α-motif (SAM) domain, and a PDZ-binding motif (Pasquale, 2008). The SAM domain is a protein interaction domain that facilitates receptors homo-dimerization and the oligomerization (Thanos et al., 1999). Moreover, biophysical and structural studies have revealed that isolated extracellular Eph and ephrin regions initially form high-affinity heterodimers around the hydrophobic loop of the ligand. Then, these dimers may form ring-like heterotetramers with lower affinity. On cell surface, Eph-ephrin complexes are further arranged into higher-order aggregates or clusters, and begin a bidirectional signaling (Himanen et al., 2001; Himanen and Nikolov, 2002; Himanen, 2012). EphB2 signals may also be propagated through the Ras binding protein AF6 and other proteins containing the SH2 domain, which bind to the C-terminus of the Eph receptors (Hock et al., 1998; Torres et al., 1998; Buchert et al., 1999). Furthermore, there are two conserved autophosphorylation sites (tyrosines 605 and 611) in the EphB2 juxtamembrane region (Zisch et al., 2000). In order to investigate their role in Src binding, Zisch et al. have mutated tyrosines 605 and 611 of EphB2 to the amino acid phenylalanine that cannot be phosphorylated (Zisch et al., 1998). However, replacing tyrosines 605 and 611 with phenylalanine reduce EphB2 kinase activity, which complicates the analysis of their role in EphB2-mediated signaling and their function as Src homology 2 (SH2) domain binding sites. In contrast, replacing them with glutamic acid, which like phosphotyrosine is negatively charged, will disrupt SH2 domain binding without impairing EphB2 kinase activity (Zisch et al., 2000). Functionally, Ephb2 is related to monocyte adhesion to endothelial cells (Vreeken et al., 2020), endothelial cell chemotaxis and branching remodeling (Salvucci et al., 2006), T-cell and B-cell activation (Nguyen et al., 2013; Yu et al., 2014; Mimche et al., 2015a), autophagic cell death (Kandouz et al., 2010; Tanabe et al., 2011), cell repulsive responses (Lin et al., 2008; Poliakov et al., 2008; Schaupp et al., 2014; Gaitanos et al., 2016; Okumura et al., 2017; Evergren et al., 2018), platelet function (Vaiyapuri et al., 2015; Berndt and Andrews, 2018; Berrou et al., 2018), angiogenesis (Sato et al., 2019), and liver fibrosis (Mimche et al., 2015b; Butler and Schmidt, 2015; Mimche et al., 2018; Chen et al., 2020; Huang et al., 2021).

FORWARD AND REVERSE SIGNALING

A distinctive characteristic of Eph-ephrin complexes is that they can generate bidirectional signals: Eph/ephrin forward signaling is triggered by activating tyrosine kinase domain after the binding of ephrin ligand, and propagates in the receptor-expressing cells, whereas Eph/ephrin reverse signaling is initiated by activating Src family kinase domain after the binding of Eph receptor, and propagates in the ligand (ephrin)-expressing cells (Surawska et al., 2004; Pasquale, 2010). Eph signaling modifies the actin cytoskeleton organization and affects the activities of intercellular adhesion molecules and integrins, thereby controlling cell morphology, adhesion, invasion, migration, and the epithelial phenotype (Pasquale, 2005; Pasquale, 2008). In addition, recent work has also discovered Eph influences on cell proliferation, survival, and special cellular functions such as insulin secretion, immune function, synaptic plasticity and bone remodeling (Pasquale, 2005).

Regarding forward signaling by EphB2 in cancer cells, although the receptor is upregulated in most cancers, its response to ephrin is silent. In some cases, Eph forward signaling that relies on ephrin may even be harmful to tumor progression. For example, the medulloblastoma cell lines with high expression of EphB2 were stimulated by ephrin-B1, the cell adhesion ability *in vitro* was significantly decreased, and the invasion ability was increased (Sikkema et al., 2012). At the same time, overexpression of EphB2 in glioma tissues and cells inhibited cell adhesion and promoted cell invasion, indicating that the overexpression of EphB2 promotes tumor progression via forward signaling (Nakada et al., 2004; Nakada et al., 2005). However, EphB2 inactivation promoted cell proliferation, motility, and invasion of bladder cancer (Lee et al., 2021). Silencing EphB2 accelerated pancreatic cancer growth by facilitating cell proliferation through triggering G1/S phase transition, indicating EphB2 forward signaling has a tumor suppressing function (Hua et al., 2011).

Unlike Eph receptors, since ephrin-Bs do not have intrinsic catalytic activity, they depend on the recruitment of signaling molecules (such as Src family kinases) to signal, which phosphorylate specific tyrosine residues in the cytoplasmic region of ephrin-Bs, leading to receptor engagement and clustering (Salvucci and Tosato, 2012; Salgia et al., 2018). Moreover, similar to the case of forward signaling, reverse signaling was also found to lead to tumor progression and suppression. For example, EphB2-ephrin-B1 promoted the invasion of pancreatic cancer cells (Tanaka et al., 2007). However, EphB2/ephrin signaling was able to suppress colorectal cancer expansion and invasion via repulsive mechanisms (Okumura et al., 2017; Evergren et al., 2018). In summary, these results on bidirectional signaling indicated that EphB2/ephrin has diverse and complex functions in different cancer types and surrounding environment. In addition, mutational inactivation of EPHB2 may also play an important role in cancer progression (Huusko et al., 2004).

EPHB2 IN VARIOUS HUMAN TUMORS

Many studies have verified that EphB2 is abnormally expressed in many cancer types **Table 1**. EphB2 is overexpressed in most tumors, such as hepatocellular carcinoma, breast cancer, glioma, and malignant mesothelioma (Leung et al., 2021; Wu et al., 2004; Nakada et al., 2004; Goparaju et al., 2013), and it functions as a tumor promoter. However, the expression of EphB2 is low in other tumors, such as colorectal cancer and bladder cancer (Xi et al., 2012; Lee et al., 2021), indicating that it exerts a tumor-

TABLE 1 | The expression levels and functions of EphB2 in different tumors.

Cancer type	EphB2 expression	Related proteins	Involved signaling pathways	Associated cellular process	Clinicopathological features	References
Gastric cancer	Upregulated	—	JAK-STAT and TP53 signaling	Promotes migration, invasion, and inhibits adhesion	Poorer overall survival	Kataoka et al. (2002); Yin et al. (2020)
	Downregulated	—	—	—	Lymph node metastasis, advanced T stage, poorer histological differentiation, poorer overall survival	Yu et al. (2011)
Prostate cancer	Downregulate; mutational inactivation	DGAT1; ATGL	—	Inhibits cell proliferation, invasion, and intracellular lipid accumulation	—	Huusko et al. (2004); Morales et al. (2021)
	Upregulated	—	—	Promotes cell proliferation, migration, invasion	—	Liu et al. (2019)
Colorectal cancer	Downregulated	c-Rel	TCF/β-catenin signaling	Inhibits migration, invasion	Higher histological tumor grade, poorer differentiation, poorer overall survival and disease-free survival	Batlle et al. (2002); Guo et al. (2006); Fu et al. (2009); Senior et al. (2010)
Breast cancer	Upregulated	TGF-β3; p53	—	Promotes migration, invasion	Poorer overall survival and disease-free survival	Wu et al. (2004); Lam et al. (2014); Husa et al. (2016)
Hepatocellular carcinoma	Upregulated	TCF1	Wnt/β-catenin signaling	-	Poorer overall survival and disease-free survival	Leung et al. (2021)
Pancreatic cancer	Upregulated	—	—	—	Lymph node metastasis, higher degree of pain, poorer overall survival	Lu et al. (2012); Chen et al., (2019)
Cutaneous squamous cell carcinoma	Upregulated	MMP1; MMP13	—	Promotes cell proliferation, migration, invasion, and angiogenesis	—	Farshchian et al. (2015)
Head and neck squamous cell carcinoma	Upregulated	STAT3	—	Promotes angiogenesis	Poorer overall survival	Sato et al. (2019)
Glioma	Upregulated	miR-204; miR-128	—	Promotes migration, invasion, and inhibits adhesion	Higher tumor grade	Nakada et al. (2004); Lin et al. (2013); Ying et al. (2013)
Glioblastoma multiforme	Upregulated	HIF-2α; circMELK; miR-593; paxillin	—	Promotes cell proliferation, migration, invasion	Poorer overall survival	Qiu et al., (2019); Zhou et al., (2021)
Medulloblastoma	Upregulated	Erk; p38; mTOR	—	Promotes migration, invasion, and inhibits adhesion	—	Sikkema et al. (2012); Bhatia et al. (2017)
Cervical cancer	Upregulated	miR-204	R-Ras signaling	Promotes cell proliferation, migration, invasion	Metastasis	Gao et al. (2014); Duan et al. (2018)
Malignant mesothelioma	Upregulated	VEGF; MMP-2; caspase-2; caspase-8	—	Promotes cell proliferation, migration, invasion, and inhibits apoptosis	—	Goparaju et al. (2013)
Bladder cancer	Downregulated	—	—	Inhibits cell proliferation, invasion	Advanced tumor stage, higher tumor grade, metastasis	Li et al. (2014); Lee et al. (2021)

(Continued on following page)

TABLE 1 | (*Continued*) The expression levels and functions of EphB2 in different tumors.

Cancer type	EphB2 expression	Related proteins	Involved signaling pathways	Associated cellular process	Clinicopathological features	References
Wilms tumor	Downregulated	—	—	—	—	Chetcuti et al. (2011)
Cholangiocarcinoma	Upregulated	FAK; paxillin	-	Promotes migration	Metastasis	Khansaard et al. (2014)
Lung adenocarcinoma	Upregulated	—	—	—	Poorer overall survival and disease-free survival	Zhao et al. (2017)
Ovarian carcinoma	Upregulated	—	—	—	Poorer overall survival	Wu et al. (2006)

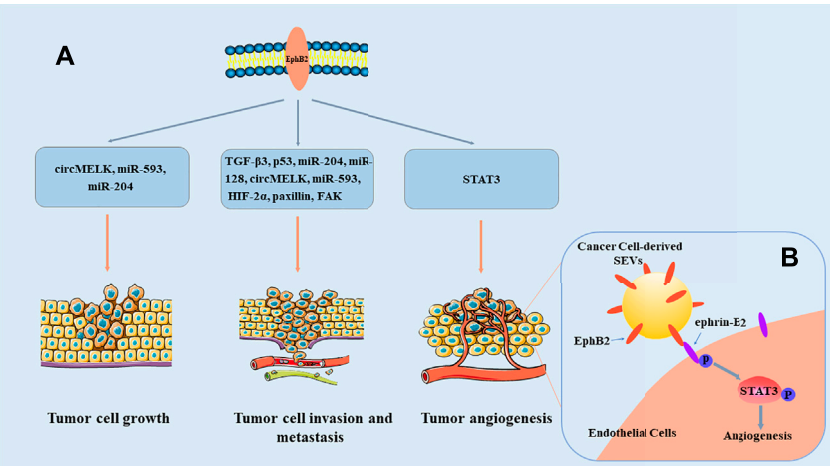

FIGURE 2 | Overview of the roles of EphB2 in cancer. **(A)** EphB2 exerts its roles in tumor cell growth, invasion and metastasis, as well as angiogenesis through multiple signaling pathways. **(B)** Model of SEV-induced angiogenesis pathway. EphB2 on cancer cell–derived small extracellular vesicles (SEVs) binds to ephrin-B2 on endothelial cells, and induces ephrin-B2 reverse signaling through downstream phosphorylation and activation of STAT3, thereby promoting angiogenesis (Sato et al., 2019).

suppression effect. These studies show that EphB2 expression is dynamically regulated in different tumor progression, and that EphB2 exerts its regulatory functions in multiple ways (**Figure 2**). Moreover, EphB2 expression is related to elevated metastatic potential, poor prognosis, and decreased survival of tumor patients (Wu et al., 2006; Yu et al., 2011; Husa et al., 2016; Koh et al., 2020). Consequently, EphB2's functional relevance and expression patterns in malignancies make this protein a potential prognostic biomarker and therapeutic target in cancer.

EphB2 in Gastric Cancer

EphB2 was found to be overexpressed in gastric cancer (GC) tissues than in adjacent or benign non-cancerous gastric tissues, including gene and protein expression (Kataoka et al., 2002; Yin et al., 2020). EphB2 activation accelerated the invasion and migration abilities of the GC cells. Conversely, EphB2 activation obviously reduced the adhesion in GC cells. Moreover, the enrichment analysis of related genes in a GC cohort showed that EphB2 may play a role by mediating the cytokine-cytokine receptor interaction, TP53 and JAK-STAT signaling pathways (Yin et al., 2020). However, the clinical significance of EphB2 in GC is controversial and contradictory so far (Kataoka et al., 2002; Lugli et al., 2005; Yu et al., 2011). Yu et al. reported that the loss of EphB2 expression in GC was significantly correlated with nodal metastasis and advanced disease stage. As the tumor grade increased, the expression rates of EphB2 lowered significantly. At the same time, univariate and multivariate analysis indicated that the loss of EphB2 expression was significantly associated with poor survival of GC patients (Yu et al., 2011). This further implies that EphB2 also serves as a tumor suppressor in GC. However, the underlying molecular mechanism that can explain this contradictory result needs further research. Furthermore, Davalos et al. found that high mutation rate of EphB2 may be related to microsatellite instability in GC compared with endometrial tumors adopting a limited sample size (Davalos et al., 2007).

EphB2 in Prostate Cancer

EphB2 expression was frequently found to be decreased in prostate cancer (PC) tissues with somatic mutational inactivation occurred in approximately 10% of sporadic tumors (Huusko et al., 2004; Robbins et al., 2011). Using nonsense-mediated RNA decay microarrays in combination with array comparative genomic hybridization, it was found

that the EphB2 gene in the PC metastatic cell line DU145 was completely inactivated (biallelic inactivation). The introduction of wild-type EPHB2 remarkably decreased clonogenic growth of DU145 cells (Huusko et al., 2004). Moreover, Morales et al. found that EphB2 expression was inversely associated with PC cell aggressiveness. EphB2 silencing promoted the proliferation of PC cells and simultaneously induced *de novo* lipid droplet (LD) accumulation in both nuclear and cytoplasmic compartments. A DGAT1-specific inhibitor (A-922500) suppressed LD accumulation induced by EphB2 loss (Morales et al., 2021). However, another study reported that the upregulation of EphB2 and Src Pathways were correlate with advanced PC. After dasatinib treatment or siRNAs knockout of Src or EphB2, the epidermal growth factor receptor (EGFR) dynamics, cell motility, and invasive capabilities of PC cells were significantly reduced. Additionally, the upregulation of partial EphB2 and Src pathways predicted poor prognosis in PC patients (Liu et al., 2019), but the paradoxical results need more thorough investigation. In addition, EphB2 was found to play a crucial role in familial PC. Loss of function mutations in the EphB2 were accompanied by an increased risk of PC development (Kittles et al., 2006).

EphB2 in Colorectal Cancer

EphB2 has been proven to be a direct transcription target of T-cell factor (TCF)/β-catenin and it was expressed at high levels in colon premalignant lesions (Batlle et al., 2002; van de Wetering et al., 2002). However, EphB2 expression was decreased in colorectal cancer (CRC). Fu et al. revealed that c-Rel serves as a transcriptional inhibitor of EphB2 and plays a positive role in EphB2 downregulation in CRC (Fu et al., 2009). Downregulation of EphB2 expression promoted the progression of CRC (Batlle et al., 2005; Oshima et al., 2008; Noberini and Pasquale, 2009) and was associated with more advanced CRC, poorer differentiation, poorer overall survival and disease-free survival (Jubb et al., 2005; Guo et al., 2006). Moreover, inactivation of EphB2 has been demonstrated to facilitate tumorigenesis caused by APC mutations in the colorectum of $APC^{Min/+}$ mice, indicating that EphB2 acts as a tumor suppressor in the large intestine (Batlle et al., 2005; Cortina et al., 2007). Consequently, although upregulated by TCF/β-catenin signaling, EphB2 inactivation seems to be a crucial requirement for CRC progression. The potential mechanism of EphB2 inactivation was considered to be genetic and epigenetic changes including aberrant promoter methylation (Alazzouzi et al., 2005), loss of heterozygosity (Oba et al., 2001; Lefeuvre et al., 2009), and/or gene mutations (Huusko et al., 2004; Alazzouzi et al., 2005; Davalos et al., 2007). Furthermore, overexpression of EphB2 inhibited CRC cell growth and activation of EphB2 receptor reduced CRC cell migration (Guo et al., 2006; Senior et al., 2010). Yet, EphB2/ephrin signaling was able to suppress CRC expansion and invasion via repulsive mechanisms (Lugli et al., 2005; Okumura et al., 2017; Evergren et al., 2018).

EphB2 in Breast Cancer

EphB2 was reported to be expressed in benign tissues, but it was significantly upregulated in breast cancer, especially in invasive and metastatic carcinomas (Wu et al., 2004; Chukkapalli et al., 2014). High EphB2 expression was correlated with poor overall survival in breast cancer patients (Wu et al., 2004; Husa et al., 2016; Ebrahim et al., 2021). However, paradoxically, although EphB2 expression induces autophagy and apoptosis, it was also found to promote cell invasion (Chukkapalli et al., 2014). To explain this duality, Kandouz et al. proposed that EphB2 stimulates autophagy, which, conversely, can promote apoptosis or invasion depending on the context. In normal circumstances, autophagy facilitates apoptosis, but when the apoptosis of cancer cells is blocked, autophagy promotes invasion (Chukkapalli et al., 2014). This mechanism could interpret the contradictory role of EphB2 receptor in breast cancer, but this theory requires further research. Furthermore, the EphB2 gene was identified as a novel transforming growth factor (TGF)-β target that is important for the TGF-β3-mediated migration and invasive of breast cancer cells, and its transcriptional activation by TGF-β3 was also suppressed by p53 (Lam et al., 2014). However, how p53 inhibits TGF-β3-induced EphB2 expression requires additional research.

EphB2 in Hepatocellular Carcinoma

EphB2 expression was found to be stepwise increased from normal liver tissues to cirrhotic liver tissues and to hepatocellular carcinoma (HCC) tissues and associated with poor prognosis (Mimche et al., 2015b; Butler and Schmidt, 2015; Leung et al., 2021). Moreover, knockout of endogenous EPHB2 showed reduced tumor growth in mice. Interestingly, EphB2 was significantly upregulated in the established sorafenib-resistant PDTXs. $EphB2^{High}$ HCC cells were found to have enhanced the traits of liver cancer stem cells (CSCs). Mechanistically, T cell factor-1 (TCF1) regulated the expression of EphB2 through promoter activation to form a positive Wnt/β-catenin feedback loop, thereby regulating cancer stemness and drug resistance. Targeting EphB2 with rAAV-8-shEphB2 inhibited HCC tumor development and obviously sensitized HCC cells to sorafenib in an HCC immunocompetent mouse model (Leung et al., 2021). Taken together, targeting the TCF1/EphB2/β-catenin pathway may act as a promising therapeutic strategy for HCC treatment.

EphB2 in Pancreatic Cancer

EphB2 was reported to be highly expressed in pancreatic cancer tissues and associated with shortened survival (Lu et al., 2012; Chen et al., 2019). Multivariate analyses showed that EphB2 was an independent prognostic factor in human pancreatic cancer. The overexpression of EphB2 and ephrin-B2 significantly increased the incidence of higher degree of pain, lymph node metastasis, and advanced classification of T factor. Moreover, in the presence of high EphB2 expression, elevated ephrin-B2 levels can cause a more aggressive tumor phenotype (Lu et al., 2012). However, another study reported that silencing EphB2 accelerated pancreatic cancer growth by promoting cell proliferation through triggering G1/S phase transition, which depended on a CyclinD1/CDK6 cell-cycle regulated signal. Similarly, inhibiting EphB2 also reduced the apoptosis of CFPAC-1 cells by upregulating Bcl-2 expression. Furthermore,

the high expression of EphB2 indicated a better response rate to Qingyihuaji formula (QYHJ) treatment in pancreatic cancer CFPAC-1 cells (Hua et al., 2011; Hua et al., 2014), but the contradictory results need more thorough research. In addition, QYHJ showed an obvious effect against the gemcitabine (GEM) resistant pancreatic cancer, which probable by inhibiting cell migration, increasing the mRNA expression of lncRNA AB209630, and decreasing the mRNA levels of EphB2, miR-373, and NANOG (Chen et al., 2019).

EphB2 in Squamous Cell Carcinoma

EphB2 overexpression was detected in head and neck squamous cell carcinoma (HNSCC) patient and correlated with poor patient survival. Functional experiments demonstrated that the expression of EphB2 in small extracellular vesicles (SEVs) regulated HNSCC angiogenesis both *in vivo* and *in vitro*, and EphB2 carried by SEVs induced ephrin reverse signaling through phosphorylation of ephrin-B and STAT3. A STAT3 inhibitor significantly reduced SEV-induced angiogenesis (Sato et al., 2019). Cutaneous squamous cell carcinoma (CSCC)-derived cell lines and tumor tissues were reported to express increased levels of EphB2 mRNA. Knockdown of EphB2 expression inhibited growth and vascularization of CSCC tumors *in vivo* and inhibited proliferation, invasion, and migration of CSCC cells (Farshchian et al., 2015). In the human CSCC cell line A431, silencing of EphB2 also induced epithelial-mesenchymal transition (EMT)-like morphological changes accompanied by an obvious upregulation of EMT-associated genes such as zinc finger E-box binding homeobox 1/2. And EphB2 plays a crucial role in facilitating the anchorage-independent growth of A431 cells by the suppression of EMT (Inagaki et al., 2019). At the same time, activation of EphB2 signaling by ephrin-B2-Fc promoted invasion of CSCC cells and stimulated production of matrix metalloproteinase-13 (MMP13) and MMP1 (Farshchian et al., 2015). Moreover, treatment of CSCC cell lines with dasatinib effectively suppressed phosphorylation of endogenous EphB2, p38 MAPK, and Src, and then inhibited phosphorylation of ERK1/2. Silencing of EphB2 expression partly rescued CSCC cells from the inhibition of dasatinib on cell viability (Farshchian et al., 2017). Furthermore, *in vitro* experiments, EphB2 small-molecule inhibitors obviously inhibited CSCC cell proliferation, migration, invasion, and induced apoptosis. In a xenograft model, EphB2 small-molecule inhibitors induced morphological changes in the EMT, thereby affecting the progression of CSCC (Li and Zhang, 2020).

EphB2 in Gliomas

EphB2 expression was reported to be significantly higher in gliomas than in normal brain tissues and was correlated with tumor grade (Nakada et al., 2004). overexpression of EphB2 inhibited cell adhesion and promoted cell invasion in glioma tissues and cells (Nakada et al., 2004; Nakada et al., 2005). Mechanistic investigations demonstrated that epigenetic silencing of miR-204 increased EphB2 expression in glioma cells and promoted EphB2-mediated invasion and migration (Ying et al., 2013). Additionally, overexpression of EphB2 decreased the capability of miR-128 to facilitate cell-cell adhesion. The wound-healing assay revealed that miR-128 obviously suppressed cell migration by EphB2 (Lin et al., 2013).

In glioblastoma multiforme (GBM), EphB2 overexpression correlated to poor overall survival in GBM patients. CircMELK could upregulate EphB2 expression by sponging miR-593, thereby promoting the proliferation, invasion, migration, and glioma stem cell (GSC) maintenance of GBM cells (Zhou et al., 2021). Moreover, Qiu et al. reported that EphB2 expression was upregulated in GBM cells under hypoxia and the stabilization of EPHB2 by hypoxia required the participation of hypoxia-inducible factor-2α (HIF-2α). The overexpression of EphB2 enhanced the invasion capability of GBM through the phosphorylation of paxillin under hypoxic conditions (Qiu et al., 2019). However, another study reported that focal adhesion kinase (FAK) activation mediated EphB2-induced actin cytoskeleton organization, focal adhesion formation, and ultimately caused GBM neurosphere cell migration, but EphB2 expression suppressed neurosphere cell proliferation (Wang et al., 2012). The phenomenon that EphB2 has both anti-proliferative and pro-migratory effects *in vivo* may reflect the migration/proliferation dichotomy of GBM, whereas its underlying molecular mechanisms are largely unclear (Giese et al., 1996; Giese et al., 2003).

EphB2 in Medulloblastoma EphB2 was reported to be overexpressed in medulloblastoma patient samples than in normal cerebellum (Sikkema et al., 2012; Coudière Morrison et al., 2013; Bhatia et al., 2017). EphB2 knockdown combined with radiation exposure induced G2/M cell cycle arrest, reduced clonogenic survival fractions, inhibited medulloblastoma cell viability, and reduced medulloblastoma cell invasion (Bhatia et al., 2017). The efficacy of this combined modality can be further tested in other pre-clinical models. Moreover, Sikkema et al. reported that stimulation with ephrin-B1 resulted in a significant decrease in cell adhesion *in vitro* and an increase in invasion ability of medulloblastoma cells expressing high levels of EphB2. Furthermore, analysis of signal transduction found that Erk, mTOR, and p38 are downstream signaling mediators, which may induce the ephrin-B1 phenotype (Sikkema et al., 2012).

EphB2 in Cervical Cancer

EphB2 expression was reported to be upregulated and significantly associated with cancer progression and stage malignancy in the cervical cancer (CC) (Narayan et al., 2007; Gao et al., 2014), and the overexpression of EphB2 induced CC cells to undergo epithelial-mesenchymal transition (EMT) and acquire stem cell-like properties by activating the R-RAS pathway (Gao et al., 2014). Moreover, Duan et al. reported that EphB2 was a direct target of miR-204 and knockdown of EphB2 obtained the inhibitory effect of miR-204 mimic on the proliferation, migration, and invasion of CC cells (Duan et al., 2018).

EphB2 in Malignant Mesothelioma

EphB2 was reported to be overexpressed in malignant mesothelioma (MM) cell lines and tumor tissues. EphB2 inhibition was involved in the decrease of cell proliferation, invasion, migration, and colony formation and the increase of apoptotic cells. Silencing the EphB2 expression is related to the

decrease of cell proliferation, migration, invasion and colony formation and the increase of apoptotic cells. Moreover, targeting EphB2 knockout in H2595 and HP-1 cell lines increased the expression of downstream targets such as caspase-2 and caspase-8, whereas vascular endothelial growth factor (VEGF) and matrix metalloproteinase (MMP-2) had decreased expression (Goparaju et al., 2013).

EphB2 in Bladder Cancer

EphB2 expression was reported to be absent or decreased in bladder cancer tissues, compared to the normal bladder tissues (Li et al., 2014; Lee et al., 2021). Low expression of EphB2 was significantly correlated with advanced clinical stage, muscular invasion, higher tumor grade, and a high incidence of cystectomy. Moreover, *in vitro* studies demonstrated that EphB2 inactivation promoted cell proliferation, motility, and invasion of bladder cancer, implying that EphB2 loss was involved in tumor metastasis and invasion of bladder cancer (Lee et al., 2021).

EphB2 in Other Tumors

EphB2 overexpression was detected in lung adenocarcinoma (AC) tissues. High expression of EphB2 was remarkably associated with poor overall survival of lung AC patients (Zhao et al., 2017). EphB2 was found to be overexpressed in ovarian carcinoma and correlated with poor prognosis (Wu et al., 2006). Moreover, EphB2 expression was reported to be increased in cholangiocarcinoma (CCA) tissues. High expression of EphB2 was remarkably associated with CCA patient's metastasis status. EphB2 suppression by siRNA obviously decreased CCA cell migration through reducing the phosphorylation level of paxillin and focal adhesion kinase (FAK) (Khansaard et al., 2014). Furthermore, EphB2 had significantly lower expression in Wilms tumor tissues compared to normal kidney tissues, but its role in Wilms tumor requires further research (Chetcuti et al., 2011).

PROSPECTS AND CONCLUSION

EphB2 is a significant member of the Eph receptor family, which was thought to be distributed on tumor cells and endothelial cells in previous researches (Salvucci et al., 2006; Wang et al., 2012). Recently, as EphB2 was found to be expressed on some immunocytes such as monocytes, T cells, and B cells, increasing researches have reported on the roles of EphB2 in immunity (Alfaro et al., 2008; Braun et al., 2011; Yu et al., 2014). Forward EphB2 signaling induced by the specific binding of ephrin-B1/B2 and EphB2 could promote monocyte activation and T-cell migration (Alfaro et al., 2008; Braun et al., 2011). In addition, transdifferentiation of human monocytes into macrophages was correlated with increased expression of EphB2, and exposure of monocytes to immobilized ephrinB2 led to phosphorylation of receptors, followed by increased expression of proinflammatory chemokines such as monocyte chemotactic protein-1/CCL2 and interleukin-8 (Braun et al., 2011). Yu et al. reported that EphB2 was involved in the activation of human naive B-cell via Notch1 and Src-p65 signaling pathways and was regulated by miR-185 (Yu et al., 2014). In this study, they used Western blot to test the expression of EphB2 on B cells, and used EphB2 siRNA interference in human B cells from healthy volunteers to evaluate the roles of EphB2 in immunoglobulin (Ig) production, cytokine secretion, and B-cell proliferation. Their demonstrated that EphB2 was scattered on naive B cells and its expression was up-regulated on activated B cells. IgG production (decreased by 26%, $p < 0.05$), TNF-α secretion (decreased by 40%, $p < 0.01$), and B-cell proliferation (decreased by 22%, $p < 0.05$) were decreased concordantly with the down-regulated EphB2 expression. Subsequently, they found that miR-185 directly targeted EphB2 mRNA and inhibited its expression. Moreover, miR-185 overexpression suppressed B-cell activation and miR-185 inhibitor promoted B-cell activation. Furthermore, abatement of EphB2 via EphB2 siRNA or miR-185 mimics attenuated the activation of Notch1 and Src-p65 signaling pathways in human B cells (Yu et al., 2014). In conclusion, it can be speculated that EphB2 might be involved in tumor immunity and this issue certainly worthy further investigation in future research. In this review, we first systematically summarized and discussed the roles of EphB2 in cancer, as well as listed researches that may deepen our understanding of how it regulates cancer progression. Overall, EphB2 serves as a tumor promoter in most cases, facilitating tumor cell proliferation, invasion, and migration through different signaling pathways. However, EphB2 expression and its specific functions in gastric cancer and prostate cancer are controversial and need to be further studied. Moreover, the relationship between EphB2 expression and clinicopathological features was summarized. In detail, the abnormal expression of EphB2 was remarkably associated with clinicopathological features, including overall survival, disease-free survival, lymph node metastasis, histological differentiation, tumor grade and stage, reflecting its potential value as a sensitive and effective biomarker for cancer diagnosis, prognosis, and therapy. Furthermore, The Eph receptor family is an attractive tumor therapeutic target. Previous studies have developed a peptide, monoclonal antibody or small molecule against EphB2 in an attempt to prevent its activation (Mao et al., 2004; Koolpe et al., 2005; Toledo-Sherman et al., 2005), which may be used as a potential treatment for cancer. Accordingly, deepening the understanding of the structure, biogenesis, and molecular mechanisms of EphB2 will provide valuable information for functional research and improving the efficiency of rational drug design.

AUTHOR CONTRIBUTIONS

WL wrote the manuscript. CY, JL, and JF coordinated and directed the project. All authors read and approved the manuscript.

REFERENCES

Alazzouzi, H., Davalos, V., Kokko, A., Domingo, E., Woerner, S. M., Wilson, A. J., et al. (2005). Mechanisms of Inactivation of the Receptor Tyrosine Kinase EPHB2 in Colorectal Tumors. *Cancer Res.* 65, 10170–10173. doi:10.1158/0008-5472.can-05-2580

Alfaro, D., Muñoz, J. J., García-Ceca, J., Cejalvo, T., Jiménez, E., and Zapata, A. (2008). Alterations in the Thymocyte Phenotype of EphB-Deficient Mice Largely Affect the Double Negative Cell Compartment. *Immunology* 125, 131–143. doi:10.1111/j.1365-2567.2008.02828.x

Arvanitis, D., and Davy, A. (2008). Eph/Ephrin Signaling: Networks. *Genes Dev.* 22, 416–429. doi:10.1101/gad.1630408

Batlle, E., Henderson, J. T., Beghtel, H., van den Born, M. M. W., Sancho, E., Huls, G., et al. (2002). β-Catenin and TCF Mediate Cell Positioning in the Intestinal Epithelium by Controlling the Expression of EphB/EphrinB. *Cell* 111, 251–263. doi:10.1016/s0092-8674(02)01015-2

Batlle, E., Bacani, J., Begthel, H., Jonkeer, S., Gregorieff, A., van de Born, M., et al. (2005). EphB Receptor Activity Suppresses Colorectal Cancer Progression. *Nature* 435, 1126–1130. doi:10.1038/nature03626

Beckmann, M. P., Cerretti, D. P., Baum, P., Vanden Bos, T., James, L., Farrah, T., et al. (1994). Molecular Characterization of a Family of Ligands for Eph-Related Tyrosine Kinase Receptors. *EMBO J.* 13, 3757–3762. doi:10.1002/j.1460-2075.1994.tb06685.x

Berndt, M. C., and Andrews, R. K. (2018). EPHB2 Regulates Platelet Activation. *Blood* 132, 2002–2004. doi:10.1182/blood-2018-09-876086

Berrou, E., Soukaseum, C., Favier, R., Adam, F., Elaib, Z., Kauskot, A., et al. (2018). A Mutation of the Human EPHB2 Gene Leads to a Major Platelet Functional Defect. *Blood* 132, 2067–2077. doi:10.1182/blood-2018-04-845644

Bhatia, S., Hirsch, K., Bukkapatnam, S., Baig, N. A., Oweida, A., Griego, A., et al. (2017). Combined EphB2 Receptor Knockdown with Radiation Decreases Cell Viability and Invasion in Medulloblastoma. *Cancer Cel. Int.* 17, 41. doi:10.1186/s12935-017-0409-7

Bonanomi, D., Chivatakarn, O., Bai, G., Abdesselem, H., Lettieri, K., Marquardt, T., et al. (2012). Ret Is a Multifunctional Coreceptor that Integrates Diffusible- and Contact-Axon Guidance Signals. *Cell* 148, 568–582. doi:10.1016/j.cell.2012.01.024

Braun, J., Hoffmann, S. C., Feldner, A., Ludwig, T., Henning, R., Hecker, M., et al. (2011). Endothelial Cell ephrinB2-Dependent Activation of Monocytes in Arteriosclerosis. *Arterioscler Thromb. Vasc. Biol.* 31, 297–305. doi:10.1161/atvbaha.110.217646

Buchert, M., Schneider, S., Meskenaite, V., Adams, M. T., Canaani, E., Baechi, T., et al. (1999). The junction-associated Protein AF-6 Interacts and Clusters with Specific Eph Receptor Tyrosine Kinases at Specialized Sites of Cell-Cell Contact in the Brain. *J. Cel. Biol.* 144, 361–371. doi:10.1083/jcb.144.2.361

Buckens, O. J., El Hassouni, B., Giovannetti, E., and Peters, G. J. (2020). The Role of Eph Receptors in Cancer and How to Target Them: Novel Approaches in Cancer Treatment. *Expert Opin. Investig. Drugs* 29, 567–582. doi:10.1080/13543784.2020.1762566

Butler, N. S., and Schmidt, N. W. (2015). Erythropoietin-producing Hepatocellular Receptor B2 Receptor Tyrosine Kinase: A Novel Regulator of Infection- and Inflammation-Induced Liver Fibrosis. *Hepatology* 62, 680–683. doi:10.1002/hep.27868

Chen, P., Wang, M., and Wang, C. (2019). Qingyihuaji Formula Reverses Gemcitabine Resistant Human Pancreatic Cancer through Regulate lncRNA AB209630/miR-373/EphB2-NANOG Signals. *Biosci. Rep.* 39:BSR20190610. doi:10.1042/BSR20190610

Chen, X., Zhang, D., Wang, Y., Chen, K., Zhao, L., Xu, Y., et al. (2020). Synergistic Antifibrotic Effects of miR-451 with miR-185 Partly by Co-targeting EphB2 on Hepatic Stellate Cells. *Cell Death Dis.* 11, 402. doi:10.1038/s41419-020-2613-y

Chetcuti, A., Aktas, S., Mackie, N., Ulger, C., Toruner, G., Alkan, M., et al. (2011). Expression Profiling Reveals MSX1 and EphB2 Expression Correlates with the Invasion Capacity of Wilms Tumors. *Pediatr. Blood Cancer* 57, 950–957. doi:10.1002/pbc.23003

Chukkapalli, S., Amessou, M., Dilly, A. K., Dekhil, H., Zhao, J., Liu, Q., et al. (2014). Role of the EphB2 Receptor in Autophagy, Apoptosis and Invasion in Human Breast Cancer Cells. *Exp. Cel. Res.* 320, 233–246. doi:10.1016/j.yexcr.2013.10.022

Cortina, C., Palomo-Ponce, S., Iglesias, M., Fernández-Masip, J. L., Vivancos, A., Whissell, G., et al. (2007). EphB-ephrin-B Interactions Suppress Colorectal Cancer Progression by Compartmentalizing Tumor Cells. *Nat. Genet.* 39, 1376–1383. doi:10.1038/ng.2007.11

Coudière Morrison, L., McClelland, R., Aiken, C., Bridges, M., Liang, L., Wang, X., et al. (2013). Deconstruction of Medulloblastoma Cellular Heterogeneity Reveals Differences between the Most Highly Invasive and Self-Renewing Phenotypes. *Neoplasia* 15, 384–398. doi:10.1593/neo.13148

Cowan, C. A., and Henkemeyer, M. (2001). The SH2/SH3 Adaptor Grb4 Transduces B-Ephrin Reverse Signals. *Nature* 413, 174–179. doi:10.1038/35093123

Davalos, V., Dopeso, H., Velho, S., Ferreira, A. M., Cirnes, L., Díaz-Chico, N., et al. (2007). High EPHB2 Mutation Rate in Gastric but Not Endometrial Tumors with Microsatellite Instability. *Oncogene* 26, 308–311. doi:10.1038/sj.onc.1209780

Davy, A., Gale, N. W., Murray, E. W., Klinghoffer, R. A., Soriano, P., Feuerstein, C., et al. (1999). Compartmentalized Signaling by GPI-Anchored Ephrin-A5 Requires the Fyn Tyrosine Kinase to Regulate Cellular Adhesion. *Genes Develop.* 13, 3125–3135. doi:10.1101/gad.13.23.3125

Duan, S., Wu, A., Chen, Z., Yang, Y., Liu, L., and Shu, Q. (2018). miR-204 Regulates Cell Proliferation and Invasion by Targeting EphB2 in Human Cervical Cancer. *Oncol. Res.* 26, 713–723. doi:10.3727/096504017x15016337254641

Ebrahim, A. S., Hailat, Z., Bandyopadhyay, S., Neill, D., and Kandouz, M. (2021). The Value of EphB2 Receptor and Cognate Ephrin Ligands in Prognostic and Predictive Assessments of Human Breast Cancer. *Int. J. Mol. Sci.* 22:8098. doi:10.3390/ijms22158098

Eph Nomenclature Committee (1997). Unified Nomenclature for Eph Family Receptors and Their Ligands, the Ephrins. Eph Nomenclature Committee. *Cell* 90, 403–404. doi:10.1016/s0092-8674(00)80500-0

Evergren, E., Cobbe, N., and McMahon, H. T. (2018). Eps15R and Clathrin Regulate EphB2-Mediated Cell Repulsion. *Traffic* 19, 44–57. doi:10.1111/tra.12531

Farshchian, M., Nissinen, L., Siljamäki, E., Riihilä, P., Toriseva, M., Kivisaari, A., et al. (2015). EphB2 Promotes Progression of Cutaneous Squamous Cell Carcinoma. *J. Invest. Dermatol.* 135, 1882–1892. doi:10.1038/jid.2015.104

Farshchian, M., Nissinen, L., Grénman, R., and Kähäri, V.-M. (2017). Dasatinib Promotes Apoptosis of Cutaneous Squamous Carcinoma Cells by Regulating Activation of ERK1/2. *Exp. Dermatol.* 26, 89–92. doi:10.1111/exd.13109

Fu, T., Li, P., Wang, H., He, Y., Luo, D., Zhang, A., et al. (2009). c-Rel Is a Transcriptional Repressor of EPHB2 in Colorectal Cancer. *J. Pathol.* 219, 103–113. doi:10.1002/path.2590

Gaitanos, T. N., Koerner, J., and Klein, R. (2016). Tiam-Rac Signaling Mediates Trans-endocytosis of Ephrin Receptor EphB2 and Is Important for Cell Repulsion. *J. Cel. Biol.* 214, 735–752. doi:10.1083/jcb.201512010

Gao, Q., Liu, W., Cai, J., Li, M., Gao, Y., Lin, W., et al. (2014). EphB2 Promotes Cervical Cancer Progression by Inducing Epithelial-Mesenchymal Transition. *Hum. Pathol.* 45, 372–381. doi:10.1016/j.humpath.2013.10.001

Giese, A., Loo, M. A., Tran, N., Haskett, D., Coons, S. W., and Berens, M. E. (1996). Dichotomy of Astrocytoma Migration and Proliferation. *Int. J. Cancer* 67, 275–282. doi:10.1002/(sici)1097-0215(19960717)67:2<275::aid-ijc20>3.0.co;2-9

Giese, A., Bjerkvig, R., Berens, M. E., and Westphal, M. (2003). Cost of Migration: Invasion of Malignant Gliomas and Implications for Treatment. *Jco* 21, 1624–1636. doi:10.1200/jco.2003.05.063

Goparaju, C., Donington, J. S., Hsu, T., Harrington, R., Hirsch, N., and Pass, H. I. (2013). Overexpression of EPH Receptor B2 in Malignant Mesothelioma Correlates with Oncogenic Behavior. *J. Thorac. Oncol.* 8, 1203–1211. doi:10.1097/jto.0b013e31829ceb6a

Guo, D. L., Zhang, J., Yuen, S. T., Tsui, W. Y., Chan, A. S. Y., Ho, C., et al. (2006). Reduced Expression of EphB2 that Parallels Invasion and Metastasis in Colorectal Tumours. *Carcinogenesis* 27, 454–464. doi:10.1093/carcin/bgi259

Himanen, J.-P., and Nikolov, D. B. (2002). Purification, Crystallization and Preliminary Characterization of an Eph-B2/ephrin-B2 Complex. *Acta Crystallogr. D Biol. Cryst.* 58, 533–535. doi:10.1107/s0907444902000264

Himanen, J.-P., Rajashankar, K. R., Lackmann, M., Cowan, C. A., Henkemeyer, M., and Nikolov, D. B. (2001). Crystal Structure of an Eph Receptor-Ephrin Complex. *Nature* 414, 933–938. doi:10.1038/414933a

Himanen, J.-P., Chumley, M. J., Lackmann, M., Li, C., Barton, W. A., Jeffrey, P. D., et al. (2004). Repelling Class Discrimination: Ephrin-A5 Binds to and Activates EphB2 Receptor Signaling. *Nat. Neurosci.* 7, 501–509. doi:10.1038/nn1237

Himanen, J. P. (2012). Ectodomain Structures of Eph Receptors. *Semin. Cel. Develop. Biol.* 23, 35–42. doi:10.1016/j.semcdb.2011.10.025

Hock, B., Bohme, B., Karn, T., Yamamoto, T., Kaibuchi, K., Holtrich, U., et al. (1998). PDZ-domain-mediated Interaction of the Eph-Related Receptor Tyrosine Kinase EphB3 and the Ras-Binding Protein AF6 Depends on the Kinase Activity of the Receptor. *Proc. Natl. Acad. Sci.* 95, 9779–9784. doi:10.1073/pnas.95.17.9779

Hua, Y.-q., Ouyang, H.-q., Chen, Z., Meng, Z.-q., Luo, J.-m., Lin, J.-h., et al. (2011). Promoted Cancer Growth by Stimulating Cell Proliferation and Decreasing Apoptosis Using a Lentivirus-Based EphB2 RNAi in Pancreatic Carcinoma CFPAC-1 Cells. *Biomed. Pharmacother.* 65, 123–131. doi:10.1016/j.biopha.2010.12.011

Hua, Y.-Q., Chen, Z., Meng, Z.-Q., Chen, H., Shen, J.-G., Wang, K., et al. (2014). High Expression of Erythropoietin-Producing Hepatoma Cell Line-B2 (EphB2) Predicts the Efficiency of the Qingyihuaji Formula Treatment in Pancreatic Cancer CFPAC-1 Cells through the EphrinB1-EphB2 Pathway. *Oncol. Lett.* 8, 17–24. doi:10.3892/ol.2014.2134

Huang, Z., Liu, S., Tang, A., Al-Rabadi, L., Henkemeyer, M., Mimche, P. N., et al. (2021). Key Role for EphB2 Receptor in Kidney Fibrosis. *Clin. Sci.* 135, 2127–2142. doi:10.1042/cs20210644

Husa, A.-M., Magić, Ž., Larsson, M., Fornander, T., and Pérez-Tenorio, G. (2016). EPH/ephrin Profile and EPHB2 Expression Predicts Patient Survival in Breast Cancer. *Oncotarget* 7, 21362–21380. doi:10.18632/oncotarget.7246

Huusko, P., Ponciano-Jackson, D., Wolf, M., Kiefer, J. A., Azorsa, D. O., Tuzmen, S., et al. (2004). Nonsense-mediated Decay Microarray Analysis Identifies Mutations of EPHB2 in Human Prostate Cancer. *Nat. Genet.* 36, 979–983. doi:10.1038/ng1408

Inagaki, Y., Tokunaga, T., Yanai, M., Wu, D., Huang, J., Nagase, H., et al. (2019). Silencing of EPHB2 Promotes the Epithelial-Mesenchymal Transition of Skin Squamous Cell Carcinoma-Derived A431 Cells. *Oncol. Lett.* 17, 3735–3742. doi:10.3892/ol.2019.10019

Jubb, A. M., Zhong, F., Bheddah, S., Grabsch, H. I., Frantz, G. D., Mueller, W., et al. (2005). EphB2 Is a Prognostic Factor in Colorectal Cancer. *Clin. Cancer Res.* 11, 5181–5187. doi:10.1158/1078-0432.ccr-05-0143

Kandouz, M., Haidara, K., Zhao, J., Brisson, M.-L., and Batist, G. (2010). The EphB2 Tumor Suppressor Induces Autophagic Cell Death via Concomitant Activation of the ERK1/2 and PI3K Pathways. *Cell Cycle* 9, 398–407. doi:10.4161/cc.9.2.10505

Kania, A., and Klein, R. (2016). Mechanisms of Ephrin-Eph Signalling in Development, Physiology and Disease. *Nat. Rev. Mol. Cel. Biol.* 17, 240–256. doi:10.1038/nrm.2015.16

Kataoka, H., Tanaka, M., Kanamori, M., Yoshii, S., Ihara, M., Wang, Y.-J., et al. (2002). Expression Profile of EFNB1, EFNB2, Two Ligands of EPHB2 in Human Gastric Cancer. *J. Cancer Res. Clin. Oncol.* 128, 343–348. doi:10.1007/s00432-002-0355-0

Khansaard, W., Techasen, A., Namwat, N., Yongvanit, P., Khuntikeo, N., Puapairoj, A., et al. (2014). Increased EphB2 Expression Predicts Cholangiocarcinoma Metastasis. *Tumor Biol.* 35, 10031–10041. doi:10.1007/s13277-014-2295-0

Kittles, R. A., Baffoe-Bonnie, A. B., Moses, T. Y., Robbins, C. M., Ahaghotu, C., Huusko, P., et al. (2006). A Common Nonsense Mutation in EphB2 Is Associated with Prostate Cancer Risk in African American Men with a Positive Family History. *J. Med. Genet.* 43, 507–511. doi:10.1136/jmg.2005.035790

Koh, H. M., Hyun, C. L., Jang, B. G., and Lee, H. J. (2020). Ephrin Receptor B2 Expression May Be a Prognostic Marker for Patients with Cancer: A Meta-Analysis. *Anticancer Res.* 40, 4309–4317. doi:10.21873/anticanres.14433

Koolpe, M., Burgess, R., Dail, M., and Pasquale, E. B. (2005). EphB Receptor-Binding Peptides Identified by Phage Display Enable Design of an Antagonist with Ephrin-like Affinity. *J. Biol. Chem.* 280, 17301–17311. doi:10.1074/jbc.m500363200

Kullander, K., and Klein, R. (2002). Mechanisms and Functions of Eph and Ephrin Signalling. *Nat. Rev. Mol. Cel Biol.* 3, 475–486. doi:10.1038/nrm856

Lam, S., Wiercinska, E., Teunisse, A. F. A. S., Lodder, K., ten Dijke, P., and Jochemsen, A. G. (2014). Wild-type P53 Inhibits Pro-invasive Properties of TGF-B3 in Breast Cancer, in Part through Regulation of EPHB2, a New TGF-β Target Gene. *Breast Cancer Res. Treat.* 148, 7–18. doi:10.1007/s10549-014-3147-8

Lee, T. H., Heo, J. H., Jeong, J.-Y., Lee, G. H., Park, D. S., and Kim, T. H. (2021). Low Expression of EphB2, EphB3, and EphB4 in Bladder Cancer: Novel Potential Indicators of Muscular Invasion. *Yonsei Med. J.* 62, 679–690. doi:10.3349/ymj.2021.62.8.679

Lefeuvre, M., Gunduz, M., Nagatsuka, H., Gunduz, E., Al Sheikh Ali, M., Beder, L., et al. (2009). Fine Deletion Analysis of 1p36 Chromosomal Region in Oral Squamous Cell Carcinomas. *J. Oral Pathol. Med.* 38, 94–98. doi:10.1111/j.1600-0714.2008.00666.x

Leung, H. W., Leung, C. O. N., Lau, E. Y., Chung, K. P. S., Mok, E. H., Lei, M. M. L., et al. (2021). EPHB2 Activates β-Catenin to Enhance Cancer Stem Cell Properties and Drive Sorafenib Resistance in Hepatocellular Carcinoma. *Cancer Res.* 81, 3229–3240. doi:10.1158/0008-5472.can-21-0184

Li, Y., and Zhang, X. (2020). Therapeutic Effects of Ephrin B Receptor 2 Inhibitors Screened by Molecular Docking on Cutaneous Squamous Cell Carcinoma. *J. Dermatol. Treat.*, 1–7. doi:10.1080/09546634.2020.1756201

Li, X., Choi, W. W., Yan, R., Yu, H., Krasnoperov, V., Kumar, S. R., et al. (2014). The Differential Expression of EphB2 and EphB4 Receptor Kinases in normal Bladder and in Transitional Cell Carcinoma of the Bladder. *PloS one* 9, e105326. doi:10.1371/journal.pone.0105326

Lin, K.-T., Sloniowski, S., Ethell, D. W., and Ethell, I. M. (2008). Ephrin-B2-induced Cleavage of EphB2 Receptor Is Mediated by Matrix Metalloproteinases to Trigger Cell Repulsion. *J. Biol. Chem.* 283, 28969–28979. doi:10.1074/jbc.m804401200

Lin, L., Chen, X., Peng, X., Zhou, J., Kung, H.-F., Lin, M. C., et al. (2013). MicroRNA-128 Promotes Cell-Cell Adhesion in U87 Glioma Cells via Regulation of EphB2. *Oncol. Rep.* 30, 1239–1248. doi:10.3892/or.2013.2596

Lisabeth, E. M., Falivelli, G., and Pasquale, E. B. (2013). Eph Receptor Signaling and Ephrins. *Cold Spring Harb Perspect. Biol.* 5:a009159. doi:10.1101/cshperspect.a009159

Liu, Y. L., Horning, A. M., Lieberman, B., Kim, M., Lin, C. K., Hung, C. N., et al. (2019). Spatial EGFR Dynamics and Metastatic Phenotypes Modulated by Upregulated EphB2 and Src Pathways in Advanced Prostate Cancer. *Cancers (Basel)* 11:1910. doi:10.3390/cancers11121910

Lu, Q., Sun, E. E., Klein, R. S., and Flanagan, J. G. (2001). Ephrin-B Reverse Signaling Is Mediated by a Novel PDZ-RGS Protein and Selectively Inhibits G Protein-Coupled Chemoattraction. *Cell* 105, 69–79. doi:10.1016/s0092-8674(01)00297-5

Lu, Z., Zhang, Y., Li, Z., Yu, S., Zhao, G., Li, M., et al. (2012). Overexpression of the B-type Eph and Ephrin Genes Correlates with Progression and Pain in Human Pancreatic Cancer. *Oncol. Lett.* 3, 1207–1212. doi:10.3892/ol.2012.650

Lugli, A., Spichtin, H., Maurer, R., Mirlacher, M., Kiefer, J., Huusko, P., et al. (2005). EphB2 Expression across 138 Human Tumor Types in a Tissue Microarray: High Levels of Expression in Gastrointestinal Cancers. *Clin. Cancer Res.* 11, 6450–6458. doi:10.1158/1078-0432.ccr-04-2458

Mao, W., Luis, E., Ross, S., Silva, J., Tan, C., Crowley, C., et al. (2004). EphB2 as a Therapeutic Antibody Drug Target for the Treatment of Colorectal Cancer. *Cancer Res.* 64, 781–788. doi:10.1158/0008-5472.can-03-1047

McClelland, A. C., Hruska, M., Coenen, A. J., Henkemeyer, M., and Dalva, M. B. (2010). Trans-synaptic EphB2-Ephrin-B3 Interaction Regulates Excitatory Synapse Density by Inhibition of Postsynaptic MAPK Signaling. *Proc. Natl. Acad. Sci.* 107, 8830–8835. doi:10.1073/pnas.0910644107

Mimche, P. N., Brady, L. M., Keeton, S., Fenne, D. S. J., King, T. P., Quicke, K. M., et al. (2015). Expression of the Receptor Tyrosine Kinase EphB2 on Dendritic Cells Is Modulated by Toll-like Receptor Ligation but Is Not Required for T Cell Activation. *PloS one* 10, e0138835. doi:10.1371/journal.pone.0138835

Mimche, P. N., Brady, L. M., Bray, C. F., Lee, C. M., Thapa, M., King, T. P., et al. (2015). The Receptor Tyrosine Kinase EphB2 Promotes Hepatic Fibrosis in Mice. *Hepatology* 62, 900–914. doi:10.1002/hep.27792

Mimche, P. N., Lee, C. M., Mimche, S. M., Thapa, M., Grakoui, A., Henkemeyer, M., et al. (2018). EphB2 Receptor Tyrosine Kinase Promotes Hepatic Fibrogenesis in Mice via Activation of Hepatic Stellate Cells. *Sci. Rep.* 8, 2532. doi:10.1038/s41598-018-20926-9

Morales, A., Greenberg, M., Nardi, F., Gil, V., Hayward, S. W., Crawford, S. E., et al. (2021). Loss of Ephrin B2 Receptor (EPHB2) Sets Lipid Rheostat by Regulating

Proteins DGAT1 and ATGL Inducing Lipid Droplet Storage in Prostate Cancer Cells. *Lab. Invest.* 101, 921–934. doi:10.1038/s41374-021-00583-9

Nakada, M., Niska, J. A., Miyamori, H., McDonough, W. S., Wu, J., Sato, H., et al. (2004). The Phosphorylation of EphB2 Receptor Regulates Migration and Invasion of Human Glioma Cells. *Cancer Res.* 64, 3179–3185. doi:10.1158/0008-5472.can-03-3667

Nakada, M., Niska, J. A., Tran, N. L., McDonough, W. S., and Berens, M. E. (2005). EphB2/R-Ras Signaling Regulates Glioma Cell Adhesion, Growth, and Invasion. *Am. J. Pathol.* 167, 565–576. doi:10.1016/s0002-9440(10)62998-7

Narayan, G., Bourdon, V., Chaganti, S., Arias-Pulido, H., Nandula, S. V., Rao, P. H., et al. (2007). Gene Dosage Alterations Revealed by cDNA Microarray Analysis in Cervical Cancer: Identification of Candidate Amplified and Overexpressed Genes. *Genes Chromosom. Cancer* 46, 373–384. doi:10.1002/gcc.20418

Nguyen, T. M., Arthur, A., Hayball, J. D., and Gronthos, S. (2013). EphB and Ephrin-B Interactions Mediate Human Mesenchymal Stem Cell Suppression of Activated T-Cells. *Stem Cell Dev.* 22, 2751–2764. doi:10.1089/scd.2012.0676

Noberini, R., and Pasquale, E. B. (2009). Proliferation and Tumor Suppression: Not Mutually Exclusive for Eph Receptors. *Cancer cell* 16, 452–454. doi:10.1016/j.ccr.2009.11.008

Oba, S. M., Wang, Y.-J., Song, J.-P., Li, Z.-Y., Kobayashi, K., Tsugane, S., et al. (2001). Genomic Structure and Loss of Heterozygosity of EPHB2 in Colorectal Cancer. *Cancer Lett.* 164, 97–104. doi:10.1016/s0304-3835(00)00716-3

Okumura, F., Joo-Okumura, A., Obara, K., Petersen, A., Nishikimi, A., Fukui, Y., et al. (2017). Ubiquitin Ligase SPSB4 Diminishes Cell Repulsive Responses Mediated by EphB2. *Mol. Biol. Cel.* 28, 3532–3541. doi:10.1091/mbc.e17-07-0450

Oshima, T., Akaike, M., Yoshihara, K., Shiozawa, M., Yamamoto, N., Sato, T., et al. (2008). Overexpression of EphA4 Gene and Reduced Expression of EphB2 Gene Correlates with Liver Metastasis in Colorectal Cancer. *Int. J. Oncol.* 33, 573–577.

Pasquale, E. B. (1991). Identification of Chicken Embryo Kinase 5, a Developmentally Regulated Receptor-type Tyrosine Kinase of the Eph Family. *Cell Regul.* 2, 523–534. doi:10.1091/mbc.2.7.523

Pasquale, E. B. (2004). Eph-ephrin Promiscuity Is Now crystal clear. *Nat. Neurosci.* 7, 417–418. doi:10.1038/nn0504-417

Pasquale, E. B. (2005). Eph Receptor Signalling Casts a Wide Net on Cell Behaviour. *Nat. Rev. Mol. Cel Biol.* 6, 462–475. doi:10.1038/nrm1662

Pasquale, E. B. (2008). Eph-ephrin Bidirectional Signaling in Physiology and Disease. *Cell* 133, 38–52. doi:10.1016/j.cell.2008.03.011

Pasquale, E. B. (2010). Eph Receptors and Ephrins in Cancer: Bidirectional Signalling and beyond. *Nat. Rev. Cancer* 10, 165–180. doi:10.1038/nrc2806

Poliakov, A., Cotrina, M. L., Pasini, A., and Wilkinson, D. G. (2008). Regulation of EphB2 Activation and Cell Repulsion by Feedback Control of the MAPK Pathway. *J. Cel. Biol.* 183, 933–947. doi:10.1083/jcb.200807151

Qiu, W., Song, S., Chen, W., Zhang, J., Yang, H., and Chen, Y. (2019). Hypoxia-induced EPHB2 Promotes Invasive Potential of Glioblastoma. *Int. J. Clin. Exp. Pathol.* 12, 539–548.

Robbins, C. M., Hooker, S., Kittles, R. A., and Carpten, J. D. (2011). EphB2 SNPs and Sporadic Prostate Cancer Risk in African American Men. *PloS one* 6, e19494. doi:10.1371/journal.pone.0019494

Royet, A., Broutier, L., Coissieux, M.-M., Malleval, C., Gadot, N., Maillet, D., et al. (2017). Ephrin-B3 Supports Glioblastoma Growth by Inhibiting Apoptosis Induced by the Dependence Receptor EphA4. *Oncotarget* 8, 23750–23759. doi:10.18632/oncotarget.16077

Salgia, R., Kulkarni, P., and Gill, P. S. (2018). EphB4: A Promising Target for Upper Aerodigestive Malignancies. *Biochim. Biophys. Acta (Bba) - Rev. Cancer* 1869, 128–137. doi:10.1016/j.bbcan.2018.01.003

Salvucci, O., and Tosato, G. (2012). Essential Roles of EphB Receptors and EphrinB Ligands in Endothelial Cell Function and Angiogenesis. *Adv. Cancer Res.* 114, 21–57. doi:10.1016/b978-0-12-386503-8.00002-8

Salvucci, O., de la Luz Sierra, M., Martina, J. A., McCormick, P. J., and Tosato, G. (2006). EphB2 and EphB4 Receptors Forward Signaling Promotes SDF-1-Induced Endothelial Cell Chemotaxis and Branching Remodeling. *Blood* 108, 2914–2922. doi:10.1182/blood-2006-05-023341

Sato, S., Vasaikar, S., Eskaros, A., Kim, Y., Lewis, J. S., Zhang, B., et al. (2019). EPHB2 Carried on Small Extracellular Vesicles Induces Tumor Angiogenesis via Activation of Ephrin Reverse Signaling. *JCI insight* 4:e132447. doi:10.1172/jci.insight.132447

Schaupp, A., Sabet, O., Dudanova, I., Ponserre, M., Bastiaens, P., and Klein, R. (2014). The Composition of EphB2 Clusters Determines the Strength in the Cellular Repulsion Response. *J. Cel. Biol.* 204, 409–422. doi:10.1083/jcb.201305037

Senior, P. V., Zhang, B. X., and Chan, S. T. F. (2010). Loss of Cell-Surface Receptor EphB2 Is Important for the Growth, Migration, and Invasiveness of a colon Cancer Cell Line. *Int. J. Colorectal Dis.* 25, 687–694. doi:10.1007/s00384-010-0916-7

Sikkema, A. H., den Dunnen, W. F. A., Hulleman, E., van Vuurden, D. G., Garcia-Manero, G., Yang, H., et al. (2012). EphB2 Activity Plays a Pivotal Role in Pediatric Medulloblastoma Cell Adhesion and Invasion. *Neuro-Oncol.* 14, 1125–1135. doi:10.1093/neuonc/nos130

Surawska, H., Ma, P. C., and Salgia, R. (2004). The Role of Ephrins and Eph Receptors in Cancer. *Cytokine Growth Factor. Rev.* 15, 419–433. doi:10.1016/j.cytogfr.2004.09.002

Tanabe, H., Kuribayashi, K., Tsuji, N., Tanaka, M., Kobayashi, D., and Watanabe, N. (2011). Sesamin Induces Autophagy in colon Cancer Cells by Reducing Tyrosine Phosphorylation of EphA1 and EphB2. *Int. J. Oncol.* 39, 33–40. doi:10.3892/ijo.2011.1011

Tanaka, M., Sasaki, K., Kamata, R., and Sakai, R. (2007). The C-Terminus of Ephrin-B1 Regulates Metalloproteinase Secretion and Invasion of Cancer Cells. *J. Cel. Sci.* 120, 2179–2189. doi:10.1242/jcs.008607

Thanos, C. D., Goodwill, K. E., and Bowie, J. U. (1999). Oligomeric Structure of the Human EphB2 Receptor SAM Domain. *Science* 283, 833–836. doi:10.1126/science.283.5403.833

Toledo-Sherman, L., Deretey, E., Slon-Usakiewicz, J. J., Ng, W., Dai, J.-R., Foster, J. E., et al. (2005). Frontal Affinity Chromatography with MS Detection of EphB2 Tyrosine Kinase Receptor. 2. Identification of Small-Molecule Inhibitors via Coupling with Virtual Screening. *J. Med. Chem.* 48, 3221–3230. doi:10.1021/jm0492204

Torres, R., Firestein, B. L., Dong, H., Staudinger, J., Olson, E. N., Huganir, R. L., et al. (1998). PDZ Proteins Bind, Cluster, and Synaptically Colocalize with Eph Receptors and Their Ephrin Ligands. *Neuron* 21, 1453–1463. doi:10.1016/s0896-6273(00)80663-7

Toth, J., Cutforth, T., Gelinas, A. D., Bethoney, K. A., Bard, J., and Harrison, C. J. (2001). Crystal Structure of an Ephrin Ectodomain. *Develop. Cel.* 1, 83–92. doi:10.1016/s1534-5807(01)00002-8

Vaiyapuri, S., Sage, T., Rana, R. H., Schenk, M. P., Ali, M. S., Unsworth, A. J., et al. (2015). EphB2 Regulates Contact-dependent and Contact-independent Signaling to Control Platelet Function. *Blood* 125, 720–730. doi:10.1182/blood-2014-06-585083

van de Wetering, M., Sancho, E., Verweij, C., de Lau, W., Oving, I., Hurlstone, A., et al. (2002). The β-Catenin/TCF-4 Complex Imposes a Crypt Progenitor Phenotype on Colorectal Cancer Cells. *Cell* 111, 241–250. doi:10.1016/s0092-8674(02)01014-0

Vreeken, D., Bruikman, C. S., Cox, S. M. L., Zhang, H., Lalai, R., Koudijs, A., et al. (2020). EPH Receptor B2 Stimulates Human Monocyte Adhesion and Migration Independently of its EphrinB Ligands. *J. Leukoc. Biol.* 108, 999–1011. doi:10.1002/jlb.2a0320-283rr

Wang, S. D., Rath, P., Lal, B., Richard, J.-P., Li, Y., Goodwin, C. R., et al. (2012). EphB2 Receptor Controls Proliferation/migration Dichotomy of Glioblastoma by Interacting with Focal Adhesion Kinase. *Oncogene* 31, 5132–5143. doi:10.1038/onc.2012.16

Wu, Q., Suo, Z., Risberg, B., Karlsson, M. G., Villman, K., and Nesland, J. M. (2004). Expression of Ephb2 and Ephb4 in Breast Carcinoma. *Pathol. Oncol. Res.* 10, 26–33. doi:10.1007/bf02893405

Wu, Q., Suo, Z., Kristensen, G. B., Baekelandt, M., and Nesland, J. M. (2006). The Prognostic Impact of EphB2/B4 Expression on Patients with Advanced Ovarian Carcinoma. *Gynecol. Oncol.* 102, 15–21. doi:10.1016/j.ygyno.2005.11.034

Xi, H.-Q., Wu, X.-S., Wei, B., and Chen, L. (2012). Eph Receptors and Ephrins as Targets for Cancer Therapy. *J. Cel. Mol. Med.* 16, 2894–2909. doi:10.1111/j.1582-4934.2012.01612.x

Yin, J., Li, Z., Ye, L., Birkin, E., Li, L., Xu, R., et al. (2020). EphB2 Represents an Independent Prognostic Marker in Patients with Gastric Cancer and Promotes Tumour Cell Aggressiveness. *J. Cancer* 11, 2778–2787. doi:10.7150/jca.38098

Ying, Z., Li, Y., Wu, J., Zhu, X., Yang, Y., Tian, H., et al. (2013). Loss of miR-204 Expression Enhances Glioma Migration and Stem Cell-like Phenotype. *Cancer Res.* 73, 990–999. doi:10.1158/0008-5472.can-12-2895

Yu, G., Gao, Y., Ni, C., Chen, Y., Pan, J., Wang, X., et al. (2011). Reduced Expression of EphB2 Is Significantly Associated with Nodal Metastasis in Chinese Patients with Gastric Cancer. *J. Cancer Res. Clin. Oncol.* 137, 73–80. doi:10.1007/s00432-010-0861-4

Yu, M., Liang, W., Wen, S., Zhao, T., Zhu, M. X., Li, H. H., et al. (2014). EphB2 Contributes to Human Naive B-cell Activation and Is Regulated by miR-185. *FASEB j.* 28, 3609–3617. doi:10.1096/fj.13-247759

Zhao, C., Wang, A., Lu, F., Chen, H., Fu, P., Zhao, X., et al. (2017). Overexpression of Junctional Adhesion Molecule-A and EphB2 Predicts Poor Survival in Lung Adenocarcinoma Patients. *Tumour Biol.* 39, 1010428317691000. doi:10.1177/1010428317691000

Zhou, F., Wang, B., Wang, H., Hu, L., Zhang, J., Yu, T., et al. (2021). circMELK Promotes Glioblastoma Multiforme Cell Tumorigenesis through the miR-593/EphB2 axis. *Mol. Ther. - Nucleic Acids* 25, 25–36. doi:10.1016/j.omtn.2021.05.002

Zisch, A. H., Kalo, M. S., Chong, L. D., and Pasquale, E. B. (1998). Complex Formation between EphB2 and Src Requires Phosphorylation of Tyrosine 611 in the EphB2 Juxtamembrane Region. *Oncogene* 16, 2657–2670. doi:10.1038/sj.onc.1201823

Zisch, A. H., Pazzagli, C., Freeman, A. L., Schneller, M., Hadman, M., Smith, J. W., et al. (2000). Replacing Two Conserved Tyrosines of the EphB2 Receptor with Glutamic Acid Prevents Binding of SH2 Domains without Abrogating Kinase Activity and Biological Responses. *Oncogene* 19, 177–187. doi:10.1038/sj.onc.1203304

Conflict of Interest: The authors declare that the research was conducted in the absence of any commercial or financial relationships that could be construed as a potential conflict of interest.

Publisher's Note: All claims expressed in this article are solely those of the authors and do not necessarily represent those of their affiliated organizations, or those of the publisher, the editors and the reviewers. Any product that may be evaluated in this article, or claim that may be made by its manufacturer, is not guaranteed or endorsed by the publisher.

frontiers in Cell and Developmental Biology

REVIEW
published: 10 February 2022
doi: 10.3389/fcell.2022.766653

Nerve Dependence in Colorectal Cancer

Lincheng Zhang[1], *Ludi Yang*[2], *Shuheng Jiang*[3]* *and Minhao Yu*[1]*

[1]*Department of Gastrointestinal Surgery, Renji Hospital, School of Medicine, Shanghai Jiao Tong University, Shanghai, China,* [2]*Department of Ophthalmology, Ninth People's Hospital, Shanghai Jiao Tong University School of Medicine, Shanghai, China,* [3]*State Key Laboratory of Oncogenes and Related Genes, Shanghai Cancer Institute, Ren Ji Hospital, Shanghai Jiao Tong University School of Medicine, Shanghai, China*

Cancerous invasion of nerves has been reported in a list of malignant tumors as a high-risk pathological feature and marker of poor disease outcome especially in neurotrophic cancers (such as in pancreas and prostate), indicating that although once neglected, nerves could have played a pivotal role in tumorigenesis and cancer progression. In colorectal cancer, perineural invasion, a specific form of tumor-nerve interaction referring to the identification of tumor cells in proximity to the nerve, has been recognized as a strong and independent prognosis predictor; denervation of autonomic nerves and enteric nerves have shown that the existence of these nerves in the gut are accompanied by promoted cancer proliferation, further supporting that nerve is a potential accomplice to shield and nurture tumor cells. However, the precise role of nerve in CRC and the pattern of interaction between CRC cells and nerve has not been unveiled yet. Here we aim to review some basic knowledge of the importance of nerves in CRC and attempt to depict a mechanistic view of tumor-nerve interaction during CRC development.

Keywords: colorectal cancer, tumor-nerve interaction, perineural invasion, mechanism, tumor microenvironment

OPEN ACCESS

Edited by:
Daniele Vergara,
University of Salento, Italy

Reviewed by:
Marina Damato,
University of Salento, Italy
Sara Sergio,
University of Salento, Italy

***Correspondence:**
Minhao Yu
fishmeangood@163.com
Shuheng Jiang
shjiang@shsci.org

Specialty section:
This article was submitted to Molecular and Cellular Oncology, a section of the journal Frontiers in Cell and Developmental Biology

Received: *29 August 2021*
Accepted: *13 January 2022*
Published: *10 February 2022*

Citation:
Zhang L, Yang L, Jiang S and Yu M (2022) Nerve Dependence in Colorectal Cancer. Front. Cell Dev. Biol. 10:766653. doi: 10.3389/fcell.2022.766653

BACKGROUND

Colorectal cancer (CRC) has been steadily ranked as one of the most common malignant tumors and a dominating cause of death in cancer patients. Although diverse pathogenic pathways have been identified in colorectal cancer, very few of them are targeted in clinical therapy.

It was not until previous decades that the significance of nerves in tumors received much attention. Recent studies have demonstrated that just as lymphovascular invasion, nerve involvement also lends support to tumor progression and dissemination, suggesting that neoplastic invasion of nerves might be another key hallmark of cancer. In clinical practice, perineural invasion (PNI), defined as at least 33% of nerve fiber circumference surrounded by cancer cells or cancer cells directly found in any layer of the nerve sheath (i.e. epineurium, perineurium or endoneurium) (Liebig et al., 2009), is most commonly used to evaluate the extent of nerve involvement. First described in head and neck cancer, the perineural invasion has now been reported in a list of malignant tumors including those in the pancreas, prostate, breast, colon and rectum, stomach, etc. Among all these cancers, despite the varying incidence of perineural invasion, PNI positive patients are remarkably susceptible to cancer progression and relapse, denoting novel pathways of tumorigenesis and metastasis to be discovered.

In colorectal cancer, perineural invasion occurs far less frequently than in pancreatic cancer, but once confirmed, it is responsible for rapid disease progression and remarkably unfavorable clinical outcomes. In most studies, detection rate of PNI in colorectal cancer stays less than 30%, suggesting a

TABLE 1 | Significance of perineural invasion in predicting prognosis.

Cancer	Stage	Treatment	Incidence of PNI(%)	Clinical significance	Ref
CRC	T1-2,N0-2,M0	Surgical resection and/or chemotherapy	2.3	PNI is an independent high-risk factor of lymph node metastasis(LNM); lymph node metastasis rate is 40.7% in PNI-positive patients compared to 19.0% in PNI-negative patients	(Lee et al., 2020; Martínez Vila et al., 2020; Mo et al., 2020)
colon	T1-T2	Surgical resection	3.4	PNI negatively influences DFS together with LNM (HR = 3.641, $p < 0.001$)	
CRC	T1	Endoscopic resection	3.8		
CRC	Tis-T1N0M0	Mixed (surgery, endoscopy, chemotherapy, radiotherapy)	11.1	PNI is among one of the predictors in the survival nomogram to predict 1-year, 3-years and 5-years OS	Liu et al. (2020)
Rectum	locally advanced(T3/T4, N+)	Surgical resection with/without neoadjuvant chemoradiotherapy	24.3	3-years DFS rate is 76.8% in PNI-negative patients compared to 26.2% in PNI-positive patient 3-years OS rate is 82.8% in PNI-negative patients compared to 31.0% in PNI positive patients($p < 0.001$)	Sun et al. (2019)
Colon	II	Surgical resection with/without adjuvant chemoradiotherapy	3.8	PNI attributes to 32.1% increase of 5-years mortality	Skancke et al. (2019)
Colon	I-III	Surgical resection with/without adjuvant chemotherapy	18.8	5-years DFS is 85.4% in PNI-negative patients compared to 57.8% in PNI-positive patients($p < 0.001$) 5-years OS rate is 76.6% in PNI-negative patients compared to 53.2% in PNI positive patients($p < 0.001$) PNI is associated with higher risk of disease recurrence and cancer death($p < 0.001$)	Leijssen et al. (2019)

DFS, disease-free survival; OS, overall survival; HR, hazard ratio; MMR, mismatched repair defects; DSS, disease-specific survival.

relatively low incidence of nerve involvement. *In-vitro* 3D migration assay also revealed that neurotrophic growth was far less frequent for colon and rectal cancer cells than pancreatic cancer cells (Liebl et al., 2013). However, these PNI-positive CRC patients suffered from severely compromised disease outcomes. As an independent risk factor of CRC prognosis, PNI culminates in more than 20% decrease in overall and disease-free survival. Several large-population studies further point out that PNI increases the risk of lymph node metastasis, another pathologic feature associated with poor disease prognosis, and cancer-related mortality. The latest studies on the association between PNI and disease prognosis are summarized in **Table 1** (Leijssen et al., 2019; Skancke et al., 2019; Sun et al., 2019; Lee et al., 2020; Liu et al., 2020; Martínez Vila et al., 2020; Mo et al., 2020). Here we review the role of nerves in colorectal cancer, identify nerve dependence in colorectal cancer and illustrate underlying molecular mechanisms of perineural invasion.

NERVES IN COLORECTAL CANCER

Colon and rectum are richly innervated by autonomic nerves and enteric nerves--presumably deal for cancer cells to take advantage of--yet the precise role of nerve in colorectal cancer has not been delineated. Colorectal distribution of nerves can be categorized into two groups: extrinsic innervation incorporates sympathetic and parasympathetic input from the brain and spinal cord, while intrinsic innervation refers to the enteric nervous system, which integrates signals from autonomic input and controls gut secretion, reabsorption and motility. Ascending and transverse colon receives sympathetic innervation through superior mesenteric plexus and parasympathetic innervation through vagus nerve; descending colon and upper rectum receives sympathetic innervation *via* inferior mesenteric plexus, lower rectum *via* inferior hypogastric plexus, with common parasympathetic input through the pelvic splanchnic nerve. Both colon and rectum are regulated by the enteric nervous system (ENS), namely the myenteric (Auerbach's) and submucosal (Meissner) plexus. Together these nerves orchestrate the normal functioning of gut **(Table 2)**.

Histopathological Changes of Nerves in CRC

Structural disarrangement of nerve tissues in CRC patients has been reported by several studies, indicating putative roles of autonomic and enteric nerves in the development of CRC. A retrospective study of 90 CRC patients tested the immunoreactivity of tyrosine hydroxylase and vesicular acetylcholine transporter respectively in the resected tissue to track down sympathetic and parasympathetic nerves. Results denoted the existence of both sympathetic and parasympathetic nerves in proximity to the tumor. Sympathetic nerves are found in the stroma closer to tumor

TABLE 2 | Physiological innervation of nerves in CRC and denervation studies.

	Nerve innervation	Location				Method of denervation	Effect of denervation
		Ascending colon	Descending colon	Upper rectum	Lower rectum		
Extrinsic	Sympathetic	Thoracic splanchnic nerve (superior mesenteric plexus)	Lumbar splanchnic nerve(inferior mesenteric plexus)	Lumbar splanchnic nerve(inferior mesenteric plexus)	Sacral splanchnic nerve(inferior hypogastric plexus)	Beta receptor blockade;	↓cancer cell proliferation and survival *in vitro*; Probably improves CRC patients' clinical outcome
	Sensory			Pelvic splanchnic nerve		/	Unclear
	Parasympathetic	Vagus nerve	Pelvic splanchnic nerve			M3R blockade	↓cancer cell proliferation, tumor number and size in vitro and in vivo.
Intrinsic	Myenteric plexus					Chagasic megacolon, BAC treatment;	↓preneoplastic and neoplastic lesions ↓risk of developing colon cancer
	Submucosal plexus					/	Unclear

site, while parasympathetic nerves are located away from tumor cells (Zhou et al., 2018). Distribution of β2A receptors appears to be denser in CRC-invaded ganglia and larger nerve bundles, compared to the nervous tissue in non-tumor sections (11). Besides, an increasingly diffuse and dense expression pattern of β2A receptors is observed from the normal colon tissue to G1, G2 and G3 differentiated adenocarcinoma. There is also a significant association between *β2* adrenergic receptor expression and tumor size, tumor invasion or lymph node metastasis. Several studies have reported abnormal morphology of enteric nerves. Significant loss of myenteric and submucosal plexuses was noticed in CRC, especially in more progressive types (Godlewski, 2010; Ciurea et al., 2017); in sigmoid and rectal cancer, disruption of normal ENS structures are observed, with an irregular border of the myenteric plexus and deformation of their structures, and, simultaneously, a larger area of extracellular matrix surrounding the myenteric plexuses with more abundant collagen fibers in tumor-infiltrated colon walls (Zauszkiewicz-Pawlak et al., 2017). Myelin-like structures that usually appear in degeneration of nerves are observed near the tumor invasion site. A marked drop in the density of enteric glial cells was also observed corresponding to the increase in tumor grading (Jaiswal et al., 2020).

Denervation Studies

Sustained efforts have been made in denervation studies to ascertain whether loss of nerve innervation would affect tumor initiation and survival, providing functional insights into the role of nerves in CRC.

Research of parasympathetic denervation mainly considers ablation of muscarinic receptors. Targeting muscarinic acetylcholine receptor 3 (M3R) through selective and non-selective antagonists (*p*-fluorohexahydro-sila-difenidol hydrochloride and atropine respectively) repressed H508 colon cancer cell proliferation by approximately 40% whilst acetylcholinesterase inhibitors were capable of stimulating tumor growth by 2 to 2.5 fold (Cheng et al., 2008), indicating participation of cholinergic signaling in tumor development. Similar inhibitory effects were also observed in murine colon cancer models as epithelial proliferation, tumor size and quantity were greatly diminished in mice deficient of CHRM3, the coding gene of M3R (Raufman et al., 2008).

Other denervation studies have been focused on enteric nerve denervation. Chagas disease, a trypanosomiasis-related disease that induces megacolon and damage to myenteric neurons, seems to be an existing example of how myenteric neuronal activity negatively associates with colon carcinogenesis. Experiments on Wistar rats suggested that chronic infection with Trypanosoma cruzi led to fewer tumors when treated with dimethylhydrazine(DMH), a specific chemical carcinogen to induce CRC (Oliveira et al., 2001). A review of histopathological findings from 894 chagasic megacolon patients revealed that none of those patients developed colon cancer(Garcia et al., 2003); previous studies on surgical specimens from Chagas patients who underwent megacolon resection confirmed a decline in the density of myenteric neurons and correspondingly reduced risk for colon cancer [(Kannen et al.,

2015)]. To prove the tumorigenic effect of myenteric nerves, *in-vivo* experimental approach has been established to mimic myenteric denervation in chagasic megacolon through benzalkonium chloride (BAC) treatment. Results showed that BAC-treated rats are less susceptible to DMH, since both preneoplastic and neoplastic lesions were reduced compared to those whose myenteric innervation were intact (Garcia et al., 1996; Vespúcio et al., 2008; Kannen et al., 2015).

Although few studies have directly investigated changes in tumors upon sympathetic denervation, many researchers have reported effects of beta receptor antagonists. Studies of multiple CRC cell lines demonstrated that beta blockade inhibits cell viability and proliferation in a dose-dependent manner, probably through EGFR-Akt/ERK1/2 pathway, cell cycle arrest and apoptosis followed by suppression of β2 signaling (Coelho et al., 2015; Chin et al., 2016). Meanwhile, various clinical studies were conducted in Europe to measure the effect of beta receptor blockers on CRC patient outcomes, but no definitive conclusion has been made. Stage-specific benefit of beta blockade at diagnosis (particularly selective beta blockers) was once detected, as overall and CRC-specific mortality markedly decreased in stage IV patients prescribed with beta blockers (Jansen et al., 2014). However, several large population-based studies have reported that long-term beta blocker usage may contribute to increased risk of CRC progression, and little association was found between pre- or post-diagnostic beta blockade and improved clinical outcomes (Jansen et al., 2012; Hicks et al., 2013; Jansen et al., 2017). Perioperative application of beta blockers, on the other hand, seems to be more promising in improving CRC patients' prognosis. The latest study demonstrated that preoperative beta blocker treatment results in reduced post-operative complications and mortality in rectal cancer (Ahl et al., 2020); it was also previously found that combine perioperative blockade of β receptor and COX2 leads to lower recurrence rate and improvement in tumor biomarkers associated with epithelial-to-mesenchymal transition, immune microenvironment and CRC-related inflammatory pathways (Haldar et al., 2020).

UNDERLYING MECHANISMS OF PERINEURAL INVASION

Initially, cancer cells were thought to spread along the nerves passively because perineural connective tissues are loose paths with low resistance. With a distensible space between nerves and outer sheaths, tumor cells might be capable of lurk in those spaces without showing any symptoms. Later, however, ultrastructural studies revealed the presence of densely organized collagen and basement membrane constituting the nerve sheath, which should have highly resisted the invasion of cancer cells, indicating that tumors could take the initiative to disseminate through nerves (Liebig et al., 2009). Through concerted efforts of neurotrophic factors, neurotransmitters, adhesion molecules, matrix metalloproteinases, glial cells and tumor stem cells, a perineural niche favoring cancerous infiltration is eventually established, and neoplastic cells are guided towards this route.

Neurotrophic Factors

Neurotrophic factors represent a list of proteins binding to tyrosine kinase receptors to activate downstream signaling pathways in the growth and differentiation of nerves, comprising nerve growth factor (NGF), brain-derived neurotrophic factor (BDNF), glial cell-derived neurotrophic factor (GDNF), neurotrophin-3 (NT-3) and neurotrophin-4/5 (NT-4/5). Their high-affinity receptors include tropomyosin-related kinase (Trk), preferring NGF, BDNF and NT-3/4, while GDNF family receptor (GFRα)/RET prefers GDNF. Each ligand-receptor complex, leading to phosphorylation of various downstream pathways including PI3K/Akt and Ras/MAPK, is responsible for recruitment of specific type of nerves during nerve development. NGF/TrkA signaling dominates in the establishment of sympathetic innervation, GDNF/GFRα in parasympathetic innervation and BDNF/TrkB in sensory innervation. Multifaceted interactions between epithelium and neurons in embryonic establishment of glandular innervation are summarized by Zahalka et al. (Zahalka and Frenette, 2020). In physiological conditions, epithelial mesenchyme secrets neurotrophins to bind their specific receptors, forming a ligand-receptor complex to be engulfed by axons and retrogradely transported to the soma, thus stimulating downstream transcription, axonogenesis, and nerve recruitment to the target organ. Once morphogenesis of their target organ is accomplished, neurotrophic factors cease to accumulate (Klein, 1994).

However, these molecules indicated in embryonic development of nervous system can be re-stimulated in the context of cancer. Neurotrophic factors such as NGF and GDNF can be released either by tumor cells or neurons (Amit et al., 2016). In colorectal cancer, abnormality in TrkA has been recurrently reported. Chromosomal rearrangement of TrkA coding gene NTRK1 produces NTRK1 fusion proteins and upregulates TrkA kinase activity, followed by oncogenic phosphorylation of downstream proteins and hypersensitivity to NGF binding. TPM3-NTRK1 is the most commonly identified fusion gene, as TrkA itself was originally separated from TPM3-TrkA fusion gene of colon carcinoma, with a detection rate of 0.5–1%. Other fusion forms such as TPR-NTRK1 and LMNA-NTRK1 have also been reported. Indeed, TrkA positive patients may represent a minority of patients with satiable response to TrkA kinase inhibitors. In resected colon adenocarcinoma, cytoplasmic immunoreactivity to TrkA was abundantly detected (Ardini et al., 2014). *In vitro* experiments confirmed the presence of typical TPM3-NTRK1 fusion gene in KM12 human CRC cell line and demonstrated strong effects of TrkA inhibitor on suppressing cancer cell proliferation. TrkA fusion protein was also discovered in a case of liver metastasis of CRC, and application of Entrectinib, a selective Trk inhibitor, managed to achieve clinical partial response (Sartore-Bianchi et al., 2016).

Other neurotrophic factors such as brain-derived neurotrophic factor (BDNF) and glial cell-derived neurotrophic factor (GDNF), have been shown to induce

tumor migration *via* upregulation of VEGF and activation of p38 and PI3K/Akt signaling pathway (Huang et al., 2014; Huang et al., 2015). *In-vitro* studies in two human colon cancer cell lines, HCT116 and SW480, proved that migratory activity increases with the concentration of BDNF and GDNF respectively, paralleled with increased expression of VEGF, MAPK and PI3K/Akt-associated proteins at transcription and translation level.

So far, it has not been fully revealed in CRC how neurotrophic factors get engaged in perineural invasion(PNI), but accumulating evidence in other types of cancer indicates crucial importance of neurotrophin signaling through the development of nerve invasion. In pancreatic cancer, GDNF signaling is a characterized mechanism of PNI (Gil et al., 2010; He et al., 2014). *In-vitro* co-culture of dorsal root ganglia and human pancreatic adenocarcinoma cell lines and *in-vivo* murine sciatic nerve models of PNI showed that nerves release GDNF, and induce polarized neurotrophic migration of cancer cells *via* downstream pathways of RET. Tumor invasion of nerves is upregulated upon GDNF induction and is greatly diminished when GDNF/GFRa1/RET pathway is suppressed. Similar changes have been reported in prostate cancer, as GFRα-1/RET binding of GDNF potentiates invasion and proliferation of cancer cells (Ban et al., 2017). NGF and GDNF were also found to be more abundantly expressed in patients with PNI and higher Gleason scores (Baspinar et al., 2017). In salivary adenoid cystic carcinoma (SACC), NT-3/TrkC signaling enhances *in-vitro* cancer cell migration in the presence of Schwann cells: A comparative study of 78 SACC and 25 normal tissue specimens demonstrated higher expression of NT-3 in tumor cells surrounding the nerves and TrkC in tumor-invaded nerves; statistics proved that level of NT-3/TrkC expression is strongly correlated with the occurrence of PNI (Li et al., 2019). BDNF/TrkB-dependent Schwann-like differentiation was also discovered in human SACC cell lines; both TrkB and S100A4, a surface marker of Schwann cell, are found to be significantly associated with PNI (Jia et al., 2015; Shan et al., 2016).

It can be concluded that neurotrophins have multifaceted roles in tumor-nerve crosstalk of PNI, as both tumor cells and neurons are able to release neurotrophic factors. These growth factors might be secreted by neoplastic epithelium in the same way as embryonic neurogenesis to summon newborn nerves to the invasive front, facilitating direct contact between cancer cells and nerves; or they might be secreted by nerves to polarize neurotrophic migration of cancer cells towards resident nerves, as indicated in pancreatic cancer, prostate cancer, SACC, etc. Further research is needed in CRC to unveil the role of neurotrophic factors in bridging tumor and nerve.

Neurotransmitters

As the main effector molecules released by nerve fibers, neurotransmitters may serve as a crucial messenger between tumor and nerve. Upregulated adrenergic signaling has been reported in colorectal cancer. As indicated in several pathology reports of CRC tissue, distribution of beta receptors appears to be denser in the tumor site (Godlewski, 2010; Ciurea et al., 2017), and such phenomenon is usually accompanied by worse prognosis. Some studies further demonstrate a direct relationship between adrenergic transmitters and tumor proliferation in CRC. An *in-vitro* study of Wong et al. shows COX-2 dependent stimulation of adrenaline on human colon adenocarcinoma HT-29 cell proliferation (Wong et al., 2011), as adrenaline activates COX-2, VEGF, PGE2 and MMP-9 downstream, which can be rescued by COX-2 inhibitors and beta receptor antagonists. Besides, adrenaline-induced COX-2 upregulation has been found to suppress immunity in coordination with inflammatory signals by enhancing expression of IDO and IL-10 in macrophages, thus attenuating the proliferation and IFN-γ production of $CD8^+$ T cells and facilitating immune escape in colon cancer (Muthuswamy et al., 2017). Han et al. have revealed the role of epinephrine in colorectal cancer as well. By targeting the CREB1-miR-373 axis and subsequent downregulation of tumor suppressor gene TIMP2 and APC, epinephrine plays a stimulatory role in the proliferation and dissemination of human colon cancer cells *in vitro* and *in vivo* (Han et al., 2020).

Cholinergic signaling via acetylcholine (Ach) and its receptors constitutes another regulating pathway of tumor-nerve crosstalk. Mounting evidence has shown that muscarinic receptor participates in the development of CRC. Muscarinic acetylcholine receptor 1 (M1R) and 3 (M3R) are the predominant types distributed in the gut, through which enteric and autonomic nervous system innervates intestinal smooth muscle tone, with M3R notably over-expressed in CRC lesions. Expression of CHRM3, coding gene of M3R robustly increased by 128 fold in colon adenocarcinoma compared with that in adjacent normal epithelium; immunostaining also shows over-expression of M3R in cancerous tissue in contrast to the unaffected epithelium (Cheng et al., 2017). CHRM3-deficient mice develop fewer and smaller colon neoplasm induced by Azoxymethane, whereas CHRM1 knockout or dual knockout didn't have much visible impact on tumor size or quantity (Cheng et al., 2014).

Due to ubiquitous distribution and multi-target effect of adrenergic and cholinergic transmitters, it would be troublesome to distinguish whether neurotransmitters support cancer development through direct local interaction with tumor or via systemic neuroendocrine signaling activated by other CRC-related events. Allen et al. have identified a feed-forward loop in ovarian cancer cells, that in response to sustained adrenergic signaling, tumor cells secrete BDNF, which then promotes intratumoral innervation via host neurotrophic receptor tyrosine kinase 2 (TrkB) receptors (Allen et al., 2018), denoting that sympathetic pathway might be an upstream inducer of tumor innervation. Parasympathetic signaling through acetylcholine promotes matrix metalloproteinase 1 (MMP1) expression, facilitating the invasion of HT29 and H508 human colon cancer cells, which can be rescued by atropine and anti-MMP1 antibody (Raufman et al., 2011). Potential mechanistic pathway downstream of M3R activation was reviewed in detail by Ali et al. (Ali et al., 2021), which involves stimulation of protein kinase C-α (PKCα), MMP1 and MMP7 transcription, EGFR signaling and PI3K/Akt pathway and ultimately contributes to tumor growth, dissemination and

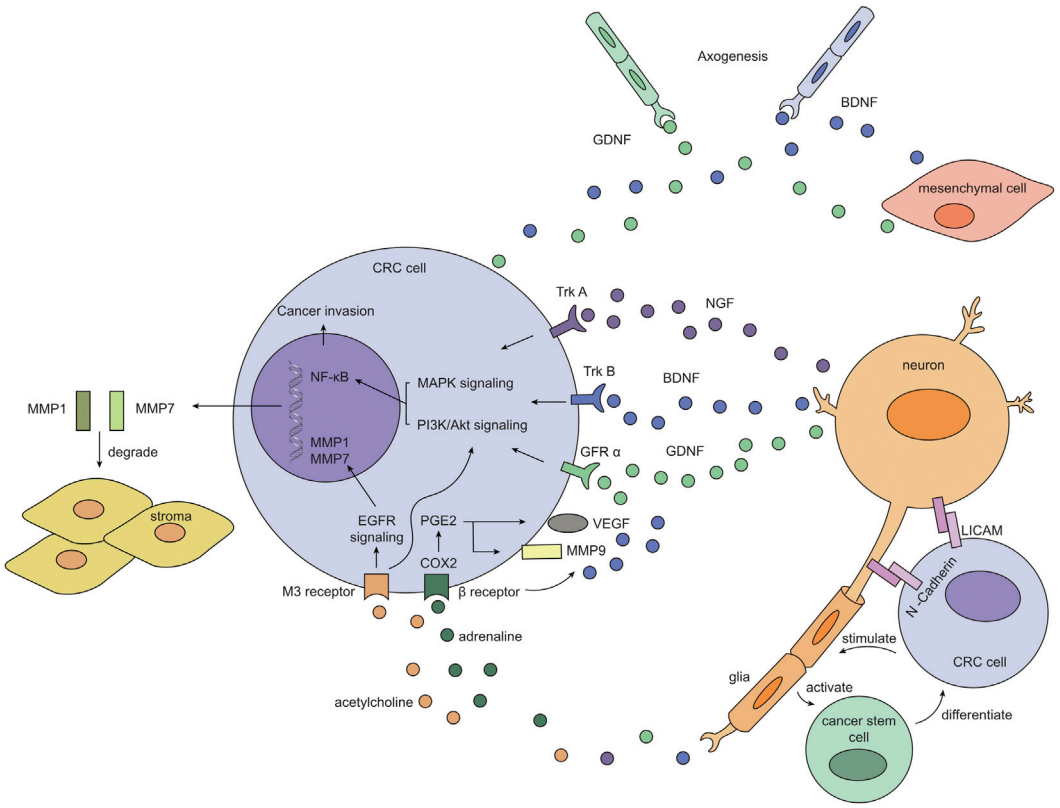

FIGURE 1 | Possible pattern of interaction between CRC cell and adjacent nerve. Neurons secret neurotrophic factors such as NGF, BDNF and GDNF, which then form signaling complex with their cognate receptors (TrkA, TrkB and GFRα respectively) on CRC cells. These complexes initiate intracellular MAPK and PI3K/Akt pathway and eventually turn on NF-κB transcription, facilitating tumor survival and invasion. Besides, neurotransmitters released by neurons also switch on growth pathways in CRC cells and prompts extracellular matrix remodeling: adrenaline binds to *β* receptor and activates PGE2/COX2 axis, resulting in increased expression of VEGF and MMP9; acetylcholine binds to M3 receptor, which upregulates EGFR signaling and downstream production of MMP1 and MMP7. 2) Tumor cells themselves and mesenchymal cells may also release BDNF and GDNF to bind TrkB and GFRα expressed on newborn nerves, assisting in neurogenesis in the tumor microenvironment, thus "placing" nerves in proximity to tumor cells. Adhesion molecules such as L1CAM and N-Cadherin are expressed on CRC cells and neurons, allowing for further migration and dissemination of cancer cells along the adjacent nerve. 3) Glia cells may be stimulated by CRC cells to activate cancer stem cell, which serves as a replenishing pool for CRC cells, constituting a positive feedback loop.

invasion. Thus, neurotransmitters and their receptors might work as a stimulator to trigger invasive acts of CRC cells, yet more studies are required to identify the role of autonomic signaling in tumor-nerve interaction.

Adhesion Molecules

During the maturation of the nervous system, a wide range of cell-matrix and cell-cell interactions are required to facilitate neuronal migration, axon/dendrite outgrowth and synaptogenesis, mainly mediated by the immunoglobulin superfamily of neural cell adhesion molecules (CAMs). L1CAM is a crucial family of adhesion molecules comprising L1 and its close homolog (CHL1), NrCAM and neurofascin. Their extracellular domain consisted of immunoglobulin (Ig)-like and fibronectin type III-homologous (FnIII) domains, specializes in modulating intercellular interaction, particularly at synaptic cleft to assist in synapse forming and functioning. L1 also stimulates signal transduction related to neuron migration and neurite outgrowth, either by serving as signaling molecule itself or as co-receptor(Schmid and Maness, 2008; Sytnyk et al., 2017). By interacting with *β1* integrin, L1 helps to upregulate cell-matrix adhesion and initiates downstream cascade, resulting in ERK1/2 MAPK signaling and transcriptional activation of a series of proteins that upregulates cell motility, including integrin and Rac1.

A handful of researchers have proposed that L1CAM represents a potential marker for cancer invasiveness and progression of CRC. It was recurrently reported that L1 expression was correlated with increased tendency of metastasis, along with advanced cancer stage, high-risk pathological features (including poor differentiation grade, solid cancer nests and tumor budding) and severely shortened survival (Boo et al., 2007; Kaifi et al., 2007; Tampakis et al., 2020; Tieng et al., 2020). Transcription of L1CAM mRNA was significantly active in the invasive front compared to the center of tumor especially in patients with nodal involvement; besides, expression levels of L1CAM and ERK1/2 in CRC tissue is associated with lymph node metastasis, indicating supportive role

of L1CAM-associated in CRC dissemination (Kajiwara et al., 2011; Fang et al., 2020). Regretfully, perineural invasion status was absent in most of these studies, making it difficult to identify whether L1 also helps tumor cells to infiltrate the nerves. Recently, it has been reported that colorectal neoplastic cells preferentially adhere to enteric neurons, supporting further dissemination of tumor cells. Through tumor-nerve adhesion mediated by L1CAM and N-Cadherin, CRC tumor cells can migrate along enteric neurons *in vitro*, representing a possible route for CRC perineural invasion due to the wide distribution of enteric nerves throughout the colon and rectum (Duchalais et al., 2018).

In pancreatic cancer, there is a strong association between L1CAM expression in cancer tissue and perineural invasion (Ben et al., 2010). By constructing *in-vitro* model of PNI, it was revealed that L1CAM secreted by Schwann cells attracts cancer cells into perineural niche via MAPK pathway and enhances expression of metalloproteinase (MMP) in cancer cells to facilitate penetration of extracellular matrix (Na'ara et al., 2019). Such process proves to be L1-dependent as neural invasion is greatly impaired after treatment of L1CAM antibody. Considering dual identity of L1CAM in nerve development and neoplastic invasion, more work remains to be done to pinpoint the position of L1CAM in neural invasion of CRC.

CONCLUDING REMARKS

Nerve dependence has been identified in several neurotrophic cancers, such as pancreatic cancer and prostate cancer, with numerous studies focused on deciphering potential mechanisms of perineural invasion. In contrast, the role of nerves in CRC has received far less attention, possibly due to low incidence of PNI in CRC (less than 30%). Currently, established models for neural invasion (Amit et al., 2016) (such as *in-vitro* dorsal root ganglia assay, 3D Schwann cell outgrowth and migration essay, etc.) are rarely applied in CRC-related studies, making it difficult to pattern nerve involvement in a systematic approach. Although the pattern of direct interaction between cancer cells and nerves has not been clearly elucidated, a handful of clues have suggested that a specialized microenvironment might be established surrounding cancer cells and adjacent nerves, with neurotrophins, neurotransmitters, adhesion molecules, matrix metalloproteinase and other mediators highly enriched in this niche **(Figure 1)**. It was also revealed that enteric glial cells, component of the neural sheath, might be activated by tumor cells to assist in expansion of cancer stem cells (Valès et al., 2019). As indicated in other types of cancers, neurotrophins may be secreted by neurons, mesenchyme or tumor cells, contributing to neurogenesis and further tumor survival or invasion; Adhesion molecules may serve as the "glue" between cancer cell and nerve to potentiate neural invasion; MMPs released by tumor cells help to degrade extracellular connective tissues, facilitating protrusion into the neural sheath; chemotaxis recruit other components and establish a favorable niche for neural tracking. Nerves may also advocate tumor growth by releasing neurotransmitters and activating multiple downstream pathways such as MAPK and PI3K/Akt signaling. Here we have illustrated the clinical significance of perineural invasion, a specific form of tumor-nerve, and we have exhibited a possible mechanistic view of nerve participation in CRC. Further studies need to be carried out to focus directly on local interaction between cancer cells and neurons or glial cells to provide solid evidence of nerve dependence in CRC.

AUTHOR CONTRIBUTIONS

All authors listed have made a substantial, direct, and intellectual contribution to the work and approved it for publication.

FUNDING

Cultivation Fund for Clinical Research of Renji Hosiptal Affiliated to Shanghai Jiao Tong University School of Medicine. (PYIII20-14).

REFERENCES

Ahl, R., Matthiessen, P., Fang, X., Cao, Y., Sjolin, G., Lindgren, R., et al. (2020). β-Blockade in Rectal Cancer Surgery. *Ann. Surg.* 271 (1), 140–146. doi:10.1097/sla.0000000000002970

Ali, O., Tolaymat, M., Hu, S., Xie, G., and Raufman, J-P. (2021). Overcoming Obstacles to Targeting Muscarinic Receptor Signaling in Colorectal Cancer. *Int. J. Mol. Sci.* 22 (2). 716. doi:10.3390/ijms22020716

Allen, J. K., Armaiz-Pena, G. N., Nagaraja, A. S., Sadaoui, N. C., Ortiz, T., Dood, R., et al. (2018). Sustained Adrenergic Signaling Promotes Intratumoral Innervation through BDNF Induction. *Cancer Res.* 78 (12), 3233–3242. doi:10.1158/0008-5472.can-16-1701

Amit, M., Na'ara, S., and Gil, Z. (2016). Mechanisms of Cancer Dissemination along Nerves. *Nat. Rev. Cancer* 16 (6), 399–408. doi:10.1038/nrc.2016.38

Ardini, E., Bosotti, R., Borgia, A. L., De Ponti, C., Somaschini, A., Cammarota, R., et al. (2014). The TPM3-NTRK1 Rearrangement Is a Recurring Event in Colorectal Carcinoma and Is Associated with Tumor Sensitivity to TRKA Kinase Inhibition. *Mol. Oncol.* 8 (8), 1495–1507. doi:10.1016/j.molonc.2014.06.001

Ban, K., Feng, S., Shao, L., and Ittmann, M. (2017). RET Signaling in Prostate Cancer. *Clin. Cancer Res.* 23 (16), 4885–4896. doi:10.1158/1078-0432.ccr-17-0528

Baspinar, S., Bircan, S., Ciris, M., Karahan, N., and Bozkurt, K. K. (2017). Expression of NGF, GDNF and MMP-9 in Prostate Carcinoma. *Pathol. - Res. Pract.* 213 (5), 483–489. doi:10.1016/j.prp.2017.02.007

Ben, Q.-W., Wang, J.-C., Liu, J., Zhu, Y., Yuan, F., Yao, W.-Y., et al. (2010). Positive Expression of L1-CAM Is Associated with Perineural Invasion and Poor Outcome in Pancreatic Ductal Adenocarcinoma. *Ann. Surg. Oncol.* 17 (8), 2213–2221. doi:10.1245/s10434-010-0955-x

Boo, Y.-J., Park, J.-M., Kim, J., Chae, Y.-S., Min, B.-W., Um, J.-W., et al. (2007). L1 Expression as a Marker for Poor Prognosis, Tumor Progression, and Short Survival in Patients with Colorectal Cancer. *Ann. Surg. Oncol.* 14 (5), 1703–1711. doi:10.1245/s10434-006-9281-8

Cheng, K., Samimi, R., Xie, G., Shant, J., Drachenberg, C., Wade, M., et al. (2008). Acetylcholine Release by Human colon Cancer Cells Mediates Autocrine

Stimulation of Cell Proliferation. *Am. J. Physiology-Gastrointestinal Liver Physiol.* 295 (3), G591–G597. doi:10.1152/ajpgi.00055.2008

Cheng, K., Shang, A. C., Drachenberg, C. B., Zhan, M., and Raufman, J.-P. (2017). Differential Expression of M3 Muscarinic Receptors in Progressive colon Neoplasia and Metastasis. *Oncotarget* 8 (13), 21106–21114. doi:10.18632/oncotarget.15500

Cheng, K., Xie, G., Khurana, S., Heath, J., Drachenberg, C. B., Timmons, J., et al. (2014). Divergent Effects of Muscarinic Receptor Subtype Gene Ablation on Murine colon Tumorigenesis Reveals Association of M3R and Zinc finger Protein 277 Expression in colon Neoplasia. *Mol. Cancer* 13, 77. doi:10.1186/1476-4598-13-77

Chin, C.-C., Li, J.-M., Lee, K.-F., Huang, Y.-C., Wang, K.-C., Lai, H.-C., et al. (2016). Selective β2-AR Blockage Suppresses Colorectal Cancer Growth through Regulation of EGFR-Akt/ERK1/2 Signaling, G1-phase Arrest, and Apoptosis. *J. Cel. Physiol* 231 (2), 459–472. doi:10.1002/jcp.25092

Ciurea, R. N., Rogoveanu, I., Pirici, D., Târtea, G.-C., Streba, C. T., Florescu, C., et al. (2017). B2 Adrenergic Receptors and Morphological Changes of the Enteric Nervous System in Colorectal Adenocarcinoma. *Wjg* 23 (7), 1250–1261. doi:10.3748/wjg.v23.i7.1250

Coelho, M., Moz, M., Correia, G., Teixeira, A., Medeiros, R., and Ribeiro, L. (2015). Antiproliferative Effects of β-blockers on Human Colorectal Cancer Cells. *Oncol. Rep.* 33 (5), 2513–2520. doi:10.3892/or.2015.3874

Duchalais, E., Guilluy, C., Nedellec, S., Touvron, M., Bessard, A., Touchefeu, Y., et al. (2018). Colorectal Cancer Cells Adhere to and Migrate along the Neurons of the Enteric Nervous System. *Cell Mol. Gastroenterol. Hepatol.* 5 (1), 31–49. doi:10.1016/j.jcmgh.2017.10.002

Fang, Q. X., Zheng, X. C., and Zhao, H. J. (2020). L1CAM Is Involved in Lymph Node Metastasis *via* ERK1/2 Signaling in Colorectal Cancer. *Am. J. Transl Res.* 12 (3), 837–846.

Garcia, S. B., Aranha, A. L., Garcia, F. R. B., Basile, F. V., Pinto, A. P. M., Oliveira, E. C. d., et al. (2003). A Retrospective Study of Histopathological Findings in 894 Cases of Megacolon: what Is the Relationship between Megacolon and Colonic Cancer. *Rev. Inst. Med. Trop. S. Paulo* 45 (2), 91–93. doi:10.1590/s0036-46652003000200007

Garcia, S. B., Oliveira, J. S. M., Pinto, L. Z., Muccillo, G., and Zucoloto, S. (1996). SHORT COMMUNICATION: The Relationship between Megacolon and Carcinoma of the colon: an Experimental Approach. *Carcinogenesis* 17 (8), 1777–1779. doi:10.1093/carcin/17.8.1777

Gil, Z., Cavel, O., Kelly, K., Brader, P., Rein, A., Gao, S. P., et al. (2010). Paracrine Regulation of Pancreatic Cancer Cell Invasion by Peripheral Nerves. *J. Natl. Cancer Inst.* 102 (2), 107–118. doi:10.1093/jnci/djp456

Godlewski, J. (2010). Morphological Changes in the Enteric Nervous System Caused by Carcinoma of the Human Large Intestine. *Folia Histochem. Cytobiol* 48 (1), 157–162. doi:10.2478/v10042-010-0029-8

Haldar, R., Ricon-Becker, I., Radin, A., Gutman, M., Cole, S. W., Zmora, O., et al. (2020). Perioperative COX2 and β-adrenergic Blockade Improves Biomarkers of Tumor Metastasis, Immunity, and Inflammation in Colorectal Cancer: A Randomized Controlled Trial. *Cancer* 126 (17), 3991–4001. doi:10.1002/cncr.32950

Han, J., Jiang, Q., Ma, R., Zhang, H., Tong, D., Tang, K., et al. (2020). Norepinephrine-CREB1-miR-373 axis Promotes Progression of colon Cancer. *Mol. Oncol.* 14 (5), 1059–1073. doi:10.1002/1878-0261.12657

He, S., Chen, C.-H., Chernichenko, N., He, S., Bakst, R. L., Barajas, F., et al. (2014). GFR 1 Released by Nerves Enhances Cancer Cell Perineural Invasion through GDNF-RET Signaling. *Proc. Natl. Acad. Sci.* 111 (19), E2008–E2017. doi:10.1073/pnas.1402944111

Hicks, B. M., Murray, L. J., Powe, D. G., Hughes, C. M., and Cardwell, C. R. (2013). β-Blocker Usage and Colorectal Cancer Mortality: a Nested Case-Control Study in the UK Clinical Practice Research Datalink Cohort. *Ann. Oncol.* 24 (12), 3100–3106. doi:10.1093/annonc/mdt381

Huang, S.-M., Chen, T.-S., Chiu, C.-M., Chang, L.-K., Liao, K.-F., Tan, H.-M., et al. (2014). GDNF Increases Cell Motility in Human colon Cancer through VEGF-VEGFR1 Interaction. *Endocr. Relat. Cancer* 21 (1), 73–84. doi:10.1530/erc-13-0351

Huang, S.-M., Lin, C., Lin, H.-Y., Chiu, C.-M., Fang, C.-W., Liao, K.-F., et al. (2015). Brain-derived Neurotrophic Factor Regulates Cell Motility in Human colon Cancer. *Endocr. Relat. Cancer* 22 (3), 455–464. doi:10.1530/erc-15-0007

Jaiswal, M., Ganapathy, A., Singh, S., Sarwar, S., Quadri, J. A., Rani, N., et al. (2020). Morphology of Enteric Glia in Colorectal Carcinoma: A Comparative Study of Tumor Site and its Proximal normal Margin. *Morphologie*. 105 (351). 267–274. doi:10.1016/j.morpho.2020.11.003

Jansen, L., Below, J., Chang-Claude, J., Brenner, H., and Hoffmeister, M. (2012). Beta Blocker Use and Colorectal Cancer Risk. *Cancer* 118 (16), 3911–3919. doi:10.1002/cncr.26727

Jansen, L., Hoffmeister, M., Arndt, V., Chang-Claude, J., and Brenner, H. (2014). Stage-specific Associations between Beta Blocker Use and Prognosis after Colorectal Cancer. *Cancer* 120 (8), 1178–1186. doi:10.1002/cncr.28546

Jansen, L., Weberpals, J., Kuiper, J. G., Vissers, P. A. J., Wolkewitz, M., Hoffmeister, M., et al. (2017). Pre- and post-diagnostic Beta-Blocker Use and Prognosis after Colorectal Cancer: Results from a Population-Based Study. *Int. J. Cancer* 141 (1), 62–71. doi:10.1002/ijc.30717

Jia, S., Wang, W., Hu, Z., Shan, C., Wang, L., Wu, B., et al. (2015). BDNF Mediated TrkB Activation Contributes to the EMT Progression and the Poor Prognosis in Human Salivary Adenoid Cystic Carcinoma. *Oral Oncol.* 51 (1), 64–70. doi:10.1016/j.oraloncology.2014.10.008

Kaifi, J. T., Reichelt, U., Quaas, A., Schurr, P. G., Wachowiak, R., Yekebas, E. F., et al. (2007). L1 Is Associated with Micrometastatic Spread and Poor Outcome in Colorectal Cancer. *Mod. Pathol.* 20 (11), 1183–1190. doi:10.1038/modpathol.3800955

Kajiwara, Y., Ueno, H., Hashiguchi, Y., Shinto, E., Shimazaki, H., Mochizuki, H., et al. (2011). Expression of L1 Cell Adhesion Molecule and Morphologic Features at the Invasive Front of Colorectal Cancer. *Am. J. Clin. Pathol.* 136 (1), 138–144. doi:10.1309/ajcp63nrbngctxvf

Kannen, V., de Oliveira, E. C., Motta, B. Z., Chaguri, A. J., Brunaldi, M. O., and Garcia, S. B. (2015). Trypanosomiasis-induced Megacolon Illustrates How Myenteric Neurons Modulate the Risk for colon Cancer in Rats and Humans. *Plos Negl. Trop. Dis.* 9 (4), e0003744. doi:10.1371/journal.pntd.0003744

Klein, R. (1994). Role of Neurotrophins in Mouse Neuronal Development. *FASEB j.* 8 (10), 738–744. doi:10.1096/fasebj.8.10.8050673

Lee, Y. J., Huh, J. W., Shin, J. K., Park, Y. A., Cho, Y. B., Kim, H. C., et al. (2020). Risk Factors for Lymph Node Metastasis in Early colon Cancer. *Int. J. Colorectal Dis.* 35 (8), 1607–1613. doi:10.1007/s00384-020-03618-7

Leijssen, L. G. J., Dinaux, A. M., Taylor, M. S., Deshpande, V., Kunitake, H., Bordeianou, L. G., et al. (2019). Perineural Invasion Is a Prognostic but Not a Predictive Factor in Nonmetastatic Colon Cancer. *Dis. Colon Rectum* 62 (10), 1212–1221. doi:10.1097/dcr.0000000000001450

Li, H., Yang, Z., Wang, W., Wang, J., Zhang, J., Liu, J., et al. (2019). NT-3/TrkC Axis Contributes to the Perineural Invasion and the Poor Prognosis in Human Salivary Adenoid Cystic Carcinoma. *J. Cancer* 10 (24), 6065–6073. doi:10.7150/jca.33635

Liebig, C., Ayala, G., Wilks, J. A., Berger, D. H., and Albo, D. (2009). Perineural Invasion in Cancer. *Cancer* 115 (15), 3379–3391. doi:10.1002/cncr.24396

Liebl, F., Demir, I. E., Rosenberg, R., Boldis, A., Yildiz, E., Kujundzic, K., et al. (2013). The Severity of Neural Invasion Is Associated with Shortened Survival in colon Cancer. *Clin. Cancer Res.* 19 (1), 50–61. doi:10.1158/1078-0432.ccr-12-2392

Liu, J., Liu, Z., Li, J., Tian, S., and Dong, W. (2020). Personalizing Prognostic Prediction in Early-Onset Colorectal Cancer. *J. Cancer* 11 (22), 6727–6736. doi:10.7150/jca.46871

Martínez Vila, C., Oliveres Montero de Novoa, H., Martínez-Bauer, E., Serra-Aracil, X., Mora, L., Casalots-Casado, A., et al. (2020). A Real World Analysis of Recurrence Risk Factors for Early Colorectal Cancer T1 Treated with Standard Endoscopic Resection. *Int. J. Colorectal Dis.* 35 (5), 921–927. doi:10.1007/s00384-020-03553-7

Mo, S., Zhou, Z., Dai, W., Xiang, W., Han, L., Zhang, L., et al. (2020). Development and External Validation of a Predictive Scoring System Associated with Metastasis of T1-2 Colorectal Tumors to Lymph Nodes. *Clin. Translational Med.* 10 (1), 275–287. doi:10.1002/ctm2.30

Muthuswamy, R., Okada, N. J., Jenkins, F. J., McGuire, K., McAuliffe, P. F., Zeh, H. J., et al. (2017). Epinephrine Promotes COX-2-dependent Immune Suppression in Myeloid Cells and Cancer Tissues. *Brain Behav. Immun.* 62, 78–86. doi:10.1016/j.bbi.2017.02.008

Na'ara, S., Amit, M., and Gil, Z. (2019). L1CAM Induces Perineural Invasion of Pancreas Cancer Cells by Upregulation of Metalloproteinase Expression. *Oncogene* 38 (4), 596–608. doi:10.1038/s41388-018-0458-y

Oliveira, E. C., Leite, M. S., Miranda, J. A., Andrade, A. L., Garcia, S. B., Luquetti, A. O., et al. (2001). Chronic Trypanosoma Cruzi Infection Associated with Low Incidence of 1,2-Dimethylhydrazine-Induced colon Cancer in Rats. *Carcinogenesis* 22 (5), 737–740. doi:10.1093/carcin/22.5.737

Raufman, J.-P., Cheng, K., Saxena, N., Chahdi, A., Belo, A., Khurana, S., et al. (2011). Muscarinic Receptor Agonists Stimulate Matrix Metalloproteinase 1-dependent Invasion of Human colon Cancer Cells. *Biochem. biophysical Res. Commun.* 415 (2), 319–324. doi:10.1016/j.bbrc.2011.10.052

Raufman, J.-P., Samimi, R., Shah, N., Khurana, S., Shant, J., Drachenberg, C., et al. (2008). Genetic Ablation of M3 Muscarinic Receptors Attenuates Murine colon Epithelial Cell Proliferation and Neoplasia. *Cancer Res.* 68 (10), 3573–3578. doi:10.1158/0008-5472.can-07-6810

Sartore-Bianchi, A., Ardini, E., Bosotti, R., Amatu, A., Valtorta, E., Somaschini, A., et al. (2016). Sensitivity to Entrectinib Associated with a Novel LMNA-NTRK1 Gene Fusion in Metastatic Colorectal Cancer. *J. Natl. Cancer Inst.* 108 (1). doi:10.1093/jnci/djv306

Schmid, R. S., and Maness, P. F. (2008). L1 and NCAM Adhesion Molecules as Signaling Coreceptors in Neuronal Migration and Process Outgrowth. *Curr. Opin. Neurobiol.* 18 (3), 245–250. doi:10.1016/j.conb.2008.07.015

Shan, C., Wei, J., Hou, R., Wu, B., Yang, Z., Wang, L., et al. (2016). Schwann Cells Promote EMT and the Schwann-like Differentiation of Salivary Adenoid Cystic Carcinoma Cells *via* the BDNF/TrkB axis. *Oncol. Rep.* 35 (1), 427–435. doi:10.3892/or.2015.4366

Skancke, M., Arnott, S. M., Amdur, R. L., Siegel, R. S., Obias, V. J., and Umapathi, B. A. (2019). Lymphovascular Invasion and Perineural Invasion Negatively Impact Overall Survival for Stage II Adenocarcinoma of the Colon. *Dis. Colon Rectum* 62 (2), 181–188. doi:10.1097/dcr.0000000000001258

Sun, Q., Liu, T., Liu, P., Luo, J., Zhang, N., Lu, K., et al. (2019). Perineural and Lymphovascular Invasion Predicts for Poor Prognosis in Locally Advanced Rectal Cancer after Neoadjuvant Chemoradiotherapy and Surgery. *J. Cancer* 10 (10), 2243–2249. doi:10.7150/jca.31473

Sytnyk, V., Leshchyns'ka, I., and Schachner, M. (2017). Neural Cell Adhesion Molecules of the Immunoglobulin Superfamily Regulate Synapse Formation, Maintenance, and Function. *Trends Neurosciences* 40 (5), 295–308. doi:10.1016/j.tins.2017.03.003

Tampakis, A., Tampaki, E. C., Nonni, A., Tsourouflis, G., Posabella, A., Patsouris, E., et al. (2020). L1CAM Expression in Colorectal Cancer Identifies a High-Risk Group of Patients with Dismal Prognosis Already in Early-Stage Disease. *Acta Oncologica* 59 (1), 55–59. doi:10.1080/0284186x.2019.1667022

Tieng, F. Y. F., Abu, N., Sukor, S., Mohd Azman, Z. A., Mahamad Nadzir, N., Lee, L. H., et al. (2020). L1CAM, CA9, KLK6, HPN, and ALDH1A1 as Potential Serum Markers in Primary and Metastatic Colorectal Cancer Screening. *Diagnostics (Basel)* 10 (7). doi:10.3390/diagnostics10070444

Valès, S., Bacola, G., Biraud, M., Touvron, M., Bessard, A., Geraldo, F., et al. (2019). Tumor Cells Hijack Enteric Glia to Activate colon Cancer Stem Cells and Stimulate Tumorigenesis. *EBioMedicine* 49, 172–188. doi:10.1016/j.ebiom.2019.09.045

Vespúcio, M. V., Turatti, A., Modiano, P., Oliveira, E. C., Chicote, S. R., Pinto, A. M., et al. (2008). Intrinsic Denervation of the colon Is Associated with a Decrease of Some Colonic Preneoplastic Markers in Rats Treated with a Chemical Carcinogen. *Braz. J. Med. Biol. Res.* 41 (4), 311–317. doi:10.1590/s0100-879x2008005000008

Wong, H. P., Ho, J. W., Koo, M. W., Yu, L., Wu, W. K., Lam, E. K., et al. (2011). Effects of Adrenaline in Human colon Adenocarcinoma HT-29 Cells. *Life Sci.* 88 (25-26), 1108–1112. doi:10.1016/j.lfs.2011.04.007

Zahalka, A. H., and Frenette, P. S. (2020). Nerves in Cancer. *Nat. Rev. Cancer* 20 (3), 143–157. doi:10.1038/s41568-019-0237-2

Zauszkiewicz-Pawlak, A., Godlewski, J., Kwiatkowski, P., and Kmiec, Z. (2017). Ultrastructural Characteristics of Myenteric Plexus in Patients with Colorectal Cancer. *Folia Histochem. Cytobiol.* 55 (1), 6–10. doi:10.5603/fhc.a2017.0003

Zhou, H., Shi, B., Jia, Y., Qiu, G., Yang, W., Li, J., et al. (2018). Expression and Significance of Autonomic Nerves and α9 Nicotinic Acetylcholine Receptor in Colorectal Cancer. *Mol. Med. Rep.* 17 (6), 8423–8431. doi:10.3892/mmr.2018.8883

Conflict of Interest: The authors declare that the research was conducted in the absence of any commercial or financial relationships that could be construed as a potential conflict of interest.

Publisher's Note: All claims expressed in this article are solely those of the authors and do not necessarily represent those of their affiliated organizations, or those of the publisher, the editors and the reviewers. Any product that may be evaluated in this article, or claim that may be made by its manufacturer, is not guaranteed or endorsed by the publisher.

frontiers in Oncology

REVIEW
published: 14 March 2022
doi: 10.3389/fonc.2022.846917

Bioelectric Dysregulation in Cancer Initiation, Promotion, and Progression

Maulee Sheth[1] *and Leyla Esfandiari*[1,2,3*]

[1] Department of Biomedical Engineering, University of Cincinnati, Cincinnati, OH, United States, [2] Department of Electrical Engineering and Computer Science, University of Cincinnati, Cincinnati, OH, United States, [3] Department of Environmental and Public Health Sciences, University of Cincinnati, Cincinnati, OH, United States

Cancer is primarily a disease of dysregulation – both at the genetic level and at the tissue organization level. One way that tissue organization is dysregulated is by changes in the bioelectric regulation of cell signaling pathways. At the basis of bioelectricity lies the cellular membrane potential or V_{mem}, an intrinsic property associated with any cell. The bioelectric state of cancer cells is different from that of healthy cells, causing a disruption in the cellular signaling pathways. This disruption or dysregulation affects all three processes of carcinogenesis – initiation, promotion, and progression. Another mechanism that facilitates the homeostasis of cell signaling pathways is the production of extracellular vesicles (EVs) by cells. EVs also play a role in carcinogenesis by mediating cellular communication within the tumor microenvironment (TME). Furthermore, the production and release of EVs is altered in cancer. To this end, the change in cell electrical state and in EV production are responsible for the bioelectric dysregulation which occurs during cancer. This paper reviews the bioelectric dysregulation associated with carcinogenesis, including the TME and metastasis. We also look at the major ion channels associated with cancer and current technologies and tools used to detect and manipulate bioelectric properties of cells.

Keywords: bioelectricity, extracellular vesicles, tumor microenvironment, membrane potential, carcinogenesis, piezo channels

OPEN ACCESS

Edited by:
Daniele Vergara,
University of Salento, Italy

Reviewed by:
Marina Damato,
University of Salento, Italy
Amilcare Barca,
University of Salento, Italy

***Correspondence:**
Leyla Esfandiari
esfandla@ucmail.uc.edu

Specialty section:
This article was submitted to Molecular and Cellular Oncology, a section of the journal Frontiers in Oncology

Received: *31 December 2021*
Accepted: *21 February 2022*
Published: *14 March 2022*

Citation:
Sheth M and Esfandiari L (2022) Bioelectric Dysregulation in Cancer Initiation, Promotion, and Progression. Front. Oncol. 12:846917. doi: 10.3389/fonc.2022.846917

Abbreviations: EV, extracellular vesicle; TME, tumor microenvironment; V_{mem}, membrane potential; EF, electric field; SMT, somatic mutation theory; TOFT, tissue organization field theory; HMEC, human mammary epithelial cell; MCF7, estrogen-receptor-positive breast cancer cell line; MDA-MB-231, estrogen-receptor-negative breast cancer cell line; ECM, extracellular matrix; EMT, epithelial mesenchymal transition; CAF, cancer associated fibroblast; GlyCl, glycine-gated chloride channel; VGCC, voltage gated calcium channel; VGSC, voltage gated sodium channel; EAG, ether-à-go-go K^+ channel; TRP, transient receptor potential; MAPK, mitogen-activated protein kinase; JNK, c-Jun N-terminal kinase; ERK, extracellular signal-regulated kinase; Pl3K/Akt, phosphatidylinositol 3-kinase/protein kinase B; MEK, mitogen-activated ERK kinase; EGF, epidermal growth factor; EGFR, epidermal growth factor receptor; GBM, glioblastoma multiforme; GSK-3ß, glycogen synthase kinase-3 ß; ITLS, induced tumor like structure; MCF10A, normal breast epithelium cell line; CTC, circulating tumor cell; DTC, disseminated tumor cell; mRNA, messenger RNA; miRNA, micro RNA; B16F1, murine melanoma cell line; 3T3, murine fibroblast cell line; OECT, organic electrochemical transistor; CHO, Chinese hamster ovary; PEDOT : PSS, poly(3,4-ethylenedioxythiophene): polystyrene sulfonate.

INTRODUCTION

Carcinogenesis, also termed oncogenesis or tumorigenesis, is rooted in two major theories or hypotheses, both significantly different from one another. The somatic mutation theory (SMT), which has been prevailing in cancer research for more than sixty years proposes that the origin of cancer can be explained by an accumulation of several DNA mutations in a single somatic cell. Tumor development is then a multistep process where successive mutations produce advantageous biological compatibilities (1). The SMT explains many features of cancer such as hereditary cancers and the success of gene-targeting cancer therapies (2). However, non-genotoxic carcinogens which induce cancer without any DNA modifications (3) and the absence of mutations in some tumors (4) contradict this theory. Alternatively, the tissue organization field theory (TOFT) proposed in 1999, hypothesizes that carcinogenesis is a problem of tissue organization instead of having a cellular level origin. Here, the carcinogenic agents disrupt the reciprocal interactions between cells that maintain tissue organization, repair, and homeostasis, hence creating altered microenvironments which allow the parenchymal cells to exercise their ability to proliferate and migrate (5).

Bioelectric regulation is an important mechanism of cell communication and dysregulation of this mechanism can result into alterations in tissue organization, fitting the tissue organization field theory of carcinogenesis. While bioelectricity has been extensively studied in cells with neural origins, its role in non-neural cell activity and functionality has only emerged more recently. With advances in understanding the underlying bioelectric mechanisms of cancer and development of molecular tools to measure and control these electric fields, we are now able to better identify the role of bioelectric signaling in carcinogenesis. Another important mechanism that facilitates intercellular communication for the maintenance of tissue homeostasis is the production and release of extracellular vesicles (EVs) by cells of different tissue types. Cancer-derived EVs play a role in all steps of carcinogenesis by mediating the communication between cancer cells and non-cancer cells as well as malignant cells and non-malignant cells within the tumor microenvironment (TME) (6). Furthermore, the production of EVs is aberrant during cancer which in turn plays an important role in disturbing the bioelectrical signaling pathways between cells.

Several review papers (7–10) focusing on the bioelectric control of one or the other aspect of cancer, such as migration or metastasis, have been published. In this paper, we provide a more extensive review of bioelectric regulation in multiple cancer processes including initiation, promotion, the tumor microenvironment, and metastasis. We also look at the major ion channels implicated in cancer and current technologies and tools used to measure and manipulate bioelectric properties of cells *in vivo*.

BIOELECTRICITY AND ENDOGENOUS ELECTRIC FIELDS – AN OVERVIEW

Membrane potential (V_{mem}) is an electrical property associated with any cell, specific to its origin and function. The electric nature of the membrane potential produces endogenous electric fields (EFs) due to the segregation of charges by molecular machines such as pumps, transporters and ion channels that are primarily located in the plasma membrane of the cell (11). These transmembrane voltage gradients have been established to control not only neural signaling *via* gap junctions, but also cell proliferation, migration, differentiation, and orientation in both, excitable and non-excitable cells (12, 13).

Depending on the presence of relative charges, all excitable and non-excitable cells possess an electric gradient across their plasma membrane (**Figure 1A**). When the cytoplasm becomes more positively charged relative to the extracellular space, the cell is said to be depolarized and will have a less negative V_{mem}. When the cytoplasm becomes more negatively charged relative to the extracellular space, the cell in said to be hyperpolarized and will have a more negative V_{mem} (**Figure 1B**). It is worthwhile to note that V_{mem} is not only a key intrinsic cellular property, but also an integral part of the microenvironment where it acts both, spatially and temporally, to guide cellular behavior (9). It does so by enabling the cells to make decisions based on the states of their neighbors (14). Physiological V_{mem} can range from -90 to -10 mV, depending on the cell type and physiological state (13, 15). Furthermore, as V_{mem} is primarily established by ion channels that are gated post-translationally, two cells that are in the exact same genetic and transcriptional states could theoretically be in very different bioelectric states (16).

BIOELECTRICITY IN CANCER PROCESSES

Bioelectric properties of cells and the electrical state of cells in the microenvironment are known to control several key behaviors of relevance to cancer (17–24). Here we first introduce some major ion channels implicated in cancer. Then we look at the role of bioelectricity in cancer initiation and progression, the tumor microenvironment, and migration and metastasis.

Ion Channels and Cancer

Ion channels are membrane proteins that create ionic concentration gradients by regulating the flow of ions across the plasma membrane. The primary function of ion channels is to maintain cellular homeostasis by regulating the inward and outward ion flux, but they are also higher order regulators of many downstream molecular signaling pathways (7). The four main ions that play a role in establishing the resting V_{mem} of a cell are: Ca^{2+}, Na^{+}, K^{+}, and Cl^{-}. The Goldman equation links the overall transmembrane potential to the concentrations and permeabilities of various ion species. The resting potential V_{mem} depends on the internal and external K^{+}, Na^{+}, and Cl^{-} concentrations, ambient temperature, and permeability of each ion specie. Alterations in ion channel expression and activity are associated with the initiation, proliferation, and metastasis of cancer cells (21, 25). For instance, there is a host of ion channels whose expression is dysregulated in cancer cells and have been found to be associated with a metastatic phenotype (7). Here, we

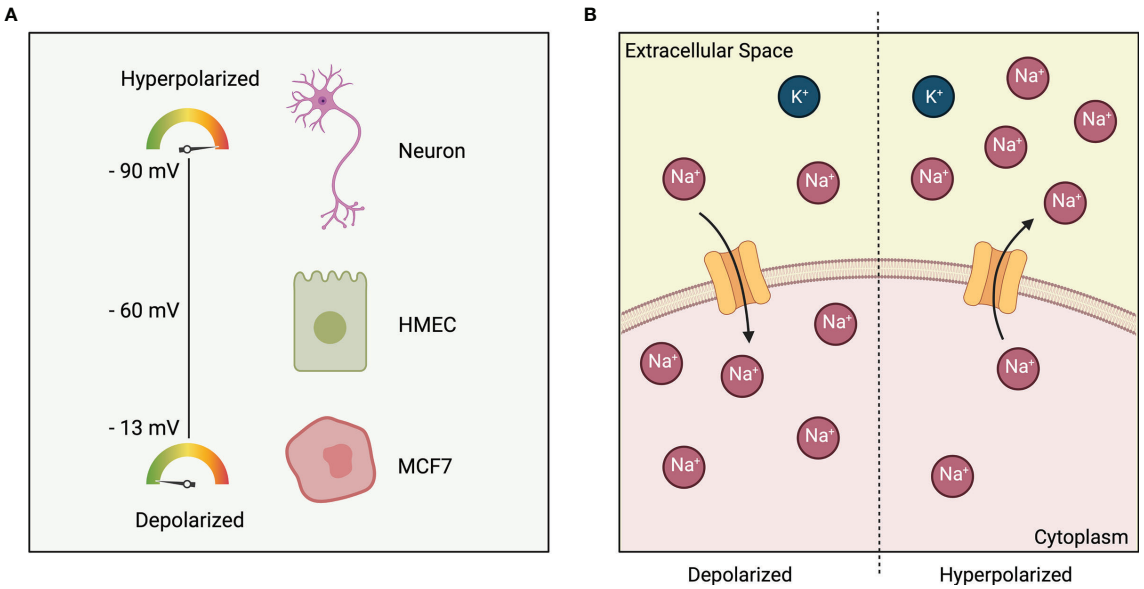

FIGURE 1 | **(A)** Polarization of cells based on cell type. Excitable cell such as neurons have a membrane potential of -90 mV. Non-excitable cells such as HMEC: Human Mammary Epithelial Cell and MCF7: Estrogen-receptor-positive breast cancer cell line are at -60 mV and -13 mV respectively. **(B)** Depolarized cell state (left) indicated by a more positive charge in the cytoplasm relative to the extracellular space. Hyperpolarized cell state (right) indicated by a less positive charge in the cytoplasm relative to the extracellular space.

summarize major ion channels responsible for the disruption of homeostasis and aberrant activation of downstream signaling pathways in cancer including voltage-gated cation channels (Ca_V, Na_V, K_V), mechanosensitive cation channels, transient receptor potential (TRP) channels, and chloride channels (CLCs). Several review papers focusing extensively on ion channels implicated in cancer can be found in literature (26–29). It is worthwhile to note that disruption in expression of these ion channels leads to deregulation in a host of different signaling pathways in cancer (27–30). Prominent ones include the mitogen-activated protein kinase (MAPK) pathways, ERK and JNK signaling pathways, Wnt/ß-catenin pathway, PI3K/Akt pathway, Notch signaling, and the Rac and Rho pathways.

Calcium Channels

Voltage-gated calcium channels (VGCCs) and transient receptor potential (TRP) ion channels are primary channels facilitating Ca^{2+} ion diffusion. VGCCs are present in human breast cancer cells but not in normal human mammary epithelial cells (HMECs) (31). Berzingi et al. studied the effect of calcium ions on cell proliferation. Upon 5 days of culture, it was found that MCF7 breast cancer cells showed almost no growth in a culture medium without Ca^{2+} ions compared with cells growing to nearly 100% confluence in a medium containing 2 mM Ca^{2+} ions. Furthermore, blocking external Ca^{2+} ions from entering the cell through voltage-gated calcium channels using Verapamil indicated that cell growth was substantially inhibited in MDA-MB-231, breast cancer cells (32). The intracellular calcium concentration is also integral for cancer cell metastasis since it regulates the cell cytoskeletal dynamics, protease activity, cell volume, and pH – all of which play a role in migration and invasion of cancer cells (33–36). Calcium is also involved in driving ECM degradation and cell invasion by promoting epithelial-mesenchymal transition (EMT) pathways and the activity of matrix metalloproteinases (37, 38). Furthermore, multiple TRP channels are regulated differently in various cancers. Expression levels of TRPC3 in some breast and ovarian tumors (39) and TRPC6 in breast, liver, stomach cancers and in glioma are elevated (40). In non-small-cell lung carcinoma cells, Ca^{2+} entry mediated by TRPC1 and its associated signaling was found to activate the Pl3K/Akt and MAPK downstream pathways and simulate proliferation (41). Some TRP channels including TRPC1 (42), TRPC3 (43), TRPC6 (44–46), TRPM2 (47–49), and TRPM8 (50, 51) also simulate apoptosis by increasing Ca^{2+} activity. Consequent increase in TRPC6-mediated Ca^{2+} entry has also been found to alter the Notch pathway, leading to tumorigenesis in human glioblastoma multiforme (GBM) and GBM-derived cell lines (52). TRPV4 is also a critical regulator of the Rho signaling pathway involved in cancer cell adhesion and migration (53).

Sodium Channels

Cancer cells can effectively use Na^+ flux to indirectly promote a metastatic phenotype. For instance, changes in Na^+ flux can create localized areas of depolarization that can drive the movement of Ca^{2+} and H^+ ions. Activity of Na^+/Ca^{2+} exchangers located in the plasma membrane of cells has also been linked to favor ECM degradation and cell invasion, as has been demonstrated in MDA-MB-231 breast cancer cells that overexpress a voltage gated sodium channel (VGSC) (54). The

expression of $Na_V1.7$ also promotes cellular invasion at the transcriptional level by epidermal growth factor (EGF) and EGF receptor (EGFR) signaling *via* the ERK1/2 pathway (55). In colon cancer cells, $Na_V1.5$ activity and the subsequent depolarization have been found to play a role in the induction of invasion-related genes through the MEK, ERK1/2 pathway (56, 57). Furthermore, a sodium-channel SCN5A has been identified as a key regulator of a genetic network that controls colon cancer invasion (57). The activity of some sodium channels has also been shown to further simulate the expression of more sodium channels in prostate and breast cancer cell lines. This allows the cells to substantially increase ion flux by creating a positive feedback loop of channel activity-induced channel expression (58). Finally, changes in the intracellular Na^+ concentration can also alter cellular pH (10). A decrease in the pH surrounding a tumor is known to influence cell adhesion *via* the formation of integrin-mediated focal adhesion contacts (59–61).

Potassium Channels

K^+ ions predominantly move from the intracellular to extracellular space through their channels to maintain the steady state resting potential of a cell. K^+ indirectly affects the V_{mem} by driving the entry of Ca^{2+} into the cell. At the same time, the proliferation of some tumor cells is dependent on voltage-gated potassium channels (62–67) that alter cell volume by affecting K^+ flow. A variety of tumor cells express $K_V10.1$ (68, 69) or $K_V11.1$ (HERG) (70) or both channels. The K^+ channel EAG has been found to be expressed in 100% of cervical cancer biopsies analyzed and overexpression of EAG in human cells has been shown to increase cell proliferation in culture (71, 72). Furthermore, overexpressing K^+ channels in breast cancer cells has been found to drive cell migration mediated by cadherin-11 and MAPK signaling (73). Calcium-dependent K^+ channel $K_{Ca}3.1$ also promoted proliferation by directly interacting with ERK1/2 and JNK signaling pathways (74). Finally, Ca^{2+} flow through TRPM8 regulates activity of Ca^{2+}-sensitive K^+ channels such as $K_{Ca}1.1$, which plays a role in migration (75, 76). In breast cancer cells, overexpression of TRPM8 increased the metastatic potential *via* activation of the AKT glycogen synthase kinase-3 ß (GSK-3ß) pathway (77).

Chloride Channels

Chloride is the main anion that accompanies the transport of cations such as calcium, sodium, and potassium. Chloride channels play an important role in cancer cell migration due to their role in maintaining cell volume (78). Cl^- channels have been revealed to have a role in glioblastomas from studies in glioma cell lines (79, 80). Studies of human prostate cancer cell lines have also shown chloride channels to play a role as key regulators of proliferation through cell size regulation (81). Chloride ion channel-4 Cl^-/H^+ exchanger has been found to enhance migration, invasion, and metastasis of glioma and colon cancer cells by regulating the cell volume (65). For instance, genetic knockdown of ClC-3 has been found to substantially reduce migration in glioma cells (82).

Piezo Channels

Piezo channels are non-selective Ca^{2+}-permeable channels whose gating can be simulated by several mechanical stimuli affecting the plasma membrane, including compression, stretching, poking, shear stress, membrane tension, and suction (83–85). A recent study has also demonstrated that Piezo channels show significant sensitivity to voltage cues and thus can also be viewed as important members of the voltage-gated ion channel family (86). Two major piezo channels – Piezo1 and Piezo2 have been identified which are mainly expressed in different tissues. Piezo channels are overexpressed in several cancers, such as breast, gastric, and bladder, whereas in other cancers, their downregulation has been described. Several studies conducted *in vitro* and *in vivo* have demonstrated that the activation of Piezo channels can drive a Ca^{2+} influx, thus modulating key Ca^{2+}-dependent signaling pathways associated with cancer cell migration, proliferation, and angiogenesis (87). Overexpression of Piezo1 has also been found to promote prostate cancer development through the activation of the Akt/mTOR pathway (88). Furthermore, the mechanistic effects of Piezo2 are associated with a Ca^{2+}-dependent upregulation of Wnt11 expression which enhances the angiogenic potential of endothelial cells in cancer *via* ß-catenin-dependent signaling (89).

Cancer Initiation and Promotion

Resting potential established by ion channel and pump proteins is important for determination of differentiation state and proliferation. One way that carcinogenesis occurs is due to the disruption of electrical gradients, or the mechanisms by which they are perceived by cells (24). V_{mem} is an important non-genetic biophysical aspect of the microenvironment that regulates the balance between normally patterned growth and carcinogenesis (7). Cancerous and proliferative tissues are generally more positively charged or depolarized than non-proliferative cells (90, 91). V_{mem} values from -10 to -30 mV correspond to more undifferentiated, proliferative, and stem-like cells (92). For instance, the resting membrane potential in normal human mammary epithelial cells (HMEC) is -60 mV. This value goes up to -13 mV in breast cancer cells isolated from patients (93). Berzingi et al. experimentally compared V_{mem} in HMEC and two different invasive ductal human carcinoma cell lines, MCF7 (estrogen-receptor-positive) and MDA-MB-231 (estrogen-receptor-negative). The results indicated that MCF7 and MDA-MB-231 cells are 30.4 mV and 27.3 mV more depolarized in comparison to HMEC cells, respectively. It was also seen that HMEC grew at a much slower rate compared to MCF7 and MDA-MB-231 (32).

Lobikin et al. used a Xenopus tadpole model to confirm the role of ion flow in oncogenesis *in vivo* by investigating the consequences of depolarizing select cell groups (67). Embryos were exposed to glycine-gated chloride channel (GlyCl) activator ivermectin to control the membrane potential of a widely distributed, sparse population of cells expressing the GlyCl channel. The membrane potential of these specific cells could be set to any desired level by manipulating external chloride

levels following ivermectin treatment. Tadpoles whose cells were depolarized were seen to exhibit excess melanocytes with a much more arborized appearance and colonize areas normally devoid of melanocytes, such as around the eyes and mouth. It was also shown that depolarization induces the up regulation of cancer relevant genes such as Sox10 and SLUG (94). Furthermore, susceptibility to oncogene-induced tumorigenesis was shown to be significantly reduced by forced prior expression of hyperpolarizing ion channels indicating that bioelectric signaling of the cellular microenvironment can both, induce and suppress, cancer-like cell behavior.

V_{mem} has been suggested as a cancer biomarker due to its role as an early indicator of tumorigenesis and is associated with tumors of diverse molecular origin (95–98). Induced tumor like structures (ITLS) can be formed in Xenopus and zebrafish embryos by mis-expressing mammalian oncogenes (Gli1, Xrel3 and KRASG12D) and mutant tumor suppressors (p53Trp248). ITLS's are formed as a result of genetic interference with signaling pathways altered in several types of cancer including basal cell carcinoma, lung cancer, leukemia, melanoma, and rhabdomyosarcoma (99–102). Fluorescence reporters of V_{mem} in the injected animals have been found to reveal unique depolarization of tumors and increased sodium content compared to healthy tissues (7, 103). Moreover, depolarized foci have a higher success rate in predicting tumor formation as compared to cancer specific antigen level in the serum. For instance, Chernet and Levin found that depolarized foci, while present in only 19-30% of oncogene-injected embryos, predict tumor formation with 50-56% success rate as compared to prostate specific antigen level in the serum, which when used as a biomarker for prostate cancer, has a 29% predictive value (104, 105).

Recently, Carvalho developed a computational model of cancer initiation, including the propagation of a cell depolarization wave in the tissue under consideration (106). This model looks at an electrically connected single layer tissue in two and three dimensions and simulates ion exchange between cells as well as between cells and the extracellular environment. It was seen that a polarized tissue with cells in quiescent state tends to change state if a large enough perturbation changes its homeostatic conditions, such as a carcinogenic event. The induced depolarized state is able to then propagate to neighboring cells in a wave like manner. The developed model shows the importance of community effects associated with cell electrical communication leading to both, short- and long-range influences and ultimately, cancer.

The Tumor Microenvironment

The microenvironment functions to guide the cell through space and to direct tissue growth through time. It also plays a significant role in the physiological outcome of a given V_{mem} input. The tumor microenvironment (TME) is a complex entity and consists of multiple cell types embedded in the extracellular matrix (ECM), including immune cells, endothelial cells and cancer associated fibroblasts (CAFs) which communicate with cancer cells and with other CAFs during tumor progression (107). One way this communication is mediated is by a plethora of bioactive molecules, including proteins, lipids, coding and non-coding RNAs, and metabolites, which are secreted into extracellular vesicles (EVs) (108, 109).

The mechanical microenvironment impacts bioelectric regulation and cell proliferation (9). An early indication of this were studies in the late 1900s which found that cells within a low cell density (fewer cell-cell contacts) exhibited reduced proliferation (110) and that cells in a confluent monolayer are more hyperpolarized than individual cells (111, 112). Similarly, chemical components of the cellular microenvironment have the ability to impact cell phenotype. Factors such as hypoxia (113) and pH (114) have been demonstrated to drive cancer progression. Moreover, hypoxic tumors exhibit more aggressive phenotypes. Tumor cells under hypoxia can produce a secretion partly in the form of EVs that modulates the microenvironment to facilitate tumor angiogenesis and metastasis (115). V_{mem} thus functions at the interface of chemical and mechanical signals by creating an electrical gradient across cells, which in turn gates voltage-sensitive channels. This creates a tightly connected communication pathway between a cell and its microenvironment (9, 116–119).

The key components of the mechanical microenvironment (**Figure 2**) are solid and fluid pressure, substratum stiffness (120–128) tissue geometry, and mechanical stress (129–131). These components of the physical microenvironment are primarily dependent on mechanosensitive calcium channels $Ca_V3.3$ (132, 133). Cells have the ability to sense the surrounding substratum by applying force through actomyosin motors in stress fibers linked to focal adhesions (134). Varying the substratum stiffness has been demonstrated to influence cellular behaviors including differentiation (122), apoptosis (126), proliferation (125), gene expression (135–137), migration (138), cell stiffness (139), and epithelial-mesenchymal transition (EMT) (127). Along with microenvironments of varying rigidity, cells also experience mechanical stress due to the dense packing of neighboring cells. Cell-cell contacts are critical for propagation of bioelectric signals *via* the transport of ions through gap junctions (140–142). The normal breast epithelium cell line MCF10A was demonstrated to respond differently to an EF *in vitro* depending on the confluency of the cell culture (143). The study observed that clustered cells are more sensitive to an EF due to increased cell-cell contacts.

Physical signals from the V_{mem} of the microenvironment also contribute to tumorigenesis (9). Furthermore, pressure activates oncogenic factors such as p38, ERK, and c-Src which are involved in the regulation of cell proliferation, differentiation, and apoptosis (132). Tumors *in vivo* are under higher pressure and are also stiffer than the surrounding tissue which creates a microenvironment that promotes cell proliferation (133). Increased pressure also enhances the invasiveness of tumor cells (121). Additionally, a key communication pathway between cells and their ECM is Integrin signaling pathway which regulates cytosolic Ca^{2+} levels (144). These cytosolic Ca^{2+} concentrations play an important role in cancer-related processes such as EMT (38), metastasis (21), and apoptosis (126, 145). For instance, inducing EMT in human breast

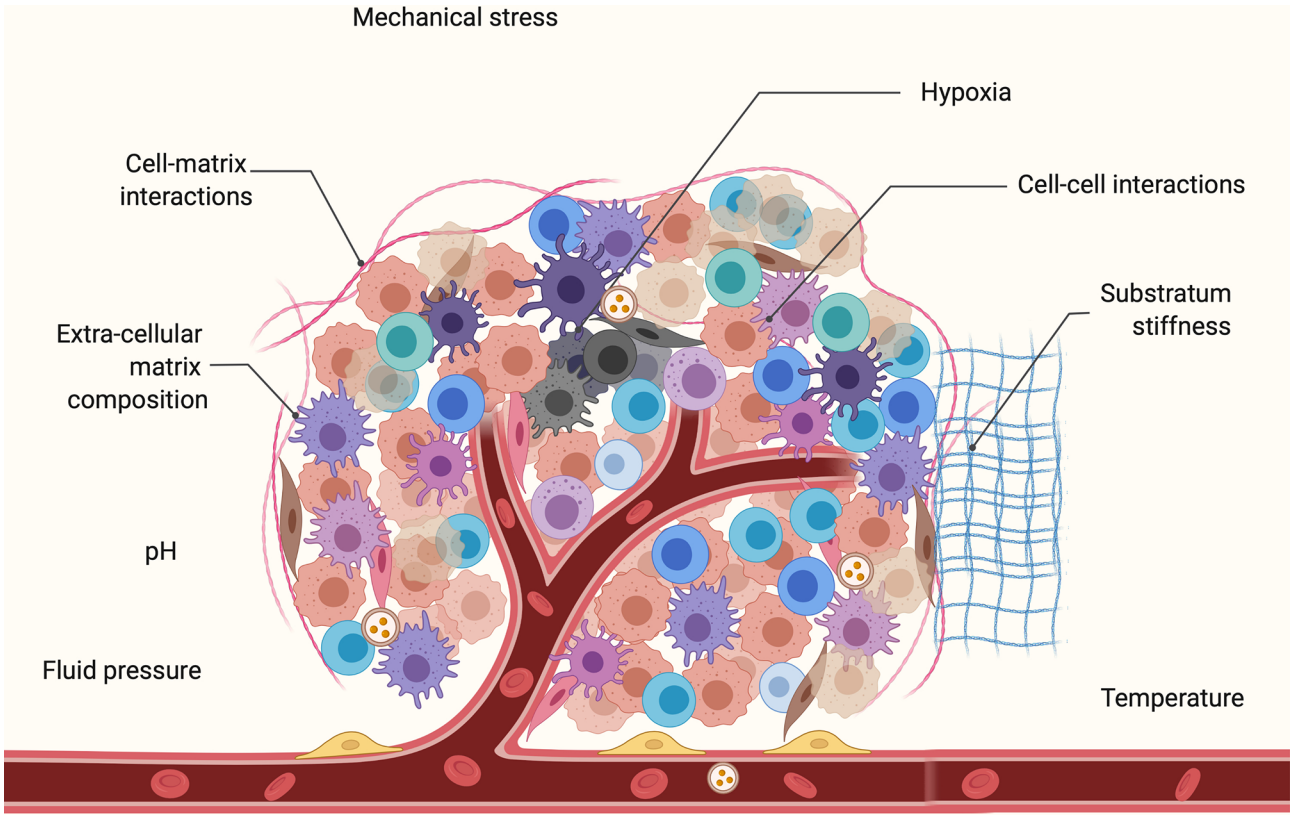

FIGURE 2 | Key components of the tumor microenvironment (TME) which comprises of multiple cell types including cancer cells, immune cells, endothelial cells, and cancer associated fibroblasts. This includes mechanical components such as fluid pressure, substratum stiffness, mechanical stress, cell-cell, and cell-matrix interactions. Also shown are some chemical components of the microenvironment such as pH, temperature, and hypoxic core of the tumor. Cell-cell and cell-TME communication is mediated by a variety of bioactive molecules during carcinogenesis.

cancer cells has been shown to upregulate cytosolic calcium levels (38).

Cell Migration and Metastasis

The dissemination of primary tumor cells to secondary organs is called metastasis. This involves cancer cells breaking away from the primary tumor, traveling through blood or lymphatic systems, and forming secondary or metastatic tumors in other parts of the body. Metastasis is a multi-step process (**Figure 3**) and involves the following events: local invasion to surrounding tissues, intravasation into the vasculature or lymphatics (where they are called circulating tumor cells or CTCs), survival and circulation in the vessels, and extravasation and colonization in a secondary organ (where they are called disseminated tumor cells or DTCs) (146, 147). Bioelectricity mediates many of the normal cell functions which are disrupted in metastasis. Factors such as ion channel expression, V_{mem}, and external EFs have been determined to regulate invasion and metastasis. Furthermore, the migration of cancer cells out of the primary tumors into local tissues through various physical barriers is driven by components of the local tumor microenvironment and executed by complex signaling pathways in the cell (10).

Cues within the TME can promote local invasion (148). For instance, an ECM protein fibronectin can attract breast cancer tumor cells to the vasculature *via* haptotaxis (directional migration in response to substrate-bound cues) to promote dissemination. During tumor invasion, constant communication occurs between tumor cells and surrounding stromal cells *via* extracellular vesicles (EVs) (115). Even upon entering a secondary tissue, the transition of a DTC into an overt metastasis is highly dependent on the local microenvironment of this organ (10). Hence, the formation of a supportive premetastatic niche, composed of ECM and resident immune cells is essential to provide nutrients and survival signals that drive DTC survival and outgrowth. Recent work suggests that tumor cells may be able to prime the premetastatic site from a distance before colonization to create a more favorable niche, for example, by secreting exosomes, a subpopulation of EVs (6). Furthermore, even within cancer cells, there is variability in the amount of depolarization. A more depolarized V_{mem} is associated with a higher metastatic potential and forced hyperpolarization of cells can reduce their migration and invasiveness (24, 141, 149, 150).

To study the effect of EFs on cell galvanotaxis, Zhu et al. employed unique probe systems to characterize cancer cell electrical properties and their migratory ability under an EF (151).

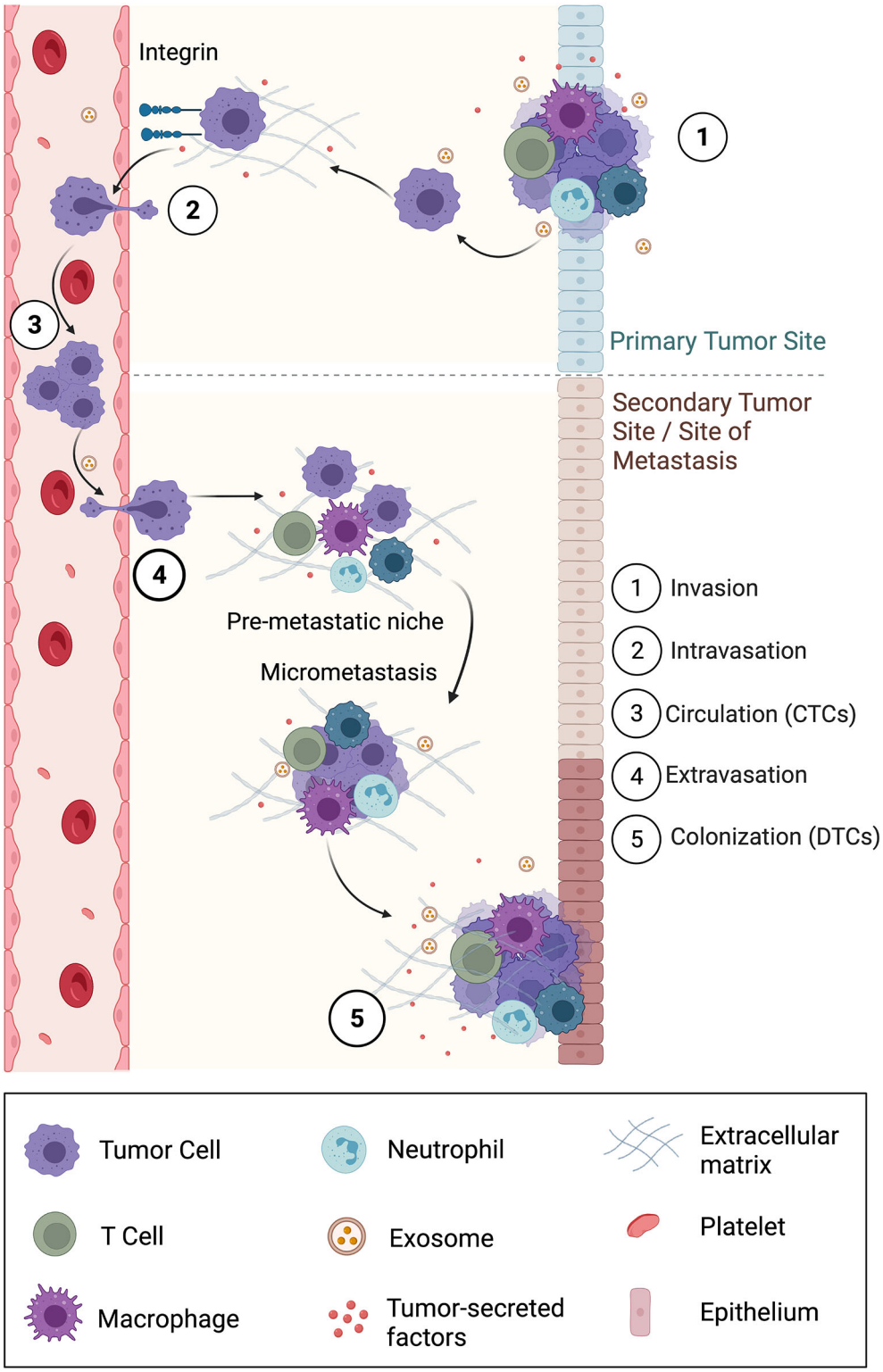

FIGURE 3 | Overview of the five-step metastatic cascade involving local invasion, intravasation into surrounding vasculature, circulation, extravasation, and finally colonization in a secondary location. Also shown is the formation of a pre-metastatic niche that supports the survival of disseminated tumor cells (DTCs) into a successful metastasis. Exosomes, a subpopulation of EVs play a primary role in carrying information from the primary site to the secondary site or site of metastasis, especially to form the pre-metastatic niche.

It was found that tumors established from 4T1, a triple-negative murine breast cancer cell line, produced heterogeneous intratumor potentials causing a flow of endogenous EFs inside and outside of the tumors, which may in turn affect cell migration behavior and ultimately contribute to cancer metastasis. Moreover, tumor electric potentials were found to increase with increase in tumor size, which is an important factor since the primary tumor size has been reported to be linked to the metastatic potential (152, 153). Finally, it was also found that metastatic sublines (m4T1) from lung, heart, axillary lymph node and spleen showed different galvanotaxis thresholds. For instance, parental 4T1 and lung metastatic cell lines were found to respond to EFs as low as 50 mV/mm, while other metastatic sublines showed an anodal migration in a field of 100 mV/mm or higher. Additionally, the migration speeds also varied among different metastatic sublines. Cancer cell monolayers were found to have a higher migration persistence (defined as the ratio of displacement to trajectory length) under EFs than that of isolated cells, suggesting that cancer cells migrated more linearly in a certain direction when responding to EFs collectively.

Interestingly, bioelectric factors override most chemical gradients and other cues in a multi-cue environment during cell migration (8). Lobikin et al. investigated a cell population termed as "instructor" cells which when depolarized, is able to direct the activity of an entirely different set of cells (7). The "instructor" cells induce metastatic phenotype in normal melanocytes by serotonergic signaling, a mechanism which mediates long-range bioelectric signaling. Furthermore, instructor cells also disrupt blood vessel patterning upon depolarization. The melanocytes were then found to acquire three properties commonly associated with metastasis – hyper-proliferation, a highly dendritic morphology, and invasion into tissues such as blood vessels, gut, and neural tube. This data illustrated the power of depolarized V_{mem} as an epigenetic initiator of widespread metastatic behavior in the absence of a centralized tumor.

APPLICATIONS

Current Devices, Materials and Technologies

Molecular-resolution tools have recently been developed for real-time detection and manipulation of bioelectric properties *in vivo* (91, 154). An important component of such investigations is the ability to track spatio-temporal distribution of V_{mem} gradients *in vivo*, over significant periods of time.

Detection of Bioelectric Properties

Microelectrodes are a common tool used to measure the electrophysiological characteristics of cells and are extremely powerful for single cell measurements. For instance, Zhu et al. used glass microelectrodes to measure intratumor potentials in subcutaneous tumors established from a triple-negative murine cancer cell line (4T1) (151). However, measurements corresponding to multicellular areas and volumes are constrained by the smaller size of these electrodes. Furthermore, the sample under study needs to be kept perfectly still (154). Fluorescent bioelectricity reporters are a more recent development which has facilitates measurement of electrophysiological properties when it is not feasible to use microelectrodes. These dyes can be used to achieve subcellular resolution, measure many cells simultaneously *in vivo*, and to track bioelectric gradients over long period of time despite cell movements and divisions (154). Chernet and Levin utilized voltage-sensitive fluorescent dyes to non-invasively detect areas of depolarization in oncogene-induced tumor structures in *Xenopus* larvae (24). A few other tools for the characterization of bioelectrical events are highly sensitive ion-selective extracellular electrode probes (105, 155) that reveal ion flux at the cell membrane, reporter proteins (156–159) and techniques that report individual ion species content such as protons (160) and sodium (161). Bioelectronic sensors or biosensors can also be used to sense electric fields, ionic concentrations, and biological markers (162–167). Based on the type of sensor, both intracellular and extracellular recordings of a single cell or a group of cells can be measured. A common transistor biosensor platform used for extracellular recordings is the organic electrochemical transistor (OECT) which is inherently sensitive to ionic species and external electric fields (14). The OECT is typically made of a poly(3,4-ethylenedioxythiophene): polystyrene sulfonate (PEDOT : PSS) mixture and has been implemented for recording of electrochemical gradients in non-excitable cells such as Caco-2 as well as excitable cells (168). Meanwhile, silicon nanowires are suitable for crossing the cell membrane and are commonly used for intracellular readings. These nanowires are synthesized with spatially controlled electrical properties. A nanoscale field effect transistor (NFET) is then created on an individual nanowire by varying the doping levels. NFETs allow localized and tuneable 3D sensing and recording of single cells and even 3D cellular networks. By having a three-dimensional probe presentation, NFETs overcome a major limitation of most traditional nanoelectronic devices which have a more planar design. Tian et al. used three-dimensional NFETs as localized bioprobes for intracellular readings in cardiomyocytes (169). While these methods are excellent tools for measuring cell electrical properties, tools that can manipulate these properties are essential to study the effects of altering cell states.

Manipulation of Bioelectric Properties

Bioactuators are a class of devices that can be used to modify cell behavior by delivering directly biophysical signals such as electrophoretic delivery of ions and small molecules targeting specific cell locations (14). Additionally, a variety of nanomaterials have been developed for reading and writing bioelectric cues in tissue. These include biocompatible piezoelectric materials and nanoparticles that alter the resting potential of cells by contact, without the use of transgenes (170–173). Warren and Payne determined that nanoparticles with amine-modified surfaces induced significant depolarization in both, Chinese Hamster Ovary (CHO) cells and HeLa cells (173).

Conductive polymers are another class of materials that can stimulate cells or tissue cultured upon them (174–176) by applying an electrical signal. Conductive polymers used in tissue engineering include conductive nanofibers, conductive hydrogels, conductive composite films, and conductive composite scaffolds fabricated using methods such as electrospinning, coating, or deposition by *in situ* polymerization (177). For instance, Jayaram et al. used PEDOT : PSS conducting polymer microwires to depolarize cells and achieve a more positive membrane potential in *E. coli* cells (170). Thourson and Payne also demonstrated the use of PEDOT : PSS microwires to control action potentials of cardiomyocytes (178). Conductive polymer microwires thus provide a minimally invasive platform to control electrical properties of cells with high spatial precision. Detailed reviews on conductive polymers have been previously published (177, 179).

As mentioned previously, treatment with ivermectin is another way to control the transmembrane potential of a select group of cells by manipulating of endogenous chloride channels (**Figure 4A**). Ivermectin targets GlyR-expressing cells and hence opens their chloride channels. Chloride ions can then be made to enter or exit the GlyR-expressing cells by manipulating the external chloride levels, thus controlling their transmembrane potential (7). For instance, a low level of chloride in the external medium would cause chloride ions to exit the cell and into the medium, hence depolarizing the cell. Lobikin et al. employed this method in frog models to regulate the membrane potential of a specific group of cells expressing GlyCl channels to desired levels and study the consequences on metastasis and tumorigenesis *in vivo*.

Another potential way to manipulate the bioelectric properties of cells is by controlling the mechanosensitive Ca^{2+}-permeable Piezo channels which have emerged as major transducers of mechanical stress into Ca^{2+} dependent signals. These mechanosensitive Piezo channels expressed on the plasma membrane are gated by various mechanical stimuli such as stiffness, compression, tension forces, and shear stress. Channel

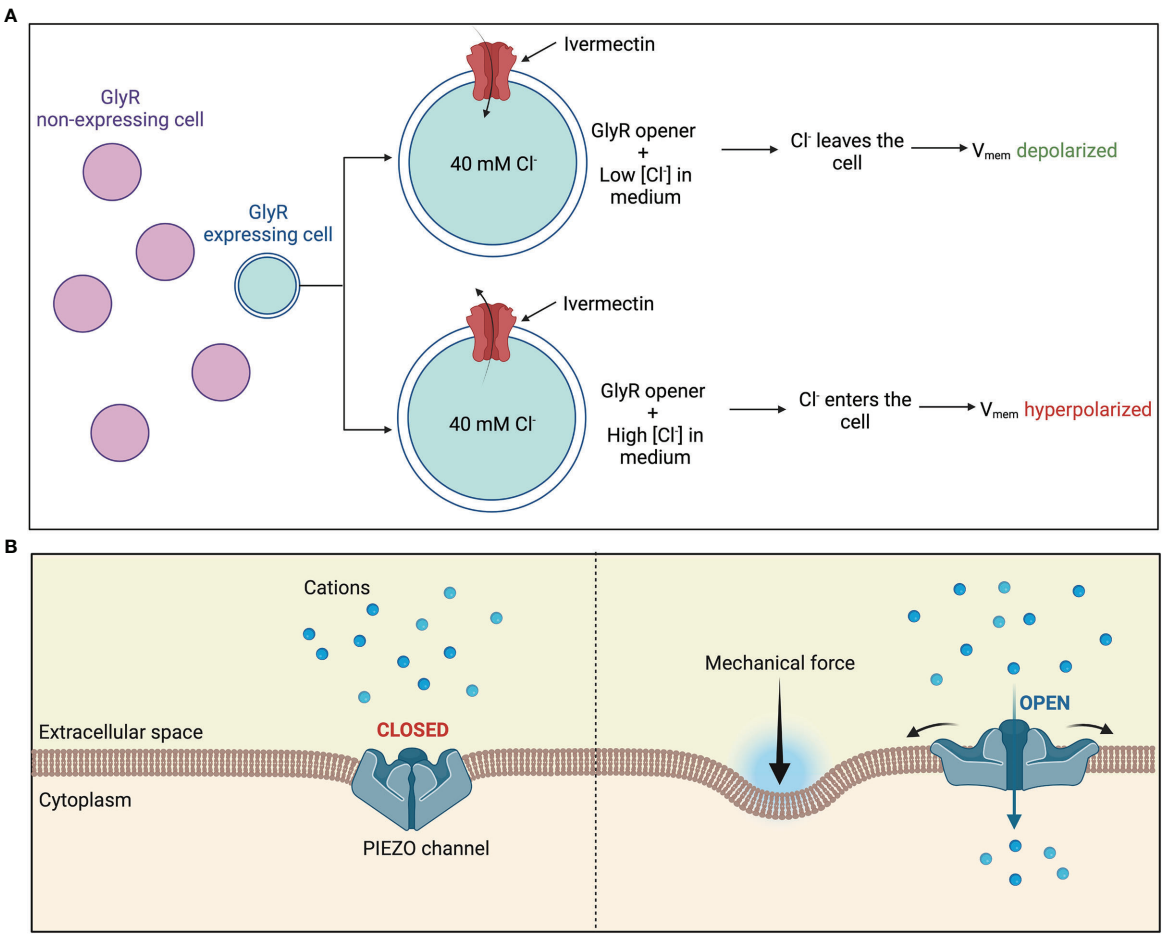

FIGURE 4 | Manipulating bioelectric properties of cells **(A)** Manipulation of endogenous chloride channels as a means of manipulating V_{mem} of a select group of cells. Treatment with ivermectin causes chloride channels in GlyR-expressing cells to open. External chloride levels are then manipulated to regulate movement of chloride flux into or out of the cytoplasm **(B)** Piezo1 and Piezo2 are mechanically activated cation channels. Application of a mechanical force causes the central pore to open, allowing an influx of positive charge into the cell.

activation then allows a Ca^{2+} influx into the cytoplasm which then mediates the cell polarity (**Figure 4B**). Piezo1 may also be pharmacologically activated by agonists such as Jedi1, Jedi2 and Yoda1 or inhibited by channel pore blockers, competitive antagonists, and peptides such as Ruthenium Red, GsMTx-4, Dooku1 and Aß peptides which distort the membrane mechanical properties (87). Han et al. demonstrated that activation of Piezo1 *via* mechanical stimuli in 1 µm using a heat-polished glass probe controlled by a piezo electric device or *via* agonist Yoda1 mediated Ca^{2+} influx in pancreatic cancer cells, resulting into a more depolarized state (88).

Extracellular Vesicles and Electricity

Extracellular vesicles (EVs) facilitate inter-cellular communication *via* delivery of proteins and nucleic acids, including microRNA (miRNA) and mRNA (180). EVs-mediated communication is vital during the establishment of planar cell polarity and the developmental patterning of tissues (181). EVs are particularly enriched in the tumor microenvironment (182, 183) and as mentioned in the previous sections of this paper, they play a special role in cancer development and progression. In a recent study, Fukuta et al. demonstrated that external stimuli such as low levels of electric field treatment that activate intracellular signaling would likely increase exosome secretion from the cells. It was seen that an electric field of 0.34 mA/cm^2 increases the secretion of these EVs from cultured cells of murine melanoma B16F1 and murine fibroblast 3T3 Swiss Albino without compromising their quality (180). These results together indicate that the bioelectric dysregulation or depolarization of cells that occurs during cancer may be responsible for the upregulation of EVs in the cancer tumor microenvironment. At the same time, the increase in production of EVs plays a role in disrupting the bioelectric homeostasis, forming a feedback loop. The change in cell state and EV production along with the interdependence of the two are major mechanisms responsible for the bioelectric dysregulation of cancer.

CONCLUSIONS

Bioelectric signaling is a growing field of study that takes us a step closer to understanding cancer as a disease, all the way from initiation to metastasis. A lot is known about cancer and its biology as per the somatic mutation theory. On the other hand, the role of electric fields in cancer processes, while strongly established over the last few decades, needs further investigation. Understanding the bioelectric mechanisms underlying cancer is especially important since it will allow us to develop new biomedical and bioengineering tools and techniques as per the tissue organization field theory. These new engineering tools, along with the existing biological knowledge will enhance our understanding of cancer and enable the development of novel treatments for patients.

Another exciting area of study is the interplay between the bioelectric dysregulation and enhancement of extracellular vesicles (EVs) within the context of the cancer microenvironment. It has been well established that EVs play a significant role in facilitating the signaling pathways involved in all processes of carcinogenesis. This paper provides a detailed review of the current knowledge about bioelectric dysregulation that underlies different processes of cancer. However, little is known about the interdependence of these two mechanisms. Furthermore, EVs, especially exosomes, have been proven to have a role in therapeutic strategies for cancer. Understanding this crosstalk will not only enhance our knowledge of cancer, but also help develop efficient exosome-based cancer immunotherapies and drug delivery vehicles.

AUTHOR CONTRIBUTIONS

MS wrote the main manuscript text and prepared all figures. LE gave suggestions and ideas on the literature search and manuscript writing. All authors contributed to the article and approved the submitted version.

FUNDING

This work has been funded by the National Science Foundation NSF CAREER ECCS (2046037).

ACKNOWLEDGMENTS

Figures 1 and **4A** were created with BioRender.com. **Figure 2** was adapted from "Tumor Microenvironment 2", by BioRender.com (2021). **Figure 3** was adapted from "Overview of Metastatic Cascade", by BioRender.com (2021). **Figure 4B** was adapted from "PIEZO Channels: How Do They Allow Mechanosensation?", by BioRender.com. (2021). **Figures 2**, **3**, and **4B** were retrieved from https://app.biorender.com/biorender-templates.

REFERENCES

1. Hanahan D, Weinberg RA. Hallmarks of Cancer: The Next Generation. *Cell* (2011) 144:646–74. doi: 10.1016/j.cell.2011.02.013
2. Vaux DL. In Defense of the Somatic Mutation Theory of Cancer. *Bioessays* (2011) 33:341–3. doi: 10.1002/bies.201100022
3. Mally A, Chipman JK. Non-Genotoxic Carcinogens: Early Effects on Gap Junctions, Cell Proliferation and Apoptosis in the Rat. *Toxicology* (2002) 180:233–48. doi: 10.1016/s0300-483x(02)00393-1
4. Versteeg R. Cancer: Tumours Outside the Mutation Box. *Nature* (2014) 506:438–9. doi: 10.1038/nature13061
5. Sonnenschein C, Soto AM. Theories of Carcinogenesis: An Emerging Perspective. *Semin Cancer Biol* (2008) 18:372–7. doi: 10.1016/j.semcancer.2008.03.012
6. Wortzel I, Dror S, Kenific CM, Lyden D. Exosome-Mediated Metastasis: Communication From a Distance. *Dev Cell* (2019) 49:347–60. doi: 10.1016/j.devcel.2019.04.011
7. Lobikin M, Chernet B, Lobo D, Levin M. Resting Potential, Oncogene-Induced Tumorigenesis, and Metastasis: The Bioelectric Basis of Cancer In Vivo. *Phys Biol* (2012) 9:65002. doi: 10.1088/1478-3975/9/6/065002

8. Funk RH. Endogenous Electric Fields as Guiding Cue for Cell Migration. *Front Physiol* (2015) 6:143. doi: 10.3389/fphys.2015.00143
9. Silver BB, Nelson CM. The Bioelectric Code: Reprogramming Cancer and Aging From the Interface of Mechanical and Chemical Microenvironments. *Front Cell Dev Biol* (2018) 6:21. doi: 10.3389/fcell.2018.00021
10. PayneSL, LevinM, OudinMJ. Bioelectric Control of Metastasis in Solid Tumors. *Bioelectricity* (2019) 1:114–30. doi: 10.1089/bioe.2019.0013
11. Simanov D, Mellaart-Straver I, Sormacheva I, Berezikov E. The Flatworm Macrostomum Lignano Is a Powerful Model Organism for Ion Channel and Stem Cell Research. *Stem Cells Int* (2012) 2012:167265. doi: 10.1155/2012/167265
12. Sundelacruz S, Levin M, Kaplan DL. Role of Membrane Potential in the Regulation of Cell Proliferation and Differentiation. *Stem Cell Rev Rep* (2009) 5:231–46. doi: 10.1007/s12015-009-9080-2
13. Blackiston DJ, McLaughlin KA, Levin M. Bioelectric Controls of Cell Proliferation: Ion Channels, Membrane Voltage and the Cell Cycle. *Cell Cycle* (2009) 8:3527–36. doi: 10.4161/cc.8.21.9888
14. Levin M, Selberg J, Rolandi M. Endogenous Bioelectrics in Development, Cancer, and Regeneration: Drugs and Bioelectronic Devices as Electroceuticals for Regenerative Medicine. *iScience* (2019) 22:519–33. doi: 10.1016/j.isci.2019.11.023
15. Al Ahmad M, Al Natour Z, Mustafa F, Rizvi T. Electrical Characterization of Normal and Cancer Cells. *IEEE Access PP* (2018) 1:25979–86. doi: 10.1109/ACCESS.2018.2830883
16. Levin M. Molecular Bioelectricity: How Endogenous Voltage Potentials Control Cell Behavior and Instruct Pattern Regulation In Vivo. *Mol Biol Cell* (2014) 25:3835–50. doi: 10.1091/mbc.E13-12-0708
17. McCaig CD, Song B, Rajnicek AM. Electrical Dimensions in Cell Science. *J Cell Sci* (2009) 122:4267–76. doi: 10.1242/jcs.023564
18. Levin M. Bioelectric Mechanisms in Regeneration: Unique Aspects and Future Perspectives. *Semin Cell Dev Biol* (2009) 20:543–56. doi: 10.1016/j.semcdb.2009.04.013
19. Rajnicek AM, Foubister LE, McCaig CD. Growth Cone Steering by a Physiological Electric Field Requires Dynamic Microtubules, Microfilaments and Rac-Mediated Filopodial Asymmetry. *J Cell Sci* (2006) 119:1736–45. doi: 10.1242/jcs.02897
20. Becchetti A. Ion Channels and Transporters in Cancer. 1. Ion Channels and Cell Proliferation in Cancer. *Am J Physiol Cell Physiol* (2011) 301:C255–265. doi: 10.1152/ajpcell.00047.2011
21. Prevarskaya N, Skryma R, Shuba Y. Ion Channels and the Hallmarks of Cancer. *Trends Mol Med* (2010) 16:107–21. doi: 10.1016/j.molmed.2010.01.005
22. Pardo LA, Contreras-Jurado C, Zientkowska M, Alves F, Stühmer W. Role of Voltage-Gated Potassium Channels in Cancer. *J Membr Biol* (2005) 205:115–24. doi: 10.1007/s00232-005-0776-1
23. Kunzelmann K. Ion Channels and Cancer. *J Membr Biol* (2005) 205:159–73. doi: 10.1007/s00232-005-0781-4
24. Chernet B, Levin M. Endogenous Voltage Potentials and the Microenvironment: Bioelectric Signals That Reveal, Induce and Normalize Cancer. *J Clin Exp Oncol Suppl* (2013) 1:S1–002. doi: 10.4172/2324-9110.S1-002
25. Arcangeli A, Crociani O, Lastraioli E, Masi A, Pillozzi S, Becchetti A. Targeting Ion Channels in Cancer: A Novel Frontier in Antineoplastic Therapy. *Curr Med Chem* (2009) 16:66–93. doi: 10.2174/092986709787002835
26. Jiang LH, Adinolfi E, Roger S. Editorial: Ion Channel Signalling in Cancer: From Molecular Mechanisms to Therapeutics. *Front Pharmacol* (2021) 12:711593. doi: 10.3389/fphar.2021.711593
27. Lang F, Stournaras C. Ion Channels in Cancer: Future Perspectives and Clinical Potential. *Philos Trans R Soc Lond B Biol Sci* (2014) 369:1638. doi: 10.1098/rstb.2013.0108
28. Litan A, Langhans SA. Cancer as a Channelopathy: Ion Channels and Pumps in Tumor Development and Progression. *Front Cell Neurosci* (2015) 9:86. doi: 10.3389/fncel.2015.00086
29. Prevarskaya N, Skryma R, Shuba Y. Ion Channels in Cancer: Are Cancer Hallmarks Oncochannelopathies? *Physiol Rev* (2018) 98(2):559–621. doi: 10.1152/physrev.00044.2016
30. Dhillon AS, Hagan S, Rath O, Kolch W. MAP Kinase Signalling Pathways in Cancer. *Oncogene* (2007) 26(22):3279–90. doi: 10.1038/sj.onc.1210421
31. Taylor JT, Huang L, Pottle JE, Pottle K, Yang Y, Zeng X, et al. Selective Blockade of T-Type Ca2+ Channels Suppresses Human Breast Cancer Cell Proliferation. *Cancer Lett* (2008) 267:116–24. doi: 10.1016/j.canlet.2008.03.032
32. Berzingi S, Newman M, Yu HG. Altering Bioelectricity on Inhibition of Human Breast Cancer Cells. *Cancer Cell Int* (2016) 16:72. doi: 10.1186/s12935-016-0348-8
33. Guéguinou M, Harnois T, Crottes D, Uguen A, Deliot N, Gambade M, et al. SK3/TRPC1/Orai1 Complex Regulates SOCE-Dependent Colon Cancer Cell Migration: A Novel Opportunity to Modulate Anti-EGFR mAb Action by the Alkyl-Lipid Ohmline. *Oncotarget* (2016) 7:36168–84. doi: 10.18632/oncotarget.8786
34. Jacquemet G, Baghirov H, Georgiadou M, Sihto H, Peuhu E, Cettour-Janet P, et al. L-Type Calcium Channels Regulate Filopodia Stability and Cancer Cell Invasion Downstream of Integrin Signaling. *Nat Commun* (2016) 7:13297. doi: 10.1038/ncomms13297
35. Hegle AP, Marble DD, Wilson GF. A Voltage-Driven Switch for Ion-Independent Signaling by Ether-À-Go-Go K+ Channels. *Proc Natl Acad Sci USA* (2006) 103:2886–91. doi: 10.1073/pnas.0505909103
36. Ouadid-Ahidouch H, Dhennin-Duthille I, Gautier M, Sevestre H, Ahidouch A. TRP Calcium Channel and Breast Cancer: Expression, Role and Correlation With Clinical Parameters. *Bull Cancer* (2012) 99:655–64. doi: 10.1684/bdc.2012.1595
37. Kohn EC, Jacobs W, Kim YS, Alessandro R, Stetler-Stevenson WG, Liotta LA, et al. Calcium Influx Modulates Expression of Matrix Metalloproteinase-2 (72-kDa Type IV Collagenase, Gelatinase a). *J Biol Chem* (1994) 269:21505–11. doi: 10.1016/S0021-9258(17)31833-1
38. Davis FM, Azimi I, Faville RA, Peters AA, Jalink K, Putney JW Jr, et al. Induction of Epithelial-Mesenchymal Transition (EMT) in Breast Cancer Cells is Calcium Signal Dependent. *Oncogene* (2014) 33:2307–16. doi: 10.1038/onc.2013.187
39. Aydar E, Yeo S, Djamgoz M, Palmer C. Abnormal Expression, Localization, and Interaction of Canonical Transient Receptor Potential Ion Channels in Human Breast Cancer Cell Lines and Tissues: A Potential Target for Breast Cancer Diagnosis and Therapy. *Cancer Cell Int* (2009) 9:23. doi: 10.1186/1475-2867-9-23
40. Ding X, He Z, Zhou K, Cheng J, Yao H, Lu D, et al. Essential Role of TRPC6 Channels in G2/M Phase Transition and Development of Human Glioma. *J Natl Cancer Inst* (2010) 102(14):1052–68. doi: 10.1093/jnci/djq217
41. Tajeddine N, Gailly P. TRPC1 Protein Channel is Major Regulator of Epidermal Growth Factor Receptor Signaling. *J Biol Chem* (2012) 287(20):16146–57. doi: 10.1074/jbc.M112.340034
42. Kusaba T, Okigaki M, Matui A, Murakami M, Ishikawa K, Kimura T, et al. Klotho is Associated With VEGF Receptor-2 and the Transient Receptor Potential Canonical-1 Ca2+ Channel to Maintain Endothelial Integrity. *Proc Natl Acad Sci USA* (2010) 107(45):19308–13. doi: 10.1073/pnas.1008544107
43. Shan D, Marchase RB, Chatham JC. Overexpression of TRPC3 Increases Apoptosis But Not Necrosis in Response to Ischemia-Reperfusion in Adult Mouse Cardiomyocytes. *Am J Physiol Cell Physiol* (2008) 294(3):C833–41. doi: 10.1152/ajpcell.00313.2007
44. Mukerji N, Damodaran TV, Winn MP. TRPC6 and FSGS: The Latest TRP Channelopathy. *Biochim Biophys Acta* (2007) 1772(8):859–68. doi: 10.1016/j.bbadis.2007.03.005
45. Sun YH, Li Q, Feng SL, Li BX, Pan ZW, Xu CQ, et al. Calcium-Sensing Receptor Activation Contributed to Apoptosis Stimulates TRPC6 Channel in Rat Neonatal Ventricular Myocytes. *Biochem Biophys Res Commun* (2010) 394(4):955–61. doi: 10.1016/j.bbrc.2010.03.096
46. Yu L, Lin Q, Liao H, Feng J, Dong X, Ye J, et al. TGF-β1 Induces Podocyte Injury Through Smad3-ERK-NF-κb Pathway and Fyn-Dependent TRPC6 Phosphorylation. *Cell Physiol Biochem* (2010) 26(6):869–78. doi: 10.1159/000323996
47. Gao Y, Lei Z, Lu C, Roisen FJ, El-Mallakh RS. Effect of Ionic Stress on Apoptosis and the Expression of TRPM2 in Human Olfactory Neuroepithelial-Derived Progenitors. *World J Biol Psychiatry* (2010) 11(8):972–84. doi: 10.3109/15622975.2010.507784

48. Hecquet CM, Malik AB. Role of H(2)O(2)-Activated TRPM2 Calcium Channel in Oxidant-Induced Endothelial Injury. *Thromb Haemost* (2009) 101(4):619–25. doi: 10.1160/TH08-10-0641
49. Massullo P, Sumoza-Toledo A, Bhagat H, Partida-Sánchez S. TRPM Channels, Calcium and Redox Sensors During Innate Immune Responses. *Semin Cell Dev Biol* (2006) 17(6):654–66. doi: 10.1016/j.semcdb.2006.11.006
50. Li Q, Wang X, Yang Z, Wang B, Li S. Menthol Induces Cell Death *via* the TRPM8 Channel in the Human Bladder Cancer Cell Line T24. *Oncology* (2009) 77(6):335–41. doi: 10.1159/000264627
51. Prevarskaya N, Zhang L, Barritt G. TRP Channels in Cancer. *Biochim Biophys Acta* (2007) 1772(8):937–46. doi: 10.1016/j.bbadis.2007.05.006
52. Chigurupati S, Venkataraman R, Barrera D, Naganathan A, Madan M, Paul L, et al. Receptor Channel TRPC6 is a Key Mediator of Notch-Driven Glioblastoma Growth and Invasiveness. *Cancer Res* (2010) 70(1):418–27. doi: 10.1158/0008-5472.CAN-09-2654
53. Thoppil RJ, Cappelli HC, Adapala RK, Kanugala AK, Paruchuri S, Thodeti CK. TRPV4 Channels Regulate Tumor Angiogenesis *via* Modulation of Rho/Rho Kinase Pathway. *Oncotarget* (2016) 7(18):25849–6. doi: 10.18632/oncotarget.8405
54. Gillet L, Roger S, Besson P, Lecaille F, Gore J, Bougnoux P, et al. Voltage-Gated Sodium Channel Activity Promotes Cysteine Cathepsin-Dependent Invasiveness and Colony Growth of Human Cancer Cells. *J Biol Chem* (2009) 284:8680–91. doi: 10.1074/jbc.M806891200
55. Campbell TM, Main MJ, Fitzgerald EM. Functional Expression of the Voltage-Gated Na+ Channel $Na_v1.7$ is Necessary for EGF-Mediated Invasion in Human non-Small Cell Lung Cancer Cells. *J Cell Sci* (2013) 126:4939 – 4949. doi: 10.1242/jcs.130013
56. House CD, Wang BD, Ceniccola K, Williams R, Simaan M, Olender J, et al. Voltage-Gated Na+ Channel Activity Increases Colon Cancer Transcriptional Activity and Invasion *Via* Persistent MAPK Signaling. *Sci Rep* (2015) 5:11541. doi: 10.1038/srep11541
57. House CD, Vaske CJ, Vaske AM, Obias V, Frank B, Luu T, et al. Voltage-Gated Na+ Channel SCN5A is a Key Regulator of a Gene Transcriptional Network That Controls Colon Cancer Invasion. *Cancer Res* (2010) 70:6957–67. doi: 10.1158/0008-5472.CAN-10-1169
58. Chioni AM, Shao D, Grose R, Djamgoz MB. Protein Kinase A and Regulation of Neonatal Nav1.5 Expression in Human Breast Cancer Cells: Activity-Dependent Positive Feedback and Cellular Migration. *Int J Biochem Cell Biol* (2010) 42:346–58. doi: 10.1016/j.biocel.2009.11.021
59. Schwab A, Fabian A, Hanley PJ, Stock C. Role of Ion Channels and Transporters in Cell Migration. *Physiol Rev* (2012) 92:1865–913. doi: 10.1152/physrev.00018.2011
60. Cardone RA, Casavola V, Reshkin SJ. The Role of Disturbed pH Dynamics and the Na+/H+ Exchanger in Metastasis. *Nat Rev Cancer* (2005) 5:786–95. doi: 10.1038/nrc1713
61. Kaverina I, Krylyshkina O, Small JV. Regulation of Substrate Adhesion Dynamics During Cell Motility. *Int J Biochem Cell Biol* (2002) 34:746–61. doi: 10.1016/s1357-2725(01)00171-6
62. Conti M. Targeting K+ Channels for Cancer Therapy. *J Exp Ther Oncol* (2004) 4:161–6.
63. Fraser SP, Grimes JA, Djamgoz MB. Effects of Voltage-Gated Ion Channel Modulators on Rat Prostatic Cancer Cell Proliferation: Comparison of Strongly and Weakly Metastatic Cell Lines. *Prostate* (2000) 44:61–76. doi: 10.1002/1097-0045(20000615)44:1<61::aid-pros9>3.0.co;2-3
64. Fukushiro-Lopes DF, Hegel AD, Rao V, Wyatt D, Baker A, Breuer EK, et al. Preclinical Study of a Kv11.1 Potassium Channel Activator as Antineoplastic Approach for Breast Cancer. *Oncotarget* (2018) 9:3321–37. doi: 10.18632/oncotarget.22925
65. Lallet-Daher H, Roudbaraki M, Bavencoffe A, Mariot P, Gackière F, Bidaux G, et al. Intermediate-Conductance Ca2+-Activated K+ Channels (IKCa1) Regulate Human Prostate Cancer Cell Proliferation Through a Close Control of Calcium Entry. *Oncogene* (2009) 28:1792–806. doi: 10.1038/onc.2009.25
66. Zhang P, Yang X, Yin Q, Yi J, Wenzhuang S, Zhao L, et al. Inhibition of SK4 Potassium Channels Suppresses Cell Proliferation, Migration and the Epithelial-Mesenchymal Transition in Triple-Negative Breast Cancer Cells. *PloS One* (2016) 11:e0154471. doi: 10.1371/journal.pone.0154471
67. Blackiston D, Adams DS, Lemire JM, Lobikin M, Levin M. Transmembrane Potential of GlyCl-Expressing Instructor Cells Induces a Neoplastic-Like Conversion of Melanocytes *via* a Serotonergic Pathway. *Dis Model Mech* (2011) 4:67–85. doi: 10.1242/dmm.005561
68. Ufartes R, Schneider T, Mortensen LS, de Juan Romero C, Hentrich K, Knoetgen H, et al. Behavioral and Functional Characterization of Kv10.1 (Eag1) Knockout Mice. *Hum Mol Genet* (2013) 22(11):2247–62. doi: 10.1093/hmg/ddt076
69. Agarwal JR, Griesinger F, Stühmer W, Pardo LA. The Potassium Channel Ether À Go-Go is a Novel Prognostic Factor With Functional Relevance in Acute Myeloid Leukemia. *Mol Cancer* (2010) 9:18. doi: 10.1186/1476-4598-9-18
70. Jehle J, Schweizer PA, Katus HA, Thomas D. Novel Roles for hERG K(+) Channels in Cell Proliferation and Apoptosis. *Cell Death Dis* (2011) 2:e193. doi: 10.1038/cddis.2011.77
71. Farias LM, Ocaña DB, Díaz L, Larrea F, Avila-Chávez E, Cadena A, et al. Ether a Go-Go Potassium Channels as Human Cervical Cancer Markers. *Cancer Res* (2004) 64:6996–7001. doi: 10.1158/0008-5472.CAN-04-1204
72. Pardo LA, del Camino D, Sánchez A, Alves F, Brüggemann A, Beckh S, et al. Oncogenic Potential of EAG K(+) Channels. *EMBO J* (1999) 18:5540–7. doi: 10.1093/emboj/18.20.5540
73. Payne SL, Ram P, Srinivasan DH, Le TT, Levin M, Oudin MJ. Potassium Channel-Driven Bioelectric Signaling Regulates Metastasis in Triple-Negative Breast Cancer. *EBioMedicine* (2022) 75:103767. doi: 10.1016/j.ebiom.2021.103767
74. Millership JE, Devor DC, Hamilton KL, Balut CM, Bruce JI, Fearson IM, et al. Calcium- Activated K+ Channels Increase Cell Proliferation Independent of K+ Conductance. *Am J Physiol Cell Physiol* (2011) 300: C792–802. doi: 10.1152/ajpcell.00274.2010
75. Turner KL, Sontheimer H. Cl- and K+ Channels and Their Role in Primary Brain Tumour Biology. *Philos Trans R Soc London Ser B Biol Sci* (2014) 369 (1638):20130095. doi: 10.1098/rstb.2013.0095
76. Wondergem R, Ecay TW, Mahieu F, Owsianik G, Nilius B. HGF/SF and Menthol Increase Human Glioblastoma Cell Calcium and Migration. *Biochem Biophys Res Commun* (2008) 372(1):210–5. doi: 10.1016/j.bbrc.2008.05.032
77. Liu J, Chen Y, Shuai S, Ding D, Li R, Luo R, et al. TRPM8 Promotes Aggressiveness of Breast Cancer Cells by Regulating EMT *via* Activating AKT/GSK-3ß Pathway. *Tumor Biol* (2014) 35:8969 – 8977. doi: 10.1007/s13277-014-2077-8
78. Jirsch J, Deeley RG, Cole SP, Stewart AJ, Fedida D. Inwardly Rectifying K+ Channels and Volume-Regulated Anion Channels in Multidrug-Resistant Small Cell Lung Cancer Cells. *Cancer Res* (1993) 53:4156–60.
79. Habela CW, Olsen ML, Sontheimer H. ClC3 is a Critical Regulator of the Cell Cycle in Normal and Malignant Glial Cells. *J Neurosci* (2008) 28:9205–17. doi: 10.1523/JNEUROSCI.1897-08.2008
80. Volkov A, Waite AJ, Wooten JD, Markin VS. Circadian Rhythms in Biologically Closed Electrical Circuits of Plants. *Plant Signal Behav* (2012) 7:282–4. doi: 10.4161/psb.18798
81. Shuba YM, Prevarskaya N, Lemonnier L, Van Coppenolle F, Kostyuk PG, Mauroy B, et al. Volume-Regulated Chloride Conductance in the LNCaP Human Prostate Cancer Cell Line. *Am J Physiol Cell Physiol* (2000) 279: C1144–1154. doi: 10.1152/ajpcell.2000.279.4.C1144
82. Cuddapah VA, Sontheimer H. Molecular Interaction and Functional Regulation of ClC-3 by Ca2+/calmodulin-Dependent Protein Kinase II (CaMKII) in Human Malignant Glioma. *J Biol Chem* (2010) 285 (15):11188–96. doi: 10.1074/jbc.M109.097675
83. Coste B, Mathur J, Schmidt M, Earley TJ, Ranade S, Petrus MJ, et al. Piezo1 and Piezo2 are Essential Components of Distinct Mechanically Activated Cation Channels. *Science* (2010) 330:55–60. doi: 10.1126/science.1193270
84. Cox CD, Bae C, Ziegler L, Hartley S, Nikolova-Krstevski V, Rohde PR, et al. Removal of the Mechanoprotective Influence of the Cytoskeleton Reveals PIEZO1 is Gated by Bilayer Tension. *Nat Commun* (2016) 7:10366. doi: 10.1038/ncomms10366
85. Ranade SS, Qiu Z, Woo SH, Hur SS, Murthy SE, Cahalan SM, et al. Piezo1, a Mechanically Activated Ion Channel, is Required for Vascular Development in Mice. *Proc Natl Acad Sci USA* (2014) 111:10347–52. doi: 10.1073/pnas.1409233111

86. Moroni M, Servin-Vences MR, Fleischer R, Sánchez-Carranza O, Lewin GR. Voltage Gating of Mechanosensitive PIEZO Channels. *Nat Commun* (2018) 9:1096. doi: 10.1038/s41467-018-03502-7
87. De Felice D, Alaimo A. Mechanosensitive Piezo Channels in Cancer: Focus on Altered Calcium Signaling in Cancer Cells and in Tumor Progression. *Cancers (Basel)* (2020) 12:1780. doi: 10.3390/cancers12071780
88. Han Y, Liu C, Zhang D, Men H, Huo L, Geng Q, et al. Mechanosensitive Ion Channel Piezo1 Promotes Prostate Cancer Development Through the Activation of the Akt/mTOR Pathway and Acceleration of Cell Cycle. *Int J Oncol* (2019) 55(3):629–44. doi: 10.3892/ijo.2019.4839
89. Yang H, Liu C, Zhou RM, Yao J, Li XM, Shen Y, et al. Piezo2 Protein: A Novel Regulator of Tumor Angiogenesis and Hyperpermeability. *Oncotarget* (2016) 7:44630–44643. doi: 10.18632/oncotarget.10134
90. Levin M. Molecular Bioelectricity in Developmental Biology: New Tools and Recent Discoveries: Control of Cell Behavior and Pattern Formation by Transmembrane Potential Gradients. *Bioessays* (2012) 34:205–17. doi: 10.1002/bies.201100136
91. Adams DS, Levin M. Endogenous Voltage Gradients as Mediators of Cell-Cell Communication: Strategies for Investigating Bioelectrical Signals During Pattern Formation. *Cell Tissue Res* (2013) 352:95–122. doi: 10.1007/s00441-012-1329-4
92. Levin M, Stevenson CG. Regulation of Cell Behavior and Tissue Patterning by Bioelectrical Signals: Challenges and Opportunities for Biomedical Engineering. *Annu Rev BioMed Eng* (2012) 14:295–323. doi: 10.1146/annurev-bioeng-071811-150114
93. Marino AA, Iliev IG, Schwalke MA, Gonzalez E, Marler KC, Flanagan CA, et al. Association Between Cell Membrane Potential and Breast Cancer. *Tumour Biol* (1994) 15:82–9. doi: 10.1159/000217878
94. Morokuma J, Blackiston D, Adams DS, Seebohm G, Trimmer B, Levin M. Modulation of Potassium Channel Function Confers a Hyperproliferative Invasive Phenotype on Embryonic Stem Cells. *Proc Natl Acad Sci USA* (2008) 105:16608–13. doi: 10.1073/pnas.0808328105
95. Cone CD. Unified Theory on the Basic Mechanism of Normal Mitotic Control and Oncogenesis. *J Theor Biol* (1971) 30:151–81. doi: 10.1016/0022-5193(71)90042-7
96. Cone CD. The Role of the Surface Electrical Transmembrane Potential in Normal and Malignant Mitogenesis. *Ann N Y Acad Sci* (1974) 238:420–35. doi: 10.1111/j.1749-6632.1974.tb26808.x
97. Binggeli R, Weinstein RC. Membrane Potentials and Sodium Channels: Hypotheses for Growth Regulation and Cancer Formation Based on Changes in Sodium Channels and Gap Junctions. *J Theor Biol* (1986) 123:377–401. doi: 10.1016/s0022-5193(86)80209-0
98. Binggeli R, Cameron IL. Cellular Potentials of Normal and Cancerous Fibroblasts and Hepatocytes. *Cancer Res* (1980) 40:1830–5.
99. Stratton MR, Fisher C, Gusterson BA, Cooper CS. Detection of Point Mutations in N-Ras and K-Ras Genes of Human Embryonal Rhabdomyosarcomas Using Oligonucleotide Probes and the Polymerase Chain Reaction. *Cancer Res* (1989) 49:6324–7.
100. Gilmore TD, Kalaitzidis D, Liang MC, Starczynowski DT. The C-Rel Transcription Factor and B-Cell Proliferation: A Deal With the Devil. *Oncogene* (2004) 23:2275–86. doi: 10.1038/sj.onc.1207410
101. McNulty SE, del Rosario R, Cen D, Meyskens FL, Yang S. Comparative Expression of NFkappaB Proteins in Melanocytes of Normal Skin vs. Benign Intradermal Naevus and Human Metastatic Melanoma Biopsies. *Pigment Cell Res* (2004) 17:173–80. doi: 10.1111/j.1600-0749.2004.00128.x
102. Clement V, Sanchez P, de Tribolet N, Radovanovic I, Ruiz i Altaba A. HEDGEHOG-GLI1 Signaling Regulates Human Glioma Growth, Cancer Stem Cell Self-Renewal, and Tumorigenicity. *Curr Biol* (2007) 17:165–72. doi: 10.1016/j.cub.2006.11.033
103. Chernet BT, Levin M. Transmembrane Voltage Potential is an Essential Cellular Parameter for the Detection and Control of Tumor Development in a Xenopus Model. *Dis Model Mech* (2013) 6:595–607. doi: 10.1242/dmm.010835
104. Thompson IM, Pauler IM, Goodman IM, Tangen IM, Lucia IM, Parnes IM, et al. Prevalence of Prostate Cancer Among Men With a Prostate-Specific Antigen Level < or =4.0 Ng Per Milliliter. *N Engl J Med* (2004) 350:2239–46. doi: 10.1056/NEJMoa031918
105. Smith DS, Humphrey PA, Catalona WJ. The Early Detection of Prostate Carcinoma With Prostate Specific Antigen: The Washington University Experience. *Cancer* (1997) 80:1852–6. doi: 10.1002/(SICI)1097-0142(19971101)80:9<1852::AID-CNCR25>3.0.CO;2-3
106. Carvalho J. A Bioelectric Model of Carcinogenesis, Including Propagation of Cell Membrane Depolarization and Reversal Therapies. *Sci Rep* (2021) 11:13607. doi: 10.1038/s41598-021-92951-0
107. Li C, Teixeira AF, Zhu HJ, Ten Dijke P. Cancer Associated-Fibroblast-Derived Exosomes in Cancer Progression. *Mol Cancer* (2021) 20:154. doi: 10.1186/s12943-021-01463-y
108. Maia J, Caja S, Strano Moraes MC, Couto N, Costa-Silva B. Exosome-Based Cell-Cell Communication in the Tumor Microenvironment. *Front Cell Dev Biol* (2018) 6:18. doi: 10.3389/fcell.2018.00018
109. Wu Q, Zhou L, Lv D, Zhu X, Tang H. Exosome-Mediated Communication in the Tumor Microenvironment Contributes to Hepatocellular Carcinoma Development and Progression. *J Hematol Oncol* (2019) 12:53. doi: 10.1186/s13045-019-0739-0
110. Todaro GJ, Green H. Quantitative Studies of the Growth of Mouse Embryo Cells in Culture and Their Development Into Established Lines. *J Cell Biol* (1963) 17:299–313. doi: 10.1083/jcb.17.2.299
111. Blennerhassett MG, Kannan MS, Garfield RE. Density-Dependent Hyperpolarization in Cultured Aortic Smooth Muscle Cells. *Am J Physiol* (1989) 256:C644–651. doi: 10.1152/ajpcell.1989.256.3.C644
112. Bossu JL, Elhamdani A, Feltz A. Voltage-Dependent Calcium Entry in Confluent Bovine Capillary Endothelial Cells. *FEBS Lett* (1992) 299:239–42. doi: 10.1016/0014-5793(92)80123-x
113. Pang MF, Siedlik MJ, Han S, Stallings-Mann M, Radisky DC, Nelson CM. Tissue Stiffness and Hypoxia Modulate the Integrin-Linked Kinase ILK to Control Breast Cancer Stem-Like Cells. *Cancer Res* (2016) 76:5277–87. doi: 10.1158/0008-5472.CAN-16-0579
114. Damaghi M, Wojtkowiak JW, Gillies RJ. pH Sensing and Regulation in Cancer. *Front Physiol* (2013) 4:370. doi: 10.3389/fphys.2013.00370
115. Yu S, Cao H, Shen B, Feng J. Tumor-Derived Exosomes in Cancer Progression and Treatment Failure. *Oncotarget* (2015) 6:37151–68. doi: 10.18632/oncotarget.6022
116. Clapham DE. Calcium Signaling. *Cell* (2007) 131:1047–58. doi: 10.1016/j.cell.2007.11.028
117. Ohkubo T, Yamazaki J. T-Type Voltage-Activated Calcium Channel Cav3.1, But Not Cav3.2, is Involved in the Inhibition of Proliferation and Apoptosis in MCF-7 Human Breast Cancer Cells. *Int J Oncol* (2012) 41:267–75. doi: 10.3892/ijo.2012.1422
118. Rothberg BS. The BK Channel: A Vital Link Between Cellular Calcium and Electrical Signaling. *Protein Cell* (2012) 3:883–92. doi: 10.1007/s13238-012-2076-8
119. Martinac B. The Ion Channels to Cytoskeleton Connection as Potential Mechanism of Mechanosensitivity. *Biochim Biophys Acta* (2014) 1838:682–91. doi: 10.1016/j.bbamem.2013.07.015
120. Discher DE, Janmey P, Wang YL. Tissue Cells Feel and Respond to the Stiffness of Their Substrate. *Science* (2005) 310:1139–43. doi: 10.1126/science.1116995
121. Piotrowski-Daspit AS, Tien J, Nelson CM. Interstitial Fluid Pressure Regulates Collective Invasion in Engineered Human Breast Tumors *via* Snail, Vimentin, and E-Cadherin. *Integr Biol (Camb)* (2016) 8:319–31. doi: 10.1039/c5ib00282f
122. Engler AJ, Sen S, Sweeney HL, Discher DE. Matrix Elasticity Directs Stem Cell Lineage Specification. *Cell* (2006) 126:677–89. doi: 10.1016/j.cell.2006.06.044
123. Kim TJ, Seong J, Ouyang M, Sun J, Lu S, Hong JP, et al. Substrate Rigidity Regulates Ca2+ Oscillation *via* RhoA Pathway in Stem Cells. *J Cell Physiol* (2009) 218:285–93. doi: 10.1002/jcp.21598
124. Kostic A, Lynch CD, Sheetz MP. Differential Matrix Rigidity Response in Breast Cancer Cell Lines Correlates With the Tissue Tropism. *PloS One* (2009) 4:e6361. doi: 10.1371/journal.pone.0006361
125. Tilghman RW, Cowan CR, Mih JD, Koryakina Y, Gioeli D, Slack-Davis JK, et al. Matrix Rigidity Regulates Cancer Cell Growth and Cellular Phenotype. *PloS One* (2010) 5:e12905. doi: 10.1371/journal.pone.0012905
126. Zhang YH, Zhao CQ, Jiang LS, Dai LY. Substrate Stiffness Regulates Apoptosis and the mRNA Expression of Extracellular Matrix Regulatory Genes in the Rat Annular Cells. *Matrix Biol* (2011) 30:135–44. doi: 10.1016/j.matbio.2010.10.008

127. Lee K, Chen QK, Lui C, Cichon MA, Radisky DC, Nelson CM. Matrix Compliance Regulates Rac1b Localization, NADPH Oxidase Assembly, and Epithelial-Mesenchymal Transition. *Mol Biol Cell* (2012) 23:4097–108. doi: 10.1091/mbc.E12-02-0166
128. Pathak MM, Nourse JL, Tran T, Hwe J, Arulmoli J, Le DT, et al. Stretch-Activated Ion Channel Piezo1 Directs Lineage Choice in Human Neural Stem Cells. *Proc Natl Acad Sci USA* (2014) 111:16148–53. doi: 10.1073/pnas.1409802111
129. Chen CS, Mrksich M, Huang S, Whitesides GM, Ingber DE. Geometric Control of Cell Life and Death. *Science* (1997) 276:1425–8. doi: 10.1126/science.276.5317.1425
130. Dike LE, Chen CS, Mrksich M, Tien J, Whitesides GM, Ingber DE. Geometric Control of Switching Between Growth, Apoptosis, and Differentiation During Angiogenesis Using Micropatterned Substrates. *In Vitro Cell Dev Biol Anim* (1999) 35:441–8. doi: 10.1007/s11626-999-0050-4
131. Vogel V, Sheetz M. Local Force and Geometry Sensing Regulate Cell Functions. *Nat Rev Mol Cell Biol* (2006) 7:265–75. doi: 10.1038/nrm1890
132. Walsh MF, Woo RK, Gomez R, Basson MD. Extracellular Pressure Stimulates Colon Cancer Cell Proliferation *via* a Mechanism Requiring PKC and Tyrosine Kinase Signals. *Cell Prolif* (2004) 37:427–41. doi: 10.1111/j.1365-2184.2004.00324.x
133. Basson MD, Zeng B, Downey C, Sirivelu MP, Tepe JJ. Increased Extracellular Pressure Stimulates Tumor Proliferation by a Mechanosensitive Calcium Channel and PKC-β. *Mol Oncol* (2015) 9:513–26. doi: 10.1016/j.molonc.2014.10.008
134. Kobayashi T, Sokabe M. Sensing Substrate Rigidity by Mechanosensitive Ion Channels With Stress Fibers and Focal Adhesions. *Curr Opin Cell Biol* (2010) 22:669–76. doi: 10.1016/j.ceb.2010.08.023
135. Provenzano PP, Inman DR, Eliceiri KW, Keely PJ. Matrix Density-Induced Mechanoregulation of Breast Cell Phenotype, Signaling and Gene Expression Through a FAK-ERK Linkage. *Oncogene* (2009) 28:4326–43. doi: 10.1038/onc.2009.299
136. Bordeleau F, Califano JP, Negrón Abril YL, Mason BN, LaValley DJ, Shin SJ, et al. Tissue Stiffness Regulates Serine/Arginine-Rich Protein-Mediated Splicing of the Extra Domain B-Fibronectin Isoform in Tumors. *Proc Natl Acad Sci USA* (2015) 112:8314–9. doi: 10.1073/pnas.1505421112
137. Branco da Cunha C, Klumpers DD, Koshy ST, Weaver JC, Chaudhuri O, Seruca R, et al. CD44 Alternative Splicing in Gastric Cancer Cells is Regulated by Culture Dimensionality and Matrix Stiffness. *Biomaterials* (2016) 98:152–62. doi: 10.1016/j.biomaterials.2016.04.016
138. Lo CM, Wang HB, Dembo M, Wang YL. Cell Movement is Guided by the Rigidity of the Substrate. *Biophys J* (2000) 79:144–52. doi: 10.1016/S0006-3495(00)76279-5
139. Tee SY, Fu J, Chen CS, Janmey PA. Cell Shape and Substrate Rigidity Both Regulate Cell Stiffness. *Biophys J* (2011) 100:L25–27. doi: 10.1016/j.bpj.2010.12.3744
140. Nogi T, Levin M. Characterization of Innexin Gene Expression and Functional Roles of Gap-Junctional Communication in Planarian Regeneration. *Dev Biol* (2005) 287:314–35. doi: 10.1016/j.ydbio.2005.09.002
141. Chernet BT, Fields C, Levin M. Long-Range Gap Junctional Signaling Controls Oncogene-Mediated Tumorigenesis in Xenopus Laevis Embryos. *Front Physiol* (2014) 5:519. doi: 10.3389/fphys.2014.00519
142. Mathews J, Levin M. Gap Junctional Signaling in Pattern Regulation: Physiological Network Connectivity Instructs Growth and Form. *Dev Neurobiol* (2017) 77:643–73. doi: 10.1002/dneu.22405
143. Lalli ML, Asthagiri AR. *2014 40th Annual Northeast Bioengineering Conference (NEBEC)*. Boston, MA: NEBEC (2014). p. 1–2.
144. Kwon MS, Park CS, Choi KR, Park CS, Ahnn J, Kim JI, et al. Calreticulin Couples Calcium Release and Calcium Influx in Integrin-Mediated Calcium Signaling. *Mol Biol Cell* (2000) 11:1433–43. doi: 10.1091/mbc.11.4.1433
145. Orrenius S, Zhivotovsky B, Nicotera P. Regulation of Cell Death: The Calcium-Apoptosis Link. *Nat Rev Mol Cell Biol* (2003) 4:552–65. doi: 10.1038/nrm1150
146. Chitty JL, Filipe EC, Lucas MC, Herrmann D, Cox TR, Timpson P. Recent Advances in Understanding the Complexities of Metastasis. *F1000Res* (2018) 7:F1000 Faculty Rev-1169. doi: 10.12688/f1000research.15064.2
147. Lambert AW, Pattabiraman DR, Weinberg RA. Emerging Biological Principles of Metastasis. *Cell* (2017) 168:670–91. doi: 10.1016/j.cell.2016.11.037
148. Oudin MJ, Weaver VM. Physical and Chemical Gradients in the Tumor Microenvironment Regulate Tumor Cell Invasion, Migration, and Metastasis. *Cold Spring Harb Symp Quant Biol* (2016) 81:189–205. doi: 10.1101/sqb.2016.81.030817
149. Chernet BT, Levin M. Transmembrane Voltage Potential of Somatic Cells Controls Oncogene-Mediated Tumorigenesis at Long-Range. *Oncotarget* (2014) 5:3287–306. doi: 10.18632/oncotarget.1935
150. Chernet BT, Adams DS, Lobikin M, Levin M. Use of Genetically Encoded, Light-Gated Ion Translocators to Control Tumorigenesis. *Oncotarget* (2016) 7:19575–88. doi: 10.18632/oncotarget.8036
151. Zhu K, Hum NR, Reid B, Sun Q, Loots GG, Zhao M. Electric Fields at Breast Cancer and Cancer Cell Collective Galvanotaxis. *Sci Rep* (2020) 10:8712. doi: 10.1038/s41598-020-65566-0
152. Sivaramakrishna R, Gordon R. Detection of Breast Cancer at a Smaller Size can Reduce the Likelihood of Metastatic Spread: A Quantitative Analysis. *Acad Radiol* (1997) 4:8–12. doi: 10.1016/s1076-6332(97)80154-7
153. Laura S, Coombs NJ, Ung O, Boyages J. Tumour Size as a Predictor of Axillary Node Metastases in Patients With Breast Cancer. *ANZ J Surg* (2006) 76:1002–6. doi: 10.1111/j.1445-2197.2006.03918.x
154. Adams DS, Levin M. General Principles for Measuring Resting Membrane Potential and Ion Concentration Using Fluorescent Bioelectricity Reporters. *Cold Spring Harb Protoc* (2012) 2012:385–97. doi: 10.1101/pdb.top067710
155. Reid B, Nuccitelli R, Zhao M. Non-Invasive Measurement of Bioelectric Currents With a Vibrating Probe. *Nat Protoc* (2007) 2:661–9. doi: 10.1038/nprot.2007.91
156. Baker BJ, Mutoh H, Dimitrov D, Akemann W, Perron A, Iwamoto Y, et al. Genetically Encoded Fluorescent Sensors of Membrane Potential. *Brain Cell Biol* (2008) 36:53–67. doi: 10.1007/s11068-008-9026-7
157. Mutoh H, Perron A, Akemann W, Iwamoto Y, Knöpfel T. Optogenetic Monitoring of Membrane Potentials. *Exp Physiol* (2011) 96:13–8. doi: 10.1113/expphysiol.2010.053942
158. Shen B, Xiang Z, Miller B, Louie G, Wang W, Noel JP, et al. Genetically Encoding Unnatural Amino Acids in Neural Stem Cells and Optically Reporting Voltage-Sensitive Domain Changes in Differentiated Neurons. *Stem Cells* (2011) 29:1231–40. doi: 10.1002/stem.679
159. Tsutsui H, Karasawa S, Okamura Y, Miyawaki A. Improving Membrane Voltage Measurements Using FRET With New Fluorescent Proteins. *Nat Methods* (2008) 5:683–5. doi: 10.1038/nmeth.1235
160. Tantama M, Hung YP, Yellen G. Imaging Intracellular pH in Live Cells With a Genetically Encoded Red Fluorescent Protein Sensor. *J Am Chem Soc* (2011) 133:10034–7. doi: 10.1021/ja202902d
161. Tseng AS, Beane WS, Lemire JM, Masi A, Levin M. Induction of Vertebrate Regeneration by a Transient Sodium Current. *J Neurosci* (2010) 30:13192–200. doi: 10.1523/JNEUROSCI.3315-10.2010
162. Fang Y, Li X, Fang Y. Organic Bioelectronics for Neural Interfaces. *J Mater Chem C* (2015) 3:6424–30. doi: 10.1039/C5TC00569H
163. Löffler S, Melican K, Nilsson KPR, Richter-Dahlfors A. Organic Bioelectronics in Medicine. *J Intern Med* (2017) 282:24–36. doi: 10.1111/joim.12595
164. Rivnay J, Owens RM, Malliaras GG. The Rise of Organic Bioelectronics. *Chem Mater* (2014) 26:679–85. doi: 10.1021/cm4022003
165. Simon DT, Gabrielsson EO, Tybrandt K, Berggren M. Organic Bioelectronics: Bridging the Signaling Gap Between Biology and Technology. *Chem Rev* (2016) 116:13009–41. doi: 10.1021/acs.chemrev.6b00146
166. Someya T, Bao Z, Malliaras GG. The Rise of Plastic Bioelectronics. *Nature* (2016) 540:379–85. doi: 10.1038/nature21004
167. Tian B, Xu S, Rogers JA, Cestellos-Blanco S, Yang P, Carvalho-de-Souza JL, et al. Roadmap on Semiconductor-Cell Biointerfaces. *Phys Biol* (2018) 15:031002. doi: 10.1088/1478-3975/aa9f34
168. Strakosas X, Bongo M, Owens RM. The Organic Electrochemical Transistor for Biological Applications. *J Appl Polymer Sci* (2015) 132(15):41735. doi: 10.1002/app.41735
169. Tian B, Cohen-Karni T, Qing Q, Duan X, Xie P, Lieber CM, et al. Three-Dimensional, Flexible Nanoscale Field-Effect Transistors as Localized Bioprobes. *Science* (2010) 329:830–4. doi: 10.1126/science.1192033

170. Jayaram DT, Luo Q, Thourson SB, Finlay AH, Payne CK. Controlling the Resting Membrane Potential of Cells With Conducting Polymer Microwires. *Small* (2017) 13:10.1002. doi: 10.1002/smll.201700789
171. Rana MA, Yao N, Mukhopadhyay S, Zhang F, Warren E, Payne C. *2016 American Control Conference (ACC)*. Boston, MA: Proc. of 2016 American Control Conference (ACC2016) (2016). p. 400–5.
172. Shin EH, Li Y, Kumar U, Sureka HV, Zhang X, Payne CK, et al. Membrane Potential Mediates the Cellular Binding of Nanoparticles. *Nanoscale* (2013) 5:5879–86. doi: 10.1039/c3nr01667f
173. Warren EA, Payne CK. Cellular Binding of Nanoparticles Disrupts the Membrane Potential. *RSC Adv* (2015) 5:13660–6. doi: 10.1039/C4RA15727C
174. Liu X, Gilmore KJ, Moulton SE, Wallace GG. Electrical Stimulation Promotes Nerve Cell Differentiation on Polypyrrole/Poly (2-Methoxy-5 Aniline Sulfonic Acid) Composites. *J Neural Eng* (2009) 6:65002. doi: 10.1088/1741-2560/6/6/065002
175. Lee JY, Lee JW, Schmidt CE. Neuroactive Conducting Scaffolds: Nerve Growth Factor Conjugation on Active Ester-Functionalized Polypyrrole. *J R Soc Interface* (2009) 6:801–10. doi: 10.1098/rsif.2008.0403
176. Jeong SI, Jun ID, Choi MJ, Nho YC, Lee YM, Shin H, et al. Development of Electroactive and Elastic Nanofibers That Contain Polyaniline and Poly(L-Lactide-Co-Epsilon-Caprolactone) for the Control of Cell Adhesion. *Macromol Biosci* (2008) 8:627–37. doi: 10.1002/mabi.200800005
177. Guo B, Ma PX. Conducting Polymers for Tissue Engineering. *Biomacromolecules* (2018) 19:1764–82. doi: 10.1021/acs.biomac.8b00276
178. Thourson SB, Payne CK. Modulation of Action Potentials Using PEDOT: PSS Conducting Polymer Microwires. *Sci Rep* (2017) 7:10402. doi: 10.1038/s41598-017-11032-3
179. Balint R, Cassidy NJ, Cartmell SH. Conductive Polymers: Towards a Smart Biomaterial for Tissue Engineering. *Acta Biomater* (2014) 10:2341–53. doi: 10.1016/j.actbio.2014.02.015
180. Fukuta T, Nishikawa A, Kogure K. Low Level Electricity Increases the Secretion of Extracellular Vesicles From Cultured Cells. *Biochem Biophys Rep* (2020) 21:100713. doi: 10.1016/j.bbrep.2019.100713
181. Lakkaraju A, Rodriguez-Boulan E. Itinerant Exosomes: Emerging Roles in Cell and Tissue Polarity. *Trends Cell Biol* (2008) 18:199–209. doi: 10.1016/j.tcb.2008.03.002
182. Rabinowits G, GerÁel-Taylor C, Day JM, Taylor DD, Kloecker GH. Exosomal microRNA: A Diagnostic Marker for Lung Cancer. *Clin Lung Cancer* (2009) 10:42–6. doi: 10.3816/CLC.2009.n.006
183. Silva J, Garcia V, Rodriguez M, Compte M, Cisneros E, Veguillas P, et al. Analysis of Exosome Release and its Prognostic Value in Human Colorectal Cancer. *Genes Chromosomes Cancer* (2012) 51:409–18. doi: 10.1002/gcc.21926

Conflict of Interest: The authors declare that the research was conducted in the absence of any commercial or financial relationships that could be construed as a potential conflict of interest.

Publisher's Note: All claims expressed in this article are solely those of the authors and do not necessarily represent those of their affiliated organizations, or those of the publisher, the editors and the reviewers. Any product that may be evaluated in this article, or claim that may be made by its manufacturer, is not guaranteed or endorsed by the publisher.

frontiers | Frontiers in Oncology

REVIEW
published: 17 May 2022
doi: 10.3389/fonc.2022.871085

Update in TIGIT Immune-Checkpoint Role in Cancer

Tiziana Annese[1,2]*, *Roberto Tamma*[2] *and Domenico Ribatti*[2]*

[1] Department of Medicine and Surgery, Libera Università del Mediterraneo (LUM) Giuseppe Degennaro University, Bari, Italy, [2] Department of Basic Medical Sciences, Neurosciences and Sensory Organs, Section of Human Anatomy and Histology, University of Bari Medical School, Bari, Italy

The in-depth characterization of cross-talk between tumor cells and T cells in solid and hematological malignancies will have to be considered to develop new therapeutical strategies concerning the reactivation and maintenance of patient-specific antitumor responses within the patient tumor microenvironment. Activation of immune cells depends on a delicate balance between activating and inhibitory signals mediated by different receptors. T cell immunoreceptor with immunoglobulin and ITIM domain (TIGIT) is an inhibitory receptor expressed by regulatory T cells (Tregs), activated T cells, and natural killer (NK) cells. TIGIT pathway regulates T cell-mediated tumor recognition *in vivo* and *in vitro* and represents an exciting target for checkpoint blockade immunotherapy. TIGIT blockade as monotherapy or in combination with other inhibitor receptors or drugs is emerging in clinical trials in patients with cancer. The purpose of this review is to update the role of TIGIT in cancer progression, looking at TIGIT pathways that are often upregulated in immune cells and at possible therapeutic strategies to avoid tumor aggressiveness, drug resistance, and treatment side effects. However, in the first part, we overviewed the role of immune checkpoints in immunoediting, the TIGIT structure and ligands, and summarized the key immune cells that express TIGIT.

Keywords: cancer, immune-checkpoint, immune-therapy, TIGIT, tumor microenvironment

OPEN ACCESS

Edited by:
Daniele Vergara,
University of Salento, Italy

Reviewed by:
Wenyan Fu,
Shanghai Jiao Tong University, China
Franziska Brauneck,
University Medical Center Hamburg-Eppendorf, Germany

***Correspondence:**
Domenico Ribatti
domenico.ribatti@uniba.it
Tiziana Annese
annese@lum.it

Specialty section:
This article was submitted to Molecular and Cellular Oncology, a section of the journal Frontiers in Oncology

Received: *07 February 2022*
Accepted: *14 April 2022*
Published: *17 May 2022*

Citation:
Annese T, Tamma R and Ribatti D (2022) Update in TIGIT Immune-Checkpoint Role in Cancer. Front. Oncol. 12:871085. doi: 10.3389/fonc.2022.871085

INTRODUCTION

Solid and hematological malignancies are complex ecosystems that arise from malfunctioning complex cellular mechanisms controlled by genetic and epigenetic factors that coordinate the cross-talk between tumor cells and the tumor microenvironment (TME) components. Among the cellular components of the TME, T cells are the second most abundant cell type after tumor-associated macrophages (TAMs) (1).

Following the development phase in the thymus, the diverse naïve T cells migrate to the secondary lymphoid organs, where they remain dormant until they are activated by recognition of the antigen-human leukocyte antigen (HLA) complex presented by the APC to their TCR (**Figure 1**). In addition to antigen recognition by TCR, naïve T cell activation is regulated by second signals known as co-stimulatory pathways, such as the well-noted CD28–CD80/CD86 and CTLA4–CD80/CD86 (3, 4). These co-stimulatory pathways have a lot of receptor/ligand pairs, also called immune checkpoints, which lead to positive signaling events, while other pathways send out negative signals (5).

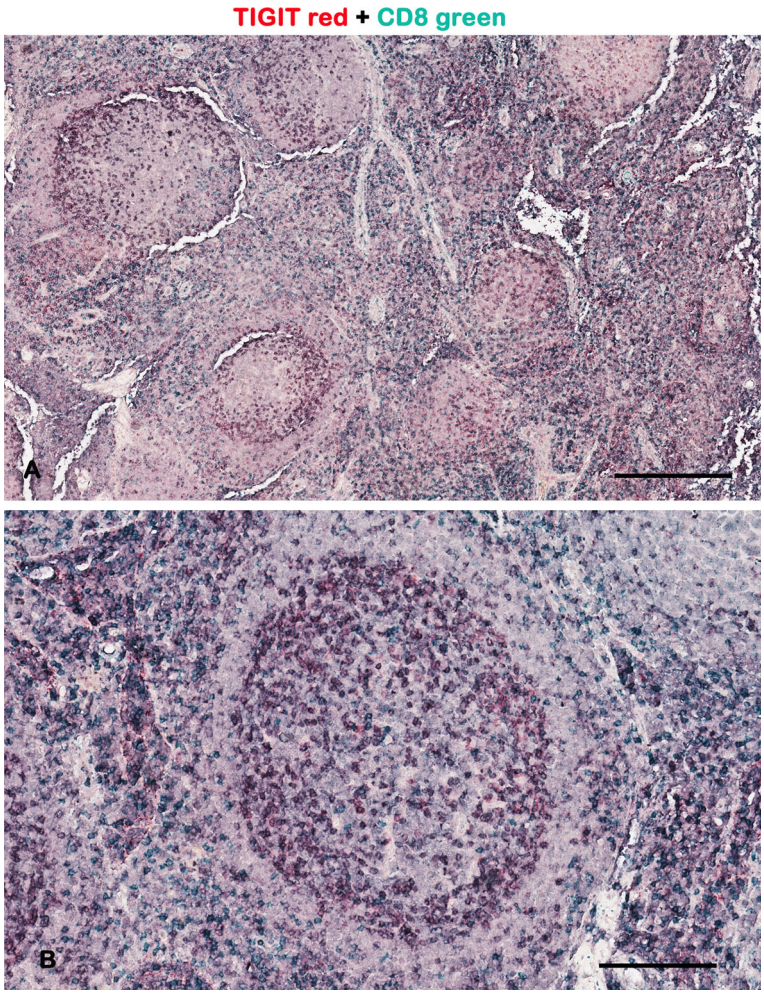

FIGURE 1 | Representative brightfield images of double IHC for TIGIT and CD8 in a lymph node. Micrographs show TIGIT staining in red, CD8 staining in green, and the colocalized TIGIT$^+$CD8$^+$ signals in purple. As demonstrated by other authors, the TIGIT$^+$ T cells are preferentially at the periphery of the germinal center (2). Scale bar: **(A)** 500 μm; **(B)** 165 μm.

CD28 is constitutively expressed on naïve CD4$^+$ and CD8$^+$ T cells, while CD80 and CD86 are inducible on APCs. CD28–CD80/CD86 pathway activates T cell responses. Other stimulatory immune checkpoints are members of the tumor necrosis factor (TNF) receptor superfamily (CD27, CD40, OX40, GITR, and CD137) or the B7–CD28 superfamily (ICOS) (6).

On the contrary, cytotoxic T-lymphocyte-associated protein 4 (CTLA4) is a negative regulatory inducible receptor for CD80/CD86 and has inhibitory effects on T cell responses, leading to T cell attenuation and tumor cell immune evasion (7). A considerable number of inhibitory immunoreceptors have been identified and studied in tumors, including but not limited to adenosine A2A receptor (A2AR), B7-H3, B7-H4, programmed death (PD-1), CTLA4, T cell immunoglobulin domain and mucin domain 3 (TIM3), T-cell immunoreceptor with immunoglobulin and ITIM domain (TIGIT), and B and T lymphocyte attenuator (BTLA) (6, 8).

Interestingly, the immune system can constrain and promote tumor development and progression (5, 9, 10). Alterations in immune checkpoint pathways result in an imbalance of positive and negative co-stimulatory signals, which increases the risk of tumorigenesis and its progression. These signals are also involved in patients' resistance to immunotherapies (9, 11).

Immune checkpoint inhibitors were developed to block checkpoints by making T cells free to attack cancer cells. These therapies are also referred to as checkpoint blockade therapies and are an emerging and attractive field to treat many cancers, but they do not work for all patients and can cause serious side effects (12). The failure of classical antitumor therapies could be attributed to the fact that most drugs currently in use primarily target tumor cells and not also TME cells. These cells are different cell types, including endothelial cells, stromal cells, and immune cells. Understanding the *in situ* cross-talk of heterogeneous tumor cells with various tumor-associated immune cells, such

as T cells, will provide critical information for improving anticancer therapies.

The immune checkpoint inhibitors are most efficacious in patients with a TME enriched in tumor-infiltrating lymphocytes (TILs) (13). TILs are deputed to tumor immunoediting ["a dynamic process wherein immunity functions not only as an extrinsic tumor suppressor but also to shape tumor immunogenicity" (14)]. Immunoediting shapes tumor fate in three steps: elimination, equilibrium, and escape. The elimination step is the immunosurveillance step, in which a competent immune system (innate and adaptive immunity) recognizes and destroys transformed cells expressing highly immunogenic antigens long before they become clinically relevant (15).

If some cancer cells evade the elimination step, they will enter the equilibrium step, in which survived tumor cells and immune cells mutually edit each other. During this adaptation time, tumor cells undergo a complex process of natural selection [similar to that described by Darwin (16)] that presses on tumor cells with traits that are better suited to the environment than others.

These natural evolution-selected tumor cell variants develop resistance to elimination and put them in the escape step (17). A progressive establishment of an immunosuppressive TME characterizes the escape step (11, 18). This is the final step when aggressive-selected tumor clones develop diverse ways to escape the immune system that mimic peripheral tolerance (8, 19, 20): prevent the response of effector T cells, TAMs, natural killer (NK) cells, and tumor-associated neutrophils (TANs) (21); down-regulate their HLA (22); induce antigen presentation defects; eliminate neoantigens; inhibit immune cell chemoattraction to the tumor site; secrete or promote the secretion of immunosuppressive cytokines (23); modulate the recruitment and expansion of immunosuppressive cells, such as regulatory T cells (Tregs); orchestrate immune cell metabolism (24); and activate immune checkpoint pathways to inhibit the emerging antitumor immune response (25).

T cells immunoediting also occurs during tumorigenesis (26, 27). At first, in order to attack and eliminate tumor cells, APCs, *via* CD28-CD80/CD86 pathway, activate T cells, but at the same time regulate pro-inflammatory mechanisms, activating inhibitory pathways by immune checkpoints (28). Among immune checkpoint inhibitors, immediately after TCR engagement, CTLA4 is upregulated and competes with CD28 to bind to CD80/CD86 on APCs, limiting autoreactive T cells, decreasing T cell priming and proliferation, inducing immune tolerance, and preventing autoimmunity (29, 30).

In the immune response, PD-1 is also expressed on activated T cells, but it acts later and interferes with T cells that have already been activated (31). When the stimulating antigen is removed, PD-1 expression on responding T cells decreases, whereas it remains increased in the opposite scenario. Like CTLA4, the PD-1–PD-L1/PD-L2 pathway recruits phosphatases to block the stimulatory signals sent by TCR and CD28–CD80/CD86, resulting in decreased T cell activation, survival, cytokine generation, and metabolism (31). Overexpression of PD-1 on tumor cells or by the cellular component of the TME with its downstream pathway is a systematic strategy used by malignancies to increase exhausted T cells and to evade immunosurveillance. The fact that PD-1 overexpression happens later means that it will only be overexpressed and activated once an inflammatory process has begun (32).

Immune checkpoint activation and an immune infiltrate enriched in Tregs were identified as the primary tumor escape mechanisms in a mouse model of hypermutated and microsatellite-instable colorectal cancer (33). According to the same study, the expansion of the TCR following PD-1 blockade potentiates immunoediting (33).

In a subtype of advanced untreated primary colorectal cancer, immune checkpoints expression has been related to immune evasion *via* neo-antigen-related mechanisms (34). This subtype was called the "stealth subtype," and immune evasion and poor prognosis have been associated with less clonal highly expressed neoantigens (HiNeo), high chromosomal instability, high immune checkpoint expression (PD-1, PD-L1, PD-L2), low neoantigen presentation (reduced HLAII), downregulation of functional $CD8^+$ T cells, and a microenvironment poor in TAMs and B cells (34, 35).

After T cell activation, also TIGIT expression increases on T cells, where it competes with CD226 (DNAM-1) for binding to their shared ligands CD112 and CD155 (36). TIGIT expression is late in the cancer-immunity cycle. It is highly expressed on specialized $CD4^+$ subsets, such as Treg and T_{FH}, and lowly expressed on $CD4^+$ and $CD8^+$ exhausted T cells (37). Moreover, $TIGIT^+CD4^+$ T cells and $TIGIT^+CD8^+$ T cells displayed a memory phenotype (37).

The timing of immune checkpoint activation is currently under investigation because there is a debate about the reactivation of primed T cells and/or novel T cells. The former depends on memory T cells and presumes the existence of pre-existing cancer-specific T cells that recognize tumor-specific antigens. The second depends on novel T cells against neo-antigens and therefore assumes that T cells are primed and recruited to tumors after the initiation of therapy (38–40). This topic is interesting in patient stratification for immune checkpoint blockades therapy since the success of these therapies relies on antigen processing and presentation (41–43).

In this context, the TIGIT immune checkpoint is emerging as a promising target for anticancer therapy alone or combined with other immune blockade therapies (44). The purpose of this review is to update the role of TIGIT in cancer progression, looking at last year's studies about its pathways that are often upregulated in immune cells and possible therapeutic strategies to avoid tumor aggressiveness, drug resistance, and treatment side effects. However, in the first part, we overviewed the TIGIT structure and ligands, and summarized the key immune cells that express TIGIT.

OVERVIEW OF TIGIT STRUCTURE AND LIGANDS

TIGIT is also known as V-set and immunoglobulin domain-containing protein 9 (VSIG9) or V-set and transmembrane

domain-containing protein 3 (VSTM3). Based on UniProt data resources, two alternatively spliced isoforms have been reported in humans.

It has an extracellular Ig-like V-type domain, a type I transmembrane domain, and a cytoplasmic domain with the immunoreceptor tyrosine-based inhibitor motif (ITIM) (45, 46) and the immunoglobulin tyrosine tail (ITT)-like motif (45, 47). ITIM modulates cellular responses by binding the SH2 domain of several SH2-containing tyrosine phosphatases, SHP1 (48) and SHP2, when phosphorylated (49).

After the extracellular ligand binding, the ITT-like domain is phosphorylated at Tyr225, binds the two cytosolic adaptor proteins Grb2 and β-arrestin2, and recruits the SH2-containing inositol phosphatase-1 (SHIP-1) that inhibits PI3K/MAPK signaling (via Grb2) (50) to reduce the NK cell effector functions (50), and TRAF6/NF-κB signaling (via β-arrestin2) to inhibit IFN-γ production (48).

Different studies show that phosphorylation of the tyrosine residue in either ITIM- (Y231) or ITT-like (Y225) motif is essential for signal transduction and the inhibitory function of TIGIT in humans (48, 50). When both tyrosine residues are mutated, the inhibitory activity of human TIGIT is completely lost (51).

TIGIT binds to nectin and nectin-like (NECL) adhesion molecules, including NECTIN-2 (CD112) (52, 53), NECTIN-3 (CD113) (45, 51), and NECL-5 (CD155) (54) to mediate cell adhesion and signaling.

TIGIT binds NECL in cis-trans, forming a receptor clustering. For instance, two TIGIT–CD155 dimers assemble into a heterotetramer with a core TIGIT–TIGIT cis-homodimer in which each TIGIT molecule binds one CD155 molecule (47).

CD112 is a cell adhesion protein involved in the modulation of T cell signaling. Two isoforms, delta and alpha, are annotated by alternative splicing. Depending on the receptor it binds to, CD112 can be either a co-stimulator or a co-inhibitor of T cell function: CD226 binding stimulates T cell proliferation and cytokine production (IL2, IL5, IL10, IL13, and IFN-γ) (55); PVRIG (also called CD112R) binding inhibits T cell proliferation (56). These interactions are competitive (57). CD112 binds with low affinity to TIGIT (46, 52). The TIGIT binds to CD112 destroys CD112–CD112 homodimer (52) and, as for TIGIT–CD155, homo- and heterodimers in the heterotetramer interact by a conserved "lock and key" binding (52). CD112 is highly expressed in bone marrow, kidney, pancreas, lung cells, and breast and ovarian cancer (58, 59).

CD113 is another cell adhesion protein that interacts with nectin and NECL molecules *via* heterophilic trans-interactions, such as CD112 at Sertoli-spermatid junctions (60). Through common signaling molecules such as SRC and RAP1, CD113 trans-interaction with CD155 activates CDC42 and RAC small G proteins (61). CD113 also establishes cell-cell junctions, such as adherens junctions and synapses (62, 63). It inhibits cell movement and proliferation by inducing endocytosis-mediated downregulation of CD155 on the cell surface (64). CD113 contributes to the morphology of the ciliary body (65). CD113 is highly expressed in the testis, placenta, kidney, liver, and lung (66). CD113, like CD112, has a low affinity for TIGIT, and their interaction prevents the self-destruction of normal cells by NK cells (46, 53).

CD155, the primary ligand for TIGIT, is also known as the Poliovirus receptor (PVR). CD155 has a "lock-and-key" motif that is essential for TIGIT binding and is highly conserved across PVR family members (47). CD155 is a glycoprotein with three extracellular immunoglobulin domains, transmembrane, and intracellular domains (67). Two splice forms, lacking the transmembrane region, have also been described as soluble or secreted isoforms that seem to compete with the membrane-anchored ones (68, 69). CD155 is highly expressed on $CD11c^+$ human dendritic cells (DCs) (70, 71), macrophages (72, 73), T (74) and B cells (75), epithelial cells (74, 76), kidneys (76), nervous system (77), intestine (78, 79), and tumor cells (80, 81). *In vivo*, the CD155–TIGIT pathway suppresses immunological responses increasing IL-10 anti-inflammatory cytokine (82, 83) and decreasing IL-12 pro-inflammatory cytokine released by DCs (46, 84). This induces a tolerogenic phenotype in T cells (85). A more detailed description of the CD155–TIGIT pathway in cancer is present in the next section.

A new NECL that exclusively binds TIGIT was recently identified, NECTIN-4 (86). TIGIT binds NECTIN-4 with high affinity, comparable to CD155 (86). NECTIN-4 is involved in cell adhesion through trans-homophilic and -heterophilic interactions, including specific interactions with NECTIN-1 (CD111) (87), does not interact with CD226, CD96, or CD112 (86), and is overexpressed in several tumors of the breast (88, 89), bladder (90), lung (91, 92), and pancreas (93, 94).

TIGIT PATHWAYS AND IMMUNE CELLS INVOLVED

TIGIT is expressed by a variety of immune cells. Its expression and related pathways have been discussed in this section.

In simple terms, TIGIT activation creates a tolerogenic microenvironment in both cell-intrinsic and cell-extrinsic ways (resumed in **Figure 2** and discussed in the following). This means that TIGIT competes directly with CD226 for binding to CD155, CD112, or CD113 ligands in the former way, or that it is involved in events that indirectly induce immunosuppressive effects, such as TIGIT's action on innate immunity cells in the second way.

CD226 is a member of the immunoglobulin superfamily and consists of an extracellular region with two IgV-like domains, a transmembrane region, a cytoplasmic region with ITT, and four putative tyrosine residues and one serine residue that are phosphorylated (95). It is mainly expressed on myeloid and lymphoid cells (96), through which promotes intercellular adhesion, lymphocyte communication, and lymphokine production, as well as enhances cellular cytotoxicity mechanisms (96).

TIGIT–CD155 in $CD4^+$ T cells induces immunosuppression inhibiting T cell proliferation directly by inducing the down-expression of T-bet, GATA3, IFN regulatory factor 4 (IRF4), and

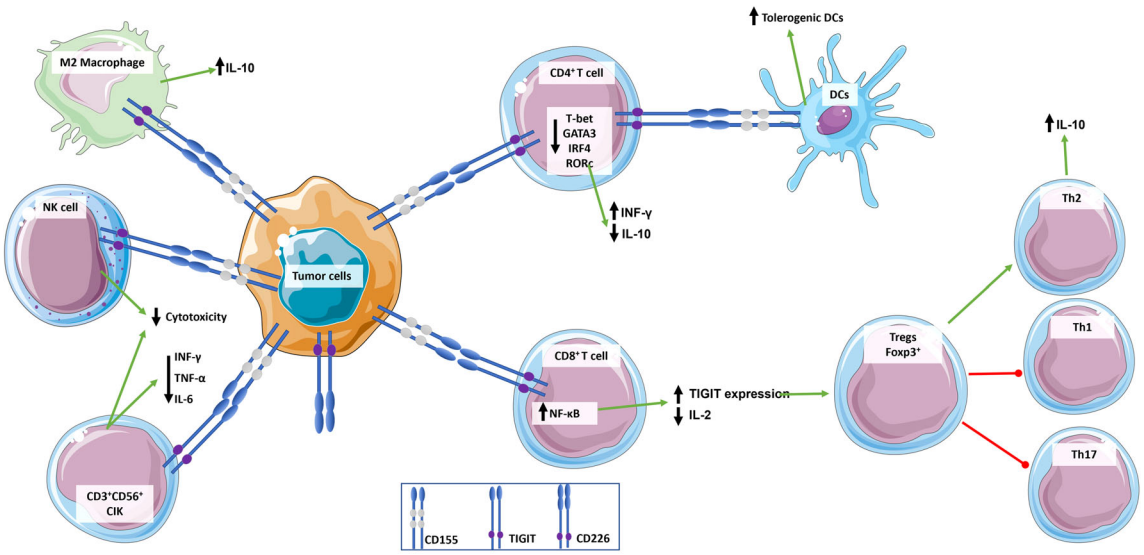

FIGURE 2 | Role of TIGIT in the regulation of immune response. TIGIT transmits inhibitory signals *via* ITIM and immunoglobulin tyrosine tail (ITT)-like motifs in its cytoplasmic domain when it is engaged. TIGIT has multiple ligands, but it binds with greater affinity to CD155, which is widely expressed by immune cells and tumor cells. CD155 expressing tumor cells bind to TIGIT expressed by immune cells inducing an immunosuppressive and tolerogenic microenvironment: $CD4^+$ T cells induce a tolerogenic phenotype in DCs, release the anti-inflammatory cytokine IL-10, and down-regulate INF-γ; $CD8^+$ T cells up-express TIGIT and down-regulate the release of pro-inflammatory cytokine IL-2, which in turn promotes a T cell immunosuppressive phenotype characterized by increase in $Foxp3^+$ Tregs and Th2 compared to pro-inflammatory Th1 and Th17; NKs cytotoxicity is suppressed; and macrophages switch to an M2 anti-inflammatory phenotype. This simplistic view does not integrate signals from the CD226/CD155 pathway.

retinoic acid-related orphan receptor c (RORc), which reduce the level of pro-inflammatory IFN-γ while increasing the level of anti-inflammatory IL-10 (97).

TIGIT–CD155 in NK cells reduces their cytotoxicity (51, 53), resulting in impaired granule polarization and IFN-γ production (50, 98). On the contrary, TIGIT blockade restored potent effector NK cells through CD226–LFA-1 signaling that increases adhesion to target cells, induces IFN-γ production by naïve $CD4^+$ T cells, and enhances the cytotoxic function of NK cells (99, 100).

TIGIT–CD155 signaling was also observed in cytokine-induced killer (CIK) cells expressing CD3 and CD56 molecules (101, 102). As observed indirectly by Zhang et al., who analyzed the literature concerning the clinical trial ongoing on renal cell carcinoma patients enrolled in integrated CIK cell immunotherapy, the TIGIT blocked enhanced CIK proliferation and the release of pro-inflammatory cytokines, such as IFN-γ, IL-6, and TNF-α (102).

TIGIT–CD155 in $CD8^+$ T cells induces immunosuppression *via* the NF-κB signaling pathway, promoting a tolerant state that is passed down across T cell generation. In this process, $CD155^+$ naïve T cells trans-interact with $TIGIT^+$ preceding tolerant T cells resulting in increased TIGIT expression and IL-2 suppression *via* Blimp1 increment (54, 103).

TIGIT–CD155 signaling was also observed in activated $Foxp3^+$ Tregs, which suppress pro-inflammatory Th1 and Th17 but not Th2 cells *via* Akt repression and FoxO1 phosphorylation, IL-10 and fibrinogen-like protein 2 overexpression (104, 105). According to this shift in immunity from Th1 and Th17 to Th2 immunity and IL-10 release, CD226 is expressed on Th1 and Th17, but not on Th2 cells, and in the former, CD226–CD155 promotes IFN-γ and IL-17 production (106, 107).

Concerning TIGIT-mediated tolerogenic microenvironment by cell-extrinsic ways, it was observed that TIGIT suppresses T cell function by enhancing the immunosuppressive function of DCs and macrophages that express TIGIT ligands such as CD155 (46, 97, 108, 109).

$TIGIT^+CD4^+$ T cells exerted immunosuppressive effects indirectly by modulating the monocyte-derived DCs cytokine production (97). TIGIT of $CD4^+$ T cells interacts with $CD155^+$ of DCs, modulating the Erk signaling pathway and increasing IL-10 production while decreasing IL-12p40 production and promoting tolerogenic DCs that suppress T cell responses (46, 97).

TIGIT was found to play a role in macrophages in an *in vitro* pig-to-human xenograft model (84). In this model, TIGIT is expressed by M2 macrophages but not by M1 macrophages or endothelial cells. At the same time, CD155 is expressed by both M1 and M2 macrophages. Here, the immunosuppressive effects of TIGIT are explained by reduced expression of pro-inflammatory cytokines, such as TNFα, IL-1β, and IL-12 in M1 *via* SHP-1 phosphorylation. In BALB/c mice, TIGIT immunomodulates $CD155^+$ pro-inflammatory M1 into IL-10-secreting anti-inflammatory M2 (85).

All of this demonstrates the intricacy of the several targets and pathways that ani-TIGIT immunotherapies must consider.

TIGIT IN CANCER PROGRESSION

Immune dysregulation may play a role in cancer progression (110). TIGIT overexpression has been found in the cellular microenvironment of several tumors, including lung (111), kidney (112), liver (113), glioma (114, 115), melanoma (116), colorectal carcinomas (117), gastric cancer (118), and neuroblastomas (119). TIGIT expression was found to be strongly associated with poor prognosis in colorectal cancer and positively correlated with pathological stages in renal clear cell carcinoma (120), kidney renal papillary cell carcinoma, and uveal melanoma (121, 122).

As explained in the introduction paragraph, immune cells interact with other microenvironment cells and the tumor cells in a cross-talk that determines the cancer features and heterogenicity (123, 124). Chronic antigen exposure, which characterizes the first part of tumorigenesis when tumor cells become detectable, stresses T cells, causing them to lose their effector function, become exhausted, and upregulate several immune inhibitor receptors (IRs) such as TIGIT (125, 126) (**Figure 3**). In various cancers, according to computational analyses, the TIGIT expression profile was related to the immune infiltration level, coupled with the expression of other IRs, including LAG3, CTLA4, PD-1, PD-L1, PD-L2, and it is related to tumor mutation burden (TMB), microsatellite instability (MSI), mismatch repair (MMR), and DNA methyltransferases (DNMTs) gene alterations in different tumors (122). Gene set enrichment analysis (GSEA) demonstrated a negative association among high TIGIT expression and cytokine-cytokine receptor interaction, chemokine signaling pathway, NK-mediated cytotoxicity, allograft rejection, INF-γ response, and IL6/JAK/STAT3 signaling (122). On the contrary, a low TIGIT expression was associated with oxidative phosphorylation and propanoate metabolism (122).

Blocking the co-expression of IRs appears to be an excellent arm of immunotherapy. TIGIT co-expression with other IRs has been widely examined on $CD8^+$ TILs and circulating T cells (116, 127). Li et al. demonstrated that distinct IRs are co-expressed on $CD8^+$ TILs in T cell exhaustion of primary cancer treatment-naïve patients comprising breast, kidney, lung, liver, cervical, esophageal, gastric, and colorectal cancer (128). Almost 50% of $CD8^+$ TILs were found PD-1^+TIGIT$^+$, indicating that TIGIT is preferentially co-expressed with PD-1 (128). Furthermore, in the same study for cervical cancer was observed that the advanced T cell differentiation ($CD27^-CCR7^-CD45RA^-$) of PD-1^+TIGIT$^+$2B4$^+$TIM3$^+$KLRG-1^-CTLA4$^-$ $CD8^+$ TILs was associated with 60% of poorly differentiated cervical cancer (128). TIGIT mono-expression was also highly present in both TILs and circulating T cells, and this is probably the cause of the side effects after systemic treatment with TIGIT blockade (128).

TIGIT and PD-1 high co-expression was observed in PBLs (peripheral blood lymphocytes), MALs (malignant ascites lymphocytes), and TILs with increased frequency in tumor proximity in matched samples of patients at first diagnosis of ovarian cancer not treated (129). Moreover, the authors also observed TIGIT and TIM3 co-expression in PBLs, MALs, and TILs but with a decreased frequency in tumor proximity (129).

Multiple IRs expression, such as PD-1, PD-L1, TIGIT, and CTLA4, was reported in detail in TILs and circulating T cells in primary breast cancer and colorectal cancer in which immune checkpoint expression was correlated with promoter

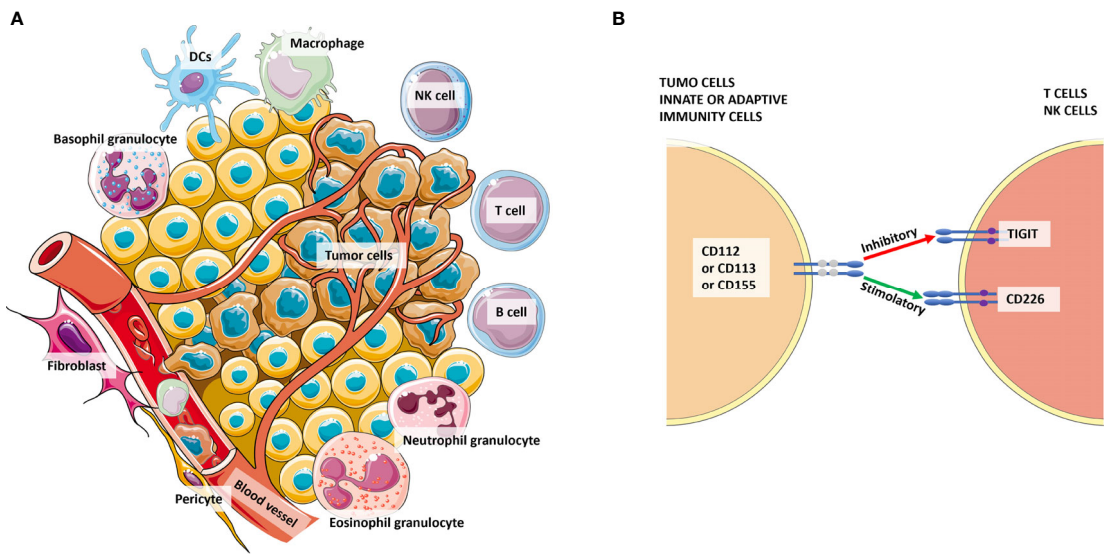

FIGURE 3 | The complexity of the tumor microenvironment and focus on TIGIT$^+$ cells. Panel **(A)** shows the major cellular components of the microenvironment that cross-talk with tumor cells. Panel **(B)** shows the competition among CD226 and TIGIT to bind their ligands CD112 or CD113 or CD155 expressed by tumor cells or antigen-presenting cells (APCs) from innate or adaptive immunity. Especially for CD155, the affinity for TIGIT is higher than its affinity for CD226. Thus, the signaling of the CD155-TIGIT synapse (red arrow) induces immunosuppression rather than effector cell activation and/or cytotoxicity.

demethylation and post-translational histone modifications (130–134). For instance, TIGIT in colorectal cancer and TIGIT plus PD-L1 in colorectal cancer and breast cancer were found hypomethylated at the gene promoter level (134).

In esophageal squamous cell carcinoma, the analysis of the RNA-seq dataset from The Cancer Genome Atlas (TCGA) database and by multiplex-immunohistochemistry reactions on patient's biopsies revealed a high expression of PD-L1 with TIM3 or TIGIT (135). This high IRs co-expression was positively correlated to a greater extent with $CD8^+$ TILs and to a lesser extent with $CD4^+$ TILs and was associated with poor overall survival (OS), TNM III/IV stage, and short restricted mean survival time (RMST) (135).

A TIGIT role in T cell exhaustion was also reported in chronic lymphocytic leukemia (CLL) (136). By flow cytometric and transcript expression analysis, Hajiasghar-Sharbaf et al. have observed a significantly high number of $TIGIT^+PD\text{-}1^+CD8^+$ T cells (136), $PD\text{-}1^+TIM3^+CD8$ T cells (137), and $PD\text{-}1^+TIM3^+CD4$ T cells (138) in CLL patients compared with control, particularly in patients with advanced TNM stage.

In both myeloid leukemia and multiple myeloma, using flow cytometry, the bone marrow resident γδ T cells, a T cell subpopulation of non-MHC-restricted, have shown TIGIT, PD-1, TIM3, and the ectonucleoside triphosphate diphosphohydrolase-1 (CD39) co-expression at a high level compared to αβ T cell but similar to that expressed on $CD8^+$ effector T cells (139). These markers were linked to signs of exhaustion, such as transcriptional reprogramming, decreased release of proinflammatory cytokines, decreased T cell proliferation, and lesser tumoricidal activity, and were associated with a lower OS for myeloid leukemia (139, 140).

In relapsed/refractory classic Hodgkin's lymphoma, a TIGIT-mediated alternative system of immune escape was demonstrated to the classic PD-1/PD-L1 (141). TIGIT and PD-L1 were found to be mutually exclusively expressed and $TIGIT^+PD\text{-}1^+CD3^+CD4^+$T cells surrounding Hodgkin Reed-Sternberg (HRS) cells were associated with advanced TNM stages (141).

IRs blockades are mainly used for T cells, but also NK cells could be a valid target for immunotherapy (142, 143). The expression pattern of immune checkpoints on NK cells isolated from peripheral blood of patients affected by hepatitis B virus-related hepatocellular carcinoma (HBV-HCC) revealed a positive correlation among the co-expression of TIGIT and TIM3 in exhausted T cells, high rate of tumor progression, and poor clinical prognosis (144).

In melanoma patients, tumor-infiltrating NK cells were present at low frequencies in metastatic melanoma, had downregulated expression of both TIGIT and CD226, and *in vitro* experiments had shown their dysfunctional phenotype with higher lytic potential but lower lytic activity compared with $TIGIT^-$ NK cells against $CD155^+$ MHC class I–deficient melanoma cells (145). Interestingly, in the same study, TIGIT blockade as a single treatment failed to reverse NK cells dysfunction, while together with IL-15 had reversed CD155-mediated NKs exhaustion and had inhibited experimental melanoma metastasis *in vivo* (145).

Despite their inhibitory effects on T cells, PD-1 and TIGIT co-expression were described in activated T cells with a cytotoxic effector phenotype and the CXCR5 overexpression (146–148). In Merkel cell carcinoma patients, the $PD\text{-}1^+TIGIT^+$ $CD8^+$ T cells circulating population was significantly associated with clinical benefit (146). Moreover, a positive trend, but not significant, was observed in melanoma patients (146). In both diseases, the monitoring of $PD\text{-}1^+TIGIT^+$ $CD8^+$ T cells was proposed as a predictive biomarker of clinical efficacy for PD-1 blockade (146).

Though under-investigated, TIGIT is also expressed in $CD4^+$ Tregs in association with an increased hypomethylation state (149, 150). In melanoma patients, increased TIGIT/CD226 ratio was observed in $CD4^+$ Tregs compared with $CD4^+$ effector T cells and was associated with highly suppressive TME and poor clinical outcomes (149). TIGIT hypomethylation was found dependent by Foxp3. It is a marker of $CD4^+$ Tregs and works as a transcriptional activator by binding to demethylated sequences containing a Forkhead-binding motif, as observed in TIGIT, MIR21, FOXP3, CTLA4, and CD25 (128, 150). Altogether, these data demonstrated that epigenetic regulators, such as demethylation inhibitors, together with immune checkpoint inhibitors, should be considered in new combined therapeutical approaches, and that the promoter methylation pattern of immune checkpoints could be a valid prognostic biomarker.

Here, we discern last year's update concerning TIGIT's role in cancer based on PubMed search [for an update concerning hematological malignances, see the review (144)]. We have also looked at studies investigating the correlation of TIGIT expression with the clinicopathological characteristics of such a tumor (such as grade, stage, and metastasis) to improve clinical diagnosis, the amount of surgical resection, prognosis determination, and target therapy. Indeed, a 2021 meta-analysis of TIGIT expression in the tumor microenvironment of various solid tumors revealed that it has prognostic value because it is associated with risk factors for OS and progression-free survival (PFS) (142). In **Table 1**, all the clinical trials evaluating anti-TIGIT immunotherapeutics started in 2021 are collected, while an in-depth discussion on TIGIT in clinical development is elegantly presented by Rotte et al. (143). (Note that there are now "new" cancers as glioblastoma and melanoma in the clinical trials and not only the "usual" lung cancers. This will give important clinical data on TIGIT blockade on different tumors).

Epigenetic modifications more and more play a role in the upregulation of immune checkpoints in cancer. Through qRT-PCR, CpG methylation, and repressive histone abundance experiments, TIGIT was found poorly expressed in primary breast cancer and adjacent non-cancerous tissues because its CpG islands at the promoter level were mostly hypermethylated (80-70%), while CpG islands of PD-L1 and LAG3 promoter were demethylated at 100% and 80-90%, respectively (130). In another study, using large-scale transcriptome data analysis of aggressive breast cancers, TIGIT was found to be highly and specifically expressed in aggressive breast cancer, and its pro-tumor activities were linked to immune-related genes (151). An in-depth analysis

TABLE 1 | Clinical trials evaluating anti-TIGIT immunotherapeutics started in 2021 (accessed on March 14, 2022).

NCT Number	Interventstions/Drug	Conditions	Status	Phases	Start Date
NCT05251948	Atezolizumab Capecitabine Oxaliplatin Tiragolumab	Gastric and gastroesophageal junction carcinoma	Recruiting	Phase 1 Phase 2	March 1, 2022
NCT05253105	TAB006 Toripalimab	Previously treated, advanced malignancies	Not yet recruiting	Phase 1	March 15, 2022
NCT05130177	Zimberelimab Domvanalimab	Melanoma	Not yet recruiting	Phase 2	March 2022
NCT05120375	BAT6021	Solid tumor	Not yet recruiting	Phase 1	Not avilable
NCT05102214	HLX301	Locally advanced or metastatic solid tumors Non-small cell lung cancer	Recruiting	Phase 2	January 2022
NCT05073484	BAT6021 BAT1308	Advanced solid tumor	Recruiting	Phase 1	October 29, 2021
NCT05060432	EOS-448 Anti-PD1 inupadenant	Advanced cancer Lung cancer Head and neck cancer Melanoma	Recruiting	Phase 1 Phase 2	September 6, 2021
NCT05061628	JS006 as Monotherapy JS006 in combination with Toripalimab	Advanced tumors	Recruiting	Phase 1	April 21, 2021
NCT05026606	Etigilimab Nivolumab	Recurrent fallopian tube clear cell adenocarcinoma Recurrent ovarian clear cell adenocarcinoma Recurrent platinum-resistant fallopian tube carcinoma Recurrent platinum-resistant ovarian carcinoma Recurrent platinum-resistant primary peritoneal carcinoma Recurrent primary peritoneal clear cell adenocarcinoma	Recruiting	Phase 2	October 1, 2021
NCT05023109	GP+PD-1+Tight	Biliary tract carcinoma	Not yet recruiting	Phase 2	September 1, 2021
NCT05019677	GP+PD-1+Tight	Intrahepatic cholangiocarcinoma	Not yet recruiting	Phase 2	September 1, 2021
NCT05014815	Ociperlimab Tislelizumab histology-based chemotherapy Placebo	Non-small cell lung cancer	Recruiting	Phase 2	November 16, 2021
NCT05009069	Radiotherapy Capecitabine Fluorouracil Atezolizumab Tiragolumab	Rectal neoplasms Rectal Cancer	Not yet recruiting	Phase 2	April 30, 2022
NCT04995523	AZD2936	Non-small cell lung carcinoma	Recruiting	Phase 1 Phase 2	September 14, 2021
NCT04952597	Ociperlimab Tislelizumab Concurrent Chemoradiotherapy	Limited stage small cell lung cancer	Recruiting	Phase 2	July 15, 2021
NCT04933227	Atezolizumab Tiragolumab Oxaliplatin Capecitabine	Stomach neoplasms Gastric cancer Gastroesophageal junction adenocarcinoma	Recruiting	Phase 2	August 6, 2021
NCT04866017	Tislelizumab Durvalumab Chemotherapy Ociperlimab	Non-small cell lung cancer	Recruiting	Phase 3	June 17, 2021
NCT04791839	Zimberelimab Domvanalimab Etrumadenant	Non-small cell lung cancer Non-small cell carcinoma Non-small cell lung cancer	Recruiting	Phase 2	August 4, 2021
NCT04761198	Etigilimab dosing Nivolumab	Solid tumor, adult Advanced solid tumor Metastatic solid tumor	Recruiting	Phase 1 Phase 2	March 23, 2021
NCT04746924	Tislelizumab Ociperlimab	Non-small cell lung cancer	Recruiting	Phase 3	June 8, 2021

(Continued)

TABLE 1 | Continued

NCT Number	Interventstions/Drug	Conditions	Status	Phases	Start Date
	Pembrolizumab Placebo				
NCT04736173	Zimberelimab Domvanalimab Carboplatin Pemetrexed Paclitaxel	Non-small cell lung cancer Nonsquamous non-small cell lung cancer Squamous non-small cell lung cancer Lung cancer	Recruiting	Phase 3	February 1, 2021
NCT04732494	Tislelizumab Ociperlimab Placebo	Esophageal squamous cell carcinoma	Recruiting	Phase 2	March 31, 2021
NCT04693234	Tislelizumab Ociperlimab	Cervical cancer	Active, not recruiting	Phase 2	March 3, 2021
NCT04672356	IBI939 Sintilimab	Advanced lung cancer	Recruiting	Phase 1	January 25, 2021
NCT04656535	AB122 AB154 Placebo	Glioblastoma	Recruiting	Early Phase 1	April 21, 2021

by the same authors revealed that TIGIT expression was positively correlated with T cells, $CD8^+$ T cells, cytotoxic T cells, NK cells, B cells, DCs, and macrophages, but negatively correlated with neutrophils, endothelial cells, and fibroblasts (151). Furthermore, TIGIT expression was positively correlated with inflammation and immune response-related genes (LCK, HCK, MHC-I, MHC-II, STAT1, and interferon) (151). Accordingly, TIGIT expression seems closely related to higher malignant pathological types of breast cancer and might be a potential biomarker of breast cancer progression.

The role of epigenetics in TIGIT expression and immunotherapeutic sensitivity was also uncovered in gastric cancer. Increased TIGIT expression in gastric cancer appears to be a favorable event (152). TIGIT expression correlates with an active immune landscape, survival and immunotherapeutic sensitivity, and favorable prognosis, according to a bioinformatics-guided analysis. Patients with high TIGIT expression respond better to immunotherapy than those with low TIGIT expression (152).

The role of TIGIT in cancer progression was updated in bladder cancer. The failure of the antitumor immune response in bladder cancer was attributed to a subset of $TIGIT^+$ Treg cells overexpressing interleukin IL-32 using single-cell sequencing technology on tissue and experiments in a mouse model (153). In support of this, the same study found that anti-TIGIT monoclonal antibodies, when used alone, have a dual effect: they boost the antitumor activities of T cells while decreasing IL-32, which in turn inhibits bladder cancer metastasis (153). Furthermore, in muscle-invasive bladder cancer, the worst clinical outcomes were attributed to a suppressive TME characterized by Th2 cells, Tregs, mast cells, neutrophils, and exhausted $TIGIT^+CD8^+$ T cells with low tumoricidal capacity that benefited from anti-PD-L1 and anti-TIGIT immunotherapy (154, 155). However, in patients with stage II of muscle-invasive bladder cancer with low $TIGIT^+$ $CD8^+$ T cell infiltrate, adjuvant chemotherapy prolongs their OS and recurrence-free survival (RFS) (155). Therefore, $TIGIT^+$ T cells have a prognostic role in clinical outcomes in bladder cancer and seem to be a predictive biomarker for inferior adjuvant chemotherapy responsiveness.

The CD155–TIGIT pathway suppresses the immune system at different levels in colorectal cancer. In colorectal cancer patients and mouse models, the TME is populated by exhausted $TIGIT^+CD8^+$ T cells with co-expression of other IRs and low levels of pro-inflammatory cytokines (IFN-γ, IL-2, TNF-α) (103, 156). Furthermore, high TIGIT expression was linked to advanced disease, early recurrence, and lower survival rates (156), and with advanced TNM stage and better disease-free survival (DFS) in colorectal cancer patients with mismatch repair deficiency (157). Another study discovered a higher $TIGIT^+CD3^+$ T cell subpopulation in the peripheral blood and cancer tissue of colorectal cancer patients than in healthy donors (121). $TIGIT^+CD3^+$T cells were exhausted cells with decreased proliferation, cytokine production, and glucose metabolism (121). TIGIT blockade, combined with PD-1 blockade, reversed these pro-tumorigenic features in the human MC38 colorectal xenograft mouse model. According to this data, GSEA computational analysis revealed that TIGIT expression in colorectal cancer drives the negative regulation of cytokine-cytokine receptor interaction pathway, chemokine signaling, and cytotoxic function of NK cells (122). *In vitro* studies have revealed that CD155–TIGIT pathway suppresses the downstream effector NF-κB, which is usually involved in the production of IFN-γ by NK cells, which in turn would activate cytotoxic $CD8^+$ T cells (103). On the contrary, the same authors demonstrated that knocking out CD155 in colorectal cancer cells promotes the effector function of tumor-infiltrating $CD8^+$ T cells, and inhibition of the CD155–TIGIT pathway suppresses the tumor growth in an *in vivo* mouse model. Overall, $TIGIT^+$ cells in colorectal cancer were linked to advanced disease, early recurrence, and lower survival rates (103).

In pancreatic cancer, the CD155–TIGIT pathway suppresses immunity and promotes immune evasion (158, 159). The cancer progression of a subset of patients with pancreatic adenocarcinoma in metastatic/advanced stages was related to high-affinity MHC-I-restricted neoepitopes expression and

exhausted TILs in the intratumoral compartment. Functional studies using orthogonal preclinical models revealed a synergistically antitumor response when TIGIT/PD-1 co-blockade was combined with CD40 agonism because they had been reinvigorated tumor-reactive T cells (158).

$TIGIT^+$ immune cells were also shown to play a role in cancer invasion and metastasis in esophageal carcinoma. A transcriptomic profile investigation followed by immunohistochemistry validation has identified the allograft inflammatory factor 1 (AIF1) gene as an unfavorable prognostic factor in this carcinoma and demonstrated that it is associated with immune infiltrates (160). In the tumor infiltrate, T cells and NK cells are affected by AIF1, which promotes TIGIT expression, and hence induces or strengthens immunotherapy resistance sustained by an immune infiltrate enriched in Th1 cells and exhausted T cells.

According to mRNA profiling of $CD8^+$ T cells in a murine model of autochthonous liver cancer, TIGIT is a hallmark of T cell exhaustion in liver cancer at various stages of their differentiation (161). TILs from patients with primary hepatocellular carcinoma and intrahepatic cholangiocarcinoma had an increased $TIGIT^+CD8^+$ T cell subpopulation. However, two subsets of these patients were identified: one had significantly higher TIGIT and PD-1 expression levels in the tumor area than the surrounding peritumoral area; whereas the other had a similar level of expression for both IRs in the tumoral and peritumoral areas (161).

In renal cell carcinoma (RCC), immunohistochemistry and flow cytometry experiments to evaluate TIGIT and PD-1 expression in circulating immune cells and TILs revealed an increased TIGIT and PD-1 expression in the tumoral area compared with adjacent normal tissue, but $TIGIT^+$ T cells and NK cells amount did not correlate with clinicopathological characteristics (age, sex, tumor diameter, Fuhrman grade, or TNM stage) (162). In contrast, a positive correlation with RCC clinicopathological characteristics was observed only for PD-1 (162).

CD155 and TIGIT were correlated with clinicopathological features in lung adenocarcinoma, in which CD155 expression was strongly associated with tumor staging and poor OS (111). TIGIT expression was associated with advanced TNM staging, which correlated with lymphatic metastasis and distant metastasis, with low antitumor immunity-related gene expression activation and poor PFS (111).

In oral squamous cell carcinoma, circulating T cells and TILs overexpressed TIGIT on $CD4^+$ and $CD8^+$ T cells, characterized by dysfunctional phenotype, including reduced proliferative capacity and low proinflammatory cytokine release (163). Higher TIGIT expression was also associated with higher T stage and nodal invasion but not with other clinicopathological variables such as age, gender, smoke/alcohol use, tumor site, and tumor differentiation (163).

Singer et al. proposed TIGIT expression as a predictive rather than prognostic biomarker for reactive tumor-infiltrating immune cells in soft sarcoma tissue in an elegant investigation on IL-15 and TIGIT blockade therapy to reactive tumor-infiltrating immune cells (164). The authors observed both activated and exhausted tumor-infiltrating NK cells and TILs and TIGIT upregulation in the TME, especially on NK cells, associated with superior distant disease recurrence-free and OS (165). Interestingly, activator and inhibitor pathways are not mutually exclusive and are a recent field of interest in targeted therapy (164, 165).

Under hypoxic conditions, HIF-1α transcript factor activation stimulates the expression of various IRs, including TIGIT. TIGIT and HIF-1α activity suppression experiments, using a siRNA carrier system, have revealed a critical role of these molecules in tumor growth, apoptosis, and metastasis in colorectal and breast cancer (166). In colorectal cancer cell line CT26 and breast cancer cell line 4T1 and in their *in vivo* mouse models, TIGIT and HIF-1α down-regulation diminished the colony formation ability and afflicted cancer cells' angiogenesis and proliferation activities, suggesting simultaneous blocking of TIGIT and HIF-1α as a potential new treatment strategy (166).

Considering all these results, it is possible to speculate that later than tumorigenesis, when the tumor already presents an immune infiltrate, immune cells, particularly T cells, upregulate TIGIT, promoting an immunosuppressive microenvironment that leads to metastasis and unfavorable prognosis. The studies with an in-depth microenvironment characterization and association with clinicopathological features point out several diverse IRs expression combined analysis that might represent an effective outcome prediction panel in cancer. However, there is much work to be done to understand in more detail TIGIT's role in the different tumor stages (e.g., initial diagnosis, progression, recurrence, metastases) in various cancers.

THERAPEUTIC STRATEGIES TARGETING TIGIT IMMUNE CHECKPOINT EXPRESSION

Cancer treatments are traditionally based on surgery, targeted therapies, chemotherapy, or radiation therapy (167). Immune inflammatory modulation-based therapy, or more simply immunotherapy, has lately emerged as a novel therapeutic arm with enormous potential, particularly in the treatment of cancer chemo-radiotherapy resistance (168, 169). Immunotherapy is a type of treatment that aids the immune system in fighting cancer and other diseases.

Immunotherapies have been shown to be effective against tumor-associated T cells that are dysfunctional. The rationale behind these therapies is that the cancer cells overexpress ligands for IRs, such as CD115, CD112, and others, to elude the immune system. Different immunotherapy strategies aim to boost the patient's antitumor immune response against malignancies minimizing T cell exhaustion and providing protective effects against recurrence and metastasis with less toxicity when compared to traditional cancer therapy (170).

Here is an update on therapeutic strategies targeting TIGIT immune checkpoint expression.

Cancer immunotherapy strategies that boost innate and adaptive immunity are being developed to achieve long-lasting

antitumor effects. Azelnidipine is a long-acting third-generation dihydropyridine calcium channel blocker that has been approved for the treatment of hypertension. However, using the molecular operating environment (MOE) by blocking and MST binding assays, molecular docking and structural analysis of CD172a and CD112 have indicated azelnidipine's potential relevance in cancer immunotherapy (171). Azelnidipine inhibits the innate checkpoint CD47/CD172a and the adaptive checkpoint TIGIT–CD112 pathways and has anti-cancer effects by increasing the infiltration and function of $CD8^+$ T cell and macrophage tumor cell phagocytosis *in vivo* and *in vitro*. This study extensively looked at the effect of TIGIT blockade on macrophages in the tumor. Tumor cells, like normal cells, can express CD47, a "do not eat me" signal that prevents $CD172a^+$ macrophages from phagocytosing them. Zhou et al. demonstrated that azelnidipine blocks CD47–CD172a signaling, reactivates macrophage phagocytosis, and improves antitumor immunity even in combination with radiotherapy, as shown in the MC38 murine colon adenocarcinoma cell line (171). A cancer immunotherapy antibody targeting both CD47 and TIGIT has been patented (WO2020259535).

Alternative anticancer treatments with a systemic approach are being developed. In a mouse model of lung adenocarcinoma, triple therapy with the RadScopal approach (high-dose radiation to primary tumors plus low-dose radiation to secondary tumors) plus anti-TIGIT and plus anti-PD-1 prolong survival and block tumor growth while decreasing $TIGIT^+$ exhausted T cells and $TIGIT^+$ Tregs (104). This approach promotes a systemic antitumor response because low-dose radiation also reduces CD155 expression on TAMs and DCs (104). Combined therapies based on immunotherapy and radiation therapy promise to reset the TME.

$TIGIT^+$ macrophages were also looked at in leukemia, in which the leukemia-associated macrophages (LAM) co-expressing TIGIT, TIM3, and LAG3 were identified as immunosuppressive M2 responsive to *in vitro* TIGIT blockade therapy that polarizes the M2 toward the M1 phenotype and improves phagocytosis of the CD47 expressing tumor cells (172, 173).

An in-depth characterization of TILs in bladder cancer using PBMC isolation and tumor single-cell isolation from fresh tumor tissue demonstrates that $PD\text{-}1^{high}TOX^+$ T cells play a key role in tumor evasion, which might be reversed by combining PD-1 and TIGIT inhibition (174).

pt?>Autophagy, a cell-intrinsic system that uses the lysosome to remove damaged organelles and proteins, plays a critical role in cellular immunity. Indeed, autophagic abnormalities linked with oncogenesis promote tumor escape by influencing cell immunogenicity, APC activity, and T cell activity (175). Artesunate, an anti-malaria drug, exerts anticancer activity by inhibiting proliferation, migration, and angiogenesis and inducing apoptosis and autophagy. Artesunate-induced autophagy was well demonstrated in human bladder cancer cells, upregulating ROS and activating the AMPK-mTOR-ULK1 axis and in uterine corpus endometrial carcinoma, enhancing NK cell cytotoxicity *via* interactions with tumor cells overexpressing CD155, and upregulating co-stimulator CD226 and downregulating co-inhibitor TIGIT (176–178).

Anti-TIGIT antibodies are used instead in more consolidated therapies. TIGIT blocked reduced tumor growth while promoting an immune infiltration enriched in effector cytokine-secreting $CD8^+$ T cells (44, 116, 127, 179).

Vibostolimab is a humanized antibody that targets TIGIT preventing its binding with CD112 and CD155. Patients with advanced solid tumors who received vibostolimab alone or combined with the anti-PD-1 pembrolizumab in a phase I clinical trial (NCT02964013) showed controllable tolerance across escalating doses and all types of advanced solid tumors assessed. Increased NK cell activation of $CD8^+$ T cells was found to have an anticancer effect in the study (180).

Etigilimab is another anti-TIGIT monoclonal antibody that is now being investigated in an open-label, multicenter, phase I/II clinical trial (NCT04761198) in patients with advanced or metastatic solid tumors for tolerance and pharmacokinetics with the anti-PD-1 nivolumab (181).

Combining anti-TIGIT and anti-PD-1 immunotherapy in metastatic melanoma has shown encouraging outcomes, with increased proliferation, cytokine generation, and degranulation of effector $CD8^+$ T cells (116).

Mono- or dual TIGIT and PD-1–PD-L1 blockade aims to take advantage of the curative potential of pre-existing tumor-primed T cells in cancer treatment by promoting $CD8^+$ T cell proliferation and function, resulting in protective memory T cells that ensure tumor rejection and avoid recurrence (182–184). Although several of these antibodies have received clinical approval, their effectiveness remains modest because immunological checkpoints and their signaling are regulated at multiple levels.

In addition to monoclonal antibodies, the most recent approach is to design T cells for TIGIT.

Hoogi et al. created a TIGIT : CD28 chimeric co-stimulatory switch receptor with the TIGIT exodomain fused to the CD28 signaling domain, which improved the activities of chimeric antigen receptor T cells by stimulating cytokine production and activating other T cell effector functions (185).

EFFICACY AND TOXICITY OF ANTI-TIGIT IMMUNE CHECKPOINT THERAPY

Even though therapeutic strategies targeting immunological checkpoints have been approved for a variety of cancer types, patients continue to have poor prognoses and suffer from immune-related adverse events (irAEs) that affect numerous organs. irAEs are secondary to the infiltration of activated T cells and can affect any organ (186, 187). Skin, gastrointestinal tract, endocrine, lungs, thyroid, pituitary and adrenal glands, and the musculoskeletal system are the most usually impacted, while nervous, renal, hematologic, ophthalmic, and cardiovascular systems are less commonly affected (188–190). Four degrees of irAEs can be distinguished based on the organs involved and the severity: patients with grade 1 irAEs show skin toxicity (<10%

body surface area) and no sign of toxicity for the gastrointestinal tract, liver, endocrine system, and lungs; patients with grade 4 of irAEs show elevated skin toxicity (> 30% body surface), hepatotoxicity, and severe symptoms of involvement of the cardiovascular, endocrine, and digestive apparatus (191). Grade 2 and 3 show intermediate signs. The management of irAEs is based on well-established clinical practice guidelines well reviewed by Barber in 2019 (192). Some irAEs are more common in immune therapy than chemotherapy, and their frequencies are positively associated with clinical efficacy, making them useful for clinical decisions (193).

To understand the efficacy and toxicity of immune checkpoint therapy, it should be noted that the types of antibodies used in anti-TIGIT therapies are very different and more or less tolerated. A murine, chimeric, humanized, or completely human IgG antibody could be used to suppress immunological checkpoints (194). The majority of anti-TIGIT antibodies in clinical trials are either humanized (such as ociperlimab, pembrolizumab, atezolizumab) or fully human (such as tiragolumab, etiligimab, ipilimumab, nivolumab, vibostolimab, domvanalimab) (195). Compared to other forms of IgG origin, humanized and completely human antibodies have increased *in vivo* tolerability but much-reduced immunogenicity (194).

Furthermore, blockade therapy efficacy depends on the antibody-dependent cellular cytotoxicity (ADCC) desired to destroy unfunctional T cells and tumor cells. ADCC is a non-phagocytic mechanism in which antibody-bound target cells are killed by innate immune cells such as NK cells, DCs, and macrophages (196). To activate ADCC, the targeted cell must express target antigens, the antibody must be preferentially IgG1 or IgG3 monoclonal because these two antibodies link any type of FcR, and the effector cell must have the Fc-gamma receptors (FcγR) (196). Concerning TIGIT, its FcγR is active in tiragolumab, ociperlimab, vibostolimab, EOS-448, etigilimab, and AGEN-1307, whereas it is inactive in domvanalimab, BMS-986207, and CASC-674 (195). However, FcγR presence or absence has not been tested for anti-TIGIT antibody clinical efficacy (197, 198).

Recently, TIGIT molecular was also used as Fc-fused protein in some reports demonstrating that TIGIT-Fc may act both as an immunosuppressor and as an immunostimulator in a microenvironment-dependent way (83, 85, 199–201). TIGIT-Fc is a dimer in which an Fc domain of an antibody is linked to the extracellular domain of TIGIT by covalent bonds. TIGIT-Fc has antibody-like features, such as a long serum half-life and efficient expression and purification *in vitro*, making it an ideal drug (46). Its action as an immunosuppressor was demonstrated *in vitro* and in a mouse model of acute allogeneic GVHD in which it decreased $CD8^+IFN\text{-}\gamma^+$ and $CD8^+$ granzyme B^+ T cells activation in a dendritic cell-dependent manner and reduced the release of IL-10 (83).

Moreover, TIGIT-Fc acts as a negative regulator of inflammation, inhibiting macrophage activation and imbalanced M1/M2 ratio in favor of M2 anti-inflammatory profile *via* c-Maf up-regulation, which promotes IL-10 transcription as demonstrated by *in vivo* and *in vitro* experiments using fibroblasts stably secreting TIGIT-Fc in the LPS shock model (85). In CLL, a tumor-supportive role of $TIGIT^+CD4^+$ T cells was observed in the presence of TIGIT-Fc *via* down-regulation of IFNγ and IL-10 production (201). Interestingly, this protumor activity of $CD4^+$ T cells was dependent on CLL cell's presence because *in vitro* experiments with $CD4^+$ T cells alone did not show any effects (201).

On the contrary, TIGIT/ligand interactions using recombinant TIGIT-Fc molecule immunostimulatory functions were shown in xenograft mouse models containing different human tumor cells (A375, A431, SK-BR-3, SK-OV-3, and H2126) co-implanted with human T cells (200). The TIGIT-Fc treatment enhanced effector NK cell functions and activated an anti-tumor T cell immune response *via* $CD4^+$ T cells preventing their exhaustion (200). Additionally, synergistic effects were observed in TIGIT-Fc plus anti-PD-L1 combined therapy (200).

Efficacy and toxicity of anti-TIGIT therapy were evaluated in the CITYSCAPE trial (NCT03563716), in which anti-TIGIT (tiragolumab) with anti-PD-L1 (atezolizumab) combined therapy were applied. The findings showed that this combined therapy in non-small cell lung cancer (NSCLC) is well tolerated when compared to CTLA4 with PD-L1 combined therapy, and that it improves responses and PFS in PD-L1–immune sensitive patients (202–205). Furthermore, despite the similar safety profiles of atezolizumab with placebo (AP) vs. atelozomab with tiragolumab (AT), 80.6% of patients in the AT group and 72% of patients in the AP group suffered irAEs. The irAEs included rash and thyroid issues, infusion reactions at the first dose, soft stool, diarrhea, and very few cases of more severe toxicities, like hepatitis (204, 205).

The anti-TIGIT vibostolimab was tested in patients with solid tumors as monotherapy or in combination with the anti-PD-L1 pembrolizumab in the phase I multicohort MK-7684-001 trial (NCT02964013). The ORR for vibostolimab monotherapy was more significant than for combination therapy in the sub-cohort of NSCLC patients with anti–PD-1–PD-L1–refractory disease (7% (95% CI, 2%-20%) vs. 5% (95% CI, <1%-18%)) (206). IrAEs were reported by 65% of patients in the same NSCLC sub-cohort, including pruritus, fatigue, rash, arthralgia, decreased appetite, and 13% also had lipase elevation and hypertension (206).

TIGIT blockade therapy may be more beneficial if it is evaluated as a first-line treatment. In February 2020, a multicenter, open-label, phase I/II study using the novel anti-TIGIT EOS884448 as monotherapy was launched in patients with previously treated advanced cancer (ovarian, head and neck, cervical, and colorectal) (NCT04335253) (207). Multiple mechanisms of action for EOS884448 were demonstrated: inhibition of TIGIT triggering activation of $TIGIT^{low}$ T cells and NK cells; depletion of immunosuppressive Treg and exhausted $TIGIT^{high}$ T cells; and reverse activation *via* FcγR engagement (207). The pharmacokinetic and pharmacodynamic analysis demonstrated that exhausted Tregs and $TIGIT^+$ T cells were depleted in a dose-dependent manner. Moreover, in this interventional study with multiple ascending-dose treatments, EOS884448 was generally well tolerated at all tested doses in patients with advanced cancer and had a promising antitumor activity as a single agent also in PD1-resistant patients. IrAEs were reported by 82% of patients, including pruritus, infusion-related reaction, fatigue pyrexia, rash macuolo-papular, eczema, and hypothyroidism (207).

Cancer patients' stratification based on tumor response to immune checkpoint inhibitors is vital even if challenging to evaluate (208, 209). In fact, patients might experience clinical pseudoprogression that can be misinterpreted as disease progression because it cannot be evaluated with the existing response-evaluation criteria (210, 211). In tumor pseudoprogression, an increase in tumor size depends on infiltrating T cells, while in proper tumor progression, the increased tumor mass is due to proliferating tumor cells (210). In 2017, the Response Evaluation Criteria in Solid Tumors (RECIST) working group published a modified set of response criteria, the immune-related response criteria (iRECIST), adapted for immunotherapy because of the importance of a standardized strategy to evaluate its effects (212, 213).

Identifying prognostic biomarkers of response to TIGIT blockade alone or in combination with other IRs is needed to improve efficacy and reduce toxicity.

CHALLENGES AND CONCLUSIONS

To summarize, in cancer, the genetic and epigenetic alterations could initiate tumorigenesis, which activates T cells and NK cells, and TME gets infiltrated by immune cells. Following T cells and NK cells upregulate TIGIT expression, which leads to an immunosuppressive TME, promoting tumor progression, immune escape, and metastases that result in poor prognosis.

Immune inflammatory modulation-based therapy is a promising therapeutic strategy against solid and hematological malignancies, but the outcomes are not largely encouraging because some tumor types remain refractory primarily to these therapies (214). $CD8^+$ T cells are extremely heterogeneous, while $CD4^+$ T cells in immunosuppression and immunotherapy are under-investigated (44). Targeting only a part of the complicated tumor system is insufficient for most cancer therapies or only in the arm of immunotherapies, so patients cannot benefit for a long time. New combined multiple targets (other co-inhibitory receptors) for immunotherapy must be explored to improve treatment.

Guidelines should be set for immunotherapy research. The results of different studies are difficult to compare due to the different designs for types of cancer, sample size, and statistical analysis. Consequently, when the results of individual studies are analyzed, they are insufficient to adopt particular and successful therapeutic interventions.

Side effects of traditional and immune checkpoint blockade therapies should be evaluated in-depth. High cytokine release and effector cell infiltration into TME cause irAEs that sometimes lead to the death of patients (215–217). Skin, gastrointestinal tract, lung, or liver are all affected by irAEs. However, the TIGIT blockade seems to have fewer side effects compared with other IRs blockades, as demonstrated in $TIGIT^{-/-}$ mouse model (218–220). In this pre-clinical model, TIGIT blockade triggers fewer irAEs than anti-PD1 or anti -CTLA4 therapies (218–220).

Anti-TIGIT therapy is now being tested in 25 clinical trials, considering only those starting from 2021 (**Table 1**), but there is still considerable work to be done to discover new and safely targetable immune checkpoints that could be effective against various malignancies.

The immunological and stromal characterization of the TME cells and their amount and spatial distribution in relation to pathology and prognosis will help patient stratification, enhance personalized cancer therapy efficiency, and overcome tumor immune evasion mechanisms.

AUTHOR CONTRIBUTIONS

This work was conceived and planned by TA. The original draft preparation and writing: TA. Review and editing: DR and RT. All authors have read and agreed to the published version of the manuscript.

FUNDING

This work was supported by Associazione "Il Sorriso di Antonio", Corato, Italy and by ARES-Centro Salute Ambiente Progetto Ionico-Salentino.

REFERENCES

1. Speiser DE, Ho PC, Verdeil G. Regulatory Circuits of T Cell Function in Cancer. *Nat Rev Immunol* (2016) 16(10):599–611. doi: 10.1038/nri.2016.80
2. Blessin NC, Simon R, Kluth M, Fischer K, Hube-Magg C, Li W, et al. Patterns of TIGIT Expression in Lymphatic Tissue, Inflammation, and Cancer. *Dis Markers* (2019) 2019:5160565. doi: 10.1155/2019/5160565
3. Sharpe AH. Mechanisms of Costimulation. *Immunol Rev* (2009) 229(1):5–11. doi: 10.1111/j.1600-065X.2009.00784.x
4. Vijayakrishnan L, Slavik JM, Illes Z, Greenwald RJ, Rainbow D, Greve B, et al. An Autoimmune Disease-Associated CTLA-4 Splice Variant Lacking the B7 Binding Domain Signals Negatively in T Cells. *Immunity* (2004) 20(5):563–75. doi: 10.1016/s1074-7613(04)00110-4
5. Gonzalez H, Hagerling C, Werb Z. Roles of the Immune System in Cancer: From Tumor Initiation to Metastatic Progression. *Genes Dev* (2018) 32(19-20):1267–84. doi: 10.1101/gad.314617.118
6. O'Neill RE, Cao X. Co-Stimulatory and Co-Inhibitory Pathways in Cancer Immunotherapy. *Adv Cancer Res* (2019) 143:145–94. doi: 10.1016/bs.acr.2019.03.003
7. Gardner D, Jeffery LE, Sansom DM. Understanding the CD28/CTLA-4 (CD152) Pathway and Its Implications for Costimulatory Blockade. *Am J Transplant* (2014) 14(9):1985–91. doi: 10.1111/ajt.12834
8. Pardoll DM. The Blockade of Immune Checkpoints in Cancer Immunotherapy. *Nat Rev Cancer* (2012) 12(4):252–64. doi: 10.1038/nrc3239
9. Schreiber RD, Old LJ, Smyth MJ. Cancer Immunoediting: Integrating Immunity's Roles in Cancer Suppression and Promotion. *Science* (2011) 331(6024):1565–70. doi: 10.1126/science.1203486
10. Dunn GP, Old LJ, Schreiber RD. The Three Es of Cancer Immunoediting. *Annu Rev Immunol* (2004) 22:329–60. doi: 10.1146/annurev.immunol.22.012703.104803
11. O'Donnell JS, Teng MWL, Smyth MJ. Cancer Immunoediting and Resistance to T Cell-Based Immunotherapy. *Nat Rev Clin Oncol* (2019) 16(3):151–67. doi: 10.1038/s41571-018-0142-8

12. Barrueto L, Caminero F, Cash L, Makris C, Lamichhane P, Deshmukh RR. Resistance to Checkpoint Inhibition in Cancer Immunotherapy. *Transl Oncol* (2020) 13(3):100738. doi: 10.1016/j.tranon.2019.12.010
13. Sharma P, Allison JP. The Future of Immune Checkpoint Therapy. *Science* (2015) 348(6230):56–61. doi: 10.1126/science.aaa8172
14. Borroni EM, Grizzi F. Cancer Immunoediting and Beyond in 2021. *Int J Mol Sci* (2021) 22(24):13275. doi: 10.3390/ijms222413275
15. Matsushita H, Vesely MD, Koboldt DC, Rickert CG, Uppaluri R, Magrini VJ, et al. Cancer Exome Analysis Reveals a T-Cell-Dependent Mechanism of Cancer Immunoediting. *Nature* (2012) 482(7385):400–4. doi: 10.1038/nature10755
16. On the Origin of Species by Means of Natural Selection, or the Preservation of Favoured Races in the Struggle for Life. *Br Foreign Med Chir Rev* (1860) 25 (50):367–404.
17. Teng MW, Galon J, Fridman WH, Smyth MJ. From Mice to Humans: Developments in Cancer Immunoediting. *J Clin Invest* (2015) 125(9):3338–46. doi: 10.1172/JCI80004
18. Mittal D, Gubin MM, Schreiber RD, Smyth MJ. New Insights Into Cancer Immunoediting and Its Three Component Phases–Elimination, Equilibrium and Escape. *Curr Opin Immunol* (2014) 27:16–25. doi: 10.1016/j.coi.2014.01.004
19. Wellenstein MD, de Visser KE. Cancer-Cell-Intrinsic Mechanisms Shaping the Tumor Immune Landscape. *Immunity* (2018) 48(3):399–416. doi: 10.1016/j.immuni.2018.03.004
20. Wu AA, Drake V, Huang HS, Chiu S, Zheng L. Reprogramming the Tumor Microenvironment: Tumor-Induced Immunosuppressive Factors Paralyze T Cells. *Oncoimmunology* (2015) 4(7):e1016700. doi: 10.1080/2162402X.2015.1016700
21. Palucka AK, Coussens LM. The Basis of Oncoimmunology. *Cell* (2016) 164 (6):1233–47. doi: 10.1016/j.cell.2016.01.049
22. Cornel AM, Mimpen IL, Nierkens S. MHC Class I Downregulation in Cancer: Underlying Mechanisms and Potential Targets for Cancer Immunotherapy. *Cancers (Basel)* (2020) 12(7):1760. doi: 10.3390/cancers12071760
23. Kohli K, Pillarisetty VG, Kim TS. Key Chemokines Direct Migration of Immune Cells in Solid Tumors. *Cancer Gene Ther* (2021) 29(1):10–21. doi: 10.1038/s41417-021-00303-x
24. Kouidhi S, Elgaaied AB, Chouaib S. Impact of Metabolism on T-Cell Differentiation and Function and Cross Talk With Tumor Microenvironment. *Front Immunol* (2017) 8:270. doi: 10.3389/fimmu.2017.00270
25. Anagnostou V, Smith KN, Forde PM, Niknafs N, Bhattacharya R, White J, et al. Evolution of Neoantigen Landscape During Immune Checkpoint Blockade in Non-Small Cell Lung Cancer. *Cancer Discovery* (2017) 7 (3):264–76. doi: 10.1158/2159-8290.CD-16-0828
26. Chen L, Flies DB. Molecular Mechanisms of T Cell Co-Stimulation and Co-Inhibition. *Nat Rev Immunol* (2013) 13(4):227–42. doi: 10.1038/nri3405
27. Mpakali A, Stratikos E. The Role of Antigen Processing and Presentation in Cancer and the Efficacy of Immune Checkpoint Inhibitor Immunotherapy. *Cancers (Basel)* (2021) 13(1):134. doi: 10.3390/cancers13010134
28. Vigano S, Perreau M, Pantaleo G, Harari A. Positive and Negative Regulation of Cellular Immune Responses in Physiologic Conditions and Diseases. *Clin Dev Immunol* (2012) 2012:485781. doi: 10.1155/2012/485781
29. Linsley PS, Greene JL, Brady W, Bajorath J, Ledbetter JA, Peach R. Human B7-1 (CD80) and B7-2 (CD86) Bind With Similar Avidities But Distinct Kinetics to CD28 and CTLA-4 Receptors. *Immunity* (1994) 1(9):793–801. doi: 10.1016/s1074-7613(94)80021-9
30. Egen JG, Allison JP. Cytotoxic T Lymphocyte Antigen-4 Accumulation in the Immunological Synapse is Regulated by TCR Signal Strength. *Immunity* (2002) 16(1):23–35. doi: 10.1016/s1074-7613(01)00259-x
31. Sharpe AH, Pauken KE. The Diverse Functions of the PD1 Inhibitory Pathway. *Nat Rev Immunol* (2018) 18(3):153–67. doi: 10.1038/nri.2017.108
32. Jiang X, Wang J, Deng X, Xiong F, Ge J, Xiang B, et al. Role of the Tumor Microenvironment in PD-L1/PD-1-Mediated Tumor Immune Escape. *Mol Cancer* (2019) 18(1):10. doi: 10.1186/s12943-018-0928-4
33. Efremova M, Rieder D, Klepsch V, Charoentong P, Finotello F, Hackl H, et al. Targeting Immune Checkpoints Potentiates Immunoediting and Changes the Dynamics of Tumor Evolution. *Nat Commun* (2018) 9(1):32. doi: 10.1038/s41467-017-02424-0
34. Sugawara T, Miya F, Ishikawa T, Lysenko A, Nishino J, Kamatani T, et al. Immune Subtypes and Neoantigen-Related Immune Evasion in Advanced Colorectal Cancer. *iScience* (2022) 25(2):103740. doi: 10.1016/j.isci.2022.103740
35. Shen R, Li P, Li B, Zhang B, Feng L, Cheng S. Identification of Distinct Immune Subtypes in Colorectal Cancer Based on the Stromal Compartment. *Front Oncol* (2019) 9:1497. doi: 10.3389/fonc.2019.01497
36. Manieri NA, Chiang EY, Grogan JL. TIGIT: A Key Inhibitor of the Cancer Immunity Cycle. *Trends Immunol* (2017) 38(1):20–8. doi: 10.1016/j.it.2016.10.002
37. Yang ZZ, Kim HJ, Wu H, Jalali S, Tang X, Krull JE, et al. TIGIT Expression Is Associated With T-Cell Suppression and Exhaustion and Predicts Clinical Outcome and Anti-PD-1 Response in Follicular Lymphoma. *Clin Cancer Res* (2020) 26(19):5217–31. doi: 10.1158/1078-0432.CCR-20-0558
38. Kvistborg P, Philips D, Kelderman S, Hageman L, Ottensmeier C, Joseph-Pietras D, et al. Anti-CTLA-4 Therapy Broadens the Melanoma-Reactive CD8+ T Cell Response. *Sci Transl Med* (2014) 6(254):254ra128. doi: 10.1126/scitranslmed.3008918
39. Yost KE, Satpathy AT, Wells DK, Qi Y, Wang C, Kageyama R, et al. Clonal Replacement of Tumor-Specific T Cells Following PD-1 Blockade. *Nat Med* (2019) 25(8):1251–9. doi: 10.1038/s41591-019-0522-3
40. Pauken KE, Godec J, Odorizzi PM, Brown KE, Yates KB, Ngiow SF, et al. The PD-1 Pathway Regulates Development and Function of Memory CD8(+) T Cells Following Respiratory Viral Infection. *Cell Rep* (2020) 31(13):107827. doi: 10.1016/j.celrep.2020.107827
41. Zaretsky JM, Garcia-Diaz A, Shin DS, Escuin-Ordinas H, Hugo W, Hu-Lieskovan S, et al. Mutations Associated With Acquired Resistance to PD-1 Blockade in Melanoma. *N Engl J Med* (2016) 375(9):819–29. doi: 10.1056/NEJMoa1604958
42. Sade-Feldman M, Jiao YJ, Chen JH, Rooney MS, Barzily-Rokni M, Eliane JP, et al. Resistance to Checkpoint Blockade Therapy Through Inactivation of Antigen Presentation. *Nat Commun* (2017) 8(1):1136. doi: 10.1038/s41467-017-01062-w
43. Zhao X, Wangmo D, Robertson M, Subramanian S. Acquired Resistance to Immune Checkpoint Blockade Therapies. *Cancers (Basel)* (2020) 12(5):1161. doi: 10.3390/cancers12051161
44. Ge Z, Peppelenbosch MP, Sprengers D, Kwekkeboom J. TIGIT, the Next Step Towards Successful Combination Immune Checkpoint Therapy in Cancer. *Front Immunol* (2021) 12:699895. doi: 10.3389/fimmu.2021.699895
45. Levin SD, Taft DW, Brandt CS, Bucher C, Howard ED, Chadwick EM, et al. Vstm3 Is a Member of the CD28 Family and an Important Modulator of T-Cell Function. *Eur J Immunol* (2011) 41(4):902–15. doi: 10.1002/eji.201041136
46. Yu X, Harden K, Gonzalez LC, Francesco M, Chiang E, Irving B, et al. The Surface Protein TIGIT Suppresses T Cell Activation by Promoting the Generation of Mature Immunoregulatory Dendritic Cells. *Nat Immunol* (2009) 10(1):48–57. doi: 10.1038/ni.1674
47. Stengel KF, Harden-Bowles K, Yu X, Rouge L, Yin J, Comps-Agrar L, et al. Structure of TIGIT Immunoreceptor Bound to Poliovirus Receptor Reveals a Cell-Cell Adhesion and Signaling Mechanism That Requires Cis-Trans Receptor Clustering. *Proc Natl Acad Sci USA* (2012) 109(14):5399–404. doi: 10.1073/pnas.1120606109
48. Li M, Xia P, Du Y, Liu S, Huang G, Chen J, et al. T-Cell Immunoglobulin and ITIM Domain (TIGIT) Receptor/Poliovirus Receptor (PVR) Ligand Engagement Suppresses Interferon-Gamma Production of Natural Killer Cells *via* Beta-Arrestin 2-Mediated Negative Signaling. *J Biol Chem* (2014) 289(25):17647–57. doi: 10.1074/jbc.M114.572420
49. Martinet L, Smyth MJ. Regulation of Immune Cell Functions Through Nectin and Nectin-Like Receptors. In: MJH Ratcliffe, editor. *Encyclopedia of Immunobiology*. Oxford: Academic Press (2016). p. 404–14.
50. Liu S, Zhang H, Li M, Hu D, Li C, Ge B, et al. Recruitment of Grb2 and SHIP1 by the ITT-Like Motif of TIGIT Suppresses Granule Polarization and Cytotoxicity of NK Cells. *Cell Death Differ* (2013) 20(3):456–64. doi: 10.1038/cdd.2012.141
51. Stanietsky N, Rovis TL, Glasner A, Seidel E, Tsukerman P, Yamin R, et al. Mouse TIGIT Inhibits NK-Cell Cytotoxicity Upon Interaction With PVR. *Eur J Immunol* (2013) 43(8):2138–50. doi: 10.1002/eji.201243072
52. Deuss FA, Gully BS, Rossjohn J, Berry R. Recognition of Nectin-2 by the Natural Killer Cell Receptor T Cell Immunoglobulin and ITIM Domain

(TIGIT). *J Biol Chem* (2017) 292(27):11413–22. doi: 10.1074/jbc.M117.786483
53. Stanietsky N, Simic H, Arapovic J, Toporik A, Levy O, Novik A, et al. The Interaction of TIGIT With PVR and PVRL2 Inhibits Human NK Cell Cytotoxicity. *Proc Natl Acad Sci USA* (2009) 106(42):17858–63. doi: 10.1073/pnas.0903474106
54. Negishi N, Sato T, Yamashita-Kanemaru Y, Shibuya K, Uchida K, Kametani Y, et al. CD155-Transducing Signaling Through TIGIT Plays an Important Role in Transmission of Tolerant State and Suppression Capacity. *Immunohorizons* (2018) 2(10):338–48. doi: 10.4049/immunohorizons.1800033
55. Pende D, Bottino C, Castriconi R, Cantoni C, Marcenaro S, Rivera P, et al. PVR (CD155) and Nectin-2 (CD112) as Ligands of the Human DNAM-1 (CD226) Activating Receptor: Involvement in Tumor Cell Lysis. *Mol Immunol* (2005) 42(4):463–9. doi: 10.1016/j.molimm.2004.07.028
56. Samanta D, Ramagopal UA, Rubinstein R, Vigdorovich V, Nathenson SG, Almo SC. Structure of Nectin-2 Reveals Determinants of Homophilic and Heterophilic Interactions That Control Cell-Cell Adhesion. *Proc Natl Acad Sci USA* (2012) 109(37):14836–40. doi: 10.1073/pnas.1212912109
57. Zhu Y, Paniccia A, Schulick AC, Chen W, Koenig MR, Byers JT, et al. Identification of CD112R as a Novel Checkpoint for Human T Cells. *J Exp Med* (2016) 213(2):167–76. doi: 10.1084/jem.20150785
58. Eberle F, Dubreuil P, Mattei MG, Devilard E, Lopez M. The Human PRR2 Gene, Related to the Human Poliovirus Receptor Gene (PVR), Is the True Homolog of the Murine MPH Gene. *Gene* (1995) 159(2):267–72. doi: 10.1016/0378-1119(95)00180-e
59. Lopez M, Aoubala M, Jordier F, Isnardon D, Gomez S, Dubreuil P. The Human Poliovirus Receptor Related 2 Protein Is a New Hematopoietic/Endothelial Homophilic Adhesion Molecule. *Blood* (1998) 92(12):4602–11. doi: 10.1182/blood.V92.12.4602
60. Inagaki M, Irie K, Ishizaki H, Tanaka-Okamoto M, Miyoshi J, Takai Y. Role of Cell Adhesion Molecule Nectin-3 in Spermatid Development. *Genes Cells* (2006) 11(9):1125–32. doi: 10.1111/j.1365-2443.2006.01006.x
61. Ogita H, Rikitake Y, Miyoshi J, Takai Y. Cell Adhesion Molecules Nectins and Associating Proteins: Implications for Physiology and Pathology. *Proc Jpn Acad Ser B Phys Biol Sci* (2010) 86(6):621–9. doi: 10.2183/pjab.86.621
62. Mizoguchi A, Nakanishi H, Kimura K, Matsubara K, Ozaki-Kuroda K, Katata T, et al. Nectin: An Adhesion Molecule Involved in Formation of Synapses. *J Cell Biol* (2002) 156(3):555–65. doi: 10.1083/jcb.200103113
63. Poon CE, Madawala RJ, Dowland SN, Murphy CR. Nectin-3 Is Increased in the Cell Junctions of the Uterine Epithelium at Implantation. *Reprod Sci* (2016) 23(11):1580–92. doi: 10.1177/1933719116648216
64. Fujito T, Ikeda W, Kakunaga S, Minami Y, Kajita M, Sakamoto Y, et al. Inhibition of Cell Movement and Proliferation by Cell-Cell Contact-Induced Interaction of Necl-5 With Nectin-3. *J Cell Biol* (2005) 171(1):165–73. doi: 10.1083/jcb.200501090
65. Inagaki M, Irie K, Ishizaki H, Tanaka-Okamoto M, Morimoto K, Inoue E, et al. Roles of Cell-Adhesion Molecules Nectin 1 and Nectin 3 in Ciliary Body Development. *Development* (2005) 132(7):1525–37. doi: 10.1242/dev.01697
66. Ozaki-Kuroda K, Nakanishi H, Ohta H, Tanaka H, Kurihara H, Mueller S, et al. Nectin Couples Cell-Cell Adhesion and the Actin Scaffold at Heterotypic Testicular Junctions. *Curr Biol* (2002) 12(13):1145–50. doi: 10.1016/s0960-9822(02)00922-3
67. Racaniello VR. Polio. In: M Schaechter, editor. *Encyclopedia of Microbiology, 3rd ed*. Oxford: Academic Press (2009). p. 459–68.
68. Baury B, Masson D, McDermott BMJr., Jarry A, Blottiere HM, Blanchardie P, et al. Identification of Secreted CD155 Isoforms. *Biochem Biophys Res Commun* (2003) 309(1):175–82. doi: 10.1016/s0006-291x(03)01560-2
69. Iguchi-Manaka A, Okumura G, Kojima H, Cho Y, Hirochika R, Bando H, et al. Increased Soluble CD155 in the Serum of Cancer Patients. *PloS One* (2016) 11(4):e0152982. doi: 10.1371/journal.pone.0152982
70. Walwyn-Brown K, Guldevall K, Saeed M, Pende D, Onfelt B, MacDonald AS, et al. Human NK Cells Lyse Th2-Polarizing Dendritic Cells *via* NKp30 and DNAM-1. *J Immunol* (2018) 201(7):2028–41. doi: 10.4049/jimmunol.1800475
71. Pende D, Castriconi R, Romagnani P, Spaggiari GM, Marcenaro S, Dondero A, et al. Expression of the DNAM-1 Ligands, Nectin-2 (CD112) and Poliovirus Receptor (CD155), on Dendritic Cells: Relevance for Natural Killer-Dendritic Cell Interaction. *Blood* (2006) 107(5):2030–6. doi: 10.1182/blood-2005-07-2696
72. Huang WC, Kuo KT, Wang CH, Yeh CT, Wang Y. Cisplatin Resistant Lung Cancer Cells Promoted M2 Polarization of Tumor-Associated Macrophages *via* the Src/CD155/MIF Functional Pathway. *J Exp Clin Cancer Res* (2019) 38(1):180. doi: 10.1186/s13046-019-1166-3
73. Kamran N, Takai Y, Miyoshi J, Biswas SK, Wong JS, Gasser S. Toll-Like Receptor Ligands Induce Expression of the Costimulatory Molecule CD155 on Antigen-Presenting Cells. *PloS One* (2013) 8(1):e54406. doi: 10.1371/journal.pone.0054406
74. Maier MK, Seth S, Czeloth N, Qiu Q, Ravens I, Kremmer E, et al. The Adhesion Receptor CD155 Determines the Magnitude of Humoral Immune Responses Against Orally Ingested Antigens. *Eur J Immunol* (2007) 37(8):2214–25. doi: 10.1002/eji.200737072
75. Azzazi MO, Hegab HM, El-Ghammaz AMS, Saber HM, Afifi YA. Impact of Serum Soluble CD155 Level at Diagnosis on Interim Response to CHOP With or Without Rituximab in Diffuse Large B Cell Lymphoma. *Clin Exp Med* (2021) 3. doi: 10.1007/s10238-021-00741-9
76. Mueller S, Wimmer E. Recruitment of Nectin-3 to Cell-Cell Junctions Through Trans-Heterophilic Interaction With CD155, a Vitronectin and Poliovirus Receptor That Localizes to Alpha(V)Beta3 Integrin-Containing Membrane Microdomains. *J Biol Chem* (2003) 278(33):31251–60. doi: 10.1074/jbc.M304166200
77. Gromeier M, Solecki D, Patel DD, Wimmer E. Expression of the Human Poliovirus Receptor/CD155 Gene During Development of the Central Nervous System: Implications for the Pathogenesis of Poliomyelitis. *Virology* (2000) 273(2):248–57. doi: 10.1006/viro.2000.0418
78. Iwasaki A, Welker R, Mueller S, Linehan M, Nomoto A, Wimmer E. Immunofluorescence Analysis of Poliovirus Receptor Expression in Peyer's Patches of Humans, Primates, and CD155 Transgenic Mice: Implications for Poliovirus Infection. *J Infect Dis* (2002) 186(5):585–92. doi: 10.1086/342682
79. Ravens I, Seth S, Forster R, Bernhardt G. Characterization and Identification of Tage4 as the Murine Orthologue of Human Poliovirus Receptor/CD155. *Biochem Biophys Res Commun* (2003) 312(4):1364–71. doi: 10.1016/j.bbrc.2003.11.067
80. Sloan KE, Eustace BK, Stewart JK, Zehetmeier C, Torella C, Simeone M, et al. CD155/PVR Plays a Key Role in Cell Motility During Tumor Cell Invasion and Migration. *BMC Cancer* (2004) 4:73. doi: 10.1186/1471-2407-4-73
81. Gao J, Zheng Q, Xin N, Wang W, Zhao C. CD155, an Onco-Immunologic Molecule in Human Tumors. *Cancer Sci* (2017) 108(10):1934–8. doi: 10.1111/cas.13324
82. Wang FF, Wang Y, Wang L, Wang TS, Bai YP. TIGIT Expression Levels on CD4+ T Cells Are Correlated With Disease Severity in Patients With Psoriasis. *Clin Exp Dermatol* (2018) 43(6):675–82. doi: 10.1111/ced.13414
83. Zhang D, Hu W, Xie J, Zhang Y, Zhou B, Liu X, et al. TIGIT-Fc Alleviates Acute Graft-Versus-Host Disease by Suppressing CTL Activation *via* Promoting the Generation of Immunoregulatory Dendritic Cells. *Biochim Biophys Acta Mol Basis Dis* (2018) 1864(9 Pt B):3085–98. doi: 10.1016/j.bbadis.2018.06.022
84. Noguchi Y, Maeda A, Lo PC, Takakura C, Haneda T, Kodama T, et al. Human TIGIT on Porcine Aortic Endothelial Cells Suppresses Xenogeneic Macrophage-Mediated Cytotoxicity. *Immunobiology* (2019) 224(5):605–13. doi: 10.1016/j.imbio.2019.07.008
85. Chen X, Lu PH, Liu L, Fang ZM, Duan W, Liu ZL, et al. TIGIT Negatively Regulates Inflammation by Altering Macrophage Phenotype. *Immunobiology* (2016) 221(1):48–55. doi: 10.1016/j.imbio.2015.08.003
86. Reches A, Ophir Y, Stein N, Kol I, Isaacson B, Charpak Amikam Y, et al. Nectin4 Is a Novel TIGIT Ligand Which Combines Checkpoint Inhibition and Tumor Specificity. *J Immunother Cancer* (2020) 8(1):e000266. doi: 10.1136/jitc-2019-000266
87. Reymond N, Fabre S, Lecocq E, Adelaide J, Dubreuil P, Lopez M. Nectin4/PRR4, a New Afadin-Associated Member of the Nectin Family That Trans-Interacts With Nectin1/PRR1 Through V Domain Interaction. *J Biol Chem* (2001) 276(46):43205–15. doi: 10.1074/jbc.M103810200
88. MR M, Cabaud O, Josselin E, Finetti P, Castellano R, Farina A, et al. Nectin-4: A New Prognostic Biomarker for Efficient Therapeutic Targeting of Primary

and Metastatic Triple-Negative Breast Cancer. *Ann Oncol* (2017) 28(4):769–76. doi: 10.1093/annonc/mdw678
89. Siddharth S, Goutam K, Das S, Nayak A, Nayak D, Sethy C, et al. Nectin-4 Is a Breast Cancer Stem Cell Marker That Induces WNT/beta-Catenin Signaling *via* Pi3k/Akt Axis. *Int J Biochem Cell Biol* (2017) 89:85–94. doi: 10.1016/j.biocel.2017.06.007
90. Hoffman-Censits JH, Lombardo KA, Parimi V, Kamanda S, Choi W, Hahn NM, et al. Expression of Nectin-4 in Bladder Urothelial Carcinoma, in Morphologic Variants, and Nonurothelial Histotypes. *Appl Immunohistochem Mol Morphol* (2021) 29(8):619–25. doi: 10.1097/PAI.0000000000000938
91. Li P, Hou F, Wang S, Luo N, Qi Y, Wang Y. A Novel NECTIN4-NTRK1 Fusion Identified in a Lung Squamous Cell Carcinoma Patient With MSI-H. *J Cancer Res Clin Oncol* (2021) 147(8):2483–6. doi: 10.1007/s00432-021-03622-6
92. Takano A, Ishikawa N, Nishino R, Masuda K, Yasui W, Inai K, et al. Identification of Nectin-4 Oncoprotein as a Diagnostic and Therapeutic Target for Lung Cancer. *Cancer Res* (2009) 69(16):6694–703. doi: 10.1158/0008-5472.CAN-09-0016
93. Challita-Eid PM, Satpayev D, Yang P, An Z, Morrison K, Shostak Y, et al. Enfortumab Vedotin Antibody-Drug Conjugate Targeting Nectin-4 Is a Highly Potent Therapeutic Agent in Multiple Preclinical Cancer Models. *Cancer Res* (2016) 76(10):3003–13. doi: 10.1158/0008-5472.CAN-15-1313
94. Nishiwada S, Sho M, Yasuda S, Shimada K, Yamato I, Akahori T, et al. Nectin-4 Expression Contributes to Tumor Proliferation, Angiogenesis and Patient Prognosis in Human Pancreatic Cancer. *J Exp Clin Cancer Res* (2015) 34:30. doi: 10.1186/s13046-015-0144-7
95. Zhang Z, Wu N, Lu Y, Davidson D, Colonna M, Veillette A. DNAM-1 Controls NK Cell Activation *via* an ITT-Like Motif. *J Exp Med* (2015) 212 (12):2165–82. doi: 10.1084/jem.20150792
96. Shibuya A, Campbell D, Hannum C, Yssel H, Franz-Bacon K, McClanahan T, et al. DNAM-1, A Novel Adhesion Molecule Involved in the Cytolytic Function of T Lymphocytes. *Immunity* (1996) 4(6):573–81. doi: 10.1016/S1074-7613(00)70060-4
97. Lozano E, Dominguez-Villar M, Kuchroo V, Hafler DA. The TIGIT/CD226 Axis Regulates Human T Cell Function. *J Immunol* (2012) 188(8):3869–75. doi: 10.4049/jimmunol.1103627
98. Sanchez-Correa B, Valhondo I, Hassouneh F, Lopez-Sejas N, Pera A, Bergua JM, et al. DNAM-1 and the TIGIT/PVRIG/TACTILE Axis: Novel Immune Checkpoints for Natural Killer Cell-Based Cancer Immunotherapy. *Cancers (Basel)* (2019) 11(6):877. doi: 10.3390/cancers11060877
99. Enqvist M, Ask EH, Forslund E, Carlsten M, Abrahamsen G, Beziat V, et al. Coordinated Expression of DNAM-1 and LFA-1 in Educated NK Cells. *J Immunol* (2015) 194(9):4518–27. doi: 10.4049/jimmunol.1401972
100. Martinet L, Ferrari De Andrade L, Guillerey C, Lee JS, Liu J, Souza-Fonseca-Guimaraes F, et al. DNAM-1 Expression Marks an Alternative Program of NK Cell Maturation. *Cell Rep* (2015) 11(1):85–97. doi: 10.1016/j.celrep.2015.03.006
101. Zhang B, Zhao W, Li H, Chen Y, Tian H, Li L, et al. Immunoreceptor TIGIT Inhibits the Cytotoxicity of Human Cytokine-Induced Killer Cells by Interacting With CD155. *Cancer Immunol Immunother* (2016) 65(3):305–14. doi: 10.1007/s00262-016-1799-4
102. Zhang Y, Ellinger J, Ritter M, Schmidt-Wolf IGH. Clinical Studies Applying Cytokine-Induced Killer Cells for the Treatment of Renal Cell Carcinoma. *Cancers (Basel)* (2020) 12(9):2471. doi: 10.3390/cancers12092471
103. Li S, Ding J, Wang Y, Wang X, Lv L. CD155/TIGIT Signaling Regulates the Effector Function of Tumor-Infiltrating CD8+ T Cell by NF-kappaB Pathway in Colorectal Cancer. *J Gastroenterol Hepatol* (2022) 37(1):154–63. doi: 10.1111/jgh.15730
104. Joller N, Lozano E, Burkett PR, Patel B, Xiao S, Zhu C, et al. Treg Cells Expressing the Coinhibitory Molecule TIGIT Selectively Inhibit Proinflammatory Th1 and Th17 Cell Responses. *Immunity* (2014) 40 (4):569–81. doi: 10.1016/j.immuni.2014.02.012
105. Lucca LE, Axisa PP, Singer ER, Nolan NM, Dominguez-Villar M, Hafler DA. TIGIT Signaling Restores Suppressor Function of Th1 Tregs. *JCI Insight* (2019) 4(3):e124427. doi: 10.1172/jci.insight.124427
106. Dardalhon V, Schubart AS, Reddy J, Meyers JH, Monney L, Sabatos CA, et al. CD226 is Specifically Expressed on the Surface of Th1 Cells and Regulates Their Expansion and Effector Functions. *J Immunol* (2005) 175(3):1558–65. doi: 10.4049/jimmunol.175.3.1558
107. Lozano E, Joller N, Cao Y, Kuchroo VK, Hafler DA. The CD226/CD155 Interaction Regulates the Proinflammatory (Th1/Th17)/Anti-Inflammatory (Th2) Balance in Humans. *J Immunol* (2013) 191(7):3673–80. doi: 10.4049/jimmunol.1300945
108. Wherry EJ, Kurachi M. Molecular and Cellular Insights Into T Cell Exhaustion. *Nat Rev Immunol* (2015) 15(8):486–99. doi: 10.1038/nri3862
109. Gorvel L, Olive D. Targeting the "PVR-TIGIT Axis" With Immune Checkpoint Therapies. *F1000Res* (2020) 9(F1000 Faculty Rev):354. doi: 10.12688/f1000research.22877.1
110. Zhang L, Pan J, Chen W, Jiang J, Huang J. Chronic Stress-Induced Immune Dysregulation in Cancer: Implications for Initiation, Progression, Metastasis, and Treatment. *Am J Cancer Res* (2020) 10(5):1294–307.
111. Sun Y, Luo J, Chen Y, Cui J, Lei Y, Cui Y, et al. Combined Evaluation of the Expression Status of CD155 and TIGIT Plays an Important Role in the Prognosis of LUAD (Lung Adenocarcinoma). *Int Immunopharmacol* (2020) 80:106198. doi: 10.1016/j.intimp.2020.106198
112. Dai S, Zeng H, Liu Z, Jin K, Jiang W, Wang Z, et al. Intratumoral Cxcl13(+) Cd8(+)T Cell Infiltration Determines Poor Clinical Outcomes and Immunoevasive Contexture in Patients With Clear Cell Renal Cell Carcinoma. *J Immunother Cancer* (2021) 9(2):e001823. doi: 10.1136/jitc-2020-001823
113. Liu X, Li M, Wang X, Dang Z, Jiang Y, Wang X, et al. PD-1(+) TIGIT(+) CD8(+) T Cells are Associated With Pathogenesis and Progression of Patients With Hepatitis B Virus-Related Hepatocellular Carcinoma. *Cancer Immunol Immunother* (2019) 68(12):2041–54. doi: 10.1007/s00262-019-02426-5
114. Hung AL, Maxwell R, Theodros D, Belcaid Z, Mathios D, Luksik AS, et al. TIGIT and PD-1 Dual Checkpoint Blockade Enhances Antitumor Immunity and Survival in GBM. *Oncoimmunology* (2018) 7(8):e1466769. doi: 10.1080/2162402X.2018.1466769
115. Xu J, Liu F, Li Y, Shen L. A 1p/19q Codeletion-Associated Immune Signature for Predicting Lower Grade Glioma Prognosis. *Cell Mol Neurobiol* (2020) 42 (3):709–22. doi: 10.1007/s10571-020-00959-3
116. Chauvin JM, Pagliano O, Fourcade J, Sun Z, Wang H, Sander C, et al. TIGIT and PD-1 Impair Tumor Antigen-Specific CD8(+) T Cells in Melanoma Patients. *J Clin Invest* (2015) 125(5):2046–58. doi: 10.1172/JCI80445
117. Masson D, Jarry A, Baury B, Blanchardie P, Laboisse C, Lustenberger P, et al. Overexpression of the CD155 Gexne in Human Colorectal Carcinoma. *Gut* (2001) 49(2):236–40. doi: 10.1136/gut.49.2.236
118. Castriconi R, Dondero A, Corrias MV, Lanino E, Pende D, Moretta L, et al. Natural Killer Cell-Mediated Killing of Freshly Isolated Neuroblastoma Cells: Critical Role of DNAX Accessory Molecule-1-Poliovirus Receptor Interaction. *Cancer Res* (2004) 64(24):9180–4. doi: 10.1158/0008-5472.CAN-04-2682
119. Tahara-Hanaoka S, Shibuya K, Kai H, Miyamoto A, Morikawa Y, Ohkochi N, et al. Tumor Rejection by the Poliovirus Receptor Family Ligands of the DNAM-1 (CD226) Receptor. *Blood* (2006) 107(4):1491–6. doi: 10.1182/blood-2005-04-1684
120. Yin X, Zhang X, Liu Z, Sun G, Zhu X, Zhang H, et al. Assessment for Prognostic Value of Differentially Expressed Genes in Immune Microenvironment of Clear Cell Renal Cell Carcinoma. *Am J Transl Res* (2020) 12(9):5416–32.
121. Shao Q, Wang L, Yuan M, Jin X, Chen Z, Wu C. TIGIT Induces (CD3+) T Cell Dysfunction in Colorectal Cancer by Inhibiting Glucose Metabolism. *Front Immunol* (2021) 12:688961. doi: 10.3389/fimmu.2021.688961
122. Wen J, Mao X, Cheng Q, Liu Z, Liu F. A Pan-Cancer Analysis Revealing the Role of TIGIT in Tumor Microenvironment. *Sci Rep* (2021) 11(1):22502. doi: 10.1038/s41598-021-01933-9
123. Zhang Y, Song J, Zhao Z, Yang M, Chen M, Liu C, et al. Single-Cell Transcriptome Analysis Reveals Tumor Immune Microenvironment Heterogenicity and Granulocytes Enrichment in Colorectal Cancer Liver Metastases. *Cancer Lett* (2020) 470:84–94. doi: 10.1016/j.canlet.2019.10.016
124. Qian J, Olbrecht S, Boeckx B, Vos H, Laoui D, Etlioglu E, et al. A Pan-Cancer Blueprint of the Heterogeneous Tumor Microenvironment Revealed by Single-Cell Profiling. *Cell Res* (2020) 30(9):745–62. doi: 10.1038/s41422-020-0355-0

125. Blackburn SD, Shin H, Haining WN, Zou T, Workman CJ, Polley A, et al. Coregulation of CD8+ T Cell Exhaustion by Multiple Inhibitory Receptors During Chronic Viral Infection. *Nat Immunol* (2009) 10(1):29–37. doi: 10.1038/ni.1679
126. Zarour HM. Reversing T-Cell Dysfunction and Exhaustion in Cancer. *Clin Cancer Res* (2016) 22(8):1856–64. doi: 10.1158/1078-0432.CCR-15-1849
127. Johnston RJ, Comps-Agrar L, Hackney J, Yu X, Huseni M, Yang Y, et al. The Immunoreceptor TIGIT Regulates Antitumor and Antiviral CD8(+) T Cell Effector Function. *Cancer Cell* (2014) 26(6):923–37. doi: 10.1016/j.ccell.2014.10.018
128. Li X, Wang R, Fan P, Yao X, Qin L, Peng Y, et al. A Comprehensive Analysis of Key Immune Checkpoint Receptors on Tumor-Infiltrating T Cells From Multiple Types of Cancer. *Front Oncol* (2019) 9:1066. doi: 10.3389/fonc.2019.01066
129. Weimer P, Wellbrock J, Sturmheit T, Oliveira-Ferrer L, Ding Y, Menzel S, et al. Tissue-Specific Expression of TIGIT, PD-1, TIM-3, and CD39 by Gammadelta T Cells in Ovarian Cancer. *Cells* (2022) 11(6):964. doi: 10.3390/cells11060964
130. Sasidharan Nair V, El Salhat H, Taha RZ, John A, Ali BR, Elkord E. DNA Methylation and Repressive H3K9 and H3K27 Trimethylation in the Promoter Regions of PD-1, CTLA-4, TIM-3, LAG-3, TIGIT, and PD-L1 Genes in Human Primary Breast Cancer. *Clin Epigenet* (2018) 10:78. doi: 10.1186/s13148-018-0512-1
131. Sasidharan Nair V, Toor SM, Taha RZ, Shaath H, Elkord E. DNA Methylation and Repressive Histones in the Promoters of PD-1, CTLA-4, TIM-3, LAG-3, TIGIT, PD-L1, and Galectin-9 Genes in Human Colorectal Cancer. *Clin Epigenet* (2018) 10(1):104. doi: 10.1186/s13148-018-0539-3
132. Syed Khaja AS, Toor SM, El Salhat H, Faour I, Ul Haq N, Ali BR, et al. Preferential Accumulation of Regulatory T Cells With Highly Immunosuppressive Characteristics in Breast Tumor Microenvironment. *Oncotarget* (2017) 8(20):33159–71. doi: 10.18632/oncotarget.16565
133. Wang W, Shen G, Wu S, Song S, Ni Y, Suo Z, et al. PD-1 mRNA Expression in Peripheral Blood Cells and its Modulation Characteristics in Cancer Patients. *Oncotarget* (2017) 8(31):50782–91. doi: 10.18632/oncotarget.15006
134. Elashi AA, Sasidharan Nair V, Taha RZ, Shaath H, Elkord E. DNA Methylation of Immune Checkpoints in the Peripheral Blood of Breast and Colorectal Cancer Patients. *Oncoimmunology* (2019) 8(2):e1542918. doi: 10.1080/2162402X.2018.1542918
135. Wang P, Chen Y, Long Q, Li Q, Tian J, Liu T, et al. Increased Coexpression of PD-L1 and TIM3/TIGIT Is Associated With Poor Overall Survival of Patients With Esophageal Squamous Cell Carcinoma. *J Immunother Cancer* (2021) 9(10):e002836. doi: 10.1136/jitc-2021-002836
136. Hajiasghar-Sharbaf R, Asgarian-Omran H, Valadan R, Hossein-Nattaj H, Shekarriz R, Zaboli E, et al. CD8+ T-Cells Co-Expressing PD-1 and TIGIT Are Highly Frequent in Chronic Lymphocytic Leukemia. *Iran J Allergy Asthma Immunol* (2021) 20(6):751–63. doi: 10.18502/ijaai.v20i6.8027
137. Taghiloo S, Allahmoradi E, Tehrani M, Hossein-Nataj H, Shekarriz R, Janbabaei G, et al. Frequency and Functional Characterization of Exhausted CD8(+) T Cells in Chronic Lymphocytic Leukemia. *Eur J Haematol* (2017) 98(6):622–31. doi: 10.1111/ejh.12880
138. Allahmoradi E, Taghiloo S, Tehrani M, Hossein-Nattaj H, Janbabaei G, Shekarriz R, et al. CD4+ T Cells are Exhausted and Show Functional Defects in Chronic Lymphocytic Leukemia. *Iran J Immunol* (2017) 14(4):257–69.
139. Brauneck F, Weimer P, Schulze Zur Wiesch J, Weisel K, Leypoldt L, Vohwinkel G, et al. Bone Marrow-Resident Vdelta1 T Cells Co-Express TIGIT With PD-1, TIM-3 or CD39 in AML and Myeloma. *Front Med (Lausanne)* (2021) 8:763773. doi: 10.3389/fmed.2021.763773
140. Jin Z, Ye W, Lan T, Zhao Y, Liu X, Chen J, et al. Characteristic of TIGIT and DNAM-1 Expression on Foxp3+ Gammadelta T Cells in AML Patients. *BioMed Res Int* (2020) 2020:4612952. doi: 10.1155/2020/4612952
141. Annibali O, Bianchi A, Grifoni A, Tomarchio V, Tafuri M, Verri M, et al. A Novel Scoring System for TIGIT Expression in Classic Hodgkin Lymphoma. *Sci Rep* (2021) 11(1):7059. doi: 10.1038/s41598-021-86655-8
142. Alfarra H, Weir J, Grieve S, Reiman T. Targeting NK Cell Inhibitory Receptors for Precision Multiple Myeloma Immunotherapy. *Front Immunol* (2020) 11:575609. doi: 10.3389/fimmu.2020.575609
143. Melaiu O, Lucarini V, Cifaldi L, Fruci D. Influence of the Tumor Microenvironment on NK Cell Function in Solid Tumors. *Front Immunol* (2019) 10:3038. doi: 10.3389/fimmu.2019.03038
144. Yu L, Liu X, Wang X, Yan F, Wang P, Jiang Y, et al. TIGIT(+) TIM-3(+) NK Cells are Correlated With NK Cell Exhaustion and Disease Progression in Patients With Hepatitis B Virusrelated Hepatocellular Carcinoma. *Oncoimmunology* (2021) 10(1):1942673. doi: 10.1080/2162402X.2021.1942673
145. Chauvin JM, Ka M, Pagliano O, Menna C, Ding Q, DeBlasio R, et al. IL15 Stimulation With TIGIT Blockade Reverses CD155-Mediated NK-Cell Dysfunction in Melanoma. *Clin Cancer Res* (2020) 26(20):5520–33. doi: 10.1158/1078-0432.CCR-20-0575
146. Simon S, Voillet V, Vignard V, Wu Z, Dabrowski C, Jouand N, et al. PD-1 and TIGIT Coexpression Identifies a Circulating CD8 T Cell Subset Predictive of Response to Anti-PD-1 Therapy. *J Immunother Cancer* (2020) 8(2):e001631. doi: 10.1136/jitc-2020-001631
147. He R, Hou S, Liu C, Zhang A, Bai Q, Han M, et al. Follicular CXCR5-Expressing CD8(+) T Cells Curtail Chronic Viral Infection. *Nature* (2016) 537(7620):412–28. doi: 10.1038/nature19317
148. Leong YA, Chen Y, Ong HS, Wu D, Man K, Deleage C, et al. CXCR5(+) Follicular Cytotoxic T Cells Control Viral Infection in B Cell Follicles. *Nat Immunol* (2016) 17(10):1187–96. doi: 10.1038/ni.3543
149. Fourcade J, Sun Z, Chauvin JM, Ka M, Davar D, Pagliano O, et al. CD226 Opposes TIGIT to Disrupt Tregs in Melanoma. *JCI Insight* (2018) 3(14):e121157. doi: 10.1172/jci.insight.121157
150. Zhang Y, Maksimovic J, Naselli G, Qian J, Chopin M, Blewitt ME, et al. Genome-Wide DNA Methylation Analysis Identifies Hypomethylated Genes Regulated by FOXP3 in Human Regulatory T Cells. *Blood* (2013) 122(16):2823–36. doi: 10.1182/blood-2013-02-481788
151. Zhang Q, Gao C, Shao J, Wang Z. TIGIT-Related Transcriptome Profile and Its Association With Tumor Immune Microenvironment in Breast Cancer. *Biosci Rep* (2021) 41(3):BSR20204340. doi: 10.1042/BSR20204340
152. Ma J. Bioinformatics-Guided Analysis Uncovers TIGIT as an Epigenetically Regulated Immunomodulator Affecting Immunotherapeutic Sensitivity of Gastric Cancer. *Cancer biomark* (2021) 33(3):349–58. doi: 10.3233/CBM-210159
153. Wu K, Zeng J, Shi X, Xie J, Li Y, Zheng H, et al. Targeting TIGIT Inhibits Bladder Cancer Metastasis Through Suppressing IL-32. *Front Pharmacol* (2021) 12:801493. doi: 10.3389/fphar.2021.801493
154. Liu Z, Zeng H, Jin K, Yu Y, You R, Zhang H, et al. TIGIT and PD-1 Expression Atlas Predicts Response to Adjuvant Chemotherapy and PD-L1 Blockade in Muscle-Invasive Bladder Cancer. *Br J Cancer* (2022) 126(9):1310–17. doi: 10.1038/s41416-022-01703-y
155. Liu Z, Zhou Q, Wang Z, Zhang H, Zeng H, Huang Q, et al. Intratumoral TIGIT(+) CD8(+) T-Cell Infiltration Determines Poor Prognosis and Immune Evasion in Patients With Muscle-Invasive Bladder Cancer. *J Immunother Cancer* (2020) 8(2):e000978. doi: 10.1136/jitc-2020-000978
156. Liang R, Zhu X, Lan T, Ding D, Zheng Z, Chen T, et al. TIGIT Promotes CD8(+)T Cells Exhaustion and Predicts Poor Prognosis of Colorectal Cancer. *Cancer Immunol Immunother* (2021) 70(10):2781–93. doi: 10.1007/s00262-021-02886-8
157. Zhou X, Ding X, Li H, Yang C, Ma Z, Xu G, et al. Upregulation of TIGIT and PD-1 in Colorectal Cancer With Mismatch-Repair Deficiency. *Immunol Invest* (2021) 50(4):338–55. doi: 10.1080/08820139.2020.1758130
158. Freed-Pastor WA, Lambert LJ, Ely ZA, Pattada NB, Bhutkar A, Eng G, et al. The CD155/TIGIT Axis Promotes and Maintains Immune Evasion in Neoantigen-Expressing Pancreatic Cancer. *Cancer Cell* (2021) 39(10):1342–60 e14. doi: 10.1016/j.ccell.2021.07.007
159. Nishi K, Ishikura S, Umebayashi M, Morisaki T, Inozume T, Kinugasa T, et al. Mutant KRAS Promotes NKG2D(+) T Cell Infiltration and CD155 Dependent Immune Evasion. *Anticancer Res* (2020) 40(8):4663–74. doi: 10.21873/anticanres.14465
160. Xu X, Wang D, Li N, Sheng J, Xie M, Zhou Z, et al. The Novel Tumor Microenvironment-Related Prognostic Gene AIF1 May Influence Immune Infiltrates and is Correlated With TIGIT in Esophageal Cancer. *Ann Surg Oncol* (2021) 29(5):2930–40. doi: 10.1245/s10434-021-10928-9
161. Ostroumov D, Duong S, Wingerath J, Woller N, Manns MP, Timrott K, et al. Transcriptome Profiling Identifies TIGIT as a Marker of T-Cell Exhaustion in Liver Cancer. *Hepatology* (2021) 73(4):1399–418. doi: 10.1002/hep.31466

162. Hong X, Wang X, Wang T, Zhang X. Correlation of T Cell Immunoglobulin and ITIM Domain (TIGIT) and Programmed Death 1 (PD-1) With Clinicopathological Characteristics of Renal Cell Carcinoma May Indicate Potential Targets for Treatment. *Med Sci Monit* (2018) 24:6861–72. doi: 10.12659/MSM.910388
163. Liu X, Li Q, Zhou Y, He X, Fang J, Lu H, et al. Dysfunctional Role of Elevated TIGIT Expression on T Cells in Oral Squamous Cell Carcinoma Patients. *Oral Dis* (2021) 27(7):1667–77. doi: 10.1111/odi.13703
164. Singer M, Wang C, Cong L, Marjanovic ND, Kowalczyk MS, Zhang H, et al. A Distinct Gene Module for Dysfunction Uncoupled From Activation in Tumor-Infiltrating T Cells. *Cell* (2016) 166(6):1500–11 e9. doi: 10.1016/j.cell.2016.08.052
165. Judge SJ, Darrow MA, Thorpe SW, Gingrich AA, O'Donnell EF, Bellini AR, et al. Analysis of Tumor-Infiltrating NK and T Cells Highlights IL-15 Stimulation and TIGIT Blockade as a Combination Immunotherapy Strategy for Soft Tissue Sarcomas. *J Immunother Cancer* (2020) 8(2):e001355. doi: 10.1136/jitc-2020-001355
166. Fathi M, Bahmanpour S, Barshidi A, Rasouli H, Karoon Kiani F, Mahmoud Salehi Khesht A, et al. Simultaneous Blockade of TIGIT and HIF-1alpha Induces Synergistic Anti-Tumor Effect and Decreases the Growth and Development of Cancer Cells. *Int Immunopharmacol* (2021) 101(Pt A):108288. doi: 10.1016/j.intimp.2021.108288
167. Debela DT, Muzazu SG, Heraro KD, Ndalama MT, Mesele BW, Haile DC, et al. New Approaches and Procedures for Cancer Treatment: Current Perspectives. *SAGE Open Med* (2021) 9:20503121211034366. doi: 10.1177/20503121211034366
168. Solomon BL, Garrido-Laguna I. TIGIT: A Novel Immunotherapy Target Moving From Bench to Bedside. *Cancer Immunol Immunother* (2018) 67(11):1659–67. doi: 10.1007/s00262-018-2246-5
169. Darvin P, Toor SM, Sasidharan Nair V, Elkord E. Immune Checkpoint Inhibitors: Recent Progress and Potential Biomarkers. *Exp Mol Med* (2018) 50(12):1–11. doi: 10.1038/s12276-018-0191-1
170. Ganesh K, Stadler ZK, Cercek A, Mendelsohn RB, Shia J, Segal NH, et al. Immunotherapy in Colorectal Cancer: Rationale, Challenges and Potential. *Nat Rev Gastroenterol Hepatol* (2019) 16(6):361–75. doi: 10.1038/s41575-019-0126-x
171. Zhou X, Jiao L, Qian Y, Dong Q, Sun Y, Zheng WV, et al. Repositioning Azelnidipine as a Dual Inhibitor Targeting CD47/SIRPalpha and TIGIT/PVR Pathways for Cancer Immuno-Therapy. *Biomolecules* (2021) 11(5):706. doi: 10.3390/biom11050706
172. Brauneck F, Fischer B, Wellbrock J, Bokemeyer C, Schulze zur Wiesch J, Haag F, et al. Blockade of Tigit on AML-Derived M2 Macrophages Results in Reprograming Into the M1 Phenotype and Enhances CD47-Mediated Phagocytosis. *Blood* (2021) 138:3351. doi: 10.1182/blood-2021-148075
173. Tseng D, Volkmer JP, Willingham SB, Contreras-Trujillo H, Fathman JW, Fernhoff NB, et al. Anti-CD47 Antibody-Mediated Phagocytosis of Cancer by Macrophages Primes an Effective Antitumor T-Cell Response. *Proc Natl Acad Sci USA* (2013) 110(27):11103–8. doi: 10.1073/pnas.1305569110
174. Han HS, Jeong S, Kim H, Kim HD, Kim AR, Kwon M, et al. TOX-Expressing Terminally Exhausted Tumor-Infiltrating CD8(+) T Cells are Reinvigorated by Co-Blockade of PD-1 and TIGIT in Bladder Cancer. *Cancer Lett* (2021) 499:137–47. doi: 10.1016/j.canlet.2020.11.035
175. Ma Y, Galluzzi L, Zitvogel L, Kroemer G. Autophagy and Cellular Immune Responses. *Immunity* (2013) 39(2):211–27. doi: 10.1016/j.immuni.2013.07.017
176. Zhang J, Zhou L, Xiang JD, Jin CS, Li MQ, He YY. Artesunate-Induced ATG5-Related Autophagy Enhances the Cytotoxicity of NK92 Cells on Endometrial Cancer Cells *via* Interactions Between CD155 and CD226/TIGIT. *Int Immunopharmacol* (2021) 97:107705. doi: 10.1016/j.intimp.2021.107705
177. Zhou X, Chen Y, Wang F, Wu H, Zhang Y, Liu J, et al. Artesunate Induces Autophagy Dependent Apoptosis Through Upregulating ROS and Activating AMPK-mTOR-ULK1 Axis in Human Bladder Cancer Cells. *Chem Biol Interact* (2020) 331:109273. doi: 10.1016/j.cbi.2020.109273
178. Yin X, Liu Y, Qin J, Wu Y, Huang J, Zhao Q, et al. Artesunate Suppresses the Proliferation and Development of Estrogen Receptor-Alpha-Positive Endometrial Cancer in HAND2-Dependent Pathway. *Front Cell Dev Biol* (2020) 8:606969. doi: 10.3389/fcell.2020.606969
179. Zhang C, Wang Y, Xun X, Wang S, Xiang X, Hu S, et al. TIGIT Can Exert Immunosuppressive Effects on CD8+ T Cells by the CD155/TIGIT Signaling Pathway for Hepatocellular Carcinoma *In Vitro*. *J Immunother* (2020) 43(8):236–43. doi: 10.1097/CJI.0000000000000330
180. Niu J, Maurice-Dror C, Lee DH, Kim DW, Nagrial A, Voskoboynik M, et al. First-In-Human Phase 1 Study of the Anti-TIGIT Antibody Vibostolimab as Monotherapy or With Pembrolizumab for Advanced Solid Tumors, Including Non-Small-Cell Lung Cancer(). *Ann Oncol* (2022) 33(2):169–80. doi: 10.1016/j.annonc.2021.11.002
181. Mettu NB, Ulahannan SV, Bendell JC, Garrido-Laguna I, Strickler JH, Moore KN, et al. A Phase 1a/B Open-Label, Dose-Escalation Study of Etigilimab Alone or in Combination With Nivolumab in Patients With Locally Advanced or Metastatic Solid Tumors. *Clin Cancer Res* (2021) 28(5):882–92. doi: 10.1158/1078-0432.CCR-21-2780
182. Walsh SR, Simovic B, Chen L, Bastin D, Nguyen A, Stephenson K, et al. Endogenous T Cells Prevent Tumor Immune Escape Following Adoptive T Cell Therapy. *J Clin Invest* (2019) 129(12):5400–10. doi: 10.1172/JCI126199
183. Grapin M, Richard C, Limagne E, Boidot R, Morgand V, Bertaut A, et al. Optimized Fractionated Radiotherapy With Anti-PD-L1 and Anti-TIGIT: A Promising New Combination. *J Immunother Cancer* (2019) 7(1):160. doi: 10.1186/s40425-019-0634-9
184. Hansen K, Kumar S, Logronio K, Whelan S, Qurashi S, Cheng HY, et al. COM902, a Novel Therapeutic Antibody Targeting TIGIT Augments Anti-Tumor T Cell Function in Combination With PVRIG or PD-1 Pathway Blockade. *Cancer Immunol Immunother* (2021) 70(12):3525–40. doi: 10.1007/s00262-021-02921-8
185. Hoogi S, Eisenberg V, Mayer S, Shamul A, Barliya T, Cohen CJ. A TIGIT-Based Chimeric Co-Stimulatory Switch Receptor Improves T-Cell Anti-Tumor Function. *J Immunother Cancer* (2019) 7(1):243. doi: 10.1186/s40425-019-0721-y
186. Gordon R, Kasler MK, Stasi K, Shames Y, Errante M, Ciccolini K, et al. Checkpoint Inhibitors: Common Immune-Related Adverse Events and Their Management. *Clin J Oncol Nurs* (2017) 21(2 Suppl):45–52. doi: 10.1188/17.CJON.S2.45-52
187. Ventola CL. Cancer Immunotherapy, Part 2: Efficacy, Safety, and Other Clinical Considerations. *P T* (2017) 42(7):452–63.
188. Brahmer JR, Lacchetti C, Thompson JA. Management of Immune-Related Adverse Events in Patients Treated With Immune Checkpoint Inhibitor Therapy: American Society of Clinical Oncology Clinical Practice Guideline Summary. *J Oncol Pract* (2018) 14(4):247–9. doi: 10.1200/JOP.18.00005
189. Puzanov I, Diab A, Abdallah K, Bingham CO3rd, Brogdon C, Dadu R, et al. Managing Toxicities Associated With Immune Checkpoint Inhibitors: Consensus Recommendations From the Society for Immunotherapy of Cancer (SITC) Toxicity Management Working Group. *J Immunother Cancer* (2017) 5(1):95. doi: 10.1186/s40425-017-0300-z
190. Okiyama N, Tanaka R. Immune-Related Adverse Events in Various Organs Caused by Immune Checkpoint Inhibitors. *Allergol Int* (2022) 71(2):169–78. doi: 10.1016/j.alit.2022.01.001
191. Spain L, Diem S, Larkin J. Management of Toxicities of Immune Checkpoint Inhibitors. *Cancer Treat Rev* (2016) 44:51–60. doi: 10.1016/j.ctrv.2016.02.001
192. Barber FD. Adverse Events of Oncologic Immunotherapy and Their Management. *Asia Pac J Oncol Nurs* (2019) 6(3):212–26. doi: 10.4103/apjon.apjon_6_19
193. Zhou C, Li M, Wang Z, An D, Li B. Adverse Events of Immunotherapy in non-Small Cell Lung Cancer: A Systematic Review and Network Meta-Analysis. *Int Immunopharmacol* (2022) 102:108353. doi: 10.1016/j.intimp.2021.108353
194. Harding FA, Stickler MM, Razo J, DuBridge RB. The Immunogenicity of Humanized and Fully Human Antibodies: Residual Immunogenicity Resides in the CDR Regions. *MAbs* (2010) 2(3):256–65. doi: 10.4161/mabs.2.3.11641
195. Rotte A, Sahasranaman S, Budha N. Targeting TIGIT for Immunotherapy of Cancer: Update on Clinical Development. *Biomedicines* (2021) 9(9):1277. doi: 10.3390/biomedicines9091277
196. Lo Nigro C, Macagno M, Sangiolo D, Bertolaccini L, Aglietta M, Merlano MC. NK-Mediated Antibody-Dependent Cell-Mediated Cytotoxicity in Solid Tumors: Biological Evidence and Clinical Perspectives. *Ann Transl Med* (2019) 7(5):105. doi: 10.21037/atm.2019.01.42

197. Chand D, Waight JD, Paltrinieri E, Dietrich S, Bushell M, Costa M, et al. Abstract 2390: FcgR Co-Engagement by Anti-TIGIT Monoclonal Antibodies Enhances T Cell Functionality and Antitumor Immune Responses. *Cancer Res* (2019) 79(13_Supplement):2390–. doi: 10.1158/1538-7445.Am2019-2390
198. Chen X, Song X, Li K, Zhang T. FcgammaR-Binding Is an Important Functional Attribute for Immune Checkpoint Antibodies in Cancer Immunotherapy. *Front Immunol* (2019) 10:292. doi: 10.3389/fimmu.2019.00292
199. Wang J, Hou H, Mao L, Wang F, Yu J, Luo Y, et al. TIGIT Signaling Pathway Regulates Natural Killer Cell Function in Chronic Hepatitis B Virus Infection. *Front Med (Lausanne)* (2021) 8:816474. doi: 10.3389/fmed.2021.816474
200. Shen X, Fu W, Wei Y, Zhu J, Yu Y, Lei C, et al. TIGIT-Fc Promotes Antitumor Immunity. *Cancer Immunol Res* (2021) 9(9):1088–97. doi: 10.1158/2326-6066.CIR-20-0986
201. Catakovic K, Gassner FJ, Ratswohl C, Zaborsky N, Rebhandl S, Schubert M, et al. TIGIT Expressing CD4+T Cells Represent a Tumor-Supportive T Cell Subset in Chronic Lymphocytic Leukemia. *Oncoimmunology* (2017) 7(1):e1371399. doi: 10.1080/2162402X.2017.1371399
202. Chauvin JM, Zarour HM. TIGIT in Cancer Immunotherapy. *J Immunother Cancer* (2020) 8(2):e000957. doi: 10.1136/jitc-2020-000957
203. Rotte A, Jin JY, Lemaire V. Mechanistic Overview of Immune Checkpoints to Support the Rational Design of Their Combinations in Cancer Immunotherapy. *Ann Oncol* (2018) 29(1):71–83. doi: 10.1093/annonc/mdx686
204. *Roche's Novel Anti-TIGIT Tiragolumab Granted FDA Breakthrough Therapy Designation in Combination With Tecentriq for PD-L1-High non-Small Cell Lung Cancer. News Release. Roche* . Available at: https://bit.ly/3hmWDm3 (Accessed April 26, 2021).
205. Rodriguez-Abreu D, Johnson ML, Hussein MA, Cobo M, Patel AJ, Secen NM, et al. Primary Analysis of a Randomized, Double-Blind, Phase II Study of the Anti-TIGIT Antibody Tiragolumab (Tira) Plus Atezolizumab (Atezo) Versus Placebo Plus Atezo as First-Line (1L) Treatment in Patients With PD-L1-Selected NSCLC (CITYSCAPE). *J Clin Oncol* (2020) 38(15_suppl):9503–. doi: 10.1200/JCO.2020.38.15_suppl.9503
206. Ahn MJ, Niu J, Kim DW, Rasco D, Mileham KF, Chung HC, et al. 1400p Vibostolimab, an Anti-TIGIT Antibody, as Monotherapy and in Combination With Pembrolizumab in Anti-PD-1/PD-L1-Refractory NSCLC. *Ann Oncol* (2020) 31:S887. doi: 10.1016/j.annonc.2020.08.1714
207. Van den Mooter TFA MA, Jungles C, Delafontaine BR, Nguyen TLA, Warot S, Truong C, et al. Preliminary Data From Phase I First-in-Human Study of EOS884448, a Novel Potent Anti-TIGIT Antibody, Monotherapy Shows Favorable Tolerability Profile and Early Signs of Clinical Activity in Immune-Resistant Advanced Cancers. In: American Association for Cancer Research (AACR) Annual Meeting 2021. *Cancer Res* (2021) 81(Suppl 13):CT118. doi: 10.1158/1538-7445.AM2021-CT118
208. Nishino M, Ramaiya NH, Hatabu H, Hodi FS. Monitoring Immune-Checkpoint Blockade: Response Evaluation and Biomarker Development. *Nat Rev Clin Oncol* (2017) 14(11):655–68. doi: 10.1038/nrclinonc.2017.88
209. McCune JS. Rapid Advances in Immunotherapy to Treat Cancer. *Clin Pharmacol Ther* (2018) 103(4):540–4. doi: 10.1002/cpt.985
210. Somarouthu B, Lee SI, Urban T, Sadow CA, Harris GJ, Kambadakone A. Immune-Related Tumour Response Assessment Criteria: A Comprehensive Review. *Br J Radiol* (2018) 91(1084):20170457. doi: 10.1259/bjr.20170457
211. Chiou VL, Burotto M. Pseudoprogression and Immune-Related Response in Solid Tumors. *J Clin Oncol* (2015) 33(31):3541–3. doi: 10.1200/JCO.2015.61.6870
212. Seymour L, Bogaerts J, Perrone A, Ford R, Schwartz LH, Mandrekar S, et al. iRECIST: Guidelines for Response Criteria for Use in Trials Testing Immunotherapeutics. *Lancet Oncol* (2017) 18(3):e143–e52. doi: 10.1016/S1470-2045(17)30074-8
213. Persigehl T, Lennartz S, Schwartz LH. iRECIST: How to do it. *Cancer Imaging* (2020) 20(1):2. doi: 10.1186/s40644-019-0281-x
214. Gun SY, Lee SWL, Sieow JL, Wong SC. Targeting Immune Cells for Cancer Therapy. *Redox Biol* (2019) 25:101174. doi: 10.1016/j.redox.2019.101174
215. Liu J, Blake SJ, Smyth MJ, Teng MW. Improved Mouse Models to Assess Tumour Immunity and irAEs After Combination Cancer Immunotherapies. *Clin Transl Immunol* (2014) 3(8):e22. doi: 10.1038/cti.2014.18
216. Boutros C, Tarhini A, Routier E, Lambotte O, Ladurie FL, Carbonnel F, et al. Safety Profiles of Anti-CTLA-4 and Anti-PD-1 Antibodies Alone and in Combination. *Nat Rev Clin Oncol* (2016) 13(8):473–86. doi: 10.1038/nrclinonc.2016.58
217. Martins F, Sofiya L, Sykiotis GP, Lamine F, Maillard M, Fraga M, et al. Adverse Effects of Immune-Checkpoint Inhibitors: Epidemiology, Management and Surveillance. *Nat Rev Clin Oncol* (2019) 16(9):563–80. doi: 10.1038/s41571-019-0218-0
218. Harjunpaa H, Blake SJ, Ahern E, Allen S, Liu J, Yan J, et al. Deficiency of Host CD96 and PD-1 or TIGIT Enhances Tumor Immunity Without Significantly Compromising Immune Homeostasis. *Oncoimmunology* (2018) 7(7):e1445949. doi: 10.1080/2162402X.2018.1445949
219. Guillerey C, Harjunpaa H, Carrie N, Kassem S, Teo T, Miles K, et al. TIGIT Immune Checkpoint Blockade Restores CD8(+) T-Cell Immunity Against Multiple Myeloma. *Blood* (2018) 132(16):1689–94. doi: 10.1182/blood-2018-01-825265
220. Kurtulus S, Sakuishi K, Ngiow SF, Joller N, Tan DJ, Teng MW, et al. TIGIT Predominantly Regulates the Immune Response *via* Regulatory T Cells. *J Clin Invest* (2015) 125(11):4053–62. doi: 10.1172/JCI81187

Conflict of Interest: The authors declare that the research was conducted in the absence of any commercial or financial relationships that could be construed as a potential conflict of interest.

Publisher's Note: All claims expressed in this article are solely those of the authors and do not necessarily represent those of their affiliated organizations, or those of the publisher, the editors and the reviewers. Any product that may be evaluated in this article, or claim that may be made by its manufacturer, is not guaranteed or endorsed by the publisher.

GLOSSARY

ADCC	antibody-dependent cellular cytotoxicity
AIF1	allograft inflammatory factor 1
CIK	cytokine-induced killer
CLL	chronic lymphocytic leukemia
CTLA4	cytotoxic T-Lymphocyte Antigen 4
DFS	disease-free survival
DCs	dendritic cells
DNMTs	DNA methyltransferases
FcγR	Fc-gamma receptors
GSEA	Gene set enrichment analysis
HiNeo	highly expressed neoantigens
IRs	inhibitor receptors
irAEs	immune-related adverse events
IRF4	IFN regulatory factor 4
ITIM	immunoreceptor tyrosine-based inhibitor motif
ITT	immunoglobulin tyrosine tail
LAM	leukemia-associated macrophages
MALs	malignant ascites lymphocytes
MHC-I	major histocompatibility complex class I
MMR	mismatch repair
MSI	microsatellite instability
NECL	nectin and nectin-like
NK	natural killer
NSCLC	non-small cell lung cancer
OS	overall survival
PBLs	peripheral blood lymphocytes
PD-1	programmed cell death protein 1
PD-L1	programmed cell death protein 1 ligand
PFS	progression-free survival
PVR	Poliovirus receptor
RCC	renal cell carcinoma
RFS	recurrence-free survival
RMST	restricted mean survival time
RORc	retinoic acid-related orphan receptor c
SHIP-1	SH2-containing inositol phosphatase-1
TAMs	tumor-associated macrophages
TANs	tumor-associated neutrophils
TCGA	The Cancer Genome Atlas
TIGIT	T-cell immunoreceptor with immunoglobulin and ITIM domain
TILs	tumor-infiltrating lymphocytes
TMB	tumor mutation burden
TME	tumor microenvironment
TNF	tumor necrosis factor
Tregs	regulatory T-cells
UCEC	uterine corpus endometrial carcinoma
VSIG9	V-set and immunoglobulin domain-containing protein 9
VSTM3	V-set and transmembrane domain-containing protein 3

frontiers | Frontiers in Oncology

REVIEW
published: 19 May 2022
doi: 10.3389/fonc.2022.871513

Targeting the Tumor Microenvironment: A Close Up of Tumor-Associated Macrophages and Neutrophils

Massimo Russo[1] *and Claudia Nastasi*[2*]

[1] *Laboratory of Cancer Metastasis Therapeutics, Department of Oncology, Mario Negri Pharmacological Research Institute (IRCCS), Milan, Italy,* [2] *Laboratory of Cancer Pharmacology, Department of Oncology, Mario Negri Pharmacological Research Institute (IRCCS), Milan, Italy*

The importance of the tumor microenvironment (TME) in dynamically regulating cancer progression and influencing the therapeutic outcome is widely accepted and appreciated. Several therapeutic strategies to modify or modulate the TME, like angiogenesis or immune checkpoint inhibitors, showed clinical efficacy and received approval from regulatory authorities. Within recent decades, new promising strategies targeting myeloid cells have been implemented in preclinical cancer models. The predominance of specific cell phenotypes in the TME has been attributed to pro- or anti-tumoral. Hence, their modulation can, in turn, alter the responses to standard-of-care treatments, making them more or less effective. Here, we summarize and discuss the current knowledge and the correlated challenges about the tumor-associated macrophages and neutrophils targeting strategies, current treatments, and future developments.

Keywords: tumor-microenvironment, macrophages, neutrophils, anti-cancer therapy, TAMs, TANs, cancer

OPEN ACCESS

Edited by:
Daniele Vergara,
University of Salento, Italy

Reviewed by:
Xiao Chen,
Wuhan University, China
Lisa Sevenich,
Georg Speyer Haus, Germany

****Correspondence:***
Claudia Nastasi
claudia.nastasi@marionegri.it

Specialty section:
This article was submitted to Molecular and Cellular Oncology, a section of the journal Frontiers in Oncology

Received: *08 February 2022*
Accepted: *11 April 2022*
Published: *19 May 2022*

Citation:
Russo M and Nastasi C (2022) Targeting the Tumor Microenvironment: A Close Up of Tumor-Associated Macrophages and Neutrophils. Front. Oncol. 12:871513. doi: 10.3389/fonc.2022.871513

1 INTRODUCTION

Cancer is a significant cause of death worldwide and does so through the ability of malignant cells to egress from the primary mass and spread to other parts of the body *via* a complex process known as metastasis. This latter can be seen as secondary cancer, as it can profoundly differ from the primary and progressively overwhelm organs leading to death.

Resistance to cancer treatment can be intrinsic to the tumor cells, but it is often conferred by non-malignant ones that make up the tumor microenvironment (TME). The importance of the TME stands within its capacity to dynamically regulate cancer progression and influence the response to treatment. For this reason, several therapies target different components of the TME, aiming to shatter at least one pillar of the palace.

The TME is considered a complex and rich multicellular environment where a tumor takes roots. It does not just include tumor cells but also many normal ones that can contribute both positively and negatively. Indeed, they can be modified by malignant cells and induced to synthesize growth factors, chemokines, matrix-degrading enzymes to enhance proliferation and invasion. They can also rearrange the stroma, avoiding the effective delivery of anti-cancer drugs, increasing interstitial fluid pressure, and changes in vascular flow (1, 2).

Many are the cell types involved: immune cells, such as dendritic cells (DCs), macrophages, T and B lymphocytes, natural killers (NKs), neutrophils, myeloid-derived suppressor cells (MDSC); stromal cells like pericytes, mesenchymal cells, cancer-associated fibroblasts (CAFs); the extracellular matrix (ECM) with many secreted molecules as cytokines, chemokines, growth factors; and the blood and lymphatic vascular networks, which are in communication with each other and the tumoral cells (**Figure 1A**).

In the light of knowledge, we understand the early days of the TME research field where therapeutics targeting each component were viewed with enormous interest (3); now, we are aware of the TME complexity, and those early perspectives were seen as overly optimistic.

Such complexity resides within several different aspects like the stage of cancer, the organ in which the tumor arises, the ontogeny of some cell populations, and their phenotype within the tumor mass and/or at the systemic level.

More recently, the knowledge of the functional role of myeloid cells (macrophages, neutrophils, MDSC) and their interactions with tumor cells has remarkably increased. The types and the relative abundance of tumor-infiltrating leukocytes define the immune landscape, and it has been shown to have prognostic value. As the increase of cytotoxic CD8+ T cells is positively correlated with survival and treatment response, the presence of myeloid cells, depending on their phenotype, could be either negative or positive (4–6). Several studies have highlighted the correlation of a specific subset of myeloid cells with more prolonged survival and better clinical responses, showing myeloid cells' heterogeneity in tumors.

The TME is well-recognized in regulating the response to therapeutic interventions conferring an intrinsic resistance or acquiring one.

High numbers of immunosuppressive cells, including tumor-associated macrophages (TAMs) and regulatory T cells (Treg), and the presence of protective niches that shield a subset of tumor cells from therapeutic effects, additionally contribute to intrinsic resistance (7–9). Few studies have revealed the pleiotropic adaptive effects on TME composition and phenotypes following different therapeutic interventions, including standard-of-care treatments and TME-directed therapies (7). These alterations lead to massive therapy-induced cell death and the correlated accumulation of immune cells, which phenotypes could be specific to the therapeutic intervention.

Both radiotherapy and chemotherapies can increase the presence of immunosuppressive TAMs in tumors, protecting the cancer cells from therapy-induced cell death, which may ultimately lead to tumor recurrence (10–13). For example, chemotherapy may also induce DNA damage in stromal cells, resulting in the activation of NF-κB contributing to therapeutic resistance (14), and radiotherapy may affect the tumor vasculature promoting cancer cell survival and radio-resistance (15); as well, specific therapies can show a synergistic effect by promoting immunogenic cell death and enhancing T cell-dependent anti-tumor immunity (16, 17).

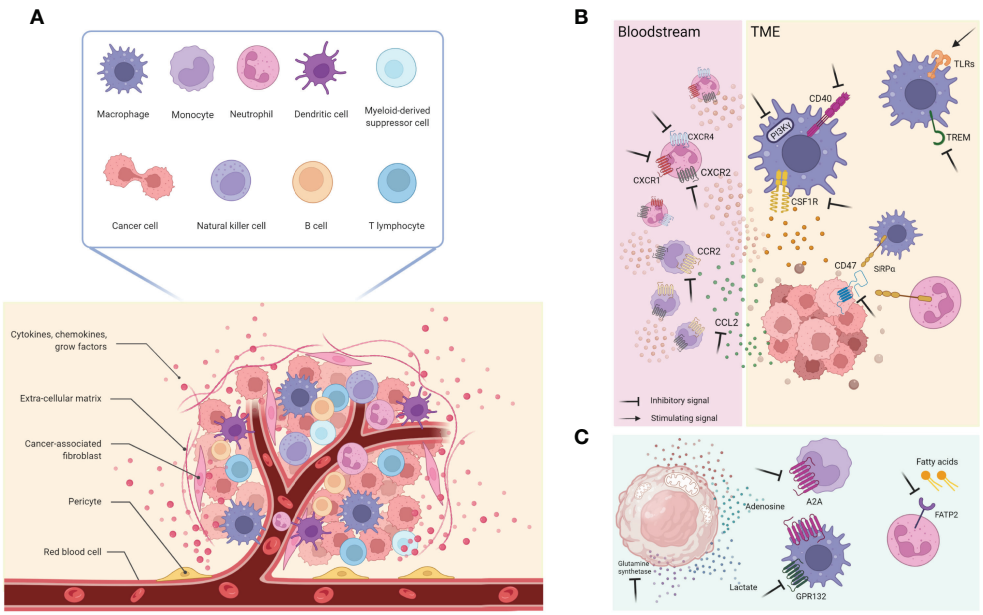

FIGURE 1 | **(A)** The TME is composed by several diverse cell types including cancer cells, immune cells (such as T and B lymphocytes, macrophages, DCs, NK cells, MDSCs, neutrophils), and stromal cells (like pericytes, mesenchymal stromal cells, fibroblasts); this architecture is also supported by the extracellular matrix and its proteins, as well as growth factors and cytokines produced by all the cellular component that, in turn, influence the TME. Together with them, blood and lymphatic vascular networks allow exchanges and nutritional supply. **(B)** General overview of cellular and molecular targets currently used and on development. **(C)** New relevant targets involving cancer cells metabolites and receptors expressed by immune cells. This figure was made with Biorender.

Given the importance of the TME in tumor progression and the efficacy of cancer treatment, in recent years, the TME has been taken as a central focus for new therapeutic strategies. These approaches mainly target TAMs, neutrophils, DCs, T cells, tumor vasculature, ECM, and CAFs. This review will focus on the myeloid cell neutrophils and macrophages, their controversial role in TME, and the clinically relevant therapeutics that are currently in use or underway.

2 MYELOID CELLS IN TUMORS

Since Rudolf Virchow recognized the immune system as an essential regulator of tumor growth, describing extensive accumulations of white cells within tumors (18), the presence of myeloid cells within the TME has raised substantial interest. Our comprehension of myeloid cells' functionality and their interaction with tumor cells has given us an epiphany in the last decades.

Great endeavours to boost T cell-directed anti-cancer immune responses have been made to date. As reported, the incidence of cancerogenesis is low in invertebrates with no T or B cells, indicating that innate immune cells are of great importance for preventing the initiation and development of cancer (19, 20).

Since the study of the TME immunophenotype had been introduced and often paired with classical oncology screenings, pathologists and oncologists had to realize the predictive value of the immune landscape based on the evidence that specific cell types are associated with distinct disease outcomes in patients. Consequently, several immune-oncology strategies have been developed to reactivate the adaptive and innate immune systems to mount a proper immune response as an alternative approach to classical anti-cancer treatments.

The opening of new clinical trials using immune checkpoint inhibitors (ICIs) (such as monoclonal antibodies (mAbs) against cytotoxic T lymphocyte antigen 4 (CTLA4), programmed cell death 1 (PD1), and PD1 ligand (PDL1), have shown complete success only on a small fraction of patients with melanoma and lung cancers, and possible reasons are still unknown (21).

In preclinical studies, TMAs can promote the recovery of tumors despite chemotherapies, radiotherapies, or biologic therapies due to the promotion of angiogenesis, maintenance of cancer stem cells, and inhibition of immune responses (22, 23). In some tumors, macrophage infiltration also interferes with the efficacy of immunotherapy, neutralizing efforts to reactivate CD8+ T cells. For this reason, several therapeutic strategies to modulate TAM function, infiltration, or activation are emerging to block resistance to conventional therapies and promote T cell-based therapies (4, 22, 24).

In parallel, recent findings studying neutrophils in cancer have opened a debate about their involvement in tumor formation, progression, and dissemination, showing a dichotomy of their role. Moreover, the importance of neutrophil recruitment in tumoral tissues was assessed on human cancer samples. It was associated with a more aggressive disease characterized by inadequate treatment response, tumor relapse, and bad prognosis (25).

3 NEUTROPHILS

3.1 About Neutrophils

Neutrophils are bone marrow (BM) granulocytic-myeloid cells and comprise 50-70% in humans and 10-30% in mice of circulating white blood cells, making the granulocytic population the first most abundant in humans and the second one in mice (B cells precede them) (26, 27). Historically, neutrophils are short-lived leukocytes that last about one day in the circulation and then cleared away by macrophages or dendritic cells in the liver, spleen, and BM (28). The granulocyte-colony stimulating factor (G-CSF) stimulates the proliferation and differentiation of neutrophil precursors into the BM and augments the mobilization of terminally differentiated neutrophils into the bloodstream (29). In fact, it regulates granulopoiesis, the *de novo* generation of neutrophils, both at the steady-state and at emergency. The latter occurs when an inflammatory stimuli (i.e. microbial infections or cancer) becomes systemic and considerably enhances the generation and the release of immature and mature neutrophils from the BM into the peripheral blood (30, 31). Alternatively, stress conditions (i.e. extensive blood loss, cancer, BM dysfunction) induce the extramedullary emergency hematopoiesis in the spleen that produces myeloid cells, monocytes, and neutrophils (32). Neutrophils developmental stages relate to their systemic trafficking. It is possible to distinguish fully mature neutrophils from pre-neutrophils and immature neutrophils using the expression of the CXC-chemokine receptor 2 (CXCR2) found only on the surface of fully differentiated neutrophils (29, 33). CXCR2 mediates signaling required for neutrophil mobilization into the peripheral blood by interacting with the IL-8 [a.k.a. Neutrophil chemotactic factor or CXC-chemokine ligand 8 (CXCL8)]. IL-8, released by endothelial cells and stromal cells of the basement membrane, acts as a chemoattractant to recruit circulating neutrophils to the site of inflammation and is required to mediate the rolling of neutrophils along the endothelium (34). Conversely to CXCR2, the CXC-chemokine receptor 4 (CXCR4) is expressed on immature neutrophils (both proliferating and mitotically inactive), where it mediates the signaling required for neutrophils retention into the BM compartment (29).

The Ly6G (Lymphocyte antigen 6G) is the key marker of neutrophils, but it is not only present on fully mature and mitotically inactive neutrophils, but also on precursors, as recently proved by 10X technology (35). Hence, it should not be considered to discriminate between immature and mature neutrophils. The distinction between those ones further relies on the gene signature level; for example, the Gata1 gene is more expressed by BM mature neutrophils than in their precursors; on the contrary, the Gata2 gene is highly expressed in premature rather than mature neutrophils (35). Nowadays, transcriptomic advances and multiparametric flow cytometry analyses revealed the presence of several neutrophil subsets both in mice and humans. The pre-neutrophil (preNeu), a committed proliferative precursor, differentiates into mitotically inactive immature (immNeu) and mature neutrophils (31). Analogously, the presence of an early neutrophil progenitor (NeP) in mouse BM

and a similar unipotent NeP in human BM (hNeP) were identified using cytometry by time of flight (CyTOF). NeP was further classified into two clusters, C1 and C2 (based on Ly6G marker), giving rise exclusively to neutrophils (35). These findings have been very recently confirmed, exploiting single-cell RNA sequencing (RNAseq), partitioned differentiating and mature subtypes of neutrophils into eight clusters (G0-G4, G5a-G5c) (33). Neutrophils are the first responders to danger signals (sterile insults or microbial infections) and are among the first mediators of inflammatory reactions. Their fast migration is mediated by danger-associated molecular patterns (DAMPs), pathogen-associated molecular patterns (PAMPs), and the activation of the Toll-like receptors (TLRs). At the injury site, they can release the content of their cytoplasmic granules or exert their protective roles by the respiratory burst producing reactive oxygen species (ROS), extruding the Neutrophil Extracellular Traps (NETs) (36), or by acting as antigen-presenting cells (APC) (37, 38).

3.2 The Controversial Role of Neutrophils in Cancer

Nowadays, the knowledge about neutrophils is constantly expanding. These cells are not only circulating grenades but also mixed populations capable of adapting and specializing in micro-environmental cues (39); thus, they exert both pro and anti-cancer activities. Notably, tumor-associated neutrophils, both primaries or secondaries, are usually referred to as TANs, even though this terminology does not relate to a specific differentiation step and activation status (40). Pertinent to metastases, the role of neutrophils is quite confounding and closely resembles the case of primary cancers. Neutrophils have been described to elicit both metastasis-promoting and -suppressing capacities, depending on the cancer type, staging, and micro-environmental signals or cancer cell-intrinsic causes. Different findings suggest their direct or indirect involvement in mediating an anti-cancer immune response early during carcinogenesis. In preclinical models, neutrophils were shown to delay primary tumor growth by releasing nitric oxide (NO) that induces cancer cell killing. The binding of the receptor tyrosine kinase MET, expressed on neutrophils, by the tumor necrosis factor-alpha (TNFα), and its ligand, the Hepatocyte growth factor (HGF), drives the nitric oxide synthase (NOS) and the consequent release of the anti-tumor inflammatory mediator (41). The neutrophil elastase (ELANE) is another extracellular protein released by human polymorphonuclear cells that can directly kill cancer cells. While human neutrophils release a catalytically active ELANE, instead murine neutrophils do not and hence fail to kill cancer cells, both *in vivo* and *in vitro* (42). A study, carried out with a mouse model spontaneously developing epithelial carcinogenesis due to the functional loss of the tumor suppressor phosphatase and tensin homolog (PTEN), neutrophils were shown to exert an inhibitory role in developing endometrial adenocarcinoma by inducing the detachment of tumor cells from the basement membrane (43), implying that PMNs can fight autochthonous tumorigenesis.

The involvement of the chemokine receptor CXCR2 in skin and intestine tumors development has been assessed when its deficiency or depletion (on $Ly6G^+$ cells) suppressed colitis-associated tumorigenesis and the formation of intestine adenomas (44). Nonetheless, the lack of a mouse model with neutrophil knockout for CXCR2 made the findings controversial. However, mouse models with selective deletion of CXCR2 in neutrophils could be generated by crossing MRP8Cre, and Cxcr2fl/fl mice (45).

PMNs are part of immune cell networks that suppress tumor formation and growth by activating T cell-mediated anti-tumor responses. During the early phase of the development of a murine sarcoma induced by 3-methylcholanthrene, neutrophils amplified the production of IL12 by macrophages, which in turn drove the release of the interferon-gamma (IFNγ) by a subset of unconventional T cells, establishing an anti-tumor immunity that led to a reduced incidence of sarcoma (46). In early-stage human lung cancer, immature neutrophils, influenced by the low concentration of INF-γ and GM-CSF in the TME, differentiated into hybrid TANs with an APC phenotype, cross-presenting tumor antigens to T cells, in turn stimulating their response and unleashing their anti-tumor action (47).

Earlier it was shown that granulocytes are equipped with anti-metastatic functions. In fact, in mice orthotopically transplanted with murine breast cancer cells 4T1, was demonstrated that tumor cells recruited neutrophils, *via* CC-motif chemokine ligand 2 (CCL2), into the pre-metastatic lungs; once arrived, neutrophils produced hydrogen peroxide (H_2O_2) that prevented the seeding of disseminated tumor cells (48). Another line of evidence reported that in human renal cancer, neutrophils were actively recruited to the metastasis sites, thanks to tumor-derived IL8 and CXCL5, exerting an anti-metastatic action (49). In these studies, neutrophils were recruited and instructed to dampen metastasis formation by a tumor-released soluble signal representing an example of tumor entrained neutrophils (TEN). Furthermore, another study revealed that MET is required for neutrophil chemo-attraction and cytotoxicity in response to HGF. Consequently, the release of HGF/MET-dependent NO by neutrophils promotes cancer cell killing, abating metastasis formation, and corresponding primary tumor growth (in several cancer models) (41).

As well, the genetic inactivation of the atypical chemokine receptors 2 (ACKR2), a scavenger for inflammatory chemokines and hence a negative regulator of inflammation (expressed in hematopoietic precursors), resulted in the release from the BM neutrophils showing higher anti-metastatic activity in mice orthotopically transplanted with 4T1 mammary carcinoma or intravenously injected with B16F10 melanoma (50).

Conversely, others demonstrated the involvement of neutrophils in the tumor formation or the growth of established primary tumors. Neutrophils might support tumor formation, incidence, and growth by exploiting several mechanisms, including the promotion of a chronic inflammatory state which was extensively studied and reviewed by others (25, 40, 51), inducing DNA damage and genome instability (52) or inducing the proangiogenic switch (53).

In the context of chemically induced tumorigenesis, PMNs amplify the DNA damage caused by urethane, a component of

cigarette smoke, in murine lungs, stimulating cancer initiation (54). Similarly, the release of ROS by neutrophils was shown to trigger oxidative DNA damage mutations causative of intestinal tumorigenesis and consequent cancer growth (55).

Neo-angiogenesis is the sprouting and growth of blood vessels into a tumor mass promoted by tumor cells and secreted growth factors and cytokines, useful for the oxygen and nutrients supply required for tumor growth (56). Primary mediators of cancer-induced neo-angiogenesis are the vascular endothelial growth factors (VEGFs) that include VEGF-A, VEGF-B, VEGF-C, VEGF-D, and placental growth factor (PLGF) and their respective receptors, the vascular endothelial growth factor receptors (VEGFRs) and the neuropilin (NRPs). Neutrophils are a reservoir of pre-formed VEGF, although they are not the principal producers of the growth factor as in the case of macrophages (57). Still, neutrophils release VEGF and other angiogenic factors such as the protein Bombina variegate peptide 8/Prokinecitin 2 (Bv8/PROK2), contributing to alternative pathways leading to new blood vessels formation (58, 59). On the contrary, neutrophils are the primary source of metalloproteinase-9 (MMP-9), which degrades the ECM and forces mesenchymal cells to release VEGF-A and other proangiogenic molecules such as the fibroblast growth factor (FGF) (60).

Another mechanisms has revealed that neutrophils, by IL1-β and matrix MMP, inhibit NK cells cytotoxicity and the disseminated tumor cells (DTCs) extravasation into the target organ, promoting their survival (61). As proof, in immunocompetent or NOD-*scid* mice, bearing E0071 breast carcinoma, neutrophils showed metastasis supporting activity *via* NK suppression, while in NSG mice (lacking of NKs), they reduced metastasis (62).

Additionally, neutrophils secrete pro-inflammatory factors (i.e., lipids and cysteinyl leukotrienes) able to favor metastatic initiating cells MICs, leading to increased metastatic competence of breast cancer cells like 4T1 (63).

It was also reported that IL-17, secreted by γδ-T cells, induces neutrophil accumulation in the lungs which, in turn, suppresses cytotoxic T cells functions, increasing pulmonary and lymph node metastasization in the KEP mouse model of spontaneous breast cancer metastasis (64). Here neutrophil depletion caused a reduction of pulmonary metastasis formation.

Interestingly, in the bloodstream has been reported an interaction between circulating tumor cells (CTCs) and white blood cells, predominantly with neutrophils. This connection seems to drive CTC cycle progression and the induction of CTCs metastatic potential (65). Such peculiar interaction could be seen a potential new target for targeting for treatment of metastatic breast cancer.

Proteomic approaches elucidated the TANs secretome, identifying transferrin as the major mitogen for tumor cells. Depletion of neutrophils inhibited lung metastasis and transferrin production in the metastatic microenvironment, while deletion of transferrin receptors suppressed the growth of lung-colonizing tumor cells (66). By these findings, preclinical models of tumors different from the mammary ones [like lung (67) and colorectal cancer (68)] produce neutrophils that support metastasis. Furthermore, others reported a pathological Notch signaling involvement in colorectal cancer cells that initiates a neutrophil-dependent, and tumor-necrosis factor (TGF)- β mediated signaling cascade leading to the appearance of metastatic disease (68).

Nonetheless, different other stimuli affect PMN cells, modulating their role in metastasis. For example, the loss of testosterone in castrated male mice impaired neutrophils' maturation and functions, thereby making them pro-metastatic in two preclinical models, while testosterone replacement restored their cytotoxic functions. These results were also observed in patients with prostate cancer undergoing androgen deprivation treatments (69).

Besides being a potent anti-tumor protein, ELASTASE is also one of the primary markers used to detect NETosis (NETs formation). NETs are extracellular, web-like structures composed of decondensed nuclear and mitochondrial DNA intertwined with cytotoxic enzymes, such as neutrophil elastase (NE) and myeloperoxidase (MPO), that usually are retained into neutrophil granules and used to neutralize pathogens like bacteria, fungi, viruses, and parasites (70). NETs formation is a mechanism that cancer cells adapt to hijack neutrophils to awake disseminated dormant cancer cells (71) or to enhance the establishment of metastases in triple-negative breast cancer murine models (72). Such a link is not only confined to hematogenous metastases but was also observed in a preclinical model of ovarian cancer, where the metastatic dissemination occurs through a transcelomatic process. By the way, it seems that the neutrophils influx into the omentum is a prerequisite for a successful metastatic dissemination. In detail, ovarian tumor-derived inflammatory factors stimulate neutrophils to NET which, in turn, binds ovarian cancer cells and promotes metastasis. In fact, omental metastasis is decreased in mice with neutrophil-specific deficiency of peptidyl-arginine deiminase 4 (PAD4), an essential enzyme for NET formation (73). Similarly, neutrophils have been shown to induce hepatocellular carcinoma (HCC) metastasis by releasing NETs that, once internalized by HCC cells, activate the TLR4 and subsequently induce cell-death resistance and enhanced invasiveness (74).

3.3 Neutrophils Interference With Anti-Cancer Therapies

Given the extensive and growing body of evidences related to the involvement of neutrophils in the formation and progression of cancer, it is relevant to understand whether they might affect anti-cancer treatments.

Immunotherapy is the latest breakthrough in anti-tumor therapy and is used to make the immune system reactive against cancers taking advantage of the blockade of immune checkpoints. In the context of cancer, immunosuppressive determinants present in the TME downregulate the immune cells' reactivity, making them exhausted or polarised toward a pro-tumor profile (75).

Antibodies against a different number of ICIs that support the expansion of type-I helper $CD4^+$ T lymphocytes and prevent the exhaustion of $CD8^+$ T cells have reached the clinic (76). Unfortunately, not all patients respond to ICIs, possibly owing to intrinsic resistance, but many usually develop acquired resistance (77).

In this context, neutrophils or, more specifically, TANs are considered contributors to the resistance to ICIs. In hot tumors (highly infiltrated with T lymphocytes), the ICIs are usually effective unless the TME is enriched with TANs, suggesting a granulocytic immunosuppressive role (78). The neutrophil pathological activation by the microenvironmental stimuli exerts detrimental effects on T cells and thus mediates the resistance to ICIs. Different neutrophil mediators are able to induce T cells exhaustion, including arginase 1, prostaglandin E2, ROS, and NO, as recently reviewed elsewhere (79).

A therapeutic strategy to restore the sensitivity to ICIs is to dampen neutrophils recruitment in the TME, hence avoiding their hijacking (80). The receptors CXCR2 and CXCR4 are central regulators of neutrophil trafficking and recruitment in tumors. In fact, the inhibition of CXCR2 in a murine model of a soft tissue sarcoma resistant to anti-PD1 treatment restored the effectiveness of the immunotherapy (81). It was also reported that the treatment with a small-molecule inhibitor of CXCR2 and CXCR1, SX-682 (SX), sensitized tumor-bearing mice to the anti-PD1 antibody. The inhibitor had no anti-tumor effect in monotherapy and was ineffective on cancer cells, independently of their positivity for CXCR1 and CXCR2 (82). These preclinical findings provided a rationale for a clinical translation, thus that ongoing clinical trials are evaluating the effectiveness of combining CXCR2 inhibitors with ICIs. SX is currently being investigated in combination with pembrolizumab and with nivolumab (both targeting PD1) for the treatment, respectively, of metastatic melanoma [NCT03161431 (83)] and metastatic pancreatic ductal adenocarcinoma [PDAC; NCT04477343 (84)]) and unresectable or metastatic colorectal cancer [NCT04599140 (85)].

Like CXCR2 inhibition, targeting CXCR4 represents a different strategy to reduce tumor recruitment and neutrophil mobilization from the BM. Accordingly, treatment with AMD3100 (plerixafor, Mozobil), a small-molecule inhibitor of CXCR4, promotes an enhanced intratumoral immune B and T cell responses in metastatic lesions in patients with microsatellite stable (MSS) colorectal cancer (CRC) or pancreatic ductal adenocarcinoma (PDA), that usually are ICIs resistant (86). Concomitantly, the clinical trial NCT02907099 (87) is studying the inhibitor of CXCR4, BL-8040, in patients with metastatic PDAC.

Pulmonary endothelial cells express CXCL12 constitutively. Treatments with AMD3100 was shown to cause neutrophilia (neutrophils in the bloodstream), decrease of neutrophils in the BM, and induce neutrophil distribution in the lungs without compromising their trafficking to inflamed sites (88). Conversely, the release of neutrophils from lungs into the bloodstream was previously observed during the treatment with AMD3100 (89). When considering the inhibition of CXCR4 in lung cancer, it needs to be considered the immunosuppressive neutrophil recruitment in the metastatic lesion and hence reduced response to ICIs.

Considering that neutrophils recruited into the tumor may acquire a tumor-supporting phenotype, the inhibition of their recruitment could be associated to the modulation of their phenotype. To this aim, a preclinical trial, on mice bearing the allografts 4T1 and LLC or transplanted with the triple-negative breast cancer line MDA-MB-231, showed that the CXCR2-inhibitor SX in combination with BinTrafusp Alpha, that simultaneously blocks PD-L1 and traps soluble TGF-β, polarize neutrophils (90, 91). SX-682 and BinTrafusp Alpha are being tested in co-administration in phase I/II trials on solid metastatic cancers (NCT04574583) (92).

A possible therapeutic strategy to induce anti-tumor neutrophils in cancer and potentiate ICIs is to potentiate the appearance of anti-tumor neutrophils, like with INF-γ. It was shown that early treatment with anti-PD1 Ab induced tumor shrinkage in mouse models of pancreatic cancer. On the contrary, delayed anti-PD1 treatment showed limited benefits associated with $CXCR2^+$ myeloid cell recruitment in response to tumor secreted CXCL8. The administration of INF-γ inhibited the tumor trafficking of $CXCR2^+$ cells, suppressing the release of tumor-derived CXCL8, ultimately enhancing anti-PD1 efficacy (93). This combination is currently investigated in a clinical trial for advanced solid tumors [NCT02614456 (94)];, which results have not been deposited yet. A general representation of cellular and molecular targets are visualized in **Figure 1B**.

Angiogenesis Inhibitors (AIs) block the formation of new blood vessels into the tumor and have been investigated in monotherapy for renal cancer and, more often, in combination with conventional chemotherapy. The VEGF/VEGFR, the angiopoietins (ANGPT) and their tyrosine kinase receptors (Tie2/Tek), or molecules mediating tumor angiogenesis, like the fibroblast growth factor (bFGF/FGF2) and platelet-derived growth factor-B (PDGF-B), have been the main targets. The humanized anti-VEGF monoclonal Ab bevacizumab, the VEGF-Trap protein aflibercept, and small molecules inhibitors of VEGF-receptors (i.e. sunitinib, sorafenib, pazopanib, and cediranib) represent examples of currently US Food and Drug Administration (FDA)-approved antiangiogenic drugs (56). The use of AIs was promising in preclinical studies but not effective in the clinical setting.

To this extent, neutrophils have been observed to sustain the resistance to therapy by generating of alternative vascularisation mechanisms. For example, tumor-infiltrating neutrophils produced the Bv8/PROK2 protein, which caused the refractoriness to anti-VEGF therapy in tumor allograft and xenograft models (95). The same was observed in a genetically engineered mouse model (GEMM), spontaneously developing colorectal cancer (CRC), and in mice bearing the colon cancer cells CT26 and Colon38. In these models, therapy resistance occurred only upon the induction of an inflammatory state by chemically-induced colitis, which caused the augmentation of the G-CSF serum levels in mice, followed by the recruitment of neutrophils into the tumor stroma and the release of Bv8/PROK2, promoting angiogenesis. Treatment with anti-GCSF

or anti- Bv8/PROK2 rescued the anti-VEGF tumor sensitivity (96). These findings indicate that the tumor responses to AI may rely on the degree of inflammation of tumor tissues.

Another study correlated the degree of neutrophils infiltrated into the metastasis with the bevacizumab treatment refractoriness and the decreased overall survival (OS), both in xenograft and syngeneic tumor models. Furthermore, the depletion of neutrophils or the use with BI-880, which targeted a different angiogenic pathway (the Tie2/Tek axis), restored the sensitivity to anti-angiogenic treatment (97). Additionally, in a preclinical model of glioblastoma, neutrophils were again found to support anti-VEGF therapy resistance in mice (98).

In contrast with these preclinical findings, the high absolute neutrophils count and high neutrophils to lymphocyte ratio (NLR) have been considered prognostic factors for antiangiogenic treatment efficacy and favorable prognosis in CRC patients, respectively (99, 100). However, the opposite is also supported in other studies (101).

Neutrophils might also indirectly promote resistance to antiangiogenic therapy and hence tumor progression. It was highlighted that TANs, but not circulating neutrophils, *via* the production of CCL2 and CCL17 and the recruitment of monocytes and Treg cells, were the cause of the refractoriness to sorafenib, the first line treatment for hepatocellular carcinomas (HCC) (102, 103). These studies do not elucidate or demonstrate whether neutrophils or the pathologically activated PMN-MDSCs were the one responsible for the acquisition of such resistance. It would be of great interest to investigate the characteristics of the neutrophil population in cancer patients undergoing anti-cancer treatments by the newly available molecular biology techniques such as RNAseq to verify each specific subset's contribution to therapy response.

Despite novel therapies, conventional cytotoxic-based chemotherapy remains the cornerstone in cancer treatment. Consequently, in preclinical and clinical trials, the effectiveness of new agents is frequently investigated with conventional chemotherapy. Neutrophils have emerged as contributors to cancer progression, reducing tumor responsiveness to the chemotherapy rather than mediating resistance. Therefore, chemotherapy might delay tumor growth, failing to induce its shrinkage. Thus, the rationale behind the co-administration of chemotherapy and immunomodulators acting on neutrophils is again to reduce their recruitment in the tumor and a likely pro-tumor polarization or convert immunosuppressive neutrophils (PMN-MDSCs) toward an anti-tumor phenotype. For example, one preclinical evidence highlighted the effectiveness of combining cisplatin, a widely known chemotherapeutic drug, with the inhibition of CXCR2 axis (104); the authors showed that the agent SB225002, that selectively inhibits CXCR2, enhanced the therapeutic effect of cisplatin in lung cancer mice models, which was associated with a significant reduction of neutrophil infiltration and enhanced CD8+ T cell anti-tumor. Supporting the benefits of combinatorial treatment, in preclinical models of PDAC, it has been tested FOLFIRINOX (composed of oxaliplatin, irinotecan, 5-FU, and leucovorin) with the small molecule PF-04136309, a CCR2 inhibitor for limiting the recruitment of monocytes-macrophages (105). This combination resulted in compensatory recruitment into the tumor of neutrophil populations highly expressing CXCR2. The combined CCR2 plus CXCR2 blockade enhanced the chemotherapeutic efficacy and improved the survival of tumor-bearing mice. Moreover, inhibiting the CXCR2 axis with the molecule SB 225002 in combination with paclitaxel retarded the growth of Lewis Lung Carcinoma (LLC) bearing mice (106). These findings are very recent, and currently, no clinical trials are using CXCR2 inhibitors with chemotherapy.

Conversely, agents exerting an immunomodulatory effect, like INF-γ, upon neutrophils have been explored. Several clinical trials are still recruiting to investigate the benefits of adding INF-γ to chemotherapy, principally phase I/II trials where the main objective is to determine the best-tolerated dose. Given the low number of patients recruited, the estimation of response parameters is considered secondary outcomes.

Patients undergoing chemotherapy frequently develop neutropenia when the absolute neutrophil count (ANC) drops below 2 $X10^9$/L. The Grade 4 neutropenia (<0.5 $X10^9$/L) represents a life-threatening event requiring patient hospitalization, treatments with antibiotics (to avoid the risk of spreading infections), and chemotherapy discontinuation, possibly favoring tumor relapse. The drop in the ANC that occurs during neutropenia usually persists for 2-3 weeks, possibly leading to a reduced abundance of neutrophils within the tumor bulk, making their targeting not feasible. The hematopoietic grow factor G-CSF (Filgrastim) is an FDA-approved drug for patients with non-myeloid malignancies, used to reduce the time for neutrophil recovery and to decrease the incidence of infections. The Granulocyte macrophage-colony Stimulating Factor (GM-CSF or Molgrastim) might represent another hematopoietic growth factor used as an immune-stimulant agent to treat neutropenic patients. A clinical trial shows that Molgrastin induced a faster neutrophil recovery and reduced hospitalization but the drug worked in a limited number of patients compared to Filgrastim, thus it is considered less effective than G-CSF. In another trial conducted on non-small-cell-lung-cancer patients, the GM-CSF was ineffective.

Alternatively, it could be hypothesized that neutrophils could be targeted based on the administered chemotherapy, since each treatment differentially affects neutrophils (e.g., cyclophosphamide and doxorubicin are drugs more myelotoxic than 5-fluorouracil or methotrexate) (107).

Chemotherapy-induced neutropenia may be considered *per se* an approach to target neutrophils by depleting their precursors in the BM. Intriguingly, neutropenia is associated with drug effectiveness and better overall survival (108), although it may cause therapy discontinuation or delayed treatment cycles. However, it is still unknown if chemotherapy-induced neutropenia and the reported outcome improvements are linked or unrelated events, and prospective trials designed *ad hoc* to evaluate this association is still lacking.

3.4 Current Strategies to Target Tumor-Associated Neutrophils

The above-mentioned strategies aim to increase the effectiveness and efficacy of the current standard of care treatments. Still, they do not represent *per se* a strategy that exploits the neutrophils' anti-cancer killing machinery, as in the case of autologous and heterologous T-cell-based therapies recognizing specific tumor antigens and mediating a direct cancer cell killing (109). Even if neutrophils are ontogenically endowed with anti-cancer properties, a tumor-promoting phenotype is more frequently observed and defined as a tumor-induced conversion subset referred to as G-MDSC. In light of this, it would be clinically relevant to find a druggable target that favor neutrophil reprogramming toward their naturally occurring anti-tumor phenotype. To this regard, the fatty acid transport protein 2 (FATP2) was recently identified as a regulator of the suppressive capacities of G-MDSCs; it is a neutrophil membrane protein implicated in the trafficking of lipids and it is overexpressed by G-MDSCs in tumor-bearing mice compared to "classical" neutrophil isolated in healthy mice. The pharmacological inhibition of FATP2 by lipofermata resulted in a delay in tumor growth of mice bearing different and etiologically unrelated tumors (namely: LLC and EL4), without affecting the proliferation of the same tumors cultured *in vitro* (**Figure 1C**). It should be noted that the *in vivo* anti-tumor effect was lost when mice were treated with lipofermata and an anti-CD8 depleting antibody or when the therapy was administered in immunodeficient (NOD/SCID) non-obese diabetic–severe mice, indicating that the anti-tumor effect is anyway mediated by T cells rather than neutrophils (110). Of note, this finding highlighted the role of the immune cells' metabolism and the influence on their polarization.

Neutrophils often share signaling cascades and extracellular receptors with other myeloid cells, such as monocytes. Using a strategy not explicitly tailored towards neutrophils might paradoxically exert detrimental effects on other myeloid cells. Hence, a more profound comprehension of neutrophils' intricate roles in tumor progression might provide new ideas for new therapeutic approaches. Despite this scary scenario, the innate immune checkpoint SIRPα/CD47, a negative regulator of myeloid cell phagocytosis, is a druggable axis which impairment showed efficacy at the preclinical levels, even though it is not a neutrophil specific target but rather a complex shared with monocyte and macrophages. For example, breast tumor-bearing mice benefitted from the combinatorial treatment with the mAb trastuzumab directed against the human epidermal receptor 2 (HER2) and the blockade of the SIRPα/CD47 checkpoint interaction that increased the killing activity of neutrophils towards antibody-opsonized cancer cells and led to tumor shrinkage caused by the antibody-dependent cell cytotoxicity (ADCC) (111) (**Figure 1C**).

As already described, several reports showed the opposite effect of neutrophils in different steps of tumor progression. Contrasting effects on metastasis formation were observed depending on the type of studied tumor. For example, after neutrophils depletion (anti-Ly6G mediated), a drastic reduction of secondary tumors (49) and a critical increment of metastatic deposits (63) were reported in Renca and 4T1 breast cancer bearing mice, respectively. This observation supports the notion of a cancer-induced alteration of the neutrophil functions. More interestingly, it suggests that comparing differences and analogies between different cancers, achieved *via* omics-based methods, might reveal new pathways involved in the pathological activation of neutrophils.

4 MACROPHAGES

4.1 About Macrophages

Macrophages, a type of white blood cell deriving from a myeloid progenitor, play essential roles in maintaining tissue homeostasis and protecting our body through several functions, such as engulfing and digesting foreign substances. Macrophages also clear away harmful matter, including cellular debris and tumor cells *in vivo*, maintaining homeostasis and limiting the entrance of pathogens (112–114).

These cells are classically categorized in the innate compartment of the immune system since they mediate a non-specific response and help initiate a specific defense mechanism, typical of adaptive immunity. In addition to stimulating the immune system, macrophages exert an immune-modulatory impact by secreting various cytokines and activating the complement system, leading to inflammation.

Depending on the microenvironment, chemokines, cytokines, and other stimuli (local anoxia, lactic acid), these cells can shape their phenotype. This led to the pragmatic description 15 years ago of two divergent forms of macrophage activation, such as M1 with immunostimulatory and anti-tumoral activity, and M2, immunosuppressive, both linked to the arms of the adaptive immune system with which they interact (T helper cells). This fundamental dichotomy has essentially formed the basis of research into macrophage activity ever since (115). Evidence indicates that macrophage phenotypes may be more appropriately described as a continuum of functional states that are signal-dependent and plastic (116), making it even more complex to classify cancers based on TME myeloid composition.

Macrophages have long been hypothesized to originate from cells of the blood compartment, deriving from hematopoietic BM precursors that would be attracted and recruited at peripheral tissues upon inflammatory conditions or tissue damage (112–114).

The understanding of macrophages ontogeny has recently undergone a profound transformation thanks to modern lineage tracing techniques. The main notable discovery is that most tissue-resident macrophages are not derived from BM progenitors, as previously thought, but instead from the yolk sac or fetal liver (117, 118). In adults, some tissue-specific macrophages exclusively derive from one source (for instance those in the intestine derive from BM). In comparison, in other tissues (i.e. the skin), different batches of macrophages derive from one source or another. Within the brain, ontogenetically distinct macrophage populations exist, including both tissue-

resident microglia and BMDMs (119). The first develops from embryonic yolk sac progenitor cells and are not replenished postnatally through peripheral mononuclear haematopoiesis (120). Also, non-parenchymal macrophages within the CNS arise during embryonic development, and are largely stable populations during adult life (121). By contrast, in response to perturbations of tissue homeostasis or pathological conditions, circulating monocytes are recruited to the brain parenchyma and give rise to BMDMs through monocytosis, particularly during tumor progression where the integrity of the blood-brain-barrier (BBB) is compromised (122).

Furthermore, the yolk sac-derived macrophages of the heart are replaced by fetal liver monocytes (118, 123). The presence of persistent embryonic populations throughout life in most tissues suggests that these tissues harbor pre-macrophages (pMACs) that can proliferate to give rise to mature macrophages (123).

Decades of shreds of evidence support that the environmental niche strongly influences macrophage gene expression and function, yet these cells remain plastic and retain the capacity to alter their phenotypes in response to new signals and situations. Phenotype is ultimately a flexible translation of multilevel cell-intrinsic and environmental signals.

Like healthy tissues, tumors also contain diverse populations of signal-responsive macrophages. Local mediators and conditions may significantly influence macrophage polarization in the tumor context as tumors have an evolving and chronic pathology that may involve dynamic environmental stresses such as hypoxia (124). Circulating precursors that are recruited into tumor tissues and subsequently differentiate into TAMs include conventional inflammatory monocytes and monocyte-related myeloid-derived suppressor cells (M–MDSCs). This latter can differentiate into mature TAMs when the signal transducer and activator of transcription 3 (STAT3) are downregulated (125); additionally, M-MDSCs contribute to the immunosuppressive tumor microenvironment, promoting tumor metastasis (126).

Of note, TAM proliferation has been observed in mouse models of sarcoma and mouse and human breast carcinomas, but this general mechanism does not seem to sustain the numbers of TAMs in growing tumors, suggesting that recruitment of circulating cells is required to maintain the TAM population (127, 128).

In a tumor setting, M1-like macrophages are currently thought to promote anti-tumor immunity, whereas M2-like TAMs stimulate angiogenesis and tissue repair (127) and suppress cytotoxic T cell function indirectly promoting tumor progression. In reality, heterogeneous macrophage populations coexist within the tumor compartment, influencing the progression of both tumor growth and the evolving immune response (124, 129). Nonetheless, a full understanding of the heterogeneity and functional states of TAMs seem now more relevant in clinical and therapeutic settings than ever before, as recently supported by the collected evidences (130).

A considerable number of questions have been raised about the relevance of macrophages' phenotype according to their lineage compared with their tissue environment, whether the replacement of yolk sac-derived or fetal liver-derived macrophages with BM-derived macrophages results in identical phenotypes, and whether macrophages from different origins can be specifically targeted. In the context of tumors, these questions are essential because not all TAMs take origin from the same organ (119, 131). For example, in pancreatic cancer models, the yolk sac-derived macrophages show a pro-tumoral phenotype opposite to the BM-derived macrophages, suggesting that origin is important (132).

Such observations underline that a different origin might be of clinical relevance, and they raise questions as to whether inhibition of BM-derived macrophage recruitment might result in compensation by yolk sac-derived and/or fetal liver-derived tissue progenitors or vice versa. Above the yet complex scenario of cancer, it seems of great importance the understand macrophage origin, heterogeneity, and dynamics in the tumor microenvironment.

4.2 The Controversial Role of Macrophages in Cancer

Macrophages can potentially mount a robust anti-tumoral response, as they can directly eliminate cancer cells if adequately activated. They can also support the adaptive immune response by presenting tumor antigens and producing chemokines and cytokines to recruit and activate cytotoxic CD8+ T cells (CTLs) and NK cells.

In the 1970s, studies demonstrated that macrophages activated by bacterial products and cytokines acquire the capacity to kill tumor cells (133–136). At least for the initial stage of cancer, TAMs have been seen as an ally, whereas when tumors progress, the TME modifies the environment and the TAMs, supporting tumor progression. It had been found that TAMs from malignant metastatic cancers promote tumor growth and metastasis (134).

Thus, early evidence suggested that macrophages could engage in a controversial dual relationship with cancer. The tumor-promoting functions of TAMs are diverse and may impact the different stages of tumor progression, from cancer initiation to metastasis, contributing to different hallmarks of cancer. Macrophages have bimodal roles in orchestrating immune responses that can either hamper or foster the effectiveness of conventional anti-cancer strategies.

In the first stages of tumor formation, macrophages are mainly tumoricidal, as they show an activated state, producing reactive oxygen and nitrogen intermediates that may contribute to DNA damage and genetic instability (55). The role of macrophages in the transition from a benign to a malignant tumor has been studied in only a few cancer models (mammary, skin, and pancreatic cancers) (137–139) and, at least in mammary tumors, premature recruitment of macrophages by overexpression of colony stimulator factor 1 (CSF1) promotes the transition to malignancy (138).

Furthermore, the presence of type II cytokines (interleukin-(IL)-4 or IL-13) in the microenvironment affect macrophage functions and phenotypes resembling those involved in tissue development and repair, with consequent suppression of anti-tumoral response switching the immune response from a cytotoxic to a supportive role (24, 140).

Macrophages also exacerbate the transition to malignancy by producing angiogenic factors, proteases, and secretion of growth factors such as epidermal growth factor, which induces cancer cell proliferation and the support of epithelial-mesenchymal transition in tumor cells (141).

TAMs are a source of additional angiogenic factors, chemokines with proangiogenic and pro-lymphangiogenic potential, and inflammatory cytokines, including placental growth factor, fibroblast growth factor 2, VEGF-C, tumor necrosis factor (TNF), IL-1β, IL-6, and chemokine (C-X-C motif) ligand 8 (CXCL8) (53). Moreover, myeloid cells produce different proteases, such as MMPs and cathepsins, that mobilize ECM-bound VEGF-A and other factors. Hypoxia, a major driver of angiogenesis in cancer tissues, induces the upregulation of hypoxia-inducible factor-1α (HIF-1α) expression and secretion of proangiogenic factors, such as VEGF-A (142). In addition, myeloid-derived VEGF-A is essential for the tumorigenic alteration of the vasculature. This alteration delays tumor progression as VEGF-A deficiency in TAMs was found to reduce angiogenesis and abnormalities in tumor vessels in mouse cancer models but to increase tumor growth (143). Accordingly, TAMs are also promoters of the neoangiogenic switch in tumors since their frequency correlates with the vascular density in preclinical tumor models and human tumors (144).

In mice, Ly6C+/CCR2+ cells, defined as inflammatory monocytes, have been shown to contribute to TAM accumulation and maintenance in a mouse mammary tumor model (145) and the establishment of pulmonary metastases derived from mouse or human breast cancer cells (146). In contrast, a protective role of patrolling monocytes, defined as Ly6C-/CX3CR1+, is shown by their inability to extravasate into tissues and differentiate into macrophages; despite that, they can rapidly accumulate within lung metastases and inhibit tumor cell seeding and growth in mouse models. Such anti-tumor functions include scavenging tumor debris, the recruitment and activation NK cells, and Th1 responses (147, 148).

M2-like macrophages can be found in the metastatic cell niche at more advanced stages, where they exert trophic functions while promoting tumor-initiating cell evasion of immune clearance (149, 150).

TAMs are major drivers of immunosuppression in the TME. Mediators released by tumor-infiltrating lymphocytes, such as Th2 cells and Treg cells (producing IL-4 and Il-10), and by tumor cells (IL-10, TGFβ, and PGE2) activate an immunosuppressive program in TAMs (151, 152). Macrophage-derived cytokines, such as IL-1, promote the recruitment and seeding of metastatic cancer cells at niche sites (146, 149). Additionally, myelomonocytic cells also promote metabolic starvation of T cells due to the activity of arginase and the production of amino acid metabolites by indoleamine 2,3-dioxygenase (IDO).

Furthermore, in mouse and human melanoma, IL-1 was shown to induce the upregulation of the expression of TET2, a DNA methylcytosine dioxygenase, which sustained the immunosuppressive functions of TAMs (153). Finally, TAMs express the ligands of checkpoint molecules, such as PD-L1, PD-L2, B7 ligands (154), and VISTA (155), which suppress adaptive T cell immune responses and promote Treg recruitment (5, 156).

In addition to primary tumors, macrophages can also assist in tumor survival and colonization at premetastatic lesions. It has been shown that macrophages are required for the early dissemination of breast cancer, and early disseminated macrophages contribute to late metastasis (157).

Macrophages promote the invasiveness and metastasis of tumor cells by expressing matrix metalloproteinases, cathepsin, urokinase, plasminogen activator, and matrix remodeling enzymes (dissolving the extracellular matrix to pave the path for a tumor cell to escape, as well as secrete IL-1ra enhancing tumor cell stemness and metastasis (158)). It has also been observed that pancreatic cancer cell-derived exosomes preferentially colocalize with macrophages in liver metastasis sites (159). Exosome-educated macrophages facilitate premetastatic niche formation *via* secretion of TGF-β (160). Additionally, exosomes produced by macrophages can transfer miRNA into cancer cells favoring metastasization in colorectal cancer and pancreatic ductal adenocarcinoma cells (160, 161). Other studies support the indispensable role of monocytes/macrophages recruited to

premetastatic niches in promoting circulating tumor cell survival and colonization in metastatic lesions (162). For instance, tumor cells of lung metastasis (derived from breast cancer) produce CCL2, recruiting and retaining monocytes/macrophages (163), likewise fibrocytes that prepare the premetastatic niche for melanoma cells by the exact mechanism (164). The inflammatory monocytes CCR2+Ly6C+, after differentiating into Ly6C– macrophages, accelerate tumor cell extravasation by generating VEGF (146).

Tissue-resident macrophages have also been demonstrated to promote or restrict metastasis. Alveolar macrophages promote hepatocellular carcinoma lung metastasis by producing the inflammatory leukotriene B4 (165) and suppressing the Th1 responses (166). Conversely, Kupffer cells engulf cancer cells to limit liver metastasis (167).

Interestingly, within the brain, evidences support that the majority of TAMs tend to be pro-tumorigenic and accumulate with higher tumor grade (168) and the dogma of a simple linear M1-M2 phenotypic balance has been disputed. Instead, many groups are focusing on defining activation and phenotype as a measure of functional diversity in brain cancers (124).

Indeed, studies in mice showed that phenotypic alteration of TAMs results in anti-tumor efficacy in glioblastoma (169, 170), whereas TAM depletion prevents brain metastasis outgrowth (171).

Lately, it has been leveraged a diverse panel of analyses to deeply interrogate the immune landscape of primary and metastatic brain cancers uncovering several pronounced differences between gliomas and brain metastasis. A significant shift in the ratio of microglia and monocytes-derived macrophages (MDMs) has been revealed between isocitrate dehydrogenase 1 and 2 (IDH) mut and IDH WT gliomas. Additionally, gliomas show an abundance of TAMs, whereas T cells were much fewer (particularly in IDH mut tumors)

confirming the notion that gliomas are immunologically cold tumors. By contrast, brain metastasis seem to accumulate more lymphocytes and neutrophils, indicating that tumors that arise within the brain shape their TME differently than cancers that metastasize from extracranial sites (172).

4.3 Macrophages Interference With Anti-Cancer Therapies

In conventional chemotherapy and radiotherapy, macrophages have boosted or limited the therapeutic effect. **Chemotherapy** can affect macrophages' functions modulating the cross-talk with the adaptive compartment, thus changing the entity of the immune responses and ultimately the therapy outcome. More than 30 years ago, an interaction was reported between the chemotherapeutic agent actinomycin D and human and murine monocytes/macrophages, afterward named "drug-dependent cellular cytotoxicity" (173). Another earlier study underlined how immunity could determine the efficacy of doxorubicin treatment (174). This latter can induce tumor cells to undergo immunogenic cell death as they express alarm signals that trigger adaptive immune responses; for instance, doxorubicin causes a massive release of ATP from tumor cells leading to the mononuclear phagocytes recruitment and their differentiation in antigen-presenting cells (APCs) (175).

Data from preclinical models suggest that myeloid cells can shift the balance of the role of immunity in the anti-tumor activity of selected chemotherapeutic agents (176), which can be leveraged to increase the efficacy of ICIs (177).

Trabectedin, a DNA-binding agent that causes DNA damage and cell-cycle arrest in tumor cells, which the EMA approves for the treatment of soft-tissue sarcomas and ovarian cancer, and by the FDA for sarcoma therapy, has shown a complex mechanism aside from the conventional ones; it indeed affects the transcription of selected genes including some that encode for inflammatory cytokines and chemokines, as well as angiogenic factors (178). The secondary and relevant effect brings delayed and prolonged responses after trabectedin treatments; thus, that cannot be explained only by the effect on cancer cells (179, 180). It has been found to activate programmed cell death (through caspase 8) *via* cell-surface receptors selectively in monocytes, inducing their apoptosis (179). Furthermore, patients with sarcoma treated with trabectedin showed a reduced TAM infiltration and decreased angiogenesis, supporting the hypothesis that the reduction of macrophages abundance is a key component of the anti-tumor activity of this drug.

However, macrophages rarely have a positive effect on responsiveness to chemotherapy. TAMs, when polarized in M2 or M2-like, can limit the effectiveness of cytotoxic agents like platinum-containing compounds, paclitaxel, and doxorubicin (10, 115, 181–183). In mouse tumor-transplantation models, M2-like macrophages, orchestrating tissue repair, were found to accumulate in perivascular areas of the tumor after chemotherapy and promoted tumor revascularization and relapse (184); recruitment of these cells was found to be CXCR4–CXCL12 dependent (184). The discrepancy of the TAMs' role in mediating the response to doxorubicin is probably a consequence of different mouse tumor models and their immunogenicity (10, 174, 181–183, 185). Patients with lymphomas treated with doxorubicin-containing regimens mirror preclinical data showing higher TAM infiltration associated with a favorable prognosis (174, 186). Similarly to these clinical associations, drugs like doxorubicin, oxaliplatin, and cyclophosphamide enhance the effect of chemotherapy through the induced immunogenic cell death (ICD), which implies the release of "eat me" signals from tumor cells promoting phagocytic and antigen-presenting capabilities (175, 176, 187, 188).

Additionally, chemotherapy can directly modulate the macrophage phenotype, reprogramming TAMs into M1-like immunostimulant cells, an effect observed with gemcitabine in pancreatic cancer (189), as well as 5-fluorouracil in colorectal cancer (190) and docetaxel in a preclinical model of breast cancer (191). Two general mechanisms seem to be responsible for the antagonistic effects of TAMs on chemotherapy outcomes. In mouse models, chemotherapy-induced tissue damage has been demonstrated to trigger the recruitment of immunosuppressive myeloid cells or elicit a pro-tumorigenic type 17 T–helper (Th17)-cell-skewed immune response promoted by IL–1 (182).

Alternatively, TAMs have been reported to protect mouse cancer stem cells (CSCs) from cytotoxicity (183, 185). Preclinical models, however, document primarily negative effects of macrophages on the responsiveness to chemotherapy; the several mechanisms identified include orchestration of an immunosuppressive response, tissue repair-related functions, nourishment of tumor cells, and pro-metastatic activity (4, 192). Accordingly, depletion of TAMs with anti-CSF1/CSF1R (CSF1 receptor) antibodies enhanced chemosensitivity to a combinatorial chemotherapeutic approach in human breast cancer xenografts (193) and a genetic mammary tumor model (194). Additionally, CSF1 expression correlates with accumulation of CD8+ T cells and CD163+ TAMs in melanoma, and anti–PD1 and anti–CSF1R combination therapy induced regression of melanoma in preclinical studies (195). Moreover, a mechanistic leap in our understanding of macrophage-specific targeting of the CSF1/CSF1R axis has been achieved in murine models of pancreatic ductal adenocarcinoma (137, 196); in fact, PD1 and CTLA4 antagonists showed limited efficacy as single agents to restrain tumor growth, but in combination with CSF1R blockade potently elicited tumor regressions, even in larger established tumors, providing a rationale to fuel the subsequent efforts to translate CSF1/1R-specific and other tumor-associated macrophage modulating therapies into the clinic (196).

Macrophage infiltration was found to be associated with chemoresistance to 5-fluorouracil in colon cancer cell lines (197), and macrophage depletion increased responsiveness to paclitaxel (PTX) treatment in breast cancer (10). Not to forget that TAMs foster chemoresistance releasing growth factors protecting tissues from chemotherapy-induced damage (183, 198). Of note, paclitaxel and doxorubicin increase the ability of perivascular macrophages to promote tumor cell metastasis.

The effect of radiotherapy on myeloid cells can also have dual implications for patient outcomes. In mouse models, the influx of monocytes into tumors following radiotherapy drives a profibrotic tissue response and might promote tumor recurrence (192, 199). Conversely, in patients, tumor regression at sites distant from the irradiated lesions — known as the 'abscopal' effect (200) — could plausibly be explained by activation of host anti-cancer immunity. In a mouse model, neoadjuvant low-dose γ–irradiation was found to set macrophage functions to an anti-tumor modality characterized by a lack of both immunosuppressive and proangiogenic activity and the production of T–cell–attracting chemokines (201). Instead, a fractionated cumulative radiation dose regimen, similar to those during cancer treatment, induced a pro-inflammatory phenotype in macrophages *in vitro* but did not alter their ability to promote cancer invasion and cancer angiogenesis (202).

Moreover, seeking to evaluate the applicability of radioimmunotherapy in experimental breast-to-brain metastasis models, it was reported that the induced immune modulation led to an increase in cytotoxic T-cell numbers and prevented the induction of lymphocyte-mediated immune suppression. Overall, radio-immunotherapy significantly improved tumor control with prolonged median survival, however recurrent brain metastases showed accumulation of blood-borne PD-L1+ myeloid cells, indicating the establishment of an immune suppressive environment to counteract re-activated T-cell responses (203). Therefore, TAMs can either reduce or amplify the magnitude of the anti-tumor effect of radiotherapy depending on context and TME; overall, data suggest that macrophage targeting in combination with radiotherapy could be a potential therapeutic strategy to modulate the stroma and allow better tumor killing, although it is not a well-explored field.

Another important determinant for the efficacy of chemotherapy and immunotherapy has emerged to be the host-microbiota (204–208). Mouse tumor models have been shown an essential role of microbial components in priming myeloid cells for the antineoplastic efficacy of platinum combined with adjuvant CpG oligonucleotides (204). Similarly, the antineoplastic activity of anthracyclines is compromised in mice with genetic inactivation of the formyl peptide receptor 1 (FPR1), a sensor of microbial components and tissue damage that is expressed in myeloid cells (209). The loss–of–function of the *FPR1* allele has been associated with unfavorable survival in patients with breast carcinoma or colorectal cancer after adjuvant chemotherapy, as well as blocking the receptor function with cyclosporin H (CsH) was shown to reduce the efficacy of anti-cancer chemotherapy against carcinogen-induced breast cancer (209, 210). Once more, myeloid cells determine the role of immunity in the anti-tumor activity of selected chemotherapeutic agents (176), which can be exploited to increase the efficacy of ICIs (177). In mouse models, repolarization of macrophages has also been reported in the context of targeted therapy, such as treatment of KIT –positive gastrointestinal stromal tumors (GISTs) with imatinib (211) and treatment of hepatocellular carcinoma with sorafenib (212).

Strategies targeting VEGF signaling are part of the current therapeutic armamentarium in oncology.

VEGF is a potent attractant of monocytes, acting *via* VEGFR–1, and its expression is upregulated in metastasis-associated macrophages in mammary carcinoma models (213). Although VEGF is a well-known chemotactic for monocytes, it did not drive the accumulation of macrophages in this model.

Nonetheless, VEGF signaling activates the CSF-1 pathway in metastasis-associated macrophages, taking that they are a major source of angiogenic factors, including VEGF; their density is also correlated to increased vasculature (214). Interestingly, the resistance of tumors to current anti-VEGF therapies is frequently associated with high levels of myeloid-cell infiltration (215). For instance, a study with 24 enrolled patients showed that the use of bevacizumab (anti-VEGF therapy) resulted in a pronounced increase in the number of TAMs and M2 macrophages compared to paclitaxel–carboplatin alone (used as neoadjuvant chemotherapy) (216). Furthermore, macrophage infiltration into human glioblastomas, resistant to anti-VEGF therapy, is correlated with a poor prognosis, but a combinatorial therapy with anti-VEGF and anti-ANG2 (angiopoietin-2) was shown to reprogram TAMs from M2 into M1 phenotype with relevant anti-tumor activity (217). Similarly, a vascular-disrupting agent 5,6-dimethylxanthenone-4-acetic acid (DMXAA), initially developed for disrupting tumor vasculature, has also been shown to activate immunostimulatory functions of TAMs, which in turn orchestrate anti-tumor response of CD8+ T cells (218).

While conventional therapies primarily target cancer cells, more recent treatments, especially mAb-based targeted therapies and immunotherapies, rely more profoundly on myeloid cells' engagement (5).

The immunotherapy field has had a rapid expansion, particularly with the discovery of ICIs. Myelomonocytic cells are a vital component of the immunosuppressive pathways targeted by ICIs and might, therefore, offer tools to predict or increase the activity of such treatments. They express PD-1 ligands PD–L1 and PD–L2, as well as the CTLA–4 ligands B7–1 (CD80) and B7–2 (CD86), and the related protein B7–H4. PD–L1 and PD–L2 are upregulated on the surface of macrophages in response to various stimuli, including cytokines and hypoxia (219, 220). TAMs present in a variety of human tumor types often expresses different levels of high levels of immune-checkpoint molecules (214). The presence of these molecules is a predictor of response to therapy, especially to ICIs (221, 222). In preclinical models, FcγR-expressing macrophages eliminated CTLA–4–positive, mAb-coated Treg cells from tumors *via* ADCC (223, 224), unleashing anti-tumor immunity. The ADCC mediated by TAMs was shown in a study where melanoma patients responders to ipilimumab (mAb anti-CTLA-4) had higher numbers of circulating CD16+ monocytes and macrophages at tumor sites and lower Treg cells (225). In general, macrophages contribute to the TME immunosuppression through several mechanisms; thus, targeting TAMs might support the efficacy of ICIs by removing

inhibitory factors for T cells (5). Up to date, neutralizing antibodies are currently US FDA-approved for the treatment of several cancers, including melanoma, advanced renal carcinoma, gastric cancer, non-small-cell lung cancer, and colorectal cancer; currently, they are also studied in combinations with other therapies such as well as studied for the treatment of solid tumors (226).

4.4 Current Strategies to Target Tumor-Associated Macrophages

TAMs can influence cancer relapse following treatment with conventional therapies; thus that several approaches have been developed to therapeutically target TAMs, from blocking the recruitment and infiltration of MDMs into the TME to interfering with TAM differentiation into tumor-promoting phenotypes and inhibiting proinflammatory cytokines and other stimuli responsible for chronic inflammation within the TME (5). Those therapies not only aim to block the ability of TAMs to promote cancer cell survival directly but can also increase cross-presentation to CD8+ T cells and thereby enhance their anti-tumoral potency.

Although TAMs are subject to tissue-specific imprinting, common strategies broadly target these cells across different organs, and many have shown promising results in preclinical models.

A considering number of these agents have entered clinical evaluation for diverse tumor types, including (i) inhibitors of CSF1R to deplete TAMs and/or alter their functions within the TME; (ii) CCL2 or CCR2 inhibitors to prevent TAMs recruitment into the TME; (iii) CD47/SIRPα complex antagonists to enhance TAM-mediated phagocytosis of cancer cells; (iv) administration of costimulatory molecules such as CD40 to enhance T-cell activation; (v) inhibitors of PI3Kγ and the triggering receptor expressed on myeloid cells 2 (TREM2) protein to reprogram TAMs toward anti-tumoral phenotypes; (vi) TLRs agonists to switch M2 phenotype into M1.

4.4.1 CSF1 Inhibitors

CSF1R is a transmembrane tyrosine kinase class III receptor that has attracted interest primarily because it is exclusively expressed by cells of the monocytic lineage, and its specific ligand CSF1 (M-CSF) is required for macrophage differentiation and survival (227). Another known ligand is IL34, which role in cancer has been less explored partly due to its relatively recent identification as an alternative ligand (228). IL34 production by chemo-resistant lung cancer cells has been reported to enhance the immunosuppressive profile of TAMs and contribute to cancer cell survival (229). Also high levels of CSF1 circulating in the serum have been correlated with poor survival of patients, in particular those with ovarian and endometrial cancers (230) (**Figure 1B**).

Several drugs, from neutralizing antibodies to small-molecule inhibitors, directed against CSF1R have been used to deplete intratumoral TAMs or promote their re-education into a tumoricidal phenotype in a context-dependent manner (169, 231). In preclinical models of multiple primary tumors, including pancreatic cancer, breast cancer, and glioblastoma, this approach resulted in anti-tumor efficacy (186, 225) and reduced breast-to-lung metastasis (10).

For instance, the occurrence of melanoma brain metastasis was significantly hindered under microglia and macrophages elimination with PLX3397, a CSF-1R inhibitor; their depletion effectively inhibited the expression of matrix metalloproteinase 3 (MMP3) and the decrease of tight junction protein zonula occludens-1 (ZO-1), correlated with myeloid cells activation (171).

In contrast to previous findings from glioblastoma mouse models, where TAMs survived CSF1R inhibition and were instead re-educated (169, 170), a recent work demonstrated that targeting TAMs with the CSF1R inhibitor BLZ945 delayed brain metastatic onset and led to an initial tumor response with transient stasis of established metastases (232).CSF1R inhibitors have also been evaluated in combination treatments in preclinical studies. In breast cancer models, the efficacy of paclitaxel (Taxol) was enhanced by CSF1R inhibitor–mediated TAM depletion (10, 233). Similarly, the effectiveness of radiotherapy and tyrosine kinase inhibitors in preclinical glioblastoma models, when CSF1R is inhibited, seems to be mediated by TAMs re-education (13, 234). Preventing the entry of MDMs into the brain TME resulted in a comparatively modest effect in glioma models (13), indicating that TAMs reeducation more than their depletion may represent a more effective strategy (231).

Multiple drugs blocking CSF1R signaling (such as trastuzumab, ARRY-382, pexidartinib, PLX7486, and BLZ945) have been tested, including in combination with conventional therapies targeting cancer cells. Combinatorial strategies have also been explored in glioblastoma models where TAM populations where targeted with CSF1R inhibitor together with radiotherapy, enhancing survival of preclinical models (13). Others have also showed that CSF1R treatment prevent the accumulation of CD11b+Ly6C- monocytes, which recruitments is usually enhanced by radiation, limiting the pro-tumorigenic TAMs generation that supports tumor progression (235).

Several other clinical studies have been published and have reported different outcomes depending on the tumor type.

4.4.2 CCL2/CCR2 Inhibitors

Chemokines usually drive monocyte recruitment and macrophages accumulation within the tumor and the expansion of the tissue-resident macrophage pool (236). In particular, CCL2 release by cancer cells leads to the recruitment not only of tissue-resident macrophages but also of CCR2+ Ly6C hi monocytes from the bloodstream that extravasate into tumor sites and differentiate into TAMs (237). High levels of CCL2 in the serum and the TME have often been associated with poor prognosis no matter the type of cancer (238, 239). Using neutralizing antibodies against CCL2 hindered the accumulation of TAMs and potentiated the anti-tumor efficacy of CD8+ T cells in the TME as the Ly6Chi monocytes were sequestered in the BM; thereby, it was shown a reduction in tumor growth and metastasis (146, 239) (**Figure 1B**). Although concerns about the long-term monotherapy efficacy were raised when its suspension triggered monocytes' recruitment to the

TME inducing lung metastasis and decreasing animals' survival (240). Carlumab/CNTO888 (a human recombinant mAb targeting CCL2) entered phase I and II trials for patients with solid tumors, including metastatic castrate-resistant prostate cancer (NCT00992186 and NCT01204996), but despite being well-tolerated, it failed to affect tumor growth significantly, and the drug was discontinued. On the other hand, several anti-CCR2 mAbs have been tested in phase I and II trials for patients with bone metastasis (NCT01015560) and with advanced pancreatic adenocarcinoma (NCT01413022). More evidence supports the need for a thoughtful rationale to bring in the clinic using such therapies as combinatorial instead of monotherapy. For instance, PF-04136309 together with chemotherapy (FOLFIRINOX) resulted in a tumor response in 49% of the patients and local tumor control in 96% (241). The lack of evident clinical efficacy and the unexpected side effects may be explained by the CCL2 boost induced by the body made to overcome the inhibition of the CCL2/CCR2 axis (242) through still-unidentified compensatory mechanisms. Moreover, angiogenesis and local proliferation of resident TAMs may also dampen the effect of CCL2/CCR2 immunotherapy (240). Thus, focusing on new targets that selectively dampen monocytes' recruitment and differentiation into pro-tumoral macrophages would be crucial to offering secondary options for unresponsive patients.

4.4.3 CD47 Antagonists

Among many pro-tumoral functions exerted by TMAs can activate the immune response and even phagocyte cancer cells (4), for instance, the CD47-SIRPα interactions (243). CD47 is a "don't eat me" immune checkpoint signaling receptor, which is constitutively expressed by normal cells and overexpressed on cancer cells (244), while CD47 binds signal regulatory protein α, expressed by TAMs, DCs and neutrophils (4). When SIRPα binds CD47, a cascade is initiated, inhibiting the phagocytic capacity of macrophages. Thus, it is believed to be important to block CD47–SIRPα interactions removes this inhibitory checkpoint signal augmenting the macrophage-mediated clearance of cancer cells (245), inducing DCs endocytosis and activation with the consequent T-cell mediated tumor clearance (243, 246, 247) (**Figure 1B**). In several preclinical models, this axis represents a promising innate immune checkpoint (243). Antibodies against CD47 are currently in the frontline of development, taken that magrolimab reduced mouse pediatric brain tumors (248), and a few others, like Hu5F9-G4, CC-90002, and ZL-1201, have started to be evaluated in patients. Along with those, several ongoing phases I studies for solid tumors and hematologic and B-cell malignancies (NCT03558139, NCT03248479, and NCT04599634), and a phase II trial (NCT02953782) for the treatment of solid tumors and advanced colorectal cancer has recently been completed but not shared yet.

4.4.4 CD40 Agonists

CD40, a TNF receptor superfamily member, is expressed on APCs and is critical for their activation and proliferation, as well as an important regulator of T cell-dependent anti-tumor immunity *via* the interaction with CD40 ligand (CD40L) mainly expressed by CD4+ T cells (249). The signaling of this axis leads to secondary and tertiary signals for proper T-cell priming, such as the upregulation of MHC molecules, costimulatory molecules (like CD80 and CD86), and the production of proinflammatory cytokines (250, 251). For these reasons, CD40 can turn upside down the immune suppression and drive anti-tumor as its blockade induce the secretion of IFNγ and a tumoricidal phenotype as demonstrated in preclinical models of pancreatic cancer and patients with cancer (252). When CD40 agonists were used in combination with CSF1R inhibition, TAMs resulted as reprogrammed, reinforcing an effective T cell response (253). Many are the monoclonal agonistic antibodies (rhuCD40L, CP-870,893, and RO7009789) that are being evaluated in several clinical trials, and few with opposite results (**Figure 1B**). While a phase I trial of CP-870,893 in patients with advanced cancer showed no clinical responses (254), an early trial of rhuCD40L in patients with advanced squamous cell cancer of the head and neck had a broad spectrum of efficacy, with some showing modest responses and only one with a long-term remission (254). More recently, the tolerability and efficacy of a CD40 antibody (APX005M) combined with chemotherapy (gemcitabine plus nab-paclitaxel), with or without nivolumab, was achieved for patients with metastatic pancreatic adenocarcinoma in a phase Ib study (255). Overall, the scattered successes in cancer therapy of different patients leave undiscovered the biological reasons that must be explored to exploit the CD40 agonist as monotherapy or in combination with other ICIs.

4.4.5 PI3K

The PI3Kγ is a myeloid-specific isoform of the PI3K family, which signaling pathway is important for regulating cell growth, survival, metabolism, angiogenesis, as its family members have important effects on the immune system. PI3Kγ acts as a key immunosuppressive pathway in myeloid cells, and its pharmacological inhibition has been studied in preclinical tumor models. Interestingly, PI3Kγ is a key regulator of TAM-mediated immunosuppression (256), and its selective inhibition increases MHC-II and IL12 expression and decreases IL10 in TAMs; as well as helping to overcome resistance to ICI, reshaping the TME and promoting CD8+ T cell recruitment and tumor regression (256, 257). Phase I and II clinical studies are now evaluating the inhibitor eganelisib (IPI-549) in diverse cancers, either as a monotherapy or in combination with ICI (NCT03719326, NCT02637531, NCT03795610, and NCT03980041). In 2020, the FDA granted eganelisib combined with ICI and chemotherapy for first-line treatment of patients with inoperable locally advanced or metastatic triple-negative breast cancer (NCT03961698). There are hundreds of ongoing clinical trials using pan-PI3K inhibitors, but only a few early-phase studies have employed specific inhibitors of the myeloid γ isoform in cancer patients (**Figure 1B**).

4.4.6 TREM

This receptor is a member of the Ig superfamily and a major signaling hub with several proteins and ligands (258). The

deficiency of TREM resulted in the reeducation of tumoral TAMs to an anti-tumoral phenotype (259, 260). TREM2 seems to be expressed in TAMs in more than 200 human cancer cases, and high levels correlate with poor outcomes in colorectal and breast cancers (259). An Ab (PY314) has been designed to deplete TREM expressing TAMs, and it is currently evaluated as monotherapy or in combination with pembrolizumab (NCT04691375) in a phase I trial (**Figure 1B**).

4.4.7 TLRs

Toll-like receptors (TLRs), which are widely expressed by innate immune, are involved primarily in activating inflammatory immune responses. The first FDA-approved TLR agonist, subsequently used in combination with anti-PD1 therapy for bladder cancer, is Bacillus Calmette-Guerin (BCG), which triggers TLR2 and TLR4 (261, 262). Up to now, many are the pieces of evidence from *in vitro* and *in vivo* preclinical studies showing the potential activity of synthetic compounds specific for the endosomal TLR3, TLR7, TLR7, TLR8, and TLR9. Those ligands induce the secretion of immunostimulatory cytokines, like the type I IFN pathway, mostly in plasmacytoid DCs (pDCs) and macrophages (263), leading to an increased production of cytokines and infiltration of CD8+ T cells. To date, only imiquimod (TLR7 specific agonist) has been approved by the FDA for the topical treatment of squamous and basal cell carcinomas; others, like poly I: C (TLR3 agonist), resiquimod and NKTR-262 (TLR7/8 agonists), and CMP-001 and tilsotolimod (TLR9 agonist), have been developed and evaluated in early-phase clinical trials, either as adjuvants for cancer vaccines to boost anti-tumor responses or in combination with other treatments (264) (**Figure 1B**). Up to now, the topical application of TLR agonists in cutaneous neoplasms or intratumoral injection into accessible lesions has been thought safe.

The analog poly-ICLC is one of the most investigated compounds in more than 100 clinical trials and a few phases of I/II trials it has been exploited in combination with ICIs therapeutics in advanced diseases or as an anti-tumor vaccine adjuvant (265). An analog of imiquimod, resiquimod (TLR7/8 agonist), was shown to induce a strong anti-tumor response (266); either its topical administration or the local injection of loaded- nanoparticles induced tumor shrinkage and protective memory (267, 268). Intratumoral injection of MEDI9197 (3M-052) (specific for TLR7/TLR8) induced macrophage repolarization and tumor regression in a mouse model of subcutaneous melanoma; a mechanism mediated by macrophages induced direct tumor cell killing *via* NO production and synergized with checkpoint inhibitors anti-CTLA4 and anti-PD-1 antibodies to inhibit tumor growth (269, 270). Another one, SD-101 binds TLR9, has also been investigated in combination with immunotherapy (271, 272). Other TLR7/8 agonists are currently in phase III trial for skin neoplasia, anal carcinoma, and cervical intraepithelial lesions (264). For instance, TLR8 agonist motolimod, in combination with cetuximab, was shown to induce partial responses in a few patients with recurrent or metastatic head and neck cancer (273). Since most clinical trials have shown TLR agonists safe and promising in the clinic, such as tumor shrinkage after their injections, they would be probably more successful when used in combination with checkpoint inhibitors to treat those cold and non-responsive tumors.

5 NEW RELEVANT TARGETS

In recent years, an increasing number of studies have highlighted the important implications of **metabolism** on the biology and functional activities of immune cells. Despite the recent advances in this field, the metabolism of neutrophils is not fully understood and need further investigations, while it is already established that changes in metabolism generally shift macrophage polarization towards a tumor-promoting phenotype (274). Accordingly, metabolic modulation has been tested as a potential strategy to reprogram TAMs towards an anti-tumor state. Many tumor-derived metabolites have been discovered, such as adenosine, glutamine, and lactate, and have been mainly studied and tested in preclinical models to assess their effects on tumors. One of the most important findings has been the crucial role of glutamine. Thus, blocking its metabolism in a mouse breast cancer model reduced tumor growth and metastases, enhancing macrophage activation and inhibiting MDSC generation (275).

In parallel, an inhibitor of the enzyme glutamine synthase, named glufosinate, has been studied. In highly metastatic mouse models of melanoma and breast and lung cancer, it reduced metastasis formation, angiogenesis, and immunosuppression reprogramming TAMs into anti-tumor effectors (276). Furthermore, lactate is highly produced in hypoxic tumors and promotes M2 macrophage polarization (277) *via* activation of the ERK/STAT3 signaling pathway or the sensor protein Gpr81/Gpr132 expressed by macrophages. Pharmacological inhibition of the ERK/STAT3 axis with selumetinib or static or the Gpr132 protein hampered lactate-induced M2 macrophage polarization and showed significant anti-tumor effects in preclinical studies (278, 279) (**Figure 1C**).

A new study recently elucidated the modulating effects of lactic acid produced by tumor cells upon the macrophages within the TME. Transcriptomic and metabolic analyses have revealed two TAMs phenotypes with different metabolic features: the pro-inflammatory major histocompatibility complex (MHC)-II hi TAMs with a hampered tricarboxylic acid (TCA) cycle and the reparative MHC-II lo TAMs with higher oxidative and glycolytic metabolism. The latter population uses lactate as an additional carbon source besides glucose, supporting oxidative metabolism. This excess of carbon is partly compensated by the reduced uptake of glutamine and enhanced TCA cycle-mediated respiration. Additionally, it profoundly affects their transcriptome increases L-arginine-catabolizing enzymes, thus enhancing the T cell suppressive capacity of these TAMs (280).

Another tumor metabolite, adenosine, influences TAMs functions and, nonetheless, stimulation of adenosine receptors hinders the differentiation of monocytes to macrophages, probably through cAMP accumulation (281). Deletion of the adenosine receptor A2A in myeloid cells has been shown to

prevent tumor progression and metastasis in melanoma tumor models (282), as well as its inhibition, enhances CD8+ T cells response in head and neck squamous cell carcinoma (283). This new field of research is appealing as well as challenging to explore as a therapeutic intervention in cancer patients as metabolic pathways are shared by all cells. Although metabolic macrophages rewiring could positively affect the combination with other treatments, the effects upon other cells of the TME need to be investigated, as well their long-term efficacy.

Other compounds have been tested, such as the histone deacetylase (HDAC) inhibitors. The selective class IIa inhibitor TMP195 has been proven to be successful in the epigenetic modulation of TAMs. In the MMTV-PyMT mammary tumor model, treatment with TMP195 stimulated macrophage-mediated phagocytosis of tumor cells and TAM reprogramming into proinflammatory immunostimulatory effectors (284). Combined treatment with TMP195 and chemotherapy or anti-PD-1 therapy resulted in increased anti-tumor effects. Additionally, a combination of low-dose adjuvant epigenetic compounds reduced metastatic spread in a preclinical metastasis model (after removing the primary tumor) (285), mainly mediated by the inhibition of myeloid cell recruitment in premetastatic niches.

Moreover, up to now, the only cell therapy approved by the FDA for hematological malignancies is the chimeric antigen receptor (CAR) T cells, genetically engineered to recognize the CD19 antigen (286). Still, the issues of the application to solid tumors are many. Classically, macrophages are more resistant to transduction procedures than lymphocytes and not many attempts to are being successful. Only one study has lightened hope, transducing an anti-HER2 CAR into primary human macrophages (CAR-Ms) (using a replication-incompetent adenovirus). They demonstrated in nude mice that the expression of the transgene reduces the volume of HER+ human tumors (287).

6 CONCLUDING REMARKS

A detailed understanding of the roles of myeloid cells in tumors has revealed their importance within the TME (5). Tumor-associated myeloid cells accumulate rapidly in tumors, where they constitute the largest population of leukocytes in tumors and, sometimes, outnumber tumor cells (256, 288). With a deeper understanding of cancer immunology, diverse strategies for the modulation of TAMs are being explored for therapeutic applications, while for neutrophils a specific strategy to modulate their phenotype has yet not been discovered; however, it is possible to affect their recruitment to ultimately avoid the detrimental effects usually observed upon their hijacking.

We must additionally look at the patient as a whole, considering the tumor as part of a circuit where microbiome, metabolism, obesity, lifestyle, and aging can alter the TME and affect treatment responsiveness.

Taken the diversity of the heterogeneity of myeloid cells within both primary tumors and their metastasis, and given the diverse targeting strategies currently used and underway, it is logical to think that characterization at the single-cell level should be included in the daily clinical practice to characterize and stratify each patient.

This approach would allow clinicians to find prognostic indicators and choose the most effective therapy based on the TME composition, lowering the cost of patient's management for the healthcare sector, in the long run. This would not only support the development of personalized medicine but also exclude immune-related toxicity profiles of specific treatments.

AUTHOR CONTRIBUTIONS

The authors contributed equally to this work, with CN being senior and correspondent. MR, writing and editinga. CN, conceptualization, original draft preparation, writing, draw figure, and editing. All authors have read and agreed to the published version of the manuscript.

ACKNOWLEDGMENTS

CN is supported by "Fondazione Beppe e Nuccy Angiolini Onlus". MR is recipient of a fellowship from "Associazione Amici del Mario Negri". We would like to thank their generous contribution.

REFERENCES

1. Dewhirst MW, Secomb TW. Transport of Drugs From Blood Vessels to Tumour Tissue. *Nat Rev Cancer* (2017) 17(12):738–50. doi: 10.1038/nrc.2017.93
2. Nia HT, Munn LL, Jain RK. Physical Traits of Cancer. In: *Science* (2020). Available at: https://www.science.org/doi/abs/10.1126/science.aaz0868. 370 (6516) doi: 10.1126/science.aaz0868
3. Joyce JA. Therapeutic Targeting of the Tumor Microenvironment. *Cancer Cell* (2005) 7(6):513–20. doi: 10.1016/j.ccr.2005.05.024
4. Mantovani A, Marchesi F, Malesci A, Laghi L, Allavena P. Tumour-Associated Macrophages as Treatment Targets in Oncology. *Nat Rev Clin Oncol* (2017) 14 (7):399–416. doi: 10.1038/nrclinonc.2016.217
5. Cassetta L, Pollard JW. Targeting Macrophages: Therapeutic Approaches in Cancer. *Nat Rev Drug Discov* (2018) 17(12):887–904. doi: 10.1038/nrd.2018.169
6. Nakamura K, Smyth MJ. Myeloid Immunosuppression and Immune Checkpoints in the Tumor Microenvironment. *Cell Mol Immunol* (2020) 17 (1):1–12. doi: 10.1038/s41423-019-0306-1
7. Klemm F, Joyce JA. Microenvironmental Regulation of Therapeutic Response in Cancer. *Trends Cell Biol* (2015) 25(4):198–213. doi: 10.1016/j.tcb.2014.11.006
8. Sharma P, Hu-Lieskovan S, Wargo JA, Ribas A. Primary, Adaptive, and Acquired Resistance to Cancer Immunotherapy. *Cell* (2017) 168(4):707–23. doi: 10.1016/j.cell.2017.01.017
9. Weissleder R, Pittet MJ. The Expanding Landscape of Inflammatory Cells Affecting Cancer Therapy. *Nat BioMed Eng* (2020) 4(5):489–98. doi: 10.1038/s41551-020-0524-y
10. DeNardo DG, Brennan DJ, Rexhepaj E, Ruffell B, Shiao SL, Madden SF, et al. Leukocyte Complexity Predicts Breast Cancer Survival and Functionally Regulates Response to Chemotherapy. *Cancer Discov* (2011) 1(1):54–67. doi: 10.1158/2159-8274.CD-10-0028

11. Takeuchi S, Baghdadi M, Tsuchikawa T, Wada H, Nakamura T, Abe H, et al. Chemotherapy-Derived Inflammatory Responses Accelerate the Formation of Immunosuppressive Myeloid Cells in the Tissue Microenvironment of Human Pancreatic Cancer. *Cancer Res* (2015) 75(13):2629–40. doi: 10.1158/0008-5472.CAN-14-2921
12. Seifert L, Werba G, Tiwari S, Giao Ly NN, Nguy S, Alothman S, et al. Radiation Therapy Induces Macrophages to Suppress T-Cell Responses Against Pancreatic Tumors in Mice. *Gastroenterology* (2016) 150(7):1659–72. doi: 10.1053/j.gastro.2016.02.070
13. Akkari L, Bowman RL, Tessier J, Klemm F, Handgraaf SM, de Groot M, et al. Dynamic Changes in Glioma Macrophage Populations After Radiotherapy Reveal CSF-1R Inhibition as a Strategy to Overcome Resistance. *Sci Trans Med* (2020) 12(552):eaaw7843. doi: 10.1126/scitranslmed.aaw7843
14. Sun Y, Campisi J, Higano C, Beer TM, Porter P, Coleman I, et al. Treatment-Induced Damage to the Tumor Microenvironment Promotes Prostate Cancer Therapy Resistance Through WNT16B. *Nat Med* (2012) 18(9):1359–68. doi: 10.1038/nm.2890
15. Moeller BJ, Cao Y, Li CY, Dewhirst MW. Radiation Activates HIF-1 to Regulate Vascular Radiosensitivity in Tumors: Role of Reoxygenation, Free Radicals, and Stress Granules. *Cancer Cell* (2004) 5(5):429–41. doi: 10.1016/S1535-6108(04)00115-1
16. Vincent J, Mignot G, Chalmin F, Ladoire S, Bruchard M, Chevriaux A, et al. 5-Fluorouracil Selectively Kills Tumor-Associated Myeloid-Derived Suppressor Cells Resulting in Enhanced T Cell-Dependent Antitumor Immunity. *Cancer Res* (2010) 70(8):3052–61. doi: 10.1158/0008-5472.CAN-09-3690
17. Galluzzi L, Humeau J, Buqué A, Zitvogel L, Kroemer G. Immunostimulation With Chemotherapy in the Era of Immune Checkpoint Inhibitors. *Nat Rev Clin Oncol* (2020) 17(12):725–41. doi: 10.1038/s41571-020-0413-z
18. Balkwill F, Mantovani A. Inflammation and Cancer: Back to Virchow? *Lancet* (2001) 357(9255):539–45. doi: 10.1016/S0140-6736(00)04046-0
19. Robert J. Comparative Study of Tumorigenesis and Tumor Immunity in Invertebrates and Nonmammalian Vertebrates. *Dev Comp Immunol* (2010) 34(9):915–25. doi: 10.1016/j.dci.2010.05.011
20. Wang J, Cao Z, Zhang X-M, Nakamura M, Sun M, Hartman J, et al. Novel Mechanism of Macrophage-Mediated Metastasis Revealed in a Zebrafish Model of Tumor Development. *Cancer Res* (2015) 75(2):306–15. doi: 10.1158/0008-5472.CAN-14-2819
21. Topalian SL, Drake CG, Pardoll DM. Immune Checkpoint Blockade: A Common Denominator Approach to Cancer Therapy. *Cancer Cell* (2015) 27(4):450–61. doi: 10.1016/j.ccell.2015.03.001
22. Ruffell B, Coussens LM. Macrophages and Therapeutic Resistance in Cancer. *Cancer Cell* (2015) 27(4):462–72. doi: 10.1016/j.ccell.2015.02.015
23. Allavena P, Digifico E, Belgiovine C. Macrophages and Cancer Stem Cells: A Malevolent Alliance. *Mol Med* (2021) 27(1):121. doi: 10.1186/s10020-021-00383-3
24. Noy R, Pollard JW. Tumor-Associated Macrophages: From Mechanisms to Therapy. *Immunity* (2014) 41(1):49–61. doi: 10.1016/j.immuni.2014.06.010
25. Mantovani A, Marchesi F, Jaillon S, Garlanda C, Allavena P. Tumor-Associated Myeloid Cells: Diversity and Therapeutic Targeting. *Cell Mol Immunol* (2021) 18(3):566–78. doi: 10.1038/s41423-020-00613-4
26. Ng LG, Ostuni R, Hidalgo A. Heterogeneity of Neutrophils. *Nat Rev Immunol* (2019) 19(4):255–65. doi: 10.1038/s41577-019-0141-8
27. O'Connell KE, Mikkola AM, Stepanek AM, Vernet A, Hall CD, Sun CC, et al. Practical Murine Hematopathology: A Comparative Review and Implications for Research. *Comp Med* (2015) 65(2):96–113.
28. Martin KR, Wong HL, Witko-Sarsat V, Wicks IP. G-CSF – A Double Edge Sword in Neutrophil Mediated Immunity. *Semin Immunol* (2021) 54:101516. doi: 10.1016/j.smim.2021.101516
29. Eash KJ, Greenbaum AM, Gopalan PK, Link DC. CXCR2 and CXCR4 Antagonistically Regulate Neutrophil Trafficking From Murine Bone Marrow. *J Clin Invest* (2010) 120(7):2423–31. doi: 10.1172/JCI41649
30. Manz MG, Boettcher S. Emergency Granulopoiesis. *Nat Rev Immunol* (2014) 14(5):302–14. doi: 10.1038/nri3660
31. Evrard M, Kwok IWH, Chong SZ, Teng KWW, Becht E, Chen J, et al. Developmental Analysis of Bone Marrow Neutrophils Reveals Populations Specialized in Expansion, Trafficking, and Effector Functions. *Immunity* (2018) 48(2):364–379.e8. doi: 10.1016/j.immuni.2018.02.002
32. Mumau MD, Vanderbeck AN, Lynch ED, Golec SB, Emerson SG, Punt JA. Identification of a Multipotent Progenitor Population in the Spleen That Is Regulated by NR4A1. *J Immunol* (2018) 200(3):1078–87. doi: 10.4049/jimmunol.1701250
33. Xie X, Shi Q, Wu P, Zhang X, Kambara H, Su J, et al. Single-Cell Transcriptome Profiling Reveals Neutrophil Heterogeneity in Homeostasis and Infection. *Nat Immunol* (2020) 21(9):1119–33. doi: 10.1038/s41590-020-0736-z
34. Baggiolini M, Walz A, Kunkel SL. Neutrophil-Activating Peptide-1/Interleukin 8, a Novel Cytokine That Activates Neutrophils. *J Clin Invest* (1989) 84(4):1045–9. doi: 10.1172/JCI114265
35. Zhu YP, Padgett L, Dinh HQ, Marcovecchio P, Blatchley A, Wu R, et al. Identification of an Early Unipotent Neutrophil Progenitor With Pro-Tumoral Activity in Mouse and Human Bone Marrow. *Cell Rep* (2018) 24(9):2329–41.e8. doi: 10.1016/j.celrep.2018.07.097
36. Ley K, Hoffman HM, Kubes P, Cassatella MA, Zychlinsky A, Hedrick CC, et al. Neutrophils: New Insights and Open Questions. *Sci Immunol* (2018) 3(30). doi: 10.1126/sciimmunol.aat4579
37. Abi Abdallah DS, Egan CE, Butcher BA, Denkers EY. Mouse Neutrophils Are Professional Antigen-Presenting Cells Programmed to Instruct Th1 and Th17 T-Cell Differentiation. *Int Immunol* (2011) 23(5):317–26. doi: 10.1093/intimm/dxr007
38. Vono M, Lin A, Norrby-Teglund A, Koup RA, Liang F, Loré K. Neutrophils Acquire the Capacity for Antigen Presentation to Memory CD4+ T Cells *In Vitro* and *Ex Vivo*. *Blood* (2017) 129(14):1991–2001. doi: 10.1182/blood-2016-10-744441
39. Nicolás-Ávila JÁ, Adrover JM, Hidalgo A. Neutrophils in Homeostasis, Immunity, and Cancer. *Immunity* (2017) 46(1):15–28. doi: 10.1016/j.immuni.2016.12.012
40. Jaillon S, Ponzetta A, Di Mitri D, Santoni A, Bonecchi R, Mantovani A. Neutrophil Diversity and Plasticity in Tumour Progression and Therapy. *Nat Rev Cancer* (2020) 20(9):485–503. doi: 10.1038/s41568-020-0281-y
41. Finisguerra V, Di Conza G, Di Matteo M, Serneels J, Costa S, Thompson AAR, et al. MET Is Required for the Recruitment of Anti-Tumoural Neutrophils. *Nature* (2015) 522(7556):349–53. doi: 10.1038/nature14407
42. Cui C, Chakraborty K, Tang XA, Zhou G, Schoenfelt KQ, Becker KM, et al. Neutrophil Elastase Selectively Kills Cancer Cells and Attenuates Tumorigenesis. *Cell* (2021) 184(12):3163–3177.e21. doi: 10.1016/j.cell.2021.04.016
43. Blaisdell A, Crequer A, Columbus D, Daikoku T, Mittal K, Dey SK, et al. Neutrophils Oppose Uterine Epithelial Carcinogenesis *via* Debridement of Hypoxic Tumor Cells. *Cancer Cell* (2015) 28(6):785–99. doi: 10.1016/j.ccell.2015.11.005
44. Jamieson T, Clarke M, Steele CW, Samuel MS, Neumann J, Jung A, et al. Inhibition of CXCR2 Profoundly Suppresses Inflammation-Driven and Spontaneous Tumorigenesis. *J Clin Invest* (2012) 122(9):3127–44. doi: 10.1172/JCI61067
45. Khaw YM, Cunningham C, Tierney A, Sivaguru M, Inoue M. Neutrophil-Selective Deletion of Cxcr2 Protects Against CNS Neurodegeneration in a Mouse Model of Multiple Sclerosis. *J Neuroinflammation* (2020) 17(1):49. doi: 10.1186/s12974-020-1730-y
46. Ponzetta A, Carriero R, Carnevale S, Barbagallo M, Molgora M, Perucchini C, et al. Neutrophils Driving Unconventional T Cells Mediate Resistance Against Murine Sarcomas and Selected Human Tumors. *Cell* (2019) 178(2):346–360.e24. doi: 10.1016/j.cell.2019.05.047
47. Singhal S, Bhojnagarwala PS, O'Brien S, Moon EK, Garfall AL, Rao AS, et al. Origin and Role of a Subset of Tumor-Associated Neutrophils With Antigen-Presenting Cell Features in Early-Stage Human Lung Cancer. *Cancer Cell* (2016) 30(1):120–35. doi: 10.1016/j.ccell.2016.06.001
48. Granot Z, Henke E, Comen EA, King TA, Norton L, Benezra R. Tumor Entrained Neutrophils Inhibit Seeding in the Premetastatic Lung. *Cancer Cell* (2011) 20(3):300–14. doi: 10.1016/j.ccr.2011.08.012
49. López-Lago MA, Posner S, Thodima VJ, Molina AM, Motzer RJ, Chaganti RSK. Neutrophil Chemokines Secreted by Tumor Cells Mount a Lung Antimetastatic Response During Renal Cell Carcinoma Progression. *Oncogene* (2013) 32(14):1752–60. doi: 10.1038/onc.2012.201
50. Massara M, Bonavita O, Savino B, Caronni N, Poeta VM, Sironi M, et al. ACKR2 in Hematopoietic Precursors as a Checkpoint of Neutrophil Release

and Anti-Metastatic Activity. *Nat Commun* (2018) 9(1):676. doi: 10.1038/s41467-018-03080-8
51. Balkwill FR, Mantovani A. Cancer-Related Inflammation: Common Themes and Therapeutic Opportunities. *Semin Cancer Biol* (2012) 22(1):33–40. doi: 10.1016/j.semcancer.2011.12.005
52. Nastasi C, Mannarino L, D'Incalci M. DNA Damage Response and Immune Defense. *Int J Mol Sci* (2020) 21(20):7504. doi: 10.3390/ijms21207504
53. De Palma M, Biziato D, Petrova TV. Microenvironmental Regulation of Tumour Angiogenesis. *Nat Rev Cancer* (2017) 17(8):457–74. doi: 10.1038/nrc.2017.51
54. Wculek SK, Bridgeman VL, Peakman F, Malanchi I. Early Neutrophil Responses to Chemical Carcinogenesis Shape Long-Term Lung Cancer Susceptibility. *iScience* (2020) 23(7):101277. doi: 10.1016/j.isci.2020.101277
55. Canli Ö, Nicolas AM, Gupta J, Finkelmeier F, Goncharova O, Pesic M, et al. Myeloid Cell-Derived Reactive Oxygen Species Induce Epithelial Mutagenesis. *Cancer Cell* (2017) 32(6):869–883.e5. doi: 10.1016/j.ccell.2017.11.004
56. Russo M, Giavazzi R. Anti-Angiogenesis for Cancer: Current Status and Prospects. *Thromb Res* (2018) 164:Supplement 1:S3–6. doi: 10.1016/j.thromres.2018.01.030
57. Albini A, Bruno A, Noonan DM, Mortara L. Contribution to Tumor Angiogenesis From Innate Immune Cells Within the Tumor Microenvironment: Implications for Immunotherapy. *Front Immunol* (2018) 9:527. doi: 10.3389/fimmu.2018.00527
58. Haibe Y, Kreidieh M, El Hajj H, Khalifeh I, Mukherji D, Temraz S, et al. Resistance Mechanisms to Anti-Angiogenic Therapies in Cancer. *Front Oncol* (2020) 10:221. doi: 10.3389/fonc.2020.00221
59. Shojaei F, Wu X, Zhong C, Yu L, Liang X-H, Yao J, et al. Bv8 Regulates Myeloid-Cell-Dependent Tumour Angiogenesis. *Nature* (2007) 450 (7171):825–31. doi: 10.1038/nature06348
60. Belotti D, Pinessi D, Taraboletti G. Alternative Vascularization Mechanisms in Tumor Resistance to Therapy. *Cancers* (2021) 13(8):1912. doi: 10.3390/cancers13081912
61. Spiegel A, Brooks MW, Houshyar S, Reinhardt F, Ardolino M, Fessler E, et al. Neutrophils Suppress Intraluminal NK Cell-Mediated Tumor Cell Clearance and Enhance Extravasation of Disseminated Carcinoma Cells. *Cancer Discov* (2016) 6(6):630–49. doi: 10.1158/2159-8290.CD-15-1157
62. Li P, Lu M, Shi J, Hua L, Gong Z, Li Q, et al. Dual Roles of Neutrophils in Metastatic Colonization are Governed by the Host NK Cell Status. *Nat Commun* (2020) 11(1):4387. doi: 10.1038/s41467-020-18125-0
63. Wculek SK, Malanchi I. Neutrophils Support Lung Colonization of Metastasis-Initiating Breast Cancer Cells. *Nature* (2015) 528(7582):413–7. doi: 10.1038/nature16140
64. Coffelt SB, Kersten K, Doornebal CW, Weiden J, Vrijland K, Hau C-S, et al. IL-17-Producing γδ T Cells and Neutrophils Conspire to Promote Breast Cancer Metastasis. *Nature* (2015) 522(7556):345–8. doi: 10.1038/nature14282
65. Szczerba BM, Castro-Giner F, Vetter M, Krol I, Gkountela S, Landin J, et al. Neutrophils Escort Circulating Tumour Cells to Enable Cell Cycle Progression. *Nature* (2019) 566:553–57. doi: 10.1038/s41586-019-0915-y
66. Liang W, Li Q, Ferrara N. Metastatic Growth Instructed by Neutrophil-Derived Transferrin. *PNAS* (2018) 115(43):11060–5. doi: 10.1073/pnas.1811717115
67. Faget J, Groeneveld S, Boivin G, Sankar M, Zangger N, Garcia M, et al. Neutrophils and Snail Orchestrate the Establishment of a Pro-Tumor Microenvironment in Lung Cancer. *Cell Rep* (2017) 21(11):3190–204. doi: 10.1016/j.celrep.2017.11.052
68. Jackstadt R, van Hooff SR, Leach JD, Cortes-Lavaud X, Lohuis JO, Ridgway RA, et al. Epithelial NOTCH Signaling Rewires the Tumor Microenvironment of Colorectal Cancer to Drive Poor-Prognosis Subtypes and Metastasis. *Cancer Cell* (2019) 36(3):319–36.e7. doi: 10.1016/j.ccell.2019.08.003
69. Markman JL, Porritt RA, Wakita D, Lane ME, Martinon D, Noval Rivas M, et al. Loss of Testosterone Impairs Anti-Tumor Neutrophil Function. *Nat Commun* (2020) 11(1):1613. doi: 10.1038/s41467-020-15397-4
70. Papayannopoulos V. Neutrophil Extracellular Traps in Immunity and Disease. *Nat Rev Immunol* (2018) 18(2):134–47. doi: 10.1038/nri.2017.105
71. Albrengues J, Shields MA, Ng D, Park CG, Ambrico A, Poindexter ME, et al. Neutrophil Extracellular Traps Produced During Inflammation Awaken Dormant Cancer Cells in Mice. *Science* (2018) 361(6409):eaao4227. doi: 10.1126/science.aao4227
72. Park J, Wysocki RW, Amoozgar Z, Maiorino L, Fein MR, Jorns J, et al. Cancer Cells Induce Metastasis-Supporting Neutrophil Extracellular DNA Traps. *Sci Transl Med* (2016) 8(361):361ra138. doi: 10.1126/scitranslmed.aag1711
73. Lee W, Ko SY, Mohamed MS, Kenny HA, Lengyel E, Naora H. Neutrophils Facilitate Ovarian Cancer Premetastatic Niche Formation in the Omentum. *J Exp Med* (2019) 216(1):176–94. doi: 10.1084/jem.20181170
74. Yang L-Y, Luo Q, Lu L, Zhu W-W, Sun H-T, Wei R, et al. Increased Neutrophil Extracellular Traps Promote Metastasis Potential of Hepatocellular Carcinoma *via* Provoking Tumorous Inflammatory Response. *J Hematol Oncol* (2020) 13(1):3. doi: 10.1186/s13045-019-0836-0
75. He X, Xu C. Immune Checkpoint Signaling and Cancer Immunotherapy. *Cell Res* (2020) 30(8):660–9. doi: 10.1038/s41422-020-0343-4
76. Kroemer G, Zitvogel L. Immune Checkpoint Inhibitors. *J Exp Med* (2021) 218 (3):e20201979. doi: 10.1084/jem.20201979
77. Jenkins RW, Barbie DA, Flaherty KT. Mechanisms of Resistance to Immune Checkpoint Inhibitors. *Br J Cancer* (2018) 118(1):9–16. doi: 10.1038/bjc.2017.434
78. Bruni D, Angell HK, Galon J. The Immune Contexture and Immunoscore in Cancer Prognosis and Therapeutic Efficacy. *Nat Rev Cancer* (2020) 20 (11):662–80. doi: 10.1038/s41568-020-0285-7
79. Faget J, Peters S, Quantin X, Meylan E, Bonnefoy N. Neutrophils in the Era of Immune Checkpoint Blockade. *J Immunother Cancer* (2021) 9(7):e002242. doi: 10.1136/jitc-2020-002242
80. Bullock K, Richmond A. Suppressing MDSC Recruitment to the Tumor Microenvironment by Antagonizing CXCR2 to Enhance the Efficacy of Immunotherapy. *Cancers* (2021) 13(24):6293. doi: 10.3390/cancers13246293
81. Highfill SL, Cui Y, Giles AJ, Smith JP, Zhang H, Morse E, et al. Disruption of CXCR2-Mediated MDSC Tumor Trafficking Enhances Anti-PD1 Efficacy. *Sci Transl Med* (2014) 6(237):237ra67. doi: 10.1126/scitranslmed.3007974
82. Sun L, Clavijo PE, Robbins Y, Patel P, Friedman J, Greene S, et al. Inhibiting Myeloid-Derived Suppressor Cell Trafficking Enhances T Cell Immunotherapy. *JCI Insight* (2019) 4(7):e126853. doi: 10.1172/jci.insight.126853
83. Syntrix Biosystems, Inc. *A Phase 1, Open-Label, Dose-Escalation With Expansion Study of SX-682 in Subjects With Metastatic Melanoma Concurrently Treated With Pembrolizumab*. clinicaltrials.gov (2021). Available at: https://clinicaltrials.gov/ct2/show/NCT03161431. Report No.: NCT03161431.
84. Dunne R. *An Open-Label Phase 1 Study to Evaluate the Safety and Tolerability of SX-682 in Combination With Nivolumab as a Maintenance Therapy in Patients With Metastatic Pancreatic Ductal Adenocarcinoma*. clinicaltrials.gov (2021). Available at: https://clinicaltrials.gov/ct2/show/NCT04477343. Report No.: NCT04477343.
85. M.D. Anderson Cancer Center. *Phase Ib/II Trial of SX-682 in Combination With Nivolumab for Refractory RAS Mutated (RAS) Microsatellite Stable (MSS) Metastatic Colorectal Cancer (mCRC) (STOPTRAFFIC-1)*. clinicaltrials.gov (2021). Available at: https://clinicaltrials.gov/ct2/show/NCT04599140. Report No.: NCT04599140.
86. Biasci D, Smoragiewicz M, Connell CM, Wang Z, Gao Y, Thaventhiran JED, et al. CXCR4 Inhibition in Human Pancreatic and Colorectal Cancers Induces an Integrated Immune Response. *PNAS* (2020) 117(46):28960–70. doi: 10.1073/pnas.2013644117
87. M.D. Anderson Cancer Center. *A Phase IIb Pilot Study to Assess the Efficacy, Safety, and Pharmacodynamics Effects of Pembrolizumab and BL-8040 in Patients With Metastatic Pancreatic Cancer*. clinicaltrials.gov (2020). Available at: https://clinicaltrials.gov/ct2/show/NCT02907099. Report No.: NCT02907099.
88. Liu Q, Li Z, Gao J-L, Wan W, Ganesan S, McDermott DH, et al. CXCR4 Antagonist AMD3100 Redistributes Leukocytes From Primary Immune Organs to Secondary Immune Organs, Lung, and Blood in Mice. *Eur J Immunol* (2015) 45(6):1855–67. doi: 10.1002/eji.201445245
89. Devi S, Wang Y, Chew WK, Lima R, A-González N, Mattar CNZ, et al. Neutrophil Mobilization *via* Plerixafor-Mediated CXCR4 Inhibition Arises From Lung Demargination and Blockade of Neutrophil Homing to the Bone Marrow. *J Exp Med* (2013) 210(11):2321–36. doi: 10.1084/jem.20130056
90. Fridlender ZG, Sun J, Kim S, Kapoor V, Cheng G, Ling L, et al. Polarization of Tumor-Associated Neutrophil Phenotype by TGF-Beta: "N1" Versus "N2" TAN. *Cancer Cell* (2009) 16(3):183–94. doi: 10.1016/j.ccr.2009.06.017

91. Horn LA, Riskin J, Hempel HA, Fousek K, Lind H, Hamilton DH, et al. Simultaneous Inhibition of CXCR1/2, TGF-β, and PD-L1 Remodels the Tumor and Its Microenvironment to Drive Antitumor Immunity. *J Immunother Cancer* (2020) 8(1):e000326. doi: 10.1136/jitc-2019-000326
92. National Cancer Institute (NCI). *Phase I/II Trial Investigating the Safety, Tolerability, Pharmacokinetics, Immune and Clinical Activity of SX-682 in Combination With BinTrafusp Alfa (M7824 or TGF-Beta "Trap"/PD-L1) With CV301 TRICOM in Advanced Solid Tumors (STAT)*. clinicaltrials.gov (2021). Available at: https://clinicaltrials.gov/ct2/show/NCT04574583. Report No.: NCT04574583.
93. Zhang M, Huang L, Ding G, Huang H, Cao G, Sun X, et al. Interferon Gamma Inhibits CXCL8-CXCR2 Axis Mediated Tumor-Associated Macrophages Tumor Trafficking and Enhances Anti-PD1 Efficacy in Pancreatic Cancer. *J Immunother Cancer* (2020) 8(1):e000308. doi: 10.1136/jitc-2019-000308
94. Fox Chase Cancer Center. *Combination Immunotherapy With Interferon-Gamma and Nivolumab for Patients With Advanced Solid Tumors: A Phase 1 Study*. clinicaltrials.gov (2019). Available at: https://clinicaltrials.gov/ct2/show/NCT02614456. Report No.: NCT02614456.
95. Shojaei F, Wu X, Malik AK, Zhong C, Baldwin ME, Schanz S, et al. Tumor Refractoriness to Anti-VEGF Treatment Is Mediated by CD11b+Gr1+ Myeloid Cells. *Nat Biotechnol* (2007) 25(8):911–20. doi: 10.1038/nbt1323
96. Itatani Y, Yamamoto T, Zhong C, Molinolo AA, Ruppel J, Hegde P, et al. Suppressing Neutrophil-Dependent Angiogenesis Abrogates Resistance to Anti-VEGF Antibody in a Genetic Model of Colorectal Cancer. *PNAS* (2020) 117(35):21598–608. doi: 10.1073/pnas.2008112117
97. Schiffmann LM, Fritsch M, Gebauer F, Günther SD, Stair NR, Seeger JM, et al. Tumour-Infiltrating Neutrophils Counteract Anti-VEGF Therapy in Metastatic Colorectal Cancer. *Br J Cancer* (2019) 120(1):69–78. doi: 10.1038/s41416-018-0198-3
98. Liang J, Piao Y, Holmes L, Fuller GN, Henry V, Tiao N, et al. Neutrophils Promote the Malignant Glioma Phenotype Through S100A4. *Clin Cancer Res* (2014) 20(1):187–98. doi: 10.1158/1078-0432.CCR-13-1279
99. Galdiero MR, Bianchi P, Grizzi F, Di Caro G, Basso G, Ponzetta A, et al. Occurrence and Significance of Tumor-Associated Neutrophils in Patients With Colorectal Cancer. *Int J Cancer* (2016) 139(2):446–56. doi: 10.1002/ijc.30076
100. Zhou G, Peng K, Song Y, Yang W, Shu W, Yu T, et al. CD177+ Neutrophils Suppress Epithelial Cell Tumourigenesis in Colitis-Associated Cancer and Predict Good Prognosis in Colorectal Cancer. *Carcinogenesis* (2018) 39 (2):272–82. doi: 10.1093/carcin/bgx142
101. Shaul ME, Fridlender ZG. Tumour-Associated Neutrophils in Patients With Cancer. *Nat Rev Clin Oncol* (2019) 16(10):601–20. doi: 10.1038/s41571-019-0222-4
102. Zhou S-L, Zhou Z-J, Hu Z-Q, Huang X-W, Wang Z, Chen E-B, et al. Tumor-Associated Neutrophils Recruit Macrophages and T-Regulatory Cells to Promote Progression of Hepatocellular Carcinoma and Resistance to Sorafenib. *Gastroenterology* (2016) 150(7):1646–1658.e17. doi: 10.1053/j.gastro.2016.02.040
103. Arvanitakis K, Mitroulis I, Germanidis G. Tumor-Associated Neutrophils in Hepatocellular Carcinoma Pathogenesis, Prognosis, and Therapy. *Cancers* (2021) 13(12):2899. doi: 10.3390/cancers13122899
104. Cheng Y, Mo F, Li Q, Han X, Shi H, Chen S, et al. Targeting CXCR2 Inhibits the Progression of Lung Cancer and Promotes Therapeutic Effect of Cisplatin. *Mol Cancer* (2021) 20(1):62. doi: 10.1186/s12943-021-01355-1
105. Nywening TM, Belt BA, Cullinan DR, Panni RZ, Han BJ, Sanford DE, et al. Targeting Both Tumour-Associated CXCR2+ Neutrophils and CCR2+ Macrophages Disrupts Myeloid Recruitment and Improves Chemotherapeutic Responses in Pancreatic Ductal Adenocarcinoma. *Gut* (2018) 67(6):1112–23. doi: 10.1136/gutjnl-2017-313738
106. Bhattacharya U, Gutter-Kapon L, Kan T, Boyango I, Barash U, Yang S-M, et al. Heparanase and Chemotherapy Synergize to Drive Macrophage Activation and Enhance Tumor Growth. *Cancer Res* (2020) 80(1):57–68. doi: 10.1158/0008-5472.CAN-19-1676
107. Crawford J, Dale DC, Lyman GH. Chemotherapy-Induced Neutropenia. *Cancer* (2004) 100(2):228–37. doi: 10.1002/cncr.11882
108. Lalami Y, Klastersky J. Impact of Chemotherapy-Induced Neutropenia (CIN) and Febrile Neutropenia (FN) on Cancer Treatment Outcomes: An Overview About Well-Established and Recently Emerging Clinical Data. *Crit Rev Oncol Hematol* (2017) 120:163–79. doi: 10.1016/j.critrevonc.2017.11.005
109. Feins S, Kong W, Williams EF, Milone MC, Fraietta JA. An Introduction to Chimeric Antigen Receptor (CAR) T-Cell Immunotherapy for Human Cancer. *Am J Hematol* (2019) 94(S1):S3–9. doi: 10.1002/ajh.25418
110. Veglia F, Tyurin VA, Blasi M, De Leo A, Kossenkov AV, Donthireddy L, et al. Fatty Acid Transport Protein 2 Reprograms Neutrophils in Cancer. *Nature* (2019) 569(7754):73–8. doi: 10.1038/s41586-019-1118-2
111. Matlung HL, Babes L, Zhao XW, van Houdt M, Treffers LW, van Rees DJ, et al. Neutrophils Kill Antibody-Opsonized Cancer Cells by Trogoptosis. *Cell Rep* (2018) 23(13):3946–3959.e6. doi: 10.1016/j.celrep.2018.05.082
112. Wynn TA, Chawla A, Pollard JW. Macrophage Biology in Development, Homeostasis and Disease. *Nature* (2013) 496(7446):445–55. doi: 10.1038/nature12034
113. Yona S, Kim K-W, Wolf Y, Mildner A, Varol D, Breker M, et al. Fate Mapping Reveals Origins and Dynamics of Monocytes and Tissue Macrophages Under Homeostasis. *Immunity* (2013) 38(1):79–91. doi: 10.1016/j.immuni.2012.12.001
114. Gordon S, Plüddemann A. The Mononuclear Phagocytic System. *Gener Divers Front Immunol* (2019) 10:1893. doi: 10.3389/fimmu.2019.01893
115. Murray PJ, Allen JE, Biswas SK, Fisher EA, Gilroy DW, Goerdt S, et al. Macrophage Activation and Polarization: Nomenclature and Experimental Guidelines. *Immunity* (2014) 41(1):14–20. doi: 10.1016/j.immuni.2014.06.008
116. Davies LC, Jenkins SJ, Allen JE, Taylor PR. Tissue-Resident Macrophages. *Nat Immunol* (2013) 14(10):986–95. doi: 10.1038/ni.2705
117. Schulz C, Gomez Perdiguero E, Chorro L, Szabo-Rogers H, Cagnard N, Kierdorf K, et al. A Lineage of Myeloid Cells Independent of Myb and Hematopoietic Stem Cells. *Science* (2012) 336(6077):86–90. doi: 10.1126/science.1219179
118. Hoeffel G, Chen J, Lavin Y, Low D, Almeida FF, See P, et al. C-Myb(+) Erythro-Myeloid Progenitor-Derived Fetal Monocytes Give Rise to Adult Tissue-Resident Macrophages. *Immunity* (2015) 42(4):665–78. doi: 10.1016/j.immuni.2015.03.011
119. Bowman RL, Klemm F, Akkari L, Pyonteck SM, Sevenich L, Quail DF, et al. Macrophage Ontogeny Underlies Differences in Tumor-Specific Education in Brain Malignancies. *Cell Rep* (2016) 17(9):2445–59. doi: 10.1016/j.celrep.2016.10.052
120. Ajami B, Bennett JL, Krieger C, Tetzlaff W, Rossi FMV. Local Self-Renewal can Sustain CNS Microglia Maintenance and Function Throughout Adult Life. *Nat Neurosci* (2007) 10(12):1538–43. doi: 10.1038/nn2014
121. Goldmann J, Kwidzinski E, Brandt C, Mahlo J, Richter D, Bechmann I. T Cells Traffic From Brain to Cervical Lymph Nodes *via* the Cribroid Plate and the Nasal Mucosa. *J Leuk Biol* (2006) 80(4):797–801. doi: 10.1189/jlb.0306176
122. Shi C, Pamer EG. Monocyte Recruitment During Infection and Inflammation. *Nat Rev Immunol* (2011) 11(11):762–74. doi: 10.1038/nri3070
123. Mass E, Ballesteros I, Farlik M, Halbritter F, Günther P, Crozet L, et al. Specification of Tissue-Resident Macrophages During Organogenesis. *Science* (2016) 353(6304):aaf4238. doi: 10.1126/science.aaf4238
124. Qian B-Z, Pollard JW. Macrophage Diversity Enhances Tumor Progression and Metastasis. *Cell* (2010) 141(1):39–51. doi: 10.1016/j.cell.2010.03.014
125. Kumar V, Cheng P, Condamine T, Mony S, Languino LR, McCaffrey JC, et al. CD45 Phosphatase Inhibits STAT3 Transcription Factor Activity in Myeloid Cells and Promotes Tumor-Associated Macrophage Differentiation. *Immunity* (2016) 44(2):303–15. doi: 10.1016/j.immuni.2016.01.014
126. Bronte V, Brandau S, Chen S-H, Colombo MP, Frey AB, Greten TF, et al. Recommendations for Myeloid-Derived Suppressor Cell Nomenclature and Characterization Standards. *Nat Commun* (2016) 7(1):12150. doi: 10.1038/ncomms12150
127. Bottazzi B, Erba E, Nobili N, Fazioli F, Rambaldi A, Mantovani A. A Paracrine Circuit in the Regulation of the Proliferation of Macrophages Infiltrating Murine Sarcomas. *J Immunol* (1990) 144(6):2409–12.
128. Campbell MJ, Tonlaar NY, Garwood ER, Huo D, Moore DH, Khramtsov AI, et al. Proliferating Macrophages Associated With High Grade, Hormone Receptor Negative Breast Cancer and Poor Clinical Outcome. *Breast Cancer Res Treat* (2011) 128(3):703–11. doi: 10.1007/s10549-010-1154-y

129. Movahedi K, Laoui D, Gysemans C, Baeten M, Stangé G, den BJV, et al. Different Tumor Microenvironments Contain Functionally Distinct Subsets of Macrophages Derived From Ly6C(high) Monocytes. *Cancer Res* (2010) 70 (14):5728–39. doi: 10.1158/0008-5472.CAN-09-4672
130. Pittet MJ, Michielin O, Migliorini D. Clinical Relevance of Tumour-Associated Macrophages. *Nat Rev Clin Oncol* (2022), 1–20. doi: 10.1038/s41571-022-00620-6
131. Chen Z, Feng X, Herting CJ, Garcia VA, Nie K, Pong WW, et al. Cellular and Molecular Identity of Tumor-Associated Macrophages in Glioblastoma. *Cancer Res* (2017) 77(9):2266–78. doi: 10.1158/0008-5472.CAN-16-2310
132. DeNardo DG, Barreto JB, Andreu P, Vasquez L, Tawfik D, Kolhatkar N, et al. CD4(+) T Cells Regulate Pulmonary Metastasis of Mammary Carcinomas by Enhancing Protumor Properties of Macrophages. *Cancer Cell* (2009) 16 (2):91–102. doi: 10.1016/j.ccr.2009.06.018
133. Evans R, Alexander P. Cooperation of Immune Lymphoid Cells With Macrophages in Tumour Immunity. *Nature* (1970) 228(5272):620–2. doi: 10.1038/228620a0
134. Mantovani A, Bottazzi B, Colotta F, Sozzani S, Ruco L. The Origin and Function of Tumor-Associated Macrophages. *Immunol Today* (1992) 13 (7):265–70. doi: 10.1016/0167-5699(92)90008-U
135. Adams DO, Hamilton TA. The Cell Biology of Macrophage Activation. *Annu Rev Immunol* (1984) 2:283–318. doi: 10.1146/annurev.iy.02.040184.001435
136. Prehn RT. The Immune Reaction as a Stimulator of Tumor Growth. *Science* (1972) 176(4031):170–1. doi: 10.1126/science.176.4031.170
137. Zhu Y, Herndon JM, Sojka DK, Kim K-W, Knolhoff BL, Zuo C, et al. Tissue-Resident Macrophages in Pancreatic Ductal Adenocarcinoma Originate From Embryonic Hematopoiesis and Promote Tumor Progression. *Immunity* (2017) 47(2):323–338.e6. doi: 10.1016/j.immuni.2017.07.014
138. Lin EY, Nguyen AV, Russell RG, Pollard JW. Colony-Stimulating Factor 1 Promotes Progression of Mammary Tumors to Malignancy. *J Exp Med* (2001) 193(6):727–40. doi: 10.1084/jem.193.6.727
139. Hanahan D, Coussens LM. Accessories to the Crime: Functions of Cells Recruited to the Tumor Microenvironment. *Cancer Cell* (2012) 21(3):309–22. doi: 10.1016/j.ccr.2012.02.022
140. Pollard JW. Trophic Macrophages in Development and Disease. *Nat Rev Immunol* (2009) 9(4):259–70. doi: 10.1038/nri2528
141. Helm O, Held-Feindt J, Grage-Griebenow E, Reiling N, Ungefroren H, Vogel I, et al. Tumor-Associated Macrophages Exhibit Pro- and Anti-Inflammatory Properties by Which They Impact on Pancreatic Tumorigenesis. *Int J Cancer* (2014) 135(4):843–61. doi: 10.1002/ijc.28736
142. Lewis JS, Landers RJ, Underwood JC, Harris AL, Lewis CE. Expression of Vascular Endothelial Growth Factor by Macrophages Is Up-Regulated in Poorly Vascularized Areas of Breast Carcinomas. *J Pathol* (2000) 192(2):150–8. doi: 10.1002/1096-9896(2000)9999:9999<::AID-PATH687>3.0.CO;2-G
143. Stockmann C, Doedens A, Weidemann A, Zhang N, Takeda N, Greenberg JI, et al. Deletion of Vascular Endothelial Growth Factor in Myeloid Cells Accelerates Tumorigenesis. *Nature* (2008) 456(7223):814–8. doi: 10.1038/nature07445
144. Leek RD, Lewis CE, Whitehouse R, Greenall M, Clarke J, Harris AL. Association of Macrophage Infiltration With Angiogenesis and Prognosis in Invasive Breast Carcinoma. *Cancer Res* (1996) 56(20):4625–9.
145. Franklin RA, Liao W, Sarkar A, Kim MV, Bivona MR, Liu K, et al. The Cellular and Molecular Origin of Tumor-Associated Macrophages. *Science* (2014) 344(6186):921–5. doi: 10.1126/science.1252510
146. Qian B-Z, Li J, Zhang H, Kitamura T, Zhang J, Campion LR, et al. CCL2 Recruits Inflammatory Monocytes to Facilitate Breast-Tumour Metastasis. *Nature* (2011) 475(7355):222–5. doi: 10.1038/nature10138
147. Hanna RN, Cekic C, Sag D, Tacke R, Thomas GD, Nowyhed H, et al. Patrolling Monocytes Control Tumor Metastasis to the Lung. *Science* (2015) 350(6263):985–90. doi: 10.1126/science.aac9407
148. Gordon SR, Maute RL, Dulken BW, Hutter G, George BM, McCracken MN, et al. PD-1 Expression by Tumour-Associated Macrophages Inhibits Phagocytosis and Tumour Immunity. *Nature* (2017) 545(7655):495–9. doi: 10.1038/nature22396
149. Joyce JA, Pollard JW. Microenvironmental Regulation of Metastasis. *Nat Rev Cancer* (2009) 9(4):239–52. doi: 10.1038/nrc2618
150. Guo X, Zhao Y, Yan H, Yang Y, Shen S, Dai X, et al. Single Tumor-Initiating Cells Evade Immune Clearance by Recruiting Type II Macrophages. *Genes Dev* (2017) 31(3):247–59. doi: 10.1101/gad.294348.116
151. Mazzoni M, Mauro G, Erreni M, Romeo P, Minna E, Vizioli MG, et al. Senescent Thyrocytes and Thyroid Tumor Cells Induce M2-Like Macrophage Polarization of Human Monocytes *via* a PGE2-Dependent Mechanism. *J Exp Clin Cancer Res* (2019) 38(1):208. doi: 10.1186/s13046-019-1198-8
152. Porta C, Consonni FM, Morlacchi S, Sangaletti S, Bleve A, Totaro MG, et al. Tumor-Derived Prostaglandin E2 Promotes P50 NF-κb-Dependent Differentiation of Monocytic MDSCs. *Cancer Res* (2020) 80(13):2874–88. doi: 10.1158/0008-5472.CAN-19-2843
153. Pan W, Zhu S, Qu K, Meeth K, Cheng J, He K, et al. The DNA Methylcytosine Dioxygenase Tet2 Sustains Immunosuppressive Function of Tumor-Infiltrating Myeloid Cells to Promote Melanoma Progression. *Immunity* (2017) 47(2):284–297.e5. doi: 10.1016/j.immuni.2017.07.020
154. Kryczek I, Zou L, Rodriguez P, Zhu G, Wei S, Mottram P, et al. B7-H4 Expression Identifies a Novel Suppressive Macrophage Population in Human Ovarian Carcinoma. *J Exp Med* (2006) 203(4):871–81. doi: 10.1084/jem.20050930
155. Wang L, Rubinstein R, Lines JL, Wasiuk A, Ahonen C, Guo Y, et al. VISTA, a Novel Mouse Ig Superfamily Ligand That Negatively Regulates T Cell Responses. *J Exp Med* (2011) 208(3):577–92. doi: 10.1084/jem.20100619
156. Ruffell B, Affara NI, Coussens LM. Differential Macrophage Programming in the Tumor Microenvironment. *Trends Immunol* (2012) 33(3):119–26. doi: 10.1016/j.it.2011.12.001
157. Linde N, Casanova-Acebes M, Sosa MS, Mortha A, Rahman A, Farias E, et al. Macrophages Orchestrate Breast Cancer Early Dissemination and Metastasis. *Nat Commun* (2018) 9(1):21. doi: 10.1038/s41467-017-02481-5
158. Wang W, Liu Y, Guo J, He H, Mi X, Chen C, et al. miR-100 Maintains Phenotype of Tumor-Associated Macrophages by Targeting mTOR to Promote Tumor Metastasis *via* Stat5a/IL-1ra Pathway in Mouse Breast Cancer. *Oncogenesis* (2018) 7(12):1–17. doi: 10.1038/s41389-018-0106-y
159. Costa-Silva B, Aiello NM, Ocean AJ, Singh S, Zhang H, Thakur BK, et al. Pancreatic Cancer Exosomes Initiate Pre-Metastatic Niche Formation in the Liver. *Nat Cell Biol* (2015) 17(6):816–26. doi: 10.1038/ncb3169
160. Yin Z, Ma T, Huang B, Lin L, Zhou Y, Yan J, et al. Macrophage-Derived Exosomal microRNA-501-3p Promotes Progression of Pancreatic Ductal Adenocarcinoma Through the TGFBR3-Mediated TGF-β Signaling Pathway. *J Exp Clin Cancer Res* (2019) 38(1):310. doi: 10.1186/s13046-019-1313-x
161. Lan J, Sun L, Xu F, Liu L, Hu F, Song D, et al. M2 Macrophage-Derived Exosomes Promote Cell Migration and Invasion in Colon Cancer. *Cancer Res* (2019) 79(1):146–58. doi: 10.1158/0008-5472.CAN-18-0014
162. Peinado H, Alečković M, Lavotshkin S, Matei I, Costa-Silva B, Moreno-Bueno G, et al. Melanoma Exosomes Educate Bone Marrow Progenitor Cells Toward a Pro-Metastatic Phenotype Through MET. *Nat Med* (2012) 18 (6):883–91. doi: 10.1038/nm.2753
163. Kitamura T, Qian B-Z, Soong D, Cassetta L, Noy R, Sugano G, et al. CCL2-Induced Chemokine Cascade Promotes Breast Cancer Metastasis by Enhancing Retention of Metastasis-Associated Macrophages. *J Exp Med* (2015) 212(7):1043–59. doi: 10.1084/jem.20141836
164. van Deventer HW, Palmieri DA, Wu QP, McCook EC, Serody JS. Circulating Fibrocytes Prepare the Lung for Cancer Metastasis by Recruiting Ly-6c+ Monocytes *Via* Ccl2. *J Immunol* (2013) 190(9):4861–7. doi: 10.4049/jimmunol.1202857
165. Nosaka T, Baba T, Tanabe Y, Sasaki S, Nishimura T, Imamura Y, et al. Alveolar Macrophages Drive Hepatocellular Carcinoma Lung Metastasis by Generating Leukotriene B4. *J Immunol* (2018) 200(5):1839–52. doi: 10.4049/jimmunol.1700544
166. Sharma SK, Chintala NK, Vadrevu SK, Patel J, Karbowniczek M, Markiewski MM. Pulmonary Alveolar Macrophages Contribute to the Premetastatic Niche by Suppressing Antitumor T Cell Responses in the Lungs. *J Immunol* (2015) 194(11):5529–38. doi: 10.4049/jimmunol.1403215
167. Kimura Y, Inoue A, Hangai S, Saijo S, Negishi H, Nishio J, et al. The Innate Immune Receptor Dectin-2 Mediates the Phagocytosis of Cancer Cells by Kupffer Cells for the Suppression of Liver Metastasis. *Proc Natl Acad Sci USA* (2016) 113(49):14097–102. doi: 10.1073/pnas.1617903113

168. Hambardzumyan D, Gutmann DH, Kettenmann H. The Role of Microglia and Macrophages in Glioma Maintenance and Progression. *Nat Neurosci* (2016) 19(1):20–7. doi: 10.1038/nn.4185
169. Pyonteck SM, Akkari L, Schuhmacher AJ, Bowman RL, Sevenich L, Quail DF, et al. CSF-1R Inhibition Alters Macrophage Polarization and Blocks Glioma Progression. *Nat Med* (2013) 19(10):1264–72. doi: 10.1038/nm.3337
170. Quail DF, Bowman RL, Akkari L, Quick ML, Schuhmacher AJ, Huse JT, et al. The Tumor Microenvironment Underlies Acquired Resistance to CSF-1R Inhibition in Gliomas. *Science* (2016) 352(6288):aad3018. doi: 10.1126/science.aad3018
171. Qiao S, Qian Y, Xu G, Luo Q, Zhang Z. Long-Term Characterization of Activated Microglia/Macrophages Facilitating the Development of Experimental Brain Metastasis Through Intravital Microscopic Imaging. *J Neuroinflammation* (2019) 16(1):4. doi: 10.1186/s12974-018-1389-9
172. Klemm F, Maas RR, Bowman RL, Kornete M, Soukup K, Nassiri S, et al. Interrogation of the Microenvironmental Landscape in Brain Tumors Reveals Disease-Specific Alterations of Immune Cells. *Cell* (2020) 181 (7):1643–1660.e17. doi: 10.1016/j.cell.2020.05.007
173. Colotta F, Peri G, Villa A, Mantovani A. Rapid Killing of Actinomycin D-Treated Tumor Cells by Human Mononuclear Cells. I. Effectors Belong to the Monocyte-Macrophage Lineage. *J Immunol* (1984) 132(2):936–44.
174. Mantovani A, Polentarutti N, Luini W, Peri G, Spreafico F. Role of Host Defense Mechanisms in the Antitumor Activity of Adriamycin and Daunomycin in Mice2. *JNCI: J Natl Cancer Inst* (1979) 63(1):61–6.
175. Ma Y, Galluzzi L, Zitvogel L, Kroemer G. Autophagy and Cellular Immune Responses. *Immunity* (2013) 39(2):211–27. doi: 10.1016/j.immuni.2013.07.017
176. Galluzzi L, Buqué A, Kepp O, Zitvogel L, Kroemer G. Immunological Effects of Conventional Chemotherapy and Targeted Anticancer Agents. *Cancer Cell* (2015) 28(6):690–714. doi: 10.1016/j.ccell.2015.10.012
177. Pfirschke C, Engblom C, Rickelt S, Cortez-Retamozo V, Garris C, Pucci F, et al. Immunogenic Chemotherapy Sensitizes Tumors to Checkpoint Blockade Therapy. *Immunity* (2016) 44(2):343–54. doi: 10.1016/j.immuni.2015.11.024
178. D'Incalci M, Badri N, Galmarini CM, Allavena P. Trabectedin, a Drug Acting on Both Cancer Cells and the Tumour Microenvironment. *Br J Cancer* (2014) 111(4):646–50. doi: 10.1038/bjc.2014.149
179. Germano G, Frapolli R, Belgiovine C, Anselmo A, Pesce S, Liguori M, et al. Role of Macrophage Targeting in the Antitumor Activity of Trabectedin. *Cancer Cell* (2013) 23(2):249–62. doi: 10.1016/j.ccr.2013.01.008
180. Germano G, Frapolli R, Simone M, Tavecchio M, Erba E, Pesce S, et al. Antitumor and Anti-Inflammatory Effects of Trabectedin on Human Myxoid Liposarcoma Cells. *Cancer Res* (2010) 70(6):2235–44. doi: 10.1158/0008-5472.CAN-09-2335
181. Dijkgraaf EM, Heusinkveld M, Tummers B, Vogelpoel LTC, Goedemans R, Jha V, et al. Chemotherapy Alters Monocyte Differentiation to Favor Generation of Cancer-Supporting M2 Macrophages in the Tumor Microenvironment. *Cancer Res* (2013) 73(8):2480–92. doi: 10.1158/0008-5472.CAN-12-3542
182. Bruchard M, Mignot G, Derangère V, Chalmin F, Chevriaux A, Végran F, et al. Chemotherapy-Triggered Cathepsin B Release in Myeloid-Derived Suppressor Cells Activates the Nlrp3 Inflammasome and Promotes Tumor Growth. *Nat Med* (2013) 19(1):57–64. doi: 10.1038/nm.2999
183. Jinushi M, Chiba S, Yoshiyama H, Masutomi K, Kinoshita I, Dosaka-Akita H, et al. Tumor-Associated Macrophages Regulate Tumorigenicity and Anticancer Drug Responses of Cancer Stem/Initiating Cells. *PNAS* (2011) 108(30):12425–30. doi: 10.1073/pnas.1106645108
184. Hughes R, Qian B-Z, Rowan C, Muthana M, Keklikoglou I, Olson OC, et al. Perivascular M2 Macrophages Stimulate Tumor Relapse After Chemotherapy. *Cancer Res* (2015) 75(17):3479–91. doi: 10.1158/0008-5472.CAN-14-3587
185. Mitchem JB, Brennan DJ, Knolhoff BL, Belt BA, Zhu Y, Sanford DE, et al. Targeting Tumor-Infiltrating Macrophages Decreases Tumor-Initiating Cells, Relieves Immunosuppression, and Improves Chemotherapeutic Responses. *Cancer Res* (2013) 73(3):1128–41. doi: 10.1158/0008-5472.CAN-12-2731
186. Kridel R, Xerri L, Gelas-Dore B, Tan K, Feugier P, Vawda A, et al. The Prognostic Impact of CD163-Positive Macrophages in Follicular Lymphoma: A Study From the BC Cancer Agency and the Lymphoma Study Association. *Clin Cancer Res* (2015) 21(15):3428–35. doi: 10.1158/1078-0432.CCR-14-3253
187. Kroemer G, Galluzzi L, Kepp O, Zitvogel L. Immunogenic Cell Death in Cancer Therapy. *Annu Rev Immunol* (2013) 31(1):51–72. doi: 10.1146/annurev-immunol-032712-100008
188. Galluzzi L, Buqué A, Kepp O, Zitvogel L, Kroemer G. Immunogenic Cell Death in Cancer and Infectious Disease. *Nat Rev Immunol* (2017) 17(2):97–111. doi: 10.1038/nri.2016.107
189. Di Caro G, Cortese N, Castino GF, Grizzi F, Gavazzi F, Ridolfi C, et al. Dual Prognostic Significance of Tumour-Associated Macrophages in Human Pancreatic Adenocarcinoma Treated or Untreated With Chemotherapy. *Gut* (2016) 65(10):1710–20. doi: 10.1136/gutjnl-2015-309193
190. Malesci A, Bianchi P, Celesti G, Basso G, Marchesi F, Grizzi F, et al. Tumor-Associated Macrophages and Response to 5-Fluorouracil Adjuvant Therapy in Stage III Colorectal Cancer. *Oncoimmunology* (2017) 6(12):e1342918. doi: 10.1080/2162402X.2017.1342918
191. Kodumudi KN, Woan K, Gilvary DL, Sahakian E, Wei S, Djeu JY. A Novel Chemoimmunomodulating Property of Docetaxel: Suppression of Myeloid-Derived Suppressor Cells in Tumor Bearers. *Clin Cancer Res* (2010) 16 (18):4583–94. doi: 10.1158/1078-0432.CCR-10-0733
192. Mantovani A, Allavena P. The Interaction of Anticancer Therapies With Tumor-Associated Macrophages. *J Exp Med* (2015) 212(4):435–45. doi: 10.1084/jem.20150295
193. Paulus P, Stanley ER, Schäfer R, Abraham D, Aharinejad S. Colony-Stimulating Factor-1 Antibody Reverses Chemoresistance in Human MCF-7 Breast Cancer Xenografts. *Cancer Res* (2006) 66(8):4349–56. doi: 10.1158/0008-5472.CAN-05-3523
194. Salvagno C, Ciampricotti M, Tuit S, Hau C-S, van Weverwijk A, Coffelt SB, et al. Therapeutic Targeting of Macrophages Enhances Chemotherapy Efficacy by Unleashing Type I Interferon Response. *Nat Cell Biol* (2019) 21 (4):511–21. doi: 10.1038/s41556-019-0298-1
195. Neubert NJ, Schmittnaegel M, Bordry N, Nassiri S, Wald N, Martignier C, et al. T Cell-Induced CSF1 Promotes Melanoma Resistance to PD1 Blockade. *Sci Transl Med* (2018) 10(436):eaan3311. doi: 10.1126/scitranslmed.aan3311
196. Ho WJ, Jaffee EM. Macrophage-Targeting by CSF1/1R Blockade in Pancreatic Cancers. *Cancer Res* (2021) 81(24):6071–3. doi: 10.1158/0008-5472.CAN-21-3603
197. Yin Y, Yao S, Hu Y, Feng Y, Li M, Bian Z, et al. The Immune-Microenvironment Confers Chemoresistance of Colorectal Cancer Through Macrophage-Derived Il6. *Clin Cancer Res* (2017) 23(23):7375–87. doi: 10.1158/1078-0432.CCR-17-1283
198. Shree T, Olson OC, Elie BT, Kester JC, Garfall AL, Simpson K, et al. Macrophages and Cathepsin Proteases Blunt Chemotherapeutic Response in Breast Cancer. *Genes Dev* (2011) 25(23):2465–79. doi: 10.1101/gad.180331.111
199. Xu J, Escamilla J, Mok S, David J, Priceman S, West B, et al. CSF1R Signaling Blockade Stanches Tumor-Infiltrating Myeloid Cells and Improves the Efficacy of Radiotherapy in Prostate Cancer. *Cancer Res* (2013) 73 (9):2782–94. doi: 10.1158/0008-5472.CAN-12-3981
200. Durante M, Reppingen N, Held KD. Immunologically Augmented Cancer Treatment Using Modern Radiotherapy. *Trends Mol Med* (2013) 19(9):565–82. doi: 10.1016/j.molmed.2013.05.007
201. Klug F, Prakash H, Huber PE, Seibel T, Bender N, Halama N, et al. Low-Dose Irradiation Programs Macrophage Differentiation to an iNOS$^+$/M1 Phenotype That Orchestrates Effective T Cell Immunotherapy. *Cancer Cell* (2013) 24(5):589–602. doi: 10.1016/j.ccr.2013.09.014
202. Teresa Pinto A, Laranjeiro Pinto M, Patrícia Cardoso A, Monteiro C, Teixeira Pinto M, Filipe Maia A, et al. Ionizing Radiation Modulates Human Macrophages Towards a Pro-Inflammatory Phenotype Preserving Their Pro-Invasive and Pro-Angiogenic Capacities. *Sci Rep* (2016) 6:18765. doi: 10.1038/srep18765
203. Niesel K, Schulz M, Anthes J, Alekseeva T, Jadranka M, Salamero-Boix A, et al. The Immune Suppressive Microenvironment Affects Efficacy of Radio-Immunotherapy in Brain Metastasis. *EMBO Mol Med* (2021) 13(5):e13412. doi: 10.15252/emmm.202013412
204. Iida N, Dzutsev A, Stewart CA, Smith L, Bouladoux N, Weingarten RA, et al. Commensal Bacteria Control Cancer Response to Therapy by Modulating

the Tumor Microenvironment. *Science* (2013) 342(6161):967–70. doi: 10.1126/science.1240527
205. Viaud S, Saccheri F, Mignot G, Yamazaki T, Daillère R, Hannani D, et al. The Intestinal Microbiota Modulates the Anticancer Immune Effects of Cyclophosphamide. *Science* (2013) 342(6161):971–6. doi: 10.1126/science.1240537
206. Vétizou M, Pitt JM, Daillère R, Lepage P, Waldschmitt N, Flament C, et al. Anticancer Immunotherapy by CTLA-4 Blockade Relies on the Gut Microbiota. *Science* (2015) 350(6264):1079–84. doi: 10.1126/science.aad1329
207. Alexander JL, Wilson ID, Teare J, Marchesi JR, Nicholson JK, Kinross JM. Gut Microbiota Modulation of Chemotherapy Efficacy and Toxicity. *Nat Rev Gastroenterol Hepatol* (2017) 14(6):356–65. doi: 10.1038/nrgastro.2017.20
208. Hayase E, Jenq RR. Role of the Intestinal Microbiome and Microbial-Derived Metabolites in Immune Checkpoint Blockade Immunotherapy of Cancer. *Genome Med* (2021) 13(1):107. doi: 10.1186/s13073-021-00923-w
209. Vacchelli E, Ma Y, Baracco EE, Sistigu A, Enot DP, Pietrocola F, et al. Chemotherapy-Induced Antitumor Immunity Requires Formyl Peptide Receptor 1. *Science* (2015) 350(6263):972–8. doi: 10.1126/science.aad0779
210. Baracco EE, Pietrocola F, Buqué A, Bloy N, Senovilla L, Zitvogel L, et al. Inhibition of Formyl Peptide Receptor 1 Reduces the Efficacy of Anticancer Chemotherapy Against Carcinogen-Induced Breast Cancer. *Oncoimmunology* (2016) 5(6):e1139275. doi: 10.1080/2162402X.2016.1139275
211. Cavnar MJ, Zeng S, Kim TS, Sorenson EC, Ocuin LM, Balachandran VP, et al. KIT Oncogene Inhibition Drives Intratumoral Macrophage M2 Polarization. *J Exp Med* (2013) 210(13):2873–86. doi: 10.1084/jem.20130875
212. Sprinzl MF, Reisinger F, Puschnik A, Ringelhan M, Ackermann K, Hartmann D, et al. Sorafenib Perpetuates Cellular Anticancer Effector Functions by Modulating the Crosstalk Between Macrophages and Natural Killer Cells. *Hepatology* (2013) 57(6):2358–68. doi: 10.1002/hep.26328
213. Qian B-Z, Zhang H, Li J, He T, Yeo E-J, Soong DYH, et al. FLT1 Signaling in Metastasis-Associated Macrophages Activates an Inflammatory Signature That Promotes Breast Cancer Metastasis. *J Exp Med* (2015) 212(9):1433–48. doi: 10.1084/jem.20141555
214. Larionova I, Tuguzbaeva G, Ponomaryova A, Stakheyeva M, Cherdyntseva N, Pavlov V, et al. Tumor-Associated Macrophages in Human Breast, Colorectal, Lung, Ovarian and Prostate Cancers. *Front Oncol* (2020), 10:566511. doi: 10.3389/fonc.2020.566511
215. Algars A, Irjala H, Vaittinen S, Huhtinen H, Sundström J, Salmi M, et al. Type and Location of Tumor-Infiltrating Macrophages and Lymphatic Vessels Predict Survival of Colorectal Cancer Patients. *Int J Cancer* (2012) 131(4):864–73. doi: 10.1002/ijc.26457
216. Vankerckhoven A, Wouters R, Mathivet T, Ceusters J, Baert T, Van Hoylandt A, et al. Opposite Macrophage Polarization in Different Subsets of Ovarian Cancer: Observation From a Pilot Study. *Cells* (2020) 9(2):305. doi: 10.3390/cells9020305
217. Kloepper J, Riedemann L, Amoozgar Z, Seano G, Susek K, Yu V, et al. Ang-2/VEGF Bispecific Antibody Reprograms Macrophages and Resident Microglia to Anti-Tumor Phenotype and Prolongs Glioblastoma Survival. *PNAS* (2016) 113(16):4476–81. doi: 10.1073/pnas.1525360113
218. Jassar AS, Suzuki E, Kapoor V, Sun J, Silverberg MB, Cheung L, et al. Activation of Tumor-Associated Macrophages by the Vascular Disrupting Agent 5,6-Dimethylxanthenone-4-Acetic Acid Induces an Effective CD8+ T-Cell–Mediated Antitumor Immune Response in Murine Models of Lung Cancer and Mesothelioma. *Cancer Res* (2005) 65(24):11752–61. doi: 10.1158/0008-5472.CAN-05-1658
219. Loke P, Allison JP. PD-L1 and PD-L2 are Differentially Regulated by Th1 and Th2 Cells. *Proc Natl Acad Sci USA* (2003) 100(9):5336–41. doi: 10.1073/pnas.0931259100
220. Noman MZ, Desantis G, Janji B, Hasmim M, Karray S, Dessen P, et al. PD-L1 Is a Novel Direct Target of HIF-1α, and Its Blockade Under Hypoxia Enhanced MDSC-Mediated T Cell Activation. *J Exp Med* (2014) 211(5):781–90. doi: 10.1084/jem.20131916
221. Relecom A, Merhi M, Inchakalody V, Uddin S, Rinchai D, Bedognetti D, et al. Emerging Dynamics Pathways of Response and Resistance to PD-1 and CTLA-4 Blockade: Tackling Uncertainty by Confronting Complexity. *J Exp Clin Cancer Res* (2021) 40(1):74. doi: 10.1186/s13046-021-01872-3
222. Tumeh PC, Harview CL, Yearley JH, Shintaku IP, Taylor EJM, Robert L, et al. PD-1 Blockade Induces Responses by Inhibiting Adaptive Immune Resistance. *Nature* (2014) 515(7528):568–71. doi: 10.1038/nature13954
223. Selby MJ, Engelhardt JJ, Quigley M, Henning KA, Chen T, Srinivasan M, et al. Anti-CTLA-4 Antibodies of IgG2a Isotype Enhance Antitumor Activity Through Reduction of Intratumoral Regulatory T Cells. *Cancer Immunol Res* (2013) 1(1):32–42. doi: 10.1158/2326-6066.CIR-13-0013
224. Stone EL, O'Brien EM. Investigating the Effect of Anti-CTLA-4 on Tumor-Infiltrating Effector T Cells. *J Immunol* (2017) 198(1 Supplement):56.12–2.
225. Romano E, Kusio-Kobialka M, Foukas PG, Baumgaertner P, Meyer C, Ballabeni P, et al. Ipilimumab-Dependent Cell-Mediated Cytotoxicity of Regulatory T Cells *Ex Vivo* by Nonclassical Monocytes in Melanoma Patients. *Proc Natl Acad Sci USA* (2015) 112(19):6140–5. doi: 10.1073/pnas.1417320112
226. Vaddepally RK, Kharel P, Pandey R, Garje R, Chandra AB. Review of Indications of FDA-Approved Immune Checkpoint Inhibitors Per NCCN Guidelines With the Level of Evidence. *Cancers (Basel)* (2020) 12(3):738. doi: 10.3390/cancers12030738
227. Perdiguero EG, Geissmann F. The Development and Maintenance of Resident Macrophages. *Nat Immunol* (2016) 17(1):2–8. doi: 10.1038/ni.3341
228. Lin H, Lee E, Hestir K, Leo C, Huang M, Bosch E, et al. Discovery of a Cytokine and its Receptor by Functional Screening of the Extracellular Proteome. *Science* (2008) 320(5877):807–11. doi: 10.1126/science.1154370
229. Baghdadi M, Wada H, Nakanishi S, Abe H, Han N, Putra WE, et al. Chemotherapy-Induced IL34 Enhances Immunosuppression by Tumor-Associated Macrophages and Mediates Survival of Chemoresistant Lung Cancer Cells. *Cancer Res* (2016) 76(20):6030–42. doi: 10.1158/0008-5472.CAN-16-1170
230. Scholl SM, Lidereau R, de la Rochefordière A, Le-Nir CC, Mosseri V, Noguès C, et al. Circulating Levels of the Macrophage Colony Stimulating Factor CSF-1 in Primary and Metastatic Breast Cancer Patients. *Pilot Study Breast Cancer Res Treat* (1996) 39(3):275–83. doi: 10.1007/BF01806155
231. Kowal J, Kornete M, Joyce JA. Re-Education of Macrophages as a Therapeutic Strategy in Cancer. *Immunotherapy* (2019) 11(8):677–89. doi: 10.2217/imt-2018-0156
232. Klemm F, Möckl A, Salamero-Boix A, Alekseeva T, Schäffer A, Schulz M, et al. Compensatory CSF2-Driven Macrophage Activation Promotes Adaptive Resistance to CSF1R Inhibition in Breast-to-Brain Metastasis. *Nat Cancer* (2021) 2(10):1086–101. doi: 10.1038/s43018-021-00254-0
233. Olson OC, Kim H, Quail DF, Foley EA, Joyce JA. Tumor-Associated Macrophages Suppress the Cytotoxic Activity of Antimitotic Agents. *Cell Rep* (2017) 19(1):101–13. doi: 10.1016/j.celrep.2017.03.038
234. Valero JG, Matas-Céspedes A, Arenas F, Rodriguez V, Carreras J, Serrat N, et al. The Receptor of the Colony-Stimulating Factor-1 (CSF-1R) Is a Novel Prognostic Factor and Therapeutic Target in Follicular Lymphoma. *Leukemia* (2021) 35(9):2635–49. doi: 10.1038/s41375-021-01201-9
235. Stafford JH, Hirai T, Deng L, Chernikova SB, Urata K, West BL, et al. Colony Stimulating Factor 1 Receptor Inhibition Delays Recurrence of Glioblastoma After Radiation by Altering Myeloid Cell Recruitment and Polarization. *Neuro Oncol* (2016) 18(6):797–806. doi: 10.1093/neuonc/nov272
236. Peña CG, Nakada Y, Saatcioglu HD, Aloisio GM, Cuevas I, Zhang S, et al. LKB1 Loss Promotes Endometrial Cancer Progression *via* CCL2-Dependent Macrophage Recruitment. *J Clin Invest* (2015) 125(11):4063–76. doi: 10.1172/JCI82152
237. Hao Q, Vadgama JV, Wang P. CCL2/CCR2 Signaling in Cancer Pathogenesis. *Cell Commun Signaling* (2020) 18(1):82. doi: 10.1186/s12964-020-00589-8
238. Lebrecht A, Grimm C, Lantzsch T, Ludwig E, Hefler L, Ulbrich E, et al. Monocyte Chemoattractant Protein-1 Serum Levels in Patients With Breast Cancer. *Tumour Biol* (2004) 25(1–2):14–7. doi: 10.1159/000077718
239. Loberg RD, Ying C, Craig M, Yan L, Snyder LA, Pienta KJ. CCL2 as an Important Mediator of Prostate Cancer Growth *In Vivo* Through the Regulation of Macrophage Infiltration. *Neoplasia* (2007) 9(7):556–62. doi: 10.1593/neo.07307
240. Bonapace L, Coissieux M-M, Wyckoff J, Mertz KD, Varga Z, Junt T, et al. Cessation of CCL2 Inhibition Accelerates Breast Cancer Metastasis by Promoting Angiogenesis. *Nature* (2014) 515(7525):130–3. doi: 10.1038/nature13862

241. Nywening TM, Wang-Gillam A, Sanford DE, Belt BA, Panni RZ, Cusworth BM, et al. Targeting Tumour-Associated Macrophages With CCR2 Inhibition in Combination With FOLFIRINOX in Patients With Borderline Resectable and Locally Advanced Pancreatic Cancer: A Single-Centre, Open-Label, Dose-Finding, non-Randomised, Phase 1b Trial. *Lancet Oncol* (2016) 17(5):651–62. doi: 10.1016/S1470-2045(16)00078-4
242. Zhao L, Lim SY, Gordon-Weeks AN, Tapmeier TT, Im JH, Cao Y, et al. Recruitment of a Myeloid Cell Subset (CD11b/Gr1 Mid) *via* CCL2/CCR2 Promotes the Development of Colorectal Cancer Liver Metastasis. *Hepatology* (2013) 57(2):829–39. doi: 10.1002/hep.26094
243. Feng M, Jiang W, Kim BYS, Zhang CC, Fu Y-X, Weissman IL. Phagocytosis Checkpoints as New Targets for Cancer Immunotherapy. *Nat Rev Cancer* (2019) 19(10):568–86. doi: 10.1038/s41568-019-0183-z
244. Zhang H, Lu H, Xiang L, Bullen JW, Zhang C, Samanta D, et al. HIF-1 Regulates CD47 Expression in Breast Cancer Cells to Promote Evasion of Phagocytosis and Maintenance of Cancer Stem Cells. *Proc Natl Acad Sci USA* (2015) 112(45):E6215–6223. doi: 10.1073/pnas.1520032112
245. Edris B, Weiskopf K, Volkmer AK, Volkmer J-P, Willingham SB, Contreras-Trujillo H, et al. Antibody Therapy Targeting the CD47 Protein Is Effective in a Model of Aggressive Metastatic Leiomyosarcoma. *Proc Natl Acad Sci USA* (2012) 109(17):6656–61. doi: 10.1073/pnas.1121629109
246. Blazar BR, Lindberg FP, Ingulli E, Panoskaltsis-Mortari A, Oldenborg PA, Iizuka K, et al. CD47 (Integrin-Associated Protein) Engagement of Dendritic Cell and Macrophage Counterreceptors Is Required to Prevent the Clearance of Donor Lymphohematopoietic Cells. *J Exp Med* (2001) 194(4):541–9. doi: 10.1084/jem.194.4.541
247. Wang Y, Wang H, Bronson R, Fu Y, Yang Y-G. Rapid Dendritic Cell Activation and Resistance to Allotolerance Induction in Anti-CD154-Treated Mice Receiving CD47-Deficient Donor-Specific Transfusion. *Cell Transpl* (2014) 23(3):355–63. doi: 10.3727/096368912X661346
248. Gholamin S, Mitra SS, Feroze AH, Liu J, Kahn SA, Zhang M, et al. Disrupting the CD47-Sirpα Anti-Phagocytic Axis by a Humanized Anti-CD47 Antibody Is an Efficacious Treatment for Malignant Pediatric Brain Tumors. *Sci Transl Med* (2017) 9(381):eaaf2968. doi: 10.1126/scitranslmed.aaf2968
249. Hernandez MGH, Shen L, Rock KL. CD40 on APCs is Needed for Optimal Programming, Maintenance, and Recall of CD8+ T Cell Memory Even in the Absence of CD4+ T Cell Help. *J Immunol* (2008) 180(7):4382–90. doi: 10.4049/jimmunol.180.7.4382
250. Richards DM, Sefrin JP, Gieffers C, Hill O, Merz C. Concepts for Agonistic Targeting of CD40 in Immuno-Oncology. *Hum Vaccin Immunother* (2020) 16(2):377–87. doi: 10.1080/21645515.2019.1653744
251. Vonderheide RH. CD40 Agonist Antibodies in Cancer Immunotherapy. *Annu Rev Med* (2020) 71:47–58. doi: 10.1146/annurev-med-062518-045435
252. Beatty GL, Chiorean EG, Fishman MP, Saboury B, Teitelbaum UR, Sun W, et al. CD40 Agonists Alter Tumor Stroma and Show Efficacy Against Pancreatic Carcinoma in Mice and Humans. *Science* (2011) 331 (6024):1612–6. doi: 10.1126/science.1198443
253. Hoves S, Ooi C-H, Wolter C, Sade H, Bissinger S, Schmittnaegel M, et al. Rapid Activation of Tumor-Associated Macrophages Boosts Preexisting Tumor Immunity. *J Exp Med* (2018) 215(3):859–76. doi: 10.1084/jem.20171440
254. Rüter J, Antonia SJ, Burris HA, Huhn RD, Vonderheide RH. Immune Modulation With Weekly Dosing of an Agonist CD40 Antibody in a Phase I Study of Patients With Advanced Solid Tumors. *Cancer Biol Ther* (2010) 10(10):983–93. doi: 10.4161/cbt.10.10.13251
255. O'Hara MH, O'Reilly EM, Varadhachary G, Wolff RA, Wainberg ZA, Ko AH, et al. CD40 Agonistic Monoclonal Antibody APX005M (Sotigalimab) and Chemotherapy, With or Without Nivolumab, for the Treatment of Metastatic Pancreatic Adenocarcinoma: An Open-Label, Multicentre, Phase 1b Study. *Lancet Oncol* (2021) 22(1):118–31. doi: 10.1016/S1470-2045(20)30532-5
256. Kaneda MM, Messer KS, Ralainirina N, Li H, Leem CJ, Gorjestani S, et al. Pi3kγ Is a Molecular Switch That Controls Immune Suppression. *Nature* (2016) 539(7629):437–42. doi: 10.1038/nature19834
257. De Henau O, Rausch M, Winkler D, Campesato LF, Liu C, Cymerman DH, et al. Overcoming Resistance to Checkpoint Blockade Therapy by Targeting PI3Kγ in Myeloid Cells. *Nature* (2016) 539(7629):443–7. doi: 10.1038/nature20554
258. Deczkowska A, Weiner A, Amit I. The Physiology, Pathology, and Potential Therapeutic Applications of the TREM2 Signaling Pathway. *Cell* (2020) 181 (6):1207–17. doi: 10.1016/j.cell.2020.05.003
259. Molgora M, Esaulova E, Vermi W, Hou J, Chen Y, Luo J, et al. TREM2 Modulation Remodels the Tumor Myeloid Landscape Enhancing Anti-PD-1 Immunotherapy. *Cell* (2020) 182(4):886–900.e17. doi: 10.1016/j.cell.2020.07.013
260. Katzenelenbogen Y, Sheban F, Yalin A, Yofe I, Svetlichnyy D, Jaitin DA, et al. Coupled scRNA-Seq and Intracellular Protein Activity Reveal an Immunosuppressive Role of TREM2 in Cancer. *Cell* (2020) 182(4):872–885.e19. doi: 10.1016/j.cell.2020.06.032
261. Pettenati C, Ingersoll MA. Mechanisms of BCG Immunotherapy and Its Outlook for Bladder Cancer. *Nat Rev Urol* (201) 15(10):615–25. doi: 10.1038/s41585-018-0055-4
262. Ji N, Mukherjee N, Morales EE, Tomasini ME, Hurez V, Curiel TJ, et al. Percutaneous BCG Enhances Innate Effector Antitumor Cytotoxicity During Treatment of Bladder Cancer: A Translational Clinical Trial. *Oncoimmunology* (2019) 8(8):1614857. doi: 10.1080/2162402X.2019.1614857
263. Fitzgerald KA, Kagan JC. Toll-Like Receptors and the Control of Immunity. *Cell* (2020) 180(6):1044–66. doi: 10.1016/j.cell.2020.02.041
264. Smith M, García-Martínez E, Pitter MR, Fucikova J, Spisek R, Zitvogel L, et al. Trial Watch: Toll-Like Receptor Agonists in Cancer Immunotherapy. *Oncoimmunology* (2018) 7(12):e1526250. doi: 10.1080/2162402X.2018.1526250
265. Kyi C, Roudko V, Sabado R, Saenger Y, Loging W, Mandeli J, et al. Therapeutic Immune Modulation Against Solid Cancers With Intratumoral Poly-ICLC: A Pilot Trial. *Clin Cancer Res* (2018) 24 (20):4937–48. doi: 10.1158/1078-0432.CCR-17-1866
266. Huang L, Xu H, Peng G. TLR-Mediated Metabolic Reprogramming in the Tumor Microenvironment: Potential Novel Strategies for Cancer Immunotherapy. *Cell Mol Immunol* (2018) 15(5):428–37. doi: 10.1038/cmi.2018.4
267. Rodell CB, Arlauckas SP, Cuccarese MF, Garris CS, Li R, Ahmed MS, et al. TLR7/8-Agonist-Loaded Nanoparticles Promote the Polarization of Tumour-Associated Macrophages to Enhance Cancer Immunotherapy. *Nat BioMed Eng* (2018) 2(8):578–88. doi: 10.1038/s41551-018-0236-8
268. Anfray C, Mainini F, Digifico E, Maeda A, Sironi M, Erreni M, et al. Intratumoral Combination Therapy With Poly(I:C) and Resiquimod Synergistically Triggers Tumor-Associated Macrophages for Effective Systemic Antitumoral Immunity. *J Immunother Cancer* (2021) 9(9): e002408. doi: 10.1136/jitc-2021-002408
269. Singh M, Khong H, Dai Z, Huang X-F, Wargo JA, Cooper ZA, et al. Effective Innate and Adaptive Antimelanoma Immunity Through Localized TLR7/8 Activation. *J Immunol* (2014) 193(9):4722–31. doi: 10.4049/jimmunol.1401160
270. Mullins SR, Vasilakos JP, Deschler K, Grigsby I, Gillis P, John J, et al. Intratumoral Immunotherapy With TLR7/8 Agonist MEDI9197 Modulates the Tumor Microenvironment Leading to Enhanced Activity When Combined With Other Immunotherapies. *J ImmunoTher Cancer* (2019) 7 (1):244. doi: 10.1186/s40425-019-0724-8
271. Frank MJ, Reagan PM, Bartlett NL, Gordon LI, Friedberg JW, Czerwinski DK, et al. *In Situ* Vaccination With a TLR9 Agonist and Local Low-Dose Radiation Induces Systemic Responses in Untreated Indolent Lymphoma. *Cancer Discov* (2018) 8(10):1258–69. doi: 10.1158/2159-8290.CD-18-0743
272. Ribas A, Medina T, Kummar S, Amin A, Kalbasi A, Drabick JJ, et al. SD-101 in Combination With Pembrolizumab in Advanced Melanoma: Results of a Phase Ib, Multicenter Study. *Cancer Discov* (2018) 8(10):1250–7. doi: 10.1158/2159-8290.CD-18-0280
273. Chow LQM, Morishima C, Eaton KD, Baik CS, Goulart BH, Anderson LN, et al. Phase Ib Trial of the Toll-Like Receptor 8 Agonist, Motolimod (VTX-2337), Combined With Cetuximab in Patients With Recurrent or Metastatic SCCHN. *Clin Cancer Res* (2017) 23(10):2442–50. doi: 10.1158/1078-0432.CCR-16-1934
274. Viola A, Munari F, Sánchez-Rodríguez R, Scolaro T, Castegna A. The Metabolic Signature of Macrophage Responses. *Front Immunol* (2019) 10:1462. doi: 10.3389/fimmu.2019.01462
275. Oh M-H, Sun I-H, Zhao L, Leone RD, Sun I-M, Xu W, et al. Targeting Glutamine Metabolism Enhances Tumor-Specific Immunity by Modulating

Suppressive Myeloid Cells. *J Clin Invest* (2020) 130(7):3865–84. doi: 10.1172/JCI131859
276. Menga A, Serra M, Todisco S, Riera-Domingo C, Ammarah U, Ehling M, et al. Glufosinate Constrains Synchronous and Metachronous Metastasis by Promoting Anti-Tumor Macrophages. *EMBO Mol Med* (2020) 12(10): e11210. doi: 10.15252/emmm.201911210
277. Manoharan I, Prasad PD, Thangaraju M, Manicassamy S. Lactate-Dependent Regulation of Immune Responses by Dendritic Cells and Macrophages. *Front Immunol* (2021) 12:691134. doi: 10.3389/fimmu.2021.691134
278. Chen P, Zuo H, Xiong H, Kolar MJ, Chu Q, Saghatelian A, et al. Gpr132 Sensing of Lactate Mediates Tumor-Macrophage Interplay to Promote Breast Cancer Metastasis. *Proc Natl Acad Sci USA* (2017) 114(3):580–5. doi: 10.1073/pnas.1614035114
279. Mu X, Shi W, Xu Y, Xu C, Zhao T, Geng B, et al. Tumor-Derived Lactate Induces M2 Macrophage Polarization *via* the Activation of the ERK/STAT3 Signaling Pathway in Breast Cancer. *Cell Cycle* (2018) 17(4):428–38. doi: 10.1080/15384101.2018.1444305
280. Geeraerts X, Bolli E, Fendt S-M, Van Ginderachter JA. Macrophage Metabolism As Therapeutic Target for Cancer, Atherosclerosis, and Obesity. *Front Immunol* (2017) 8:289. doi: 10.3389/fimmu.2017.00289
281. Vigano S, Alatzoglou D, Irving M, Ménétrier-Caux C, Caux C, Romero P, et al. Targeting Adenosine in Cancer Immunotherapy to Enhance T-Cell Function. *Front Immunol* (2019), 10:925. doi: 10.3389/fimmu.2019.00925
282. Cekic C, Day Y-J, Sag D, Linden J. Myeloid Expression of Adenosine A2A Receptor Suppresses T and NK Cell Responses in the Solid Tumor Microenvironment. *Cancer Res* (2014) 74(24):7250–9. doi: 10.1158/0008-5472.CAN-13-3583
283. Ma S-R, Deng W-W, Liu J-F, Mao L, Yu G-T, Bu L-L, et al. Blockade of Adenosine A2A Receptor Enhances CD8+ T Cells Response and Decreases Regulatory T Cells in Head and Neck Squamous Cell Carcinoma. *Mol Cancer* (2017) 16(1):99. doi: 10.1186/s12943-017-0665-0
284. Guerriero JL, Sotayo A, Ponichtera HE, Castrillon JA, Pourzia AL, Schad S, et al. Class IIa HDAC Inhibition Reduces Breast Tumours and Metastases Through Anti-Tumour Macrophages. *Nature* (2017) 543(7645):428–32. doi: 10.1038/nature21409
285. Lu Z, Zou J, Li S, Topper MJ, Tao Y, Zhang H, et al. Epigenetic Therapy Inhibits Metastases by Disrupting Premetastatic Niches. *Nature* (2020) 579 (7798):284–90. doi: 10.1038/s41586-020-2054-x
286. Frigault MJ, Maus MV. State of the Art in CAR T Cell Therapy for $CD19^+$ B Cell Malignancies. *J Clin Invest* (2020) 130(4):1586–94. doi: 10.1172/JCI129208
287. Klichinsky M, Ruella M, Shestova O, Lu XM, Best A, Zeeman M, et al. Human Chimeric Antigen Receptor Macrophages for Cancer Immunotherapy. *Nat Biotechnol* (2020) 38(8):947–53. doi: 10.1038/s41587-020-0462-y
288. Schmid MC, Avraamides CJ, Dippold HC, Franco I, Foubert P, Ellies LG, et al. Receptor Tyrosine Kinases and TLR/IL1Rs Unexpectedly Activate Myeloid Cell Pi3kγ, A Single Convergent Point Promoting Tumor Inflammation and Progression. *Cancer Cell* (2011) 19(6):715–27. doi: 10.1016/j.ccr.2011.04.016

Conflict of Interest: The authors declare that the research was conducted in the absence of any commercial or financial relationships that could be construed as a potential conflict of interest.

Publisher's Note: All claims expressed in this article are solely those of the authors and do not necessarily represent those of their affiliated organizations, or those of the publisher, the editors and the reviewers. Any product that may be evaluated in this article, or claim that may be made by its manufacturer, is not guaranteed or endorsed by the publisher.

frontiers | Frontiers in Oncology

REVIEW
published: 31 May 2022
doi: 10.3389/fonc.2022.886440

Overcoming Resistance to Checkpoint Inhibitors: Natural Killer Cells in Non-Small Cell Lung Cancer

Maria Gemelli[1], *Douglas M. Noonan*[2,3], *Valentina Carlini*[2], *Giuseppe Pelosi*[2,4], *Massimo Barberis*[5], *Riccardo Ricotta*[1]* *and Adriana Albini*[6]*

[1] Istituto di Ricovero e Cura a Carattere Scientifico (IRCCS) MultiMedica, Milan, Italy, [2] Istituto di Ricovero e Cura a Carattere Scientifico (IRCCS) MultiMedica Science and Technology Park, Milan, Italy, [3] Immunology and General Pathology Laboratory, Department of Biotechnology and Life Sciences, University of Insubria, Varese, Italy, [4] Department of Oncology and Hemato-Oncology, University of Milan, Milan, Italy, [5] Department of Pathology, European Institute of Oncology (IEO) Istituto di Ricovero e Cura a Carattere Scientifico (IRCCS), Milan, Italy, [6] European Institute of Oncology (IEO) Istituto di Ricovero e Cura a Carattere Scientifico (IRCCS), Milan, Italy

OPEN ACCESS

Edited by:
Daniele Vergara,
University of Salento, Italy

Reviewed by:
Sara Bravaccini,
Scientific Institute of Romagna for the Study and Treatment of Tumors (IRCCS), Italy
Nayoung Kim,
University of Ulsan, South Korea

***Correspondence:**
Adriana Albini
adriana.albini@ieo.it
Riccardo Ricotta
riccardo.ricotta@multimedica.it

Specialty section:
This article was submitted to Molecular and Cellular Oncology, a section of the journal Frontiers in Oncology

Received: *28 February 2022*
Accepted: *27 April 2022*
Published: *31 May 2022*

Citation:
Gemelli M, Noonan DM, Carlini V, Pelosi G, Barberis M, Ricotta R and Albini A (2022) Overcoming Resistance to Checkpoint Inhibitors: Natural Killer Cells in Non-Small Cell Lung Cancer. Front. Oncol. 12:886440. doi: 10.3389/fonc.2022.886440

Immune checkpoint inhibitors (ICIs) have revolutionized cancer treatments over the last 10 years, with even increasing indications in many neoplasms. Non-small cell lung cancer (NSCLC) is considered highly immunogenic, and ICIs have found a wide set of applications in this area, in both early and advanced lines of treatment, significantly changing the prognosis of these patients. Unfortunately, not all patients can benefit from the treatment, and resistance to ICIs can develop at any time. In addition to T lymphocytes, which are the major target, a variety of other cells present in the tumor microenvironment (TME) act in a complex cross-talk between tumor, stromal, and immune cells. An imbalance between activating and inhibitory signals can shift TME from an "anti-" to a "pro-tumorigenic" phenotype and vice versa. Natural killer cells (NKs) are able to recognize cancer cells, based on MHC I (self and non-self) and independently from antigen presentation. They represent an important link between innate and adaptive immune responses. Little data are available about the role of pro-inflammatory NKs in NSCLC and how they can influence the response to ICIs. NKs express several ligands of the checkpoint family, such as PD-1, TIGIT, TIM-3, LAG3, CD96, IL1R8, and NKG2A. We and others have shown that TME can also shape NKs, converting them into a pro-tumoral, pro-angiogenic "nurturing" phenotype through "decidualization." The features of these NKs include expression of CD56, CD9, CD49a, and CXCR3; low CD16; and poor cytotoxicity. During ICI therapy, tumor-infiltrating or associated NKs can respond to the inhibitors or counteract the effect by acting as pro-inflammatory. There is a growing interest in NKs as a promising therapeutic target, as a basis for adoptive therapy and chimeric antigen receptor (CAR)-NK technology. In this review, we analyzed current evidence on NK function in NSCLC, focusing on their possible influence in response to ICI treatment and resistance development, addressing their prognostic and predictive roles

and the rationale for exploiting NKs as a tool to overcome resistance in NSCLC, and envisaging a way to repolarize decidual NK (dNK)-like cells in lung cancer.

Keywords: natural killer, non-small cell lung cancer, tumor microenvironment, checkpoint inhibitors, inflammation, angiogenesis, polarization, resistance

1 INTRODUCTION

Immunotherapy has become a milestone in the treatment of almost all kinds of neoplasms, both solid and hematologic. While chemotherapy is aimed to kill cancer cells, immunotherapy stimulates the immune system to react against tumors (1). The concept of cancer immunotherapy is based on the finding that tumor cells, normally recognized and neutralized by T cells, can develop mechanisms to evade the host's immune surveillance. Thus, inhibition of negative regulators of T-cell function may increase the activation of the immune system, inducing a subsequent enhancement of antitumor responses as well (1). Great progress has been made from the first attempts with cancer vaccines leading to the approval of the more recent immune checkpoint inhibitors (ICIs). Among these, the first therapeutic molecules to be developed and to have brought a clinical improvement are the anti-cytotoxic T-lymphocyte antigen 4 (CTLA-4), also known as CD152, and the anti-programmed death receptor-1/programmed death ligand-1 (PD-1/PD-L1) antibodies. These agents, alone or in combination, are routinely used in clinical practice for the treatment of many solid tumors, such as lung cancer, urothelial and renal cell carcinoma, head and neck tumors, melanoma, and mismatch repair deficient colon cancer (2). ICIs act by blocking the activation of tumor-induced inhibitory pathways: the first one (anti-CTLA-4) mostly at the early stage of naïve T-cell activation, at the site of antigen presentation in lymph nodes, and the latter (anti-PD-1/PD-L1) at the advanced stage of a T-cell immune response, directly in the tumor microenvironment (TME) (3), as depicted in **Figure 1**. In addition to PD-1/PD-L1 and CTLA-4, other checkpoint molecules such as the T-cell immunoglobulin and mucin domain 3 (TIM-3), lymphocyte activation gene-3 (LAG3), T-cell immunoglobulin and immunoreceptor tyrosine-based inhibitory motif (ITIM) domain (TIGIT), and, more

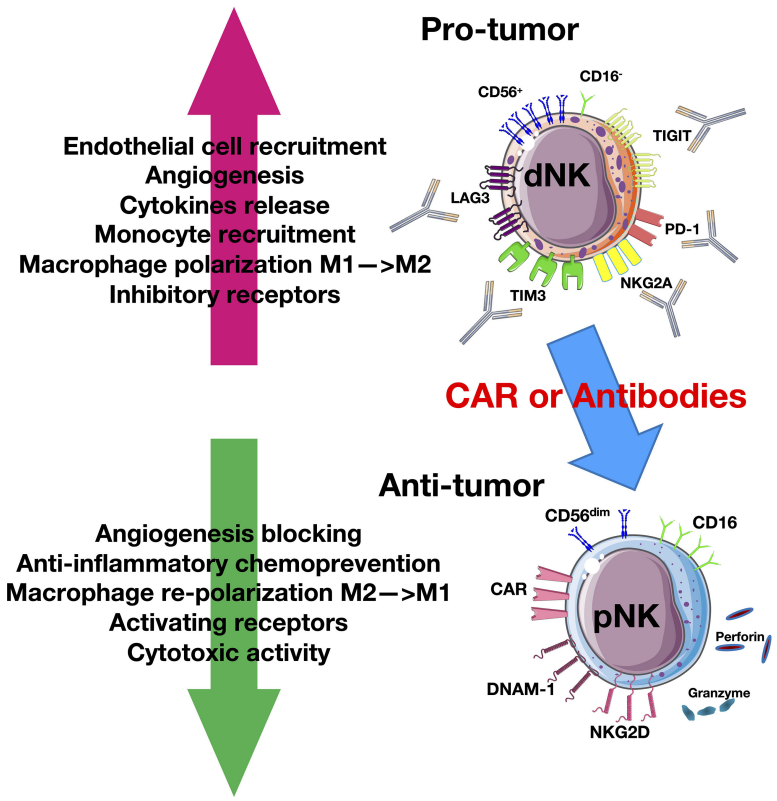

FIGURE 1 | Natural killer cell (NK) plasticity in cancer. Tumor cells and tumor microenvironment (TME) induce a pro-tumor $CD56^{+}CD16^{-}$ decidual-like phenotype that expresses inhibitory receptors. The blockade of these receptors or the use of chimeric antigen receptor (CAR) or adaptive therapy can reverse this mechanism by switching NKs into antitumor cytotoxic $CD56^{dim}CD16^{+}$ cytotoxic phenotype that can release granzyme and perforin.

recently, V-domain immunoglobulin suppressor of T-cell activation (VISTA) have been explored as potential targets for the development of new agents for cancer immunotherapy (4). Non-small cell lung cancer (NSCLC), the most common cause of cancer-related death worldwide, is considered a highly immunogenic neoplasm. ICIs have found a wide range of applications in this oncologic field, in both early and advanced lines of treatment, dramatically changing the prognosis of these patients in many cases (5–12). Unfortunately, not all patients can benefit from this treatment, and resistance can occur even in individuals who were previously responsive (13, 14). Several explanations have been provided for the lack of efficacy of ICIs, one of which is related to the low presence of T lymphocytes to be reactivated by targeting the immune checkpoints. The fine balance between activating and suppressing signals of the immune system plays a pivotal role in promoting or, conversely, counteracting cancer onset and progression. Tumor-infiltrating T lymphocytes have emerged as important prognostic and predictive factors in many types of cancer. In particular, the percentage of $CD8^+$ T lymphocytes as well as the $CD4^+/CD8^+$ ratio and the polarization toward an anti-cancer T-helper response (Th1 vs. Th2), seem to correlate with better prognosis and improved response to ICIs in melanoma, breast, and lung cancers (15–17). Another reason lies in the complex interaction existing between innate immunity, stromal, and tumor cells in TME, which is crucial in regulating tumor formation, growth, invasion, and metastasis. The importance of tumor-associated macrophages (TAMs) in tumor response has been recently understood. Some preliminary observations propose that polarization toward a pro-tumorigenic M2 phenotype correlates with worse prognosis and increased risk of recurrence after resection in different types of cancer, including lung tumors; more recent evidence also suggests a possible negative predictive role for response to ICIs (15, 18). We have been working for a long time on tumor-associated natural killer cells (NK) (TA-NKs). Despite their crucial role in immunity, limited data are evaluable about their role to modulate the response to immunotherapy. In this review, we want to summarize and discuss the data currently available on the behavior of NKs under ICI treatment, their role in resistance to treatment and possible strategies to exploit their function as a therapeutic target, and their potential re-polarization into killers, with a focus on NSCLC.

2 NATURAL KILLER CELL PHENOTYPE AND BIOLOGY

NKs are lymphoid cells of the innate immune system, representing about 20% of total peripheral blood (PB) circulating lymphocytes. Since their discovery in the 1970s, they have aroused growing interest thanks to their potent cytolytic function against tumor cells or virus-infected cells without previous antigen sensitization or immunologic memory (19–21). T-cell immunity requires recognition of specific antigens presented through major histocompatibility complex (MHC) class I and class II proteins by $CD8^+$ and $CD4^+$ T cells (22, 23), respectively, while NKs recognize as "non-self", tumor cells that have lost their MHC class I molecules (19, 20). Furthermore, they are primary producers of interferon-gamma (IFN-γ), the most potent stimulus for MHC expression and antigen presentation, acting as a cross-talk between innate and adaptive responses. Recently, NKs have been recategorized as type 1 in the larger family of innate lymphoid cells (ILCs) (24–26).

NKs exert both cytotoxic and regulatory activities. On the one hand, they induce apoptosis and cell death through the release of perforin and granzyme by their intracytoplasmic granules; on the other hand, they orchestrate innate response through the secretion of immunomodulatory soluble factors, such as cytokines and chemokine, which act on hematopoietic cell recruitment and activation (24–28).

Two major immunophenotypic subpopulations of NKs, which differ in morphology and function, have been identified in PB based on the relative expression of the CD56 and CD16 antigen surface markers. The first subset, the $CD56^{dim}CD16^+$, accounts for 95% of NKs in PB, and, when it comes into contact with virus-infected cells or tumor cells expressing low levels of MHC class I or other ligands, exhibits high cytotoxic activity through perforin and granzyme release. The other subset, the $CD56^{bright}CD16^-$, represents only 5% of NKs circulating in PB, but it is the majority of NKs in secondary lymphoid tissues and shows low cytotoxic potential and efficient production of cytokines, such as the tumor necrosis factor (TNF)-alpha and the granulocyte macrophage colony-stimulating factor (GM-CSF), both of which play a crucial role in the modulation of an immune response, particularly in chronic inflammation. These cells are considered as a less differentiated form than the "terminally differentiated" $CD56^{dim}CD16^+$, subtype (29). In fact, when exposed to interleukin (IL)-2, IL-12, and/or IL-15, they can differentiate into granules secreting $CD56^{dim}CD16^+$ NKs (30–32).

NKs dynamically circulate between organs and the bloodstream to exert their immunosurveillance activity (33, 34). Among organs, the lungs have the highest contents of NKs, mostly the $CD56^{dim}CD16^+$ subtype (34–37). An analysis performed on NKs isolated from bronchoalveolar lavage of normal lungs underlined that pulmonary NKs are mainly functionally inactive and show a weaker response to immune stimulation, as a consequence of local inhibitory influences (38). However, in response to proper stimuli, such as IL-2, lung NK activity is completely restored. This suggests that pulmonary alveolar macrophages can regulate lung NK activity for the maintenance of physiological homeostasis (38), as the lungs are continuously exposed to novel antigens (38, 39).

The third type of NKs showing a $CD56^{bright}CD16^-$ phenotype and the expression of killer-cell immunoglobulin-like receptors (KIR) receptor, CD69, and CD49a on the cell surface has been recently described (35, 40, 41). About 15% of tissue-resident NKs in the lungs are $CD56^{bright}CD16^-CD49a^+$, with a high ability to secrete IFN-γ (40). This can be considered a "decidual" phenotype (dNK), recapitulating an NK type first described in

the decidua and which has a crucial role in the tolerance of the embryo and the spiral artery formation (42–45). The dNK was observed in many cancers, both infiltrating and in PB. In cancer patients, it acts in a "pro-tumorigenic" way, inducing tolerance and proving nurturing function, similar to what happens with the embryo (42).

3 NATURAL KILLER CELLS IN NON-SMALL CELL LUNG CANCER AND MODULATION BY THE TUMOR MICROENVIRONMENT

NKs were found to be an important part of the TME in various cancer types, able to modulate the immune response and affect prognosis, particularly in lung cancer (35–37, 40, 41, 46–48). Although these cells normally carry out immune surveillance and have the function of destroying tumor cells, they can also act as tumor-promoting inflammatory leukocytes. This is in large due to the modulation by both the tumor itself and the TME, which is constituted by various immune cells, fibroblasts, extracellular matrix, growth factors, and endothelial and vascular cells: an imbalance between activating and inhibitory signals can determine whether NKs will exert their cytotoxic activity or remain inactive or even become pro-tumor (46). Intratumorally, NKs have a prognostic significance in lung cancer: high NK infiltration was positively correlated with survival rate in patients who underwent surgery in early stages, and in particular, increased NK infiltration was found in squamous cell carcinoma (SCC), in non-smoking patients, and lower-stage tumors (T1–T2 and limited nodal involvement) (46).

In NSCLC patients, NKs were found at the invasive margin of tumor samples (35, 48). Tumor-infiltrating NKs (TI-NKs) in lung cancer are mostly of the $CD56^{bright}CD16^{-}$ subset and exhibit low cytotoxic potential as well as high cytokine production capability. They are mainly present in the tumor stroma, particularly in the alveolar and peri-bronchovascular interstitium, without direct interaction with tumor cells, suggesting a major role in the orchestration of the immune response rather than killing effect (36, 48). In contrast, the percentage of cytotoxic $CD56^{dim}CD16^{+}$ NKs is lower in lung cancer compared to normal tissue, probably as a result of the modulation by TME, and it is related to MHC class I expression, as it is higher in MHC I-deficient tumors.

TME can directly contribute to the bloodstream recruitment and the accumulation of $CD56^{bright}CD16^{-}$ NKs at the tumor site by promoting a switch in chemokine expression. In particular, the number of $CD56^{bright}$ NKs infiltrating NSCLC is correlated with a downregulation of C-X-C Motif Chemokine Ligand (CXCL)2, the chemokine specifically attracting $CD56^{dim}$ NKs, and overexpression of the chemokines preferentially attracting $CD56^{bright}$ NKs, CXCL9, CXCL10, and C-C Motif Chemokine Ligand (CCL)19. These chemokines, through the binding to C-X-C Motif Chemokine Receptor (CXCR)3, promote low-cytotoxic $CD56^{bright}$ NK recruitment, ultimately leading to tumor escape (34). TI-NKs show a deep alteration of their phenotype, with overexpression of CXCR3 receptor and downregulation of CD57 mature NK marker, and have profound defects in their ability to activate granzyme B degranulation and IFN-γ production (49).

Whether the presence of TI-NKs and their tumor-specific characterization affect prognosis and treatment sensitivity is largely unknown. A high proportion of TI-NKs have been associated with longer progression-free survival (PFS) in advanced and resected early-stage NSCLC, in both squamous and adenocarcinoma (50–52). Conversely, in a recent meta-analysis performed on NKs infiltrating solid tumors, including four studies on lung cancer, no correlation was found between the degree of NK infiltration and overall survival (OS) in patients from stage I to IV (53). However, the small sample size, the high variability in methods used for analysis, and the large differences in stages and histological profiles in all these studies make it difficult to draw definitive conclusions. Furthermore, such heterogeneous results might depend on the dual nature of the NKs themselves, since, against all the "dogmas" on terminal differentiation, they can switch from a cytotoxic antitumor activity to an exhausted pro-tumoral function under pressure and modulation of tumor and TME.

TME is composed of a multitude of immune cells, in addition to T and B cells, macrophages, granulocytes, mast cells, fibroblasts and extracellular matrix, secreting growth factors, activating or inhibitory cytokines, and chemokines and proteases, all of which are in dynamic spatial and temporal evolution. An imbalance in cellular and soluble inhibitory factors results in the establishment of a pro-tumoral microenvironment, which in turn supports tumor growth, progression, and resistance. NKs have pleiotropic functions, and given their dual nature between innate and adaptive immunity, TME may deeply affect their function to contrast or to support tumor growth and promote immune escape. As in other observed malignancies, TI-NKs derived from NSCLC displayed an impaired degranulation activity and INF-γ production when exposed to tumor cells than NKs present in normal lung tissue or circulating in the bloodstream (48, 54). Furthermore, T1-NKs produce placental-derived growth factor (PIGF), vascular endothelial growth factor (VEGF), and IL-8/CXCL8, particularly in SCC (37). We found that the $CD56^{+}CD16^{-}$ NKs represented the predominant subset in samples from 31 surgically resected NSCLC and a minor subset in samples from adjacent normal lung tissue and PB (37). We also observed that NK supernatants derived from NSCLC samples induced endothelial cell chemotaxis and formation of capillary-like structures *in vitro*, particularly evident in SCC patients and absent in controls (37). Taken together, these data suggest that in NSCLC, and particularly in SCC, NKs act as proangiogenic cells with a mechanism at least in part mediated by transforming growth factor-beta (TGF-beta). TI-NKs infiltrating the tumors have been shown to have a phenotype characterized by $CD56^{bright}CD16^{-}$/low CD94/NK group 2 member A $(NKG2A)^{+}$ perforin low (36, 37, 47) and decreased expression of CD337/NK protein (NKp)30, NKp80/KLRF1, CD226/DNAX accessory molecule (DNAM-1), CD16, and

CD85j/Ig-like transcript (ILT2) inhibitory receptors. TI-NKs in NSCLC patients show uniformly poor cytotoxicity and acquire a pro-angiogenic dNK-like phenotype, described as VEGF+ CXCL8+ PlGF+ (37, 42, 47). This NK subtype was observed in many cancers, in both infiltrating tumoral tissues and the PB (37, 41, 42, 47). In cancer, these cells lack the ability to kill malignant cells and directly act in a "pro-tumorigenic" way, inducing immune tolerance and providing nurturing function (37, 42, 47), similar to what happens in the embryo.

The production of pro-angiogenic factors not only is limited to TI-NKs but also is observed in PB NKs (tumor-associated NKs (TA-NKs)) (37, 42, 47). TA-NKs present similar phenotypic characteristics compared to TI-NKs (37, 41, 42, 47, 55, 56). The presence of these NKs in PB results in a potent systemic pro-tumorigenic effect even in early-stage small-size carcinomas, especially for the SCC (37, 47). The TME interacts with the immune system and may impair NK activity through different strategies, including the production of inhibitory cytokines, such as TGF-beta and IL-10, the high infiltration of peritumoral monocytes/macrophages, which can induce the polarization of NK toward a pro-tumorigenic phenotype, and the inhibition of natural cytotoxicity receptor (NCR) expression, mainly NKp30, NKp44, and NKp46 (57–59). Here we describe the main mechanisms involved.

3.1 Decidual Natural Killer Cells

As reported above, dNK cells are a third NK subset that has recently been described and differs from the PB subset at both functional and phenotypical levels. They show a $CD56^{bright}CD16^{-}$ phenotype, a characteristic expression profile of KIR receptors, various chemokine receptors, and tissue residency markers CD9 and CD49a on the cell surface (43–45). CD9 is a member of the tetraspanin family, which is associated with different integrin adhesion receptors and modulates cell migration, invasion, and adhesion. CD9 is upregulated by TGF-beta (60) and is also characteristic of exosomes (61) CD49a constitutes the alpha-subunit of the alpha1beta1 integrin receptor (VLA1), which binds collagen IV present in basement membranes and is involved in regulating cell cytotoxic activity, migration, and adhesion (43).

This NK subtype was first identified in the as decidual placenta and uterus and for this reason called dNKs (43, 62). dNKs are highly proangiogenic and have a fundamental function in decidual vascularization and spiral artery formation, through the secretion of proangiogenic cytokines like PlGF, angiogenin, CXCL8, VEGF, and angiopoietins 1 and 2 (44, 63–66). When added to tumor cell xenografts, dNK cells can stimulate neoangiogenesis and tumor growth (63). dNKs play also an important role in maintaining immune homeostasis: acting as an immunosuppressant and losing their killing ability, they create a microenvironment protected by the recognition of the immune system and capable of tolerating the growth of the embryo (43–45).

Similar mechanisms occur in tumors; cancer cells can shape the TME, converting immune cells from a cytolytic to a tolerant and nurturing phenotype (42). dNK cells with proangiogenic decidual features have been described in lung cancer and other tumors, such as colorectal and prostate cancers (42). The dNK cell decidual marker CD9 is expressed by TI-NKs of melanoma, colorectal cancer, breast cancer, and glioblastoma (41, 42, 55, 56, 67–70). The chemokine receptor CXCR3, another dNK marker, is expressed in TI-NKs of colorectal cancer, breast cancer, melanoma, and glioblastoma (42, 49, 67–69), while CXCR4 in NK is upregulated in neuroblastoma and prostate cancer (42, 71). TA-NKs express CD9 and $CD49^{+}$ in NSCLC, prostate cancer, and melanoma (41, 42, 56, 69), and CXCR4 is present in TA-NKs of prostate cancer (56). TME induces accumulation of $CD56^{bright}CD16^{-}$ poorly cytotoxic NKs, promotes their survivorship and NK decidualization, and reprograms them to resume embryonic activity finalized to tumor immune escape and growth (42). TME can exert this function through the release of a large number of proangiogenic factors, like adenosine (ADO), hypoxia, prostaglandin E2 (PGE-2), glycodelin-A (GdA), HLA-G, and galectin-1 (42). Among these molecules, TGF-beta seems to be the most potent cytokine inducing immune response downregulation and NK decidualization, and it is found to be upregulated in many tumor types (60, 72, 73).

$CD56^{bright}CD16^{-}$ NKs represent the predominant subset in resected NSCLC and show proangiogenic features, such as VEGF, P1GF, and IL-8 secretion, particularly evident in SCC (37, 42, 47). In our previous publications, we showed that supernatants derived from TI-NKs and TA-NKs can induce endothelial cell chemotaxis and capillary formation *in vitro* (37). NKs expressing decidual-like markers, such as CD49a and CD9, have also been found in pleural effusion from primary and metastatic tumors, including lung cancer. These cells showed compromised degranulation activity and IFN-γ production and enhanced VEGF secretion, which was partially restored with the addition of IL-2 (37, 74).

Our data suggest that tissue inhibitors of metalloproteases (TIMPs) might counteract cancer-induced NK polarization, by restoring the expression of activation markers like NKG2D and reducing the expression of exhaustion markers such as CD9, CD49a, and the T-cell immunoglobulin and mucin-domain containing-3 (TIM-3) (75). Taken together, these and many other results suggest an important role for NK polarization in tumor growth and invasion, including in NSCLC. Understanding these mechanisms is fundamental for the development of new therapeutic strategies. A blockade of decidualization could constitute a new therapeutic target, not only in lung cancer but also in other malignancies sharing this phenomenon.

3.2 Activating and Inhibitory Receptors

A mechanism by which TME may shape NKs into a non-cytotoxic phenotype is the reduction of activating NK receptors and the induction of inhibitory receptors on the cell surface. The tolerance toward self-healthy cells is mediated by HLA molecules that bind to inhibitory HLA NK receptors, mainly KIRs and CD94/NKG2A, mitigating NK cytotoxic ability (36, 48). NKG2A is an inhibitory member of the NKG2 family and is expressed on $CD56^{high}$ NKs (76, 77). The non-classical MHC class I molecule HLA-E is the major ligand of $NKG2A^{-}CD94$ (76–78). High NKG2A expression on the cell surface is a marker of NK exhaustion and correlates with a worse

prognosis (76–79). This goes in parallel with the downregulation of NCRs such as NKp30, NKp44, and NKp46, by a mechanism that is supposed to depend on cell-to-cell contact (76–79). Upregulation of inhibitory NK receptors occurs in cancer (76–78). As for "decidualization," TGF-beta is the most potent stimulus to induce upregulation of inhibitory T-cell receptors (TCRs) and downregulation of the activating ones on NKs (60, 72, 73). Lung cancer produces a high amount of TGF-beta, and the circulating levels of this factor correlate with prognosis (48) and diagnostic effects for patients with early-stage NSCLC (80).

Inhibitory checkpoints have an important role in maintaining homeostasis and usually are not expressed by resting NKs, but in cancer and other pathological condition, their production is induced by the interaction of ligands released by tumor cells, to allow immune escape.

Among these, TIGIT is an important co-inhibitory receptor of the immunoglobulin superfamily expressed by NKs (81). Together with CD96, TIGIT binds to CD155 and CD112 resulting in NK and T-cell inhibition (82). Like TIGIT, TIM-3 has been investigated as a marker of T-cell exhaustion because it is frequently co-expressed with PD-1 and has recently been found overexpressed in circulating NKs of advanced lung cancer (83). Moreover, TIM-3 is overexpressed in $CD3^{-}CD56^{+}$ NKs, and it is higher in patients with advanced lung adenocarcinoma (nodal involvement or T3–T4); this overexpression is correlated with shorter OS. Interestingly, blocking TIM-3 alone or in combination with an anti-PD1 may reverse the NK exhaustion (84).

Beyond a well-established regulatory role in T-cell activation, overexpression of LAG3 was associated with decreased NK function in mouse models. However, this has not been confirmed in humans, so further studies might focus on T-cell regulation for LAG3 rather than NK function (85–87).

NK activation is partially controlled by KIRs upon binding with their ligands, primarily the HLA-C molecules. KIRs are a large family that comprehends several inhibitory receptors, which bind to different allotypes of MHC complexes. Through this binding, KIRs activate intracellular inhibitory signals that prevent NK activation (88). The importance of KIR inhibition has been demonstrated in acute myeloid leukemia (AML) patients in whom allogeneic transplantation of stem cells having a mismatch between KIRs on donor NKs and recipient MHC class I molecules was likely to reactivate NK antitumor function, leading to improved relapse-free survival and OS. The results suggest that blocking the interaction between KIRs and MHC class I results in NK activation and subsequent eradication of the residual leukemia clones (89).

PD-1 is one of the most important immune checkpoints, with relevant clinical applications. PD-1 was first described in T cells, but it is also expressed in NKs (90–92). Like other checkpoint regulators, its primary role is to maintain cell homeostasis. However, cancer cells can express their ligand (PD-L1) and, together with other inhibitory immune cells, like the regulatory T cells (Tregs), can release TGF-beta to induce PD-1 expression on NKs, thereby escaping the immune response (90–92). Furthermore, PD-L1 expressing circulating epithelial tumor cells CETCs have been detected in 82% of lung cancer patients. PD-L1 positive CETCs could be a potential biomarker to select patients for treatment with PD-1/PD-L1 inhibitors, and may be a direct target of anticancer treatment (93).

All these receptors are currently under investigation in clinical trials as targets.

3.3 Alterations of Natural Killer Cell Metabolism

NK metabolism might be impaired in TI-NKs, limiting NK cytotoxic activity. TME plays a major role even in this context, as it consumes a large number of nutrients, such as glucose and glutamine, and releases TGF-beta, which in turn reduces NK glycolysis and oxidative phosphorylation, decreasing NK activity (94). Inhibition of the TGF-beta pathway restores NK metabolism, underlying its importance in TME regulation (94). The enzyme fructose-1,6-biphosphates 1 (FBP1) is upregulated by TGF-beta during cancer progression, resulting in functional NK impairment (95). An FBP1 inhibitor has recently been developed and showed preclinical evidence of restoring NK function (95). In addition to low glucose concentrations, TME is characterized by other conditions that can decrease NK function, like hypoxia and acidic pH (96). Moreover, hypoxia can reduce NK surface expression of activating receptors such as NKG2D, and the resulting high level of hypoxia-inducible factor 1 alpha (HIF-1 alpha) is correlated with a worse prognosis in NSCLC (97). This is possibly due to adenosine and lactate accumulation that block NK activation and cytotoxicity, increasing the number of regulatory inhibitory cells like Tregs and myeloid-derived suppressor cells (MDSCs) (97). Natural Polyphenols can exerts antitumor activity and circumvent anti-PD-1 resistance (98). We have investigated the effects of a polyphenol rich olive mill wastewater derived polyphenols on the immune-microenvironment of lung cancer to overcome resistance (99).

4 NATURAL KILLER CELLS AS A POTENTIAL PREDICTIVE BIOMARKER FOR IMMUNOTHERAPY IN NON-SMALL CELL LUNG CANCER

4.1 Natural Killer Cells and Anti-PD-1/PD-L1

ICIs targeting the PD-1/PD-L1 axis are now a milestone in the treatment of NSCLC (**Figures 2**, **3**), both as a single agent and in combination therapies (5, 6, 10–12, 100). In the lung, there are two main subtypes of NSCLC, namely, adenocarcinoma and SCC, for which immunotherapy may be a valuable strategy for the treatment of driver-negative metastatic patients (101). The WHO guidelines have emphasized the importance of the precise subclassification of NSCLC in both resection specimens and small-sized diagnostic material, the utility of immunohistochemical biomarkers in the accurate diagnosis and subclassification of NSCLC, and the critical role of

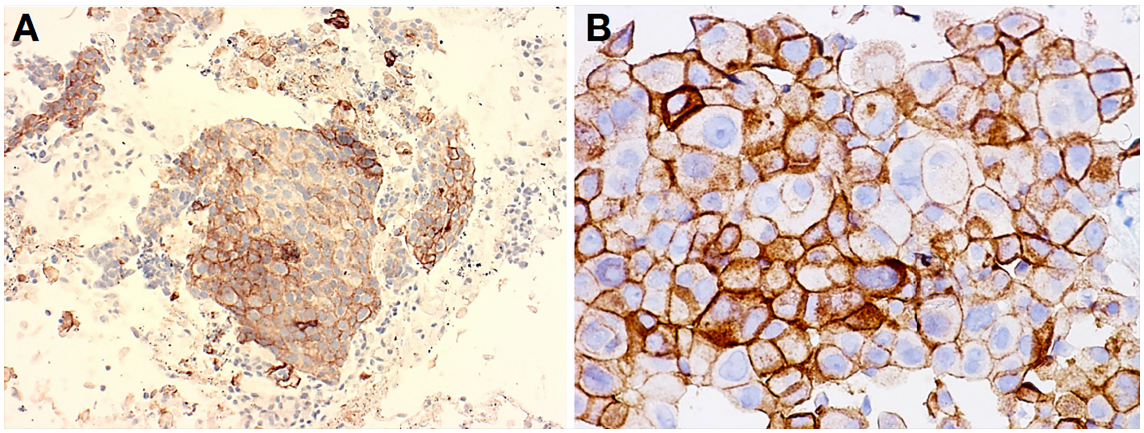

FIGURE 2 | Lung adenocarcinoma obtained with EBUS-TBNA procedure **(A)** and pleural effusion (cell block) **(B)**. These two cases of metastatic adenocarcinoma to a mediastinal lymph node **(A)** and pleura cavity **(B)** featured solid-clumped patterns of growth, which turned out positive for TTF1 and negative for p40, thus confirming the correct subtyping as required by the current WHO guidelines (not shown). When tumors were made to react with antibodies to PD-L1 within companion kits, clusters of tumor cells unequivocally revealed membrane decoration in more than 50% of them, thus suggesting amenability of immunotherapy. Clone Agilent-Dako 22C3 was developed in Autostainer Link 48, with original magnification at ×400 **(A)**, while Ventana-Roche clone SP263 was developed in BenchMark Ultra IHC at ×200 **(B)**.

molecular characterization for targeted therapy (102). The use of a marker of adenocarcinoma, such as thyroid transcription factor 1 (TTF1), and a marker of squamous cell differentiation, such as p40, is recommended as a two-hit, sparing-material minimalist antibody panel approach for reliably subtyping tumors (103). In clinical practice, after subtyping, the suitability for immune checkpoint axis-based immunotherapy is usually evaluated by means of the immunohistochemical detection of PD-L1 on tumor cells, which turned out to be a potential predictor of response to inhibitors especially when it is higher than 50%

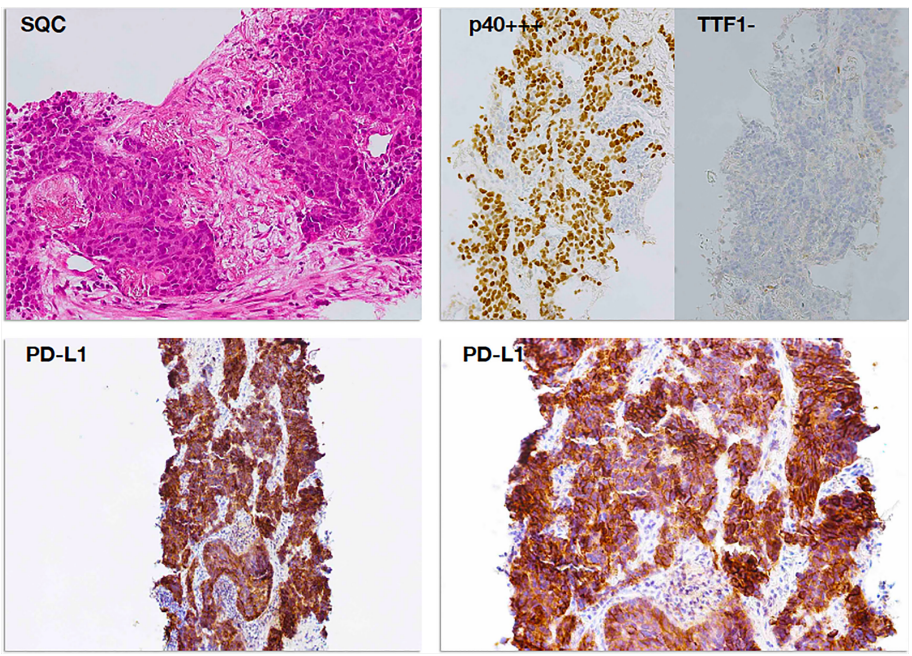

FIGURE 3 | PD-L1 immunostaining in a case of squamous cell carcinoma (SCC). Poorly differentiated squamous cell carcinoma (top left panel, H&E staining) was readily subtyped by means of immunoreactivity for p40 (p40+++) and negativity for TTF1 (TTF1–), according to the current WHO guidelines (top right panel). Diffuse and intense membrane immunostaining for PD-L1 was observed in tumor cells, already evident at lower magnification (×100, bottom left panel) and then confirmed at higher magnification (×200, bottom right panel) as membrane decoration in over 95% of tumor cells.

(104). The immunohistochemical reaction to PD-L1, which is quantified as the percentage of immunolabeled cells on the membrane independent of its completeness or intensity (realizing the so-called tumor proportion score) (104), is shown in **Figure 2** for adenocarcinoma and **Figure 3** for SCC. In clinical practice, it is usual to substitute the immune checkpoint axis by means of the immunohistochemical detection of PD-L1 on cancer cells, which is a potential predictor of response to inhibitors, especially when it is higher than 50 (104). PD-L1 expression is highly variable among different malignancies, and it can be very heterogeneous even in the same tumor, with different levels of expression depending on the area considered, as shown in **Figures 2** and **3** (104). Recent studies demonstrated that NKs play a crucial role in tumoral response to ICIs. PD-1 is expressed by NKs in PB and TME in multiple cancers, including lung cancer (90–92). After binding to PD-L1, PD-1-positive NKs become unpaired in mouse and human models, suggesting that downregulation of this pathway plays an important role not only in T cells but also in other immune cells of the TME. By PD-1/PD-L1 blockade, ICIs partially restore the normal NK activity, highlighting the therapeutic and predictive potential of PD-1-positive NKs (105–107). Interestingly, PD-1/PD-L1 blockade may also influence NK activity by inducing a Treg downregulation, Treg inhibit NK function and survival through TGF-beta release (105, 106). Several mouse models showed that the therapeutic effect was NK-dependent in MHC-deficient tumors, while in MHC-expressing tumors (T-cell sensitive), NK depletion has the same effect as $CD8^+$ T-cell depletion (105). Accordingly, mice lacking both T cells and NKs do not develop any response after PD-1 blockade (108). NKs can influence response to ICIs also triggering antibody-dependent cell-mediated cytotoxicity (ADCC) against cancer cells in *in vitro* models, as the Fc gamma receptor (Fcγ) on NKs is an integral part of the ADCC mechanism (109). Furthermore, NKs can stimulate the migration and survival of $CD141^+$ dendritic cells (DCs) *via* chemokines and cytokine production (i.e., CCL5, XCL-1, or lymphotactin, FLT3-Ligand) (110). Finally, NKs release a great amount of IFN-γ, which can induce PD-L1 expression on tumor cells, increasing sensitiveness to ICI (110).

In conclusion, PD-1 is an important regulator of NK function, and its blockade was shown to enhance NK activity leading to increased tumor control. Moreover, NKs were shown to play a role in response to PD-1–PD-L1-based therapies against tumors both sensitive and resistant to T cell-mediated cytotoxicity.

Due to their central role in immune response, NKs may be involved in predicting tumor response to immunotherapy. An NK-related gene expression profile performed on NSCLC patients treated with nivolumab or pembrolizumab was found to be correlated to treatment response and PFS (111). In another prospective trial of nivolumab in NSCLC, patients who achieved clinical benefit showed higher baseline functionally active circulating NKs compared to non-responders. Circulating NK numbers progressively increased during PD-1 blockade in responders, counterbalanced by a reduction in circulating Tregs (112).

Furthermore, stratification of patients by quantification of NK receptors from blood samples could be a useful prognostic and predictive tool: low expression of Natural Cytotoxicity Triggering Receptor (NCR) 1 and 3 correlated with worse prognosis in NSCLC and PD-L1-positive (>5%) patients, and low NCR3 expression correlated with the worse outcome to anti-PD1 (113).

As it is well known that NKs are primary producers of IFN-γ, the best overall response rate (ORR) to nivolumab has been reported in advanced NSCLC patients with higher expression of the IFN-γ target gene (114).

An exploratory analysis of the phase II randomized POPLAR trial showed that NSCLC patients with high T-effector–IFN-γ-associated gene expression had improved OS with atezolizumab compared to docetaxel (115). Circulating levels of IFN-γ might reflect the activation of the IFN-γ signaling and could be an easy tool to monitor patients during treatment. In a prospective study on 26 NSCLC patients treated with pembrolizumab or nivolumab, increased blood levels of IFN-γ and in addition other cytokines (TNF-alpha, IL-1β, IL-2, IL-4, IL-6, and IL-8) at the time of diagnosis and 3 months after the start of the treatment were significantly correlated with improved response to immunotherapy and prolonged OS, while no correlation with PD-L1 expression was found (116). However, robust data on the specific contribution of NKs in response to anti-PD-1/PD-L1 drugs in NSCLC are limited. Further prospective studies are needed to assess the predictive role in this context, and no data are available on the modulation of NKs under concomitant chemotherapy and immunotherapy.

4.2 Natural Killer Cells and Anti-CTLA-4

The CTLA-4 is abundantly expressed by Tregs and, upon stimulation, by cytotoxic T cells (9, 100). While interest in the role of innate immunity in anti-PD-1/PD-L1 therapy is growing, little is known about NKs in CTLA-4-based therapies. Although under IL-2 stimulation murine NKs can exhibit CTLA-4 on their surface, this does not happen in humans (117, 118).

Anti-CTLA-4 seems to increase intratumor NK levels in melanoma murine models, positively affecting response, especially when treatment was combined with IL-2 (119). In melanoma patients, high levels of intratumor NKs in pretreatment tumor samples were correlated to improved outcomes of anti-CTLA-4 (120), and survival rate was correlated with low levels of IL-15 in the serum. In PB of patients with malignant pleural mesothelioma (MPM), a reduction of $CD56^{dim}$ effector NKs was observed as compared to healthy controls, but the levels of these cells increased after therapy with tremelimumab, an anti-CTLA-4 monoclonal antibody (mAb) (121). Similar results were reported in melanoma patients after treatment with ipilimumab (122).

Treg downregulation upon anti-CTLA-4 therapy can result in reduced Treg-mediated NK inhibition (123). Taken together, these data suggest a possible interplaying role between CTLA-4 blockade and NKs. These observations might be useful, as combination therapy of nivolumab, ipilimumab, and standard chemotherapy has recently been approved in clinical practice as a

first-line option for metastatic NSCLC. A combination of multiple checkpoints might overcome NK resistance to a single agent and restore NK immunity. However, to date, no data are available in this field.

5 NATURAL KILLER CELLS AS A TARGET OF NEW THERAPEUTIC STRATEGIES

Resistance to anti-PD-1/PD-L1 and anti-CTLA-4 ICIs can occur during treatment, as a result of the exhaustion of immunological targets or the activation of alternative pathways, under pressure and dynamic changes of the TME. Thus, there is an urgent need for the development of new pharmacological agents able to block these evasion mechanisms. As for PD-1/PD-L1 and anti-CTLA 4, blocking other cancer-dependent inhibitory pathways, either through single agents or in combinations with other ICIs, is one of the most studied strategies to obtain disease control. Mobilization of NKs, which can coordinate the anticancer response together with T cells, may also be a promising therapeutic strategy. As reported above, NKs have a crucial role in tumor response and are also possibly implicated in response to immunotherapy. Many efforts have been made to target NKs as therapeutic agents. NK immunotherapy can be approached from two directions: the activation of endogenous NKs currently circulating or resident within normal or tumor tissues or the administration of activated autologous or allogeneic NKs. **Tables 1** and **2** summarize ongoing clinical trials with ICIs and adoptive or chimeric antigen receptor (CAR)-NK therapy in NSCLC. Most of the targets that are being explored by new ICIs are expressed on NKs.

5.1 Inhibitors of Natural Killer Cell Receptors in Non-Small Cell Lung Cancer

As exhausted TI-NKs or TA-NKs express inhibitory receptors on their cell surface, one strategy to overcome resistance is to target in order to restore NKs to their antitumoral activity (**Figure 4**).

5.1.1 Anti-KIR

Monoclonal antibodies targeting KIR inhibitory receptors KIR2DL1–3 have been developed. They mimic the "missing-

TABLE 1 | Current clinical trials with checkpoint inhibitors in NSCLC.

Identifier	Drug	Phase	Study design	Setting	Status
TIGIT					
NCT04294810 SKYSCRAPER-01	Tiragolumab	III	Tiragolumab + atezolizumab vs. placebo + atezolizumab	Untreated advanced NSCLC PD-L1 pos.	Active, recruiting
NCT03563716 CITYSCAPE-01	Tiragolumab	II	Tiragolumab + atezolizumab vs. placebo + atezolizumab	Untreated advanced	Active, not recruiting
NCT04746924	Ociperlimab	III	Ociperlimab + tislelizumab vs. pembrolizumab in PD-L1 ≥ 50%	Untreated advanced PD-L1 pos.	Active, recruiting
NCT05102214	HLX301	I/II	HLX301 (bi-specific: TIGIT and PD-1) single-arm multicohort	Previously treated solid tumors	Active, recruiting
KIR					
NCT01714739	Lirilumab	I/II	Lirilumab + nivolumab or nivolumab and ipilimumab	Pretreated solid tumors	Completed
NCT03347123	Lirilumab	I/II	Lirilumab + nivolumab + epacadostat	Pretreated solid tumors	Completed
TIM-3					
NCT03708328	RO7121661	I	RO7121661 (Bi-specific: TIM-3 and PD-1) single arm dose escalation phase + expansion cohort	Advanced solid tumors	Active, recruiting
NCT03744468	BGB-A425	I/II	BGB-A425+ tislelizumab multicohort	Stage III-IV NSCLC PD-L1 positive	Active, recruiting
LAG-3					
NCT02966548	Relatlimab	I	Relatlimab + nivolumab	Pretreated, metastatic solid tumors	Active, not recruiting
NCT01968109	Relatlimab	II	Relatlimab + nivolumab	Solid tumors (I or II line NSCLC)	Active, not recruiting
NCT03459222	Relatlimab	I/II	Relatlimab + nivolumab + ipilimumab	Solid tumors	Not recruiting
NCT03625323	IMP321 (eftilagimod alpha)	II	Eftilagimod alpha + pembrolizumab	I or II line NSCLC	Active, not recruiting
NCT04623775	Relatlimab	II	Relatlimab + nivolumab + Chemotherapy vs. nivolumab + chemotherapy	First-line stage IV NSCLC	Active, recruiting
NCT04205552	Relatlimab	II	Relatlimab + nivolumab vs. nivolumab	Neoadjuvant stage IB–IIIA NSCLC	Active, recruiting
NKG2A					
NCT03822351	Monalizumab	II	Durvalumab/monalizumab/oleclumab Following chemo-radiotherapy	Stage III NSCLC	Active, not recruiting
NCT05061550	Monalizumab	II	Durvalumab/monalizumab/oleclumab	Neo/adjuvant stage IB–IIIA NSCLC	Active, not recruiting

The table shows phase I–III ongoing clinical trials on new checkpoint inhibitors acting on NK.
NK, natural killer cell; NSCLC, non-small cell lung cancer.

TABLE 2 | Current clinical trials on adoptive and CAR-NK therapy in NSCLC.

Identifier	Type of NK	Patient number	Phase	Drugs	Setting	Current status
NCT04990063	Autologous	20	I	Natural killer cells (NKs) and gamma delta T cells (γδT cells) + chemotherapy	Advanced NSCLC	Active, recruiting
NCT02843204	Allogenic	109	I/II	Allogenic NK + pembrolizumab	Advanced pretreated NSCLC	Completed
NCT02118415	Autologous	90	II	Hsp70-peptide TKD/IL-2 activated, autologous NKs	Maintenance therapy, unresectable stage III NSCLC after chemo-radiotherapy	Suspended
NCT04616209	Allogenic	24	I/II	Allogeneic PB103 and standard cancer treatment	Stage IIIB–C/IV	Active, recruiting
NCT04872634	Allogenic	24	I/II	SNK01 + chemotherapy ± cetuximab	Advanced NSCLC, pretreated with TKI	Active, recruiting
NCT03656705	CAR-NK	5	I	Chimeric costimulatory converting receptor (CCCR)-modified NK92 cells in previously treated advanced non-small cell lung carcinoma	Advanced pretreated NSCLC	Enrolling by invitation
NCT03841110	Allogenic	37	I	FT500 (allogeneic, iPSC-derived NK) monotherapy or plus pembrolizumab/nivolumab/atezolizumab	Advanced pretreated NSCLC	Active, recruiting
NCT04440735	BIKE	100	I	DSP107(SIRPα-4-1BBL) + Atezolizumab	Advanced refractory NSCLC	Active, recruiting
NCT04050709	CAR-NK	16	I	PD-L1 t-haNK	Pretreated solid tumors	Active, not recruiting

The table summarizes the ongoing trials on genetically modified and non-genetically modified adoptive cell therapy with NKs.
NK, natural killer cell; NSCLC, non-small cell lung cancer; TKI, tyrosine kinase inhibitor.

self" response by blocking the interaction between KIR2DL and the natural ligand HLA-C. Lirilumab is a fully humanized IgG4 that binding with high affinity to KIR2DL1–3 receptors, expressed in about half of TI-NKs and TA-NKs, blocks the interaction with HLA-C. Lirilumab was first investigated on hematologic malignancies (124), but it showed initial efficacy and a favorable safety profile also in a phase I basket trials comprising various tumor types (breast, ovarian, pancreatic, and endometrial cancers) (125). A combination of lirilumab and nivolumab showed promising activity in the SCC of the head and neck (126). Lirilumab is under investigation in various solid tumors, including NSCLC, alone or in combination with nivolumab and epacadostat in a multicohort phase I–II study (NCT03347123).

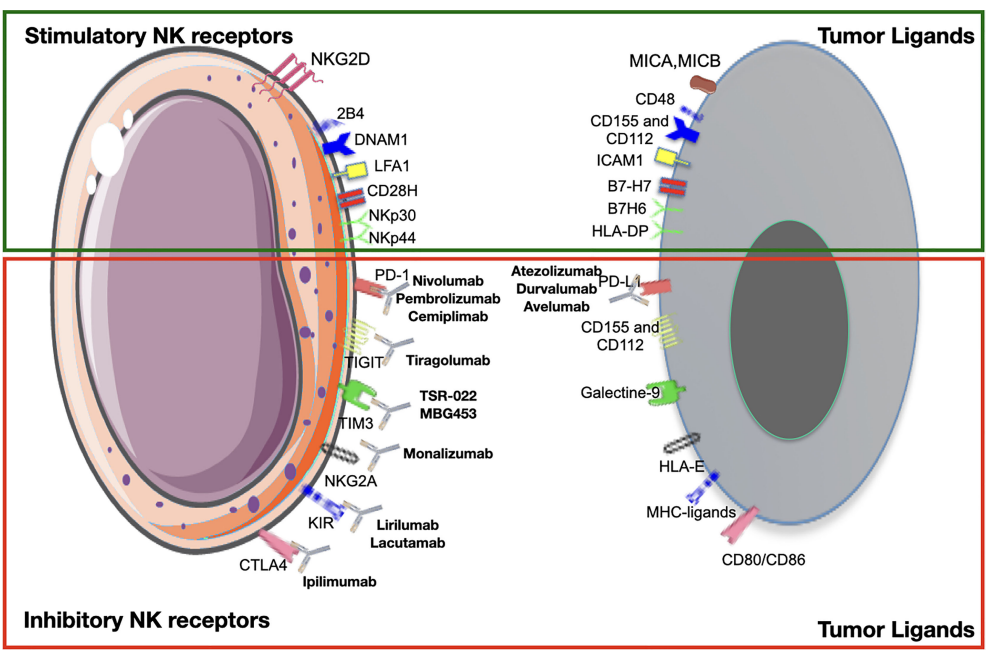

FIGURE 4 | Activating and inhibitory receptors on natural killer cells (NKs) and their ligands on tumor cells. Checkpoint inhibitors bind to inhibitory receptors on NKs, preventing the link with their ligands on tumor cells and vice versa. Here are reported the major pathways and monoclonal antibodies currently used in clinical practice or under evaluation in clinical trials.

5.1.2 Anti-NGK2A

NKG2A is another inhibitory receptor expressed on the NK surface (76, 77). After interaction with a non-classical MHC class I molecule, it forms heterodimers with CD94 leading to the activation of inhibitory intracellular signals. As reported above, NKG2A is overexpressed on NKs in many types of cancers and is related to worse prognosis and immunotherapy resistance. This has encouraged the development of a specific monoclonal antibody blocking this pathway, called monalizumab (76, 77). Furthermore, when combined with anti-PD-1, monalizumab can stimulate also $CD8^+$ T-cell antitumor activity (76, 77). Monalizumab is currently under investigation in combination with durvalumab in solid tumors and in particular in NSCLC (NCT02671435, NCT03833440).

5.1.3 Anti-TIM-3

Preclinical evidence suggests that TIM-3 blockade alone or in combination with PD-1 inhibitors can reverse the functional impairment of TIM-3+ T cells (127, 128). An increase in TIM-3+ circulating NKs has been reported in lung cancer, associated with immune suppressive TME, NK killing activity inhibition, and the more aggressive disease form, suggesting that it could be a possible therapeutic target in NSCLC (84). Preclinical data demonstrated that TIM-3 blockade is effective not only in counter-modulating dysfunctional $CD8^+$ T cells and Tregs but also in restoring NK cytotoxic activity and TNF-alpha and IFN-γ production in lung cancer (83). Therapeutic TIM-3 antibodies are currently being evaluated in phase I trials either as single-agent treatment or in combination therapy [NCT03744468, NCT03708328]. Furthermore, a bi-specific antibody targeting both PD-1 and TIM-3, AZD7789, has recently been developed and is currently under investigation in a phase I trial in patients with different solid tumors, including lung cancer [NCT03708328].

5.1.4 Anti-LAG3

Although the specific role of LAG-3 in human NKs is still unclear, the therapeutic blockade of this checkpoint receptor remains appealing due to its interaction with both NK and T cells, particularly in combination with PD-1 inhibitors. Certain clinical-grade inhibitors (IMP321, BMS-986016) are currently under investigation in ongoing phase I and II trials (129).

5.1.5 Anti-TIGIT

TIGIT is an inhibitory receptor expressed on $CD8^+$ T cells, Tregs, and NKs and has gained increasing attention as a promising novel pharmacological target for cancer immunotherapy. Binding to its ligands CD155 and CD112 (or nectin-2) expressed by tumor cells and antigen-presenting cells in the TME, TIGIT induces anergy of T cells and NKs, immune suppression, and tumor escape (130). The combination of the anti-TIGIT antibody, tiragolumab, with atezolizumab showed encouraging results in NSCLC. In preclinical models, the combination of anti-TIGIT and anti-PD-L1 synergistically improved tumor control and survival (131). The randomized phase II CITYSCAPE compares the first-line treatment with tiragolumab plus atezolizumab with atezolizumab alone in metastatic NSCLC patients, stratified for histology and selected for PD-L1 expression (132). The combination of tiragolumab and atezolizumab significantly improved ORR (37% versus 21%) and PFS (median PFS (mPFS) 5.42 versus 3.58), independently from the histology, with a greater magnitude benefit in patients with PD-L1 > 50% (133). The blockade of TIGIT could be an interesting chemo-sparing strategy; however, longer follow-up and phase III trials are required.

5.2 BiKEs and TriKEs

Bi- and Tri-specific T-cell engagers (BiTEs and TriTEs) are bi- or tri-valent antibodies constituted by two or three single-chain Fc fragments, respectively, that create a link between T cells and tumor cells (134). T cells lack Fcγ receptors, so normal monoclonal antibodies are not able to directly recruit T cells (135). Thanks to their two or three chains, BiTEs and TriTEs can recognize both one or two tumor antigens and one CD3 molecule, associated with the TCR, at the same time resulting in T-cell activation (136). This is an intriguing strategy to re-activate exhausted T cells induced by long-term exposure to tumor antigens. More recently, the same mechanism has been designed for bi- or tri-specific killer–cell engagers (BiKEs and TriKEs) to recruit and activate NKs in the TME and to promote tumor lysis. These molecules are built up by two (BiKEs) or three (TriKEs) single-chain variable fragments (scFv) with different heavy and light antibody chains connected through short peptide linkers (137). These can be considered "NK cell adaptors"; they usually target an activating receptor, like NKp46 and CD16 on NKs and a tumor antigen, such as CD19, CD20, or endothelial growth factor receptor (EGFR) and Fc fragments (138). Compared to monoclonal antibodies, BiKEs and TriKEs present some important advantages, such as higher biodistribution, due to their small size, lower immunogenicity, and great flexibility (139). AFM24 is a bispecific EGFR/CD16A innate cell engager antibody that has shown preclinical activity in controlling tumor growth in *in vitro* and mouse models of EGFR-positive tumors, independently from the presence of EGFR mutation (140). TriKEs have the ulterior advantage of targeting two different molecules, preventing an eventual downregulation of one selected molecule on target tumor cells (137). A new generation of TriKEs and TetraKEs (with four functional domains) has been designed to incorporate an IL-15 moiety, with the aim of promoting NK activation, *in vivo* persistence, and proliferation. However, most of these agents are only in preclinical development, and further studies are needed before testing them in a clinical setting.

5.3 Adoptive Natural Killer Cell Therapy

5.3.1 Non-Genetically Modified

An alternative approach to the systemic activation of NKs is to directly introduce activated NKs into patients. This adaptive transfer of NKs is the most direct way to restore and improve the function of the immune system. NKs can be autologous or allogenic as derived from PB mononuclear cells (PBMCs) or stem cells (umbilical cord blood and embryonic stem cells) or NK lines. Following isolation, NKs can be activated by exposure to cytokines or other stimulating factors or by genetically engineered manipulation (141, 142). To assess the feasibility of

autologous NK transfer, a study was designed in patients with advanced NSCLC and treated with a combination of docetaxel and *ex vivo* expanded autologous NK. However, it failed to demonstrate a real therapeutic benefit of the combination, probably due to poor NK activity *in vivo* (143). Even though autologous NKs can be efficiently expanded and activated *in vitro*, the unsuccessful result of this study suggests that this approach is probably not a feasible treatment modality (42, 143, 144). Compared to autologous NKs, allogeneic NKs have a longer persistence *in vivo*, which corresponds to an improved response to treatment but is burdened with a higher risk of graft-versus-host disease (145). Adaptive allogenic or alloreactive transfer results in MHC-I and KIR ligand mismatch and efficient immune response, as reported first in AML (146). Following AML, clinical studies testing the adaptive transfer of mismatched alloreactive NKs as a form of immunotherapy showed low toxicity and initial therapeutic efficacy also in solid tumors including NSCLC (147, 148). In advanced NSCLC, repetitive infusions of alloreactive donor NKs resulted in encouraging disease control in many patients, highlighting its potential use in this setting (149). Furthermore, the combination of allogenic adaptive NK therapy with pembrolizumab led to improved OS and PFS (median OS (mOS) 15.5 vs. 13.3 months; mPFS 6.5 vs. 4.3 months; $p < 0.05$) as compared to pembrolizumab alone in pretreated advanced NSCLC patients. The survival advantage was particularly evident in PD-L1-positive patients (>50%) (149).

To expand the therapeutic use of alloreactive NKs, human NK lines have been generated as a renewable source of NKs. The human NK line NK-92 (150) is highly cytotoxic against a variety of cancer types, and it is under investigation also in phase I trials in solid tumors, such as melanoma (151, 152). The NK-92 cell line has been used as a source of NKs for adaptive transfer and modified for improved efficacy and target specificity, with genetic manipulation or cytokine activation prior to adaptive transfer. In a phase I basket trial, infusion of NK-92 cells was particularly active in patients with lung cancer patients: three of four small cell lung cancer (SCLC) and NSCLC patients in the study have tumor response according to Response Evaluation Criteria in Solid Tumors (RECIST) criteria or long-lasting disease control with the adaptive transfer of IL-2 activated NK-92 cells (153). A hypothesis about this particular sensitivity in lung cancer patients is that NKs reside in the lung prior to circulating following intravenous administration (142). These could represent an intriguing strategy to develop in dedicated clinical trials.

5.3.2 Chimeric Antigen Receptor–Natural Killer Cells

Genetically modified NKs present enhanced specificity and activity against the target. One of these methods that are founding increasing interest is the construction of CARs based on NKs instead of T lymphocytes (154). CAR-T cells are now widely used in clinical practice, mostly in hematological malignancies, but this technology has also been applied to macrophages and NKs to enhance efficacy and limit possible toxicity (155). In fact, CAR-NK administration is not associated with the development of cytokine release syndrome, neurotoxicity or graft-versus-host response, and other side effects, which makes it a very attractive therapeutic option (156).

The sources of NKs usable for CAR-NK are the same as for adaptive therapy: PB or umbilical cord NKs or cell lines, such as NK-92. Recently, a CAR-NK was created using NK-92-derived cell lines carrying on the surface the immune checkpoint anti-B7-H3: in xenograft models, it showed significant inhibition of tumor growth and increased survival, providing a proof of concept for its development in the clinical setting (157). Another interesting new chimeric costimulatory converting receptor was built up by modified NK92 and constituted by the extracellular domain of PD-1, transmembrane and cytoplasmatic NKG2D domain, and cytoplasmic domain of the TNF receptor superfamily member 4–1BB (TNFRSF9/CD1377). It is able to counteract the immunosuppressive action of PD-1 and showed preclinical *in vitro* anti-humoral activity against human lung cancer H1299 cells (158). Delta-like ligand 3 (DLL3) is overexpressed in most SCLC and may be used as a target for CAR-NKs therapy. In a recent study, DLL3-positive SCLC cell lines have been cocultured with DLL3-CAR-NK-92, and the construct was proved to have a high cytolytic effect (158). This report explored the potential in the treatment of SCLC. Furthermore, the DLL3-CAR NK-92 showed improved cytotoxicity also against lung metastasis in tumor models with good tolerance and in subcutaneous tumor models of SCLC (158).

CONCLUSION

Cancer treatment with ICIs of PD-1/PD-L1 and CTLA-4 is widely used in clinical practice, but, unfortunately, it shows limited efficacy in a variety of patients due to secondary resistance or non-response. In physiological conditions, NKs play an important role in the immune response against the tumor. However, following neoplastic transformation, cancer cells and TME act by modulating NK functions inducing the switch toward a pro-tumor phenotype (42, 144). TME can influence the treatment response and effectiveness of ICIs, and a growing amount of evidence suggest that NKs can act as a predictor as well as a prognostic factor (42, 144). NKs have been shown to play a crucial role in metastatic tumor surveillance in both NSCLC and SCLC. In recent years, the application of NK and CAR-NK immunotherapy has brought significant progress in the field of cancer therapy, with the latest clinical trials showing tremendous potential (155). Although the clinical focus of NK therapy is largely hematopoietic malignancies, conceivable progression of NK immunotherapy in the treatment of lung cancer has also emerged.

The lung cancer cells and the TME can polarize NKs into pro-inflammatory, pro-angiogenic decidual-like subsets (42, 155). Therefore, although the application of NK therapy as a standalone agent or in combination with other therapeutic modalities is a rapidly evolving field that is producing promising results, the possibility of turning the tumor and TME into a non-lytic phenotype has to be taken into account.

The findings summarized in this review have yet to be fully confirmed in more in-depth clinical settings, but they highlight a potential diagnostic and therapeutic modality in a field with limited therapeutic options and an invariably low survival rate.

Curbing NK pro-inflammatory switch in cancer is pivotal in the success of immunotherapy with ICI.

AUTHOR CONTRIBUTIONS

Conceptualization: AA, MG, and RR. Writing—original draft preparation: MG and AA. Writing—review and editing: AA, RR, DN, VC, MB, and GP. Figures: AA, MG, DN, GP, and MB. All authors have read and agreed to the published version of the manuscript.

FUNDING

DM was the recipient of the Ministero della Salute COVID-2020-12371849 and the Italian Ministry of University and Research PRIN 2017 grant 2017NTK4HY. AA is the recipient of a research contract in progress from Stazione Zoologica (ADViSE Project; PG/2018/0494374) and Azienda Agricola Fattoria La Vialla, Castiglion Fibocchi, Arezzo (Italy). This work has also been supported by the Italian Ministry of Health Ricerca Corrente—IRCCS MultiMedica to MG, GP, and RR and IRCCS IEO to AA.

ACKNOWLEDGMENTS

We like to thank Dr. Paola Corradino for the bibliography.

REFERENCES

1. Yang Y. Cancer Immunotherapy: Harnessing the Immune System to Battle Cancer. *J Clin Invest* (2015) 125(9):3335–7. doi: 10.1172/JCI83871
2. Vaddepally RK, Kharel P, Pandey R, Garje R, Chandra AB. Review of Indications of FDA-Approved Immune Checkpoint Inhibitors Per Nccn Guidelines With the Level of Evidence. *Cancers (Basel)* (2020) 12(3):738–57. doi: 10.3390/cancers12030738
3. Wei SC, Levine JH, Cogdill AP, Zhao Y, Anang NAS, Andrews MC, et al. Distinct Cellular Mechanisms Underlie Anti-Ctla-4 and Anti-Pd-1 Checkpoint Blockade. *Cell* (2017) 170(6):1120–33.e17. doi: 10.1016/j.cell.2017.07.024
4. Nowak EC, Lines JL, Varn FS, Deng J, Sarde A, Mabaera R, et al. Immunoregulatory Functions of Vista. *Immunol Rev* (2017) 276(1):66–79. doi: 10.1111/imr.12525
5. Antonia SJ, Villegas A, Daniel D, Vicente D, Murakami S, Hui R, et al. Durvalumab After Chemoradiotherapy in Stage Iii Non-Small-Cell Lung Cancer. *N Engl J Med* (2017) 377(20):1919–29. doi: 10.1056/NEJMoa1709937
6. Borghaei H, Paz-Ares L, Horn L, Spigel DR, Steins M, Ready NE, et al. Nivolumab Versus Docetaxel in Advanced Nonsquamous Non-Small-Cell Lung Cancer. *N Engl J Med* (2015) 373(17):1627–39. doi: 10.1056/NEJMoa1507643
7. Gandhi L, Rodriguez-Abreu D, Gadgeel S, Esteban E, Felip E, De Angelis F, et al. Pembrolizumab Plus Chemotherapy in Metastatic Non-Small-Cell Lung Cancer. *N Engl J Med* (2018) 378(22):2078–92. doi: 10.1056/NEJMoa1801005
8. Herbst RS, Baas P, Kim DW, Felip E, Perez-Gracia JL, Han JY, et al. Pembrolizumab Versus Docetaxel for Previously Treated, Pd-L1-Positive, Advanced Non-Small-Cell Lung Cancer (Keynote-010): A Randomised Controlled Trial. *Lancet* (2016) 387(10027):1540–50. doi: 10.1016/S0140-6736(15)01281-7
9. Paz-Ares L, Ciuleanu TE, Cobo M, Schenker M, Zurawski B, Menezes J, et al. First-Line Nivolumab Plus Ipilimumab Combined With Two Cycles of Chemotherapy in Patients With Non-Small-Cell Lung Cancer (Checkmate 9la): An International, Randomised, Open-Label, Phase 3 Trial. *Lancet Oncol* (2021) 22(2):198–211. doi: 10.1016/S1470-2045(20)30641-0
10. Paz-Ares L, Vicente D, Tafreshi A, Robinson A, Soto Parra H, Mazieres J, et al. A Randomized, Placebo-Controlled Trial of Pembrolizumab Plus Chemotherapy in Patients With Metastatic Squamous Nsclc: Protocol-Specified Final Analysis of Keynote-407. *J Thorac Oncol* (2020) 15(10):1657–69. doi: 10.1016/j.jtho.2020.06.015
11. Reck M, Rodriguez-Abreu D, Robinson AG, Hui R, Csoszi T, Fulop A, et al. Pembrolizumab Versus Chemotherapy for Pd-L1-Positive Non-Small-Cell Lung Cancer. *N Engl J Med* (2016) 375(19):1823–33. doi: 10.1056/NEJMoa1606774
12. Rittmeyer A, Barlesi F, Waterkamp D, Park K, Ciardiello F, von Pawel J, et al. Atezolizumab Versus Docetaxel in Patients With Previously Treated Non-Small-Cell Lung Cancer (Oak): A Phase 3, Open-Label, Multicentre Randomised Controlled Trial. *Lancet* (2017) 389(10066):255–65. doi: 10.1016/S0140-6736(16)32517-X
13. Nowicki TS, Hu-Lieskovan S, Ribas A. Mechanisms of Resistance to Pd-1 and Pd-L1 Blockade. *Cancer J* (2018) 24(1):47–53. doi: 10.1097/PPO.0000000000000303
14. Karasarides M, Cogdill AP, Robbins PB, Bowden M, Burton EM, Butterfield LH, et al. Hallmarks of Resistance to Immune-Checkpoint Inhibitors. *Cancer Immunol Res* (2022) 10(4):372–83. doi: 10.1158/2326-6066.CIR-20-0586
15. Bremnes RM, Busund LT, Kilvaer TL, Andersen S, Richardsen E, Paulsen EE, et al. The Role of Tumor-Infiltrating Lymphocytes in Development, Progression, and Prognosis of Non-Small Cell Lung Cancer. *J Thorac Oncol* (2016) 11(6):789–800. doi: 10.1016/j.jtho.2016.01.015
16. Burugu S, Asleh-Aburaya K, Nielsen TO. Immune Infiltrates in the Breast Cancer Microenvironment: Detection, Characterization and Clinical Implication. *Breast Cancer* (2017) 24(1):3–15. doi: 10.1007/s12282-016-0698-z
17. Oble DA, Loewe R, Yu P, Mihm MCJr. Focus on Tils: Prognostic Significance of Tumor Infiltrating Lymphocytes in Human Melanoma. *Cancer Immun* (2009) 9:3.
18. Pan Y, Yu Y, Wang X, Zhang T. Tumor-Associated Macrophages in Tumor Immunity. *Front Immunol* (2021) 12:775758. doi: 10.3389/fimmu.2021.775758
19. Moretta A, Locatelli F, Moretta L. Human Nk Cells: From Hla Class I-Specific Killer Ig-Like Receptors to the Therapy of Acute Leukemias. *Immunol Rev* (2008) 224:58–69. doi: 10.1111/j.1600-065X.2008.00651.x
20. Vivier E, Tomasello E, Baratin M, Walzer T, Ugolini S. Functions of Natural Killer Cells. *Nat Immunol* (2008) 9(5):503–10. doi: 10.1038/ni1582
21. Freud AG, Mundy-Bosse BL, Yu J, Caligiuri MA. The Broad Spectrum of Human Natural Killer Cell Diversity. *Immunity* (2017) 47(5):820–33. doi: 10.1016/j.immuni.2017.10.008
22. Blum JS, Wearsch PA, Cresswell P. Pathways of Antigen Processing. *Annu Rev Immunol* (2013) 31:443–73. doi: 10.1146/annurev-immunol-032712-095910
23. Kobayashi KS, van den Elsen PJ. Nlrc5: A Key Regulator of Mhc Class I-Dependent Immune Responses. *Nat Rev Immunol* (2012) 12(12):813–20. doi: 10.1038/nri3339
24. Vacca P, Munari E, Tumino N, Moretta F, Pietra G, Vitale M, et al. Human Natural Killer Cells and Other Innate Lymphoid Cells in Cancer: Friends or Foes? *Immunol Lett* (2018) 201:14–9. doi: 10.1016/j.imlet.2018.11.004
25. Spits H, Artis D, Colonna M, Diefenbach A, Di Santo JP, Eberl G, et al. Innate Lymphoid Cells–a Proposal for Uniform Nomenclature. *Nat Rev Immunol* (2013) 13(2):145–9. doi: 10.1038/nri3365
26. Spits H, Cupedo T. Innate Lymphoid Cells: Emerging Insights in Development, Lineage Relationships, and Function. *Annu Rev Immunol* (2012) 30:647–75. doi: 10.1146/annurev-immunol-020711-075053
27. Bruno A, Pagani A, Pulze L, Albini A, Dallaglio K, Noonan DM, et al. Orchestration of Angiogenesis by Immune Cells. *Front Oncol* (2014) 4:131. doi: 10.3389/fonc.2014.00131

28. Noonan DM, De Lerma Barbaro A, Vannini N, Mortara L, Albini A. Inflammation, Inflammatory Cells and Angiogenesis: Decisions and Indecisions. *Cancer Metastasis Rev* (2008) 27(1):31–40. doi: 10.1007/s10555-007-9108-5
29. Cooper MA, Fehniger TA, Caligiuri MA. The Biology of Human Natural Killer-Cell Subsets. *Trends Immunol* (2001) 22(11):633–40. doi: 10.1016/S1471-4906(01)02060-9
30. Morandi F, Horenstein AL, Chillemi A, Quarona V, Chiesa S, Imperatori A, et al. Cd56brightcd16- Nk Cells Produce Adenosine Through a Cd38-Mediated Pathway and Act as Regulatory Cells Inhibiting Autologous Cd4 + T Cell Proliferation. *J Immunol* (2015) 195(3):965–72. doi: 10.4049/jimmunol.1500591
31. Schleypen JS, Von Geldern M, Weiss EH, Kotzias N, Rohrmann K, Schendel DJ, et al. Renal Cell Carcinoma-Infiltrating Natural Killer Cells Express Differential Repertoires of Activating and Inhibitory Receptors and Are Inhibited by Specific Hla Class I Allotypes. *Int J Cancer* (2003) 106(6):905–12. doi: 10.1002/ijc.11321
32. Farrar MA, Schreiber RD. The Molecular Cell Biology of Interferon-Gamma and Its Receptor. *Annu Rev Immunol* (1993) 11:571–611. doi: 10.1146/annurev.iy.11.040193.003035
33. Malmberg KJ, Carlsten M, Bjorklund A, Sohlberg E, Bryceson YT, Ljunggren HG. Natural Killer Cell-Mediated Immunosurveillance of Human Cancer. *Semin Immunol* (2017) 31:20–9. doi: 10.1016/j.smim.2017.08.002
34. Carrega P, Bonaccorsi I, Di Carlo E, Morandi B, Paul P, Rizzello V, et al. Cd56(Bright)Perforin(Low) Noncytotoxic Human Nk Cells Are Abundant in Both Healthy and Neoplastic Solid Tissues and Recirculate to Secondary Lymphoid Organs *Via* Afferent Lymph. *J Immunol* (2014) 192(8):3805–15. doi: 10.4049/jimmunol.1301889
35. Marquardt N, Kekalainen E, Chen P, Kvedaraite E, Wilson JN, Ivarsson MA, et al. Human Lung Natural Killer Cells Are Predominantly Comprised of Highly Differentiated Hypofunctional Cd69(-)Cd56(Dim) Cells. *J Allergy Clin Immunol* (2017) 139(4):1321–30.e4. doi: 10.1016/j.jaci.2016.07.043
36. Carrega P, Morandi B, Costa R, Frumento G, Forte G, Altavilla G, et al. Natural Killer Cells Infiltrating Human Nonsmall-Cell Lung Cancer Are Enriched in Cd56 Bright Cd16(-) Cells and Display an Impaired Capability to Kill Tumor Cells. *Cancer* (2008) 112(4):863–75. doi: 10.1002/cncr.23239
37. Bruno A, Focaccetti C, Pagani A, Imperatori AS, Spagnoletti M, Rotolo N, et al. The Proangiogenic Phenotype of Natural Killer Cells in Patients With Non-Small Cell Lung Cancer. *Neoplasia* (2013) 15(2):133–42. doi: 10.1593/neo.121758
38. Robinson BW, Pinkston P, Crystal RG. Natural Killer Cells Are Present in the Normal Human Lung But Are Functionally Impotent. *J Clin Invest* (1984) 74(3):942–50. doi: 10.1172/JCI111513
39. Weissman DN, deShazo RD, Banks DE. Modulation of Natural Killer Cell Function by Human Alveolar Macrophages. *J Allergy Clin Immunol* (1986) 78(4 Pt 1):571–7. doi: 10.1016/0091-6749(86)90073-4
40. Cooper GE, Ostridge K, Khakoo SI, Wilkinson TMA, Staples KJ. Human Cd49a(+) Lung Natural Killer Cell Cytotoxicity in Response to Influenza a Virus. *Front Immunol* (2018) 9:1671. doi: 10.3389/fimmu.2018.01671
41. Bruno A, Bassani B, D'Urso DG, Pitaku I, Cassinotti E, Pelosi G, et al. Angiogenin and the Mmp9-Timp2 Axis Are Up-Regulated in Proangiogenic, Decidual Nk-Like Cells From Patients With Colorectal Cancer. *FASEB J* (2018) 32(10):5365–77. doi: 10.1096/fj.201701103R
42. Albini A, Noonan DM. Decidual-Like Nk Cell Polarization: From Cancer Killing to Cancer Nurturing. *Cancer Discovery* (2021) 11(1):28–33. doi: 10.1158/2159-8290.CD-20-0796
43. Jabrane-Ferrat N. Features of Human Decidual Nk Cells in Healthy Pregnancy and During Viral Infection. *Front Immunol* (2019) 10:1397. doi: 10.3389/fimmu.2019.01397
44. Santoni A, Zingoni A, Cerboni C, Gismondi A. Natural Killer (Nk) Cells From Killers to Regulators: Distinct Features Between Peripheral Blood and Decidual Nk Cells. *Am J Reprod Immunol* (2007) 58(3):280–8. doi: 10.1111/j.1600-0897.2007.00513.x
45. Vacca P, Moretta L, Moretta A, Mingari MC. Origin, Phenotype and Function of Human Natural Killer Cells in Pregnancy. *Trends Immunol* (2011) 32(11):517–23. doi: 10.1016/j.it.2011.06.013
46. Jin S, Deng Y, Hao JW, Li Y, Liu B, Yu Y, et al. Nk Cell Phenotypic Modulation in Lung Cancer Environment. *PloS One* (2014) 9(10):e109976. doi: 10.1371/journal.pone.0109976
47. Bruno A, Ferlazzo G, Albini A, Noonan DM. A Think Tank of Tink/Tanks: Tumor-Infiltrating/Tumor-Associated Natural Killer Cells in Tumor Progression and Angiogenesis. *J Natl Cancer Instit* (2014) 106(8):1–13. doi: 10.1093/jnci/dju200
48. Platonova S, Cherfils-Vicini J, Damotte D, Crozet L, Vieillard V, Validire P, et al. Profound Coordinated Alterations of Intratumoral Nk Cell Phenotype and Function in Lung Carcinoma. *Cancer Res* (2011) 71(16):5412–22. doi: 10.1158/0008-5472.CAN-10-4179
49. Lavin Y, Kobayashi S, Leader A, Amir ED, Elefant N, Bigenwald C, et al. Innate Immune Landscape in Early Lung Adenocarcinoma by Paired Single-Cell Analyses. *Cell* (2017) 169(4):750–65.e17. doi: 10.1016/j.cell.2017.04.014
50. Soo RA, Chen Z, Yan Teng RS, Tan HL, Iacopetta B, Tai BC, et al. Prognostic Significance of Immune Cells in Non-Small Cell Lung Cancer: Meta-Analysis. *Oncotarget* (2018) 9(37):24801–20. doi: 10.18632/oncotarget.24835
51. Takanami I, Takeuchi K, Giga M. The Prognostic Value of Natural Killer Cell Infiltration in Resected Pulmonary Adenocarcinoma. *J Thorac Cardiovasc Surg* (2001) 121(6):1058–63. doi: 10.1067/mtc.2001.113026
52. Villegas FR, Coca S, Villarrubia VG, Jimenez R, Chillon MJ, Jareno J, et al. Prognostic Significance of Tumor Infiltrating Natural Killer Cells Subset Cd57 in Patients With Squamous Cell Lung Cancer. *Lung Cancer* (2002) 35(1):23–8. doi: 10.1016/s0169-5002(01)00292-6
53. Nersesian S, Schwartz SL, Grantham SR, MacLean LK, Lee SN, Pugh-Toole M, et al. Nk Cell Infiltration Is Associated With Improved Overall Survival in Solid Cancers: A Systematic Review and Meta-Analysis. *Transl Oncol* (2021) 14(1):100930. doi: 10.1016/j.tranon.2020.100930
54. Le Maux Chansac B, Moretta A, Vergnon I, Opolon P, Lecluse Y, Grunenwald D, et al. Nk Cells Infiltrating a Mhc Class I-Deficient Lung Adenocarcinoma Display Impaired Cytotoxic Activity Toward Autologous Tumor Cells Associated With Altered Nk Cell-Triggering Receptors. *J Immunol* (2005) 175(9):5790–8. doi: 10.4049/jimmunol.175.9.5790
55. Holtan SG, Creedon DJ, Thompson MA, Nevala WK, Markovic SN. Expansion of Cd16-Negative Natural Killer Cells in the Peripheral Blood of Patients With Metastatic Melanoma. *Clin Dev Immunol* (2011) 2011:316314. doi: 10.1155/2011/316314
56. Gallazzi M, Baci D, Mortara L, Bosi A, Buono G, Naselli A, et al. Prostate Cancer Peripheral Blood Nk Cells Show Enhanced Cd9, Cd49a, Cxcr4, Cxcl8, Mmp-9 Production and Secrete Monocyte-Recruiting and Polarizing Factors. *Front Immunol* (2020) 11:586126. doi: 10.3389/fimmu.2020.586126
57. Garcia-Iglesias T, Del Toro-Arreola A, Albarran-Somoza B, Del Toro-Arreola S, Sanchez-Hernandez PE, Ramirez-Duenas MG, et al. Low Nkp30, Nkp46 and Nkg2d Expression and Reduced Cytotoxic Activity on Nk Cells in Cervical Cancer and Precursor Lesions. *BMC Cancer* (2009) 9:186. doi: 10.1186/1471-2407-9-186
58. Wu Y, Kuang DM, Pan WD, Wan YL, Lao XM, Wang D, et al. Monocyte/Macrophage-Elicited Natural Killer Cell Dysfunction in Hepatocellular Carcinoma Is Mediated by Cd48/2b4 Interactions. *Hepatology* (2013) 57(3):1107–16. doi: 10.1002/hep.26192
59. Zhang QF, Yin WW, Xia Y, Yi YY, He QF, Wang X, et al. Liver-Infiltrating Cd11b(-)Cd27(-) Nk Subsets Account for Nk-Cell Dysfunction in Patients With Hepatocellular Carcinoma and Are Associated With Tumor Progression. *Cell Mol Immunol* (2017) 14(10):819–29. doi: 10.1038/cmi.2016.28
60. Fionda C, Stabile H, Cerboni C, Soriani A, Gismondi A, Cippitelli M, et al. Hitting More Birds With a Stone: Impact of Tgf-Beta on Ilc Activity in Cancer. *J Clin Med* (2020) 9(1):2–14. doi: 10.3390/jcm9010143
61. Hoshino A, Kim HS, Bojmar L, Gyan KE, Cioffi M, Hernandez J, et al. Extracellular Vesicle and Particle Biomarkers Define Multiple Human Cancers. *Cell* (2020) 182(4):1044–61.e18. doi: 10.1016/j.cell.2020.07.009
62. Vento-Tormo R, Efremova M, Botting RA, Turco MY, Vento-Tormo M, Meyer KB, et al. Single-Cell Reconstruction of the Early Maternal-Fetal Interface in Humans. *Nature* (2018) 563(7731):347–53. doi: 10.1038/s41586-018-0698-6
63. Hanna J, Goldman-Wohl D, Hamani Y, Avraham I, Greenfield C, Natanson-Yaron S, et al. Decidual Nk Cells Regulate Key Developmental Processes at the Human Fetal-Maternal Interface. *Nat Med* (2006) 12(9):1065–74. doi: 10.1038/nm1452
64. Lash GE, Schiessl B, Kirkley M, Innes BA, Cooper A, Searle RF, et al. Expression of Angiogenic Growth Factors by Uterine Natural Killer Cells

During Early Pregnancy. *J Leukoc Biol* (2006) 80(3):572–80. doi: 10.1189/jlb.0406250
65. Montaldo E, Vacca P, Chiossone L, Croxatto D, Loiacono F, Martini S, et al. Unique Eomes(+) Nk Cell Subsets Are Present in Uterus and Decidua During Early Pregnancy. *Front Immunol* (2015) 6:646. doi: 10.3389/fimmu.2015.00646
66. Wallace AE, Fraser R, Gurung S, Goulwara SS, Whitley GS, Johnstone AP, et al. Increased Angiogenic Factor Secretion by Decidual Natural Killer Cells From Pregnancies With High Uterine Artery Resistance Alters Trophoblast Function. *Hum Reprod* (2014) 29(4):652–60. doi: 10.1093/humrep/deu017
67. Close HJ, Stead LF, Nsengimana J, Reilly KA, Droop A, Wurdak H, et al. Expression Profiling of Single Cells and Patient Cohorts Identifies Multiple Immunosuppressive Pathways and an Altered Nk Cell Phenotype in Glioblastoma. *Clin Exp Immunol* (2020) 200(1):33–44. doi: 10.1111/cei.13403
68. Shaim H, Shanley M, Basar R, Daher M, Gumin J, Zamler DB, et al. Targeting the Alphav Integrin/Tgf-Beta Axis Improves Natural Killer Cell Function Against Glioblastoma Stem Cells. *J Clin Invest* (2021) 131(14):e142116. doi: 10.1172/JCI142116
69. Levi I, Amsalem H, Nissan A, Darash-Yahana M, Peretz T, Mandelboim O, et al. Characterization of Tumor Infiltrating Natural Killer Cell Subset. *Oncotarget* (2015) 6(15):13835–43. doi: 10.18632/oncotarget.3453
70. de Andrade LF, Lu Y, Luoma A, Ito Y, Pan D, Pyrdol JW, et al. Discovery of Specialized Nk Cell Populations Infiltrating Human Melanoma Metastases. *JCI Insight* (2019) 4(23):e133103. doi: 10.1172/jci.insight.133103
71. Castriconi R, Dondero A, Bellora F, Moretta L, Castellano A, Locatelli F, et al. Neuroblastoma-Derived Tgf-Beta1 Modulates the Chemokine Receptor Repertoire of Human Resting Nk Cells. *J Immunol* (2013) 190(10):5321–8. doi: 10.4049/jimmunol.1202693
72. Cerdeira AS, Rajakumar A, Royle CM, Lo A, Husain Z, Thadhani RI, et al. Conversion of Peripheral Blood Nk Cells to a Decidual Nk-Like Phenotype by a Cocktail of Defined Factors. *J Immunol* (2013) 190(8):3939–48. doi: 10.4049/jimmunol.1202582
73. Keskin DB, Allan DS, Rybalov B, Andzelm MM, Stern JN, Kopcow HD, et al. Tgfbeta Promotes Conversion of Cd16+ Peripheral Blood Nk Cells Into Cd16- Nk Cells With Similarities to Decidual Nk Cells. *Proc Natl Acad Sci USA* (2007) 104(9):3378–83. doi: 10.1073/pnas.0611098104
74. Bosi A, Zanellato S, Bassani B, Albini A, Musco A, Cattoni M, et al. Natural Killer Cells From Malignant Pleural Effusion Are Endowed With a Decidual-Like Proangiogenic Polarization. *J Immunol Res* (2018) 2018:2438598. doi: 10.1155/2018/2438598
75. Albini A, Gallazzi M, Palano MT, Carlini V, Ricotta R, Bruno A, et al. Timp1 and Timp2 Downregulate Tgfbeta Induced Decidual-Like Phenotype in Natural Killer Cells. *Cancers (Basel)* (2021) 13(19):4955. doi: 10.3390/cancers13194955
76. Andre P, Denis C, Soulas C, Bourbon-Caillet C, Lopez J, Arnoux T, et al. Anti-Nkg2a Mab Is a Checkpoint Inhibitor That Promotes Anti-Tumor Immunity by Unleashing Both T and Nk Cells. *Cell* (2018) 175(7):1731–43.e13. doi: 10.1016/j.cell.2018.10.014
77. Vacca P, Pietra G, Tumino N, Munari E, Mingari MC, Moretta L. Exploiting Human Nk Cells in Tumor Therapy. *Front Immunol* (2019) 10:3013. doi: 10.3389/fimmu.2019.03013
78. Borst L, van der Burg SH, van Hall T. The Nkg2a-Hla-E Axis as a Novel Checkpoint in the Tumor Microenvironment. *Clin Cancer Res* (2020) 26(21):5549–56. doi: 10.1158/1078-0432.CCR-19-2095
79. Sun C, Xu J, Huang Q, Huang M, Wen H, Zhang C, et al. High Nkg2a Expression Contributes to Nk Cell Exhaustion and Predicts a Poor Prognosis of Patients With Liver Cancer. *Oncoimmunology* (2017) 6(1):e1264562. doi: 10.1080/2162402X.2016.1264562
80. Ye X, Zhang N, Jin Y, Xu B, Guo C, Wang X, et al. Dramatically Changed Immune-Related Molecules as Early Diagnostic Biomarkers of Non-Small Cell Lung Cancer. *FEBS J* (2020) 287(4):783–99. doi: 10.1111/febs.15051
81. Harjunpaa H, Guillerey C. Tigit as an Emerging Immune Checkpoint. *Clin Exp Immunol* (2020) 200(2):108–19. doi: 10.1111/cei.13407
82. Anderson AC, Joller N, Kuchroo VK. Lag-3, Tim-3, and Tigit: Co-Inhibitory Receptors With Specialized Functions in Immune Regulation. *Immunity* (2016) 44(5):989–1004. doi: 10.1016/j.immuni.2016.05.001
83. Xu L, Huang Y, Tan L, Yu W, Chen D, Lu C, et al. Increased Tim-3 Expression in Peripheral Nk Cells Predicts a Poorer Prognosis and Tim-3 Blockade Improves Nk Cell-Mediated Cytotoxicity in Human Lung Adenocarcinoma. *Int Immunopharmacol* (2015) 29(2):635–41. doi: 10.1016/j.intimp.2015.09.017
84. Gallois A, Silva I, Osman I, Bhardwaj N. Reversal of Natural Killer Cell Exhaustion by Tim-3 Blockade. *Oncoimmunology* (2014) 3(12):e946365. doi: 10.4161/21624011.2014.946365
85. Datar I, Sanmamed MF, Wang J, Henick BS, Choi J, Badri T, et al. Expression Analysis and Significance of Pd-1, Lag-3, and Tim-3 in Human Non-Small Cell Lung Cancer Using Spatially Resolved and Multiparametric Single-Cell Analysis. *Clin Cancer Res* (2019) 25(15):4663–73. doi: 10.1158/1078-0432.CCR-18-4142
86. Mishra AK, Kadoishi T, Wang X, Driver E, Chen Z, Wang XJ, et al. Squamous Cell Carcinomas Escape Immune Surveillance *Via* Inducing Chronic Activation and Exhaustion of Cd8+ T Cells Co-Expressing Pd-1 and Lag-3 Inhibitory Receptors. *Oncotarget* (2016) 7(49):81341–56. doi: 10.18632/oncotarget.13228
87. Miyazaki T, Dierich A, Benoist C, Mathis D. Independent Modes of Natural Killing Distinguished in Mice Lacking Lag3. *Science* (1996) 272(5260):405–8. doi: 10.1126/science.272.5260.405
88. Trambas CM, Griffiths GM. Delivering the Kiss of Death. *Nat Immunol* (2003) 4(5):399–403. doi: 10.1038/ni0503-399
89. Ruggeri L, Capanni M, Casucci M, Volpi I, Tosti A, Perruccio K, et al. Role of Natural Killer Cell Alloreactivity in Hla-Mismatched Hematopoietic Stem Cell Transplantation. *Blood* (1999) 94(1):333–9. doi: 10.1182/blood.V94.1.333.413a31_333_339
90. Niu C, Li M, Zhu S, Chen Y, Zhou L, Xu D, et al. Pd-1-Positive Natural Killer Cells Have a Weaker Antitumor Function Than That of Pd-1-Negative Natural Killer Cells in Lung Cancer. *Int J Med Sci* (2020) 17(13):1964–73. doi: 10.7150/ijms.47701
91. Pesce S, Greppi M, Tabellini G, Rampinelli F, Parolini S, Olive D, et al. Identification of a Subset of Human Natural Killer Cells Expressing High Levels of Programmed Death 1: A Phenotypic and Functional Characterization. *J Allergy Clin Immunol* (2017) 139(1):335–46.e3. doi: 10.1016/j.jaci.2016.04.025
92. Tumino N, Martini S, Munari E, Scordamaglia F, Besi F, Mariotti FR, et al. Presence of Innate Lymphoid Cells in Pleural Effusions of Primary and Metastatic Tumors: Functional Analysis and Expression of Pd-1 Receptor. *Int J Cancer* (2019) 145(6):1660–8. doi: 10.1002/ijc.32262
93. Schott DS, Pizon M, Pachmann U, Pachmann K. Sensitive Detection of PD-L1 Expression on Circulating Epithelial Tumor Cells (CETCs) Could be a Potential Biomarker to Select Patients for Treatment With PD-1/PD-L1 Inhibitors in Early and Metastatic Solid Tumors. *Oncotarget* (2017) 8(42):72755–72. doi: 10.18632/oncotarget.20346
94. Zaiatz-Bittencourt V, Finlay DK, Gardiner CM. Canonical Tgf-Beta Signaling Pathway Represses Human Nk Cell Metabolism. *J Immunol* (2018) 200(12):3934–41. doi: 10.4049/jimmunol.1701461
95. Cong J, Wang X, Zheng X, Wang D, Fu B, Sun R, et al. Dysfunction of Natural Killer Cells by Fbp1-Induced Inhibition of Glycolysis During Lung Cancer Progression. *Cell Metab* (2018) 28(2):243–55.e5. doi: 10.1016/j.cmet.2018.06.021
96. Lardner A. The Effects of Extracellular Ph on Immune Function. *J Leukoc Biol* (2001) 69(4):522–30. doi: 10.1189/jlb.69.4.522
97. Li C, Lu HJ, Na FF, Deng L, Xue JX, Wang JW, et al. Prognostic Role of Hypoxic Inducible Factor Expression in Non-Small Cell Lung Cancer: A Meta-Analysis. *Asian Pac J Cancer Prev* (2013) 14(6):3607–12. doi: 10.7314/apjcp.2013.14.6.3607
98. Messaoudene M, Pidgeon R, Richard C, Ponce M, Diop K, Benlaifaoui M, et al. A Natural Polyphenol Exerts Antitumor Activity and Circumvents Anti-PD-1 Resistance Through Effects on the Gut Microbiota. *Cancer Discov* (2022) 12(4):1070–87. doi: 10.1158/2159-8290.CD-21-0808
99. Gallazzi M, Festa M, Corradino P, Sansone C, Albini A, Noonan DM. An Extract of Olive Mill Wastewater Downregulates Growth, Adhesion and Invasion Pathways in Lung Cancer Cells: Involvement of CXCR4. *Nutrients* (2020) 12(4):903. doi: 10.3390/nu12040903

100. Hellmann MD, Paz-Ares L, Bernabe Caro R, Zurawski B, Kim SW, Carcereny Costa E, et al. Nivolumab Plus Ipilimumab in Advanced Non-Small-Cell Lung Cancer. *N Engl J Med* (2019) 381(21):2020–31. doi: 10.1056/NEJMoa1910231
101. Grant MJ, Herbst RS, Goldberg SB. Selecting the Optimal Immunotherapy Regimen in Driver-Negative Metastatic NSCLC. *Nat Rev Clin Oncol* (2021) 18(10):625–44. doi: 10.1038/s41571-021-00520-1
102. Nicholson AG, Tsao MS, Beasley MB, Borczuk AC, Brambilla E, Cooper WA, et al. The 2021 WHO Classification of Lung Tumors: Impact of Advances Since 2015. *J Thorac Oncol* (2022) 17(3):362–87. doi: 10.1016/j.jtho.2021.11.003
103. Yatabe Y, Dacic S, Borczuk AC, Warth A, Russell PA, Lantuejoul S, et al. Best Practices Recommendations for Diagnostic Immunohistochemistry in Lung Cancer. *J Thorac Oncol* (2019) 14(3):377–407. doi: 10.1016/j.jtho.2018.12.005
104. Tsao MS, Kerr KM, Kockx M, Beasley MB, Borczuk AC, Botling J, et al. Pd-L1 Immunohistochemistry Comparability Study in Real-Life Clinical Samples: Results of Blueprint Phase 2 Project. *J Thorac Oncol* (2018) 13(9):1302–11. doi: 10.1016/j.jtho.2018.05.013
105. Hsu J, Hodgins JJ, Marathe M, Nicolai CJ, Bourgeois-Daigneault MC, Trevino TN, et al. Contribution of Nk Cells to Immunotherapy Mediated by Pd-1/Pd-L1 Blockade. *J Clin Invest* (2018) 128(10):4654–68. doi: 10.1172/JCI99317
106. Oyer JL, Gitto SB, Altomare DA, Copik AJ. Pd-L1 Blockade Enhances Anti-Tumor Efficacy of Nk Cells. *Oncoimmunology* (2018) 7(11):e1509819. doi: 10.1080/2162402X.2018.1509819
107. Trefny MP, Kaiser M, Stanczak MA, Herzig P, Savic S, Wiese M, et al. Pd-1 (+) Natural Killer Cells in Human Non-Small Cell Lung Cancer Can Be Activated by Pd-1/Pd-L1 Blockade. *Cancer Immunol Immunother* (2020) 69(8):1505–17. doi: 10.1007/s00262-020-02558-z
108. Liu Y, Cheng Y, Xu Y, Wang Z, Du X, Li C, et al. Increased Expression of Programmed Cell Death Protein 1 on Nk Cells Inhibits Nk-Cell-Mediated Anti-Tumor Function and Indicates Poor Prognosis in Digestive Cancers. *Oncogene* (2017) 36(44):6143–53. doi: 10.1038/onc.2017.209
109. Boyerinas B, Jochems C, Fantini M, Heery CR, Gulley JL, Tsang KY, et al. Antibody-Dependent Cellular Cytotoxicity Activity of a Novel Anti-Pd-L1 Antibody Avelumab (Msb0010718c) on Human Tumor Cells. *Cancer Immunol Res* (2015) 3(10):1148–57. doi: 10.1158/2326-6066.CIR-15-0059
110. Barry KC, Hsu J, Broz ML, Cueto FJ, Binnewies M, Combes AJ, et al. A Natural Killer-Dendritic Cell Axis Defines Checkpoint Therapy-Responsive Tumor Microenvironments. *Nat Med* (2018) 24(8):1178–91. doi: 10.1038/s41591-018-0085-8
111. Prat A, Navarro A, Pare L, Reguart N, Galvan P, Pascual T, et al. Immune-Related Gene Expression Profiling After Pd-1 Blockade in Non-Small Cell Lung Carcinoma, Head and Neck Squamous Cell Carcinoma, and Melanoma. *Cancer Res* (2017) 77(13):3540–50. doi: 10.1158/0008-5472.CAN-16-3556
112. Mazzaschi G, Facchinetti F, Missale G, Canetti D, Madeddu D, Zecca A, et al. The Circulating Pool of Functionally Competent Nk and Cd8+ Cells Predicts the Outcome of Anti-Pd1 Treatment in Advanced Nsclc. *Lung Cancer* (2019) 127:153–63. doi: 10.1016/j.lungcan.2018.11.038
113. Fend L, Rusakiewicz S, Adam J, Bastien B, Caignard A, Messaoudene M, et al. Prognostic Impact of the Expression of Ncr1 and Ncr3 Nk Cell Receptors and Pd-L1 on Advanced Non-Small Cell Lung Cancer. *Oncoimmunology* (2017) 6(1):e1163456. doi: 10.1080/2162402X.2016.1163456
114. Gettinger SN, Wurtz A, Goldberg SB, Rimm D, Schalper K, Kaech S, et al. Clinical Features and Management of Acquired Resistance to Pd-1 Axis Inhibitors in 26 Patients With Advanced Non-Small Cell Lung Cancer. *J Thorac Oncol* (2018) 13(6):831–9. doi: 10.1016/j.jtho.2018.03.008
115. Fehrenbacher L, Spira A, Ballinger M, Kowanetz M, Vansteenkiste J, Mazieres J, et al. Atezolizumab Versus Docetaxel for Patients With Previously Treated Non-Small-Cell Lung Cancer (Poplar): A Multicentre, Open-Label, Phase 2 Randomised Controlled Trial. *Lancet* (2016) 387(10030):1837–46. doi: 10.1016/S0140-6736(16)00587-0
116. Boutsikou E, Domvri K, Hardavella G, Tsiouda D, Zarogoulidis K, Kontakiotis T. Tumour Necrosis Factor, Interferon-Gamma and Interleukins as Predictive Markers of Antiprogrammed Cell-Death Protein-1 Treatment in Advanced Non-Small Cell Lung Cancer: A Pragmatic Approach in Clinical Practice. *Ther Adv Med Oncol* (2018) 10:1758835918768238. doi: 10.1177/1758835918768238
117. Lang S, Vujanovic NL, Wollenberg B, Whiteside TL. Absence of B7.1-Cd28/Ctla-4-Mediated Co-Stimulation in Human Nk Cells. *Eur J Immunol* (1998) 28(3):780–6. doi: 10.1002/(SICI)1521-4141(199803)28:03<780::AID-IMMU780>3.0.CO;2-8
118. Stojanovic A, Fiegler N, Brunner-Weinzierl M, Cerwenka A. Ctla-4 Is Expressed by Activated Mouse Nk Cells and Inhibits Nk Cell Ifn-Gamma Production in Response to Mature Dendritic Cells. *J Immunol* (2014) 192(9):4184–91. doi: 10.4049/jimmunol.1302091
119. Hutmacher C, Gonzalo Nunez N, Liuzzi AR, Becher B, Neri D. Targeted Delivery of Il2 to the Tumor Stroma Potentiates the Action of Immune Checkpoint Inhibitors by Preferential Activation of Nk and Cd8(+) T Cells. *Cancer Immunol Res* (2019) 7(4):572–83. doi: 10.1158/2326-6066.CIR-18-0566
120. Tallerico R, Cristiani CM, Staaf E, Garofalo C, Sottile R, Capone M, et al. Il-15, Tim-3 and Nk Cells Subsets Predict Responsiveness to Anti-Ctla-4 Treatment in Melanoma Patients. *Oncoimmunology* (2017) 6(2):e1261242. doi: 10.1080/2162402X.2016.1261242
121. Sottile R, Tannazi M, Johansson MH, Cristiani CM, Calabro L, Ventura V, et al. Nk- and T-Cell Subsets in Malignant Mesothelioma Patients: Baseline Pattern and Changes in the Context of Anti-Ctla-4 Therapy. *Int J Cancer* (2019) 145(8):2238–48. doi: 10.1002/ijc.32363
122. Tietze JK, Angelova D, Heppt MV, Ruzicka T, Berking C. Low Baseline Levels of Nk Cells May Predict a Positive Response to Ipilimumab in Melanoma Therapy. *Exp Dermatol* (2017) 26(7):622–9. doi: 10.1111/exd.13263
123. Jie HB, Schuler PJ, Lee SC, Srivastava RM, Argiris A, Ferrone S, et al. Ctla-4 (+) Regulatory T Cells Increased in Cetuximab-Treated Head and Neck Cancer Patients Suppress Nk Cell Cytotoxicity and Correlate With Poor Prognosis. *Cancer Res* (2015) 75(11):2200–10. doi: 10.1158/0008-5472.CAN-14-2788
124. Kohrt HE, Thielens A, Marabelle A, Sagiv-Barfi I, Sola C, Chanuc F, et al. Anti-Kir Antibody Enhancement of Anti-Lymphoma Activity of Natural Killer Cells as Monotherapy and in Combination With Anti-Cd20 Antibodies. *Blood* (2014) 123(5):678–86. doi: 10.1182/blood-2013-08-519199
125. Vey N, Karlin L, Sadot-Lebouvier S, Broussais F, Berton-Rigaud D, Rey J, et al. A Phase 1 Study of Lirilumab (Antibody Against Killer Immunoglobulin-Like Receptor Antibody Kir2d; Iph2102) in Patients With Solid Tumors and Hematologic Malignancies. *Oncotarget* (2018) 9(25):17675–88. doi: 10.18632/oncotarget.24832
126. Hanna GJ, O'Neill A, Shin KY, Wong K, Jo VY, Quinn CT, et al. Neoadjuvant and Adjuvant Nivolumab and Lirilumab in Patients With Recurrent, Resectable Squamous Cell Carcinoma of the Head and Neck. *Clin Cancer Res* (2022) 28(3):468–78. doi: 10.1158/1078-0432.CCR-21-2635
127. Anderson AC. Tim-3: An Emerging Target in the Cancer Immunotherapy Landscape. *Cancer Immunol Res* (2014) 2(5):393–8. doi: 10.1158/2326-6066.CIR-14-0039
128. Sakuishi K, Apetoh L, Sullivan JM, Blazar BR, Kuchroo VK, Anderson AC. Targeting Tim-3 and Pd-1 Pathways to Reverse T Cell Exhaustion and Restore Anti-Tumor Immunity. *J Exp Med* (2010) 207(10):2187–94. doi: 10.1084/jem.20100643
129. Sun H, Sun C. The Rise of Nk Cell Checkpoints as Promising Therapeutic Targets in Cancer Immunotherapy. *Front Immunol* (2019) 10:2354. doi: 10.3389/fimmu.2019.02354
130. Rotte A, Jin JY, Lemaire V. Mechanistic Overview of Immune Checkpoints to Support the Rational Design of Their Combinations in Cancer Immunotherapy. *Ann Oncol* (2018) 29(1):71–83. doi: 10.1093/annonc/mdx686
131. Johnston RJ, Comps-Agrar L, Hackney J, Yu X, Huseni M, Yang Y, et al. The Immunoreceptor Tigit Regulates Antitumor and Antiviral Cd8(+) T Cell Effector Function. *Cancer Cell* (2014) 26(6):923–37. doi: 10.1016/j.ccell.2014.10.018
132. Liu SV, Camidge DR, Gettinger SN, Giaccone G, Heist RS, Hodi FS, et al. Atezolizumab (Atezo) Plus Platinum-Based Chemotherapy (Chemo) in Non-Small Cell Lung Cancer (Nsclc): Update From a Phase Ib Study. *J Clin Oncol* (2017) 35:9092. doi: 10.1200/JCO.2017.35.15_suppl.9092

133. Rodriguez-Abreu D, Johnson ML, Hussein MA, Cobo M, Patel AJ, Secen NM, et al. Primary Analysis of a Randomized, Double-Blind, Phase Ii Study of the Anti-Tigit Antibody Tiragolumab (Tira) Plus Atezolizumab (Atezo) Versus Placebo Plus Atezo as First-Line (1l) Treatment in Patients With Pd-L1-Selected Nsclc (Cityscape). *J Clin Oncol* (2020) 38(15):9503. doi: 10.1200/JCO.2020.38.15_suppl.9503
134. Tian Z, Liu M, Zhang Y, Wang X. Bispecific T Cell Engagers: An Emerging Therapy for Management of Hematologic Malignancies. *J Hematol Oncol* (2021) 14(1):75. doi: 10.1186/s13045-021-01084-4
135. Nagorsen D, Baeuerle PA. Immunomodulatory Therapy of Cancer With T Cell-Engaging Bite Antibody Blinatumomab. *Exp Cell Res* (2011) 317 (9):1255–60. doi: 10.1016/j.yexcr.2011.03.010
136. Brischwein K, Parr L, Pflanz S, Volkland J, Lumsden J, Klinger M, et al. Strictly Target Cell-Dependent Activation of T Cells by Bispecific Single-Chain Antibody Constructs of the Bite Class. *J Immunother* (2007) 30 (8):798–807. doi: 10.1097/CJI.0b013e318156750c
137. Hodgins JJ, Khan ST, Park MM, Auer RC, Ardolino M. Killers 2.0: Nk Cell Therapies at the Forefront of Cancer Control. *J Clin Invest* (2019) 129 (9):3499–510. doi: 10.1172/JCI129338
138. Gauthier L, Morel A, Anceriz N, Rossi B, Blanchard-Alvarez A, Grondin G, et al. Multifunctional Natural Killer Cell Engagers Targeting Nkp46 Trigger Protective Tumor Immunity. *Cell* (2019) 177(7):1701–13.e16. doi: 10.1016/j.cell.2019.04.041
139. Wingert S, Reusch U, Knackmuss S, Kluge M, Damrat M, Pahl J, et al. Preclinical Evaluation of Afm24, a Novel Cd16a-Specific Innate Immune Cell Engager Targeting Egfr-Positive Tumors. *MAbs* (2021) 13(1):1950264. doi: 10.1080/19420862.2021.1950264
140. Sivori S, Pende D, Quatrini L, Pietra G, Della Chiesa M, Vacca P, et al. Nk Cells and Ilcs in Tumor Immunotherapy. *Mol Aspects Med* (2021) 80:100870. doi: 10.1016/j.mam.2020.100870
141. Leung W. Infusions of Allogeneic Natural Killer Cells as Cancer Therapy. *Clin Cancer Res* (2014) 20(13):3390–400. doi: 10.1158/1078-0432.CCR-13-1766
142. Souza-Fonseca-Guimaraes F, Cursons J, Huntington ND. The Emergence of Natural Killer Cells as a Major Target in Cancer Immunotherapy. *Trends Immunol* (2019) 40(2):142–58. doi: 10.1016/j.it.2018.12.003
143. Yang YJ, Park JC, Kim HK, Kang JH, Park SY. A Trial of Autologous *Ex Vivo*-Expanded Nk Cell-Enriched Lymphocytes With Docetaxel in Patients With Advanced Non-Small Cell Lung Cancer as Second- or Third-Line Treatment: Phase Iia Study. *Anticancer Res* (2013) 33(5):2115–22.
144. Cozar B, Greppi M, Carpentier S, Narni-Mancinelli E, Chiossone L, Vivier E. Tumor-Infiltrating Natural Killer Cells. *Cancer Discovery* (2021) 11(1):34–44. doi: 10.1158/2159-8290.CD-20-0655
145. Sahin U, Beksac M. Natural Killer Cell-Mediated Cellular Therapy of Hematological Malignancies. *Clin Hematol Int* (2019) 1(3):134–41. doi: 10.2991/chi.d.190623.001
146. Ruggeri L, Capanni M, Urbani E, Perruccio K, Shlomchik WD, Tosti A, et al. Effectiveness of Donor Natural Killer Cell Alloreactivity in Mismatched Hematopoietic Transplants. *Science* (2002) 295(5562):2097–100. doi: 10.1126/science.1068440
147. Dranoff G. Cytokines in Cancer Pathogenesis and Cancer Therapy. *Nat Rev Cancer* (2004) 4(1):11–22. doi: 10.1038/nrc1252
148. Guillerey C, Huntington ND, Smyth MJ. Targeting Natural Killer Cells in Cancer Immunotherapy. *Nat Immunol* (2016) 17(9):1025–36. doi: 10.1038/ni.3518
149. Lin M, Luo H, Liang S, Chen J, Liu A, Niu L, et al. Pembrolizumab Plus Allogeneic Nk Cells in Advanced Non-Small Cell Lung Cancer Patients. *J Clin Invest* (2020) 130(5):2560–9. doi: 10.1172/JCI132712
150. Gong JH, Maki G, Klingemann HG. Characterization of a Human Cell Line (Nk-92) With Phenotypical and Functional Characteristics of Activated Natural Killer Cells. *Leukemia* (1994) 8(4):652–8.
151. Arai S, Meagher R, Swearingen M, Myint H, Rich E, Martinson J, et al. Infusion of the Allogeneic Cell Line Nk-92 in Patients With Advanced Renal Cell Cancer or Melanoma: A Phase I Trial. *Cytotherapy* (2008) 10(6):625–32. doi: 10.1080/14653240802301872
152. Tam YK, Miyagawa B, Ho VC, Klingemann HG. Immunotherapy of Malignant Melanoma in a Scid Mouse Model Using the Highly Cytotoxic Natural Killer Cell Line Nk-92. *J Hematother* (1999) 8(3):281–90. doi: 10.1089/106161299320316
153. Tonn T, Schwabe D, Klingemann HG, Becker S, Esser R, Koehl U, et al. Treatment of Patients With Advanced Cancer With the Natural Killer Cell Line Nk-92. *Cytotherapy* (2013) 15(12):1563–70. doi: 10.1016/j.jcyt.2013.06.017
154. Shimasaki N, Jain A, Campana D. Nk Cells for Cancer Immunotherapy. *Nat Rev Drug Discovery* (2020) 19(3):200–18. doi: 10.1038/s41573-019-0052-1
155. Daher M, Rezvani K. Outlook for New Car-Based Therapies With a Focus on Car Nk Cells: What Lies Beyond Car-Engineered T Cells in the Race Against Cancer. *Cancer Discovery* (2021) 11(1):45–58. doi: 10.1158/2159-8290.CD-20-0556
156. Liu E, Marin D, Banerjee P, Macapinlac HA, Thompson P, Basar R, et al. Use of Car-Transduced Natural Killer Cells in Cd19-Positive Lymphoid Tumors. *N Engl J Med* (2020) 382(6):545–53. doi: 10.1056/NEJMoa1910607
157. Yang S, Cao B, Zhou G, Zhu L, Wang L, Zhang L, et al. Targeting B7-H3 Immune Checkpoint With Chimeric Antigen Receptor-Engineered Natural Killer Cells Exhibits Potent Cytotoxicity Against Non-Small Cell Lung Cancer. *Front Pharmacol* (2020) 11:1089. doi: 10.3389/fphar.2020.01089
158. Pockley AG, Vaupel P, Multhoff G. Nk Cell-Based Therapeutics for Lung Cancer. *Expert Opin Biol Ther* (2020) 20(1):23–33. doi: 10.1080/14712598.2020.1688298

Conflict of Interest: The authors declare that the research was conducted in the absence of any commercial or financial relationships that could be construed as a potential conflict of interest.

Publisher's Note: All claims expressed in this article are solely those of the authors and do not necessarily represent those of their affiliated organizations, or those of the publisher, the editors and the reviewers. Any product that may be evaluated in this article, or claim that may be made by its manufacturer, is not guaranteed or endorsed by the publisher.

frontiers | Frontiers in Oncology

ORIGINAL RESEARCH
published: 06 July 2022
doi: 10.3389/fonc.2022.879405

m^{6}A Regulator-Based Methylation Modification Patterns Characterized by Distinct Tumor Microenvironment Immune Profiles in Rectal Cancer

Kaili Liao[1†], Jialing Hu[2†], Yu Huang[3†], Siji Yu[3†], Qijun Yang[4], Fan Sun[1], Chengfeng Wu[5], Yunqi Cheng[4], Wenyige Zhang[4], Xue Zhang[4], Hongyu Li[4] and Xiaozhong Wang[1]*

[1] Jiangxi Province Key Laboratory of Laboratory Medicine, Jiangxi Provincial Clinical Research Center for Laboratory Medicine, Department of Clinical Laboratory, The Second Affiliated Hospital of Nanchang University, Nanchang, China, [2] Department of Emergency medicine, The Second Affiliated Hospital of Nanchang University, Nanchang, China, [3] School of Advanced Manufacturing of Nanchang University, Nanchang, China, [4] Queen Mary College of Nanchang University, Xuefu Road, Nanchang, Nanchang, China, [5] Department of Vascular Surgery, The Second Affiliated Hospital of Nanchang University, Nanchang, China

OPEN ACCESS

Edited by:
Francesca Pirini,
Scientific Institute of Romagna for the Study and Treatment of Tumors (IRCCS), Italy

Reviewed by:
Giorgia Marisi,
Scientific Institute of Romagna for the Study and Treatment of Tumors (IRCCS), Italy
Josefa Leon,
Fundación para la Investigación Biosanitaria de Andalucía Oriental (FIBAO), Spain

***Correspondence:**
Xiaozhong Wang
wangxzlj@126.com

†These authors share first authorship

Specialty section:
This article was submitted to Molecular and Cellular Oncology, a section of the journal Frontiers in Oncology

Received: 12 March 2022
Accepted: 23 May 2022
Published: 06 July 2022

Citation:
Liao K, Hu J, Huang Y, Yu S, Yang Q, Sun F, Wu C, Cheng Y, Zhang W, Zhang X, Li H and Wang X (2022) m^{6}A Regulator-Based Methylation Modification Patterns Characterized by Distinct Tumor Microenvironment Immune Profiles in Rectal Cancer. Front. Oncol. 12:879405. doi: 10.3389/fonc.2022.879405

Background: Previous studies reported the related role of RNA n6-methyladenosine (m6A) modification in tumorigenesis and development. However, it is not clear whether m6A modification also plays a potential role in the immune regulation of rectal cancer (RC) and the formation of tumor microenvironment.

Methods: In this study, we screened 23 m6A regulatory factors from 369 rectal cancer specimens, further determined the modification patterns of m6A in RC, and systematically linked these modification patterns with the characteristics of TME cell infiltration. The principal component analysis (PCA) algorithm was used to evaluate the m6A modification pattern of a single tumor related to immune response.

Results: Three different m6A modification patterns were found in the measurement results, which are related to different clinical results and biological pathways. TME identification results show that the identified m6A pattern is closely related to immune characteristics. According to the m6Ascore extracted from m6A-related signature genes, RC patients were divided into high and low score subgroups combined with tumor mutation burden. Patients with high tumor mutation burden and higher m6Ascore have a significant survival advantage and enhanced immune infiltration. Further analysis showed that patients with higher m6Ascore had higher PD-L1 expression levels and showed better immune response and lasting clinical benefits.

Conclusions: M6A modification plays a crucial role in the formation of TME diversity and complexity. The evaluation of the m6A modification mode will help us to enhance our understanding of the characteristics of TME infiltration and provide new insights for more effective immunotherapy strategies.

Keywords: rectal cancer, M6A modification, tumor microenvironment, immune profiles, immunotherapy

INTRODUCTION

Rectal cancer is a malignant tumor that occurs in the lower part of the large intestine, accounting for 30-40% of colorectal cancer (CRC) (1, 2). There are approximately 700,000 confirmed cases of rectal cancer each year in the world, and the annual death toll is approximately 310,000 (3). Although the colon and rectum are anatomically related, there are significant differences in recurrence rates and treatment options between cancer types (4). Therefore, the determination of reliable prognostic biomarkers to improve the prognosis of rectal cancer has important clinical biological significance. The molecular mechanism of the occurrence and development of malignant tumors is one of the current research hotspots. RC is a major social health problem and occupies a special position in tumor diseases. The interaction network jointly established by immune cells, endothelial cells, mesenchymal fibroblasts and matrix-related molecules in the tumor and surrounding tissues constitutes the TME (5). Tumor cells in TME can directly or indirectly invade tissues through blood vessels and lymphatic vessels, and infiltrating cells can induce immune responses by releasing cytokines, cytokine receptors and other factors, and affect tumor progression (6–9). However, the role of TME and the specific biological mechanism of potential therapeutic response are still unclear (10).

In recent years, the study of post-transcriptional gene regulation in eukaryotes has opened up new fields. So far, more than 100 different chemical modifications have been discovered for post-transcriptional modification (11). The methylation of messenger RNA to form m6A is considered to be the most abundant internal modification in messenger RNA and has become a wide-ranging regulatory mechanism that controls gene expression in various physiological processes (12–16). m6A modification is a dynamic and reversible process in mammalian cells. It is installed by m6A methyltransferases, removed by m6A demethylases, and recognized by reader proteins. The process is regulated by methyltransferase, demethylase and binding protein, also known as "writer", "erasers" and "reader" (17, 18). Post-transcriptional modification has become an important regulator of various physiological processes and disease progression, and has attracted increasing attention in biological science research. In addition, in terms of molecular mechanism, m6A participates in almost all steps of RNA metabolism, including translation, degradation, splicing, export and folding of mRNA (19, 20).

Recent literature has reported the interaction between TME infiltration of immune cells and m6A modification, which cannot be fully explained by the mechanism of RNA degradation. Studies have shown that m6A methylation of dendritic cells and YTHDF1 regulate anti-tumor immunity, further supporting the view that decreased YTHDF1 expression may be related to T cell inflammation and tumor microenvironment (21). Another study showed that m6A mRNA demethylase FTO regulates the tumorigenicity of melanoma and the response to PD-1 blockade, and plays an important role in the response to immunotherapy (22). In addition, it is reported that Mettl3-mediated m6A modification plays an important role in promoting the maturation and activation of dendritic cells, which may promote cancer immunotherapy (23). However, the above research is limited to one or two m6A modulators and cell types, and the anti-tumor effect requires the interaction of multiple tumor suppressor factors. Therefore, the systematic evaluation of the infiltration characteristics of TME cells mediated by multiple m6A regulatory factors will comprehensively strengthen our understanding of TME immune regulation.

In this study, we screened the genomic information of 369 rectal cancer samples from The Cancer Genome Atlas (TCGA) (167) and Gene-Expression Omnibus (GEO) databases (203), systematically evaluated m6A modification patterns, and deeply understood the potential connection between m6A modification patterns and TME cell infiltration characteristics. Three different m6A modification modes are summarized. What is interesting is that the TME characteristics of these three modes are highly consistent with the immune exclusion phenotype, the immune inflammation phenotype and the immune desert phenotype, respectively. This indicates that the role of m6A modification in shaping individual tumor microenvironmental characteristics is a promising method. To this end, we established a scoring system to quantify the m6A modification patterns of individual patients.

MATERIALS AND METHODS

Collect and Organize of Expression Datasets Obtained From Public Databases

With the rapid development of precision medicine, researchers are increasingly using statistical algorithms to explore new diagnosis and treatment goals. We retrospectively collected gene expression data and related data of RC samples from the GEO database (https://www.ncbi.nlm.nih.gov/geo/), TCGA (https://cancergenome.nih.gov/) public data sets and clinical characteristics data. In short, the study collected TCGA and GSE87211 cohorts for further analysis. Through Protein-Protein Interaction (PPI) network analysis, the key nodes in the differentially expressed proteins were found and visualized by Cytoscape.

Consensus Molecular Cluster Analysis of Twenty-Three m6A Regulators

In the process of cluster analysis, the cohort with fewer m6A regulatory factors was not included. Twenty-three regulatory factors were extracted from the TCGA and GSE87211 cohorts to identify different m6A modification patterns mediated by m6A

Abbreviations: m6A, N6-methyladenosine; RC, rectal cancer; TME, tumor microenvironment; PCA, principal component analysis; CRC, colorectal cancer; TCGA, The Cancer Genome Atlas; GEO, Gene-Expression Omnibus; GSVA, Gene set variation analysis; GO, Gene Ontology; KEGG, Kyoto encyclopedia of genes and genomes; ssGSEA, single sample gene set enrichment analysis; DEGs, differentially expressed genes; DCs, Dendritic cells; TLS, tertiary lymphatic structure; NK, natural killer; ICB, Immunological checkpoint blockade; PD-L1, programmed death receptor ligand 1; CNV, copy variation; MDSCs, myeloid-derived suppressor cells.

regulatory factors. 23 m6A regulators including 8 writers (METTL3, METL14, METL16, WTAP, VIRMA, ZC3H13, RBM15 and RBM15B), 2 erasers (FTOA and ALKBH5), 13 readers (YTHDC1, YTHDC2, YTHDF1, YTHDF2, YTHDF3, HNRNPC, FMR1, LRPPRC, HNRNPA2B1, IGFBP1, IGFBP2, IGFBP3 and RBMX). Subsequently, we applied an unsupervised cluster analysis method to determine different m6A modification patterns based on the expression of 23 m6A regulatory factors, and classified patients for further analysis. The number and stability of clustering are determined by the consensus clustering algorithm. We use the Consensus Cluster Plus package to repeat the above steps to ensure the stability of the classification results.

Gene Set Variation Analysis (GSVA) and Gene Ontology (GO) Kyoto Encyclopedia of Genes and Genomes (KEGG) Annotation

In order to study the biological process differences between the m6A modification modes, we used the "GSVA" R package to perform GSVA enrichment analysis. GSVA is a non-parametric, unsupervised method, usually used to estimate changes in pathways and biological process activity in expression data sets (24). The adjusted P value <0.05 indicates that the difference is statistically significant. We used cluster Profiler R package to annotate m6A-related genes with a cutoff value of FDR <0.05. And ggplot was used to visualize the enrichment analysis.

Estimation of m6A Modification Pattern in Immune Cell Infiltration

We used single sample gene set enrichment analysis (ssGSEA) to evaluate the relative abundance of each cell infiltration in RC TME. According to published research methods, the gene set of each TME infiltrating immune cell type is labeled (25, 26). Immune cell subtypes include activated CD4 T cells, activated B cells, mast cells, monocytes, etc (25). The enrichment score calculated by ssGSEA analysis represents the relative abundance of each TME infiltrated cell in each sample.

Screening of m6A Differentially Expressed Genes (DEGs)

In order to identify m6A-related genes, we divided patients into three different m6A modification modes based on the expression of 23 m6A regulatory factors. The empirical Bayesian method was used to quantitatively analyze the DEGs between different modification modes (27). The significance standard for determining DEG is the corrected P value <0.001.

Construction of the m6Ascore

We constructed a scoring system to evaluate the m6A modification pattern of individual patients with rectal cancer-m6A gene characteristics to quantify the m6A modification pattern of individual tumors, and named it m6Ascore. In simple terms, first normalize DEGs from different m6Aclustered samples in the sample, using unsupervised clustering method to analyze the extracted overlapping DEGs, then use consensus clustering algorithm to determine the number and stability of gene clusters, and use univariate Cox. The regression model performs prognostic analysis on each gene in the signature. Genes with significant prognosis were extracted for subsequent analysis. PCA analysis is performed on the final gene expression profile, and principal component 1 and principal component 2 are selected as the signature scores. The advantage of this method is that the score is concentrated on the set with the largest correlation (or irrelevant) gene block in the set, and the weight of the gene contribution that is not tracked with other set members is reduced. Then, we use a method similar to the previous study to define the m6Ascore (28, 29): m6Sig score=∑(PC1i+PC2i), where is the final expression of the m6A phenotype-related genes.

Statistical Analysis

For quantitative data, the statistical significance of normally distributed variables was estimated by Student's t test, and the Wilcoxon rank sum test was used for non-normally distributed variables. For the comparison of more than two groups, the nonparametric method uses the Kruskal-Wallis test, the parametric method uses the one-way analysis of variance. The Kaplan-Meier survival analysis and the Cox proportional hazard model, and the R package "Survminer" are used to analyze the relationship between the m6A modification model and the prognosis Relationship. The measurement cut function in the "survival" software package was used to stratify the samples into high m6Sig score subgroups and low m6Ascore subgroups. P <0.05 is considered statistically significant.

RESULTS

Genetic Variation of m6A Regulators in Rectal Cancer

In this study, we studied the role of 23 m6A RNA methylation regulation genes in RC ("writer": METTL3, METTL14, METTL16, WTAP, VIRMA, ZC3H13, RBM15 and RBM15B; "reader": YTHDC1 YTHDC2, YTHDF1, YTHDF2, YTHDF3, HNRNPC, FMR1, LRPPRC, HNRNPA2B1, IGFBP1, IGFBP2, IGFBP3 and RBMX; there are also " erasers": FTO and ALKBH5). We first determined the incidence of somatic mutations in 23 m6A regulatory factors in RC. 15 of 137 samples (10.95%) experienced genetic changes in m6A regulatory factors, including missense mutations, nonsense mutations, and Multi -Hit and Splice-site. Among them, ZC3H13 has the highest mutation frequency, followed by RBM15 and YTHDC1. WTAP, ZC3H13, VIRMA, HNRNPA2B1, IGFBP1, IGFBP3 and ALKBH5 have no mutations (**Figure 1A**). Next, we conducted an in-depth analysis of the position of the copy variation (CNV) of the 23 m6A regulatory factors on the chromosome, as shown in (**Figure 1B**). In order to determine whether genetic variation affects the expression of m6A regulatory factors in RC patients, we studied the expression levels of regulatory factors in normal and RC samples and found that, compared with normal control samples, METTL14, METTL16, WTAP, YTHDC1, YTHDC2, YTHDF3, HNRNPC, FTO, and ALKBH5 were significantly down-regulated in tumor samples, while METTL13, RBM15,

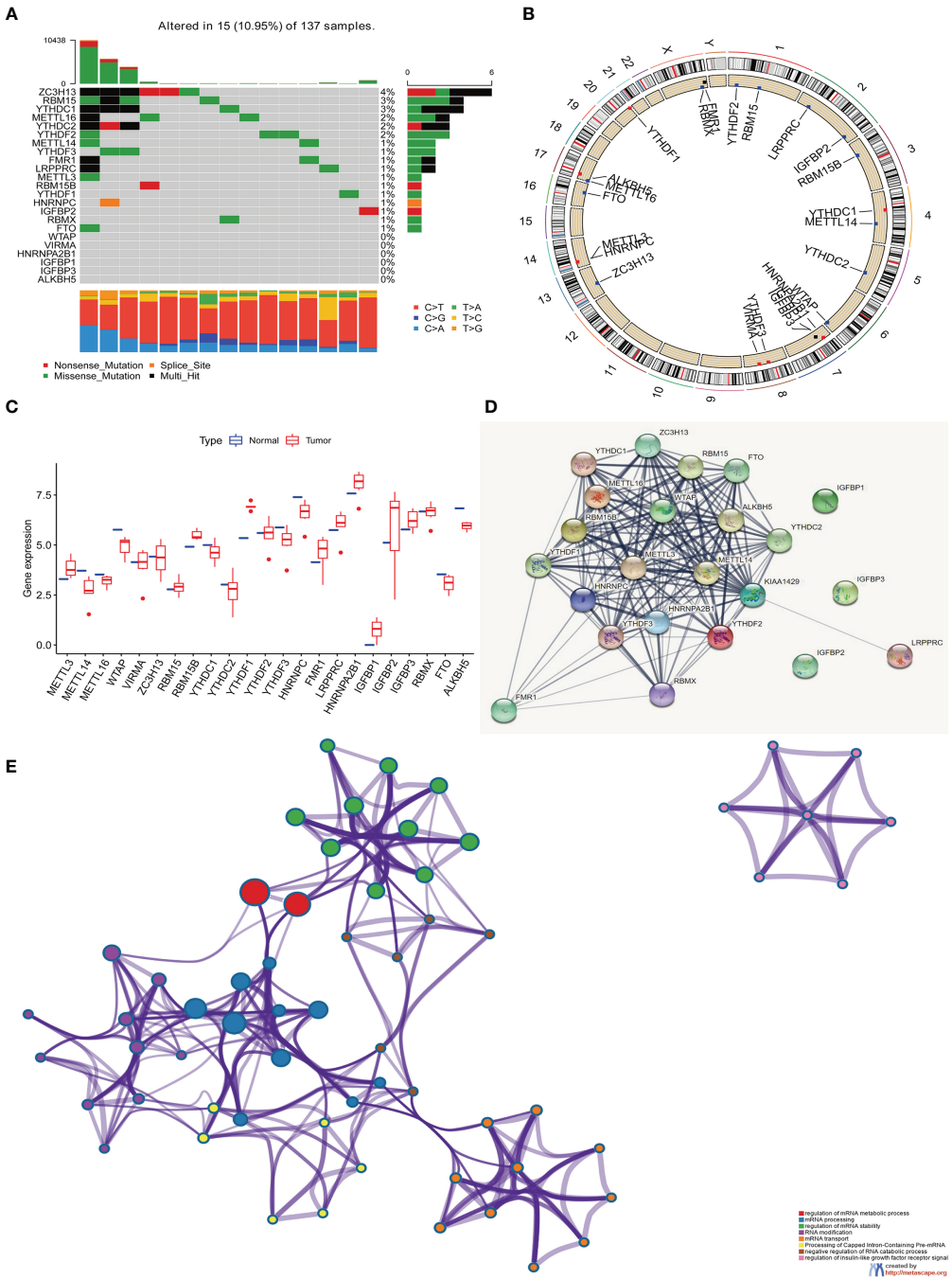

FIGURE 1 | The genetic and expression variant landscape of m^{6}A regulators in rectal cancer. **(A)** The mutation frequency of 23 m^{6}A regulatory factors in 137 rectal cancer patients in the TCGA-RC cohort. Each column represents an .individual patient. The bar graph above shows TMB, and the numbers on the right indicate the mutation frequency of each regulatory factor. The bar graph on the right shows the proportion of each variant type and the four different colors indicates four variant types with legends showing in the bottom of the figure. The stacked bar graph below shows the proportion of different single nucleotide mutation in each sample, with annotation on the right showing six colors representing six different mutations. **(B)** Use the GSE87211 cohort to locate the changes of m^{6}A regulatory factor CNV on 23 chromosomes. **(C)** The expression of 23 m6A regulatory factors in normal tissues and rectal tissues. Tumor, red; normal, blue. The upper and lower ends of the box represent a quarter of the value range. The line in the box represents the median value, and the black dots represent the outliers. **(D)** The protein protein interaction network(PPI) demonstrated the interaction between 23 m^{6}A regulatory factors, including 23 nodes and 104edges. **(E)** The enrichment analysis of 23 m^{6}A regulatory factors. These m^{6}A regulatory factors have a rich regulatory role in the metabolism of mRNA, primarily involved in the mRNA metabolic process, mRNA processing and mRNA stability.

RBM15B, FMR1, LRPPRC, HNRNPA2B1, IGFBP1, IGFBP2, and IGFBP3 were significantly up-regulated in tumor samples (**Figure 1C**). In order to further study the role of 23 m6A regulatory factors in RC, we created PPI and visualized it with Cytoscape software, including 23 nodes and 104 edges (**Figure 1D**). These regulatory factors are abundant in the process of regulation of mRNA metabolism process and mRNA stability, RNA modification and mRNA transport are many important ways (**Figure 1E**).

The above analysis shows that there are significant differences and connections in the genome and transcriptome landscape of m6A regulatory factors between normal and RC samples. Therefore, the expression changes and genetic variation of m6A regulatory factors play an important role in regulating the occurrence and development of RC. In view of the relatively high mutation frequency of the author's gene ZC3H13, we analyzed the expression differences of 23 m6A regulatory factors in ZC3H13 wild-type (**Supplementary Figures 1A–W**).

The Relationship Between the High and Low Expression Groups of 23 m6A Regulators and the Overall Survival of Rectal Cancer

On the TCGA and GSE87211 data sets with OS data and clinical information, the Kaplan-Meier method was used to analyze the prognosis of the survival curves of 23 m6A regulatory factors. The results showed that the expression of 19 m6A regulatory factors was related to prognosis. In short, compared with the low expression group of corresponding regulatory factors, HNRNPC, RBM15, RBMX, FMR1, LRPPRC, YTHDF2, HNRNPA2B1, YTDC2, RBM15B, YTHDF1, IGFBP1 and The METTL16 high expression group showed a significant survival advantage. In contrast, FTO, IGFBP2, IGFBP3, YTHDF3, ZC3H13, WTAP and METTL13 showed significant survival advantages in their corresponding low expression groups (**Figures 2A–S** and **Table 1**).

m6A Methylation Modification Patterns Mediated by 23 Regulators

We are trying to further determine whether the connection between writers, erasers and readers plays a key role in the formation of different m6A modification patterns, and is related to the formation of TME cell infiltration characteristics and the incidence and progression of cancer. Based on these assumptions, we use the R package of Consensus Cluster Plus to classify patients with qualitatively different m6A modification patterns based on the expression of 23 m6A regulatory factors (**Supplementary Figures 2A–L**). In order to explore the interaction between the 23 m6A regulators in RC patients, the connection between the regulators and their prognostic value, we constructed a m6A regulator network (**Figure 3A**). As we expected, not only the expression of m6A regulatory factors of the same functional category showed a significant correlation, but also a significant correlation among writers, erasers and readers (**Figure 3A**). Among these m6A regulatory factors, the m6A binding protein IGFBP1 has attracted our attention because of its significant correlation with prognosis and immune infiltration (30). Our KaplanMeier survival analysis (p=0.041) showed that patients in the IGFBP1 high expression group had a good prognosis, and we also determined that IGFBP1 was significantly related to the prognosis (**Figure 3B**). We also analyzed the unsupervised aggregation of 23 m6A regulatory factors in the GSE87211 rectal cancer cohort and the TCGA cohort. The survival status, tumor stage, gender, age, project, and m6Acluster were used as patient annotations (**Figure 3C**). The results showed that most elderly male patients with advanced survival in ZC3H13, LRPPRC, HNRNPA2B1 and RBMX were highly expressed in m6Aclusters-A, and METTL14, YTHDC1, YTHDC2, YTHDF3 and in ALKBH5, most young male patients with late-stage survival are highly expressed in m6Aclusters-B, while most young male patients with late-stage survival in VIRMA, YTHDF1, FMR1, IGFBP1, IGFBP2, IGFBP3, and FTO are highly expressed in m6Aclusters-C (**Figure 3C**). The results show that there is an inseparable connection between m6A regulatory factors and clinical characteristics. In addition, the principal component analysis (PCA) of the transcriptome profiles of the three m6A modification patterns showed that the transcriptomes of different modification patterns are significantly different (**Figure 3D**).

Characteristics of m6A Modification Mode

In order to determine the biomolecule changes under the three different m6A modification modes, we performed GSVA enrichment analysis on the gene set, as shown in **Figures 3E, F**, **4A**. The results showed that m6Acluster-A was significantly enriched in Nucleotide excision repair, RNA polymerase, degradation, Cell cycle, Base excision repair, One carbon pool by folate, DNA replication, and Homologous recombination (**Figures 3E, F**). m6Acluster-B is used in FC epsilon Ri, GNRH, calcium and neurotrophin signaling pathway, aldosterone regulated sodium reabsorption, long term potentiation and depression, proximal tubule bicarbonate reclamation, starch and sucrose, fatty acid, retinol, ascorbate and aldarate metabolism, vascular muscle contraction, and endocytosis and other processes are significantly enriched (**Figures 3E**, **4A**). However, m6Acluster-C is significantly enriched in Toll like and Nod receptor signaling pathway, mismatch repair, DNA replication, cell cycle, nuclear excision repair, RNA polymerase and homologous recombination (**Figures 3F**, **4A**).

In addition, we also analyzed the infiltration of TME cells (**Figure 4B**). We noticed that m6Aclusters-C has abundant innate immune cell infiltration, including natural killer cells, MDSC, regulatory T cells, neutrophils, and type 2 T cells. Helper cells, Immature dendritic cell, and CD56 bright and dim natural killer cell. We also noticed significant increases in Activated B cell, Eosinophils, Immature B cell, Macrophages, Mast cells and Monocytes in m6Aclusters-B. However, it is surprising that m6Aclusters-A is significantly higher than m6Aclusters-B and m6Aclusters-C. The degree of infiltration in immune cells is low.

Furthermore, in the above results, it is found that there is a strong positive correlation between IGFBP1 and YTHDF1 (**Figure 3A**). Previous studies have shown that the m6A

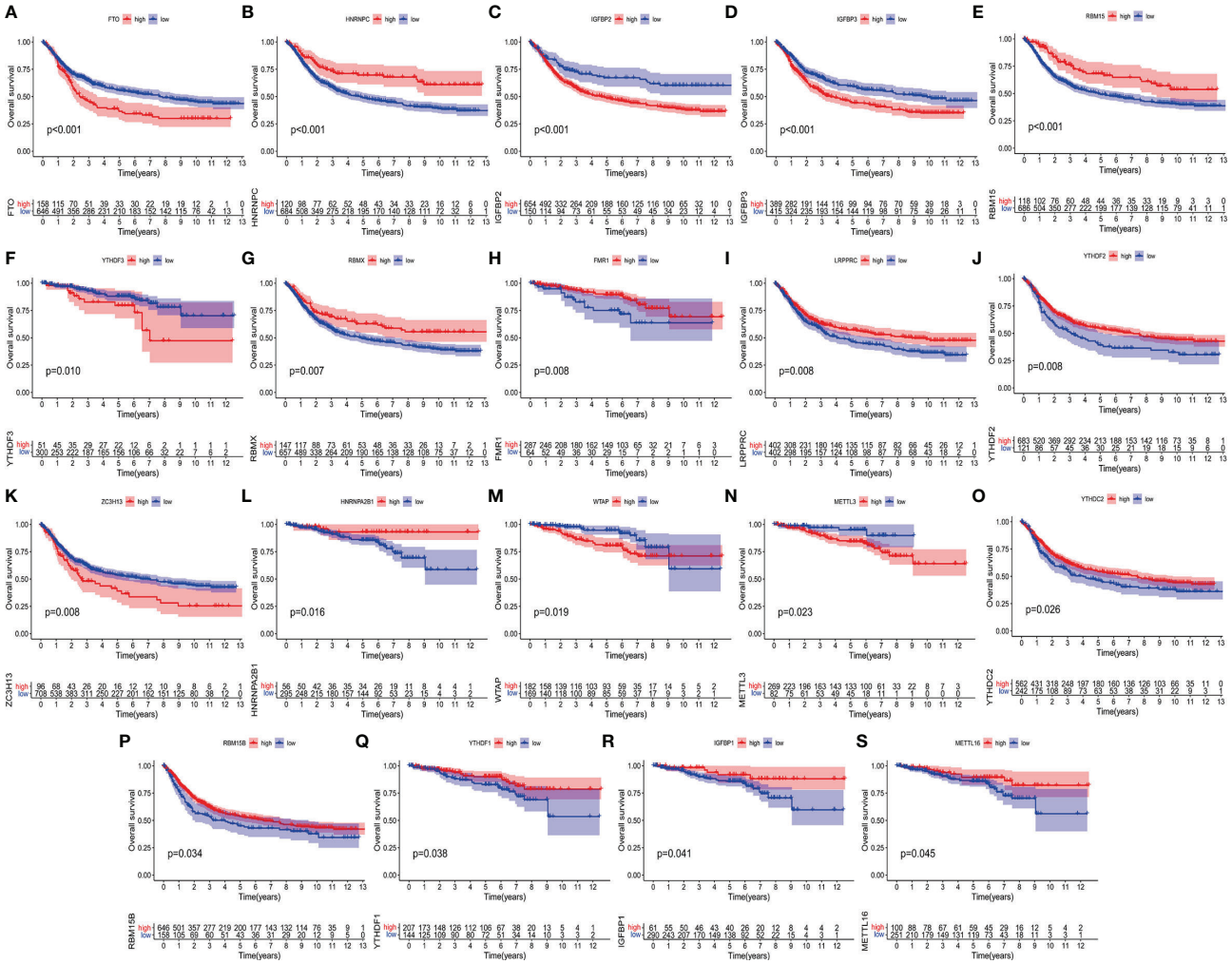

FIGURE 2 | Kaplan-Meier curves of 19 m^{6}A regulatory factors in patients with rectal cancer. **(A–S)** Each figure represents the comparison of the overall survival in patients with higher and low expression of a specific gene and the gene name is shown in the top of each figure. The ordinate shows the survival probability and the abscissa shows the years of survival of the patients. The number of patients in high- and low-expression groups are shown in the bottom of each figure. Log-rank test P<0.05 indicates that the difference is statistically significant.

regulatory factor YTHDF1 mediates the activation of dendritic cells (DC) and the mechanism of CD8+ T cell antigen cross-priming by enhancing the translation of cathepsin (lysosomal protease that degrades antigens in the phagosome) mRNA encoding. Interestingly, this study noticed that IGFBP1 was significantly increased in immune infiltration in Activated B cell, Eosinophils, Immature B cell, Macrophages, Mast cells and Monocytes (**Figure 4B**).

GSVA analysis showed that IGF2BP1 is involved in FC epsilon ri, GNRH, calcium and neurotrophin signaling pathway, aldosterone regulated sodium reabsorption, long term potentiation and depression, proximal tubule bicarbonate reclamation, starch and sucrose, fatty acid, retinol, ascorbate and aldarate metabolism, vascular muscle Significantly enriched during contraction, and endocytosis (**Figures 3E, F**, **4A**). In summary, we speculate that IGFBP1 may cooperate with YTHDF1 to mediate methylation modification, thereby inhibiting the activation of DCs and cytotoxic T lymphocytes, hindering the anti-tumor immune response in tumors.

m6A Phenotype-Related DEGs in Rectal Cancer

The above study classified m6A-regulated gene expression consensus clustering algorithm into three m6A-modified phenotypes, but the potential genetic changes and expression perturbations in these phenotypes are still unclear. Therefore, it is necessary to further analyze the possible m6A-related transcriptional expression changes of the three m6A modification patterns in RC. We used the empirical Bayes method to determine the overlapping differentially expressed genes (DEGs) among the three m6A modification patterns. Expressed as a Venn diagram, the inclusion of 779 DEGs

TABLE 1 | Analysis of 23 m6A regulatory factors through univariate Cox regression.

id	HR	HR.95L	HR.95H	p-value
METTL3	1.3705	0.6186	3.0366	0.4374
METTL14	0.8918	0.4358	1.8253	0.7541
METTL16	0.4158	0.1555	1.1119	0.0804
WTAP	2.7722	0.9954	7.7205	0.0510
VIRMA	0.7447	0.3319	1.6713	0.4748
ZC3H13	1.0227	0.6227	1.6798	0.9292
RBM15	0.9465	0.4822	1.8579	0.8730
RBM15B	0.9631	0.4989	1.8593	0.9109
YTHDC1	1.0778	0.7387	1.5726	0.6975
YTHDC2	1.1251	0.6651	1.9033	0.6602
YTHDF1	0.7173	0.3680	1.3983	0.3293
YTHDF2	1.1000	0.3771	3.2083	0.8615
YTHDF3	0.9860	0.4498	2.1614	0.9719
HNRNPC	1.0862	0.3652	3.2308	0.8818
FMR1	0.4990	0.2426	1.0262	0.0588
LRPPRC	0.6365	0.3369	1.2028	0.1641
HNRNPA2B1	0.6183	0.2274	1.6808	0.3460
IGFBP1	0.9685	0.8126	1.1544	0.7210
IGFBP2	1.0951	0.8981	1.3353	0.3691
IGFBP3	1.2071	0.8644	1.6858	0.2693
RBMX	0.8887	0.3850	2.0514	0.7822
FTO	1.2640	0.8290	1.9274	0.2763
ALKBH5	1.4732	0.5645	3.8446	0.4285

represents the key distinguishing index of the three m6A modification modes (**Figure 4C**). And we analyzed the expression of 23 m6A regulatory factors in 3 gene clusters (**Figure 4D**). The results show that compared with gene Cluster-B, the expression of ZC3H13, LRPPRC, HNRNPA2B1 and RBMX in gene Cluster C were significantly higher. YTHDC1, YTHDC2, YTHDF3 and ALKBH5 in gene Cluster-B was higher than the other two gene clusters. Compared with gene Cluster-A and gene Cluster-B, VIRMA, YTHDF1, FMR1, IGFBP1, IGFBP2, IGFBP3 and FTO were significantly increased in gene Cluster-C.

In addition, we also analyzed three clinicopathological characteristics, and we found that male patients with advanced clinical stages (N1-3, T3-T4) less than or equal to 65 years old are mainly concentrated in gene Cluster-C. Male patients over 65 years old are mainly concentrated in gene Cluster-B (**Figure 4E**). Next, we will conduct follow-up research and analysis on these characteristic genes, GO enrichment analysis shows: in extracellular matrix organization, extracellular structure organization, positive regulation of inflammatory response, collagen-containing extracellular matrix, complex of collagen trimers, extracellular matrix structural constituent conferring tensile strength, extracellular matrix structural constituent, growth factor binding and RAGE. The biological process of receptor binding is significantly more common (**Figures 5A, B**). KEGG enrichment analysis showed that: Fatty acid degradation and metabolism, Retinol and Sulfur metabolism and Protein digestion and absorption biological processes are significantly enriched (**Figures 5C, D**). Next, we use the R package to further analyze the pathway enrichment of 23 m6A regulatory factors, and visualize it with ggpolt, and get similar results (**Figure 5E**). The enrichment analysis of various cellular pathways was shown in circle plot (**Figure 5F**) and another circle plot indicated the enrichment analysis of metabolism (**Figure 5G**). The above further confirmed that the overlapping dimer has m6A modification and immune characteristics, similar to the characteristics of m6A-related genes. We noticed that there are significant differences in m6A regulatory gene expression among the three m6A gene signature subgroups, which is consistent with the expected results of m6A methylation modification patterns.

Construction and Application of m6Ascore

The above results indicate that m6A methylation modification plays a crucial regulatory role in the TME landscape. However, these results are based on patient populations and are not suitable for evaluating the m6A methylation modification pattern of a single patient. In addition, considering that the research process may be interfered by individual heterogeneity and complexity, we have constructed a set of the scoring scheme for quantifying the m6A modification pattern of individual patients with rectal cancer was named m6Ascore. The alluvial map is used to illustrate the workflow of m6Ascore construction (**Figure 6A**). In order to better illustrate the characteristics of m6A signatures, we also tested the correlation between known signatures and m6Ascore (**Figure 6B**). These results indicate that gene Cluster-C has the highest m6Ascore, followed by gene Cluster-A and gene Cluster-B (**Figure 6C**). It is worth noting that m6Acluster-A, m6Acluster-B and m6Acluster-C obtained similar results (**Figure 6D**).

In addition, we tried to explore the significance of m6Ascore in clinical work. We first analyzed the relationship between m6Ascore and patient survival status, and found that m6Ascore had no significant difference between survival and death groups (p=0.18) (**Figure 6E**). Previous studies have shown that there is a close relationship between tumor genome cell mutations and immunotherapy response. Therefore, we explored

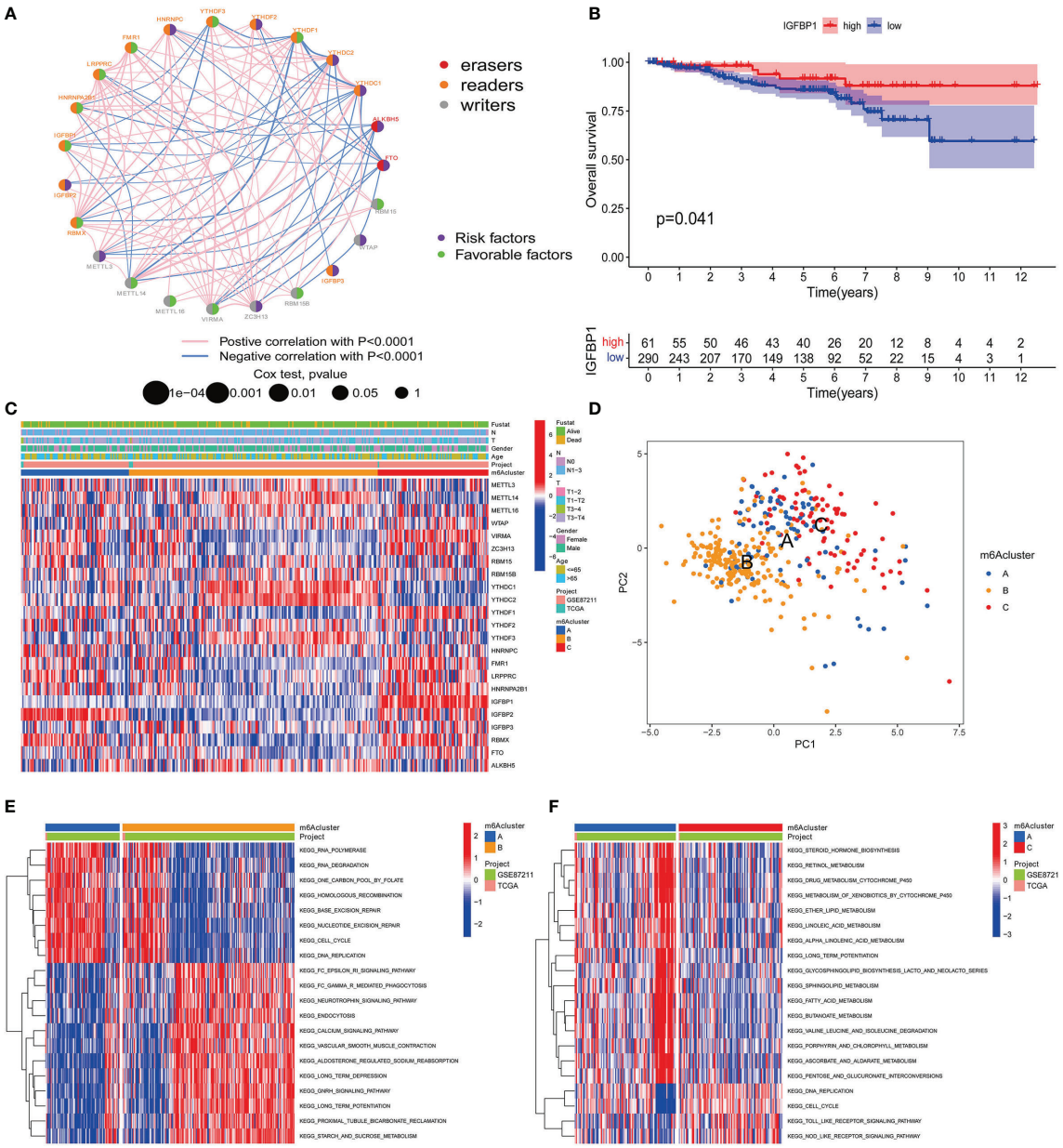

FIGURE 3 | m6A methylation modification patterns and related clinical features. **(A)** The interaction of m^{6}A regulatory factors in rectal cancer. The size of the circle represents the influence of each adjusting factor on the prognosis, and the range of the calculated value of the Log-rank test is p<0.0001, p<0.001, p<0.01, p<0.05, p<1. The purple dots in the circle indicate prognostic risk factors; the green dots in the circle indicate prognostic protective factors. The line connecting the regulators represents the interaction between them, and the thickness represents the relative strength between the regulators. Blue is a negative correlation, and pink is a positive correlation. The regulatory factors ("eraser", "reader", and "writer") are marked in red, brown, and gray, respectively. **(B)** Kaplan-Meier curve of the patient group with high and low expression of IGFBP1. The number of high and low expression groups of patients were indicated in the bottom. Log-rank test, P = 0.041. **(C)** Unsupervised aggregation of 23 m^{6}A regulatory factors in the GSE87211 rectal cancer cohort. Survival status, tumor stage, gender, age, project and m^{6}Acluster are used as patient annotations. On the right, the bar with two colors indicates the level of gene expression and red color represents high expression while blue represents low expression. m6A cluster A–C were shown in blue, yellow and red, respectively. **(D)** Principal component analysis of the transcriptome profiles of the three m6A modification patterns. Blue dots represent m6A cluster A, yellow represent m6A cluster B and red represent m6A cluster C. **(E, F)** KEGG enrichment analysis shows the activation status of biological pathways with different m^{6}A modification modes. Heat maps are used to visualize these biological processes. Red represents activated pathways and blue represents inhibited pathways. Take rectal cancer GSE87211 cohort as sample annotation. **(E)** m^{6}Acluster A vs m^{6}Acluster B; **(F)** m^{6}Acluster A vs m^{6}Acluster C.

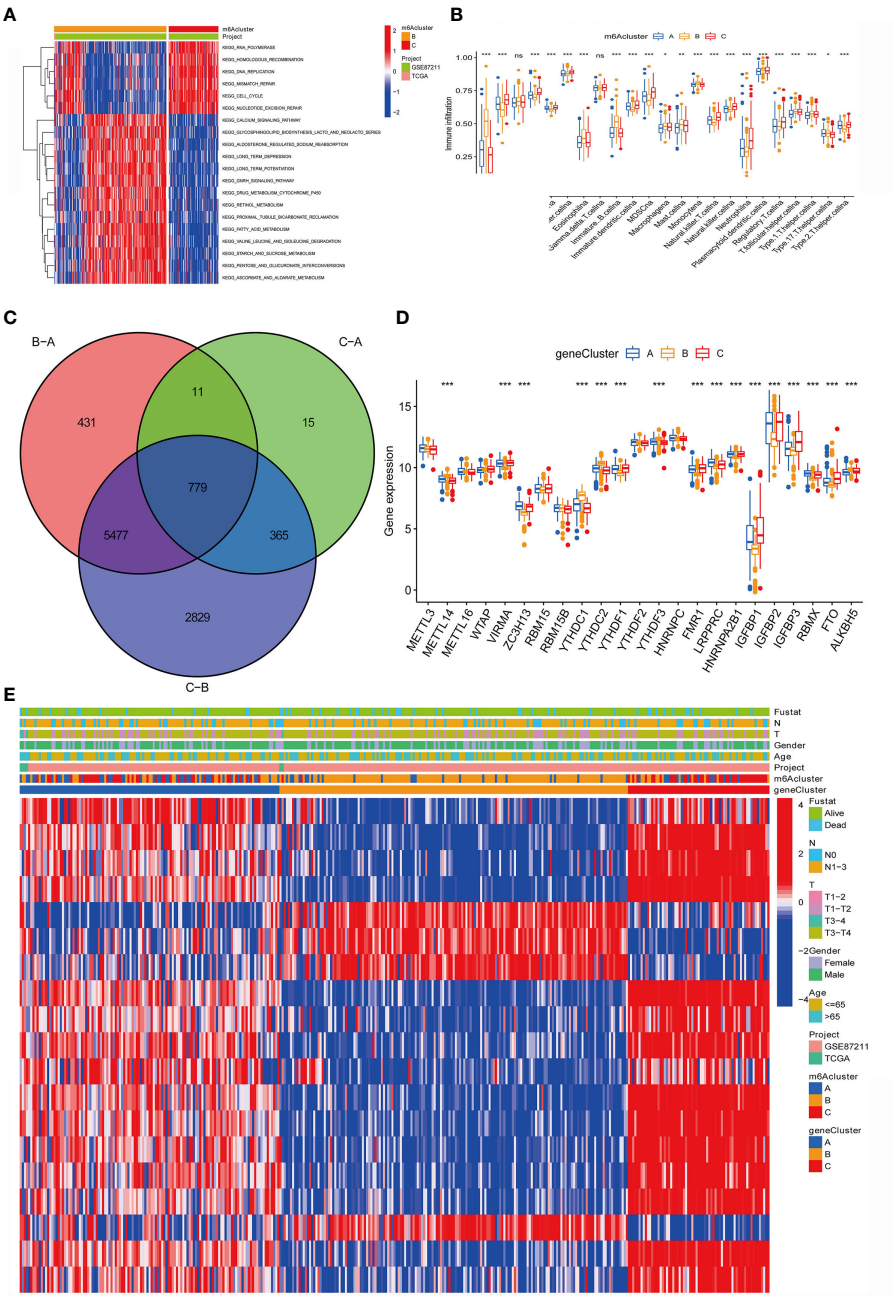

FIGURE 4 | Construction of m^{6}A differential gene expression and gene cluster. **(A)**The heat maps show the differences in KEGG enrichment analysis results between the m^{6}Acluster B and m^{6}Acluster C. **(B)** The abundance of each TME infiltrated cell in the three m6A modification modes. The upper and lower ends of the box represent a quarter of the value range. The line in the box represents the median value, and the dots outside the boxes and their vertical lines represent the outliers. The ordinate shows the immune infiltration while the abscissa represents various types of immune cells. Asterisks indicate statistical P values (*P < 0.05; **P < 0.01; ***P < 0.001). "ns" means "no significance". **(C)** 779 m^{6}A-related differentially expressed genes (DEGs) are displayed in the intersection of Venn diagram among the three m^{6}A clusters. The red circle represents the DEGs between patients of m6A cluster B and cluster A. The green circle represents the DEGs between patients of m6A cluster C and cluster A. The purple circle represents the DEGs between patients of m6A cluster B and cluster C. **(D)** Expression of 23 m^{6}A regulatory factors in three gene clusters. The upper and lower ends of the box represent a quarter of the value range. The line in the box represents the median value, and the black dots represent the outliers. The ordinate represents the level of gene expression in a gene cluster while the abscissa represents the 23 m6A regulatory factors. Asterisks indicate statistical P values (*P < 0.05; **P < 0.01; ***P < 0.001). One-way ANOVA was used to test the statistical differences among the three gene clusters. **(E)** Unsupervised aggregation in the GSE87211 rectal cancer cohort, using survival status, tumor stage, gender, age, project, m^{6}Acluster, and gene cluster as patient annotations. Red represents high expression of regulatory factors, and blue represents low expression.

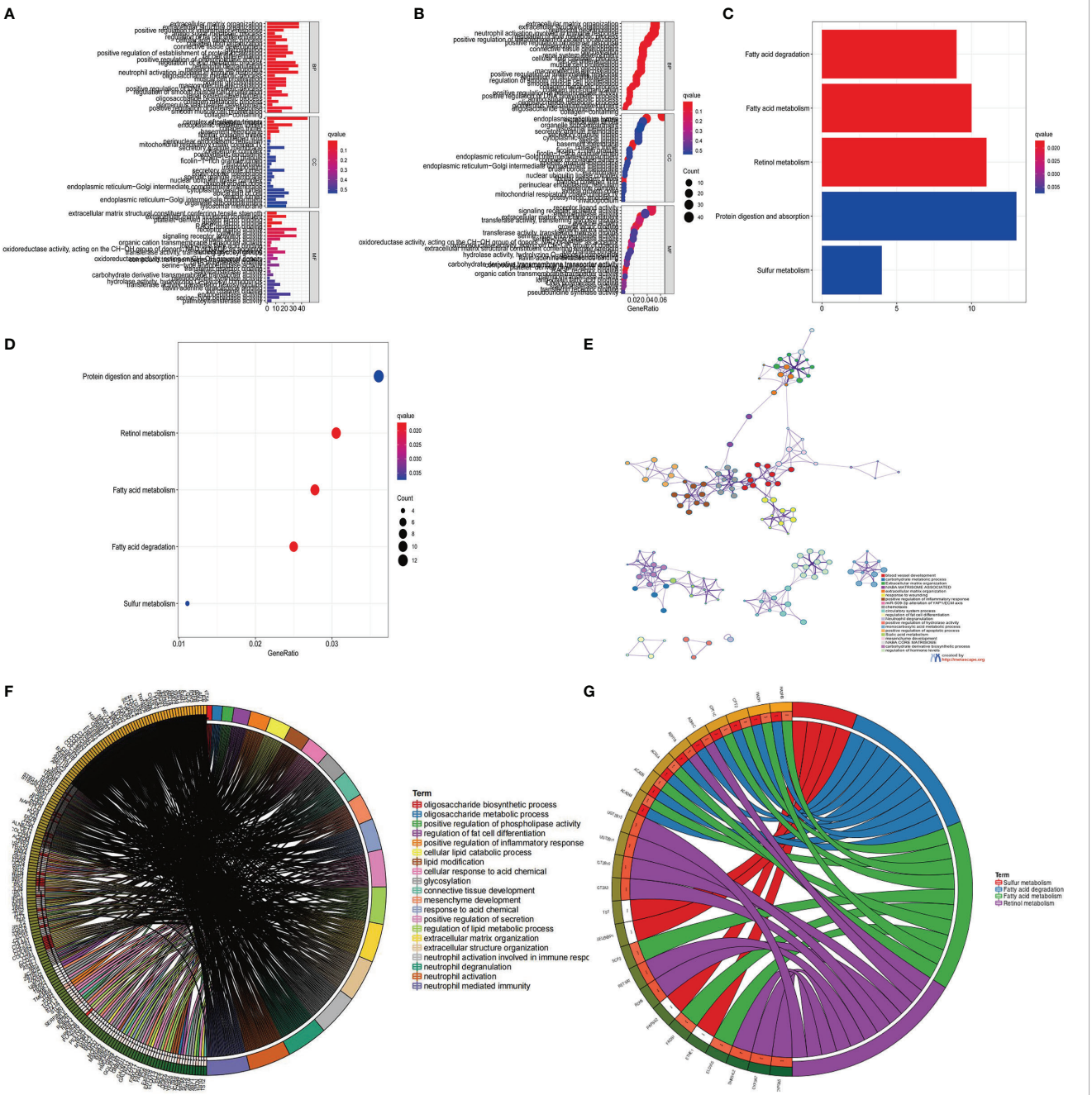

FIGURE 5 | KEGG and GO enrichment analysis of m6A related genes. **(A, B)** GO enrichment analysis for functional annotation of m^{6}A-related genes. The color depth of the histogram represents the number of enriched genes. **(C, D)** KEGG enrichment analysis for the functional annotation of m^{6}A-related genes. The color depth of the histogram represents the number of enriched genes. **(E)** The interaction of pathways of 23 m6A regulatory factors. The circles of different colors represent different types of pathways and the lines linking them represent their interaction. **(F)** Circle plot showing the enrichment analysis of various pathways. **(G)** Circle plot showing the enrichment analysis of different metabolic pathways.

the distribution of tumor mutation burden in different m6Sig score groups and found that regardless of the status of m6A, the H-TMB group had a better prognosis (**Figure 6F**). Further analysis showed that in the H-TMB group, there was no significant difference in the prognosis of patients in the H-m6Ascore and L-m6Ascore, while in the L-TMB group, the H-m6Ascore group had a better prognosis than the L-m6Ascore group(p=0.003) (**Figure 6G**). This is consistent with the results of previous studies, that is, high mutation load is positive correlation with in immune evasion and tumor cell

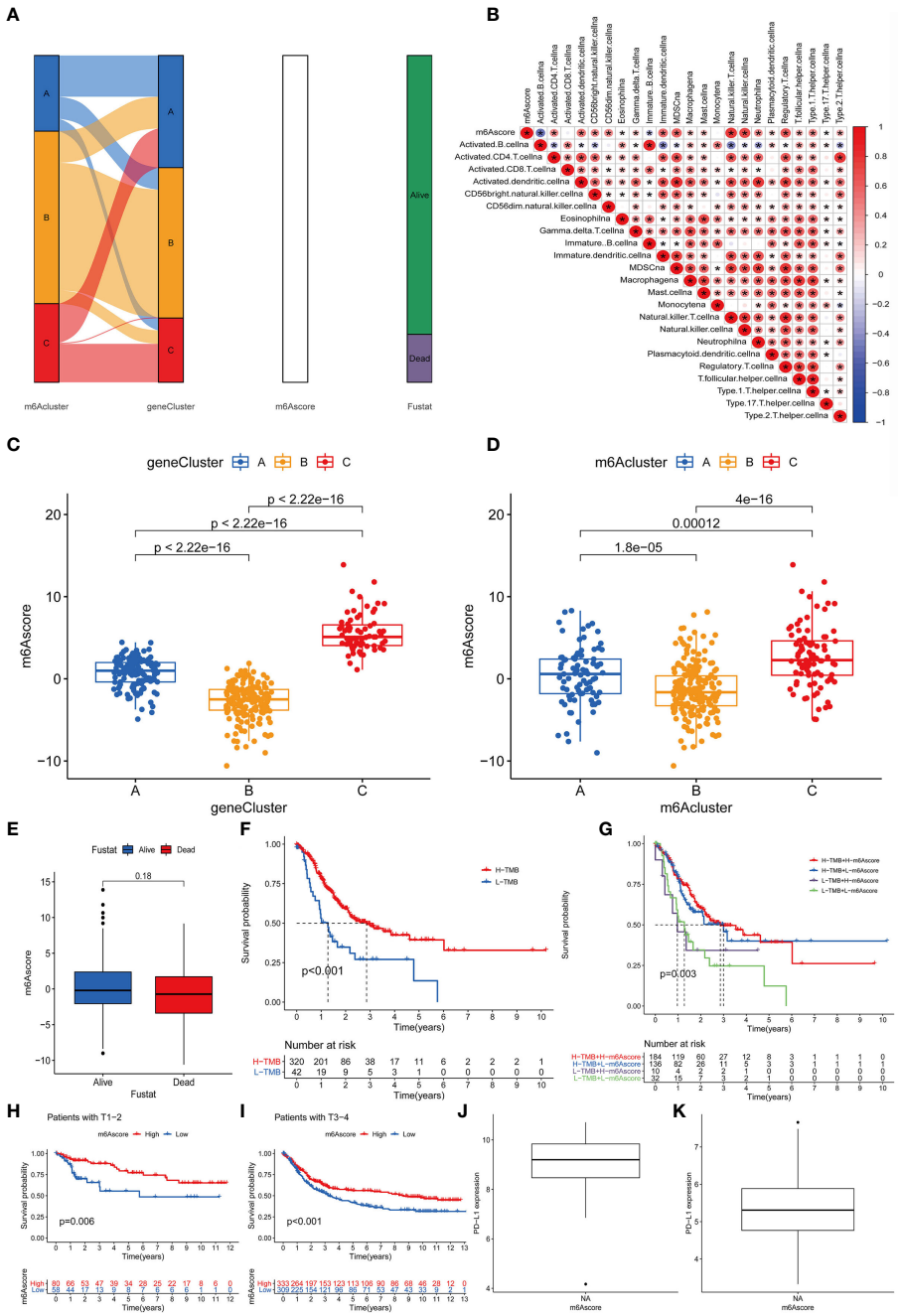

FIGURE 6 | Construction of m6A score and analysis of related modification patterns and clinical treatment effect of m6A score. **(A)** The alluvial map shows the changes of m^{6}Aclusters, gene clusters, m^{6}Ascore and survival status. **(B)** Using Spearman analysis, the correlation between m6score and known gene characteristics in the GSE87211 cohort. Blue is a negative correlation, and red is a positive correlation P values (*P <0.05; **P <0.01; ***P <0.001). **(C)** The difference of gene clusters among the three gene clusters in the GSE87211 cohort. The ordinate represents the m6A score while the abscissa shows the gene cluster A–C. Kruskal Wallis test was used to compare the statistical differences between the three gene clusters (P<0.001). **(D)** The difference of m^{6}Acluster among the three gene clusters in the GSE87211 cohort. The ordinate indicates the m6A score while the abscissa shows the three m6A cluster A–C. Kruskal Wallis test was used to compare the statistical differences between the three gene clusters (P<0.001). **(E)** The difference of m6Ascore between different survival states in the GSE87211 cohort. **(F)** Kaplan-Meier curve of TMB high and low patients in the TCGA cohort, Log-rank test, P<0.001. The numbers of patients with high and low TMB were shown in the bottom. **(G)** Kaplan-Meier curve of patients with high and low TMB-m6Ascore in the TCGA cohort, Log-rank test, P=0.003. **(H)** Kaplan-Meier curve of patients with high and low m6Ascore in patients with T1-2 stage of rectal cancer. Log-rank test, P = 0.006. **(I)** Kaplan-Meier curve of patients with high and low m6Ascore in patients with rectal cancer T3-4 stage. Log-rank test, P<0.001. **(J, K)** PD-L1 expression difference in m6Ascore group.

proliferation (31). Finally, we further evaluated the relationship of m6Ascore in tumor staging of T1-2 and T3-4 patients, and the results showed that the prognosis of patients with stage T1-2 ($p=0.006$) and stage T3-4($p<0.001$) is better under high m6Ascore (**Figures 6H, I**). The above results strongly suggest that m6Ascore can represent the change pattern of m6A and predict the prognosis of RC patients. These data allow us to more fully describe the impact of m6Ascore classification on genomic variation and reveal the possible complex interactions between individual cell mutations and m6A modifications.

The Role of m6Ascore in Predicting Immunotherapeutic Benefits

Next, consider that PD-L1 is a mature biomarker predicting response to anti-PD-1/L1 treatment, the emergence of immunotherapy represented by PD-L1 and PD-1 block is undoubtedly a major breakthrough in cancer treatment. We further compared the relationship between different m6Ascore and PD-L1 expression level and found that the higher the m6Ascore, the higher the PD-L1 expression level (**Figures 6J, K**). In summary, our research results show that there is a close relationship between m6Ascore and immune response, which can be used in clinical work to evaluate immune response and further predict the prognosis of patients.

DISCUSSION

Many recent studies have shown that m6A modification interacts with m6A regulatory factors and plays a vital role in immune, inflammation and cancer treatment (22, 32, 33). So far, most published studies have focused on unilateral studies of TME cell types and regulatory factors, but the overall characterization of TME infiltration mediated by the combined action of multiple m6A regulatory factors is far from enough. Therefore, it is of great significance to further explore the role of different m6A modification modes in TME cell infiltration, which will help us to improve our understanding of the anti-tumor immune response of TME and open up a new path for the immunotherapy of malignant tumors.

In this study, we summarized three different m6A methylation modification patterns, which have their own unique characteristics of TME cell infiltration. m6Aclusters-C has a rich infiltration of innate immune cells, including natural killer cells, MDSC, regulatory T cells, neutrophils, type 2 T helper cells, Immature dendritic cells, and CD56 bright and dim natural killer cells. We also noticed significant increases in Activated B cell, Eosinophilna, Immature B cell, Macrophagena, Mast cellna and Monocytena in m6Aclusters-B. However, it is surprising that m6Aclusters-A is significantly higher than m6Aclusters-B and m6Aclusters-C. The degree of infiltration in immune cells is low. Previous studies have shown that the tumor microenvironment plays an essential role in tumor progression and the effect of immunotherapy. CD8+ T lymphocytes are triggered by specific dendritic cells in the tertiary lymphatic structure (TLS) located in the tumor. Other cell types (such as CD4+ T cells) may also contribute to immune surveillance, thereby enhancing the anti-cancer immune response ability (34). The baseline levels of tumor-infiltrating CD8+ T cells, CD4+ T cells, and NK cells are related to the likelihood of an immune response (35–37). The intratumoral immune landscape, including memory cells, cytotoxic cells [CD8+ T cells, natural killer (NK) cells and NK T (NKT) cells] and immunosuppressive cells [Tregs and myeloid-derived suppressor cells (MDSCs)], quantitative Immune core prognostic markers predict survival more accurately than standard TNM staging (25).

In addition, we also analyzed the enrichment of m6A modification patterns in immune-related biological pathways. m6Acluster-A is significantly enriched in Nucleotide excision repair, cell cycle regulation and Homologous recombination. The feature of m6Acluster-B is that it is significantly enriched in the process of calcium and neurotrophin signaling pathway, aldosterone regulated sodium reabsorption and endocytosis. And m6Acluster-C is significantly enriched in Toll like and Nod receptor signaling pathway, mismatch repair, and DNA replication. Combination studies have shown that mismatch repair defects and Toll like signaling pathway both lead to higher tumor mutation burden and immune response (38–41). The TME is also related to the response to immune checkpoint block (ICB) therapy. Our research is consistent with the above results. Considering the individual heterogeneity of m6A modification, it is necessary to quantify the m6A modification pattern of a single tumor. In view of that, we have established a scoring system to evaluate the m6A modification patterns of individual rectal cancer patients-m6A gene signature, in order to better guide the treatment strategies of individual rectal cancer patients. The results showed that m6Ascore of m6Acluster-C was the highest, followed by m6Acluster-A and m6Acluster-B. In addition, gene clusters constructed from differentially expressed genes (DEGs) identified from different m6A modification patterns have obtained similar results to m6A modification clusters. We also analyzed the prognosis of the m6Ascore high and low groups and found that the high m6Ascore group has a clear survival advantage. This further shows that m6Ascore is a promising tool, and m6Ascore is a prognostic biomarker for RC.

Tumor mutation burden correlates with immunotherapy response (42), in addition, it has been confirmed that programmed death receptor ligand 1 (PD-L1) interacts with the tumor microenvironment to mediate tumor immune escape. PD-L1 inhibitors are a hot spot in tumor immunotherapy in recent years. They can restore the activity of T cells and enhance the body's immune response (43). Here we found that m6Ascore, the higher the expression of PD-L1, which means that m6Ascore can guide immunotherapy. It is worth noting that we also found that m6Ascore can be used to assess the clinicopathological characteristics of patients, including survival status, gender, age, and tumor stage. This research provides a new perspective for the development of new drugs and immunotherapy, and brings hope to the precise treatment of clinical malignant tumors, the identification of different tumor immunophenotypes, and the improvement of individualized tumor immunotherapy.

It must be admitted that our analysis also has potential limitations. First of all, our study is retrospective. Therefore, a prospective cohort of RC patients receiving immunotherapy is

needed to verify our results. Secondly, the newly discovered regulatory factors need to be incorporated into the model in future research to optimize the accuracy of the m6A modification pattern. In addition, it is necessary to explore a suitable rectal cancer data set to verify the effect of m6Ascores from various clinical aspects, so as to further strengthen our conclusions. In summary, in this study, for the first time, we constructed 23 RNA methylation regulators with rectal cancer as the research object, analyzed the m6A modification patterns of 369 rectal cancer samples, and systematically compared these modification patterns with the characteristics of TME cell infiltration are related to clinicopathological characteristics. This research helps to enhance our understanding of the characteristics of TME infiltration and provides new insights for more effective individualized immunotherapy strategies.

DATA AVAILABILITY STATEMENT

The datasets presented in this study can be found in online repositories. The names of the repository/repositories and accession number(s) can be found in the article/**Supplementary Material**.

AUTHOR CONTRIBUTIONS

KL, JH,YH and SY have contributed equally to this work and share first authorship. KL and JH: Design research direction, Writing papers; YH and SY: Data analysis, Drawing figures; QY, FS, CW, YC, WZ, XZ and HL: Searching for references, Helping to write papers; XW: Review and revise the papers, Guidance article writing. All authors contributed to the article and approved the submitted version.

FUNDING

This study was funded by the Natural Science Foundation of China. (No. 81860034 to XW).

SUPPLEMENTARY MATERIAL

The Supplementary Material for this article can be found online at: https://www.frontiersin.org/articles/10.3389/fonc.2022.879405/full#supplementary-material

Supplementary Figure 1 | The expression of 23 m^6A regulatory factors in ZC3H13 Wild. **(A–W)** The upper and lower ends of the box represent a quarter of the value range. The line in the box represents the median value, and the black dots represent the outliers.

Supplementary Figure 2 | Unsupervised cluster analysis of m^6A regulatory factors. **(A)** Consensus matrix legend. **(B–I)** Consensus matrices of the TCGA and GSE87211 cohort for k = 2-9. **(J)** The consensus graph of CDF value K=2-9. **(K)** CDF curve with CDF value K=2-9. **(L)** CDF value K=2-9 in the tracking plot of the samples.

REFERENCES

1. Conde-Muíño R, Cuadros M, Zambudio N, Segura-Jiménez I, Cano C, Palma P. Predictive Biomarkers to Chemoradiation in Locally Advanced Rectal Cancer. *BioMed Res Int* (2015) 2015:921435. doi: 10.1155/2015/921435
2. Siegel RL, Miller KD, Jemal A. Cancer Statistics, 2019. *CA: Cancer J Clin* (2019) 69:7–34. doi: 10.3322/caac.21551
3. Bray F, Ferlay J, Soerjomataram I, Siegel RL, Torre LA, Jemal A. Global Cancer Statistics 2018: GLOBOCAN Estimates of Incidence and Mortality Worldwide for 36 Cancers in 185 Countries. *CA: Cancer J Clin* (2018) 68:394–424. doi: 10.3322/caac.21492
4. Schmoll HJ, Van Cutsem E, Stein A, Valentini V, Glimelius B, Haustermans K, et al. ESMO Consensus Guidelines for Management of Patients With Colon and Rectal Cancer. A Personalized Approach to Clinical Decision Making. *Ann Oncol* (2012) 23:2479–516. doi: 10.1093/annonc/mds236
5. Giraldo NA, Sanchez-Salas R, Peske JD, Vano Y, Becht E, Petitprez F, et al. The Clinical Role of the TME in Solid Cancer. *Br J cancer* (2019) 120:45–53. doi: 10.1038/s41416-018-0327-z
6. Xiong Y, Wang K, Zhou H, Peng L, You W, Fu Z. Profiles of Immune Infiltration in Colorectal Cancer and Their Clinical Significant: A Gene Expression-Based Study. *Cancer Med* (2018) 7:4496–508. doi: 10.1002/cam4.1745
7. Liu Z, Zhu Y, Xu L, Zhang J, Xie H, Fu H, et al. Tumor Stroma-Infiltrating Mast Cells Predict Prognosis and Adjuvant Chemotherapeutic Benefits in Patients With Muscle Invasive Bladder Cancer. *Oncoimmunology* (2018) 7:e1474317. doi: 10.1080/2162402X.2018.1474317
8. Tahmasebi Birgani M, Carloni V. Tumor Microenvironment, A Paradigm in Hepatocellular Carcinoma Progression and Therapy. *Int J Mol Sci* (2017) 18(2):405. doi: 10.3390/ijms18020405
9. Wu J, Liang C, Chen M, Su W. Association Between Tumor-Stroma Ratio and Prognosis in Solid Tumor Patients: A Systematic Review and Meta-Analysis. *Oncotarget* (2016) 7:68954–65. doi: 10.18632/oncotarget.12135
10. Junttila MR, de Sauvage FJ. Influence of Tumour Micro-Environment Heterogeneity on Therapeutic Response. *Nature* (2013) 501:346–54. doi: 10.1038/nature12626
11. Krug RM, Morgan MA, Shatkin AJ. Influenza Viral mRNA Contains Internal N6-Methyladenosine and 5'-Terminal 7-Methylguanosine in Cap Structures. *J Virol* (1976) 20:45–53. doi: 10.1128/jvi.20.1.45-53.1976
12. Desrosiers R, Friderici K, Rottman F. Identification of Methylated Nucleosides in Messenger RNA From Novikoff Hepatoma Cells. *Proc Natl Acad Sci U S A* (1974) 71:3971–5. doi: 10.1073/pnas.71.10.3971
13. Lavi S, Shatkin AJ. Methylated Simian Virus 40-Specific RNA From Nuclei and Cytoplasm of Infected BSC-1 Cells. *Proc Natl Acad Sci U S A* (1975) 72:2012–6. doi: 10.1073/pnas.72.6.2012
14. Wei CM, Moss B. Methylated Nucleotides Block 5'-Terminus of Vaccinia Virus Messenger RNA. *Proc Natl Acad Sci U S A* (1975) 72:318–22. doi: 10.1073/pnas.72.1.318
15. Furuichi Y, Morgan M, Shatkin AJ, Jelinek W, Salditt-Georgieff M, Darnell JE. Methylated, Blocked 5 Termini in HeLa Cell mRNA. *Proc Natl Acad Sci U S A* (1975) 72:1904–8. doi: 10.1073/pnas.72.5.1904
16. Adams JM, Cory S. Modified Nucleosides and Bizarre 5'-Termini in Mouse Myeloma mRNA. *Nature* (1975) 255:28–33. doi: 10.1038/255028a0
17. Quah HM, Chou JF, Gonen M, Shia J, Schrag D, Saltz LB, et al. Pathologic Stage is Most Prognostic of Disease-Free Survival in Locally Advanced Rectal Cancer Patients After Preoperative Chemoradiation. *Cancer* (2008) 113:57–64. doi: 10.1002/cncr.23516
18. Liu Q, Gregory RI. RNAmod: An Integrated System for the Annotation of mRNA Modifications. *Nucleic Acids Res* (2019) 47:W548–w555. doi: 10.1093/nar/gkz479
19. Liu N, Zhou KI, Parisien M, Dai Q, Diatchenko L, Pan T. N6-Methyladenosine Alters RNA Structure to Regulate Binding of a Low-Complexity Protein. *Nucleic Acids Res* (2017) 45:6051–63. doi: 10.1093/nar/gkx141
20. Han D, Liu J, Chen C, Dong L, Liu Y, Chang R, et al. Anti-Tumour Immunity Controlled Through mRNA M(6)A Methylation and YTHDF1 in Dendritic Cells. *Nature* (2019) 566:270–4. doi: 10.1038/s41586-019-0916-x

21. Yang S, Wei J, Cui YH, Park G, Shah P, Deng Y, et al. M(6)A mRNA Demethylase FTO Regulates Melanoma Tumorigenicity and Response to Anti-PD-1 Blockade. *Nat Commun* (2019) 10:2782. doi: 10.1038/s41467-019-10669-0
22. Wang H, Hu X, Huang M, Liu J, Gu Y, Ma L, et al. Mettl3-Mediated mRNA M(6)A Methylation Promotes Dendritic Cell Activation. *Nat Commun* (2019) 10:1898. doi: 10.1038/s41467-019-09903-6
23. Hänzelmann S, Castelo R, Guinney J. GSVA: Gene Set Variation Analysis for Microarray and RNA-Seq Data. *BMC Bioinf* (2013) 14:7. doi: 10.1186/1471-2105-14-7
24. Charoentong P, Finotello F, Angelova M, Mayer C, Efremova M, Rieder D, et al. Pan-Cancer Immunogenomic Analyses Reveal Genotype-Immunophenotype Relationships and Predictors of Response to Checkpoint Blockade. *Cell Rep* (2017) 18:248–62. doi: 10.1016/j.celrep.2016.12.019
25. Jia Q, Wu W, Wang Y, Alexander PB, Sun C, Gong Z, et al. Local Mutational Diversity Drives Intratumoral Immune Heterogeneity in Non-Small Cell Lung Cancer. *Nat Commun* (2018) 9:5361. doi: 10.1038/s41467-018-07767-w
26. Ritchie ME, Phipson B, Wu D, Hu Y, Law CW, Shi W, et al. Limma Powers Differential Expression Analyses for RNA-Sequencing and Microarray Studies. *Nucleic Acids Res* (2015) 43:e47. doi: 10.1093/nar/gkv007
27. Zhang B, Wu Q, Li B, Wang D, Wang L, Zhou YL. M(6)A Regulator-Mediated Methylation Modification Patterns and Tumor Microenvironment Infiltration Characterization in Gastric Cancer. *Mol Cancer* (2020) 19:53. doi: 10.1186/s12943-020-01170-0
28. Zeng D, Li M, Zhou R, Zhang J, Sun H, Shi M, et al. Tumor Microenvironment Characterization in Gastric Cancer Identifies Prognostic and Immunotherapeutically Relevant Gene Signatures. *Cancer Immunol Res* (2019) 7:737–50. doi: 10.1158/2326-6066.CIR-18-0436
29. Xu T, Gao S, Liu J, Huang Y, Chen K, Zhang X. MMP9 and IGFBP1 Regulate Tumor Immune and Drive Tumor Progression in Clear Cell Renal Cell Carcinoma. *J Cancer* (2021) 12:2243–57. doi: 10.7150/jca.48664
30. Chen H, Chong W, Wu Q, Yao Y, Mao M, Wang X. Association of LRP1B Mutation With Tumor Mutation Burden and Outcomes in Melanoma and Non-Small Cell Lung Cancer Patients Treated With Immune Check-Point Blockades. *Front Immunol* (2019) 10:1113. doi: 10.3389/fimmu.2019.01523
31. Li XC, Jin F, Wang BY, Yin XJ, Hong W, Tian FJ. The M6a Demethylase ALKBH5 Controls Trophoblast Invasion at the Maternal-Fetal Interface by Regulating the Stability of CYR61 mRNA. *Theranostics* (2019) 9:3853–65. doi: 10.7150/thno.31868
32. Zhao Q, Zhao Y, Hu W, Zhang Y, Wu X, Lu J, et al. M(6)A RNA Modification Modulates PI3K/Akt/mTOR Signal Pathway in Gastrointestinal Cancer. *Theranostics* (2020) 10:9528–43. doi: 10.7150/thno.42971
33. Fridman WH, Zitvogel L, Sautès-Fridman C, Kroemer G. The Immune Contexture in Cancer Prognosis and Treatment. *Nat Rev Clin Oncol* (2017) 14:717–34. doi: 10.1038/nrclinonc.2017.101
34. Topalian SL, Taube JM, Anders RA, Pardoll DM. Mechanism-Driven Biomarkers to Guide Immune Checkpoint Blockade in Cancer Therapy. *Nat Rev Cancer* (2016) 16:275–87. doi: 10.1038/nrc.2016.36
35. Borst J, Ahrends T, Bąbała N, Melief CJM, Kastenmüller W. CD4(+) T Cell Help in Cancer Immunology and Immunotherapy. *Nat Rev Immunol* (2018) 18:635–47. doi: 10.1038/s41577-018-0044-0
36. Hsu J, Hodgins JJ, Marathe M, Nicolai CJ, Bourgeois-Daigneault MC, Trevino TN, et al. Contribution of NK Cells to Immunotherapy Mediated by PD-1/PD-L1 Blockade. *J Clin Invest* (2018) 128:4654–68. doi: 10.1172/JCI99317
37. Le DT, Durham JN, Smith KN, Wang H, Bartlett BR, Aulakh LK, et al. Mismatch Repair Deficiency Predicts Response of Solid Tumors to PD-1 Blockade. *Sci (New York NY)* (2017) 357:409–13. doi: 10.1126/science.aan6733
38. Bhatia S, Miller NJ, Lu H, Longino NV, Ibrani D, Shinohara MM, et al. Intratumoral G100, A TLR4 Agonist, Induces Antitumor Immune Responses and Tumor Regression in Patients With Merkel Cell Carcinoma. *Clin Cancer Res* (2019) 25:1185–95. doi: 10.1158/1078-0432.CCR-18-0469
39. Uthaman S, Pillarisetti S, Hwang HS, Mathew AP, Huh KM, Rhee JH, et al. Tumor Microenvironment-Regulating Immunosenescence-Independent Nanostimulant Synergizing With Near-Infrared Light Irradiation for Antitumor Immunity. *ACS Appl Materials Interfaces* (2021) 13:4844–52. doi: 10.1021/acsami.0c20063
40. Jiang Y, Wan Y, Gong M, Zhou S, Qiu J, Cheng W. RNA Demethylase ALKBH5 Promotes Ovarian Carcinogenesis in a Simulated Tumour Microenvironment Through Stimulating NF-κb Pathway. *J Cell Mol Med* (2020) 24:6137–48. doi: 10.1111/jcmm.15228
41. Corrò C, Dutoit V, Koessler T. Emerging Trends for Radio-Immunotherapy in Rectal Cancer. *Cancers* (2021) 13(6):1374. doi: 10.3390/cancers13061374
42. Sun J, Zheng Y, Mamun M, Li X, Chen X, Gao Y. Research Progress of PD-1/PD-L1 Immunotherapy in Gastrointestinal Tumors. *Biomedicine Pharmacotherapy* (2020) 129:110504. doi: 10.1016/j.biopha.2020.110504
43. Dammeijer F, van Gulijk M, Mulder Evalyn E, et al. Dammeijer Floris,van Gulijk Mandy, Mulder Evalyn E, et al. The PD-1/PD-L1-Checkpoint Restrains T cell Immunity in Tumor-Draining Lymph Nodes. *Cancer Cell* (2020) 38:685-700.e8. doi: 10.1016/j.ccell.2020.09.001

Conflict of Interest: The authors declare that the research was conducted in the absence of any commercial or financial relationships that could be construed as a potential conflict of interest.

Advantages of publishing in Frontiers

OPEN ACCESS
Articles are free to read for greatest visibility and readership

FAST PUBLICATION
Around 90 days from submission to decision

HIGH QUALITY PEER-REVIEW
Rigorous, collaborative, and constructive peer-review

TRANSPARENT PEER-REVIEW
Editors and reviewers acknowledged by name on published articles

Frontiers
Avenue du Tribunal-Fédéral 34
1005 Lausanne | Switzerland

Visit us: www.frontiersin.org
Contact us: frontiersin.org/about/contact

REPRODUCIBILITY OF RESEARCH
Support open data and methods to enhance research reproducibility

DIGITAL PUBLISHING
Articles designed for optimal readership across devices

FOLLOW US
@frontiersin

IMPACT METRICS
Advanced article metrics track visibility across digital media

EXTENSIVE PROMOTION
Marketing and promotion of impactful research

LOOP RESEARCH NETWORK
Our network increases your article's readership